Komitet Krystalografii PAN
Polskie Towarzystwo Krystalograficzne
Politechnika Wrocławska
Instytut Niskich Temperatur i Badań Strukturalnych PAN

64 Konwersatorium Krystalograficzne

Polish Crystallographic Meeting

Warsztaty Naukowe PTKryst

Sesja Naukowa Sekcji Młodych Krystalografów PTKryst

5 - 7 VII 2023

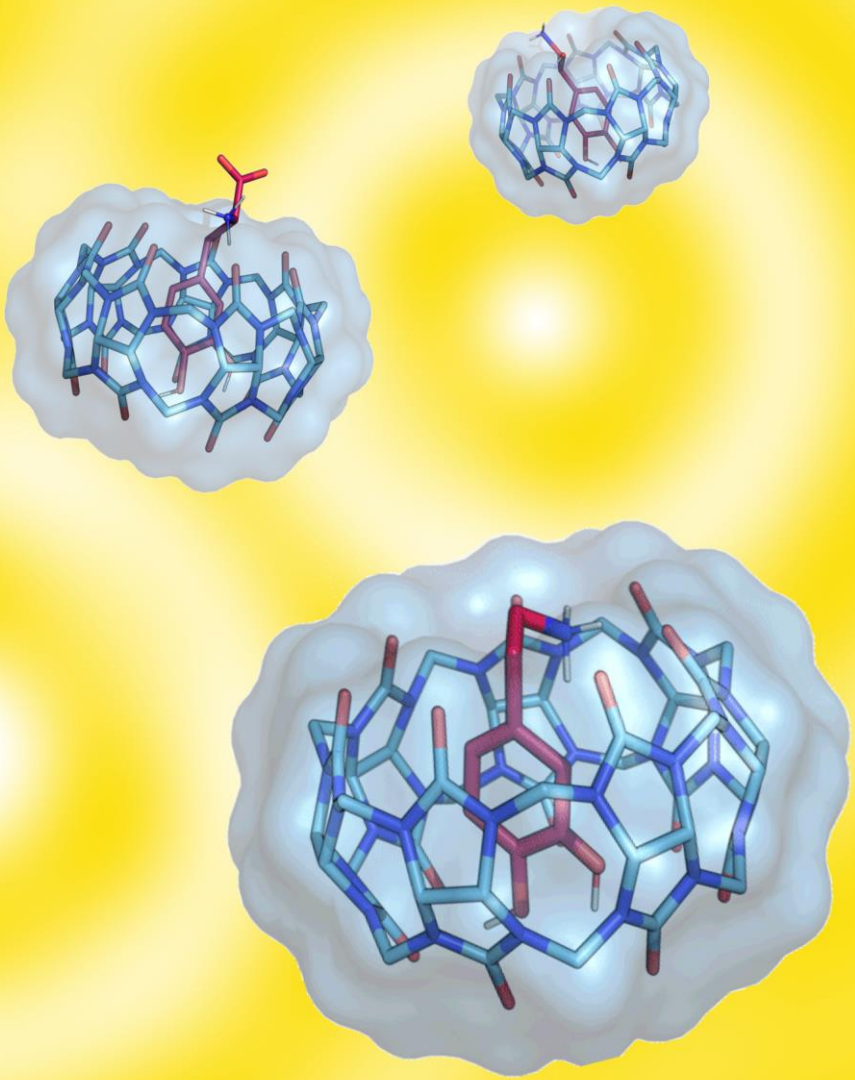

64 Konwersatorium Krystalograficzne

Warsztaty Naukowe PTKryst i Sesja Sekcji Młodych Krystalografów PTKryst

5 VII – 7 VII 2023 r.

Program
Streszczenia komunikatów
Lista uczestników i autorów prac

Organizatorzy:
Komitet Krystalografii PAN
Politechnika Wrocławska: Wydział Chemiczny i Wydział Elektroniki, Fotoniki i Mikrosystemów
Instytut Niskich Temperatur i Badań Strukturalnych PAN we Wrocławiu
Polskie Towarzystwo Krystalograficzne

Sponsorzy Konwersatorium:

Rigaku Europe SE

Sponsor Warsztatów i Sesji Młodych Krystalografów PTKryst:

Komitet Organizacyjny:
Marek Wołcyrz – przewodniczący, Marek Daszkiewicz - zastępca przewodniczącego, Piotr Młynarz, Jarosław Serafińczuk, Kinga Suwińska, Dorota Kowalska, Vasyl Kinzhybalo, Anna Gągor, Tamara Bednarchuk, Piotr Rejnhardt, Dawid Drozdowski, Magdalena Rowińska, Konrad Dyk, Ewa Bukowska

Redakcja:
Marek Wołcyrz, Dorota Kowalska

Wydawca:
Instytut Niskich Temperatur i Badań Strukturalnych PAN, Wrocław
oraz Komitet Krystalografii PAN

ISBN 978-83-966642-1-1

Tematyka Konwersatorium obejmuje badania podstawowe i stosowane dotyczące idealnej i realnej struktury kryształów prowadzone za pomocą promieniowania rentgenowskiego uzyskiwanego zarówno tradycyjnymi metodami jak i w synchrotronach, badania przy użyciu neutronów i elektronów, zagadnienia symetrii, przemian fazowych i wzrostu kryształów, nowe metody badawcze i obliczeniowe oraz wszelkie inne aspekty krystalografii. Konwersatorium stanowi forum wymiany poglądów wszystkich polskich krystalografów.

Ilustracja na okładce: Kompleksy CB[7] z dopaminą, L-noradrenaliną i L-DOPA – z komunikatu O-7 autorstwa Eweliny Zaorskiej i Maury Malińskiej.

PROGRAM KONWERSATORIUM I WARSZTATÓW POLSKIEGO TOWARZYSTWA KRYSTALOGRAFICZNEGO
PROGRAMME OF THE MEETING AND PCA WORKSHOP

Środa, 5 lipca 2023 r. / Wednesday, July 5, 2023

9:00 – 13:30	**WARSZTATY NAUKOWE PTKryst / PCA WORKSHOP** **Practical electron crystallography using Rigaku XtaLAB Synergy-ED instrument** **Jakub Wojciechowski** Rigaku Europe SE, Neu-Isenburg	**W**
15:00 – 19:30	**SESJA NAUKOWA SEKCJI MŁODYCH KRYSTALOGRAFÓW POLSKIEGO TOWARZYSTWA KRYSTALOGRAFICZNEGO / SCIENTIFIC SESSION OF THE YOUNG CRYSTALLOGRAPHERS SECTION OF THE POLISH CRYSTALLOGRAPHIC ASSOCIATION**	**S**

Czwartek, 6 lipca 2023 r. / Thursday, July 6, 2023

9:00 – 9:30	**OTWARCIE KONWERSATORIUM / OPENING CEREMONY** **UROCZYSTE WRĘCZENIE NAGRÓD LAUREATOM V OGÓLNOPOLSKIEJ OLIMPIADY KRYSTALOGRAFICZNEJ/ AWARDS GIVEAWAY TO THE WINNERS OF 5TH NATIONAL CRYSTALGRAPHIC OLYMPIAD**	
	SESJA PLENARNA 1 / PLENARY SESSION 1	
9:30 – 9:50	**Grygoriy Dmytriv**, Nazar Pavlyuk, Volodymyr Pavlyuk, Helmut Ehrenberg **Crystallography and art: on examples of core-shell structures** Ivan Franko National University of Lviv; Jan Długosz University in Częstochowa; Karlsruhe Institute of Technology, Eggenstein-Leopoldshafen	**O-1**
9:50 – 10:10	**Andrzej Katrusiak**, Kinga Roszak **Preference for low-density high-pressure polymorphs of DL-menthol** Faculty of Chemistry, Adam Mickiewicz University, Poznań	**O-2**
10:10 – 10:20	**Szymon Sobczak**, Andrzej Katrusiak **High-pressure synthesis of novel perovskites** Adam Mickiewicz University, Poznań	**O-3**

10:20 – 10:40	**Jarosław Serafińczuk** **Wysokorozdzielcza dyfrakcja rentgenowska w badaniach warstw epitaksjalnych prowadzona od krawędzi próbki** Katedra Nanometrologii, Politechnika Wrocławska; Sieć Badawcza Łukasiewicz - PORT Polskie Centrum Rozwoju Technologii, Wrocław	**O-4**
10:40 – 11:00	**Zbigniew Kaszkur**, Ilia Smirnov **Nanocrystallography *in situ* (Nanopowder diffraction *in situ*)** Institute of Physical Chemistry PAS, Warszawa	**O-5**
11:00 – 11:30	**PRZERWA / BREAK**	
	SESJA PLENARNA 2 / PLENARY SESSION 2	
	Sesja specjalna dedykowana Profesorowi Januszowi Lipkowskiemu z okazji 80-rocznicy urodzin **Special session dedicated to Professor Janusz Lipkowski on the occasion of his 80th birthday**	
11:30 – 11:40	**Kinga Suwińska** **Jubileusz Profesora Janusza Lipkowskiego - wprowadzenie do sesji specjalnej** Uniwersytet Kardynała Stefana Wyszyńskiego w Warszawie	**O-6**
11:40 – 11:55	Ewelina Zaorska, **Maura Malińska** **Unlocking the secrets of molecular recognition in aqueous solutions: a study on the properties of cucurbit[7]uril and neurotransmitters/ amino acids complexes** Wydział Chemii, Uniwersytet Warszawski	**O-7**
11:55 – 12:05	**Armand Budzianowski**, Katarzyna Betlejewska-Kielak, Elżbieta Bednarek, Katarzyna Michalska, Jan K. Maurin **Characterization of the flurbiprofen-β-cyclodextrin inclusion complex by X-ray techniques** National Centre for Nuclear Research, Otwock; Department of Synthetic Drugs, National Medicines Institute, Warsaw; Falsified Medicines and Medical Devices Department, National Medicines Institute, Warsaw	**O-8**
12:05 – 12:25	**Vasyl Kinzhybalo**, Marta Otręba, Jakub Wojciechowski, Miłosz Siczek, Katarzyna Ślepokura **Combining X-ray and electron diffraction for dehydration and structural description of sodium hypodiphosphates** Institute of Low Temperature and Structure Research, Polish Academy of Sciences, Wroclaw; University of Wroclaw, Faculty of Chemistry; Rigaku Europe SE, Neu Isenburg	**O-9**
12:25 – 12:35	**Urszula Maciołek**, Ewaryst Mendyk, Marcin Kuśmierz, Anna E. Kozioł **Kwercetyna jako synton supramolekularny w układach dwuskładnikowych** Instytut Nauk Chemicznych, Wydział Chemii, Uniwersytet Marii Curie-Skłodowskiej, Lublin	**O-10**
12:35 – 12:55	G. J. Reiss, M. Wyshusek, **I. S. Konovalova** **What is the actual supramolecular architecture of theophylline polymorphs and co-crystals with water and iodine from energetic viewpoint?** SSI "Institute for Single Crystals", National Academy of Science of Ukraine, Kharkiv; Bioinorganic Chemistry, Heinrich-Heine-University, Düsseldorf	**O-11**

12:55 – 13:05	**Katarzyna Jarzembska** **Tracing of transient species *via* combined crystallographic and spectroscopic methods – new perspectives from the XFEL Centers of Excellence initiative** Department of Chemistry, University of Warsaw	**O-12**
13:05 – 15:00	**PRZERWA / BREAK**	
	SESJA PLENARNA 3 / PLENARY SESSION 3	
15:00 – 15:20	**Jakub Wojciechowski**, Khai Truong, Christian Goeb, Christian Schürmann, Robert Bücker, Mathias Meyer, Fraser White **Rigaku advances in X-ray and electron crystallography** Rigaku Europe SE, Neu-Isenburg	**O-13**
15:20 – 15:40	Maciej Grzywa, **Sebastian Machowski** **Określanie struktury z użyciem wysokiej jakości danych rentgenowskiej dyfrakcji proszkowej** Testchem Radlin; Rigaku Europe SE, Neu-Isenburg	**O-14**
15:40 – 16:00	Eddy Martin**, Vernon Smith** **Latest development in SC-XRD from Bruker AXS** Bruker AXS GmbH	**O-15**
16:00 – 16:20	**Lei Ding**, Marco Sommariva, Milen Gateshki **Hard-radiation laboratory X-ray powder diffraction** Malvern Panalytical B.V., Almelo	**O-16**
16:20 – 16:40	**Kamil Urbański** **Mozliwości badawcze XRD poza warunkami otoczenia** Anfon Paar Poland, Warszawa	**O-17**
16:40 – 17:00	**Szymon Stolarek,** A. Cheminal, B. Faure, S. Rodrigues, P. Panine **Extending measuring length (and time) scales of laboratory SAXS/WAXS beamlines** Xenocs SAS, Grenoble	**O-18**
17:00 – 17:20	**Maja Zupancic** **Expanding single crystal design space using temperature and vacuum in the CrystalBreeder** Technobis Crystallization Systems, Alkmaar	**O-19**
17:30 – 20:00	**SESJA PLAKATOWA A / POSTER SESSION A**	

Piątek, 7 lipca 2023 r. / Friday, July 7, 2023

SESJA PLENARNA 4 / PLENARY SESSION 4

9:00 – 9:15 **O-20**

<u>**Joanna Loch**</u>, Paulina Worsztynowicz, Joanna Śliwiak, Barbara Imiołczyk, Kinga Pokrywka, Mateusz Chwastyk, Marta Grzechowiak, Mirosław Gilski, Mariusz Jaskólski

Structural characterization of *Rhizobium etli* thermostable L-asparaginase ReAIV

Faculty of Chemistry, Jagiellonian University, Krakow; Institute of Bioorganic Chemistry, Polish Academy of Sciences, Poznań; Institute of Physics, Polish Academy of Sciences, Warsaw; Faculty of Chemistry, Adam Mickiewicz University, Poznań

9:15 – 9:30 **O-21**

<u>**Mirosław Gilski**</u>, Julian C.-H. Chen, Changsoo Chang, Maciej Kubicki, Mariusz Jaskólski, Andrzej Joachimiak

What to do with a vast amount of protein diffraction data at an extremely high resolution of 0.38Å

Institute of Bioorganic Chemistry, Polish Academy of Sciences, Poznań; Faculty of Chemistry, A. Mickiewicz University, Poznań; Structural Biology Center, Biosciences Division, Argonne National Laboratory

9:30 – 9:50 **O-22**

Leszek Błaszczyk, Marcin Ryczek, Bimolendu Das, Martyna Pluta, Magdalena Bejger, Kazuhiko Nakatani, <u>**Agnieszka Kiliszek**</u>

Analiza strukturalna RNA powtórzeń G2C4 związanych ze stwardnieniem zanikowym bocznym i otępieniem czołowo-skroniowym: polimorfizm strukturalny RNA oraz jego potencjał do oddziaływania z syntetycznymi cząsteczkami

Instytut Chemii Bioorganicznej PAN, Poznań

9:50 – 10:10 **O-23**

<u>**Marta K. Dudek**</u>, Maura Malińska, Agata Jeziorna, Piotr Paluch, Justyna Zając, Rafał Dolot

An uneven fight with elusive polymorphs of meloxicam

Centre of Molecular and Macromolecular Studies, Polish Academy of Sciences, Łódź; Department of Chemistry, University of Warsaw

10:10 – 10:25 **O-24**

<u>**Dawid Drozdowski**</u>, Anna Gągor, Mirosław Mączka

Two-dimensional hybrid perovskites with (110)-oriented layers and large octahedra tilting

Institute of Low Temperature and Structure Research, Polish Academy of Sciences, Wrocław

10:25 – 10:40 **O-25**

<u>**Maria Książek**</u>, Marek Weselski, Aleksandra Półrolniczak, Andrzej Katrusiak, Damian Paliwoda, Joachim Kusz, Robert Bronisz

Pressure induced spin crossover in the two-dimensional coordination polymer of mixed crystals $[Fe(bbtr)_3](BF_4)_{2x}(ClO4)_{2(1-x)}$ ($0 \leq x \leq 1$)

Institute of Physics, University of Silesia, Chorzów; Faculty of Chemistry, University of Wrocław; Faculty of Chemistry, Adam Mickiewicz University of Poznań; LCC, CNRS and University of Toulouse

10:40 – 10:55 **O-26**

<u>**Kornel Roztocki**</u>

Unusual properties of flexible MOFs and their applicability in gas storage and separation

Adam Mickiewicz University, Poznań

11:00 – 13:00 **SESJA PLAKATOWA B / POSTER SESSION B**

13:00 – 15:00 **PRZERWA / BREAK**

SESJA PLENARNA 5 / PLENARY SESSION 5

15:00 – 15:20 **O-27**

Maciej Kozak, Tomasz Kołodziej, Joanna Sławek, Grzegorz Gazdowicz, Agnieszka Klonecka, Jarosław Wiechecki, Adriana Wawrzyniak

SOLCRYS - PX beamline at SOLARIS NSRC - updated design and progress in construction

SOLARIS National Synchrotron Radiation Centre, Jagiellonian University, Kraków; Department of Biomedical Physics, Faculty of Physics, Adam Mickiewicz University, Poznań; Faculty of Physics, Astronomy and Applied Computer Science, Jagiellonian University, Kraków; Doctoral School of Exact and Natural Sciences, Jagiellonian University, Kraków

15:20 – 15:35 **O-28**

Anna A. Hoser, Toms Rekis, Helena Butkiewicz, Karlis Berzins, Anders Ø. Madsen

Revisiting the thermodynamics of phase transition in the jumping crystal L-pyroglutamic acid: insights from dynamic quantum crystallography and spectroscopy

Faculty of Chemistry, University of Warsaw; Department of Pharmacy, Copenhagen University

15:35 – 15:45 **O-29**

Svitlana Shishkina, Anna Shaposhnik, Vitalii Rudiuk, Igor Levandovskiy

New polymorphic modifications of 6-methyluracil: experimental and quantum chemical study for the practical use

State Scientific Institution, "Institute for Single Crystals" of the National Academy of Sciences of Ukraine, Kharkiv; Farmak JSC, Kyiv; National Technical University of Ukraine “Igor Sikorsky Kyiv Polytechnic Institute”

15:45 – 16:00 **O-30**

Monika K. Krawczyk

Nietypowa faza w krysztale trifenylosilanolu jako wynik szybkiego chłodzenia (flash cooling)

Instytut Fizyki Doświadczalnej, Uniwersytet Wrocławski

16:00 – 16:15 **O-31**

Marcin Oszajca, Anabel Berenice Gonzalez Guillen, Marlena Gryl, Wiesław Łasocha

Solving a past conundrum – a peek into a class of carboxylic group-based molybdates

Wydział Chemii Uniwersytetu Jagiellońskiego, Kraków

16:15 – 16:30 **O-32**

Wojciech Paszkowicz, Hanna Dąbkowska, Tomasz Rygier

Determination of iron distribution in inhomogeneous $Ca_3CrFeGe_3O_{12}$ garnet

Institute of Physics, Polish Academy of Sciences, Warsaw; McMaster University, Brockhouse Institute for Materials Research, Hamilton; Warsaw University of Technology, Faculty of Materials Science and Engineering

16:30 – 16:45 **O-33**

Ilia Smirnov, Zbigniew Kaszkur, Armin Hoell

Analysis of twinning in *fcc* nanoparticles by X-ray diffraction: a multidomain XRD approach

Institute of Physical Chemistry PAS, Warsaw; Helmholtz-Zentrum Berlin für Materialien und Energie

16:45 – 17:00 **WRĘCZENIE DYPLOMÓW ZA NAJLEPSZE PREZENTACJE PLAKATOWE – ZAKOŃCZENIE KONWERSATORIUM**

GRANTING DIPLOMAS FOR THE BEST POSTER PRESENTATIONS – CLOSING CEREMONY

17:00 **WALNE ZEBRANIE SPRAWOZDAWCZE POLSKIEGO TOWARZYSTWA KRYSTALOGRAFICZNEGO / GENERAL ASSEMBLY MEETING OF THE POLISH CRYSTALLOGRAPHIC ASSOCIATION**

REFERATY PLENARNE
ORAL SESSIONS

O-1

CRYSTALLOGRAPHY AND ART: ON EXAMPLES OF CORE-SHELL STRUCTURES

Grygoriy Dmytriv[1], Nazar Pavlyuk[1,2], Volodymyr Pavlyuk[1,2], Helmut Ehrenberg[3]

[1] Ivan Franko National University of Lviv,
Kyryla & Mefodia str. 6, 79005 Lviv, Ukraine,
[2] Jan Długosz University in Częstochowa,
al. Armii Krajowej 13/15, 42200 Częstochowa, Poland
[3] Karlsruhe Institute of Technology,
Hermann-von-Helmholtz-Platz 1 D-76344 Eggenstein-Leopoldshafen, Germany

When people talk about the beauty of crystals, they usually mean their outer shape. For example, many famous diamonds in the world even have their own names and stories [1]. The structure of the crystals from the inside is no less beautiful, even if it is a single crystal of an intermetallic compound up to 0.5×0.5×0.5 mm in size. As an example, we will consider several magnesium intermetallic compounds with a core-shell structure.

Earlier crystal structures of three compounds were presented at the 25th Congress and General Assembly of the International Union of Crystallography in Prague, Czech Republic (August 14-22, 2021): $Li_{20}Mg_6Cu_{13}Al_{42}$ (sp. gr. $Im\bar{3}$, a = 13.8451(2) Å), $Mg_9Ni_6Ga_{14}$ (sp. gr. $Fd\bar{3}m$, a = 19.8621(1) Å), Mg_3Ni_2Ga (sp. gr. $Fd\bar{3}m$, a = 11.4886(17) Å) [2]. This year new crystal structure of such type compound $MgMn_4Ga_{18}$ (sp. gr. $P4/mmm$, a = 6.3116(9) Å, c = 9.944(2) Å) [3] was placed on official Happy New Year postcard of Department of Inorganic Chemistry, Ivan Franko National University of Lviv (Fig. 1).

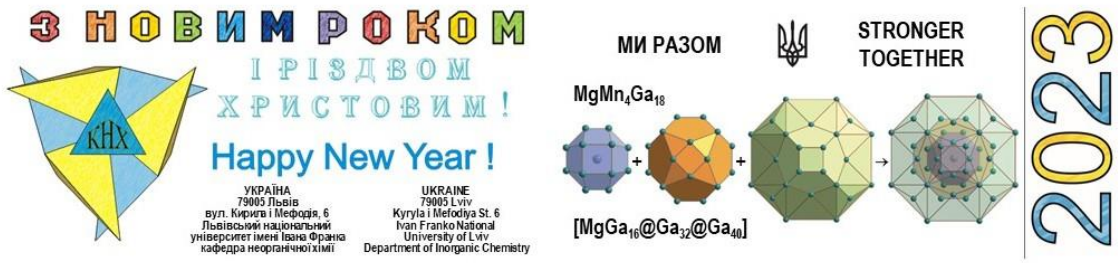

Fig. 1. Happy New Year postcard of Department of Inorganic Chemistry, Ivan Franko National University of Lviv.

Unfortunately, by some chemists such type of structure was described as “matryoshka clusters” [4]. We want to show on our intermetallic compounds with core-shell structures that this definition is not correct and must be changed. First of all this definition is completely wrong from the point of view of symmetry of such type of compounds, which have higher level of symmetry. From this point of view, there are at least three other concepts for describing compounds with core-shell clusters. The first concept is Chinese puzzle balls, the second is “Durchbrochener Polyeder” and the third is Johannes Kepler’s Platonic Solids model of the Solar system from Mysterium Cosmographicum (Fig. 2).

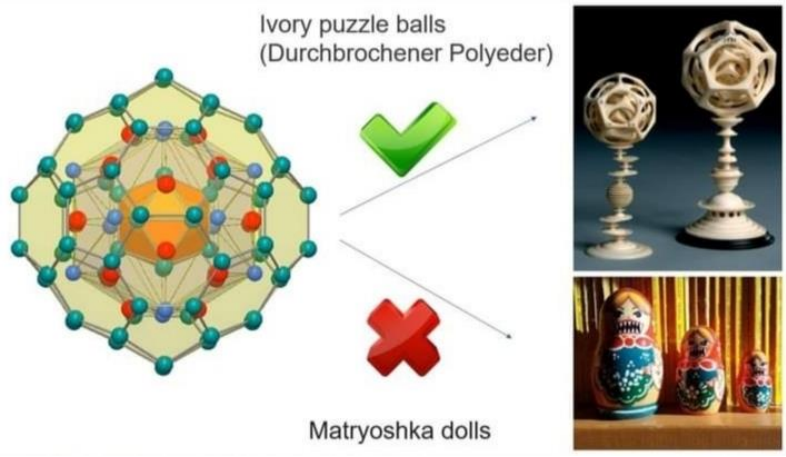

Fig. 2. Correct and incorrect way for a description of core-shell structures by art objects.

This work was partially supported by the Simons Foundation (Award Number: 1037973).

References

[1] https://en.wikipedia.org/wiki/List_of_diamonds.
[2] G. Dmytriv, N. Pavlyuk, V. Pavlyuk, H. Ehrenberg, *Acta Cryst*. *A*, **77** (2021) C543.
[3] N. Pavlyuk, G. Dmytriv, V. Pavlyuk, I. Chumak, S. Indris, B. Schwarz, H Ehrenberg, *Acta Cryst*. *C*, **78** (2022) 455.
[4] X. Huang, J. Zhao, Y. Su, Z. Chen, R. B. King, *Scientific Reports*, **4** (2014) 6915.

O-2

PREFERENCE FOR LOW-DENSITY HIGH-PRESSURE POLYMORPHS OF DL-MENTHOL

Andrzej Katrusiak and Kinga Roszak

Faculty of Chemistry, Adam Mickiewicz University, Poznań

High-temperature polymorphs are intuitively connected with the density reduction, but numerous exceptions show that this is not a general rule. For example, the transformation between the low-temperature low-density resorcinol polymorph α and high-temperature high-density polymorph β, the first structurally characterized polymorphs of organic compounds in the 1930s [1-3], the transition between strongly deformed guanidinium nitrate phases [4] or the ferroelectric-paraelectric phases of KH_2PO_4 and of similar KDP-type (OH···O bonded) compounds [5] contradict the generality of temperature-density relation. However, the pressure-density relation, that high-pressure phases must be more dense than the low-pressure ones, is usually considered a general one. Here we present new experimental evidence of the low-density phases in situ crystallized under the high-pressure conditions. Two new polymorphs β and γ of bis-3-nitrophenyl disulphide $(3\text{-}NO_2\text{-}PhS)_2$ were nucleated under high-temperature high-pressure conditions from the quickly cooled sample in a diamonds-anvil cell; the crystals recovered to ambient conditions had their density significantly lower than that of polymorph α crystallized under the atmospheric conditions, according to our X-ray diffraction determination [6]. More recently, we established that another compound, DL-menthol, displays a preference to form a lower-density polymorph β when crystallized either in isothermal or isochoric conditions above 0.4 GPa [7]. These observations show that the pressure-volume relations between condensed phases can be more complicated than usually assumed.

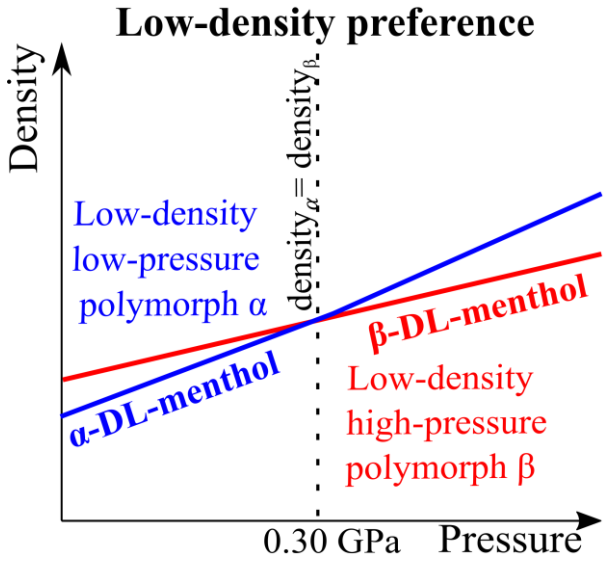

Fig. 1 Low-density preference of DL-menthol.

References
[1] J. M. Robertson, *Proc. Roy. Soc. London A*, **157** (1936) 79–99.
[2] J. M. Robertson, A. R. Ubbelhode, *Proc. Roy. Soc. London A*, **167** (1938) 122–135.
[3] F. Safari, A. Katrusiak, *J. Phys. Chem. C*, **125** (2021) 23501–23509.
[4] A. Katrusiak, M. Szafrański, *J. Mol. Struct.*, **378** (1996) 205–223.
[5] A. Katrusiak, *Phys. Rev. B.*, **48** (1993) 2992–3002.
[6] S. Sobczak, P. Ratajczyk, A. Katrusiak, *Chem. Eur. J.*, **27** (2021) 10769–10779.
[7] K. Roszak, A. Katrusiak, *IUCrJ*, **10** (2023) 341–351.

O-3

HIGH-PRESSURE SYNTHESIS OF NOVEL PEROVSKITES

Szymon Sobczak, Andrzej Katrusiak

Adam Mickiewicz University, ul. Uniwersytetu Poznanskiego 8, 61-614 Poznań, Poland

The energy required to induce a chemical reaction can be delivered to a reactant system through various forms such as light, heat, or electric potential. However, it's also possible to activate reactions using mechanical force. The mechanical energy, supplied by techniques like ball-milling, generates friction, stress, and strain, often resulting in the formation of fine powder or amorphous solid. Importantly, similar effects can be also observed when the reactant are compressed in hydrostatic pressure for example in a diamond anvil cell (DAC).[1]

Here, we demonstrate a high-pressure protocol for obtaining novel perovskite materials *via* two distinct approaches. The first approach, called a *'bottom-up*' synthesis, involves the dissolution of PbI_2 in an aqueous solution of HI at high-pressure, allowed for formation of the elusive, up to this point, iodoplumbic acid. Structural analysis at high-pressure revealed two hydrated hydronium salts with compositions $[H_3O][PbI_3] * nH_2O$ (n = 3, 4) in form of single crystals.[2] The second approach, a 'top-down' method, involves the pressure-induced disproportionation of $DmaFe^{2+}Fe^{3+}For_6$ (where Dma represents $(CH_3)_2NH_2^+$) to form $Dma_3Fe^{2+}3Fe^{3+}For_{12}\cdot CO_2$, which is stable under ambient conditions.[3]

Literatura

[1] A. Katrusiak, *Acta Cryst. B.*, **75** (2019) 918–926.
[2] Sobczak, S.; Fidelli, A. M.; Do, J.-L.; Demopoulos, G. P.; Moores, A.; Friscic, T.; Katrusiak, A. 10.26434/chemrxiv.14369813.
[3] S. Sobczak, A. Katrusiak *Inorg. Chem.*, **58** (2019) 11773–1178.

O-4

WYSOKOROZDZIELCZA DYFRAKCJA RENTGENOWSKA W BADANICH WARSTW EPITAKSLAJNYCH PROWADZONA OD KRAWĘDZI PRÓBKI

Jarosław Serafińczuk

Katedra Nanometrologii, Politechnika Wrocławska, Janiszewskiego 11/17, 50-372 Wrocław, Polska
Sieć Badawcza Łukasiewicz - PORT Polskie Centrum Rozwoju Technologii, Stabłowicka 147, 54-066 Wrocław, Polska

Wysokorozdzielcza dyfraktometria rentgenowska jest podstawową metodą pomiarową stosowaną w badaniach strukturalnych warstw i struktur epitaksjalnych. W konfiguracji wysoko rozdzielczej monochromator Bartelsa daje rozbieżność wiązki padającej na kryształ równą 12 sekund kątowych. W torze wiązki odbitej otwarta konfiguracja detektora jest używana do pomiarów krzywych odbić (RC), natomiast zastosowanie analizatora dwukrystalicznego pozawala na pomiary map węzłów sieci odwrotnej (RLM). Takie konfiguracje pomiarowe pozwalają na badanie monokrystalicznych struktur półprzewodnikowych, w tym: niskowymiarowych studni kwantowych (QW), kropek kwantowych (QDs), struktur laserowych itp. Analiza wyników pomiaru RC i RLM pozwala na wyznaczenie podstawowych parametrów struktury m.in.: grubości i składu warstw, stopnia relaksacji, parametrów sieciowych, wielkość bloków krystalicznych i mozaikowatość silnie niedopasowanych struktur, a także gęstość dyslokacji, odkształceń i naprężeń w warstwach epitaksjalnych. Ponadto pomiary i analiza map węzłów sieci odwrotnej płaszczyzn prostopadłych do powierzchni próbki wykorzystując geometrię krawędziową pozwala na określanie kształtu niskowymiarowych struktur jakimi są kropki kwantowe. W takiej analizie głównym problemem jest pomiar płaszczyzn prostopadłych do powierzchni próbki. W standardowej konfiguracji HR-XRD pomiar takich płaszczyzn dla silnie zorientowanych próbek jest praktycznie niemożliwy. Aby uniknąć tego problemu, płaszczyzny o dużym kącie nachylenia (np. powyżej 60 stopni) są badane za pomocą geometrii skośnej (rys. 1).

Zastosowanie pomiarów prowadzonych od krawędzi próbki pozwala na pomiar i analizę takich płaszczyzn, a przede wszystkim na przestrzenne rozdzielenie efektów obserwowanych w wynikach badań. W szczególności pozwala na niezależne wyznaczenie parametru sieci prostopadłej do kierunku wzrostu, rozdzielenie mozaikowatości pochylenia i skrętu [1], obliczenie gęstości dyslokacji krawędziowych [2] czy odkształceń resztkowych [3] w strukturze oraz analizę kształtu QDs. Ponadto tego typu pomiary ujawniają różnice w parametrach sieciowych poszczególnych warstw [4], które nie zawsze są widoczne przy konwencjonalnych pomiarach wykonywanych z powierzchni próbki. Ten typ pomiarów został opracowany w Laboratorium Badań Strukturalnych PWr i jest od lat stosowany w analizie struktur epitaksjalnych - głównie niedopasowanych materiałów III-N jak (Ga, Al)N ale także struktur niskowymiarowych (QW i QD) materiałów III-V.

O-4

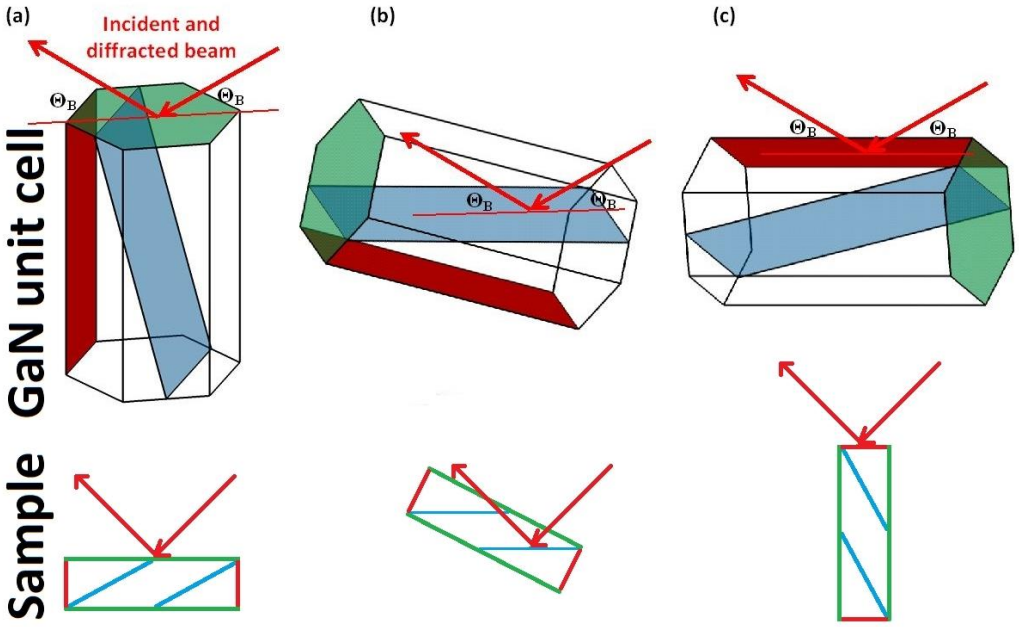

Rys. 1. Geometria pomiarów XRD: a) klasyczne pomiary z powierzchni próbki; b) geometria skośna; c) pomiary w geometrii krawędziowej.

References

[1] J. Serafinczuk, *Cryst. Res. Technol.*, **51** (2016) 276–281.

[2] J. Serafinczuk, K. Moszak, L. Pawlaczyk, W. Olszewski, D. Pucicki, R. Kudrawiec, D. Hommel, *J. Alloys Compd.*, **825** (2020) 153838.

[3] J. Serafinczuk, L. Pawlaczyk, K. Moszak, D. Pucicki, R. Kudrawiec, D. Hommel, submitted to *Materials Characterisation* (2021).

[4] R. Kucharski, M. Zajac, A. Puchalski, T. Sochacki, M. Bockowski, JL. Weyher, M. Iwinska, J. Serafinczuk, R. Kudrawiec, Z. Siemiątkowski, *J. Cryst. Growth*, **427** (2015) 1–6.

O-5

NANOCRYSTALLOGRAPHY IN SITU (NANOPOWDER DIFFRACTION IN SITU)

Zbigniew Kaszkur and Ilia Smirnov

Institute of Physical Chemistry PAS, ul. Kasprzaka 44/52, 01-224 Warszawa

The last decades surge of interest in nanomaterials spurs efforts to determine their structure and its evolution. To this end the Large Scale Facilities (Synchrotrons, FELs) develop crystallographic methods applicable to nanoparticles (Coherent Diffraction Imaging, serial crystallography). Recently also electron diffraction developes into atomic structure determination (3D electron diffraction). All these methods have own limitations. However many nanomaterials are available in powder form and methods of powder diffraction are widely used although with no sufficient care to specific methodology constraints. This presentation aims at reviewing these constraints focusing at:

- the use of Debye summation formula vs. crystal phase analysis;
- applicability of Lorentz factor [3];
- effects of surface relaxation and chemisorption [3];
- strain in fcc nanocrystals.
- from stacking faults and multiple nano-domains to a stable decahedra and icosahedra.
- from fcc Warren's [1] phenomenologic analysis to a realistic models (stacking probabilities vs. number of nanodomains [2]).

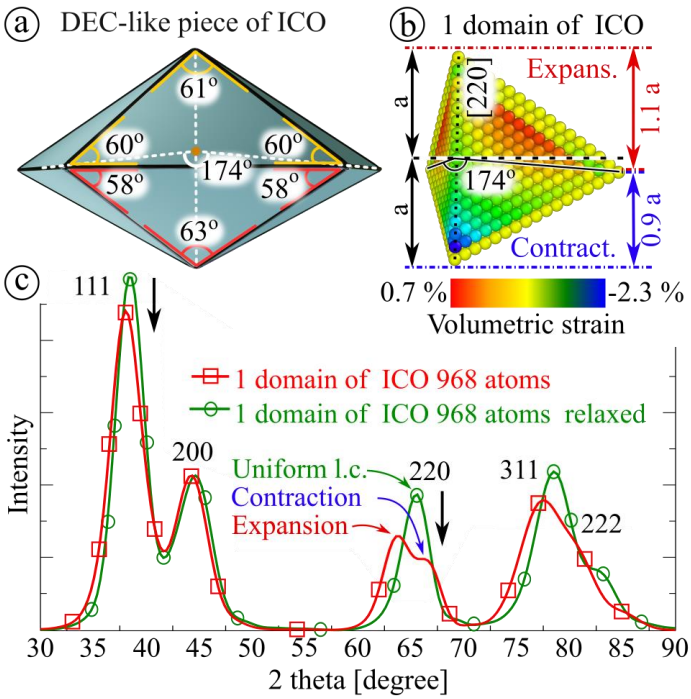

Fig.1. Illustration of the strain distribution in icosahedron: a) change of optimal plane angles in decahedron-like piece of icosahedron. The red angles correspond to the lower part of the cluster (close to the center), the yellow angles correspond to the upper part of the cluster; b) the volumetric strain distribution in the one piece (domain); c) comparison of the calculated XRD patterns of the strained and relaxed one domain of icosahedron (968 atoms). The influence of a "double lattice" parameter on the diffraction pattern can be seen from the 220 double peak [3].

O-5

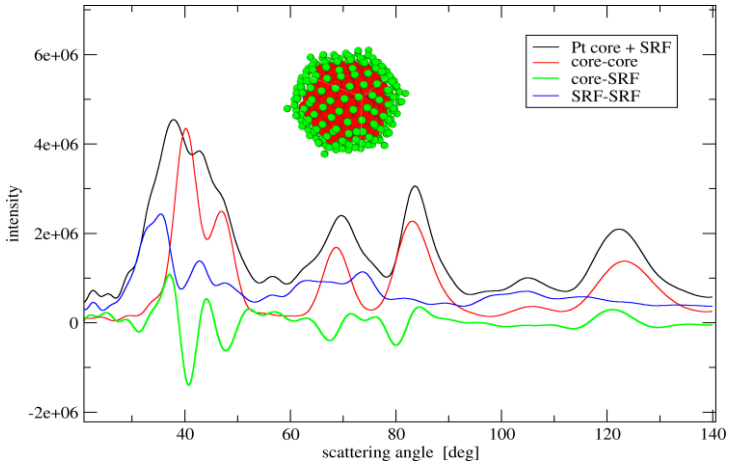

Fig. 2. Powder diffraction pattern (Cu Kα radiation) of Pt−PtO_2 core-shell(SRF) nanocrystal of 2nm size (black line) with contribution from core-core distances (red line), SRF-SRF distances (mimicking PtO_2) (blue line) and core-SRF distances (green line) [4].

The above figure shows that small size nanomaterials cannot be analyzed via Rietveld method. The Rietveld method is unable to treat structures with continuous profile of the lattice parameters, epitaxially contacting phases etc. This comes from the pattern treatment as as a sum of patterns of a separated crystal phases. In reality the diffraction pattern is formed by contributions from interatomic distances. When Rietveld approach considers two phases A and B, it accounts for distances A-A and B-B. The contribution from A-B distances is included in Debye summation formula but not in Rietveld's. The consequences are important for small nanocrystals where one can consider two phases: the core and the surface. The pattern were calculated using Cluster program [5]

References

[1] B. E. Warren *X-Ray Diffraction* , Addison-Wesley, Reading, MA, 1969,.
[2] I.Smirnov, Z.Kaszkur, A.Hoell, *Nanoscale.* **15** (2023) , 8633, DOI: 10.1039/d3nr00456b.
[3] Z. Kaszkur, I.Smirnov, https://doi.org/10.48550/arXiv.2212.06926 (2022) .
[4] Z.Kaszkur, comment, https://doi.org/10.48550/arXiv.2212.10434 (2022).
[5] Z.Kaszkur, B. Mierzwa (2022). Program Cluster, http://kaszkur.net.pl/program-cluster/, Accessed: 2022-12-12.

O-6

PROFESOR JANUSZ S. LIPKOWSKI

Kinga Suwińska

Uniwersytet Kardynała Stefana Wyszyńskiego w Warszawie,
K. Wóycickiego 1/3, 01-938 Warszawa

Janusz Stanisław Lipkowski, ur. 3 lutego 1943 roku w Warszawie, absolwent VI-go Liceum Ogólnokształcącego im. Tadeusza Reytana w Warszawie, ukończył z wyróżnieniem studia na Wydziale Chemii Uniwersytetu Warszawskiego w 1965 roku ze specjalnością krystalografia (promotor prof. Ludwik Chrobak). Po ukończeniu studiów dostał skierowanie do pracy w Instytucie Badań Jądrowych na Żeraniu (Warszawa) do Zakładu Chemii Analitycznej, którym w tamtym czasie kierował prof. Jerzy Minczewski, gdzie pracował do końca 1965 roku.

Od 1 stycznia 1966 wrócił na Wydział Chemii UW gdzie przez dwa lata był asystentem w Katedrze Krystalografii, a następnie, w roku 1968, rozpoczął studia doktoranckie w Instytucie Chemii Fizycznej PAN w Warszawie. W ciągu następnych czterech lat pod kierunkiem prof. Wiktora Kemuli, w laboratorium dyfraktometrii, które zaczął tworzyć dr Wiesław Wolfram, prowadził badania nad sorpcyjnymi właściwościami klatratów tworzonych przez kompleksy Wernera, które to badania zakończyły się pracą doktorską p.t. Klatraty tworzone przez kompleks Ni(NCS)2(4-metylopirydyna)4 jako sorbenty chromatograficzne obronioną w 1972 roku.

Kontynuował badania nad zależnością struktury i właściwości sorpcyjnych klatratów również w następnych latach, najpierw na podoktorskim stażu naukowym w Parmie (Włochy), gdzie nawiązał trwającą następnie przez wiele lat współpracę z prof. Giovannim Andreettim oraz prof. Mario Nardellim, a następnie, jako adiunkt, w IChF PAN. W tym czasie dr Janusz Lipkowski zaczął budować własny zespół badawczy, którego głównym zadaniem badawczym były badania strukturalne. Tematyka ta stanowiła również podstawę pracy habilitacyjnej Współzależność budowy i właściwości fizykochemicznych klatratów tworzonych przez kompleksy koordynacyjne MeX_2A_4 przedłożonej Radzie Naukowej Instytutu Chemii Fizycznej PAN, na podstawie której w 1983 roku uzyskał stopień naukowy doktora habilitowanego. Jednocześnie, równolegle z badaniami związków klatratowych, zaczyna rozwijać tematykę związaną z inkluzją molekularną, poszerzając zainteresowania naukowe o związki typu eterów koronowych i cyklodekstryn, a następnie kaliksarenów i kaliksrezorcynarenów. W 1990 roku uzyskuje tytuł profesora nauk chemicznych.

W 1978 roku dr Janusz Lipkowski został kierownikiem Zakładu Fizykochemicznych Metod Analitycznych w IChF PAN. Od tego czasu datuje się kompleksowy rozwój badań nad związkami inkluzyjnymi w Zakładzie, zarówno metodami strukturalnymi, jak i, we współpracy z innymi zespołami, metodami analitycznymi – chromatograficznymi, elektrochemicznymi, termochemicznymi. Jednocześnie dr Lipkowski zaczyna rozwijać współpracę międzynarodową, zapoczątkowaną zorganizowaniem

w 1980 roku w Jachrance k/Warszawy z jego inicjatywy Międzynarodowego Sympozjum *Clathrate Compounds and Molecular Inclusion Phenomena*. Od tego momentu zaczyna się błyskawicznie rozwijać kariera międzynarodowa dr. Lipkowskiego. Na wspomnianym sympozjum podjęto trzy ważne inicjatywy: (1) aby *sympozjum Clathrate Compounds and Molecular Inclusion Phenomena* było pierwszym z serii sympozjów organizowanych co dwa lata w różnych krajach na całym świecie, (2) aby wydać monograficzną publikację *Inclusion Compounds*, która opisywałaby aktualny *state-of-art* w tej dziedzinie oraz (3) aby utworzyć nowe czasopismo *Journal of Inclusion Compounds* (obecnie *Journal of Inclusion Phenomena and Molecular Recognition in Chemistry*).

Równolegle z szybko rozwijającą się karierą naukową prof. Lipkowski awansował na szczeblach administracyjnych. W 1982 roku, jeszcze jako doktor, zostaje zastępcą dyrektora Instytutu, najpierw ds. ogólnych, a od kadencji 1986 ds. naukowych. W 1992 roku został wybrany przez Radę Naukową Instytutu Chemii Fizycznej PAN dyrektorem naczelnym i funkcję tę pełnił nieprzerwanie do roku 2003, kiedy został powołany na stanowisko wiceprezesa Polskiej Akademii Nauk.

Dorobek naukowy prof. Lipkowskiego to ponad 370 publikacji w renomowanych czasopismach naukowych, kilkaset prac konferencyjnych oraz kilkanaście rozdziałów w opracowaniach monograficznych.

Od 1998 roku był członkiem korespondentem, a od 2013 roku jest członkiem rzeczywistym Polskiej Akademii Nauk. W latach 2003–2006 pełnił funkcję pierwszego wiceprezesa PAN. Był Przewodniczącym Rady Kuratorów Wydziału III Nauk Ścisłych i Nauk o Ziemi PAN (2011–2014) i przez dwie kadencje przewodniczącym Komitetu Chemii PAN (2007–2010, 2011–2014). Od 2012 roku jest członkiem korespondentem Polskiej Akademii Umiejętności. Od 1991 roku jest członkiem Towarzystwa Naukowego Warszawskiego a w latach 2007-2020 pełnił funkcję Prezesa TNW. Jest też członkiem wielu polskich i zagranicznych towarzystw naukowych.

W 1997 roku otrzymał doktorat honoris causa Instytutu Chemii Nieorganicznej Rosyjskiej Akademii Nauk w Nowosybirsku. W 2001 roku został honorowym profesorem Syberyjskiego Oddziału Rosyjskiej Akademii Nauk, a w 2019 roku również Uniwersytetu Technicznego w Ningbo (Chiny). Został odznaczony Złotym Krzyżem Zasługi (1975), Krzyżem Kawalerskim Orderu Odrodzenia Polski (2002) i Orderem Honoru Republiki Mołdawii (2006).

Prof. Janusz Lipkowski jest znakomitym naukowcem, a jednocześnie świetnym organizatorem życia naukowego. Ale przede wszystkim jest człowiekiem o wysokiej kulturze osobistej, wspaniałym przełożonym i kolegą. Ma szerokie zainteresowania i rozmaite talenty, z których chcę tu wymienić trzy: talent do nauki języków obcych – posługuje się biegle angielskim, rosyjskim i włoskim, talent fotograficzny oraz talent muzyczny. Niewiele osób wie, że potrafi on bardzo dobrze grać na keyboardzie, a nawet komponuje własne utwory muzyczne. Prof. Janusz Lipkowski jest prawdziwym człowiekiem renesansu.

O-7

UNLOCKING THE SECRETS OF MOLECULAR RECOGNITION IN AQUEOUS SOLUTIONS: A STUDY ON THE PROPERTIES OF CUCURBIT[7]URIL AND NEUROTRANSMITTERS/AMINO ACIDS COMPLEXES

Ewelina Zaorska and Maura Malińska

Wydział Chemii, Uniwersytet Warszawski, ul. Pasteura 1, 02-093 Warszawa

Molecular recognition in aqueous environments is a fundamental step in essentially any biological process. However, biological processes are very complex and difficult to unravel because of many overlapping phenomena. Therefore, we study molecular recognition in synthetic macrocycles that are water soluble and possess hydrophobic cavities. This study investigates the interaction between the macrocyclic host molecule cucurbit[7]uril (CB[7]) and neurotransmitters (NRs) or amino acids (AAs). By examining the reversible binding of nine complexes formed in solution, using techniques such as isothermal titration calorimetry, computational investigations, and X-ray diffraction (XRD) studies on crystallized complexes (Fig. 1.), we aim to gain insights into the underlying factors responsible for CB[7]'s exceptional selectivity.

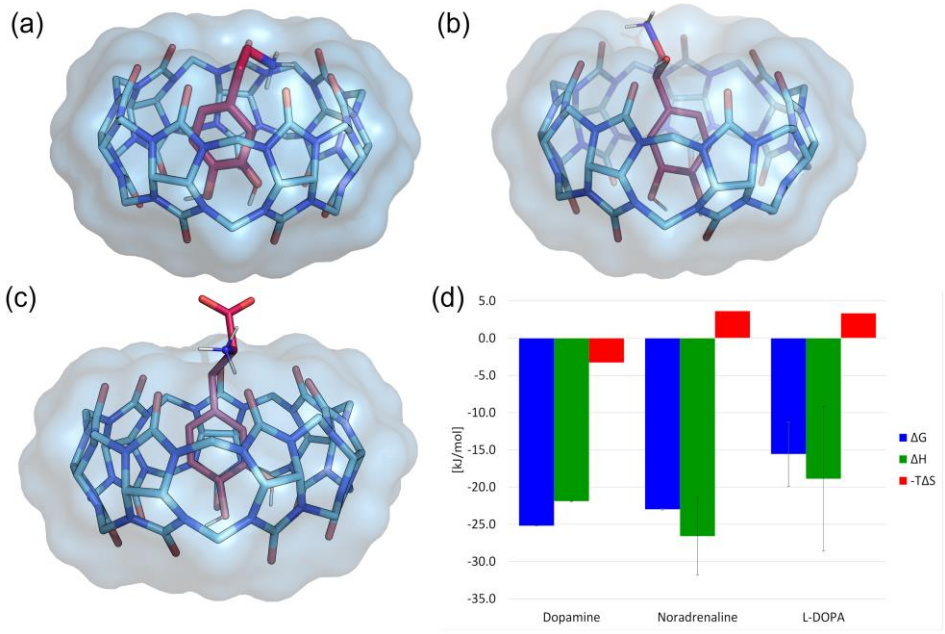

Fig. 1. CB[7] complexes with dopamine (a), L-noradrenaline (b), and L-DOPA (c). Only polar hydrogen atoms are shown. Thermodynamic parameters of CB[7] binding with dopamine, L-noradrenaline, and L-DOPA (d).

Interestingly, when analyzing the gas-phase interaction energies between the CB[7] host and guest, we observe a negative correlation with binding affinities. This indicates a diminished significance of non-covalent interactions between the polar side chains in the presence of water. Additionally, by considering the position of the

hydroxyl group in the ligands and analyzing hydrogen bond formations using XRD structures, we investigated the impact on the free energy of hydrogen bond formations. Our findings reveal that the transfer of hydrophobic groups from the bulk solution into the hydrophobic CB[7] cavity encounters fewer obstacles from desolvation penalties. Consequently, the formation of hydrogen bonds has a negative impact on the free energy of binding, while the burial of hydrophobic parts within the cavity results in higher binding affinities in water. These findings highlight the critical role of hydrophobic effects in molecular recognition and provide insights into the behavior of hydrophobic moieties in aqueous environments.

In summary, this study elucidates the captivating world of molecular recognition in aqueous environments. By examining the CB[7]-NR and CB[7]-AA complexes, we uncover the factors contributing to CB[7]'s high selectivity, with NRs exhibiting superior binding affinities. The interplay between hydrophobic effects and hydrogen bonding, along with the influence of guest solvation, offers new insights into ligand and drug design strategies. These findings have the potential to advance our understanding of molecular recognition processes and pave the way for more efficient and effective structure-based drug design.

O-8

CHARACTERIZATION OF THE FLURBIPROFEN-β-CYCLODEXTRIN INCLUSION COMPLEX BY X-RAY TECHNIQUES

Armand Budzianowski[1], Katarzyna Betlejewska-Kielak[2], Elżbieta Bednarek[3], Katarzyna Michalska[2*], and Jan K. Maurin[3]

[1] National Centre for Nuclear Research, A. Sołtana 7, 05-400 Otwock, Poland; Armand.Budzianowski@ncbj.gov.pl
[2] Department of Synthetic Drugs, National Medicines Institute, Chełmska 30/34, 00-725 Warsaw, Poland; k.kielak@nil.gov.pl
[3] Falsified Medicines and Medical Devices Department, National Medicines Institute, Chełmska 30/34, 00-725 Warsaw, Poland; (E.B.) e.bednarek@nil.gov.pl (J.K.M.) j.maurin@nil.gov.pl (K.M) k.michalska@nil.gov.pl; Tel.: +48-(22)-841-18-88 (ext. 369)

The most popular cyclodextrin is β-cyclodextrin (β-CD), a cyclic oligosaccharide formed from seven D-glucose units linked by α (1-4) linkages, resulting in a hollow truncated cone shape. It has a hydrophobic cavity that can accommodate lipophilic molecules. Cyclodextrins complexation is widely used in pharmaceuticals to improve drug properties such as solubility, dissolution rate, chemical and physical stability and hence bioavailability, and to reduce irritation and toxicity.

Flurbiprofen (FP) is used in a tablet form at doses up to 400 mg/day. It has severe gastrointestinal side effects when administered orally and due to poor solubility in water a low bioavailability *in vivo*.

The aims of this study were: (i) to obtain FP/β-CD inclusion complexes by one or more complexation methods, (ii) to grow a single crystal when XRPD and NMR methods confirmed the formation of the inclusion complexes, and (iii) to comprehensively investigate the FP/β-CD inclusion complex by XRPD, NMR and X-ray single crystal techniques [1].

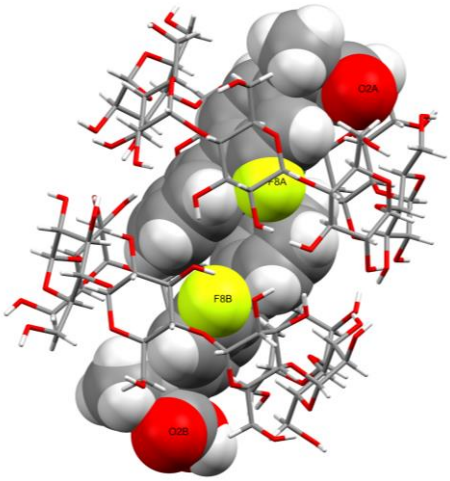

Single crystal data and structure refinement were obtained for the fulbiprofen-cyclodextrin complex (see Figure), fulbiprofen and cyclodextrin.

Literatura

[1] K. Betlejewska-Kielak, E. Bednarek, A. Budzianowski, K. Michalska, J. K. Maurin, *Journal of Molecular Structure*, **1285** (2023) 135450. DOI: 10.1016/j.molstruc.2023.135450

O-9

COMBINING X-RAY AND ELECTRON DIFFRACTION FOR DEHYDRATION AND STRUCTURAL DESCRIPTION OF SODIUM HYPODIPHOSPHATES

Vasyl Kinzhybalo[a], Marta Otręba[b], Jakub Wojciechowski[c], Miłosz Siczek[b], Katarzyna Ślepokura[b]

[a] Institute of Low Temperature and Structure Research, Polish Academy of Sciences, 2 Okólna, 50-422 Wroclaw
[b] University of Wroclaw, Faculty of Chemistry, 14 F. Joliot-Curie, 50-383 Wroclaw
[c] Rigaku Europe SE, Hugenottenallee 167, D-63263 Neu Isenburg, Germany

Crystal engineering is known to be a fascinating field with its hidden routes, tricks and know-hows leading to new crystal forms preparation [1]. Crystal-makers are constantly looking for new techniques to broaden the crystal structure landscape [2]. Dehydration as a particular case of desolvation has shown its effectiveness in obtaining of the new crystal forms (possibly otherwise inaccessible) both in organic and inorganic materials. Different stimuli can be used to induce dehydration like increased temperature, decreased pressure, immersion in anhydrous solvents or mechanochemical synthesis. Depending on the nature of the material, dehydration may proceed as single-crystal-to-single-crystal, single-crystal-to-micropowder, single-crystal-to-nanopowder or even as a transformation to amorphous solid. Unfortunately in most cases monocrystal fracturing takes place, especially in case of inorganic compounds. Monocrystal quality deterioration is a challenge for crystallographers, therefore structure elucidation requires involvement of non-routine techniques like electron diffraction and microsample powder diffraction, that are being currently enabled by state-of-the-art diffractometers.

In the last years hypodiphosphates (PPs), both organic and inorganic, have been studied in terms of their synthesis, spectroscopy, crystallochemistry, experimental electron density distribution, phase transitions and dehydration [3]. Among other things, it was shown that a SC-to-SC dehydration of tetrabutylammonium hypodiphosphate leads to reorganization of hydrogen bond network and consequent change in PP anion conformation from energetically-favoured staggered into very seldom occurring eclipsed form [4].

The majority of synthetic routes of PP leads to sodium hypodiphosphates. Usually red phosphorus is treated by various oxidizing agents to produce the mixture of phosphoric acids which are next neutralized by NaOH to different pH values (depending on the procedure) to produce sparingly soluble $Na_2(H_2P_2O_6)\cdot 6H_2O$ or $Na_4(P_2O_6)\cdot 10H_2O$. Unfortunately, their crystallization may sometimes lead to formation of by-products – another sodium hypodiphosphates. Additionally, and not uncommonly for inorganic compounds, the same or very similar crystallization conditions may result in different thermodynamically or kinetically advantaged polymorphs, pseudopolymorphs, metastable forms or even more different crystal compositions. Hydrated salts may also undergo spontaneous dehydration even at room temperature and it all impedes proper identification of the obtained product.

The throughout structural analysis of crystalline hydrated sodium hypodiphosphates and their dehydration products covered thirteen substances of the following compositions: $Na(H_3P_2O_6)$ (**1** and **2**), $Na(H_3P_2O_6)\cdot H_2O$ (**3**), $Na_2(H_2P_2O_6)$ (**4**),

$Na_2(H_2P_2O_6)\cdot 2H_2O$ (**5**), $Na_2(H_2P_2O_6)\cdot 6H_2O$ (**6** and **7**), $Na_5(HP_2O6)(H_2P_2O_6)\cdot 21H_2O$ (**8**), $Na_3(HP_2O_6)$ (**9** and **10**), $Na_3(HP_2O_6)\cdot 9H_2O$ (**11**), $Na_4(P_2O_6)$ (**12**) and $Na_4(P_2O_6)\cdot 10H_2O$ (**13**). They have been characterized by variable-temperature optical microscopy, thermogravimetry, single-crystal and powder X-ray diffraction (SCXRD, PXRD), as well as 3D electron diffraction (3D-ED). Crystalline salts **1**-**9**, **11** and **13** have been obtained in typical solution-crystallization processes. Anhydrous $Na_4(P_2O_6)$ (**12**), which could not be grown either from a solution or from a melt, has been obtained via dehydration of $Na_4(P_2O_6)\cdot 10H_2O$ (**13**). The crystal structure of **12** has been determined by 3D-ED and powder diffraction data. Dehydrations of $Na(H_3P_2O_6)\cdot H_2O$ (**3**), $Na_2(H_2P_2O_6)\cdot 6H_2O$ (both **6** and **7**), $Na_3(HP_2O_6)\cdot 9H_2O$ (**11**) and $Na_4(P_2O_6)\cdot 10H_2O$ (**13**), were monitored by TGA, variable-temperature microscopy and powder or microsample powder X-ray diffraction (μ-PXRD), and turned out to be one-step, destructive transformations, resulting in almost pure triclinic form of $Na(H_3P_2O_6)$ (**1**), $Na_2(H_2P_2O_6)$ (**4**), α-$Na_3(HP_2O_6)$ (**9**) and $Na_4(P_2O_6)$ (**12**) (Fig. 1), respectively.

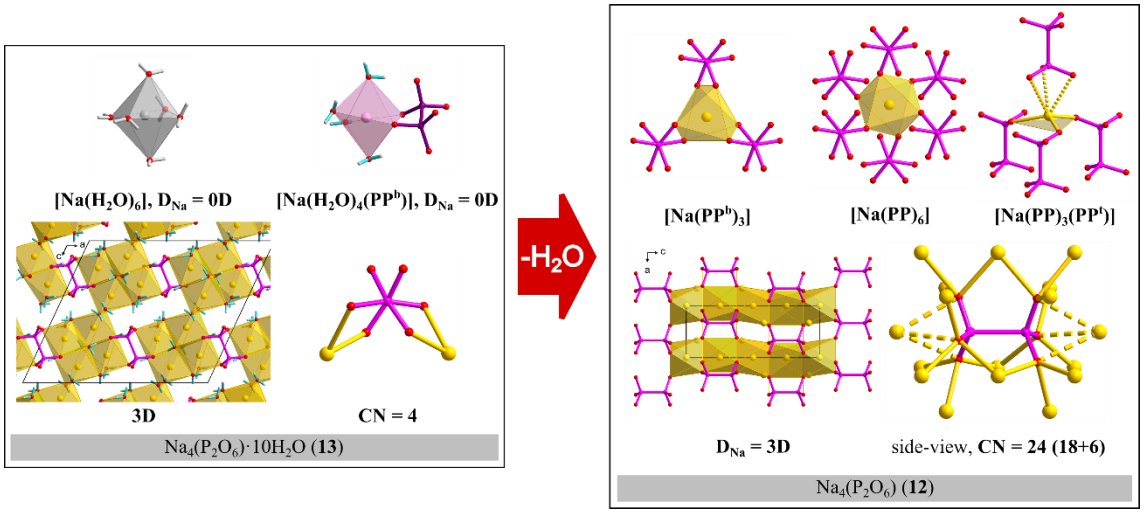

Fig. 1. Structural changes observed during dehydration of $Na_4(P_2O_6)\cdot 10H_2O$ (**13**) to $Na_4(P_2O_6)$ (**12**).

Acknowledgement

This research was partially performed under a cooperation agreement between Rigaku Polska Sp. z o.o. and University of Wrocław (agreement No. 1/2021).

Literature

[1] D. Braga, F. Grepioni, *Angew. Chem. Int. Ed.* **43** (2004) 4002–4011.
[2] G. R. Desiraju, *Acta Crystallogr.* **B73** (2017) 775–778.
[3] V. Kinzhybalo, M. Otręba, K. Ślepokura, T. Lis, *Wiad. Chem.*, **75** (2021) 423–466.
[4] M. Emami, K. A. Ślepokura, M. Trzebiatowska, N. Noshiranzadeh, V. Kinzhybalo, *CrystEngComm* **20** (2018) 5209–5219.

O-10

KWERCETYNA JAKO SYNTON SUPRAMOLEKULARNY W UKŁADACH DWUSKŁADNIKOWYCH

Urszula Maciołek, Ewaryst Mendyk, Marcin Kuśmierz i Anna E. Kozioł

Instytut Nauk Chemicznych, Wydział Chemii, Uniwersytet Marii Curie-Skłodowskiej, Pl. Marii Curie-Skłodowskiej 3, 20-031 Lublin

Cząsteczka kwercetyny (3,5,7,3',4'-pentahydroksyflawonu) ze względu na swoją budowę chemiczną ma wiele możliwości oddziaływań niekowalencyjnych (Rys. 1). Grupy hydroksylowe i grupa karbonylowa mogą uczestniczyć w oddziaływaniach zarówno wewnątrz- jak i międzycząsteczkowych, jako donory i akceptory w wiązaniach wodorowych. Z tego powodu należy uznać kwercetynę za bardzo labilny synton, wykazujący polimorfizm strukturalny [1].

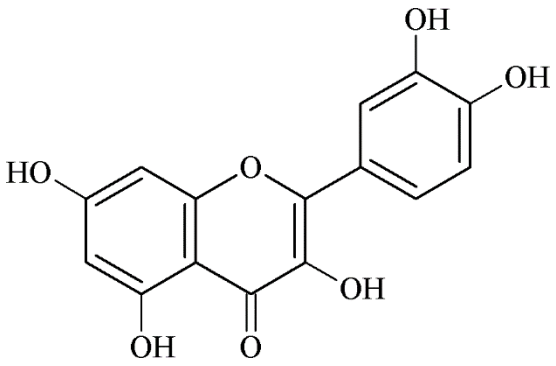

Rys. 1. Wzór strukturalny kwercetyny.

Dwuskładnikowe ko-kryształy kwercetyny otrzymano z zastosowaniem syntezy mechanochemicznej w obecności niewielkiej ilości rozpuszczalnika (acetonitrylu), a później poddano je rekrystalizacji. Jako ko-formery zastosowano związki heterocykliczne z atomami azotu i tlenu (dwie pirydylowe pochodne benzofuranu i fenantrolinę) oraz pochodną aniliny (o-dianizydynę) [2]. Rentgenowska analiza strukturalna monokryształów oraz spektroskopie FT-IR i FT-Raman wykazały utworzenie wiązań wodorowych O-H…N i N-H…O z udziałem grup hydroksylowych kwercetyny i atomów azotu ko-formerów. We wszystkich ko-kryształach w cząsteczce kwercetyny obserwuje się stały motyw dwóch wewnątrzcząsteczkowych wiązań wodorowych O3-H…O4…H5-O. Metodę XPS wykorzystano do badania dynamiki wiązań wodorowych. Rentgenowska analiza strukturalna wykazała obecność obojętnych cząsteczek w strukturze ko-kryształów. Natomiast dla dwóch ko-kryształów w warunkach doświadczalnych XPS (wysoka próżnia – 5×10^{-9} mbar, stała czasowa $\sim10^{-15}$–10^{-16}) obserwuje się w wiązaniach wodorowych częściowe przeniesienie protonu grupy hydroksylowej do azotu pirydyny (O… H^{+}N) (Rys. 2).

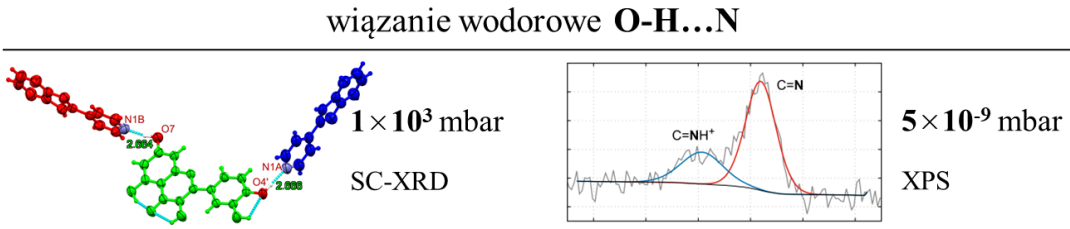

Rys. 2. Widmo N1s XPS dla ko-kryształu. Przeniesienie protonu w ko-krysztale.

Literatura

[1] R. Dubey, G.R. Desiraju, *IUCrJ*, **2** (2015) 402.
[2] U. Maciołek, doktorat (2019).

O-11

WHAT IS THE ACTUAL SUPRAMOLECULAR ARCHITECTURE OF THEOPHYLLINE POLYMORPHS AND CO-CRYSTALS WITH WATER AND IODINE FROM ENERGETIC VIEWPOINT?

G. J. Reiss[b], M. Wyshusek[b] and I. S. Konovalova[a,b]*

[a] SSI "Institute for Single Crystals", National Academy of Science of Ukraine, 60 Nauky ave., Kharkiv, 61001, Ukraine
[b] Bioinorganic Chemistry, Heinrich-Heine-University Dusseldorf, Universitatsstrasse 1, 40225 Dusseldorf, Germany

**e-mail: ikonovalova0210@xray.isc.kharkov.com*

The natural product theophylline (Fig. 1) was firstly isolated from an extract of the leaves from the tea plant [1,2]. Nowadays theophylline is sometimes used as pharmaceutical agent due to its effects on the respiratory system [2,3]. However, despite the popularity and seeming study of this type of compounds, the literature provides only data on their properties and methods of synthesis. There is no enough information on the ability of theophylline to form certain types of intermolecular interactions in spite of that the theophylline has five polymorphic modifications, which limits its use in pharmaceutical applications. Because the theophylline molecule is conformationally rigid, only the so-called orientational polymorphism we can discuss. Therefore, it is really important to analyse and compare intermolecular interactions in all polymorphic modifications and we furthermore includes the co-crystals with water and iodine in this study.

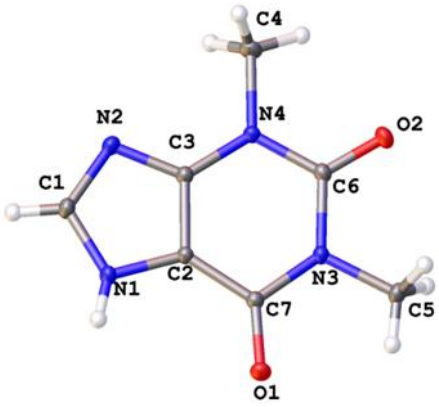

Fig. 1. Molecular structure of theophylline according to X-ray diffraction data.

All modern approaches to the molecular crystal structure analysis base on the comparison of the geometric characteristics of intermolecular interactions. However, these approaches are useless in many cases: a lot of weak interactions presence, the specific directed interactions absence *etc*.

In the case of theophylline and the aforementioned co-crystals the presence of classical strong (N-H...O/N, stacking) and weak (N/C-H…π) types of intermolecular interactions complicates the description of the crystal structures. It is difficult to define

the main structural motif in the solid state just on the basis of geometrical considerations. It is not clear which interaction has the energetically dominating role in the crystal structure.

The crystal packing analysis from energetic viewpoint provides detailed information about the organization of these crystals depending on the weak intermolecular interactions. It indicates that even small difference in weak interactions leads to the formation of polymorphic modifications.

Literature

[1] A. Kossel, *Ber. Dtsch. Chem. Ges.*, **21** (1888) 2164.
[2] A. Kossel, *Z. Physiol. Chem*., **13** (1889) 298.
[3] C. G. A. Persson, *J. Allergy Clin. Immunol*., **78 (**1986) 780.
[4] Z. M. Sofian, F. Benaouda, J. T. W. Wang, Y. Lu, D. J. Barlow, P. G. Royall, D. B. Farag, K. M. Rahman, K. T. Al Jamal, B. Forbes, S. A. A. Jones, *Adv. Ther*., **3 (**2020) 2.

O-12

TRACING OF TRANSIENT SPECIES VIA COMBINED CRYSTALLOGRAPHIC AND SPECTROSCOPIC METHODS – NEW PERSPECTIVES FROM THE XFEL CENTERS OF EXCELLENCE INITIATIVE

Katarzyna Jarzembska

Department of Chemistry, University of Warsaw, Żwirki i Wigury 101, Warsaw, Poland

The network of X-ray Free-Electron Laser Centers of Excellence (XFEL CoE) has been established this year to provide substantive and organizational support to the Polish scientific community in the use of the European XFEL (EuXFEL). It brings together scientists with experience in research using XFELs, whose knowledge and commitment constitutes support for new Polish users of this infrastructure. The activities planned within the project include for instance: conducting training in the research techniques related to potential experiments using the EuXFEL source, organization of workshops and conferences dedicated to XFEL science, organization and financing of internships at EuXFEL, or supporting preliminary research indispensable to prepare high-quality research proposals for measurement time on EuXFEL.

In the current contribution the initiative will be presented in detail, with the introduction of the four Centers of Excellence in Poland and their role. We will present current possibilities of time-resolved photocrystallography for small-molecule crystals. The results of our latest synchrotron studies dedicated to photoactive transition-metal complexes in the solid state will serve as examples. The XFEL research perspectives for crystallographers will be discussed.

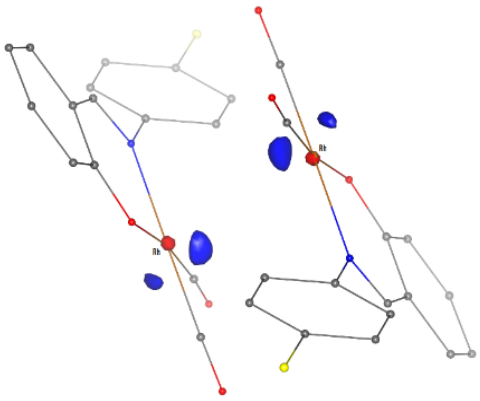

Fig. 1. Photodifference map for dicarbonyl (4-bromo-N-salicylideneaniline)rhodium(I); blue isosurfaces represent influx of electron density of at least 0.35 e·A^{-3}.

Acknowledgements: NSC (Poland), Support for Polish EuXFEL users–Supervision, Part II (2022-26), Ministry of Science and Education (Poland), South African National Research Foundation (137759), SONATA BIS (2020/38/E/ST4/00400), Advanced Photon Source, BioCARS beamline (R24GM111072) NIH (U.S.). Development of TR setup at BioCARS possible via collaboration with Philip Anfinrud (NIH/NIDDK).

O-13

RIGAKU ADVANCES IN X-RAY AND ELECTRON CRYSTALLOGRAPHY

Jakub Wojciechowski, Khai Truong, Christian Goeb, Christian Schürmann, Robert Bücker, Mathias Meyer, Fraser White

Rigaku Europe SE, Hugenottenallee 167, 63263 Neu-Isenburg, Germany

The latest range of Rigaku Oxford Diffraction instrument configurations will be summarized and illustrated with a number of particular examples in application. Rigaku technology advantages like HyPix Arc series detectors and the Dual Wavelength rotating anode sources with novel configurations will be highlighted combined with the applications of Intelligent Goniometer Head and XtalCheck-S plate/xyz stage attachments.

Furthermore the update on the XtaLAB Synergy-ED, the first commercially available electron diffractometer will show the lates improvement in CrysAlis^{Pro} and novel application enabled by LT cryo-transfer stage.

Fig. 1. XtaLAB Synergy-S (left), XtaLAB Synergy-R (middle), and XtaLAB Synergy-ED (right).

O-14

OKREŚLANIE STRUKTURY Z UŻYCIEM WYSOKIEJ JAKOŚCI DANYCH RENTGENOWSKIEJ DYFRAKCJI PROSZKOWEJ

Maciej Grzywa, Sebastian Machowski

Rigaku Europe SE, Neu-Isenburg; Testchem Radlin

Określenie struktury krystalicznej jest kluczowym elementem charakterystyki każdego nowego związku. W większości przypadków struktury krystaliczne są rozwiązywane przy użyciu metod monokrystalicznych. Jednak nie wszystkie związki krystalizują w postaci monokryształów o wystarczającej wielkości i jakości. Alternatywą jest zastosowanie metod dyfrakcji proszkowej. W przypadku dyfrakcji proszkowej bardzo ważnym punktem analizy strukturalnej jest uzyskanie wysokiej jakości danych dyfrakcyjnych. Wysokiej jakości dane uzyskuje się za pomocą instrumentów Rigaku wyposażonych w rotującą anodę, monochromator Johanssona i wysokiej klasy detektory. W prezentacji zostaną przedstawione przykłady danych zebranych za pomocą dyfraktometru SmarLab XE oraz przykłady analizy strukturalnej w SmartLab Studio II, w tym etapy takie jak: indeksowanie, określanie grup przestrzennych, wyznaczanie modelu krystalicznego i udokładnianie metoda Rietvelda.

O-15

LATEST DEVELOPMENTS IN SC-XRD FROM BRUKER AXS

Eddy Martin, Vernon Smith

Bruker AXS GmbH

The D8 QUEST and D8 VENTURE are Bruker's tried and tested systems for SC-XRD, and are a proven platform for new developments. Having the latest technology and methods in your instrument ensures you always obtain the most accurate structures from small molecule, macromolecule and solid state crystals. This presentation will provide a thorough overview of the state of the art in SC-XRD.

O-16

HARD-RADIATION LABORATORY X-RAY POWDER DIFFRACTION

Lei Ding, Marco Sommariva, Milen Gateshki

Malvern Panalytical B.V., Almelo, The Netherlands

Laboratory X-ray powder diffractometers are typically equipped with Cu radiation, which support a wide range of applications. However, for specific applications, higher energy X-ray radiation sources such as Mo and Ag tubes can provide significant insights and even allow to perform experiments that are unfeasible with Cu radiation. Hard-radiation X-ray sources are useful to access larger Q space and enable higher penetration in materials, particularly essential for pair distribution function analysis and in situ/operando experiments at multiple/extreme environments.

Conventionally, one has to carry out hard-radiation X-ray experiments at synchrotron radiation sources, but state of the art developments on X-ray source, optics and detector technologies allow a variety of hard radiation experiments on a laboratory diffractometer. The Malvern Panalytical Empyrean platform with hard radiation X-ray sources and efficient detectors is a multipurpose diffractometer supporting the applications from crystallography, pair-distribution function to operando battery study and in situ high-temperature/pressure measurements. In this lecture, the basics and advantages of hard-radiation X-rays on the Empyrean system will be presented. Then, an overview will be presented about the wide range of hard-radiation X-ray applications and how to perform the experiments as well as data analysis using HighScore Plus software for some specific applications.

O-17

MOŻLIWOŚCI BADAWCZE XRD POZA WARUNKAMI OTOCZENIA

Kamil Urbański

Anton Paar Poland Sp. z o.o., ul. Hołubcowa 123, 02-854 Warszawa

Najwyższa jakość pomiarów dyfrakcyjnych - Nowoczesny i zautomatyzowany dyfraktometr proszkowy XRDynamic 500 zapewnia najwyższą dostępną jakość pomiarów w swojej klasie za sprawą implementacji nowatorskich koncepcji. Wysoka rozdzielczość zagwarantowana jest dzięki szerokiemu promieniowi goniometru oraz zapewnieniu próżni na ścieżce optycznej wiązki rentgenowskiej. Doskonały stosunek sygnału do szumu wynika z powstrzymania rozpraszania wiązki przez powietrze, pozwalając na otrzymywanie doskonałej jakości dyfraktogramów nawet dla najbardziej złożonych próbek proszkowych.

Rys. 1. Dyfraktometr proszkowy XRDynamic 500

Przystawki do badań poza warunkami otoczenia - XRDynamic 500 jest wszechstronną platformą idealnie współpracująca z przystawkami do badań dyfrakcyjnych poza warunkami otoczenia. Przeprowadzanie badań strukturalnych próbek w warunkach zmiennej temperatury, atmosfery, wilgotności czy napięcia nigdy nie było prostsze. Zmiana konfiguracji urządzenia oraz projektowanie eksperymentów non-ambient jest niezwykle wygodne. Przystawki są automatycznie rozpoznawane i w pełni sterowalne z poziomu oprogramowania sterującego dyfraktometrem.

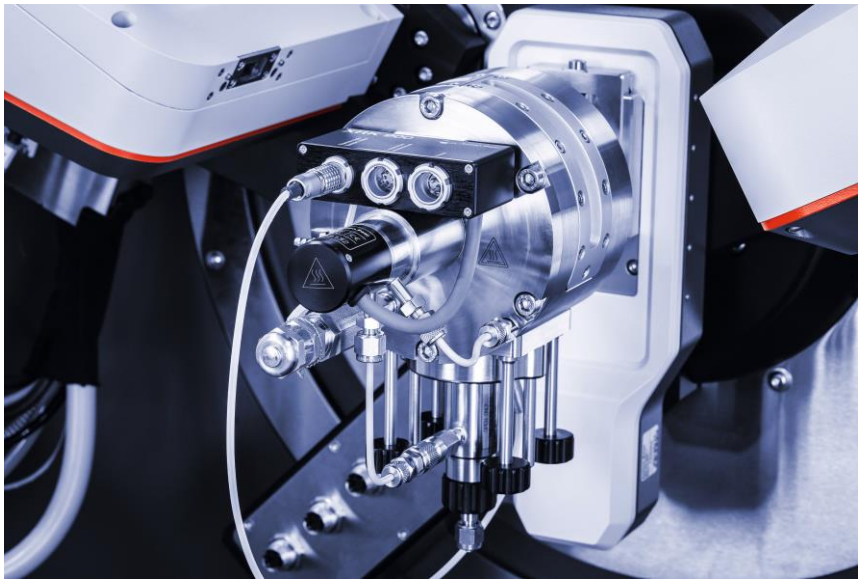

Rys. 2. Komora reakcyjna XRK 900

Szereg możliwości badawczych – poznaj potencjał przystawek do badań poza warunkami otoczenia od Anton Paar za sprawą raportów aplikacyjnych z wykorzystania komory reakcyjnej XRK 900, komory wysokotemperaturowej HTK 16N oraz komory niskotemperaturowej TTK 600. Daj zainspirować się do wykorzystania różnorodnych rozwiązań non-ambient do badania Twoich próbek i zaspokojenia unikalnych potrzeb badawczych.

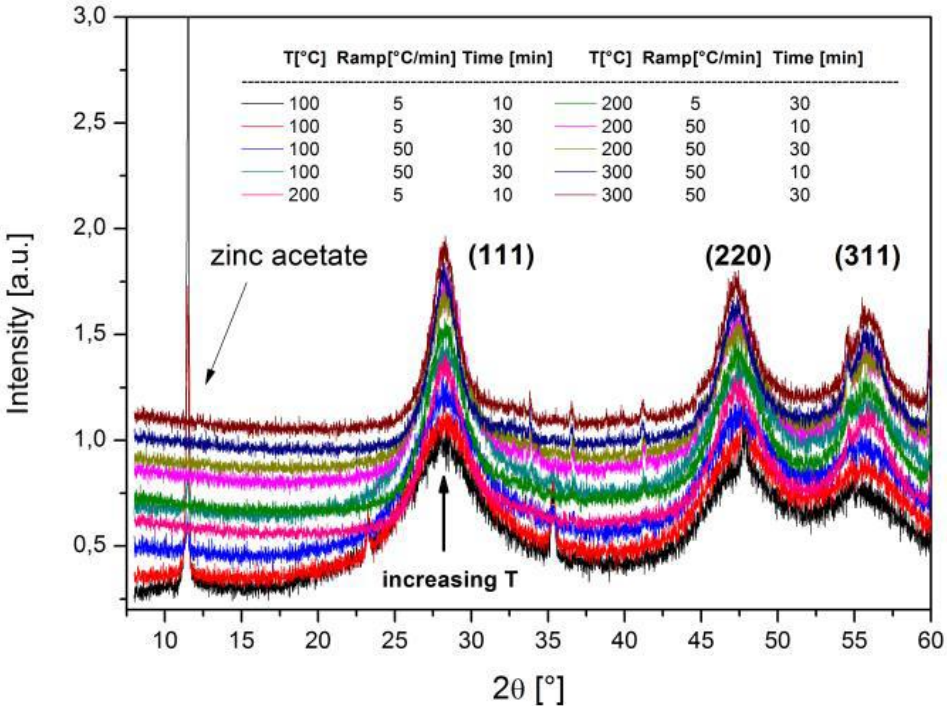

Rys. 3. Dyfraktogramy nanoczastek tlenku cynku syntezowanego in-situ w komorze XRK 900

O-18

EXTENDING MEASURING LENGTH (AND TIME) SCALES OF LABORATORY SAXS/WAXS BEAMLINES

S. Stolarek , A. Cheminal, B. Faure , S. Rodrigues, P. Panine

Xenocs SAS, 1-3 Allée du Nanomètre, Grenoble, France

State of the art laboratory SAXS/WAXS instruments used for soft matter or nanomaterials structural characterization are typically made of high brightness microfocus sources coupled to in-vacuum hybrid pixel detectors for low noise and high dynamic range detection. The achievable characteristic length scales are typically from few hundred nanometers down to atomic scale ($2\theta \geq 60°$) using standard Copper radiation source ideal for characterization of polymers, nanoparticles, colloids surfactants, proteins or lipid-based systems. More recently laboratory beamlines with motorized change of sample to detector distance and multi-radiation sources have been introduced respectively for maximum automation, flexibility, or improved measuring performances for inorganic samples.

We will present the latest developments of the Xeuss 3.0 a (GI-)SAXS/WAXS/ USAXS beamline for the laboratory with new advanced options extending measuring length scales up to more than 5 orders of magnitude in Q (wave-vector). This includes a fully retractable Bonse Hart USAXS attachment and a motorized dedicated WAXS detector collecting up to $2\theta=90°$ on both isotropic and anisotropic samples. Different measurement examples will be presented such as SAXS and WAXS characterization in transmission and grazing incidence of metallic samples or hierarchical materials characterization using sequential SAXS/WAXS/USAXS.

In addition, we present newly developed measuring configurations for heterogenous or composite materials: a focused incident beam channel for mapping SAXS/WAXS applications and an X-ray imaging module to detect defects or region of interest for further X-ray scattering analysis.

The described beamline is made of a large and versatile sample chamber, and we will review recent examples of in-situ environmental studies.

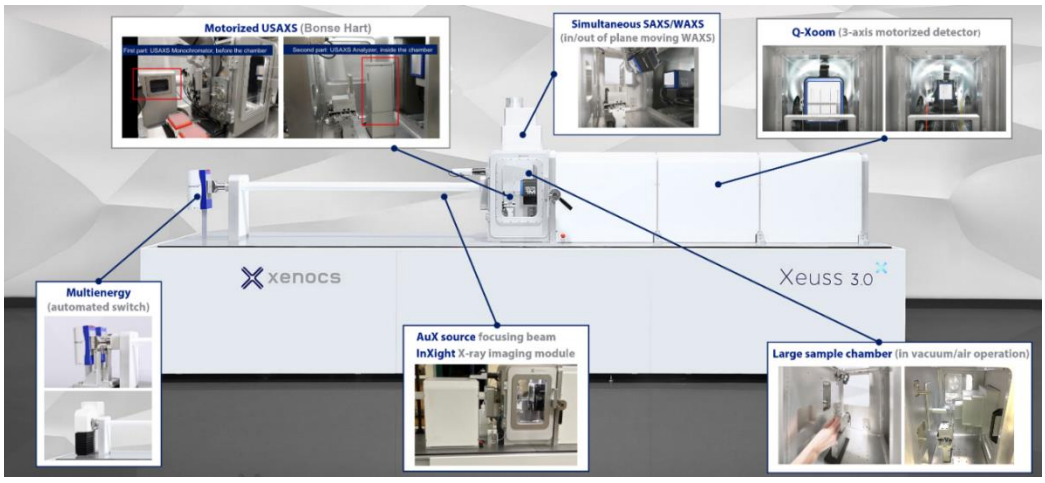

Fig. 1. Xeuss 3.0 laboratory beamline with insets showing advanced measuring options or features described.

O-19

EXPANDING SINGLE CRYSTAL DESIGN SPACE USING TEMPERATURE AND VACUUM IN THE CRYSTALBREEDER

Maja Zupancic

Technobis Crystallization Systems, Pyrietstraat 2, 1812 SC Alkmaar, Netherlands

Single crystal X-ray diffraction (SCXRD) is a powerful tool employed in a plethora of scientific areas. Information obtained using SCXRD can be used to identify solid forms and generate predicted powder patterns with significant regulatory and legal implications for new molecules. Therefore, the quality of the SCXRD data collected needs to be high, which is usually related to the quality of the single crystal sample used.

Growing single crystals can be considered an art form that requires skill and knowledge of techniques and molecules in order to conduct experiments. However, there is still a large amount of randomness in single crystal growing experiments, and parameters and procedures that produce crystalline material the first time might not do so on subsequent tries. This can be attributed to the fact that many procedures used, such as evaporation, ripening, and vapour diffusion, have not changed since their inception and thus lack proper control. Additionally, they depend on solvent properties, which can limit the design space.

We show here how the CrystalBreeder instrument can be used to expand the design space of single crystal experiments by controlling temperature and pressure. Using these, it is possible to use solvents, which previously could not be used in vapor diffusion and evaporation due to low vapor pressure. Increasing temperature and applying vacuum it is possible to control the rate of diffusion and evaporation, thereby applying a level of control over single crystal experiments and improving the quality of crystals and removing randomness.

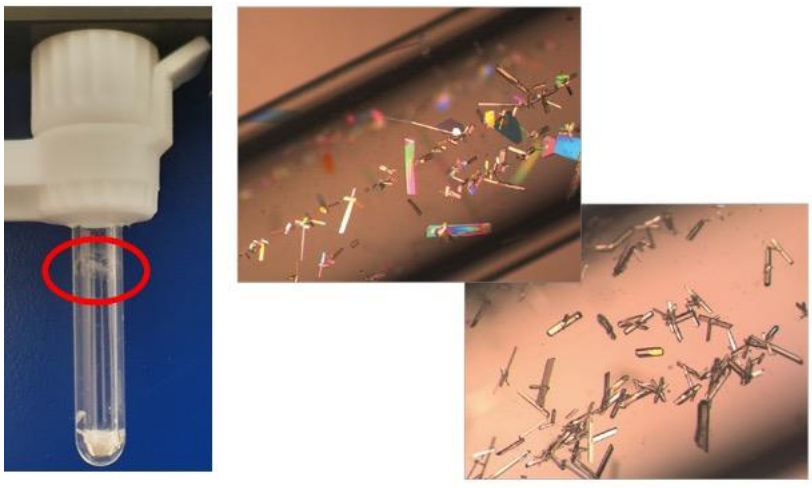

Rys. 1. Salicylamide crystals grown by sublimation in CrystalBreeder.

O-20

STRUCTURAL CHARACTERIZATION OF *RHIZOBIUM ETLI* THERMOSTABLE L-ASPARAGINASE ReAIV

Joanna Loch[1], Paulina Worsztynowicz[2], Joanna Sliwiak[2], Barbara Imiolczyk[2], Kinga Pokrywka[2], Mateusz Chwastyk[3], Marta Grzechowiak[2], Mirosław Gilski[2,4], Mariusz Jaskólski[2,4]

[1] *Faculty of Chemistry, Jagiellonian University, Krakow, Poland*
[2] *Institute of Bioorganic Chemistry, Polish Academy of Sciences, Poznań, Poland*
[3] *Institute of Physics, Polish Academy of Sciences, Warsaw, Poland*
[4] *Faculty of Chemistry, Adam Mickiewicz University, Poznań, Poland*

L-Asparaginases catalyze the metabolically essential amidohydrolysis of L-Asn to L-Asp and NH_3 [1]. The genome of *Rhizobium etli*, which is a nitrogen fixing bacterial symbiont of the leguminous common bean, encodes two L-asparaginases: the recently characterized inducible and thermolabile enzyme ReAV [2] and the constitutive and thermostable protein ReAIV (Fig. 1). In this work [3], we have determined five crystal structures (resolution from 1.30 to 2.50 Å) of the constitutive ReAIV enzyme, showing that despite low level of sequence identity it is a structural ortholog of the inducible ReAV protein. Systematic investigations of L-asparaginases are important from the medicinal point of view, as enzymes with sufficiently high substrate affinity are potential drug candidates for the treatment of several forms of leukemia.

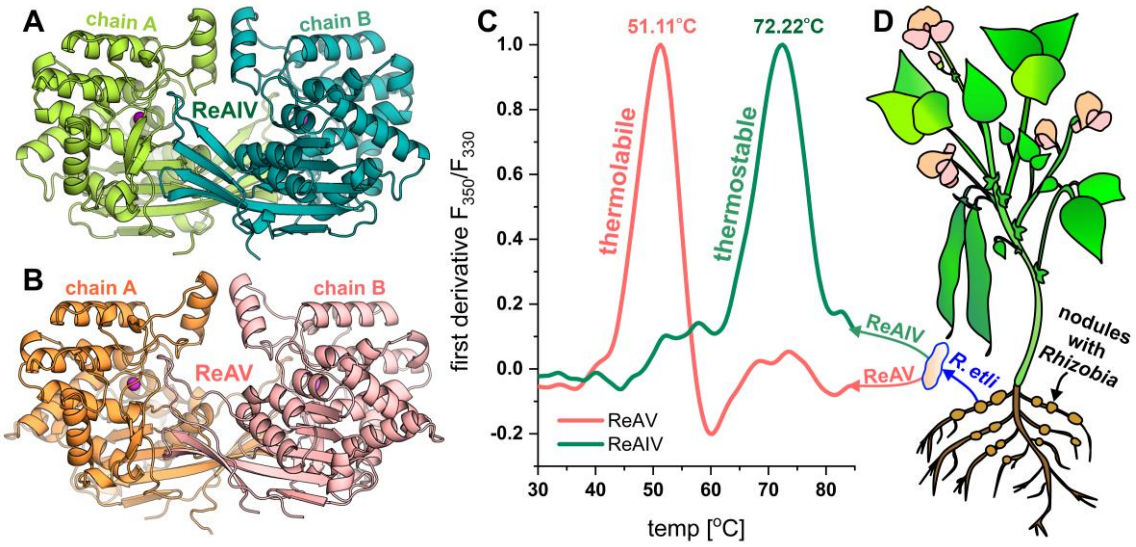

Fig. 1. Crystal structures of the (A) ReAIV and (B) ReAV (PDB: 7os5) dimers. (C) Thermal stability of ReAIV and ReAV determined by nanoDSF. (D) Scheme of typical nitrogen fixing legume plant with root nodules containing bacteroids form the *Rhizobia* genus (among them *R. etli*).

ReAIV has a sequence of 335 residues that is by 32 residues shorter than ReAV. The shortening of the ReAIV sequence is not the effect of random residue deletions but arises from the removal of three segments from the ReAV sequence: of loops 211-217 and 275-284, and of the C-terminus 350-367. All the determined structures show that the biological assembly of ReAIV is a C_2-symmetric homodimer with two identical

active sites (Fig. 1A) consisting of a zinc coordination sphere and two catalytic tandems formed by Ser47-Lys50 and Ser79-Lys256. The zinc coordination sphere in ReAIV is created by Lys137, two cysteine residues, Cys134 and Cys188, and a water molecule w1. Water w1 is H-bonded to the nearby side chains of Asp186 and Ser47. Near the active site of ReAIV there is an interesting Cys242 residue. In most of the structures, this residue is oxidized, although the role of this modification is not clear. Analysis of the ReAIV crystal structures, in which as many as 14 "snapshots" of the protein chain and the active site are visualized, allowed us to identify several distinct conformational states of the active site residues, and to arrange them in a movie-like sequence illustrating the changes of the enzyme during a conjectural catalytic cycle.

Careful inspection of the electron density maps also revealed the presence of three clusters of structural water molecules, buried in three internal cavities in the protein core. The water molecules in all three cavities act as "drops of glue", cementing the protein core. Thus, all these water molecules are likely to play an important role in the increased thermal stability of ReAIV. Interestingly, the water-filled cavities of ReAIV are all located in the close proximity of the regions important for the catalytic apparatus.

With the discovery of the ReAIV and ReAV L-asparaginases, interesting questions arise concerning the evolutionary origin of these enzymes. Since these L-asparaginases are similar in fold to Penicillin Binding Proteins (PBPs) and serine β-lactamases, it is possible that they have evolved from those cell-wall-metabolism-related bacterial proteins. A pan-genomic analysis of the bacterial kingdom revealed that ReAV (but not ReAIV) orthologs are rarely found in *Rhizobia* and that the presence ReAV in *R. etli* seems to be the result of a Horizontal Gene Transfer (HGT) from *Burkholderia* [4].

Work supported by National Science Centre (NCN) grant 2020/37/B/NZ1/03250

References

[1] J.I. Loch, M. Jaskolski, *IUCrJ*, **8** (2021) 514-531.
[2] J.I. Loch, B. Imiolczyk, J. Sliwiak, A. Wantuch, M. Bejger, M. Gilski, M. Jaskolski, *Nat. Commun.*, **12** (2021) 6717.
[3] J.I. Loch, P. Worsztynowicz, J. Sliwiak, B. Imiolczyk, K. Pokrywka, M. Chwastyk, M. Grzechowiak, M. Gilski, M. Jaskolski, *Acta Cryst.*, D**79** (2023) submitted.
[4] A. Zielezinski, J.I. Loch, W.M. Karlowski, M. Jaskolski, *Sci. Rep.*, **12** (2022) 15797.

O-21

WHAT TO DO WITH A VAST AMOUNT OF PROTEIN DIFFRACTION DATA AT AN EXTREMELY HIGH RESOLUTION OF 0.38Å

Mirosław Gilski[1,2], Julian C.-H. Chen[3], Changsoo Chang[3], Maciej Kubicki[2], Mariusz Jaskólski[1,2] & Andrzej Joachimiak[3]

[1] Institute of Bioorganic Chemistry, Polish Academy of Sciences, Poznan, Poland
[2] Faculty of Chemistry, A. Mickiewicz University, Poznan, Poland
[3] Structural Biology Center, Biosciences Division, Argonne National Laboratory, Argonne, IL 60439, USA

The goal of structural studies is to determine the crystal structure accurately and gain detailed insights into the studied structure. The quality of the crystal structure depends on the resolution and quality of the diffraction data. Small molecules can achieve a resolution of about 0.8 Å, but larger molecules like proteins and nucleic acids do not diffract so well, mainly due to their size and disordered solvent. Currently, the Protein Data Bank (PDB) contains 1009 structures (0.5%) with resolutions below 1 Å, 70 structures (0.035%) below 0.8 Å, and only 5 structures (0.0025%) below 0.6 Å, including two crambin structures and one Z-DNA structure.

Crambin is a small protein found in *Crambe abyssinica* seeds and its crystals exhibit excellent X-ray scattering properties. It exists in two isoforms, PL and SI, differing by two amino acids (Pro/Ser22 and Leu/Ile25). The natural mixture of both forms yields the best diffraction, achieving a record-breaking resolution of 0.48 Å in the entire PDB [1]. In contrast, crystals of the pure PL or SI forms exhibit less effective scattering.

Ten years ago, several sets of crambin diffraction data were successfully collected at the 19-ID beamline of Structural Biology Center, Advanced Photon Source (APS) Argonne, achieving a remarkable resolution of 0.37 Å. Collecting this data was a significant challenge, involving modifications to the beamline setup and the use of 30 keV X-ray radiation (at wavelength of 0.4 Å. [2].

Despite extensive efforts, the full utilization of the collected data has not been achieved yet. The structure was solved, but refinement of such an extreme high-resolution structure requires dedicated protocols to address additional aspects and problems revealed during detailed data analysis. The main challenges include disturbance of monochromaticity caused by higher harmonics due to the use of the Si(333) reflection of the monochromator instead of the standard Si(111), as well as detector absorption corrections for high-angle reflections.

In the past year, the project aiming to obtain the most precise crambin structure has been resumed. Remarkable technological advancements, particularly in low-noise X-ray detectors, allow for the repetition of the experimental phase of the project utilizing the current beamline capabilities. A new diffraction data for crambin crystals were collected using the PILATUS3 X 6M detector. Data were collected for dozens of crystals at three temperatures: 15 K, 100 K, and 293 K. High- and low-resolution data were collected separately. For 15K data collection, detector was lowered for 220 mm to

collect high-angle reflections, but completeness in such setting was below 50%. The whole dataset size exceeded 300 GB and requires a labor-intensive analysis.

Standard data processing protocols were insufficient for such cases, and the preliminary results were unsatisfactory. While some crystals diffract to resolutions of about 0.4 Å, obtaining a complete dataset requires merging and scaling data from multiple crystals, which always affects data quality - a crucial aspect of this project. Additionally, efforts are underway to collect new crambin diffraction data using a diffractometer equipped with a rotating molybdenum anode, which theoretically allows for obtaining diffraction with a maximum resolution on the order of 0.38 Å. Further data collection aims to achieve a complete dataset from a single crystal by utilizing the advantages of a kappa goniometer geometry and exploring the possibility of collecting extreme high-resolution data using home radiation sources.

Efforts continue to push the boundaries of high-resolution protein structure determination and advance our understanding of subatomic-level structures.

References

[1] Schmidt, A., Teeter, M., Weckert, E. & Lamzin, V. S. *Acta Cryst., F***67** (2011) 424–428.
[2] Rosenbaum, G., Ginell, S.L. & Chen, J.C.H. *J. Synchrotron Rad*., **22** (2015) 172–174.

O-22

ANALIZA STRUKTURALNA RNA POWTÓRZEŃ G2C4 ZWIĄZANYCH ZE STWARDNIENIEM ZANIKOWYM BOCZNYM I OTĘPIENIEM CZOŁOWO-SKRONIOWYM: POLIMORFIZM STRUKTURALNY RNA ORAZ JEGO POTENCJAŁ DO ODDZIAŁYWANIA Z SYNTETYCZNYMI CZĄSTECZKAMI

Leszek Błaszczyk, Marcin Ryczek, Bimolendu Das, Martyna Pluta, Magdalena Bejger, Kazuhiko Nakatani i Agnieszka Kiliszek

Instytut Chemii Biorganicznej PAN, ul. Noskowskiego 12/14, 61-704 Poznań

Stwardnienie zanikowe boczne oraz otępienie czołowo-skroniowe (ALS/FTD) są nieuleczalnymi chorobami neurodegeneracyjnymi. Zaliczają się do grupy chorób wywołanych nadmiernym zwielokrotnieniem sekwencji powtarzających się występujących w obrębie niektórych genów. Najczęstszą przyczyną rozwoju rodzinnej choroby ALS/FTD jest mutacja genu *C9orf72,* który zlokalizowany jest na chromosomie 9p21. Region promotorowy tego genu zawiera sekwencję mikrosatelitarną składającą się z sześcionukleotydowych powtórzeń (HRE) 5'-GGGGCC-3'/5'GGCCCC-3'. Typowo w genie znajduje się kilka powtórzeń HRE. Mogą jednak ulec zwielokrotnieniu, do wielu tysięcy kopii, co rozpoczyna proces chorobotwórczy. Obecność zwielokrotnionych powtórzeń ma negatywny efekt zarówno na poziomie DNA, RNA jak i białka, prowadząc do skomplikowanego oraz wieloczynnikowego patomechanizmu ALS/FTD.

Na poziomie RNA zmutowane fragmenty transkryptów przyjmują drugo- i trzeciorzędowe struktury mające zdolność do nadmiernego wiązania białek, tworzenia jądrowych złogów oraz stanowią matrycę do translacji toksycznych polipeptydów. Znajomość struktur sześcionukleotydowych powtórzeń jest istotna dla zrozumienia patomechanizmu choroby oraz rozwoju farmakoterapii. Struktury przestrzenne mogą stanowić matryce, do projektowania małych cząsteczek oddziałujących z docelowym RNA w celu hamowania procesu chorobotwórczego.

W ramach badań prowadzonych nad powtórzeniami HRE wyznaczyliśmy dwa modele krystalograficzne: natywnej cząsteczki RNA zawierającej sekwencję GGCCCC (G2C4) oraz jej kompleks z syntetyczną cząsteczką ANP77 (dimer 2-amino-1,8,-naftarydyny). Przeprowadziliśmy również badaniach biofizyczne w celu scharakteryzowania oddziaływania RNA-ligand przy użyciu kalorymetrii różnicowej, spektrometrii mas oraz dichroizmu kołowego. Modele przestrzenne pokazały, że natywna cząsteczka RNA utworzyła skomplikowaną strukturę tripleksu składającego się z czterech nici oligomeru. Natomiast w strukturze kompleksu RNA-ligand obserwujemy jedną cząsteczka ligandu, która związała się do jednego z końców tripleksu. ANP77 oddziałuje bezpośrednio z dwiema resztami cytozyn tworząc dwie pseudo-kanoniczne pary typu Watsona-Cricka. Uzyskane wyniki demonstrują bogactwo i polimorfizm strukturalny powtórzeń HRE i stanowią matrycę dla projektowania leków na ALS/FTD. Ponadto model kompleksu RNA-ligand pokazuje potencjał cząsteczki ANP77 do rozpoznawania reszt cytozyny znajdujących się w określonym kontekście strukturalnym. Właściwość ta może zostać wykorzystana do projektowania związków wiodących celowanych na RNA przy użyciu narzędzi do przewidywań *in silico*.

Przedstawione badania są prowadzone z grantów Narodowego Centrum Nauki: UMO-2022/45/B/NZ7/03543 and UMO-2017/26/E/NZ1/00950.

O-23

AN UNEVEN FIGHT WITH ELUSIVE POLYMORPHS OF MELOXICAM

Marta K. Dudek[1], Maura Malińska[2], Agata Jeziorna[1], Piotr Paluch[1], Justyna Zając[1], Rafał Dolot[1]

[1] *Centre of Molecular and Macromolecular Studies, Polish Academy of Sciences, Sienkiewicza 112, 90-363 Łódź*
[2] *Department of Chemistry, University of Warsaw, Pasteura 1, 02-093 Warsaw*

In 1994 prof. A. Gavezzotti published a paper entitled '*Are crystal structures predictable*' and gave a very succinct answer '*No*' in its opening line, claiming that this could be the shortest paper ever written [1]. Since then an enormous progress has been made in computational crystal structure prediction (CSP) methods, facilitating polymorph screening and reducing a risk of late-appearing polymorphs. At the same time, CSP still suffers from a number of issues, among which the problem of how to realize in practice what has been predicted in a computer is not the least [2]. In CSP crystal energy landscape of a molecule is generated, which is usually a plot of crystal energies *vs* densities, in which each point corresponds to a different crystal structure. Nothing is said, however, in which conditions any of the generated structures can be crystallized in a laboratory, or even is it at all possible to experimentally obtain all of them.

The presented work is a part of an effort to bridge a gap between computational predictions and practical ways of their realization using elusive polymorphs of meloxicam (MLX) as a case study. Out of four neat polymorphs of MLX only the commercially available form I is fully characterized structurally by single crystal X-Ray diffraction [3], while forms II, III and V remain elusive. Our numerous crystallization attempts to obtain these forms by repeating procedures disclosed in a patent failed and led us to employ CSP calculations to indicate possible new crystallization pathways. The obtained crystal energy landscape featured primarily structures stabilized by NH…O=S dimers, present also in commercial form I, but several low energy and low density structures stabilized by NH…N dimers were also found (Fig. 1).

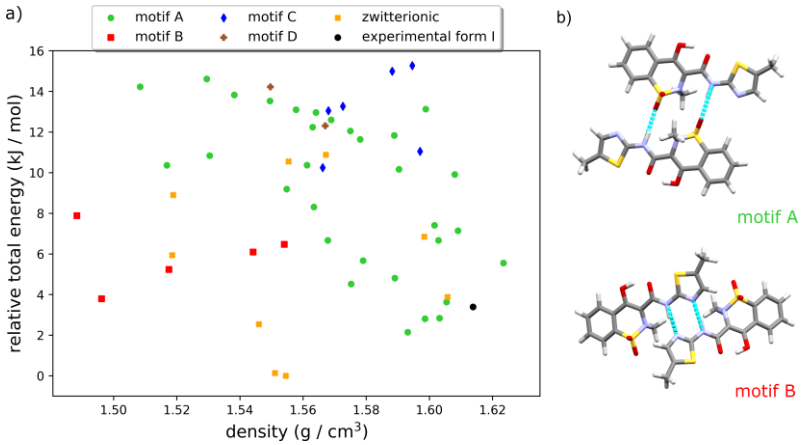

Fig. 1. (a) The lowest energy part of the CSP PBE-MBD energy landscape for MLX; (b) two hydrogen bond motifs found in the predicted lowest energy structures build by neutral MLX molecules.

The results of CSP calculations were used to guide crystallization effort. First, it was suggested to explore desolvation experiments which have a capacity to lead to low density structures, as well as crystallization in the presence of additives capable of influencing the formation of hydrogen bonds. This approach led us to propose new and efficient crystallization methods to obtain three elusive forms of MLX.

The crystallization experiments resulted also in growing a single crystal of form III of MLX, enabling its crystal structure solution by single-crystal X-Ray diffraction. The remaining forms II and V were found to notoriously crystallize as microcrystalline powders, efficiently hindering their structure elucidation. In such cases alternative crystal structure determination methods, such as microED and NMR crystallography are particularly helpful [4, 5]. Indeed, CSP-supported NMR crystallography enabled crystal structure determination of form II of MLX, while microED led us to crystal structure determination of form V, which was found to be a Z'=4 polymorph, in agreement with solid-state NMR measurements (Fig. 2). All elusive structures were found to be stabilized by NH…N dimers, as suggested by crystallization guiding CSP calculations.

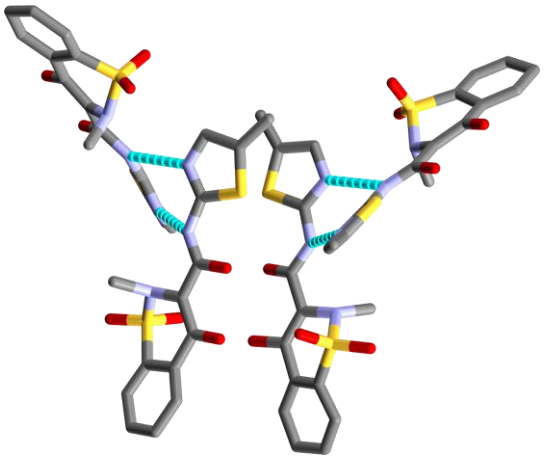

Fig. 2. Four symmetry-inequivalent molecules of MLX building an asymmetric part of a unit cell of MLX form V determined from microED measurements. The two dimers of MLX are stabilized by motif B hydrogen bond.

This work was possible due to the financial support of the Polish National Science Centre under Sonata grant No. UMO-2018/31/D/ST4/01995. The Authors gratefully acknowledge PLGrid infrastructure for providing resources within the computational grant no. PLG/2022/015813.

Literatura

[1] A. Gavezzotti. *Acc. Chem. Res.*, **27** (1994) 309.
[2] A. J. Cruz-Cabeza, N. Feeder, R. J. Davey. *Commun. Chem.*, **3** (2020) 142.
[3] G. F. Fabiola, V. Pattabhi, S. G. Manjunatha, G. V. Rao and K. Nagarajan. *Acta Cryst. C*, **54** (1998) 2003.
[4] C. J. H. Smalley, H. E. Hoskyns, C. E. Hughes, D. N. Johnstone, T. Willhammar, M. T. Young, C. J. Pickard, A. J. Logsdail, P. A. Midgley, K. D. M. Harris. *Chem. Sci.*, **13** (2022) 5277.
[5] M. K. Dudek, P. Paluch, E. Pindelska. *Acta Cryst. B*, **76** (2020) 322.

O-24

TWO-DIMENSIONAL HYBRID PEROVSKITES WITH (110)-ORIENTED LAYERS AND LARGE OCTAHEDRA TILTING

Dawid Drozdowski, Anna Gągor, Mirosław Mączka

Institute of Low Temperature and Structure Research Polish Academy of Sciences, ul. Okólna 2, 50-422 Wrocław

Hybrid organic-inorganic perovskites (HOIPs) have gained significant attention in materials science due to their potential applications in solar cells, photodetectors, and light-emitting devices. While three-dimensional (3D) lead halide HOIPs of the ABX_3 formula, with methylammonium (MA^+) and formamidinium (FA^+) at the 'A' site, revealed outstanding photovoltaic performance, they suffer from poor outdoor stability [1]. To address this issue, researchers have explored the use of layered (2D) analogues with improved stability and superior optoelectronic properties when compared to their 3D counterparts. In 2D HOIPs (A_2BX_4), the octahedra layers are separated by organic spacers, exhibiting a quantum well character that enhances certain optoelectronic properties, *e.g.*, photoluminescence quantum yield (PLQY). Moreover, 2D HOIPs can be easily tuned through compositional engineering, offering greater flexibility compared to 3D analogues or conventional semiconductors. One may distinguish three families of 2D perovskite phases, *i.e.*, Ruddlesden–Popper (RP), Dion–Jacobson (DJ), and Alternating Cation in the Interlayer space compounds (ACI) [2]. The other way of classification is based on the 'slicing' of 3D parental structure along particular crystallographic planes, namely (001)-, (110)- or (111)-oriented. The ACI-type compounds are the rarest and the most attractive for light-emitting applications, whereas (110)-oriented types demonstrate broadband white-light emission with large Stokes shifts [3, 4].

Contemporary knowledge about both groups remains limited. In this contribution, we report the synthesis and crystal structure-physiochemical properties relationship in $IMMHyPbX_4$ (X = Br, Cl) 2D HOIPs of the ACI type (IM=imidazolium, MHy = methylhydrazinium) [5]. It is worth noting that the chlorine analogue is the first ever reported (110)-type lead chloride 2D perovskite with two monovalent organic cations, while for bromines 7 compounds of such type have been reported hitherto [6]. XRD studies combined with the DSC measurements revealed the existence of two temperature-controlled crystal phases – high-temperature (HT) phase (**I**) and low-temperature (LT) phase (**II**) described in $P2/c$ and $P2_1/c$ space groups, respectively (Fig. 1). The **I** → **II** phase transition is associated with a translational symmetry breaking and formation of the 2*b* superstructure, and occurs at 344.5 K (375.4 K) for Br^- (Cl^-) compound in the cooling mode. In **I**, the organic moieties are heavily disordered, while in **II** the IM^+ is ordered and MHy^+ gradually stabilises its position on further cooling. This ordering results in the creation of the network of possible hydrogen bonds (HBs), bringing the largest tilting of octahedra layers and the lowest distances of adjacent Pb atoms within the layers among all the reported lead halides of this structural type (143° and 7.96 Å for Cl^- analogue at 100 K). These distortions manifest themselves in optical properties, leading to broadband photoluminescence (PL, full width at half maximum *ca*. 170 nm) with large Stokes shifts (up to 250 nm) and, for the first time within the ACI family, white-light PL emission observed for Br- compound at 200 K (T ~ 5226 K) [5]. The reorientational motions of MHy^+ also affected the electrical properties, revealed in the dipolar relaxation process.

Our findings highlight the crucial role of crystal structure examination in understanding the physiochemical properties of crystalline solids and open the path for further exploration of this intriguing subclass of 2D HOIPs with practical applications, especially in the optoelectronic scope.

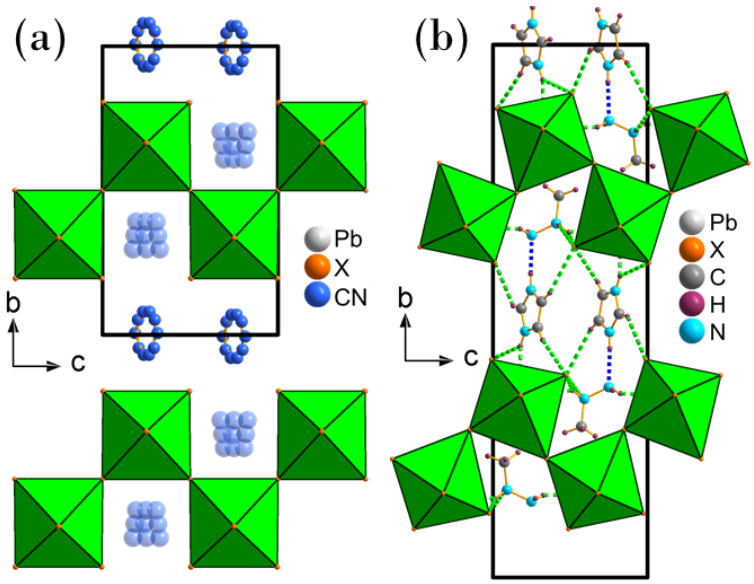

Fig. 1. Crystal structure of IMMHyPbX_4 (X = Br, Cl) compounds in (a) HT phase **I** and (b) LT phase **II** at 100 K. Dashed lines denote possible HBs interaction.

This research was supported by the Polish National Science Centre (project No. 2019/35/B/ST5/00043)

Literature

[1] S. Shao, M. Loi, *Adv. Mater. Inter.*, 7 (**2020**) 1901469.
[2] C. M. M. Soe et al., *J. Am. Chem. Soc.*, 139 (**2017**) 16297–16309.
[3] C. Katan, N. Mercier, J. Even, *Chem. Rev.*, 119 (**2019**) 3140–3192.
[4] E.R. Dohner, E.T. Hoke, H.I. Karunadasa, *J. Am. Chem. Soc.*, 136 (**2014**) 1718–1721.
[5] D. Drozdowski, K. Fedoruk, A. Kabański, M. Mączka, A. Sieradzki, A. Gągor, *J. Mater. Chem. C*, 11 (**2023**) 4907–4915.
[6] E.I. Marchenko, S.A. Fateev, A.A. Petrov, V.V. Korolev, A. Mitrofanov, A.V. Petrov, E.A. Goodilin, A.B. Tarasov, *Chem. Mater.*, 32 (**2020**) 7383–7388.

O-25

PRESSURE INDUCED SPIN CROSSOVER IN THE TWO-DIMENSIONAL COORDINATION POLYMER OF MIXED CRYSTALS $[Fe(bbtr)_3](BF4)_{2x}(ClO_4)_{2(1-x)}$ ($0 \leq x \leq 1$)

Maria Książek[1], Marek Weselski[2], Aleksandra Półrolniczak[3], Andrzej Katrusiak[3], Damian Paliwoda[4], Joachim Kusz[1], Robert Bronisz[2]

[1] Institute of Physics, University of Silesia, 1 75 Pułku Piechoty, 41-500 Chorzów
[2] Faculty of Chemistry, University of Wrocław, 14 F. Joliot – Curie, 50-383 Wrocław
[3] Faculty of Chemistry, Adam Mickiewicz University of Poznań, 8 Uniwersytetu Poznańskiego, 61-614 Poznań
[4] LCC, CNRS and University of Toulouse, 205 Route de Narbonne, 31077 Toulouse

Cooling of $[Fe(bbtr)_3](BF_4)_2$ (bbtr = 1,4-di(1,2,3-triazol-1-yl)butane) triggers very slow spin crossover below 80 K ($T_{1/2}^{\downarrow}$=76 K). In the isostructural perchlorate analogue $[Fe(bbtr)_3](ClO_4)_2$ spin crossover during cooling is preceded by phase transition at 125 K. Studies of the mixed crystals $[Fe(bbtr)_3](BF_4)_{2x}(ClO_4)_{2(1-x)}$ ($0.1 \leq x \leq 0.9$) showed that a decrease in the content of perchlorate anions in the tetrafluoroborate host causes that observed P-3 → P-1 phase transition for $x \geq 0.5$ disappears for lower x values, however, thermally induced spin crossover still occurs.

Mentioned above observation is supported by the results of pressure-dependent studies of $[Fe(bbtr)_3](BF_4)_{2x}(ClO_4)_{2(1-x)}$ ($0.1 \leq x \leq 0.9$) mixed crystals carried out at room temperature under UV/VIS spectroscopy monitoring. Initially, an application of pressure up to ca. 0.5 GPa does not involve the appearance of $^1A_1 \rightarrow {}^1T_1$ band characteristic for LS form. Elevation of the pressure causes an appearance of LS form and then a very sluggish increase of LS molar ratio up to about 0.9 GPa. Further pressure triggers a very abrupt spin crossover. Obtained results showed that enforcing spin crossover in terafluoroborate ($p_{1/2}$ = 1.08 GPa) requires higher pressure than for perchlorate ($p_{1/2}$ = 1.0 GPa), which means higher stabilization of the LS form in that last one. Thus, it remains in agreement with the results of magnetic studies showing that at 300K perchlorate achieves $T_{1/2}$ for slightly lower pressure than tetrafluoroborate. It can conclude that the linearity of this dependence indicates the same mechanism of spin crossover under high pressure conditions for all studied samples.

The crystal structures determined at pressure 1.064 GPa for perchlorate and 1.212 GPa for tetrafluoroborate indicate the occurrence of P-3 → P-1 phase transition. The average Fe-N distances are equal to 2.0 and 2.0 Å, respectively, that is, the spin crossover is practically completed. It is clearly visible that, unlike ambient pressure, the mechanism of spin crossover under high pressure conditions is very similar for both complexes. Moreover, obtained results confirm that for perchlorate mechanism of spin crossover was changed upon transition from ambient pressure, where structural phase transition preceded spin crossover, to higher pressures where spin crossover starts before phase transition.

O-26

UNUSUAL PROPERTIES OF FLEXIBLE MOFS AND THEIR APPLICABILITY IN GAS STORAGE AND SEPARATION

Kornel Roztocki

Adam Mickiewicz University, Uniwersytetu Poznańskiego 8, 61-614 Poznań, Poland

e-mail: kornel.roztocki@amu.edu.pl

The spatiotemporal adaptivity of flexible metal-organic frameworks gives rise to novel phenomena that are not observed in their rigid counterparts. This not only broadens our knowledge about the universe of porous materials but may also have practical implications in gas storage, separation, or sensing technologies.

In first part, we will discuss a stimuli responsive terpyridine MOF which, upon desolvation, transforms into the closed phase, and then to the open shape-memory phase after the first CO_2 (195 K) adsorption-desorption cycle (Fig. 1).[1] Based on comprehensive *in situ* experimental studies (SC-XRD and PXRD) and DFT energetic considerations combined with the literature reports, we recommend dividing shape-memory MOFs into two categories, responsive and non-responsive, depending on the transformability of gas-free reopen pore phase into the collapsed phase. The presented DFT approach is the first example of a theoretical methodology describing the shape-memory MOFs and thus paving the way for further development in this field. Moreover, we emphasize the essential role of multicycle physisorption experiments as well as the development of theoretical tools for further discoveries and understanding of shape-memory porous materials, including various types of flexible porous materials, such as noncovalent, covalent, and metal-organic frameworks.

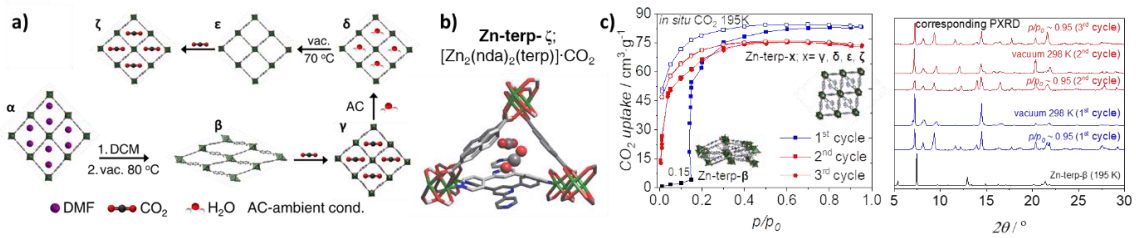

Fig. 1. **a**) Schematic illustration of the SC-SC phase transformation triggered by several subsequent stimuli. **b**) CO_2 binding sites involving anions and N-donor linkers resolved from *in situ* SC-XRD data collected during adsorption. **c**) Three CO_2 adsorption (full symbols) and desorption (open symbols) cycles at 195 K juxtaposed with calculated and experimental PXRD patterns.

Second part concerns two isostructural pillared-layer dynamic MOF that differ only in one atom bridging the benzenocarboxylate linker.[2] Through a presented synthetic approach, we convert the CO_2-induced stepwise transformation into a continuous process (Fig. 2a). This is the first example in which a one-atom exchange in a flexible MOF changes the 2nd order phase transformation to 1st order. we not only mechanistically understand the switchability of those flexMOFs by state-of-the art *in situ* powder X-ray diffraction measurements, but we also show the superiority of continuous structural transformation in CH_4 storage and CH_4/CO_2 separation at 298 K (Fig. 2b,c).

O-26

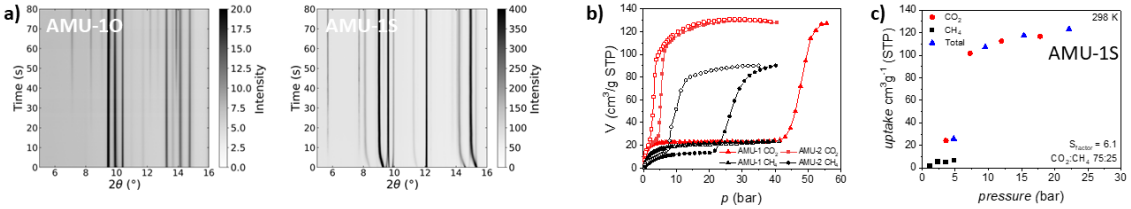

Fig. 2. **a**) *In situ* time-resolved PXRD during the CO_2 adsorption at 195K, **b**) single-gas adsorption measurements for AMU-1X at 298 K. Isothermal multicomponent adsorption experiments for CO_2/CH_4 compositions in AMU-1S at 298 K.

Acknowledgment: National Science Centre (NCN, Poland; Grants no. 2020/36/C/ST4/00534).

References

[1] K. Roztocki* *et al.*, *ACS Mater. Lett.*, **5**(4) (2023) 1256–1260.
[2] K. Roztocki* *et al.*, submitted.

O-27

SOLCRYS - PX BEAMLINE AT SOLARIS NSRC - UPDATED DESIGN AND PROGRESS IN CONSTRUCTION

Maciej Kozak[1,4], Tomasz Kołodziej[1], Joanna Sławek[1], Grzegorz Gazdowicz[1], Agnieszka Klonecka[1,3,4], Jarosław Wiechecki[1], Adriana Wawrzyniak[1]

[1] SOLARIS National Synchrotron Radiation Centre, Jagiellonian University, ul. Czerwone Maki 98, 30-392 Kraków, Poland
[2] Department of Biomedical Physics, Faculty of Physics, Adam Mickiewicz University, ul. Uniwersytetu Poznańskiego 2, 61-614 Poznań, Poland
[3] Faculty of Physics, Astronomy and Applied Computer Science, Jagiellonian University, ul. Łojasiewicza 11, 30-348 Kraków, Poland
[4] Doctoral School of Exact and Natural Sciences, Jagiellonian University, Kraków, Poland

The construction of new part of the experimental hall at the SOLARIS National Synchrotron Radiation Centre (JU Kraków, Poland) creates the possibility of construction of long experimental synchrotron beamlines, allowing for effective focusing of hard X-rays obtained from insertion devices. Completion of the hall extension is planned for November 2023. The SOLCRYS project, involving the construction of a research beamline for diffraction studies and SAXS measurements, was located in a new part of the experimental hall from the very beginning. The construction of this beamline was originally designed on the basis of the 4 Tesla superconducting wiggler, and the supplier of this system, selected in an open tender was to be the Budker Institute of Nuclear Physics (Novosibirsk, Russia).

Unfortunately, Russia's aggression against Ukraine in February 2022 resulted in the termination of the contract for the construction and installation of this insertion device and the need to search again for the new source of synchrotron radiation (alternative wiggler) for the SOLCRYS beamline. In the currently updated concept of the SOLCRYS beamline, the radiation source planned to be installed in the straight section 02 of the SOLARIS storage ring is a 3-pole wiggler operating at 3 Tesla. The tender for the supply of this device has been announced, and we are currently at the final stage of analyzing the submitted offers. The current concept of the construction of the SOLCRYS diffraction beamline assumes locating it as the sole recipient of the synchrotron radiation generated by the wiggler, which will allow to obtain a high-intensity stream of photons. However, the SAXS line has been moved and will be located at a bending magnet.

In the lecture, the updated technical and construction parameters of the SOLCRYS beamline and the planned research capabilities will be presented. Technological data and the status of the SAXS line will be updated.

O-28

REVISITING THE THERMODYNAMICS OF PHASE TRANSITION IN THE JUMPING CRYSTAL L-PYROGLUTAMIC ACID: INSIGHTS FROM DYNAMIC QUANTUM CRYSTALLOGRAPHY AND SPECTROSCOPY

Anna A. Hoser[1], Toms Rekis[2], Helena Butkiewicz[1], Karlis Berzins[2], Anders Ø. Madsen[2]

[1] Faculty of Chemistry, University of Warsaw, Pasteura1, 02-093 Warsaw, Poland.
[2] Department of Pharmacy, Copenhagen University, Copenhagen, Denmark

Over the past decade, extensive research has been conducted on the thermosalient phenomenon, employing a wide range of experimental techniques. While the molecular mechanism behind the jumping phenomenon has been well characterized, less attention has been given to the preceding dynamics.

The thermosalient effect in L-pyroglutamic acid was investigated by Panda et al [1]. This system exhibits three enantiotropically related polymorphs, namely α', α, and β. The solid-state phase transitions from α' to α (around 110 K) and from α to β (within the range of 350-370 K) both involve the jumping phenomenon. These phase transitions exhibit reversibility but display significant hysteresis, with the majority of crystals remaining intact during heating cycles.

In this study, we aim to explore the lattice dynamics of the α and β polymorphs through a combination of X-ray diffraction, Raman spectroscopy, and periodic DFT calculations. Building upon our previous work, we have demonstrated that lattice-dynamical models refined using X-ray diffraction data can provide insights into the thermodynamic properties of molecular crystals, an approach we refer to as dynamic quantum crystallography[2-4]. Furthermore, the low-frequency lattice vibrations obtained from this approach were complemented by low-frequency Raman spectroscopy (LFR).

The lattice dynamical models derived from density functional theory (DFT) calculations for the polymorphs of L-pyroglutamic acid exhibit excellent agreement with the results obtained from low-frequency Raman (LFR) spectroscopy. Frequencies obtained from DFT calculations were refined against X-ray data (normal mode refinement (NoMoRe)). Notably, we have demonstrated that the frequencies obtained through NoMoRe can be effectively utilized for estimating entropy.

Scheme 1. From lattice dynamics to thermodynamic properties.

In the specific case of L-pyroglutamic acid, our findings suggest that form β is stabilized by entropy at elevated temperatures, which is in agreement with experimental observations. Leveraging this understanding, we are able to make predictions regarding the phase transition temperature. By considering the entropy contribution, we gain

valuable insights into the thermodynamic behavior of L-pyroglutamic acid and its polymorphs.

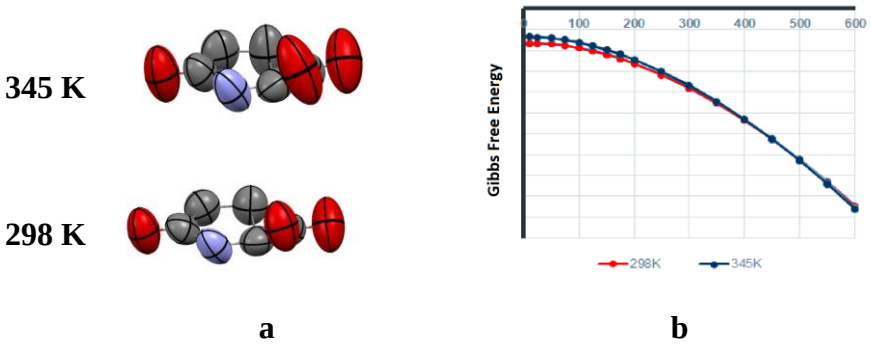

Fig. 1. (a) Anisotropic displacement parameters (ADPs) at 298K and at 345K (b) Gibbs free energies obtained for both polymorph from frequencies from NoMoRe.

Financial support from Polish National Science Centre (SONATA17 grant 2021/43/D/ST4/03136) is kindly acknowledged.

Literature

[1] Panda, Runčevski, Husain, Dinnebier, Naumov, *J. Am. Chem. Soc.*, **137**(5) (2015) 1895–1902.
[2] Hoser A. A., Madsen A. Ø., *Acta Cryst A*, A**72** (2016) 206–214.
[3] Hoser A. A., Sztylko M.,Trzybiński D., Madsen A. Ø. *Chem. Commun.*, **57** (2021) 9370–9373.
[4] Hoser A. A., Rekis T., Madsen A. Ø. *Acta Cryst. B Struct Sci Cryst Eng Mater*., **78** (2022) 416–424.

O-29

NEW POLYMORPHIC MODIFICATIONS OF 6-METHYLURACIL: EXPERIMENTAL AND QUANTUM CHEMICAL STUDY FOR THE PRACTICAL USE

Svitlana Shishkina[a], Anna Shaposhnik[a], Vitalii Rudiuk[b], Igor Levandovskiy[c]

[a] State Scientific Institution, "Institute for Single Crystals" of the National Academy of Sciences of Ukraine, 60 Nauky Ave., Kharkiv, Ukraine
[b] Farmak JSC, 63 Kyrylivska str., Kyiv, Ukraine
[c] National Technical University of Ukraine "Igor Sikorsky Kyiv Polytechnic Institute", 37 Pobedy ave., Kyiv, Ukraine

The thorough study of crystalline forms of 6-methyluracil (**6MU**), which affects the regulation of lipid peroxidation and wound healing, leds to finding of two new polymorphic modifications that can be formed in the technological process due to temperature violations (see Figure below). For two previously known and two new polymorphic modifications, the conditions for their preparation were studied. The structure of all polymorphic modifications of **6MU** was unambiguously established by the single-crystal X-ray diffraction study. The obtained crystalline forms have also been characterized by the powder X-ray diffraction method, differential scanning calorimetry method and IR spectroscopy.

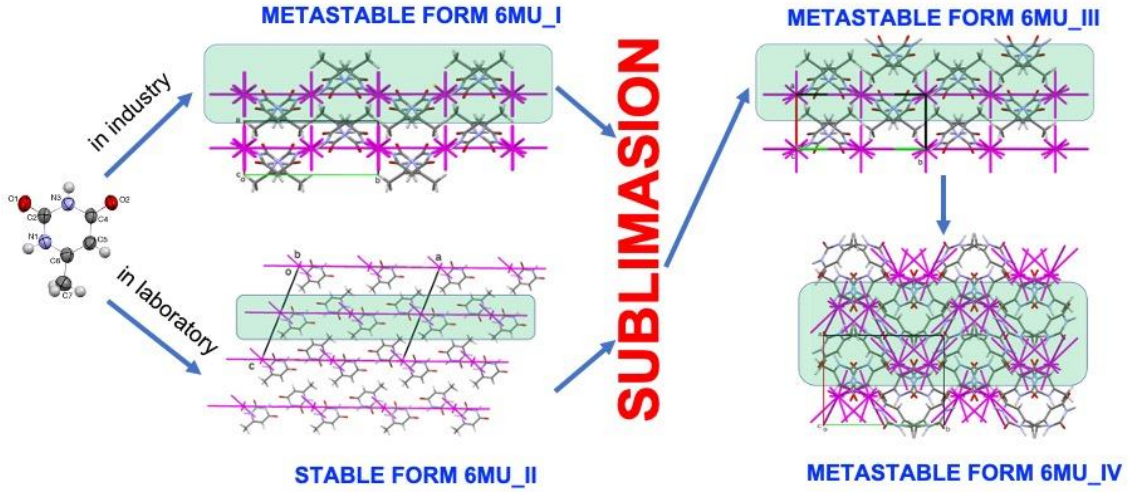

The calculations of pairwise interactions between molecules, as well as calculations of the lattice energies in periodic approximation, have shown that the **6MU_II** polymorphic form is the most stable, while the **6MU_I** form used in the pharmaceutical industry and the new forms **6MU_III** and **6MU_IV**, which can be formed by sublimation, are metastable. In all the polymorphic modifications, the centrosymmetric dimer formed by two N–H…O hydrogen bonds between **6MU** molecules is a dimeric building unit (DBU) of the crystal structure. The calculations of pairwise interaction energies between DBUs have revealed that the studied crystalline forms have layered structure. The comparison of interaction energies of DBU_0 with its neighbors within the layer and with ones belonging to neighboring layers allows us to

conclude that the most stable **6MU_II** form has the most anisotropic "energetic" structure. The interaction energy of DBU_0 with its neighbors within the layer parallel to the (001) crystallographic plane, is more than three times higher than the interaction energy with the molecules of the neighboring layer. The metastable polymorphic forms of **6MU** obtained under more nonequilibrium conditions (stirring or sublimation) have much more isotropic "energetic" structure. The interaction energy of DBU_0 with its neighbors within the layer parallel to the (100) crystallographic plane is almost two times higher than with the molecules of the neighboring layer in the **6MU_I** and **6MU_III** structures. In the most unstable polymorph **6MU_IV**, the layer is highly corrugated, and the energies of DBU_0 interactions within the layer and with the adjacent layer are very close.

The pharmaceutical industry uses the metastable polymorphic form **6MU_I** and two new metastable forms, **6MU_III** and **6MU_IV**, may be formed during technological process. Therefore, the possibility of these structures to be deformed under external influence such as mechanical stress or pressure during tableting was evaluated using quantum chemical modeling. It was shown that any structure deformation leads to significant decrease in the distances between closest atoms belonging to the neighboring layers. This fact allows to conclude that the metastable polymorphic forms of **6MU** cannot undergo a polymorphic transition under external influence and can be used in the technological process without any limitations.

Literature

[1] S. V. Shishkina, A. M. Shaposhnik, V. V. Dyakonenko, V. M. Baumer, V. V. Rudiuk, I. B. Yanchuk, I. A. Levandovskiy, *ACS Omega*, accepted for publication.

O-30

NIETYPOWA FAZA W KRYSZTALE TRIFENYLOSILANOLU JAKO WYNIK SZYBKIEGO CHŁODZENIA (FLASH COOLING)

Monika K. Krawczyk

Instytut Fizyki Doświadczalnej, Uniwersytet Wrocławski
Pl. M. Borna 9, 50-204 Wrocław

Odkryto nową, nietypową fazę (II) w krysztale trifenylosilanolu (Ph_3SiOH), która indukowana jest pod wpływem szybkiego chłodzenia z temperatury pokojowej do 100 K [1]. Na obrazach dyfrakcyjnych obserwowano liczne dodatkowe refleksy wskazujące na podwojenie objętości komórki elementarnej w stosunku do komórki fazy pierwotnej (I), której struktura jest znana. Struktura fazy II jest w pełni uporządkowana, w przeciwieństwie do struktury fazy I. Istotny jest fakt, że nowa faza II nie jest obserwowana, gdy kryształ Ph_3SiOH chłodzony jest powoli do temperatury 100 K, ale kryształ pozostaje w fazie pierwotnej (I) o mniejszej komórce elementarnej. Natomiast stopniowe ogrzewanie kryształu znajdującego się w fazie II powoduje powrót do fazy I w temperaturze około 150 K. Kryształ trifenylosilanolu jest stabilny i ulega wielokrotnym cyklom szybkiego chłodzenia/ogrzewania.

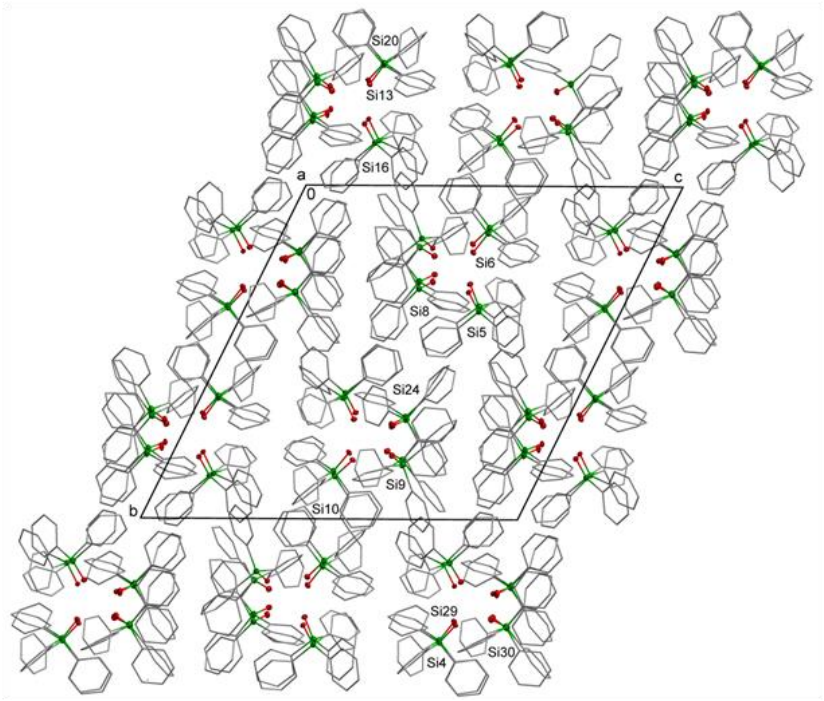

Rys. Upakowanie w krysztale Ph_3SiOH dla fazy II. Elipsoidy drgań atomów Si i O przedstawiono z 50% prawdopodobieństwem. Atomy H usunięto dla przejrzystości rysunku.

Literatura

[1] M. K. Krawczyk, *Acta Cryst. B.*,**79** (2023) 245.

O-31

SOLVING A PAST CONUNDRUM – A PEEK INTO A CLASS OF CARBOXYLIC GROUP-BASED MOLYBDATES

Marcin Oszajca, Anabel Berenice Gonzalez Guillen, Marlena Gryl, Wiesław Łasocha

Wydział Chemii Uniwersytetu Jagiellońskiego, ul. Gronostajowa 2, 30-387 Kraków

Polyoxomolybdates tend to systematically yield new and exciting structures due to the versatile bonding arrangements provided by the molybdate condensation. This process gives rise to a class of polyanions, consisting of multiple molybdenum centers surrounded by a typically octahedral arrangement of ligands, that combine in a variety of ways to form anionic entities differing in relative arrangement of molybdenum centers, dimensionality of the assemblies (clusters, fibers, layers) as well as counterions and/or accompanying molecules present in the structures (solvents or others)

The attractiveness of these compounds lays in the potential applications usually derived from their ability to act as redox catalysts[1] or from their propensity for photochromism[2]. Other reported applications are related with antiviral[3] and cancer treatments[4]. These materials commonly do not form crystals of sufficient size for single crystal-based diffraction experiments and thus their structures are often solved using powder diffraction based methods.

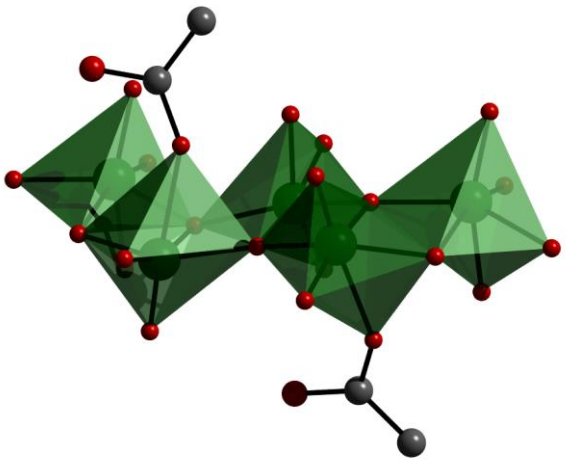

Fig. 1. Visualization of the crystal structure of the acetic acid-containing molybdate material.

The presentation will detail how solving the structure of an old material[5] (Fig. 1) that kept showing up in different, relatively unrelated syntheses led to a new approach to the synthesis of molybdate based materials with carboxylic-groups-containing-molecules present in the structures. The obtained structures will be discussed along with some properties that have been determined for the new materials.

O-31

Literature
[1] M. Oszajca, W. Nitek, A. Rafalska-Łasocha, K. Pamin, J. Połtowicz, W. Lasocha, *J. Mol Struct.* **1273** (2022) 134292. 10.1016/j.molstruc.2022.134292.
[2] F. Arnaud-Neu, M.J. Schwing-Weill, *J. Less-Common Met*., **36** (1974) 71-78.
[3] T. Ito, K. Sunada, T. Nagai, H. Ishiguro, R. Nakano, Y. Suzuki, A. Nakano, H. Yano, T. Isobe, S. Matsushita, A. Nakajima, *Acta Cryst. Z.*, **21** (2001) 201.
[4] A. Sławińska, M Tyszka-Czochara, P. Serda, M. Oszajca, M. Ruggiero-Mikołajczyk, K. Pamin, B. Napruszewska, E. Prochownik, W. Lasocha, *Mater.*, **15** (2022) 5976, 10.3390/ma15175976.
[5] W. Lasocha, *ICDD Grant-In-Aid* (2009).

O-32

DETERMINATION OF IRON DISTRIBUTION IN INHOMOGENEOUS $Ca_3CrFeGe_3O_{12}$ GARNET

Wojciech Paszkowicz[1], Hanna Dąbkowska[2], and Tomasz Rygier[1*]

[1]Institute of Physics, Polish Academy of Sciences, Warsaw, al. Lotników 32/46, Poland
[2]McMaster University, Brockhouse Institute for Materials Research, Hamilton, Canada
**present address: Warsaw University of Technology, Faculty of Materials Science and Engineering, Warsaw, Poland*

For some materials such as tooth enamel or solid electrolytes, a distribution of unit cell size is their inherent property. Diffraction peaks of more or less inhomogeneous solid solutions typically exhibit either broadened or irregular-shape. Such reflections are not satisfactorily modelled by classical shape functions; although modelling of a weakly asymmetric peak can be performed using a model built from two phases of the same structure and slightly differing lattice parameters (for an example see [1]), procedure of this kind does not provide detailed information on distribution of lattice parameters. Diffraction patterns of such inhomogeneous materials can be used for extracting information about the lattice parameter distribution. This information can serve for evaluation of the distribution of components of the given solid solution. The principles of approach allowing for the evaluation and effectiveness of this method have been demonstrated for diffraction data of $(1\text{-}x)\cdot CuMoO_4$(III) + $x\cdot CuWO_4$ solid solution, collected at a synchrotron beamline [2].

The aim of the present study is demonstration, that a modern laboratory instrument employing a linear detectors provides data of sufficiently good statistics for using the described approach, for an example when the extremely high resolution available at synchrotron beamlines is not critical. In this study, we present its application for the case of an inhomogeneous garnet solid solution. Namely, it is shown that it is possible to characterize the inhomogeneity of $Ca_3CrFeGe_3O_{12}$ crystal, using just the low-resolution laboratory data. The powder samples were prepared from single crystals grown by the flux method. The peak shape of the side samples, $Ca_3Cr_2Ge_3O_{12}$ and $Ca_3Fe_2Ge_3O_{12}$, was easily modelled by the pseudo-Voigt function. However, for the mixed crystal, the peak shape showed both, large broadening and shape irregularity. For calculations, this sample was considered as a mixture, of components of $Ca_3(Cr_{1-x}Fe_x)_2Ge_3O_{12}$ formula, each component having a different x value. The Rietveld refinement yielded a distribution of a large x extent. The average Fe content of the resulting mixture model nearly ideally corresponds to the expected $Ca_3CrFeGe_3O_{12}$ formula. The applied computational procedure can be useful in characterizing various polycrystalline materials showing a discernible distribution of lattice parameters.

References

[1] Scherb, T. et al. *J. Appl. Crystallogr.*, **49**(3) (2016) 997.
[2] Ehrenberg, H. et al., *J. Physics: Condens. Matt.*, **14**(36) (2002) 8573.

O-33

ANALYSIS OF TWINNING IN FCC NANOPARTICLES BY X-RAY DIFFRACTION: A MULTIDOMAIN XRD APPROACH

Ilia Smirnov[a], Zbigniew Kaszkur[a], Armin Hoell[b]

[a] Institute of Physical Chemistry, ul. Kasprzaka 44/52, 01-224 Warsaw, Poland
[b] Helmholtz-Zentrum Berlin für Materialien und Energie, Hahn-Meitner-Platz 1, 14109 Berlin, Germany

The appearance of twin/stacking faults in nanoparticles creates strains affecting the catalytic, optical, and electrical properties of nanomaterials. Currently, there is a lack of experimental tools for a numeric characterization of these defects in samples. Therefore, many structure–property correlations are poorly understood.

Recently [1] we report the exploration of the twinning effect on the XRD pattern and its practical application. We developed a new approach focused on the special mutual orientation of periodic fcc segments, domains. Using computational simulations, we found that the more domains, the smaller the height ratio of 220 to 111 diffraction peaks. This effect was indirectly predicted more than 50 years ago by Warren [2] and observed later [3]. However, it has not been systematically studied beyond one dimensional twinning and stacking of low probability.

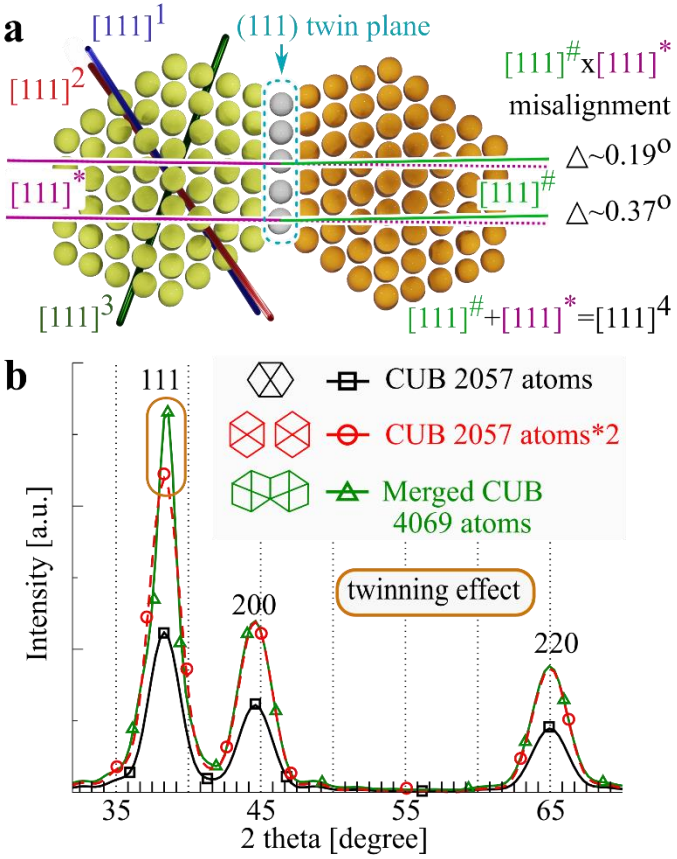

Fig. 1. (a) Two gold cuboctahedra (CUB) merged via the (111) plane, view along [−110]. (b) XRD diffraction patterns calculated for regular relaxed: gold CUB, gold CUB multiplied by 2 and two merged Au CUBs. The 111 height of the merged CUBs is 1.2 times greater than the doubled height of the regular CUB.

We analyzed the effect of multiple twinning on the quantitative features of the diffraction pattern and developed a special multidomain XRD (MDXRD) based method for the bulk morphology analysis. MDXRD allow one to estimate the average number of ideally periodic segments, domains (fcc segments without twin or stacking faults) inside an average cluster in a powder sample.

To verify the multidomain XRD method, we have meticulously analysed 11 samples (Au and AuPt nanoparticles). For each sample, we analysed the mean volume weighted size and the average number of domains. To assess the MDXRD accuracy, we compared its results with those obtained by reference methods: transmission electron microscopy (TEM) and small-angle X-ray scattering (SAXS). Nine of these 11 samples show the direct applicability of MDXRD: all three techniques were in good agreement. Meantime remaining two samples serve as examples of the limitations of the method.

So far, the main driving tool for structure – properties correlations in NPs studies is TEM (cryo/3D), which cannot be used as a routine tool. Therefore, this niche remains available only to a small number of scientific groups worldwide. Our approach is more versatile, operates on statistically meaningful amounts of NPs, and can be easily applied in numerous types of (catalytic, optical, electrical) studies and for different fcc samples, which will eventually interest a wide range of scientists. We believe that the multidomain XRD approach is an important step towards revealing the structure – properties correlations in NPs studies.

References

[1] I.Smirnov, Z.Kaszkur, A.Hoell, *Nanoscale*, **15** (2023) 8633-8642.
[2] B. E. Warren X-Ray Diffraction , Addison-Wesley, Reading, MA, 1969.
[3] A. Cervellino , C. Giannini , A. Guagliardi and D. Zanchet , *Eur. Phys. J.*, B**41** (2004) 485-493.

PLAKATY – SESJA A
POSTERS – SESSION A

A-1

INITIAL STRUCTURAL STUDIES OF DOMESTICATED AVIAN SERUM ALBUMINS

Kajetan Duszyński, Anna Bujacz, Grzegorz Bujacz

Institute of Molecular and Industrial Biotechnology, Faculty of Biotechnology and Food Sciences, Lodz University of Technology, Stefanowskiego 2/22, 90-537 Łódź

Albumins are water-soluble transport proteins found in the body fluids of all vertebrates. Among serum albumins, the structure of human serum albumin (HSA) has been known for over 20 years [1,2], and the structures of several mammalian albumins (MSA) have been determined in the last 10 years [3,4].

We have started structural investigation of albumins from lower evolutionary species and have determined crystal structures of first three domesticated avian serum albumins (ASA): chicken (ChSA) 2,56 Å in space group $C222_1$, turkey (TSA) 1,70 Å in C2 and 2,23 Å in $P2_1$, and duck (DSA) 1.77 Å in C2. We chose poultry serum albumins to obtain three-dimensional structures, which structural changes observation are important for the selective ligand binding by albumins. This information can be used to identify compounds, which should not be used in animal farming, as the animals can accumulate hormones, toxins, drugs and metabolites. Consumption of the meat of such animals can be dangerous to human health, causing diseases and allergies.

Serum albumins, in general, are difficult proteins to crystallize, and in the case of avian albumins, the use of *in situ* seeding crystallization has helped to obtain well diffracting crystals.

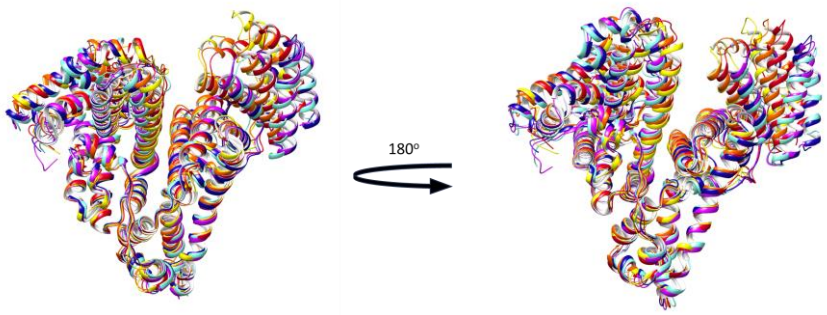

Fig. 1 Superposed crystal structures of 3 ASA and 3 representatives of MSA. The colors are as follows: DSA – light blue, TSA – deep blue, ChSA – purple, LSA (4F5V) – yellow, HSA (6M5D) – orange, ESA (4F5T) – red.

Avian serum albumins, like mammalian ones, also have a helical structure with a characteristic heart shape. However, a comparison of their structures shows significant diversity within the third and the first domains.

The presented research is a part of a grant application OPUS 25 submitted to NCN in 2023.

References

[1] Curry S. *Drug Metab Pharmacokinet.*, **24** (2009) 342–357.
[2] Ito S., Senoo A., Nagatoishi S., Ohue M., Yamamoto M. *J. Med. Chem.*, **63** (2020) 14045–14053.
[3] Bujacz, A. *Acta Crystallogr. Sect. D Struct. Biol.*, **68** (2012) 1278–1289.
[4] Bujacz A., Talaj J.A., Zielinski K., Pietrzyk-Brzezinska A.J., Neumann P. *Acta Crystallogr. Sect. D Struct. Biol.*, **73** (2017) 896–909.

A-2

STRUCTURAL AND FUNCTIONAL STUDIES OF EcAIII MUTANTS POSSESSING DIFFERENT SUBSTITUTIONS AT THE ENTRANCE TO THE ACTIVE SITE

Anna Ściuk, Krzysztof Lewiński[1], Mariusz Jaskólski[3,4], Joanna Loch[1]

[1] Faculty of Chemistry, Jagiellonian University, Krakow, Poland
[2] Jagiellonian University, Doctoral School of Exact and Natural Sciences, Krakow, Poland
[3] Institute of Bioorganic Chemistry, Polish Academy of Sciences, Poznan, Poland
[4] Faculty of Chemistry, A. Mickiewicz University, Poznan, Poland

L-asparaginases are enzymes that catalyze the decomposition of L-Asn into L-Asp and ammonia. L-asparaginases are used in the treatment of acute lymphoblastic leukemia. However, due to their severe side effects, new therapeutic L-asparaginases are highly needed. Class 2 L-asparaginases belong to the Ntn-hydrolase family and develop enzymatic activity in the autoproteolytic maturation process. Although their affinity for the substrate is relatively low, genetic engineering, in particular site-directed mutagenesis, could potentially improve it. Some studies of structure-function relationships in Class 2 L-asparaginases are available; however, many aspects of the maturation process or catalytic mechanism remain unresolved. Therefore, the main objective of our project was to explore the role of selected residues in the activity of Class 2 L-asparaginases.

To design new variants, sequence conservation near the catalytic threonine triad was analyzed using pangenomic analysis and methodology described previously [1]. Five of the most preferred substitutions at position 200 in the EcAIII sequence were identified. Next, a series of EcAIII new variants, i.e., M200I, M200L, M200K, M200T, and M200W were produced. For purified proteins, biochemical, biophysical, and structural studies were performed. The nanoDSF experiment showed reduced T_m for variants M200K and M200L. It was possible to crystallize most of the new variants, and the determined crystal structures revealed interesting rearrangements of the active site, especially in variant M200W. Crystallographic studies were supported by extensive bioinformatic analysis to discover the origins of structural changes and substrate affinity observed in EcAIII mutants.

Work supported by National Science Centre (NCN) grant 2020/38/E/NZ1/00035

References

[1] A. Zielezinski, J.I. Loch, W.M. Karlowski, M. Jaskolski, *Sci Rep* **12**, (2022) 15797.

A-3

MULTIDIMENSIONAL ANALYSIS OF MODULATED STRUCTURES OF MACROMOLECULES ON THE EXAMPLE OF HYP-1/ANS PROTEIN COMPLEX

Joanna Śmietańska[1,*], Joanna Śliwiak[2], Mariusz Jaskólski[2,3], Mirosław Gilski[2,3], Zbigniew Dauter[4], Radosław Strzałka[1], Janusz Wolny[1]

[1] Faculty of Physics and Applied Computer Science, AGH University of Science and Technology, Krakow, Poland
[2] Center for Biocrystallographic Research, Institute of Bioorganic Chemistry, Polish Academy of Sciences, Poznan, Poland
[3] Department of Crystallography, Faculty of Chemistry, A. Mickiewicz University, Poznan, Poland
[4] Synchrotron Radiation Research Section, MCL, National Cancer Institute, Argonne National Laboratory, Argonne, IL, USA

**e-mail: joanna.smietanska@fis.agh.edu.pl*

The phenomenon of structure modulation is relatively well understood in small-molecule crystallography, but its occurrence in macromolecular protein crystals has been surprising. Physical manifestations of this phenomenon include the observation of additional reflections between major Bragg peaks on diffraction images. This requires specialized methods of multidimensional analysis to correctly index diffraction images and describe the structure. Existing methods of solving and refining structures routinely used in protein crystallography are inadequate for comprehensive analysis of modulated structures. The lack of appropriate tools for the analysis of macromolecular modulated structures leads to serious problems in the proper indexing and processing of diffraction data, and then constructing a complete model of the structure with satisfactory divergence indices. So far, it has been possible to carry out a complete structural analysis only for a few modulated protein crystals. These include complexes of the Hyp-1 protein from St. John's wort (*Hypericum perforatum*) with the fluorescent ligand ANS (8-anilinonaphthalene-1-sulfonate) [1]. Depending on crystallization conditions, the Hyp-1/ANS protein complexes can form crystals with seven- (7Hyp/ANS) or nine-fold structure modulation (9Hyp/ANS) along the c direction of the *C*2 space group [2].

In present study, modulated structure of Hyp-1/ANS protein complex, designated 7Hyp/ANS, with seven-fold modulation along the **c**-axis and 28 independent protein molecules in an extended supercell [3] was analyzed. The current research includes detailed analysis of the diffraction data of modulated Hyp-1/ANS crystals, refinement and methodical description and refinement of the 7Hyp/ANS structure in multidimensional space. In the process of refinement of the 7Hyp/ANS structure, specialized software developed in the Matlab environment was used. Dropping the simplified assumption of modulation dimensionality and introducing additional corrections to account for the disorder in the structure made it possible to obtain new models and improve their divergence rates. The developed package was then extended with further modules that allowed visualization of the data and introduction of corrections related to thermal vibrations of the crystal lattice (phonons).

A-3

Literature

[1] J. Sliwiak, M. Jaskólski, Z. Dauter, A.J. McCoy, R.J. Read, Likelihood-based molecular-replacement solution for a highly pathological crystal with tetartohedral twinning and sevenfold translational noncrystallographic symmetry, *Acta Cryst. D*, **70** (2014) 471–480.

[2] J. Sliwiak, Z. Dauter, M. Jaskólski, Crystal Structure of Hyp-1, a *Hypericum perforatum* PR-10 Protein, in Complex with Melatonin, *Front Plant Sci.*, **7** (2016) 668.

[3] J. Sliwiak, Z. Dauter, M. Kowiel, A.J. McCoy, R.J. Read, M. Jaskólski, ANS complex of St John's wort PR-10 protein with 28 copies in the asymmetric unit: a fiendish combination of pseudosymmetry with tetartohedral twinning, *Acta Cryst.* ***D***, **71** (2015) 829–843.

A-4

INFLUENCE OF POSTTRANSCRIPTIONAL MODIFICATIONS ON RNA STRUCTURES: CRYSTALLOGRAPHIC AND THERMODYNAMIC ANALYSIS OF "NATIVE" MOLECULES

Antonina Gonet[1], Martyna Mateja-Pluta[2], Magdalena Bejger[2] and Agnieszka Kiliszek[2]

[1] Faculty of Biology, A.Mickiewicz University, Poznań, Poland
[2] Institute of Bioorganic Chemistry, Polish Academy of Sciences, Poznań, Poland

Years of extensive research on ribonucleic acid (RNA) have revealed the significance of its role in various cellular processes. RNA intermediates in protein synthesis (mRNA), act as an effector molecule in this process (tRNA, rRNA) and can directly affect gene expression (miRNA, lncRNA). The ubiquity of the RNA's functions comes from its structural richness derived from four nucleotides (A, C, G, U) and their canonical pairing. Furthermore, posttranscriptional modifications of nucleotides extended the possibilities of RNA folding, and thus the spectrum of structural variations. Comparing the three-dimensional models of modified sequences to their "native" counterparts can help to describe the impact of the modification on RNA structure and function. Hence, conducting more crystallographic studies on RNA molecules is crucial, particularly considering their limited number.

Our study is focused on natural uridine modification and its role in RNA folding using crystallographic analysis. Here, we present two crystal structures of unmodified RNA. Both oligomers, named *RNA1* and *RNA2*, were chemically synthesized and purified. They are semi-complementary hexamers forming duplexes. The *RNA1* crystallizes in $P6_3$ space group while *RNA2* in R32. The resolution of collected data was 1.39 Å and 1.34 Å, respectively. In the structure of *RNA2* three Sr^{2+} ions were identified. One was bound in the major groove of the RNA helix while two others were involved in interactions between symmetry-related molecules. The impact of Sr^{2+} ions on the thermal stability of RNA was further evaluated using Differential Scanning Calorimetry (DSC). Moreover, the UV-melting analysis was employed to calculate thermodynamic parameters of both RNA duplexes.

In the future, the crystallographic models of *RNA1* and *RNA2* will be compared with RNA structures containing pseudouridine and methylpseudouridine in order to identify structural changes associated with the presence of modification.

A-5

STUDY ON CRYSTAL STRUCTURES OF B- AND T-LYMPHOCYTE ATTENUATOR WITH MONOCLONAL ANTIBODIES – STRUCTURE-ACTIVITY RELATIONSHIP ANALYSIS AND MOLECULAR DYNAMICS

Marta Karpiel[1,2], Justyna Kalinowska-Tłuścik[1]

[1] Jagiellonian University, Faculty of Chemistry, 2 Gronostajowa Str., 30-387 Krakow, Poland
[2] Jagiellonian University, Doctoral School of Exact and Natural Sciences, 11 Lojasiewicza Str., 30-348 Krakow, Poland

B- and T-lymphocyte attenuator (BTLA) is a transmembrane protein, a member of the immunoglobulin-like superfamily. With its ligand, the herpes virus entry mediator (HVEM), a member of the tumor necrosis factor receptor (TNFR) superfamily, it belongs to the immune checkpoint regulatory system. BTLA is expressed on the T-cells surface, while HVEM is exposed on healthy and tumor cells. Those two proteins' mutual recognition play a crucial role in cancer development. The formation of the protein-protein complex inhibits T-cell activity against cancer cells, allowing their escape from the immune system surveillance. Thus, the development of immune checkpoint blockade therapies is essential to enhance organisms' antitumor responses [1]. To date, only monoclonal antibodies or HVEM-originated peptide inhibitors are reported. A deep understanding of the intermolecular interactions of the BTLA binding regions may initiate the search for plausible small-molecular inhibitors of the BTLA-HVEM immune checkpoint.

Apart from the BTLA-HVEM crystal structure published in 2005 (PDB ID 2AW2 [2]), three new crystal structures of BTLA complexes with monoclonal antibodies 22B3 (PDB ID 8F6O), 25F7 (PDB ID 8F6L) and 23C8 (PDB ID 8F60) [3], determined at 2.31Å, 1.85 Å, and 1.64 Å resolution, respectively, were deposited within Protein Data Bank (PDB) [4]. In the presented study, those structures were analyzed and *ab initio* molecular dynamics (MD) simulations were performed using the GROMACS (GROningen MAchine for Chemical Simulation) software [5] and the CHARMM36 force field [6]. Data obtained from MD simulations suggests the protein-protein complexes' stability in a water environment. Additionally, the BTLA conformational changes in all studied complexes were compared and analyzed.

Each antibody binds to different BTLA regions. Electron density maps investigation show that coordinates of atoms in residues engaged in the protein-protein complexes formation were determined with sufficient precision. The differences in binding modes were carefully studied to provide useful information about the key BTLA residues and regions which can serve as starting point to design small-molecular inhibitors of the BTHL-HVEM immune checkpoint.

A-5

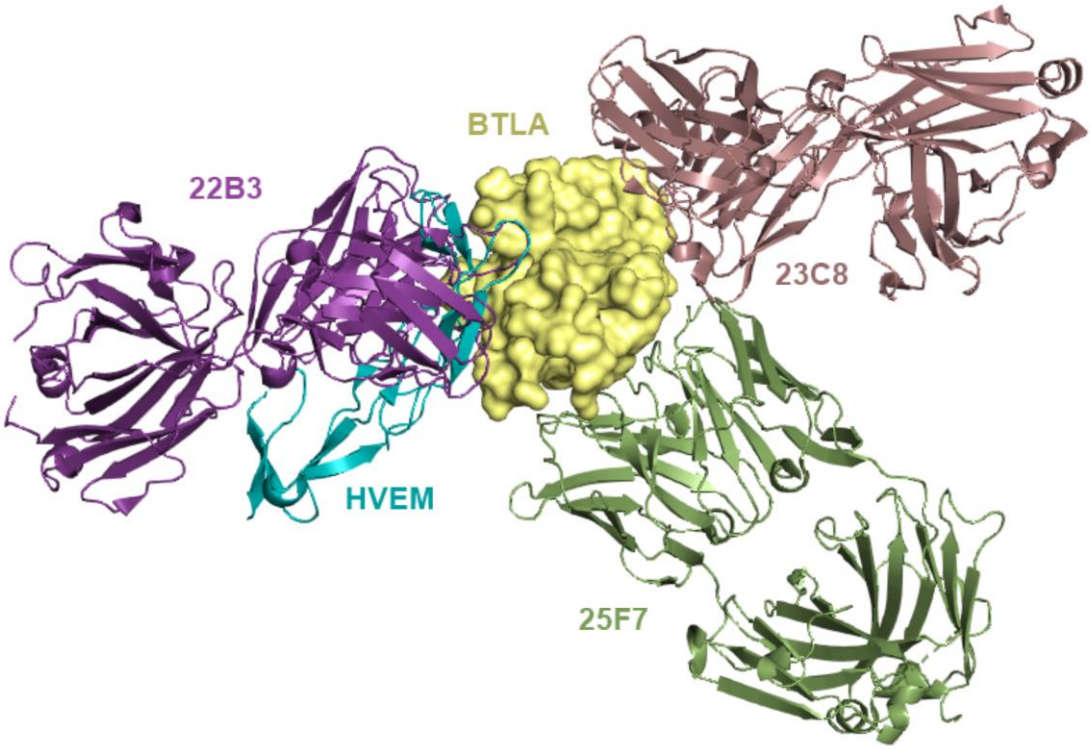

Fig. 1. The crystal structure alignment of the BTLA (yellow surface representation) complexes with HVEM (blue cartoon representation) and monoclonal antibodies (22B3 purple; 25F7 green; 23C8 brown) (PDB IDs 2AW2, 8F6O, 8F6L and 8F60, respectively).

References

[1] M. Spodzieja *et al.*, *Int. J. Mol. Sci.*, **21** (2020) 636.
[2] D.M. Compaan, L.C. Gonzalez, I. Tom *et al.*, *J Biol Chem*., **280** (2005) 39553–39561.
[3] T.C. Cheung, S. Atwell, L. Bafetti *et al*. *Structure*, **25** (2023) S0969–2126(23)00166-1.
[4] H.M. Berman, J. Westbrook, Z. Feng *et al.*, *Nucleic acids research*, **28** (2000) 235–242.
[5] D. Van Der Spoel *et al.*, *J. Comput. Chem.*, **26** (2005) 1701–1718.
[6] J. Huang, A.D. MacKerell, *J. Comput. Chem.*, **25** (2013) 2135-2145.

A-6

STRUCTURAL CONSEQUENCES OF CHANGES IN THE ACTIVE SITE OF *ESCHERICHIA COLI* TYPE III L-ASPARAGINASE

Marta Kilichowska[1], Krzysztof Lewiński[1], Mariusz Jaskólski[2,3] and Joanna Loch[1]

[1] Faculty of Chemistry, Jagiellonian University in Krakow, Gronostajowa 2, 30-387 Krakow, Poland,
[2] Faculty of Chemistry, A. Mickiewicz University, Uniwersytetu Poznanskiego 8, 61-614 Poznan, Poland
[3] Institute of Bioorganic Chemistry, Polish Academy of Sciences, Zygmunta Noskowskiego 12/14, 61-704 Poznan, Poland

L-asparaginases are enzymes catalyzing the hydrolysis of L-asparagine to L-aspartate and ammonia. In 20th century these biocatalysts found their application in the therapy of Acute Lymphoblastic Leukemia (ALL) [1]. Currently, there are only two of these proteins available as drugs, both belonging to type II L-asparaginases. The advantage of type II enzymes is their very high substrate affinity (K_M in μM range). Such a high affinity to L-asparagine is required for the therapeutic effect of the enzymes [2]. However, administration of type II L-asparaginases often brings about severe adverse reactions, connected with their side L-glutaminase activity or an allergic response [2].

Type III L-asparaginases (so-called plant-type, but present in all domains of life) comprise a different family of proteins. On the contrary to type II, instead of L-glutaminase co-activity, they exhibit β-aspartylpeptidase co-activity, which is assumed to be their primary role in nature [3]. The exact catalytic mechanism of type III L-asparaginases hasn't been determined to date. Lack of L-glutaminase activity, as well as structure different than type II, are interesting properties in terms of searching for novel therapeutic enzymes. Type III enzymes, however, exhibit lower substrate affinity (K_M in mM range), which renders their medical application impossible in their wild-type (WT) form.

In this study modifications were introduced to the active site of *Escherichia coli* L-asparaginase of type III (EcAIII). Three mutants were constructed, each with a serine substitution of a different catalytic threonine (T179S, T197S, T230S). Each of the modified proteins, together with the WT form, were subject to co-crystallization experiments. Of the examined proteins, two mutants (T179S and T230S) and WT enzyme yielded crystals of quality sufficient for X-ray data collection (Fig. 1).

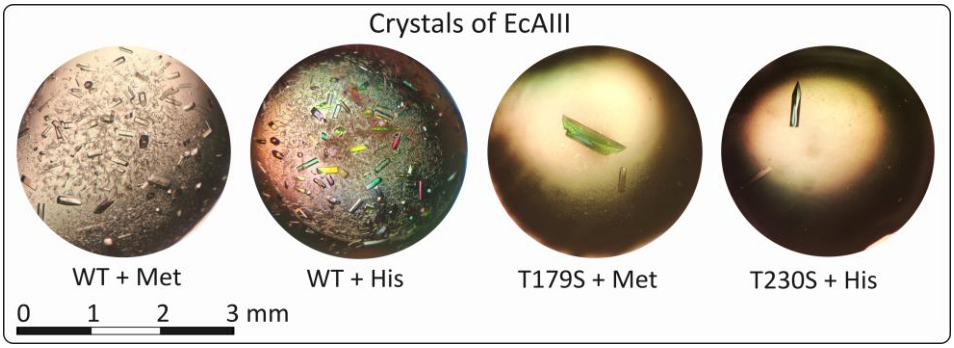

Fig. 1. Crystals of EcAIII.

A-6

Four crystal structures were determined: T179S (1.60 Å), T230S (2.14 Å) and WT (1.94 Å and 2.23 Å). X-ray data collection on WT EcAIII was performed using crystals obtained by co-crystallization with putative inhibitors: histidine and methionine. In both cases interesting conformational changes of R207 (Fig. 2) or E234 were observed. Despite structural changes, no electron density suggesting the presence of an inhibitor in the active site was detected. The structure of EcAIII mutant T179S revealed interesting changes resulting from the modification of the N-terminal nucleophile. Determined structure confirms that mutation T179S prevents efficient autoproteolytic maturation of the enzyme and reveals unusual position of the linker region in the catalytically inactive precursor. In the structure of variant T230S modification of residue 230 was confirmed with no significant structural changes. Such results suggest that the increased K_M of the protein [4] in comparison to the WT form is the consequence of the serine substitution itself.

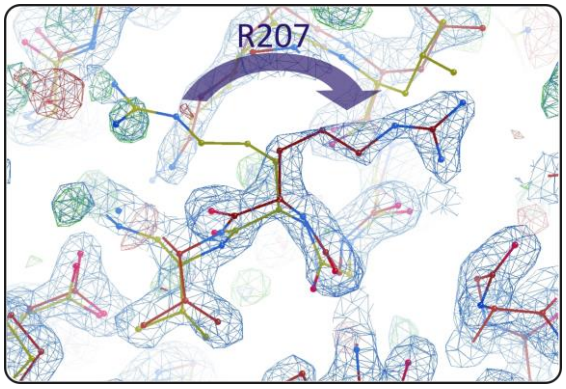

Fig. 2. Crystal structure of WT EcAIII with flipped R207 (red) in superposition with reference structure (PDB ID: 2zal; yellow). Electron density maps were contoured at 1.50σ (2FoFc) and 3.00σ (FoFc).

References

[1] L. Maese, R. E. Rau, *Front Pediatr.*, **10** (2022).
[2] M. H. G. Fonseca, T. da Silva Fiúza, S. T. B. *et al.*, *Biomed. Pharmactorer. Z.*, **139** (2021) 111616.
[3] K. Michalska, M. Jaskólski, *Acta Biochim. Polon.* **53** (2006) 627.
[4] M. Kilichowska, unpublished results.

A-7

ODDZIAŁYWANIA MIĘDZYCZĄSTECZKOWE I ICH WPŁYW NA WŁAŚCIWOŚCI FLUORESCENCYJNE POCHODNYCH 3,6-DIAZA-9-BORAFLUORENU

Jan Adamek, Sergiusz Luliński, Krzysztof Durka, Paulina Marek-Urban

[a] *Wydział Chemiczny, Politechnika Warszawska, ul. Noakowskiego 3, 00-664 Warszawa*
[b] *Wydział Chemii, Uniwersytet Warszawski, ul. Pasteura 1, 02-093 Warszawa*

Obecnie dynamiczny rozwój przeżywa rynek wyświetlaczy opartych na technologii OLED. Kluczowym elementem diody elektroluminescencyjnej jest warstwa, która emituje światło pod wpływem przyłożonego napięcia. Jedną z klas związków mogących służyć jako składniki takich warstw są kompleksy boroorganiczne, składające się z dwóch aromatycznych układów z atomem boru w charakterze łącznika [1]. Tego typu układy poza zastosowaniem w roli materiałów elektroluminescencyjnych i transportujących elektrony w diodach OLED mogą służyć również jako fotokatalizatory, sensory oraz materiały światłoczułe.

W ramach prezentowanych badań zsyntezowano szereg chelatowych kompleksów boroorganicznych zawierających nowy, wysoce elektronoakcpetorowy rdzeń 3,6-diaza-9-borafluorenowy. Związki te wykazują fluorescencję w zakresie światła od fioletowoniebieskiego do zielonego, z wydajnościami kwantowymi dochodzącymi do wartości 73%. Tego typu układy mogą wykazywać właściwości fotouczulające związane ze zjawiskiem przejścia międzysystemowego [2]. Przeprowadzone badania aktywności fotokatalitycznej generowania tlenu singletowego potwierdzają tę hipotezę.

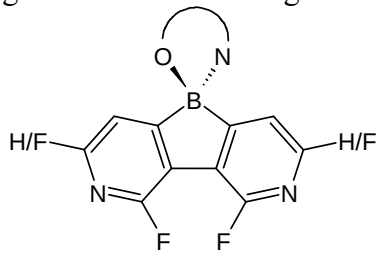

Rys. 1. Wzór ogólny prezentowanych kompleksów.

Struktury molekularne siedmiu kompleksów zostały określone metodą rentgenostrukturalną. We wszystkich związkach atom boru jest 4−koordynacyjny i charakteryzuje się geometrią typu spiro, przy czym płaszczyzny rdzenia boracyklicznego i ligandu są zorientowane względem siebie w przybliżeniu prostopadle. Taka geometria przeciwdziała typowemu dla aromatycznych związków luminescencyjnych wygaszaniu fluorescencji wywołanemu przez agregację (ACQ), co znajduje potwierdzenie w analizie oddziaływań międzycząsteczkowych prezentowanych układów. Ponadto dwa otrzymane związki charakteryzują się dodatkowymi maksimami emisji w ciele stałym, co można powiązać z oddziaływaniami noszącymi znamiona J–agregacji w ich strukturze.

Literatura

[1] Y. Rao, S. Wang, *Inorg. Chem.*, **50** (2011) 12263–12274.
[2] K. Durka et al., *J. Org. Chem.*, **86** (2021) 12714–12722.

A-8

CONTROL OF CRYSTAL STRUCTURES THROUGH PH-DEPENDENT CRYSTALLIZATION OF 4-SULFANTOCALIX[6]ARENE

Julia Alberska, Ewelina Zaorska and Maura Malińska

Wydział Chemii, Uniwersytet Warszawski, ul. Pasteura 1, 02-093 Warszawa

The macrocyclic cavity and hydrophobic interior of supramolecular structures such as calixarenes proclaim reversible binding of different organic molecules. 4-sulfanatocalix[6]arene (SOX6) are water-soluble macrocycles that have application in metal ions binding, crystallization aid for proteins, sensing and extraction.

It has been observed that the choice of pH buffer affects the crystallization outcome, leading to the formation of either SOX6 hydrates or alkali metal salts. The resulting crystal structures exhibit different charge states for the SOX6 ions, ranging from -2 to -8. In all of these crystal structures, the SOX6 macrocycles adopt a specific conformation that resembles a double partial cone. This conformation is achieved by the inversion center in the crystal structure, where the anion is located. The cone structure is formed by three adjacent SO3 groups pointing "up" and three pointing "down." This arrangement is stabilized by intramolecular hydrogen bonding interactions within the macrocycle.

The crystals of SOX6 exhibit a layered structure, meaning that the SOX6 ions are organized in alternating layers with solvent molecules. The specific solvent molecules present in these layers can vary depending on the conditions of crystallization. Overall, the pH-dependent crystallization of 4-sulfantocalix[6]arene offers a versatile approach to control the formation of different crystal structures

A-9

NEW ADDUCTS OF VITAMIN B6 WITH ALIPHATIC DICARBOXYLIC ACIDS

Mateusz Gołdyn[a], Weronika Nowak[a], Elżbieta Bartoszak-Adamska*[a], Anna Komasa[a], Karolina Babijczuk[a], Weronika Pielach[a], Zofia Dega-Szafran[a], Daria Larowska-Zarych[a,b]

[a] *Faculty of Chemistry, Adam Mickiewicz University, Uniwersytetu Poznańskiego 8, 61-614 Poznań*

[b] *Faculty of Chemistry, University of Warsaw, Żwirki i Wigury 101, 02-089 Warsaw*

**e-mail: ela@amu.edu.pl*

Pyridoxine (3-hydroxy-4,5-bis(hydroxymethyl)-2-methylpyridine) is one of the forms of vitamin B6. Vitamin B6 affects the proper functioning of the nervous system, supports the immune system, heart rate, blood pressure, muscle contractions. It also participates in the metabolism of amino acids and the formation of red blood cells.[1] Three hydroxyl groups that are proton donors and one basic nitrogen atom that is a proton acceptor make pyridoxine an extremely active base for the formation of adducts with acidic molecules. The pK_a values of phenolic hydroxyl and pyridine nitrogen are 5.00 and 8.96, respectively.[2]

Dicarboxylic acids are often used in research of new pharmaceutical salts or cocrystals.[3-6] Oxalic acid, is one of the strongest carboxylic acids. This is due to the mutual inductive effect of the two carboxyl groups.[7]

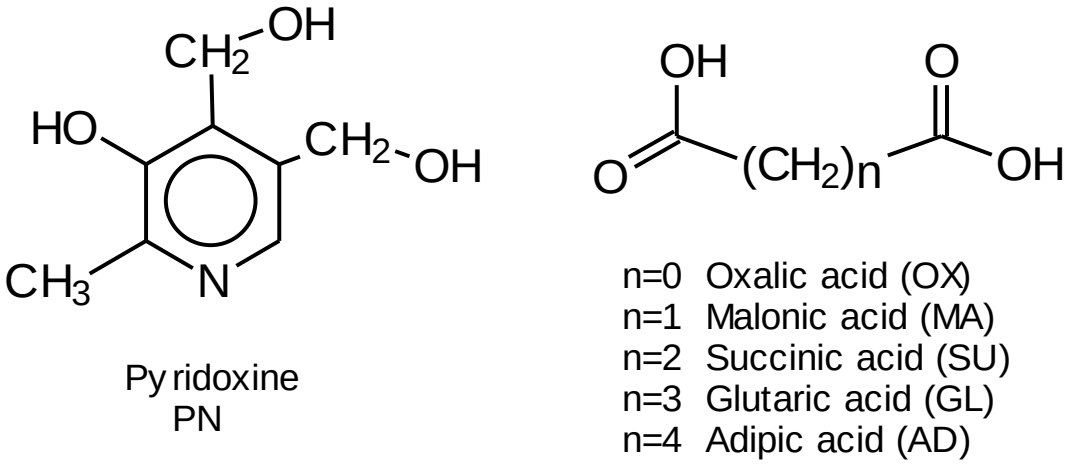

Fig. 1. Structures and acronyms of the investigated compounds

New pyridoxine adducts with five aliphatic dicarboxylic acids: oxalic, OX, malonic, MA, succinic, SU, glutaric GL, and adipic (AD) were synthesized and structurally characterized (Fig.1).

The stoichiometry of the first three adducts: PN-OX, PN-MA and PN-SU is 1:1. In their crystal structure, pyridoxinium moiety is linked to the monoanion of the dicarboxylic acid, through the N–H···OOC hydrogen bonds. The donor···acceptor

distance vary from 2.706(1) to 2.785(1) Å. In contrast, pyridoxine and adipic acid form salt in a 2:1 stoichiometric ratio. In this salt, two pyridoxinium cations are connected with C_i-symmetric adipate dianion via short N–H···OOC H-bonds of 2.632(2) Å. A more complex adduct (2:1:1) was obtained in a case of cocrystallization of vitamin B6 with glutaric acid. In the crystal network of bis(pyridoxinium) glutarate glutaric acid, two pyridoxinium cations interact with symmetric glutarate dianion through the N-H···O hydrogen bonds of 2.703(2) Å. Additionally, glutaric acid molecule is linked to the carboxylate group of glutarate anion by short O-HO hydrogen bond of 2.507(2) Å.

In the structure optimized at the APF-D/6-311++G(d,p) level of theory, when the PCM model for solvated molecule by water was applied, the proton transfer from acid to pyridoxine was predicted for the complexes with oxalic, malonic and glutaric acids. The N–H···OOC and COOH···N interactions in the 2:1:1 adduct with glutaric acid was confirmed by the molecular electrostatic surface map (MEP).

Based on the TGA and DSC measurements, it was found that the thermal decomposition runs continuously and there is no dependence on the chain length of the acid used.

Acknowledgements

MG thanks the National Science Centre (grant PRELUDIUM no. 2021/41/N/ST5/00503) for financial support. WN thanks Adam Mickiewicz University for funds from the Initiative of Excellence – Research University (IDUB) program obtained in the PhD Minigrants competition (research grant no. 054/13/SNŚ/0016). The computations supported in part by PL-Grid Infrastructure were performed at the Poznań Supercomputing and Networking Center.

References

[1] S. Mooney, J.-E. Leuendorf, C. Hendrickson and H. Hellmann, *Molecules*, 2009, **14** (2009) 329–351.
[2] V. R. Williams and J. B. Neilands, *Arch. Biochem. Biophys.*, **53** (1954) 56–70.
[3] L. Wang, S. Liu, J.-M. Chen, Y.-X. Wang and C. C. Sun, *Mol. Pharm.*, **18** (2021) 1758–1767.
[4] P. Sanphui, S. Tothadi, S. Ganguly and G. R. Desiraju, *Mol. Pharm.*, **10** (2013) 4687–4697.
[5] A. N. Manin, A. P. Voronin, K. V. Drozd, A. V. Churakov and G. L. Perlovich, *Acta Cryst.. Sect. C Struct. Chem.*, **74** (2018) 797–806.
[6] A. Hamideh, Z. Rahman, S. Dharani, T. Khuroo, E. M. Mohamed, M. T. H. Nutan, I. K. Reddy and M. A. Khan, *Pharm. Dev. Technol.*, **26** (2021) 455–463.
[7] D. Enkelmann, G. Lipinski and K. Merz, *Eur. J. Inorg. Chem.*, **2021** (2021) 3367–3372.

A-10

CRYSTAL STRUCTURES OF OXYTETRACYCLINE HYDROCHLORIDE: POLYMORPHS OR SOLVATES?

Teresa Bizoń, Helena Butkiewicz, Anna Hoser, Maura Malińska

[1] *Faculty of Chemistry, University of Warsaw,*
Pastera 1, 02-093 Warsaw, Poland

In recent years, there has been a growing interest in the polymorphism of drugs within the pharmaceu- tical industry. In particular, polymorphism has a significant impact on the solubility and stability of active pharmaceutical ingredients (API). Consequently, different forms can affect drug efficacy, bioavailability and safety [1]. Moreover, the issue of antimicrobial resistance remains of the utmost importance, emphasizing the need to expand our knowledge in the field of antibiotics.

Oxytetracycline hydrochloride (OxyCl) is a commonly prescribed antibiotic from the tetracyclines fami- ly which is know for its bacteriostatic properties against a wide range of bacteria, particularly for cutaneous and minor infections [2]. However, limited information is available regarding the polymorphic forms of OxyCl. Previous research by Bueno et al. (2020) [2] identified four different forms, including three stable solid forms and one metastable form, without determining their precise crystal structures. Since 1965, only one form of OxyCl has been known, crystallizing in $P2_12_12_1$ space group [3].

Our aim is to address the knowledge gap regarding OxyCl polymorphs structures by crystallizing various forms of OxyCl and oxytetracycline dihydrate as monocrystals. The crystallization process involved examination of different solvents. Resulting single crystals were subjected to SCXRD (single-crystal X-ray diffraction) analyses, which revealed that polymorphic structures of form III and IV are not true polymorphs but methanol and ethanol solvates, which crystallize in the $P6_1$ space group.

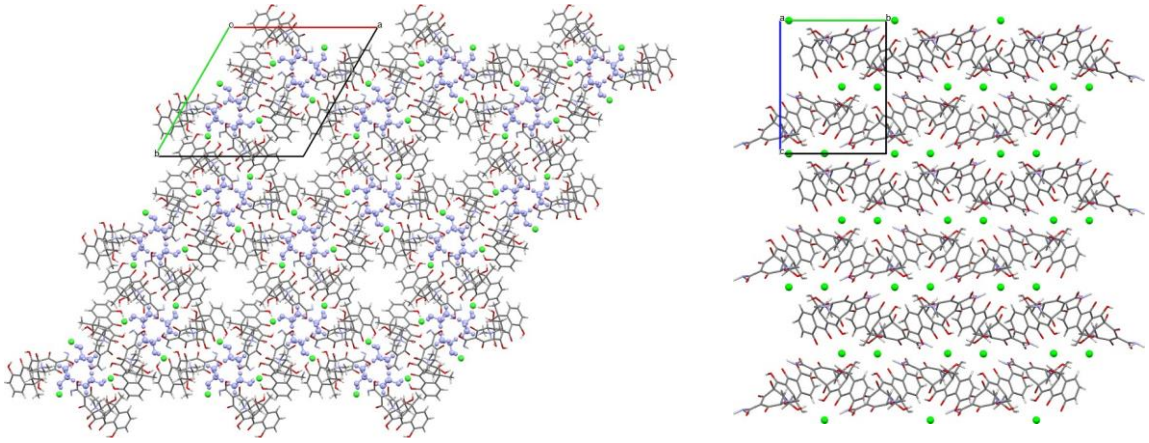

(a) (b)

Fig. 1. Crystal structures of (a) OxyCl ethanol solvate viewed along crystallographic *c* axis and (b) OxyCl obtained in 1965 viewed along crystallographic *a* axis. [3]. Green balls and purple molecules represent chloride anions and ethanol respectively.

A-10

Financial support from Polish National Science Centre (SONATA17 grant 2021/43/D/ST4/03136) is kindly acknowledged.

Literature

[1] A. Llinàs, J. M. Goodman, Polymorph control: past, present and future, *Drug Discovery Today*, **13**(5–6) (2008) 198–210.
[2] M. S. Bueno *et al*. Exploring solid forms of oxytetracycline hydrochloride, *International Journal of Pharmaceutics*, **585** (2020) 119496.
[3] H. Cid-Dresdner, The crystal structure of terramycin hydrochloride, $C_{22}H_{24}N_2O_9$ HCl, *Zeitschrift für Kristallographie*, **121**(2–4) (1965) 170–189.

A-11

MAGNETIC AND DIELECTRIC PROPERTIES DETERMINED BY CRYSTAL AND MICROSTRUCTURE OF DOPED $SrFe_{12}O_{19}$ HEXAFERRITE NANOCERAMICS

Andrzej Hilczer[1], Ewa Markiewicz[1+] and Adam Pietraszko[2]

[1] Institute of Molecular Physics, PAS, Poznań, Poland
[2] Institute of Low Temperature and Structure Research, PAS, Wrocław, Poland

M-hexaferrites ($A^{2+}Fe_{12}O_{19}$) exhibit unusual crystal structure consisting of antiferromagnetic unit cell containing two electric dipoles, switchable along the hexagonal *c* axis only. Foreign ion doping of the M-hexaferrites was found to be selective: rare earth ions substitute A^{2+} ions, whereas nonmagnetic $^{3+}$ ions substitute Fe^{3+} ions responsible for magnetic properties. M-hexaferrites which can be prepared by ceramic technology are highly interesting for applications. Heterogeneity of ferrite ceramics: highly conducting grain interiors and poorly conducting grain boundaries.

We aimed at study of a modification of collinear magnetic mode in a $SrFe_{12}O_{19}$ with nonmagnetic $^{3+}$ ions. To study the effect of deformation oxygen octahedra we substituted the Fe^{3+} ions with Sc^{3+} (ionic radius $r_{Sc} > r_{Fe}$) and Al^{3+} ions ($r_{Al} < r_{Fe}$). The size effect in magnetic and dielectric behavior we studied for nanoceramics prepared $Sr_{0.95}Nd_{0.05}Fe_{12-x}Sc_xO_{19}$ using citric sol-gel method [1] and $Sr_{0.95}Nd_{0.05}Fe_{12-x}Al_xO_{19}$ made by hydrothermal synthesis [2]. Single phase systems of $P6_3/mmc$ (controlled by XRD X'Pert PANanalytical and Rietveld method) were obtained for Sc^{3+} with *x* from 0 to 1.56 and Al^{3+} for *x* from 0 to 1.08. SEM studies of the microstructure (FEI Nova NanoSEM, 5 keV) showed that Sc doped SrM consisted of agglomerates nanocrystallites ~ 50 – 100 nm thick, whereas Al doped SrM contain agglomerated nanocrystallites ~ 10 – 20 nm thick [3].

Magnetic properties were studied with Physical Property Measurement System (Quantum Design PPMS) and Alpha-A High Performance Frequency Analyzer (Novocontrol GmbH) and E4991A RF Impedance/Material Analyzer, Agilent were used for dielectric measurements.

Literature

[1] A. Hilczer, K. Pasińska, *JALCOM*, **852** (2021) 156969.
[2] A. Hilczer, K. Pasińska, E. Markiewicz, A. Pietraszko, B. Andrzejewski, Ferroelectrics, **534** (2018) 129.
[3] A. Hilczer, Monografia, IFMPAN (2021).

A-12

HIGH-PRESSURE SINGLE-CRYSTAL X-RAY DIFFRACTION STUDIES OF MODEL RH COMPOUNDS EXHIBITING METALLOPHILIC INTERACTIONS IN THE SOLID STATE

Patryk Borowski[1], Damian Paliwoda[2], Carla Pretorius[3], Alice Brink[3], Andreas Roodt[3], Radosław Kamiński[1], Katarzyna N. Jarzembska[1]

[1] *Department of Chemistry, University of Warsaw, Żwirki i Wigury 101, 02-089 Warsaw, Poland*
[2] *European Spallation Source, Partikelgatan 2, 224 84 Lund, Sweden*
[3] *University of the Free State, Nelson Mandela Drive, 9300 Bloemfontein, South Africa*

High pressure X-ray crystallography constitutes an important tool to study behavior of various materials at extreme conditions (*e.g.* pressure-induced phase transitions), as well as to monitor structure-property relationships in crystals. In the current study a series of high pressure single crystal XRD experiments were conducted for two well-defined rhodium(I) complexes (Figure 1). The primary aim of the study was to thoroughly investigate high-pressure impact on metallophilic Rh···Rh interactions propagating in the examined crystal structures and further the effect of the observed structural changes on spectroscopic properties of the rhodium(I) organometallic compounds. Therefore, molecular structures under various pressure values, charge distribution, metal---metal interactions, and spectroscopic features were analysed both experimentally and computationally. For instance, in the case of **Rh-dbm** (Fig.1a) two types of Rh···Rh contacts can be distinguished. The shorter distance is equal to 3.5517(5) Å, whereas the longer one to 3.6279(5) Å at ambient conditions. Both distances shorten along with the elevated pressure converging to about 2.9 at 10 GPa.

(a) (b)

Fig. 1. Schematic representation of the studied Rh(I) complexes, (a) **Rh-dbm** and (b) **Rh-CNacac**.

ACKNOWLEDGEMENT
The authors thank the SONATA BIS grant (No. 2020/38/E/ST4/00400) of the National Science Centre in Poland. University of Warsaw, for financial support. The Wrocław Centre for Networking and Supercomputing (grant No. 285) is gratefully acknowledged for providing computational facilities. The in-house X-ray diffraction experiments were carried out at the Department of Physics, University of Warsaw, on a Rigaku Oxford Diffraction SuperNova diffractometer, which was co-financed by the European Union within the European Regional Development Fund (POIG.02.01.00-14.122/09)

A-13

SYNTHESIS AND CRYSTAL STRUCTURES OF TWO POLYMORPHIC FORMS OF 4-METHYL-2-PHENYL-5*H*-PYRIDO[1,2-*a*]PYRIMIDO[4,5-*d*]PYRIMIDIN-5-ONE

Iwona Bryndal[1], Anna Pyra[2], Marcin Mączyński[1]

[1] *Department of Organic Chemistry and Pharmaceutical Technology, Faculty of Pharmacy, Wroclaw Medical University, 211A Borowska, 50-556 Wrocław*
[2] *Faculty of Chemistry, University of Wroclaw, 14 Joliot-Curie, 50-383 Wrocław*

Pyrimidopyrimidine systems are of great interest due to their diverse biological activity. Here, we report the synthesis details and structural characterization of newly obtained pyrido[1,2-*a*]pyrimido[4,5-*d*]pyrimidin-5-one derivative.

In the pyridonopyrimidine derivative synthesis reaction, ethyl 4-methyl-2-phenyl-6-sulfanylidene-1,6-dihydropyrimidine-5-carboxylate was treated with 2-amino-pyridine and heated at 130 °C for about 3 hours. The final reaction product was obtained by purification by extraction from chloroform and then crystallization from acetone. This compound was analyzed by MS, NMR and IR. This allowed to conclude that under the conditions of synthesis, ethyl 4-methyl-2-phenyl-6-[(pyridin-4-yl)amino]pyrimidine-5-carboxylate undergoes intramolecular cyclization, resulting in the formation of 2-phenyl-4-methyl-5*H*-pyrido-[1,2-*a*]pyrimido[4,5-*d*]pyrimidin-5-one. The structure was confirmed by single-crystal X-ray diffraction method. After recrystallization from ethanol, two types of light yellow crystals, needles and plates were obtained, in a percentage ratio of about 70:30, which turned out to be two polymorphic forms of 2-phenyl-4-methyl-5*H*-pyrido-[1,2-*a*]pyrimido[4,5-*d*]pyrimidine-5-one.

Polymorph **I** (needle) crystallizes in the orthorhombic system in the space group $P2_12_12_1$ with one molecule in the asymmetric part of the unit cell (Fig. 1). In the structure of this polymorph, molecules are connected to others mainly by weak C−H···N interactions.

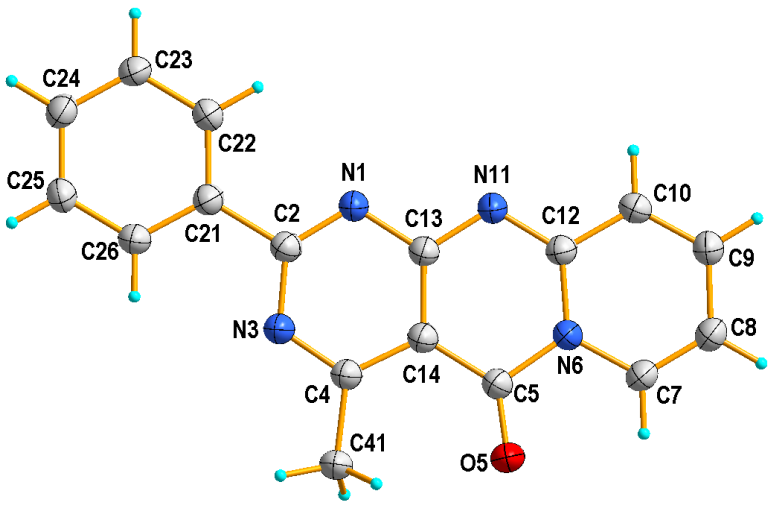

Fig. 1. View of the asymmetric unit of the polymorphic form **I**, showing the atom-numbering scheme and displacement ellipsoids drawn at the 50% probability level.

A-13

Polymorph **II** (plate) crystallizes in the monoclinic system in space group $P2_1/c$ and contains two independent molecules (A and B) in the asymmetric part of the unit cell. Molecules A and B differ from each other in geometrical parameters as well as in conformation. The C−H···O intermolecular interactions link molecules A into a zig-zag chain, which is also formed by molecules B.

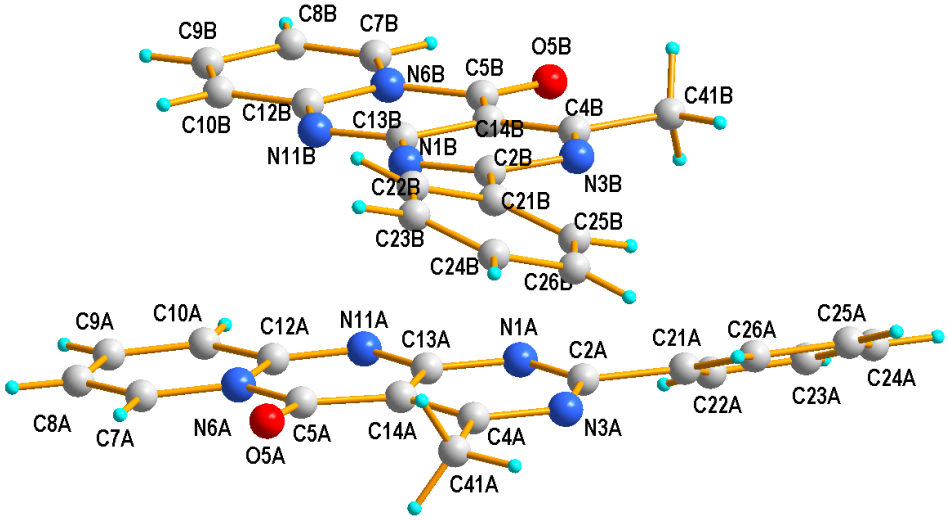

Fig. 2. View of the asymmetric unit of the polymorphic form **II**, showing the atom-numbering scheme and displacement ellipsoids drawn at the 50% probability level.

A-14

SYNTEZA I BADANIA POLIAMIDOWYCH RECEPTORÓW MAKROCYKLICZNYCH JAKO MATRYC STABILIZUJĄCYCH KLASTRY WODY W CIELE STAŁYM

Magdalena Ceborska[1], Kajetan Dąbrowa[2]

[1] Instytut Nauk Chemicznych, Wydział Matematyczno-Przyrodniczy UKSW, ul. Wóycickiego 1/3, 01-938 Warszawa
[2] Instytut Chemii Organicznej PAN, ul. Kasprzaka 44/52, 01-224 Warszawa

Niedomknięte kryptandy należą do klasy receptorów makrocyklicznych, strukturalnie spokrewnionych z dobrze znanymi kryptandami, są jednak znacznie bardziej labilne niż ich sztywne analogi, dzięki czemu są w stanie dopasować swój kształt do bardzo wymagających cząsteczek gości [1].

Ostatnio wykazaliśmy, że 26-członowe niedomknięte kryptandy mogą stabilizować w swojej strukturze klastry wody [2,3,4].

W swoich badaniach skupiamy się na wpływie zmian strukturalnych w budowie poliamidowych receptorów makrocyklicznych na ich zdolność do stabilizacji różnych asocjatów wody w ciele stałym.

Wykazaliśmy, że dla niedomkniętych kryptandów posiadających w podstawniku lariatowym grupę fenylową podstawioną przez grupę elektronoakceptorową ($-NO_2$), jak również grupę elektronodonorową (–OMe) następuje stabilizacja oktameru wody składającego się z cyklicznego tetrameru i czterech cząsteczek wody przyłączonych do każdego rogu tetrameru (Rys. 1a). Badania strukturalne wykazały, że w przypadku niedomkniętego kryptandu posiadającego w podstawniku lariatowym niepodstawioną grupę fenylową powstaje łańcuch wodny stabilizowany przez dwie cząsteczki niedomkniętego kryptandu (Rys. 1b).

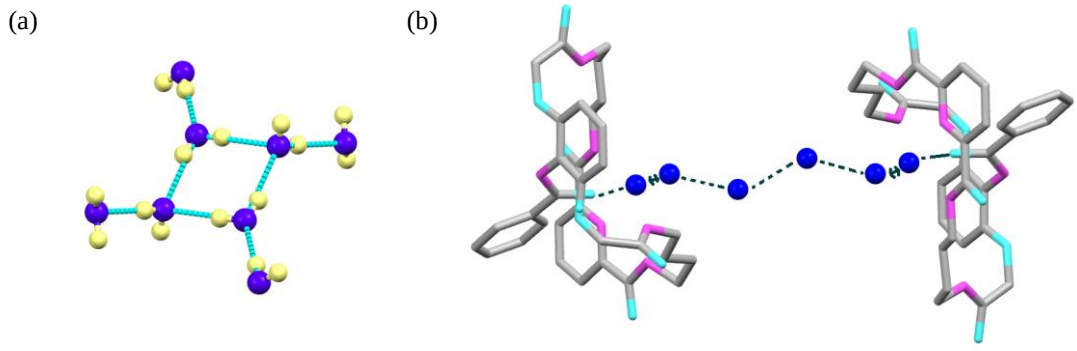

Rys. 1. Struktury wody stabilizowane przez niedomknięte kryptandy (a) oktamer (b) łańcuch wodny.

Literatura

[1] P. Niedbała, M. Ceborska, M. Mehmet, W. Ignacak, J. Jurczak, K. Dąbrowa, *Materials*, **15** (2022) 692.
[2] K. Dąbrowa, M. Ceborska, J. Jurczak, *Cryst. Growth Des.*, **14** (2014) 4906.
[3] K. Dąbrowa, M. Ceborska, J. Jurczak, *Supramol. Chem.*, **30** (2018) 464.
[4] K. Dąbrowa, M. Ceborska, J. Jurczak, *Molecules*, **26** (2021) 2787.

A-15

SYNTHESIS, CHARACTERIZATION, CRYSTAL STRUCTURE, AND HIRSCHFELD SURFACE ANALYSIS OF A NEW MOLYBDENUM(VI) COMPLEX

Rahman Bikas[a], Neda Heydari[b], Magdalena Grzegórska[c] and Anna Kozakiewicz-Piekarz[c]

[a] Department of Chemistry, Faculty of Science, Imam Khomeini International University, 34148-96818, Qazvin, Iran
[b] Department of Chemistry, Faculty of Science, University of Zanjan, 45371-38791, Zanjan, Iran
[c] Department of Biomedical and Polymer Chemistry, Faculty of Chemistry, Nicolaus Copernicus University in Toruń, Toruń, Poland

Intermolecular interactions are so important interactions in crystal engendering and chemical sciences. These interactions have a considerable effect on the stabilization of the crystal packing and they also play vital roles in biological systems. Due to this, studying intermolecular interactions in the crystal structure of crystalline materials has attracted considerable attention during the last decade. Hirschfeld surface analysis is one of the best and newest ways to investigate intra- and inter-molecular interactions in crystal structures [1]. In this method, intermolecular interactions are checked from a new aspect. For example, the distances from the interior and exterior atoms relative to the surface are revealed by specific colors, which makes this analysis more significant than previous methods. Another prominent feature of this analysis is the provision of intermolecular contacts in a 2D diagram [2].

Here, we describe the synthesis and spectroscopic properties of a new molybdenum(VI) complex, $[MoO_2L(CH_3OH)]$ (**1**) with tridentate ONO-donor hydrazone ligand. The complex was obtained from the reaction of MoO_3 with hydrazone ligand (H_2L = (*E*)-4-amino-*N*′-(3-ethoxy-2-hydroxy-benzylidene)benzohydrazide). The structure of **1** was determined by SC-X-ray analysis which revealed it has free amine functionality ($Ph{-}NH_2$). Due to the presence of free amine functionality, coordinated methanol, and also Mo=O groups in the structure of the complex, there are several strong and directed intermolecular hydrogen bond interactions in the crystal structure of this compound (Fig. 1). These interactions were further studied by Hirschfeld surface analysis.

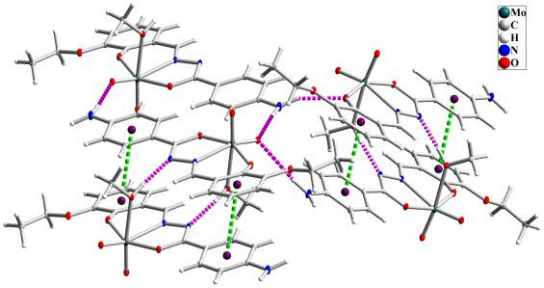

Fig. 1. Intermolecular O–H···N and N–H···O hydrogen bond interactions (pink dashed lines) and π···π interactions (green dashed lines) in the crystal structure of complex **1**.

Literatura

[1] B.R. Chavda, B.N. Socha, S.B. Pandya, K.P. Chaudhary, *et al*., *J. Mol. Struct.*, **1228** (2021) 129777.
[2] J.J. McKinnon, M.A. Spackman, A.S. Mitchell, *Acta Cryst. B*, **60** (2004) 627.

A-16

STUDIES OF BIOMIMETIC Fe(III) COMPLEXES WITH N_2O LIGAND

Karolina Kałduńska, Maja Mielcarz, Andrzej Wojtczak

Faculty of Chemistry, Nicolaus Copernicus University in Toruń, 87-100 Toruń, Poland

The constant development of civilization requires the search for newer and better solutions, but very often inspirations and even ready-made ideas can be found in nature. Recent years have shown that the trend of introducing biomimetics not only to everyday life but also to scientific research continues. D-electron metal complexes are a very important group of compounds that are used in virtually every branch of industry [1].

Metalloenzymes are proteins containing d-electron metal ions in the active center, which act as cofactors stabilized by binding to the amino acid residues of the side chains. Moreover, metalloproteins are characterized by specific catalytic properties, and the conducted catalysis is limited by optimal conditions of enzymatic activity. Biomimetic compounds of d-electron metals are usually characterized by the analogy of the first coordination sphere to the catalytic center of the selected enzyme, which is often correlated with similar chemical properties. Obtaining a complex compound with enzymatic properties makes it possible to use the biomimetic catalysis process in conditions previously unavailable for the native enzyme [2].

Iron(III) complexes are an example of such biomimetics, which can catalyze various processes, including the conversion of aromatic rings. The assisted conversion occurs with mechanisms analogous to catechol dioxygenases (CD). Intra- and extradiol CDs catalyze the oxidative aerobic decomposition of catechol rings [2].

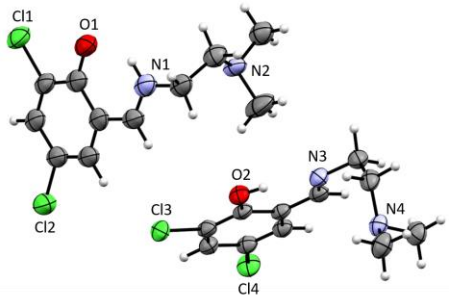

Fig. 1. Ligand.

Complexes of N_2O ligand with Fe(III) have been synthesized as analogs of the active site of catechol dioxygenase. Low-temperature structural tests were performed for the obtained single crystals on the XtaLAB Synergy-S diffractometer by Rigaku. The data were processed using the CrysAlisPro software [3], and the structures were solved by direct methods and refined using the SHELX-2017 software package [4].

References

[1] Vincent, J. F. V.; Bogatyreva, O. A.; Bogatyrev N. R.; Bowyer, A.; Pahl A.-K. Biomimetics: its practice and theory. *J R Soc Interface*., **3**(9) (2006) 471–482.
[2] Kałduńska, K.; Kozakiewicz, A.; Wujak, M.; Wojtczak, A. Biological Inspirations: Iron Complexes Mimicking the Catechol Dioxygenases. *Materials*, **14** (2021) 3250.
[3] Oxford Diffraction Ltd. CrysAlisPro. CrysAlisPro 2010.
[4] G. M. Sheldrick, *Acta Cryst. C*, **71** (2015) 3–8.

A-17

SYNTHESIS, CRYSTAL STRUCTURE, AND CATALYTIC ACTIVITY OF ANIONIC DINUCLEAR VANADIUM(V) COMPLEXES WITH HYDRAZONE LIGANDS

Rahman Bikas[a], Neda Heydari[b], Fatemeh Soltani[a], Anna Kozakiewicz-Piekarz[c]

[a] Department of Chemistry, Faculty of Science, Imam Khomeini International University, 34148-96818, Qazvin, Iran
[b] Department of Chemistry, Faculty of Science, University of Zanjan, 45371-38791, Zanjan, Iran
[c] Department of Biomedical and Polymer Chemistry, Faculty of Chemistry, Nicolaus Copernicus University in Toruń, Toruń, Poland

Hydrazones by having N-N and NH-C(=O)- units in their structure are a class of flexible and attractive N- and O- donor ligands in synthetic coordination chemistry [1]. Hydrazone complexes usually show good catalytic activity and they have high stability in catalytic oxidation reactions [2]. Dihydrazone ligands, by having two hydrazone donor units connected by a linker, can form dinuclear or multinuclear complexes [3]. The coordination chemistry of dihydrazones can be greatly influenced by the variety of aromatic [4] and aliphatic [5] linkers that connect two hydrazone groups. Therefore, the synthesis and characterization of new coordination compounds with dihydrazone ligands have attracted considerable attention in recent years. On the other hand, vanadium is an important metal in oxidation reactions and its complexes with hydrazone ligands have been widely used in catalytic reactions [6].

In this report, we describe the synthesis, characterization, and crystal structure of two anionic dinuclear vanadium(V) complexes with general formula of $(NH_4)_2[(VO_2)_2L^1]$ (**1**) and $(NH_4)_2[(VO_2)_2L^2]$ (**2**) which have been obtained by the reaction of NH_4VO_3 with dihydrazone ligands (H_4L^1 = *N'*^{3},*N'*^{5}-bis((*E*)-2-hydroxy-3-methoxybenzylidene)-2,6-dimethylpyridine-3,5-dicarbohydrazide and H_4L^2 = *N'*^{3},*N'*^{5}-bis((*2E,3Z*)-4-hydroxy-4-phenylbut-3-en-2-ylidene)-2,6-dimethylpyridine-3,5-dicarbohydrazide). The ligands and complexes have been characterized by spectroscopic methods and the structures of vanadium complexes have been determined by single crystal X-ray analysis. These studies indicated that the obtained complexes are anionic and two ammonium cations are present as counter ions in their composition. Therefore, there are several strong and directed intermolecular hydrogen bonds in the crystal structure of these compounds. The synthesized complexes have been used in the oxidation of thioanisole by H_2O_2 and the results showed they can efficiently oxidize it to sulfoxide. The effects of some influencing parameters like temperature, solvent, and the ratio of reagents were investigated in the selective oxidation of sulfides by **1** and **2** and they can also influence the catalytic activity of these compounds [7].

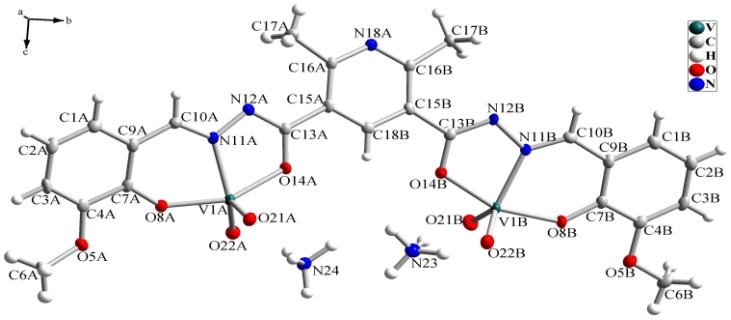

Fig. 1. Molecular structure of complex $(NH_4)_2[(VO_2)_2L^1]$ (**1**).

References

[1] T. Gebretsadik, Q. Yang, J. Wu and J. Tang, *Coord. Chem. Rev*., **431** (2021) 213666.
[2] T. Jiao,G. Wu,Y. Zhang, L. Shen, Y. Lei, C.Y. Wang, A. C. Fahrenbach and H. Li, *Angew. Chem. Int. Ed*., **59** (2020) 18350.
[3] V. Tamilthendral, R. Ramesh and J. G. Malecki, *New J. Chem*., **46** (2022) 21568.
[4] Z. Ashbridge, S. D. P. Fielden, D. A. Leigh, L. Pirvu, F. Schaufelberger and L. Zhang, *Chem. Soc. Rev*., **51** (2022) 7779.
[5] A. G. Orrillo and R. L. E. Furlan, *Angew. Chem. Int. Ed.*, **16** (2022) e202201168.
[6] R. R. Langeslay, D. M. Kaphan, C. L. Marshall, P. C. Stair, A. P. Sattelberger and M. Delferro, *Chem. Rev*., **119** (2019) 2128.
[7] F. Soltani, R. Bikas, N.Heydari, A. Kozakiewicz-Piekarz, *New J. Chem.*, **47** (2023) 6102.

A-18

STRUKTURA SOLI IBUPROFENU Z PIRYMETAMINĄ

Marta S. Krawczyk

Wydział Farmaceutyczny, Uniwersytet Medyczny im. Piastów Śląskich we Wrocławiu, ul. Borowska 211, 50-556 Wrocław

Kokryształy i sole substancji leczniczych stanowią obiecującą alternatywę dla farmaceutyków, dzięki możliwościom wpływania na poprawę ich właściwości fizykochemicznych i farmakologicznych. Odpowiednio dobrane komponenty mogą współkrystalizować oddziałując ze sobą poprzez sieci wiązań wodorowych i innych słabych oddziaływań. Prowadząc badania nad kompleksami i solami substancji z grupy niesteroidowych leków przeciwzapalnych (NLPZ), otrzymano sól ibuprofenu z pirymetaminą (Rysunek). Ibuprofen jest jednym z najpopularniejszych obecnie leków należących do NLPZ. Pirymetamina wykazuje działanie przeciwbakteryjne i przeciwpasożytnicze i jest stosowana głównie w leczeniu malarii oraz toksoplazmozy [1]. Prowadzone są też badania nad jej właściwościami przeciwnowotworowymi [2].

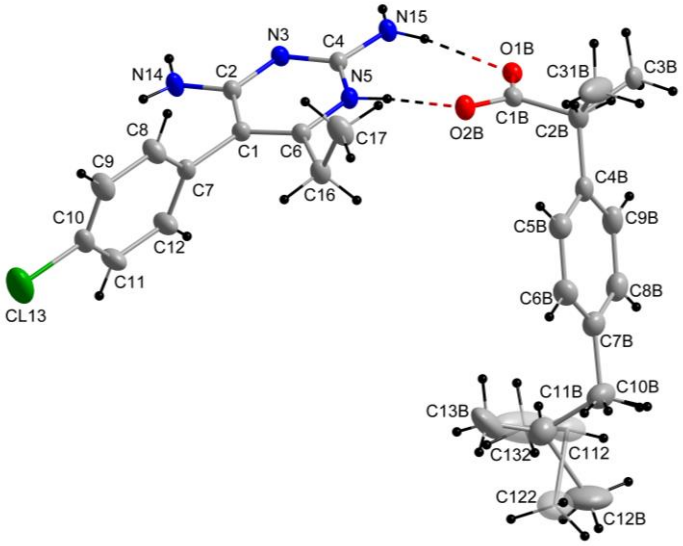

Rys. Oddziaływanie anionu i kationu w strukturze soli ibuprofenu z pirymetaminą.

W krysztale soli ibuprofenu z pirymetaminą kationy oddziałują z anionami poprzez wiązania wodorowe typu N–H···O, tworząc łańcuchy rozciągające się wzdłuż kierunku [001]. Dodatkowo kationy pirymetaminy oddziałują ze sobą poprzez wiązania wodorowe N–H···N.

Literatura

[1] R. R. Ben-Harari, E. Goodwin, J. Casoy, *Drugs in R&D*, **17** (2017) 523.
[2] S. Ramchandani, C.D. Mohan, J.R. Mistry, Q. Su, I. Naz, K.S. Rangappa, K.S. Ahn, *IUBMB Life*, **74**(3) (2022) 198.

A-19

STRUCTURAL ANALYSIS IN CHIRAL COPPER(II) – 1,2-DIAMINOCYCLOHEXANE COMPLEXES

Julia Reszkowska, Maciej Lewandowski, Tadeusz M. Muzioł

Nicolaus Copernicus University in Toruń,
ul. Gagarina 7, 87-100 Toruń

The structural analysis is important tool in supramolecular chemistry, crystal engineering, solid state and material chemistry. It allows for description of crystal structures and enables finding structure-properties relationships of new multifunctional compounds sharing *e.g.* magnetism with porosity, chirality, luminescent properties [1]. Chirality might be introduced by different approaches, e.g. by selection of the chiral ligand. It offers a new perspective on design and preparation of magnetochiral materials and study of magnetochiral effects.

We synthesized copper(II) complexes with 1,2-diaminocyclohexane being simple diamine ligand showing bidentate coordination. We aimed to obtain chiral magnets *via* the chirality introduced by chiral ligand – (1R,2R)-(-)-cyclohexanediamine (dach). Crystals of $[Cu(dach)Cl_2]\cdot 2H_2O$ (**1**) and $[Cu(dach)_2(H_2O)](SO_4)\cdot 0.67H_2O$ (**2**) were prepared by slow evaporation of the solvent. The data collection was performed using XtaLAB Synergy, Dualflex with HyPix detector, CuKα radiation λ = 1.54184 Å. XAS experiments were performed on PIRX (previously PEEM/XAS beamline of National Synchrotron Radiation Centre SOLARIS (Kraków) for $L_{2,3}$ edges of Cu).

In $[Cu(R,R\text{-dach})Cl_2]\cdot 2H_2O$ (**1**) copper(II) ion is found in [4+2] coordination mode with four nitrogen atoms in the equatorial base and two elongated axial Cu-Cl bonds. In the packing between molecules are found cavities which are occupied by crystallization water molecules. In $[Cu(dach)_2(H_2O)](SO_4)\cdot 0.67H_2O$ (**2**) copper(II) is found in distorted square pyramidal environment with the axial position occupied by the water molecule. Cavities of the crystal network are filled with crystallization water molecules and sulfate anions.

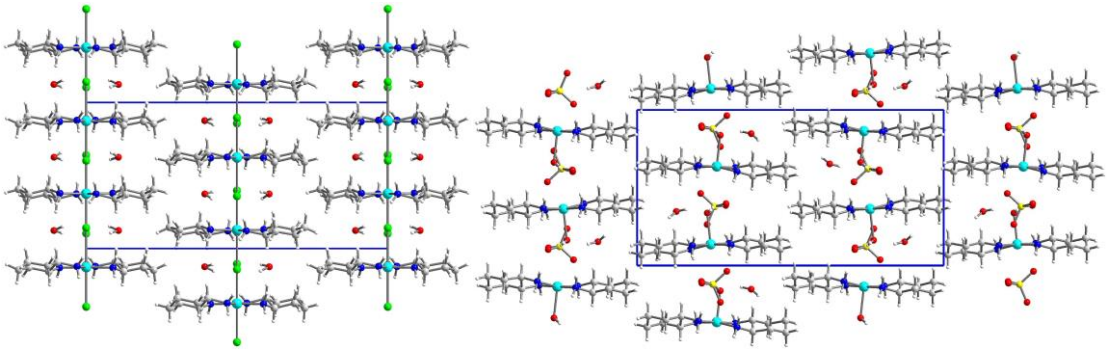

Rys. 1. Packing in $[Cu(R,R\text{-dach})Cl_2]\cdot 2H_2O$ (**1**) (left) and $[Cu(R,R\text{-dach})_2(H_2O)](SO_4)\cdot 0.67H_2O$ (**2**) (right).

Literatura

[1] M. Pilkington, S. Decurtins, in: *Comprehensive Coordination Chemistry II*, eds. J.A. McCleverty, T.J. Meyer, Elsevier, 2003, vol. 7, ch. 7.4 (High Nuclearity Clusters: Clusters and Aggregates With Paramagnetic Centers: Cyano and Oxalato Bridged Systems), pp. 177-229.

A-20

CONTROLLING ELASTIC PROPERTIES AND AMORPHIZATION IN METAL-ORGANIC POLYMERS THROUGH FLEXIBLE LINKERS

Aleksandra Półrolniczak, Szymon Sobczak and Andrzej Katrusiak

Department of Materials Chemistry, Faculty of Chemistry, Adam Mickiewicz University, Uniwersytetu Poznańskiego 8, 61-614 Poznań, Poland

e-mail: aleksandra.polrolniczak@amu.edu.pl

Metal-organic polymers have gained significant attention in various technological applications due to their diverse functionalities.[1] However, understanding their physical properties and predicting their behaviour remains challenging.[2] In this study, we focused on the role of flexible linkers in controlling the compression and deformation of metal-organic polymers. Specifically, we explored the performance of 1,6-hexanediamine (HDA), an aliphatic diamine ligand known for its conformational flexibility. HDA is commonly used in the synthesis of organic materials, plastics, and detergents due to its safety and versatility.[3] By coordinating with different metal cations, HDA linkers enable the formation of three-dimensional frameworks.

Our study investigates the compression behaviour and structural transformations of coordination polymers (CPs), based on the 1,6-hexanediamine (HDA) as a ligand capable of conformational switching. The study explores three CPs: $Cd(HDA)_2(NO_3)_2$, $Cd_2(HDA)_3(NO_3)_4$, and $Cu(HDA)_2(MeCN)_2{\cdot}2BF_4$ (Fig. 1). These CPs exhibit interesting phase transitions and transformations under pressure.

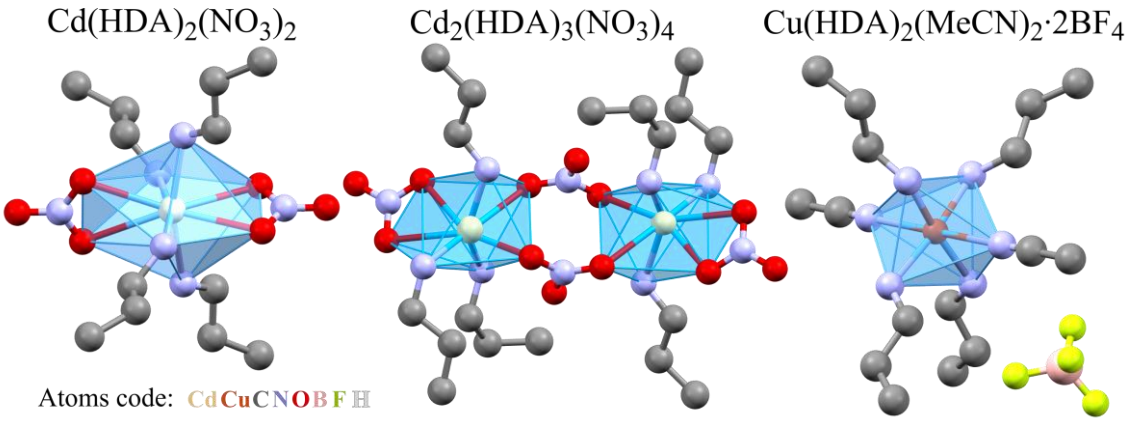

Fig. 1. Three coordination polymers with HDA linkers; their halves coordinating one metal cation are shown, and the H-atoms are omitted for clarity.

These structural transformations were accompanied by conformational changes in the HDA linkers, as well as modifications in the coordination schemes around the metal centres. This dynamic behaviour of the linkers contributed to the enhanced capability of the frameworks to absorb external stress. The results highlight the compression mechanism and structural responses of metal-organic polymers, for exploring their elastic properties and understanding their structure-property relationships.

References
[1] H. C. Zhou, J. R. Long and O. M. Yaghi, *Chem. Rev.*, **112** (2012) 673–674.
[2] M. Safaei, M. M. Foroughi, N. Ebrahimpoor, S. Jahani, A. Omidi and M. Khatami, *TrAC - Trends Anal. Chem.*, **118** (2019) 401–425.
[3] C. W. Chen, Z. Y. Yang, H. C. Yang, Y. Z. Hsieh, C. Liu, Y. C. Chuang, J. J. Le, S. P. Rwei, I. J. Hsu and H. H. Chen, *Polymer*, **232** (2021) 124162.

This work was supported by funding from the Polish National Science Centre: PRELUDIUM 18 No. UMO-2019/35/N/ST5/01838 and grant POWR.03.02.00-00-I026/16 co-financed by the EU European Social Fund under the Operational Program Knowledge Education Development.

A-21

HIGH-PRESSURE AND HIGH-TEMPERATURE PHASES OF SELENOUREA

Kinga Roszak and Andrzej Katrusiak

Department of Materials Chemistry, Faculty of Chemistry, Adam Mickiewicz University, Uniwersytetu Poznańskiego 8, 61-614 Poznań

Selenourea ($SeC(NH_2)_2$) is an important metabolite and chemical agent [1-3]. Its polymorph α, which is stable under normal conditions, is unique due to the complex structure comprising nine independent molecules (Z' = 9) in the asymmetric unit [4-6]. The recently revealed polymorph β, stable above 0.21 GPa, contains two independent molecules (Z' = 2). The recrystallization under high pressure also induces a partial stochastic hydration in phase α; the recrystallization from the aqueous solution above 0.21 GPa favors the formation of duotritohydrate $3SeC(NH_2)_2 \cdot 2H_2O$, unknown under normal conditions [4]. Meanwhile, relatively little is known about the thermal behavior of $SeC(NH_2)_2$. Two crystal structures determined at 100 K [6] and 173 K [5] are both consistent with phase α (*i.e.* space group $P3_1$, Z' = 9) [4-5]. Our differential scanning calorimetry (DSC) measurements revealed a first-order phase transition at 381 K and a new solid selenourea phase γ stable below the melting point at 473 K [7]. The structural mechanism of this transition involves intermolecular hydrogen bonds NH Se and NH N, aggregating the molecules into helices and the helices into a three-dimensional framework. The lattice projections along *c* of selenourea phases α and γ are related by a similarity transformation, which is connected with the qualitative differences between intermolecular interactions in the structures of these phases and to the origin of the large number of independent molecules in phase α.

References

[1] S. Hariharan, S. Dharmaraj, *Inflammopharmacology*, **28** (2020) 667–695.
[2] M. Koketsu, H. Ishihara, *Curr. Org. Synth*., **3** (2006) 439–455.
[3] J. Zheng, Y. Shibata, A. Tanaka, *Anal. Bioanal. Chem*., **374** (2002) 348–353.
[4] K. Roszak, A. Katrusiak, *Acta Cryst. B*, 77 (2021) 449–455.
[5] J.S. Rutherford, C. Calvo, *Z. Kristallogr. New Cryst. Struct*., **128** (1969) 229–258.
[6] Z. Luo, Z. Dauter, *PLoS One*, **12** (2017) e0171740.
[7] K. Roszak, A. Katrusiak, *Acta Cryst. B*, **79** (2023) 64–72.

A-22

CHARGE-TRANSFER BENZOQUINONE:CATECHOL COMPLEXES UNDER HIGH PRESSURE

Hien Quy Le, Michalina Rusek and Andrzej Katrusiak

Faculty of Chemistry, Adam Mickiewicz University, Uniwersytetu Poznanskiego 8, Poznan 61-614, Poland

New charge-transfer complexes of para-benzoquinone (*p*Bq) and catechol (Ct) have been reported. Compounds *p*Bq and Ct preferentially co-crystallize to a 1:1 brown complex (α-*p*Bq:Ct), with the molecules alternatively stacked into columns. We have revealed the accelerated aging reaction of α-*p*Bq:Ct, leading to an orange *p*Bq:2Ct complex. High-pressure experiments shown transition converting the catechol conformers syn into anti in a markedly darker new phase β-*p*Bq:Ct. This conversion extensively extends the transition hysteresis between phases α- and β-*p*Bq:Ct. At about 2.5 GPa, a radical complex γ-*p*Bq:Ct is formed and above 3.0 GPa it gradually transforms into the black amorphous phase δ-*p*Bq:Ct (Fig. 1).

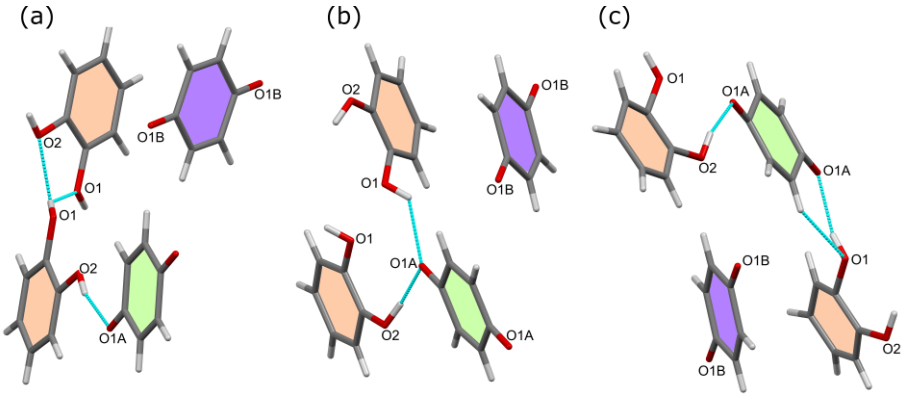

Fig. 1 H-bonds (cyan dotted lines) in the structure of phase α-*p*Bq:Ct at 0.1 MPa (a); in phase β-*p*Bq:Ct at 0.8 GPa (b) and in phase γ-*p*Bq:Ct at 2.5 GPa (c).

The high-pressure measurements were carried out in a modified diamond anvil cell (DAC) [1]. Pressure in the DAC was calibrated using the ruby fluorescence method with a Photon Control spectrometer, affording an accuracy of 0.02 GPa. [2]. The sample crystal and several ruby chips were mounted in the DAC chamber and filled up with Daphne oil 7575 used as the pressure-transmitting medium, hydrostatic to about 4 GPa at room temperature, [3] and the DAC was closed and compressed.

References

[1] L. Merrill, W. A. Bassett, *Rev. Sci. Instrum.*, **45** (1974) 290–294.
[2] G. J. Piermarini, S. Block, J. D. Barnett, R. A. Forman, *J. Appl. Phys.*, **46** (1975) 2774–2780.
[3] D. Staško, J. Prchal, M. Klicpera, S. Aoki, K. Murata, *High Pressure Res.*, **40** (2020) 525–536.

A-23

BORACYKLICZNE TRIADY DONOR-AKCEPTOR-DONOR OPARTE O SZKIELET BODIPY

Jakub Tyborowski[a], Paulina H. Marek-Urban[a,b], Krzysztof Woźniak[b], Krzysztof Durka[a]

[a] *Wydział Chemiczny, Politechnika Warszawska, ul. Noakowskiego 3, 00-554 Warszawa*
[b] *Wydział Chemii, Uniwersytet Warszawski, ul. Pasteura 1, 02-093 Warszawa*

Fotouczulacze to szeroka grupa substancji stosowanych w terapii fotodynamicznej – nowoczesnej metodzie leczenia nowotworów[1]. Poza zastosowaniami medycznymi związki te mogą być wykorzystywane jako fotokatalizatory w reakcjach chemicznych oraz w procesach oczyszczania wody lub powietrza[2]. Swoje szerokie zastosowanie fotouczulacze zawdzięczają zdolności do generowania reaktywnych form tlenu. W wyniku interakcji z cząsteczkami wzbudzonego fotouczulacza (w stanie trypletowym) cząsteczki tlenu trypletowego ($^3O_2$) ulegają wzbudzeniu do stanu singletowego ($^1O_2$).

Przykładem fotouczulaczy jest grupa boroorganicznych kompleksów typu BODIPY. Jedną ze strategii umożliwiających zwiększenie efektywności generowania stanów trypletowych jest zastosowanie efektu ciężkiego atomu, który zwiększa prawdopodobieństwo przejścia międzysystemowego (ISC), wzbronionego kwantowymi regułami wyboru. W 2017 roku zaproponowano alternatywne podejście, niewymagające stosowania ciężkich atomów, których wprowadzenie zmniejsza trwałość molekuły i podnosi jej ciemną cytotoksyczność[3], polegające na konstrukcji związków charakteryzujących się architekturą donor-akceptor (Rys. 1). W ich przypadku przejście ze stanu singletowego do trypletowego odbywa się za pośrednictwem stanu z przeniesieniem ładunku (CT), a prawdopodobieństwo przejścia ISC jest zwiększane przez ortogonalną budowę cząsteczki. Nasz zespół zaproponował inny wariant układu donor-akceptor (Rys. 1), w którym przeniesiono część donorową na atom boru, tworząc kompleks o geometrii *spiro*[4].

W niniejszej prezentacji przedstawiono właściwości triady donor-akceptor-donor, będącej połączeniem wspomnianych strategii. Celem badań było określenie wpływu jednoczesnego wprowadzenia dwóch różnych donorów na zdolności fotokatalityczne triad. Badane związki zostały scharakteryzowane spektroskopowo i strukturalnie.

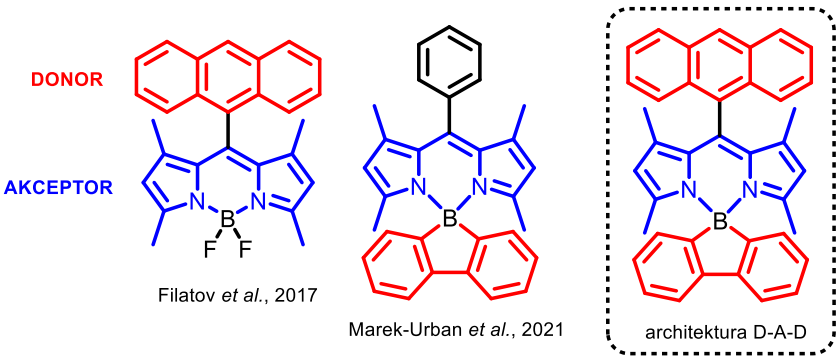

Rys. 1 Schemat budowy omawianych związków.

A-23

Finansowanie badań w ramach projektu OPUS 20 „Efektywne fotouczulacze oparte na sztywnych układach boroorganicznych jako generatory tlenu singletowego” (2020/39/B/ST4/02370).

Literatura

[1] Jonathan P. Celli, *et al.*, *Chem. Rev.*,**110**(5) (2010) 2795–2838.
[2] Sanchita Shah, *et al.*, *Eur. J.*, **24**(70) (2018) 18788−18794.
[3] Mikhail A. Filatov, *et al.*, *J. Am. Chem. Soc.*, **139**(18) (2017) 6282–6285.
[4] Paulina H. Marek-Urban, *et al.*, *J. Org. Chem.*, **86**(18) (2021) 12714-12722.

A-24

STRUKTURY KRYSTALICZNE NOWYCH KOMPLEKSÓW ZŁOTA STABILIZOWANYCH PRZEZ LIGAND SILANOTIOLANOWY O DUŻEJ ZAWADZIE STERYCZNEJ

Anna Ciborska*, Anna Dołęga

Katedra Chemii Nieorganicznej, Wydział Chemiczny, Politechnika Gdańska
ul. Narutowicza 11/12, 80-233 Gdańsk

**e-mail: anna.ciborska@pg.edu.pl*

Kompleksy srebra(I) i złota(I) znajdują zastosowanie w nanotechnologii i medycynie. Wzrost zainteresowania tymi związkami wynika z ich aktywności biologicznej oraz potencjalnego zastosowania, jako prekursorów materiałów i leków przeciwdrobnoustrojowych [1,2]. Zarówno kompleksy srebra jak i kompleksy złota z ligandami tiolanowymi wykazują tendencję do tworzenia klastrów i struktur polimerowych oraz innych układów supramolekularnych [3,4].

W naszych dotychczasowych badaniach nad silanotiolanowymi kompleksami srebra(I) rolę liganda S-donorowego pełniła reszta $(dippO)_3SiS^-$ (dipp = 2,6-diizopropylofenyl) o dużej zawadzie sterycznej, pozwalająca na otrzymanie względnie stabilnych kompleksów metali zarówno jedno- jak i wielordzeniowych oraz polimerów koordynacyjnych [5–7]. Obecnie przedstawiamy wyniki badań strukturalnych silanotiolanowych kompleksów złota(I).

W wyniku reakcji $AuCl(PPh)_3$ z tris(2,6-diizopropylofenoksy)silanotiolem otrzymano bezbarwne kryształy jednordzeniowego związku **1**, który posłużył, jako substrat do kolejnych syntez. W reakcji z nadmiarem trimetylofosfiny otrzymano jednordzeniowy związek **2**, gdzie zaszła wymiana liganda trifenylofosfinowego na mniejszy ligand trimetylofosfinowy.

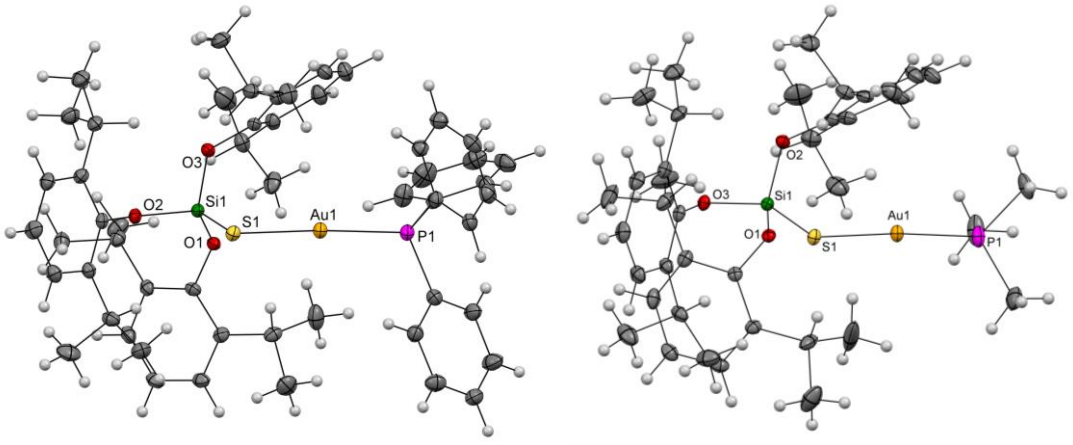

Rys. 1. Struktury molekularne silanotiolanowych kompleksów złota(I):**[$Ph_3PAuSSi(Odipp)_3$] 1**, wybrane długości wiązań (Å): Au1-P1 2.2499(11), Au1-S1 2.3042(11), S1-Si1 2.0744(16); wybrane kąty walencyjne (°): P1-Au1-S1 171.70(4), Si1-S1-Au1 102.77(6); **[$Me_3PAuSSi(Odipp)_3$] 2**, wybrane długości wiązań (Å): Au1-P1 2.2437(13), Au1-S1 2.3132(12), S1-Si1 2.0660(16); wybrane kąty walencyjne (°): P1-Au1-S1 175.55(4), Si1-S1-Au1 97.94(6).

A-24

Reakcja silanotiolanowego kompleksu złata(I) **1** z nadmiarem 1,4 bis(difenylofosfino)butanu (dppb) prowadzi do dwurdzeniowego kompleksu **3**, w którym atomy złota są połączone poprzez mostkujący ligand difosfinowy. W strukturze krystalicznej molekularnego kompleksu **3** na część symetrycznie niezależną przypada pół cząsteczki. Układ dwurdzeniowy odtwarzany jest przez odbicie względem środka symetrii, zaś środek symetrii znajduje się w środku łańcucha dppb. Ponadto w strukturę tego związku wbudowują się cząsteczki toluenu.

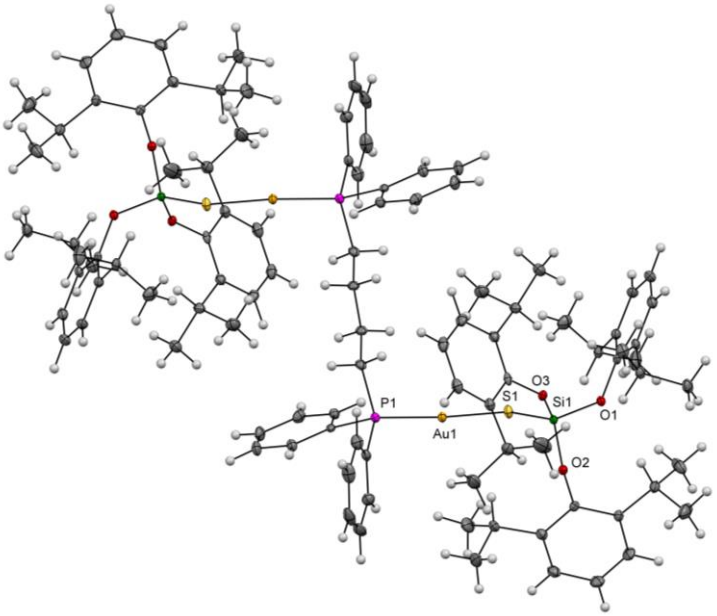

Rys. 2. Struktura molekularna silanotiolanowego kompleksu złota(I), dla czytelność pominięto cząsteczki rozpuszczalnika. Elipsoidy drgań termicznych 30%. **[(dppb){AuSSi(Odipp)$_3$}$_2$] 3**, wybrane długości wiązań (Å): Au1-P1 2.2509(9), Au1-S1 2.3099(9), S1-Si1 2.0776(13); wybrane kąty walencyjne (°): P1-Au1-S1 174.48(3), Si1-S1-Au1 104.48(5).

dipp – 2,6-diizopropylofenyl
dppb – 1,4 bis(difenylofosfino)butan

Literatura

[1] S. Simon, Le T Phung, G. Silver, *J. Ind. Microbiol. Biotechnol*., **33** (2006) 627.
[2] E.R.T. Tiekink, *Crit. Rev. Oncol.*, (2002).
[3] L.S. Ahmed, J. R. Diworth, J. R. Miller, N. Wheatley, *Inorganica Chim. Acta*, **278** (1998) 229.
[4] R. R. Nasaruddin, T. Chen, N. Yan, J. Xie, *Coord. Chem. Rev.*, **368** (2018) 60.
[5] A. Dołęga, W. Marynowski, K. Baranowska, M. Śmiechowski, J. Stangret, *Inorg. Chem.*, **51** (2012) 836.
[6] A. Ciborska, Z. Hnatejko, K. Kazimierczuk, A. Mielcarek, A. Wiśniewska, A. Dołęga, *Dalton Trans*., **46** (2017) 11097.
[7] A. Pladzyk, D. Kowalkowska-Zedler, A. Ciborska, A. Schnepf, A. Dołęga, *Coord. Chem. Rev*., **437** (2021) 213761.

A-25

STRUCTURAL STUDIES OF UREA CLATHRES WITH ALIPHATIC DIAMINES

Anna Sadocha, Kamila Urbaniak, Michał K. Cyrański and Arkadiusz Ciesielski

University of Warsaw, Faculty of Chemistry, Pasteura 1 02-093 Warsaw

Urea is an incredibly intriguing molecule, due to its extensive applications in various fields, including pharmacy, agriculture, and industry. It exhibits a significant versatility in forming a wide range of systems, from simple ones to highly complex compounds, like macrocycles. Furthermore, it has the ability to arrange themselves into channel clathrates with linear molecules such as aliphatic hydrocarbons and their derivatives.

The first documented example of such clathrate is the urea-1-octanol system, while the exploration of its structures only began in the 1980s. These clathrates exhibit an architecture of hexagonal infinite channels, wherein guest molecules are loosely bound. Moreover, they are often highly disordered. Crystallization of these compounds typically occurs in the $P6_1$ or $P6_5$ space groups, resulting in enantiomorphic crystal forms. This phenomenon arises from the formation of helical structures, facilitated by the hydrogen bonds formed between urea molecules and their neighboring counterparts.

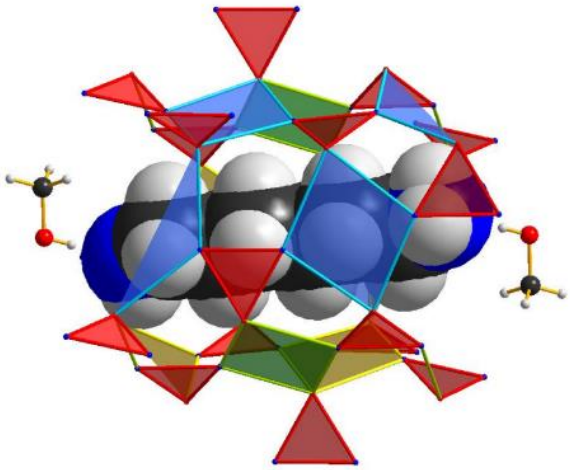

Fig. 1 Urea clathrate with 1,6-diaminohexane

The objective of the research was to obtain and perform structural analysis of finite urea clathrates with aliphatic diamines. Six urea clathrates were synthesized using 1,*n*-diaminoalkanes (where $n = 3 \div 8$). These clathrates form channels whose length is fitted to the dimensions of the diamines. The amine groups interact by hydrogen bonds with a solvent molecule, methanol, leading to stabilization of the system. Interestingly, in addition to chiral tubes composed of urea molecules, centrosymmetric ones can also be formed. The variation in topology observed in these systems can be attributed to the presence of a minimal motif consisting of four urea molecules. This motif gives rise to a distinctive rhombus shape, with the edges formed by hydrogen bonds between the four urea molecules. The relative arrangement of these compounds determines whether the

resulting system is chiral or centrosymmetric. Importantly, it has been demonstrated that the topology of urea channels in these clathrates is governed by this fundamental motif, ultimately influencing the overall crystal architecture.

References

[1] M. F. Bengen, *Angew. Chem*., **6** (1951) 207.

A-26

STRUKTURA KRYSTALICZNA NOWEGO SILANOTIOLANU CYNKU(II) Z 1,4-BIS(3-AMINOPROPYLO)PIPERAZYNĄ

Bartosz Cieśla, Łukasz Ponikiewski, Agnieszka Pladzyk

Katedra Chemii Nieorganicznej, Wydział Chemiczny, Politechnika Gdańska, ul. Narutowicza 11/12, 80-233 Gdańsk

Od wielu lat szczególną uwagę poświęca się badaniu wpływu oddziaływań niekowalencyjnych, takich jak wiązania wodorowe na strukturę krystaliczną związków chemicznych [1]. W tym celu, w syntezie układów koordynacyjnych opartych na jonach metali, stosuje się różne ligandy, między innymi takie, które jedynie pośrednio wpływają na generowanie wspomnianych oddziaływań. Przykładem takiego związku jest tri-*tert*-butoksysilanotiol (tBuO)$_3$SiSH, który jako S-donorowy ligand chętnie koordynuje do jonów metali, a swoją budową wymusza aranżację przestrzenną pozostałych ligandów podstawionych na centrum metalicznym [2, 3].

Ostatnio w naszej grupie badawczej zajmowaliśmy się badaniem właściwości strukturalno-spektralnych zsyntezowanych heteroleptycznych silanotiolanowych pochodnych kadmu i cynku. Związki te dodatkowo zawierały pochodne piperazyny w roli ligandów N-donorowych. W wyniku naszych prac otrzymaliśmy szereg nowych związków zarówno jedno- jak i wielordzeniowych [4].

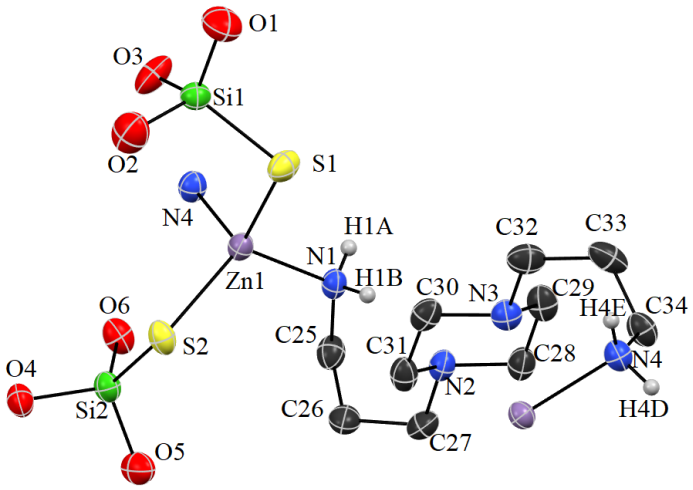

Rys. 1. Struktura molekularna części asymetrycznej związku **1**. Dla czytelności rysunku pominięto grupy *tert*-butylowe i atomy wodoru niezaangażowane w tworzenie wiązań wodorowych. Elipsoidy drgań termicznych 50%.

Jednym z otrzymanych związków jest [Zn{SSi(tBuO)$_3$}$_2$($C_{10}H_{24}N_4$)]$_n$ **1** o strukturze jednowymiarowego polimeru koordynacyjnego (Rys. 1). Synteza **1** przebiegła z użyciem Zn(acac)$_2$, (tBuO)$_3$SiSH i 1,4-bis(3-aminopropylo)piperazyny (bapp). Związek **1** krystalizuje w układzie jednoskośnym i grupie przestrzennej $P2_1/c$. Centrum metaliczne każdego meru przyjmuje nieznacznie zniekształconą geometrię tetraedryczną (τ_4=0,91, τ_4'=0,91 [5, 6]) o rozpiętości kątów między 100,48(13)° dla N_1–Zn_1–N_4^i (*i*: x, -y+3/2, z-1/2), a 116,57(4)° dla S_2–Zn_1–S_1. Rdzeń koordynacyjny

o wzorze ZnN_2S_2 tworzony jest przez koordynujące do jonu metalu reszty tri-*tert*-butoksysilanotiolanowe pełniące rolę ligandów S-terminalnych (Rys 1.). Sfera koordynacyjna jonów Zn(II) jest dopełniona przez mostkujące cząsteczki aminy, które koordynują jedynie poprzez atomy azotu pierwszorzędowych grup aminowych. Długości wiązań Zn–N, Zn–S, Si–O oraz Si–S są wartościami zbliżone do tych obserwowanych w dotychczas otrzymanych heteroleptycznych silanotiolanach cynku [3]. Łańcuch polimeru układa się na kształt wygiętej wstęgi. Tym samym, centra metaliczne w łańcuchu oddalone są naprzemiennie na odległość Zn···Zn 8,879(9) i 9,884(6) Å.

Za specyficzny sposób organizacji struktury krystalicznej związku **1** odpowiedzialne są przede wszystkim licznie występujące oddziaływania wodorowe. Donorem wszystkich wiązań wodorowych tworzących się w obrębie pojedynczego łańcucha polimerowego jest cząsteczka bapp. Są to oddziaływania typu $N_{bapp}–H\cdots N_{bapp}$ (*D*···*A* 2,897(4) i 2,969(4) Å) oraz $N_{bapp}–H\cdots O_{TBST}{}^{i}$ (*i*: x, -y+3/2, z-1/2) (*D*···*A* 3,028(5) i 3,098(5) Å) tworzące odpowiednio motywy R(8) i R(6) (Rys 2.) [7].

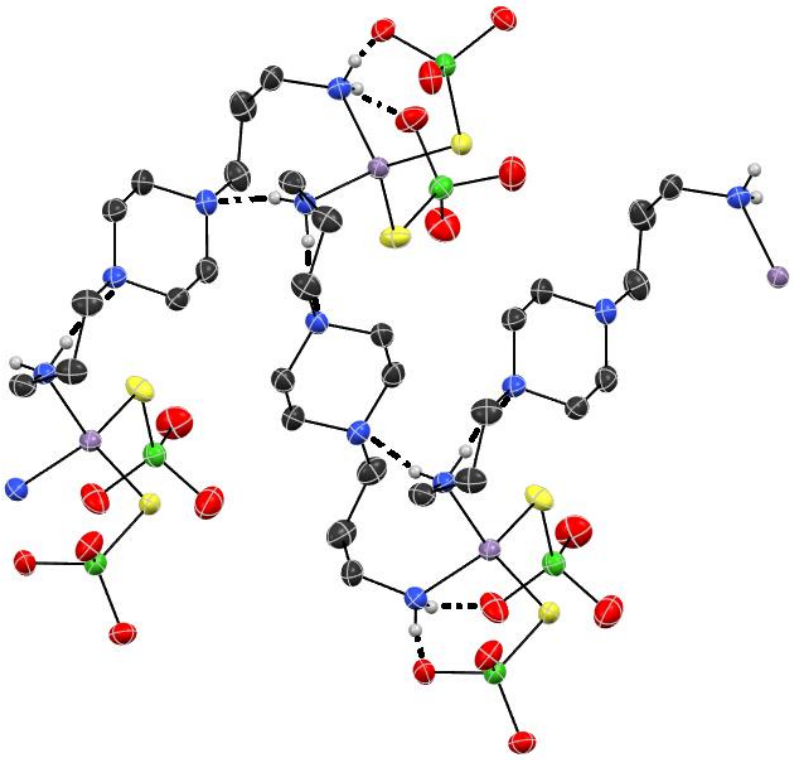

Rys 2. Oddziaływania wodorowe w strukturze krystalicznej związku **1**. Dla czytelności rysunku pominięto grupy *tert*-butylowe i atomy wodoru niezaangażowane w tworzenie wiązań wodorowych. Elipsoidy drgań termicznych 50%.

Literatura

[1] Desiraju, G. R. *J. Am. Chem. Soc.*, **135** (2013) 9952–9967.
[2] Wojnowski W. *et al. Z annorg. allg. Chem.*, **403** (1974) 186-192.
[3] Pladzyk, A. *et al. Coord. Chem. Rev.*, **433** (2021) 213761.
[4] Kowalkowska-Zedler, D. *et al. Acta Crystallogr. C Struct. Chem.,* (2023) – przyjęta do druku.
[5] Okuniewski, A. *et al. Polyhedron*, **90** (2015) 47-57.
[6] Rosiak, D. *et al. Polyhedron*, 146 (2018) 35–41.
[7] Berenstein, J. *et al. Angew. Chem. Int. Ed. Engl.*, **34** (1995) 1555-1573.

A-27

SYNTEZA I ANALIZA STRUKTURY KRYSTALICZNEJ KOMPLEKSU ALFA-CYKLODEKSTRYNY Z KWASEM P-AMINOBENZOESOWYM

Patryk Czapnik i Magdalena Małecka

Uniwersytet Łódzki, Wydział Chemii, Katedra Chemii Fizycznej, Zakład Chemii Biofizycznej, ul Pomorska 163/165, 90-236 Łódź

Kwas p-aminobenzoesowy jest organicznym związkiem z grupy aminokwasów biorącym udział m.in. w syntezie kwasu foliowego [1]. Charakterystyczna budowa sprzyja zdolności inkludowania się wewnątrz hydrofobowej wnęki cyklodekstryny [2, 3].

Celem przeprowadzonych badań było uzyskanie monokryształów kompleksu inkluzyjnego tego kwasu z α-cyklodekstryną oraz wyznaczenie struktury krystalicznej powstałego kompleksu inkluzyjnego za pomocą monokrystalicznego dyfraktometru rentgenowskiego Oxford XtaLAB Synergy-S. Wykonano również badania spektrometrią FT-IR metodą transmisyjną z KBr oraz różnicowym kalorymetrem skaningowym (DSC) celem potwierdzenia procesu kompleksowania kwasu wewnątrz hydrofobowej wnęki makrocykla.

W części asymetrycznej komórki elementarnej obserwuje się 1 cząsteczkę kompleksu inkluzyjnego oraz 4 cząsteczki wody (Rys. 1.). Zbadany kompleks tworzy się w stosunku stechiometrycznym 1:1 i stabilizowany jest przez liczne wiązania wodorowe, które są odpowiedzialne również za specyficzne ułożenie warstwowe. Pierścienie cyklodekstryn ułożone są w znacznej części w sposób „głowa do głowy”, a kolejne warstwy kompleksów układają się według schematu ABAB (Rys. 2.). Każdy z pierścieni cyklodekstryn otoczony jest przez 6 innych torusów z nią sąsiadujących (Rys. 3.). Wartości podstawowych danych krystalograficznych zostały przedstawione w Tabeli 1.

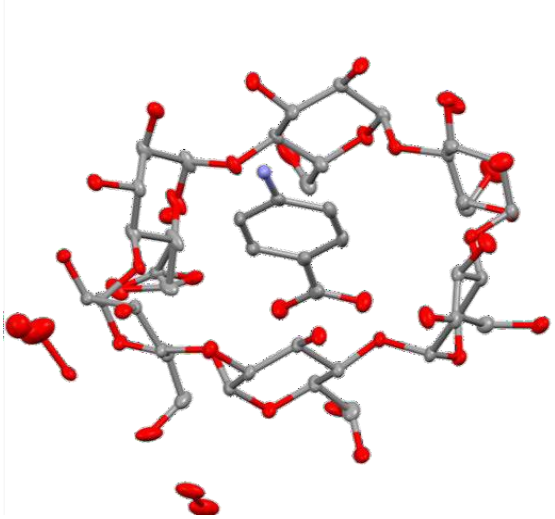

Rys. 1. Struktura molekularna kompleksu inkluzyjnego.

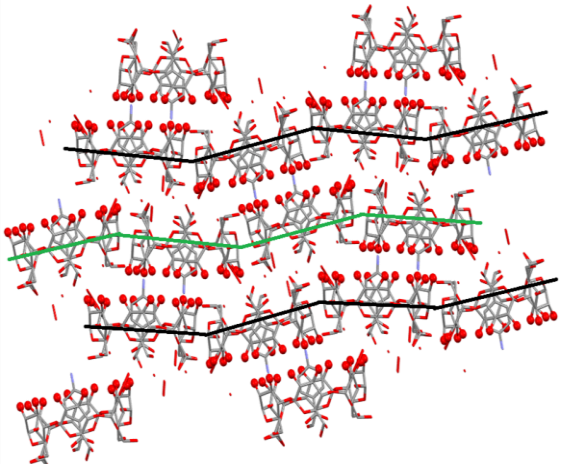

Rys. 2. Schemat ułożenia warstw kompleksów inkluzyjnych.

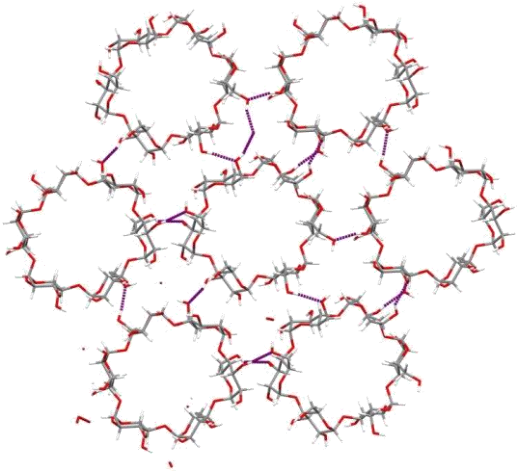

Rys. 3. Ułożenie kompleksów inkluzyjnych w płaszczyźnie.

Tab. 1. Podstawowe dane krystalograficzne.

a [Å]	13,4505(1)
b [Å]	15,4519(1)
c [Å]	24,6570(2)
α = β = γ [°]	90
T [K]	100
V [Å^3]	5124,61(7)
G.P.	$P2_12_12_1$
R1	0,0337(9422)
wR2	0,0909(9772)
S	1,059

Literatura

[1] Brown G., The Biosynthesis of Folic Acid, *Journal of Biological Chemistry*, **237**(2) (1962) 536-540.
[2] Jun S. W., Kim J. S., Kim M. S., Park H. J., Sibeum L., Woo J. S., Hwang S. J., *European Journal of Pharmaceutics and Biopharmaceutics*, **66**(3) (2007) 413-421.
[3] Crini G., *Chemical Reviews*, **114**(21) (2014) 10940-10975.

A-28

A PLETHORA OF HOST-GUEST CRYSTAL FORMS

Oksana Danylyuk*, Helena Butkiewicz and Kateryna Kravets

Institute of Physical Chemistry Polish Academy of Sciences, Kasprzaka 44/52, 01-224 Warsaw, Poland

**e-mail: odanylyuk@ichf.edu.pl*

Host-guest systems have been widely explored to design and create various supramolecular materials, where molecular guest is sheltered in the confined space of the host. In the confined nanospace the trapped guest molecules can adopt unusual conformations and make peculiar interactions which they do not experience in other environments. In the last decade there has been more and more experimental evidences that generally assumed fast and direct route from molecular recognition in host-guest systems towards isolation of the single thermodynamic product (*crystallization*) is not always so obvious. In reality at least some of the host-guest systems are not characterized by a single crystal structure, but by ensemble of various crystal forms. The structural landscape can embrace crystallization of metastable and equilibrium supramolecular assemblies, that can sometimes be spatially and temporary resolved, Fig. 1. The situation is additionally complicated by solute(s)-solvent interactions, as in aqueous supramolecular chemistry water cannot be treated as pure spectator in the molecular recognition between host and guest.

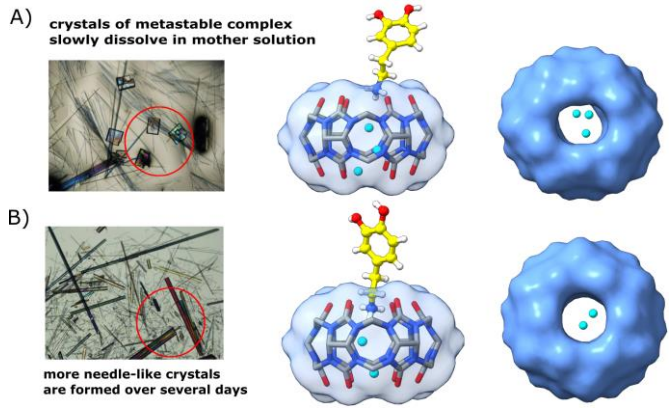

Fig. 1. Concomitant crystallization of two crystal forms of cucurbit[6]uril-dopamine complexes – prisms of the metastable complex and needles of thermodynamically preferred complex.

Here the host-guest systems of pathway-dependent molecular recognition and crystallization will be discussed [1, 2]. The crystallization pathway can be variable of different factors, such as kinetic trapping, presence of the cosolvent, pH, temperature, additives, *etc*. It is time to shift our focus from 'visible interactions' in one crystal structure to the appreciation of many subtle effects playing combined role in the host-guest complexation and crystallization.

Literature

[1] O. Danylyuk, V.P. Fedin, V. Sashuk, *Chem. Commun.*, **49** (2013) 1859.
[2] O. Danylyuk, M. Worzakowska, J. Osypiuk-Tomasik, V. Sashuk, Kedra-Krolik, *CrystEngComm*,, **22** (2020) 634.

A-29

DEHYDRATION-AIDED STRUCTURAL STUDIES REVEAL NEW (PSEUDO)POLYMORPHS OF cGMP, Na(cGMP) AND $Mg(cGMP)_2$

Wojciech Dudziak, **Katarzyna Ślepokura**

University of Wrocław, Faculty of Chemistry, 14 F. Joliot Curie, 50-383, Wrocław

3′:5′-Cyclic guanosine monophosphate (cGMP) is a cyclic nucleotide of vital biological significance, acting as a second messenger in many signal cascades within human cells. It responds to e.g. cytokines, hormones and neurotransmitters and mediates such processes as excretion, calcium homeostasis, muscle relaxation, and nucleic acid synthesis [1,2]. Despite its vast role in the human body, the solid-state behaviour of cGMP and its salts has not been thoroughly investigated.

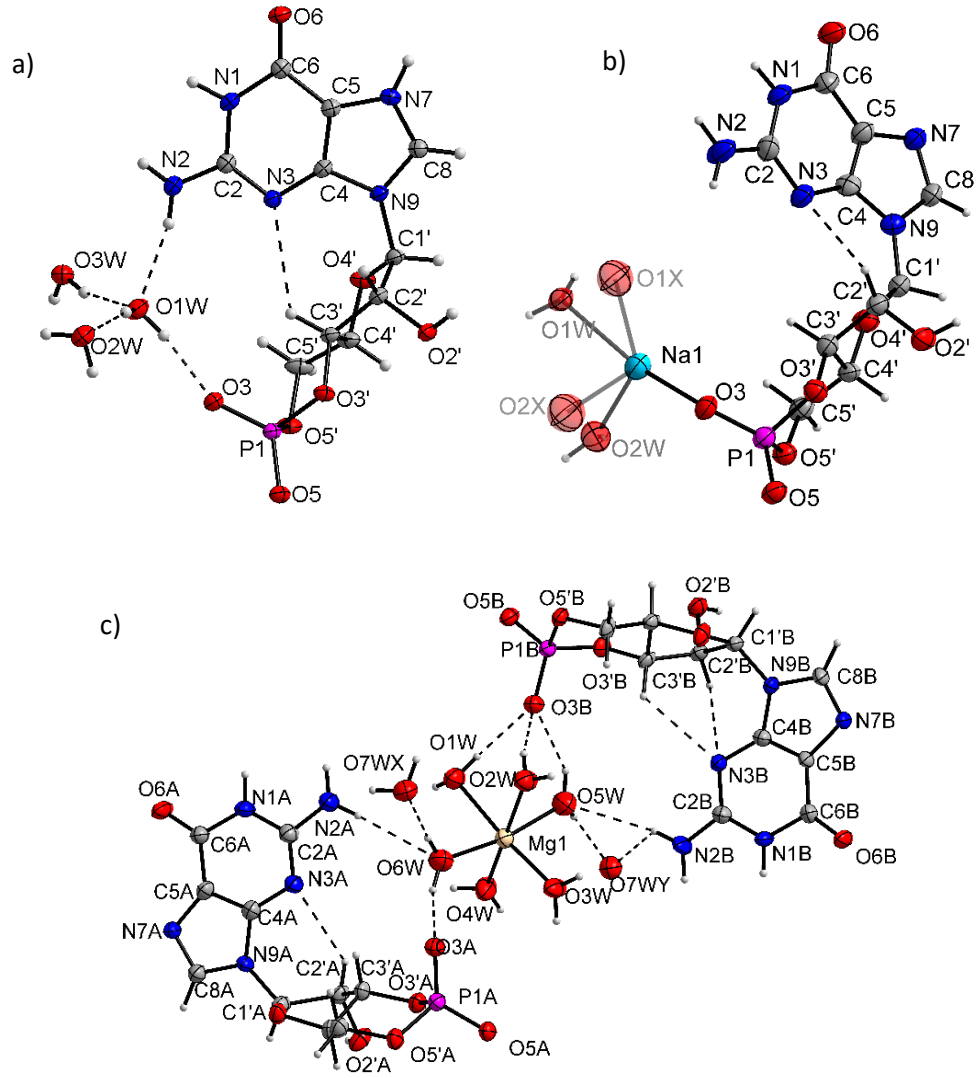

Fig. 1. Asymmetric units of some of the obtained crystals; a) β-cGMP·$3H_2O$, b) Na(cGMP)·$2H_2O$, c) $[Mg(H_2O)_6](cGMP)_2 \cdot H_2O$.

A-29

Dehydration is sometimes employed as a strategy to improve diffraction quality of crystals of macromolecules (such as nucleic acids or proteins). It is however quite uncommon for small organic compounds, such as cGMP. Surprisingly, this study showed that in some cases, partial dehydration of the obtained single crystals yielded new crystalline forms, which diffracted better that their more hydrated counterparts. Using both typical solution crystallization and post-crystallization dehydration, seven new crystalline forms were obtained (see Fig. 1):

(1) cGMP·5H_2O, for which a temperature-driven phase transition was described, and low-temperature phase was determined,
(2) cGMP·4H_2O,
(3) β-cGMP·3H_2O (which may be formed by dehydration of cGMP·5H_2O),
(4) γ-cGMP·3H_2O (formed by dehydration of cGMP·4H_2O),
(5) sodium salt Na(cGMP)·2H_2O (obtained when Na(cGMP)·4H_2O dehydrated),
(6) magnesium salt [Mg(H_2O)$_6$](cGMP)$_2$·3H_2O,
(7) partially dehydrated magnesium salt [Mg(H_2O)$_6$](cGMP)$_2$·H_2O.

During the dehydration of Na(cGMP)·4H_2O crystal, significant rearrangement of sodium coordination sphere along with the formation of new Na–O(cGMP) bonds were observed, while the structurally characterized product of the magnesium salt dehydration revealed no changes in the coordination environment of the Mg^{2+} ion. In all crystals, strong π-π interactions between guanine rings were observed (see Fig. 2), which Sponer *et al.* suggested as a possible explanation for cGMP's unique ability to spontaneously oligomerize under suitable conditions [3].

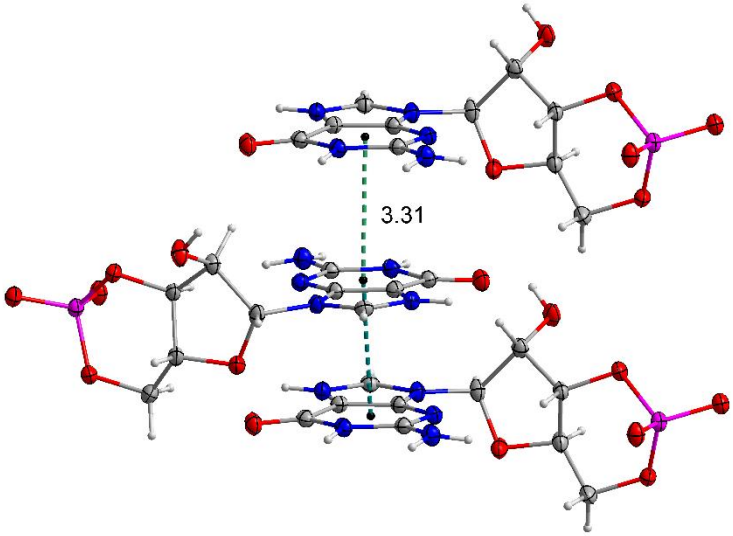

Fig. 2. Distance (Å) between neighbouring guanosine rings in the crystal of β-cGMP·3H_2O.

Literature

[1] A. M. Fajardo, G. A. Piazza, H. N. Tinsley, *Cancers (Basel)*, **6** (2014) 436-458.
[2] N. Pasmanter, F. Iheanacho, M. F. Hashimi, *Biochemistry, Cyclic GMP*. In StatPearls (Internet). StatPearls Publishing, (last updated 2023).
[3] J. E. Sponer, S. J., J. Vyravsky, O. Sedo, Z. Zdrahal, G. Costanzo, E. D. Mauro, S. Wunnava, D. Braun, R. Matyasek, A. Kovarik, *ChemSystemsChem*, **3** (2021) e2100017.

A-30

CRYSTAL STRUCTURE OF $EuNi_5Ge_3$

Bohdana Belan[1], Mariya Dzevenko[2], Marek Daszkiewicz[3], Roman Gladyshevskii[1]

[1] Department of Inorganic Chemistry, Ivan Franko National University of Lviv, Kyryla i Mefodia Str. 6, 79005 L'viv, Ukraine
[2] Kruty Heroes Lviv Lyceum with Intensive Military and Physical Training, Pasichna Str. 68, 79038 L'viv, Ukraine
[3] Institute of Low Temperature and Structure Research, Polish Academy of Sciences, ul. Okólna 2, 50-422 Wrocław, Poland

Interactions of the components in the Er-Ni-Ge ternary system has been studied previously at T = 670 K. According to the authors [1], the eight intermetallic compounds have been found at the temperature of investigation [2]. However, some white area is still in this system. Thus, during the detailed study of the Er-Ni-Ge system the new ternary germanide has been found. Therefore, in the present report we describe the results of the crystal structure investigation of the $EuNi_5Ge_3$ compound, which is the first representative of a new structure type.

A sample of nominal composition $Eu_{11}Ni_{56}Ge_{33}$ was synthesized from high-purity elements (Eu ≥ 99.9 wt.%, Ni ≥ 99.999 wt.%, and Ge ≥ 99.999 wt.%) by arc-melting under a purified argon atmosphere, using Ti as a getter and a tungsten electrode. The alloy was remelted two times to ensure homogeneity. The ingot was annealed at 670 K in an evacuated quartz ampoule for 720 h and subsequently quenched in cold water. The weight loss during the preparation of the sample was less than 1 % of the total mass, which was 2 g. The single crystals were selected by mechanical fragmentation from the sample. They exhibit metallic lustre whereas the ground powders are dark grey. The composition of the investigated single crystal was analyzed by EDS employing a scanning electron microscope (FEINovaNonoSEM 230) equipped with an EDAX Genesis XM4 spectrometer. The experimentally determined composition of the grain is rather close to the composition calculated from the structure refinement. The crystal structure of the $EuNi_5Ge_3$ compound was investigated by X-ray single-crystal diffraction. X-ray diffraction was performed at room temperature on an Xcalibur Atlas CCD diffractometer (Mo$K\alpha$ radiation). The structure was solved by direct methods and refined by the SHELX-2018/3 program package [3] with anisotropic atomic displacement parameters.

The compound crystalizes in its own structure type: space group *Pnma*, Pearson symbol *oS*72, Z = 4; a = 11.2373(3), b = 3.88161(9), c = 24.0927(6) Å, V = 1050.89(4) Å^3; $R1$ = 0.0231, $wR2$ = 0.0395, for 1761 independent reflections with $I > 2\sigma(I)$ and 109 variables. The final atomic positional and displacement parameters of the compound are listed in the Table 1.

The majority of interatomic distances are in good agreement with the sum of atomic sizes. The coordination sphere for the both Eu atoms consists of 23 atoms of all types. The coordination number of nickel atoms are 11-13, and germanium atoms 9-10. The structure of $EuNi_5Ge_3$ germanide can be described as framework from nickel and germanium atoms with whole which are centered by the europium atoms (Fig. 1).

Table 1. Atomic coordinates and thermal displacement parameters for $EuNi_5Ge_3$.

Atom	Wyckoff Site	*x*	*y*	*z*	U_{eq}, Å^2
Eu1	4*c*	0.40011(2)	1/4	0.10226(2)	0.00674(6)
Eu2	4*c*	0.39277(2)	3/4	0.33779(2)	0.00849(6)
Ni1	4*c*	0.60611(6)	1/4	0.41648(3)	0.00796(13)
Ni2	4*c*	0.50197(6)	1/4	0.23256(3)	0.00971(13)
Ni3	4*c*	0.70710(6)	3/4	0.35167(3)	0.00833(13)
Ni4	4*c*	0.40910(6)	3/4	0.00179(3)	0.00802(13)
Ni5	4*c*	0.78410(6)	1/4	0.27448(3)	0.00947(13)
Ni6	4*c*	0.08388(6)	3/4	0.34538(3)	0.00851(13)
Ni7	4*c*	0.19932(6)	1/4	0.40838(3)	0.00818(12)
Ni8	4*c*	0.50982(6)	3/4	0.46799(3)	0.00831(13)
Ni9	4*c*	0.64350(6)	3/4	0.25338(3)	0.00904(13)
Ni10	4*c*	0.27970(6)	3/4	0.48469(3)	0.00951(13)
Ge1	4*c*	0.58638(5)	3/4	0.05708(2)	0.00702(10)
Ge2	4*c*	0.27876(5)	1/4	0.55038(2)	0.00701(10)
Ge3	4*c*	0.18591(5)	1/4	0.31214(2)	0.00756(10)
Ge4	4*c*	0.60194(5)	1/4	0.31940(2)	0.00771(11)
Ge5	4*c*	0.39517(4)	1/4	0.44186(2)	0.00757(10)
Ge6	4*c*	0.39461(5)	3/4	0.20293(2)	0.00897(11)

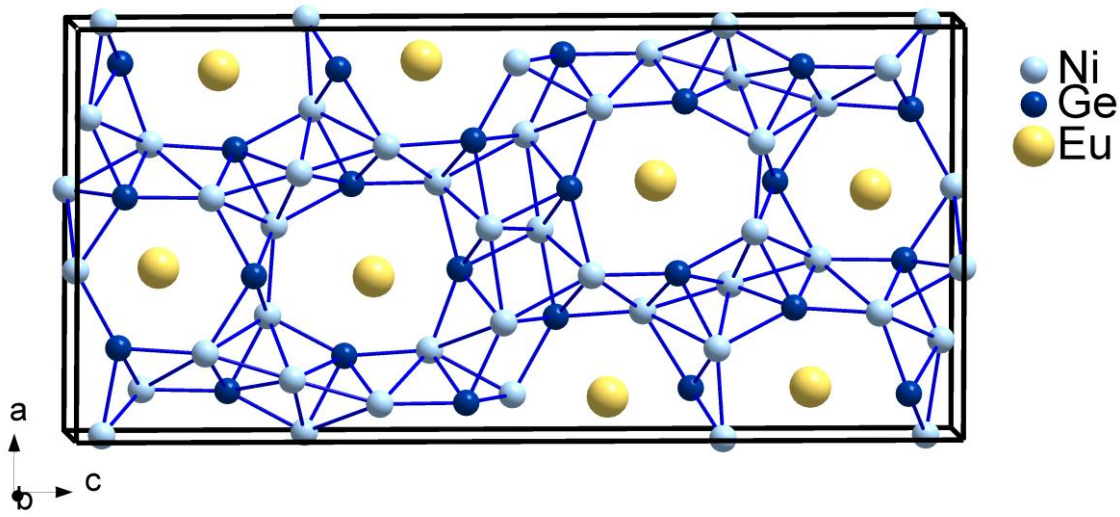

Fig. 1. A projection of the $EuNi_5Ge_3$ unit cell on *ac*-plane and view of the coordination polyhedra of the atoms.

ACKNOWLEDGMENTS. This study was performed under the research international project in Ivan Franko National University of Lviv “Search of new structure types”, registration number: HX-010123

Literatura

[1] Bodak, O.i., Oniskovets, B.D., Goral, O.E.(1987). The Eu-Ni-Ge system. Dopovidi Akademii Nauk Ukrainskoi RSR, Seriya B: Geologichni, Khimichni ta Biologichni Nauki, **8** (1987) 46.
[2] Villars P., Cenzual K., Eds. *Pearson’s Crystal Data: Crystal Structure Database for Inorganic Compounds* (release 2018/19); ASM International®: Materials Park, Ohio (USA), 2018.
[3] G.M. Sheldrick, *Acta Crystallogr. A*, **64** (2015) 3–8.

A-31

CATALYTIC HYDROLYSIS OF GOLD(III) WITH 2-CYANOPYRIDINE COMPLEX, STRUCTURAL ANALYSIS OF REACTION PRODUCTS AND THEIR ANTI-MICROBIAL ACTIVITY ASSESSMENT

Maciej Ejnik[a,*], Karolina Gutmańska[a], Piotr Bruździak[b], Anna Ciborska[a], Anna Brillowska-Dąbrowska[c], Anna Dołęga[a]

[a] *Department of Inorganic Chemistry, Faculty of Chemistry, Gdansk University of Technology, Narutowicza 11/12, 80-233 Gdańsk*
[b] *Department of Physical Chemistry, Faculty of Chemistry, Gdansk University of Technology, Narutowicza 11/12, 80-233 Gdańsk*
[c] *Department of Molecular Biotechnology and Microbiology, Faculty of Chemistry, Gdansk University of Technology, Narutowicza 11/12, 80-233 Gdańsk*

**e-mail: s185339@student.pg.edu.pl*

As a part of our previous study of gold(III) complexes with isomeric cyanopyridines [1] we continued research of chemistry of complex with 2-cyanopyridine as a ligand. We observed formation of different products, depending on complexation reaction conditions. Specifically, the previously reported complex of gold(III) with 2-cynaopyridine was the least favored product, while an ionic pair of tetrachloroauric(III) anion with a cation consisting of two 2-cyanopyridinic rings, with delocalized proton between them was isolated as the main product (Fig. 1, compound **1**). We also discovered, that after prolonged exposure to heat, in the presence of water, another compound is formed, namely a complex of gold(III) and picolinamide as a bidentate ligand (Fig. 1, compound **2**).

Here we report the results of structural analysis of two compounds, previously discussed ionic pair and complex of gold(III) with picolinamide (respectively compound **1** and compound **2**, Fig. 1), as well as their anti-microbial activity assessment.

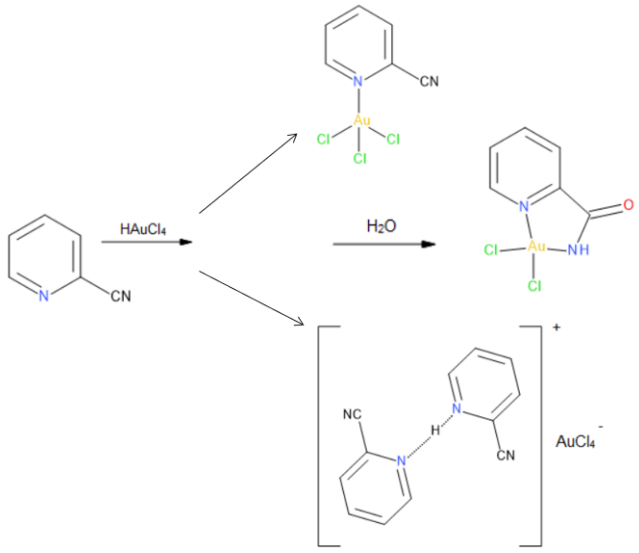

Fig. 1. Different products of the reaction of chloroauric acid with 2-cyanopyridine.

Compound **1** (Fig. 2, left side) crystallizes in a *P*-1 symmetry group of a triclinic system with a = 7.545(2) Å, b = 8.0759(16) Å, c = 15.103(3) Å, α = 96.074(16) °, β= 100,834(3)°, γ = 115.61(2) °. The Au1 atom is bonded to four chlorine atoms by bonds, one of which slightly differs by length: Au1-Cl1 2,272(2) Å, Au1-Cl2 2,271(3) Å, Au1-Cl4 2,279(2) Å, whereas fourth bond is significantly longer Au1-Cl3 2,287(2) Å. The square planar geometry of chloroauric anion remained unchanged in comparison to the chloroauric acid crystalline structure. Interestingly, discussed compound crystallizes in a different system, compared to chloroauric acid - triclinic compared to monoclinic.

Compound **2** (Fig. 2, right side) crystallizes in a $P2_1/c$ symmetry group of a monoclinic system with a = 8.685(5) Å, b = 5.909(3) Å, c = 16,905(8) Å, β= 91,54(5)°. The gold atom is characterized by coordination number C.N. = 4, the geometric index parameter τ_4' [2], for the discussed compound is equal to 0,085, indicating a slightly distorted square planar geometry. The central Au1 atom is bonded to two chlorine atoms by bonds, slightly differing in length (Au1-Cl1 2.2904(16) Å and Au1-Cl2 2.2512(16) Å) and to two nitrogen atoms (Au1-N1 2.024(5) Å and Au1-N2 1.977(4) Å).

Our preliminary results confirm the activity of a gold(III) complex with picolinamide against selected strains of pathogenic bacteria and fungi. The strongest inhibitory effect was observed for the Gram-positive bacteria *S. aureus* and *S. epidermis*. Moderate inhibitory activity was observed for the other bacteria (*E. coli*, *S. enterica*, *C. glabrata*, *P. aeruginosa*).

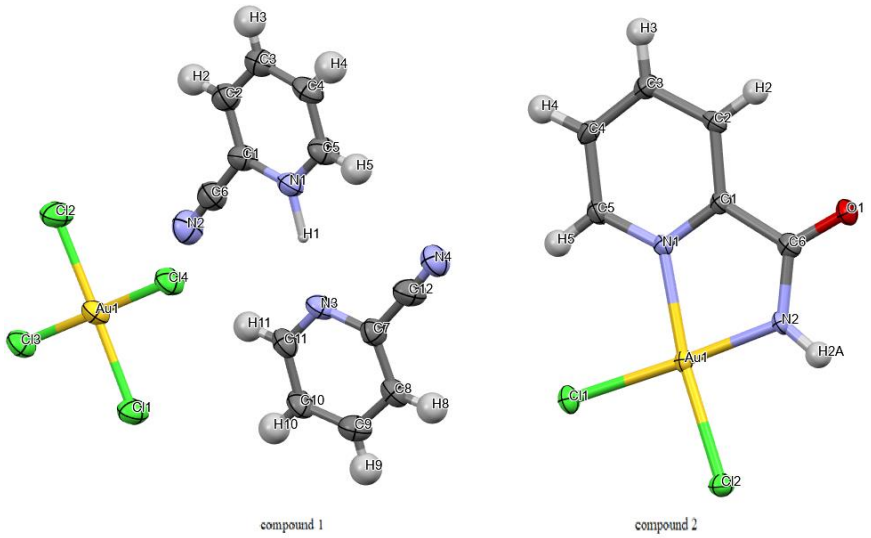

Fig 2. Molecular structures of compound **1** and compound **2**.

Research financed by the "Excellence Initiative - Research University" program of the Gdańsk University of Technology: TECHNETIUM TALENT MANAGEMENT GRANTS 14/1/2022/IDUB/III.4c/Tc.

References

[1] M. Ejnik, A. Ciborska, A. Dołęga, *The results of synthesis and structural analysis of gold(III) complexes with 3-cyanopyridine, and 2-cyanopyridine*. 63 Konwersatorium Krystalograficzne, Wrocław, 29 VI-1 VII 2022, streszczenia, P-13, 60.

[2] D. Rosiak, A. Okuniewski, J. Chojnacki, *Polyhedron*,, **146** (2018) 35.

A-32

TEMPERATURE-CONTROLLED SELF-ASSEMBLY OF FUNCTIONAL SILVER(I) COORDINATION POLYMERS

Julia Fiszer[a], Sabina W. Jaros[a], Chris H. J. Franco[b], Alexander M. Kirillov[b] and Piotr Smoleński[a]

[a] Faculty of Chemistry, University of Wrocław, ul. F. Joliot-Curie 14, 50-383 Wrocław, Poland
[b] Centro de Química Estrutural, Institute of Molecular Sciences, Departamento de Engenharia Química Instituto Superior Tecnico, Universidade de Lisboa, Av. Rovisco Pais, 1049-001 Lisbon Portugal

Coordination polymers (CP) and their porous subgroup known as metal-organic frameworks (MOFs) are important compounds with a broad spectrum of properties, which define their application as luminescent, catalytic, and magnetic materials [1], as well as in the fields of gas storage, drug release, and medicinal chemistry [2,3]. Although self-assembly methods are common for generating functional metal-organic networks, the control over the self-assembly processes, final structural types, and properties is still challenging in many cases and requires further improvement.

Our research is focused on developing functional silver(I)-based coordination polymers. Here, we report the self-assembly synthesis of two new CPs, $[Ag(\mu\text{-dca})(\mu\text{-PTA})]_n$ (**1**) and $[Ag_2(\mu\text{-dca})(\mu_3\text{-dca})(\mu_3\text{-PTA})]_n$ (**2**), driven by a water-soluble aminophosphine, 1,3,5-triaza-7-phosphaadamantane (PTA), and dicyanamide anion (dca^-). The self-assembly process of their formation and the dimensionality of the resulting 2D or 3D structures are controlled by the reaction temperature. The compound **1** obtained at 60 °C crystallizes in the orthorhombic system, space group P*bca*, and consists of 2D V-shaped layers driven by the μ-PTA and μ-dca^- linkers. The self-assembly at 25 °C results in the 3D compound **2** that crystallizes in the monoclinic system, space group $P2_1/c$. In contrast to **1**, the structure of **2** is more complex and composed of two independent crystallographic silver(I) ions in addition to two coordination modes (μ_2- and μ_3-) of dicyanamide(1−) and the μ_3-PTA ligand. Both new silver(I) products were characterized by standard methods, including FT-IR, TGA, elemental analysis, singe-crystal, and powder X-ray diffraction. Bioactivity studies on the obtained coordination polymers are currently in progress.

References

[1] The Chemistry of Metal–Organic Frameworks: Synthesis, Characterization, and Applications (Ed. S. Kaskel), Wiley, 2016.
[2] S. W. Jaros, A. Krogul-Sobczak, B. Bażanów, M. Florek, D. Poradowski, D. S. Nesterov, U. Śliwińska-HilL, A. M. Kirillov, P. Smoleński, *Inorg. Chem.*, **60** (2021) 15435.
[3] T.Baati, L. Njim, F.,Neffati, A. Kerkeni, M. Bouttemi, R. Gref, M. F. Najjar, A. Zakhama, P. Couvreur, C. Serre, P. Horcajada, *Chem. Sci.*, **4** (2013) 1597.

We thank the National Science Center (SONATA Grant No. 2019/35/D/ST5/01155, Poland) and the FCT (PTDC/QUI-QIN/29697/2017, LA/P/0056/2020, and UIDB/00100/2020) for the financial support.

A-33

SYNTEZA I STRUKTURA 2,6-DIHYDROKSY-1,3,5,7-TETRA (DIFENYLOFOSFINOILO)-BICYKLO[3.3.1]NONA-2,6-DIENU

Sławomir Frynas, Daniel Kamiński

Katedra Chemii Organicznej i Krystalochemii, ul. Gliniana 33, 20-614 Lublin

Związki alkenylofosforowe zawierające w swojej strukturze wiązanie C-P to cząsteczki o dużym znaczeniu syntetycznym z powodu ich licznych zastosowań w różnych dziedzinach chemii. Związki te są prekursorami wielu nowych cząsteczek o dużym znaczeniu biologicznym.[1] Podstawione tlenki alkenylofosfin znajdują szerokie zastosowanie w syntezie chemicznej i chemii materiałowej [2,3]. Jedną z uniwersalnych metod syntezy α,β-nienasyconych tlenków winylofosfin okazała się być reakcja Knoevenagela pomiędzy pochodnymi kwasu fosfinoilooctowego **1** i aldehydami [4]. W reakcjach **1** z paraformaldehydem otrzymano z wysokimi wydajnościami niepodstawione tlenki winylofosfin, natomiast w reakcjach **1** z aldehydami aromatycznymi uzyskano oczekiwane α,β-nienasycone tlenki winylofosfin.

Analogiczna reakcja 1,3-bis(difenylofosfinoilo)acetonu **2** z paraformaldehydem miała na celu uzyskanie tlenku **4** posiadającego w swojej strukturze dwa terminalne wiązania podwójne. Nieoczekiwanie jedynym produktem reakcji okazał się być związek o nieznanej strukturze. Wydzielony produkt zanalizowano za pomocą spektroskopii NMR. Zaproponowano dwie struktury produktu **3** i **5**. Analiza rentgenostrukturalna pozwoliła na przypisanie właściwej struktury **3** otrzymanego produktu.

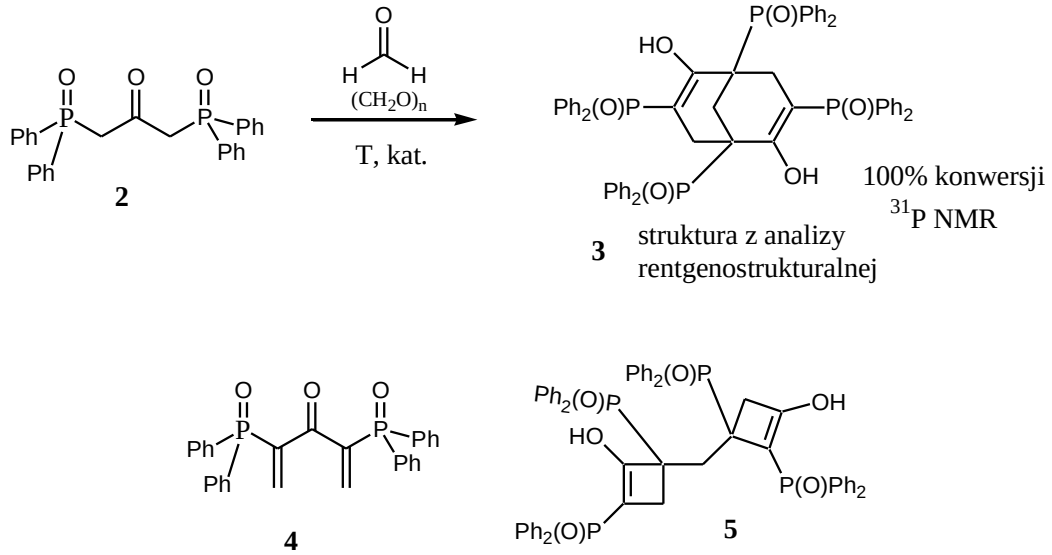

2 **3** **4** **5**

Rys 1. Reakcja 1,3-bis(difenylofosfinoilo)acetonu **2** z paraformaldehydem.

Literatura

[1] G. P. Horsman, D. L. Zechel, *Chem. Rev*., **117** (2017) 5704.
[2] A. M.Gonzalez-Nogal, P. Cuadrado, M. A Sarmentero, *Tetrahedron*, **66** (2010) 9610.
[3] C. Queffelec, M. Petit, P. Janvier, D. A.Knight, B. Bujoli, *Chem. Rev.*, **112** (2012) 3777.
[4] K. Dziuba, S. Frynas, K. Szwaczko, *Synthesis*, **53** (2021) 2142.

A-34

CALCIUM ZIG-ZAG COORDINATION POLYMERS WITH NONSTEROIDAL ANTI-INFLAMMATORY DRUGS (KETOPROFEN AND MEFENAMIC ACID)

Michał Gacki[a], Karolina Kafarska[a], Izabela Korona-Głowniak[b], Patrycja Schab[a], Jakub M. Wojciechowski[c], Wojciech M. Wolf[a]

[a] *Institute of General and Ecological Chemistry, Faculty of Chemistry, Lodz University of Technology, 116 Zeromskiego Street, 90-924 Lodz, Poland,*
[b] *Department of Pharmaceutical Microbiology, Medical University of Lublin, Chodźki 1, 20-093 Lublin, Poland,*
[c] *Rigaku Europe SE, Hugenottenallee 167, 63263 Neu-Isenburg, Germany*

Nonsteroidal anti-inflammatory drugs (NSAIDs) are among the most frequently prescribed pharmaceuticals to reduce pain and inflammation. Their activity is based on the inhibition of cyclooxygenases COX–1 and COX–2 which hamper conversion of the arachidonic acid to prostaglandins and are responsible for anti-inflammatory action [1]. Side effects are related to the well-known ability of COX–1 to prompt gastric irritations [2]. The therapeutic value of those drugs may be improved by their complexation with carefully selected metal cations [3].

This communication presents X-ray structures of three calcium complexes with ketoprofen (Hket) and mefenamic acid (Hmef). Supramolecular structures of all compounds are dominated by one-dimensional (1-D) polymeric zig-zag chains which include carboxylate chelating-bridged (μ_2-η^2:η^1) Ca^{2+} centers.

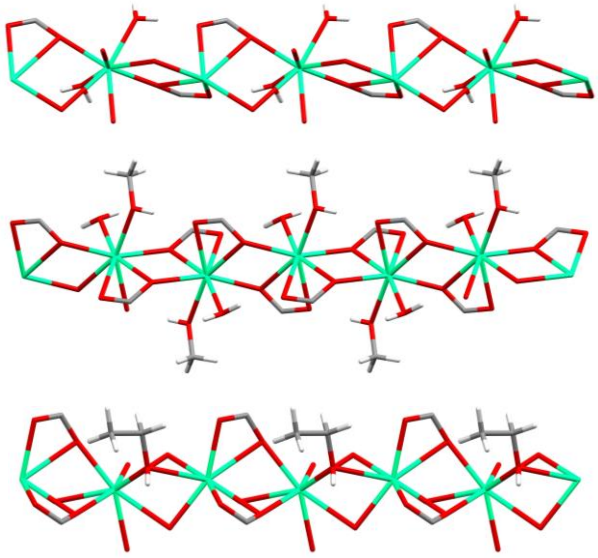

$[Ca(ket)_2 \cdot (H_2O)_2]_n$

$[Ca(mef)_2 \cdot MeOH \cdot H_2O]_n$

$\{[Ca(mef)_2 \cdot EtOH] \cdot H_2O\}_n$

Fig 1. Polymeric zig-zag chains in calcium complexes.

References

[1] S. Wongrakpanich, A. Wongrakpanich, K. Melhado, J. Rangaswami, *Aging Dis.*, **9** (2018) 143–150.
[2] M. Ahmadi, S. Bekeschus, K.D. Weltmann, T. von Woedtke, K. Wende, *RSC Med Chem*., **13** (2022).
[3] C.N. Banti, S.K. Hadjikakou, *Eur J Inorg Chem*., **2016** (2016) 3048–3071.

A-35

TYRAMINE AS A PROLIFIC COFORMER IN CRYSTAL ENGINEERING

Szymon Grabowski[a,b] and Marlena Gryl[a]

[a] Faculty of Chemistry, Jagiellonian University, Gronostajowa 2, Kraków, 30-387, Poland
[b] Doctoral School of Exact and Natural Sciences, Jagiellonian University, Prof. Łojasiewicza 11, Kraków, 30-348 Poland

Prolific cofomers in crystal engineering can be defined as building blocks showing a remarkable ability to create multicomponent solids (co-crystals/salts) with various components. Such molecules are extremely interesting from the crystal engineering perspective as they enable the design of materials containing molecules unwilling to cocrystallize. It is vital to understand the nature of prolific coformers, particularly the interactions formed in their structures. This analysis might lead to a better understanding and controlling the crystallization process.[1,2,3]

Tyramine is a molecule that crystallizes with many components[4], creating a variety of salts and co-crystals reported in the Cambridge Structural Database. Here we present crystal structures of two new organic salts containing tyramine: I – with L-pyroglutamic acid; III – with aminohippuric acid. Results were compared with the known crystal phase of tyraminium (R)-mandelate. Asymmetric units are shown in Fig. 1. In each case, proton transfer occurred between carboxylic and amino groups.

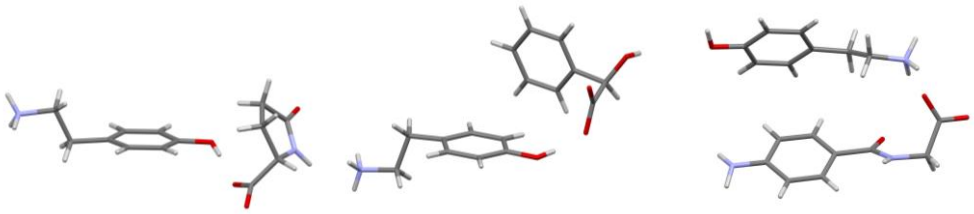

Figure 1. Asymmetric units of (I) – left, (II) – middle and (III) – right.

Structure analysis results showed that the tyramine alkyl chain's conformational flexibility contributes to its prolific performance. In (I), (II) and (III), the torsion angle between atoms in tyramine alkyl chain is different, which indicates the capability of tyraminium cation to fit to another component during molecular self-organization. For each structure also Hirshfeld surface analysis was performed and results were compared to examine possible interaction schemes created by tyramine. Fingerprint plots are shown in Fig. 2.

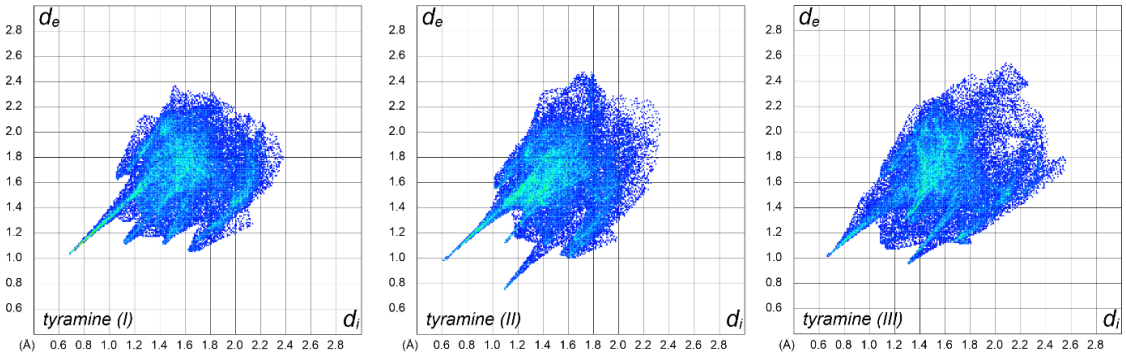

Figure 2. Fingerprint plots for tyramine cation in (I), (II) and (III).

Some differences are visible in the low d_i and d_e values region, where the characteristic spikes should occur. $O_i \cdots H_e$ interactions nature varies in each case: for (I) they are hydrogen bonds, for (II) – weak C—H···O interactions and for (III) – both of them.

For (I) and (II), experimental and theoretical electron density analysis was performed to quantify intermolecular interactions. For (III), only topological analysis based on theoretical data was conducted because the obtained crystals were unsuitable for high-resolution X-ray diffraction measurements. Estimated interaction energies and values of electron density at critical points differed for tyramine cation in each structure. Especially for (II), tyramine···acid interactions are of less importance for crystal packing than for (I) and (III), where these interactions are crucial. It shows that tyramine demonstrates not only conformational but also synthon formation flexibility which is another vital factor causing its prolific abilities.[5]

Literatura

[1] Zhang, S.-W. & Yu, L. (2015). Vol. *Advances in Organic Crystal Chemistry: Comprehensive Reviews 2015*, edited by R. Tamura & M. Miyata. pp. 337–353. Springer.
[2] Zhang, S. W., Harasimowicz, M. T., De Villiers, M. M. & Yu, L. *J. Am. Chem. Soc.*, **135** (2013) 18981–18989.
[3] Zhang, S. W., Kendrick, J., Leusen, F. J. J. & Yu, L. *J. Pharm. Sci.i*, **103** (2014) 2896–2903.
[4] Briggs, N. E. B., Kennedy, A. R. & Morrison, C. A. *Acta Crystallogr. Sect. B Struct. Sci.*, **68** (2012) 453–464.
[5] Grabowski, S. & Gryl, M., in preparation for publication.

A-36

STRUKTURA KRYSTALICZNA FENAZYNY Z KWASEM 3,4,5-TRIHYDROKSYBENZOESOWYM

Natalia Halaba, Kinga Wzgarda-Raj

Wydział Chemii Uniwersytetu Łódzkiego, Zakład Chemii Teoretycznej i Strukturalnej, ul. Pomorska 163/165, 90-236 Łódź

Fenazyna to heterocykliczny wielopierścieniowy związek chemiczny z grupy barwników azynowych, zbudowany z dwunastu węgli, ośmiu wodorów oraz dwóch azotów. Wykorzystywana jest do produkcji farmaceutyków, barwników oraz do uzyskania wtórnych wodnych baterii cynkowych [1-2]. Pochodne tego związku wykazują szeroki zakres właściwości biologicznych, takich jak: przeciw-drobnoustrojowe, przeciwnowotworowe, przeciwutleniające, przeciwmalaryczne, czy neuroprotekcyjne [1].

Celem przeprowadzonych badań było otrzymanie nowych struktur krystalicznych fenazyny z wybranymi kwasami organicznymi. Wykonano kilka krystalizacji w wyniku których uzyskano kokryształ fenazyny z kwasem 3,4,5-trihydroksybenzoesowym oraz cząsteczkami wody. Ponadto, wykonano analizę geometryczną wiązań wodorowych.

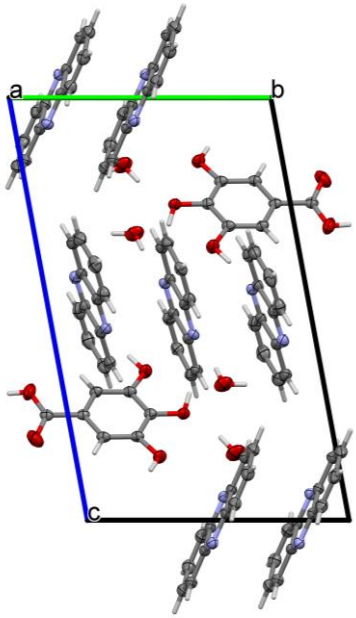

Rys. 1. Upakowanie kokryształu w komórce elementarnej wzdłuż kierunku krystalograficznego [100].

Literatura

[1] A. Chaudhary, J.M. Khurana, *Research on Chemical Intermediates*, **44** (2018) 1045.
[2] Q. Wang, Y. Liu, P. Chen, *Journal of Power Sources*, **468** (2020) 228401.

A-37

SYNTHESIS AND CRYSTAL STRUCTURE OF RHENIUM(I)-M(I) (M = K OR Na) COORDINATION POLYMERS

Rahman Bikas[a], Neda Heydari[b], Tadeusz Lis[c]

[a] Department of Chemistry, Faculty of Science, Imam Khomeini International University, 34148-96818, Qazvin, Iran
[b] Department of Chemistry, Faculty of Science, University of Zanjan, Zanjan, Iran
[c] Faculty of Chemistry, University of Wroclaw, Joliot-Curie 14, Wroclaw 50-383, Poland

Cyanide is a powerful bridging ligand that can strongly coordinates to the metal ions and show interesting interactions in the structure of the coordination compounds. Cyanide coordination compounds have been mainly synthesized by using its salts with various metal ions (like KCN, NaCN, $KAg(CN)_2$, CuCN, *etc*.) and due to this, it can strongly form mixed metal coordination compounds. Recently, we have reported the crystal structure of mixed metal cyandio bridged Re(I)-Ag(I) [1] and Re(I)-Cu(I) [2] coordination compounds. Here, we describe the synthesis, crystal structure and spectroscopic properties of two mixed metal Re(I)-M(I), M = K or Na, coordination polymers with general formular of $[ReK(PPh_3)_2(CO)_2(\mu\text{-}CN)_2(\mu\text{-}OHCH_3)_2(CH_3OH)]_n$ (**1**) and $[ReNa(PPh_3)_2(CO)_2(\mu\text{-}CN)_2(\mu\text{-}OHCH_3)_2(CH_3OH)]_n$ (**2**). These 1D coordination polymers were synthesized by the reaction of KCN or NaCN with $[Re(PPh_3)_2(CO)_2(OAc)]$ under reflux condition in methanol solvent. The colorless single crystals of these compounds were obtained by thermal gradient method. The air stable crystals were characterized by spectroscopic methods and their structures were determined by single crystal X-ray analysis. Structural studies indicated that these compounds are cyanido bridged Re(I)-M(I) coordination polymers. Two Re and two M metal ions (M = K or Na) are connected by four cyanide bridges to form a rectangular like Re_2-M_2 unit. This unit is further connected to the neighboring units by methanol bridges to form a 1D coordination polymer (see Figure 1). In the crystal structure of compound **1** strong C-K interaction can be observed between C=C bond of one of the phenyl rings of PPh_3 ligand and potassium ion which further stabilizes the crystal structure of this compound. This interaction is absent in the structure of compound **2** that has a Na ion instead of K.

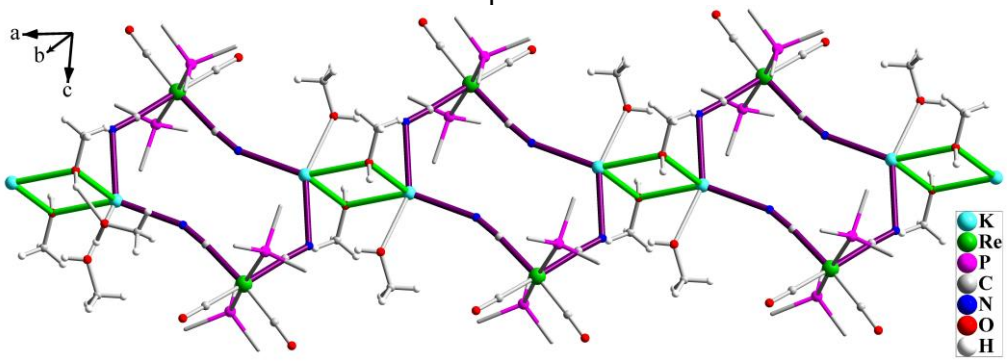

Fig. 1. 1D polymeric chain of compound **1**. Phenyl rings of PPh_3 are omitted for clarity.

References

[1] M.K. Krawczyk, R. Bikas, M.S. Krawczyk, T. Lis, *CrystEngComm*, **19** (2017) 3138-3144.
[2] M.K. Krawczyk, R. Bikas, M.S. Krawczyk, T. Lis, *J. Organomet. Chem*., **908** (2020) 121065.

A-38

NEW CRYSTAL STRUCTURES OF NORFLOXACIN

Valeryia Hushcha, Lilianna Chęcińska

Faculty of Chemistry, University of Lodz, Pomorska 163/165, 90-236 Łódź

Quinolones, as well as their derivatives fluoroquinolones, are a large group of compounds that contain a 4-quinolone moiety. They are characterized by a wide range of action, easy bioavailability, and high safety; therefore, these compounds have been readily used in human and veterinary medicine for over half a century [1].

The mechanism of action of quinolones is to inhibit DNA synthesis by blocking enzymes in bacterial cells. Inhibition of the activity of enzymes leads to DNA damage and blockage of numerous cellular processes, which in turn leads to the death of a bacterial cell. Therefore, quinolones are classified as bactericidal drugs [2].

Norfloxacin (1-ethyl-6-fluoro-1,4-dihydro-4-oxo-7-(1-piperazinyl)-3-quinoline-carbo-xylic acid, NFX) (Fig.1) belongs to fluoroquinolone antibiotics; it is active against Gram-negative and Gram-positive bacteria. It is widely prescribed in respiratory and urinary tract infections [3].

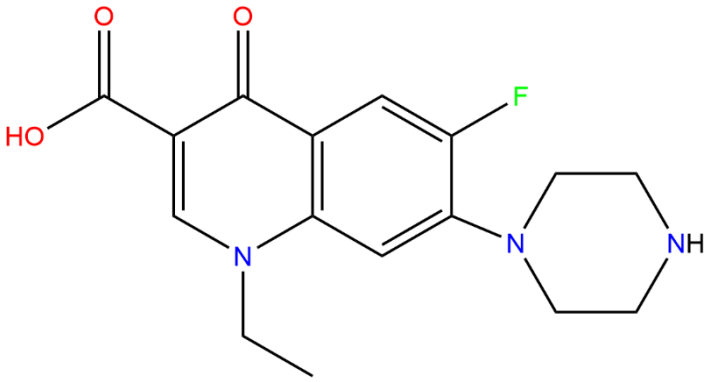

Fig. 1. Structure of norfloxacin.

The aim of the presented research was to obtain new multicomponent crystals of norfloxacin with pyridine-2,3-dicarboxylic acid, pyridine-2,6-dicarboxylic acid and pyridazine-3-carboxylic acid; their crystal and molecular structures have been determined using single-crystal X-ray diffraction analysis.

Literatura

[1] S. Roy, N. R. Goud, N. J. Babu, J. Iqbal, A. K. Kruthiventi, A. Nangia, *Crystal Growth & Design*., **8** (2008) 4343–4346
[2] C. M. Oliphant, G. M. Green, *Am. Fam. Physician*., **65** (2002) 455.
[3] P. C. Appelbaum, P. A. Hunter, *Int. J. Antimicrob. Agents*., **16** (2000) 5–16.

A-39

2,2'- DITIOBISPIRAZYNA – STRUKTURA KRYSTALICZNA I ANALIZA KONFORMACYJNA

Natallia Husik, Kinga Wzgarda-Raj, Justyna Dominikowska, Agnieszka Rybarczyk-Pirek

Katedra Chemii Fizycznej, Wydział Chemii, Uniwersytet Łódzki, Pomorska 163/165, 90-236 Łódź

Wiązania disiarczkowe biorą udział w stabilizacji struktury trzeciorzędowej białek. Wiązania te utworzone pomiędzy dwiema grupami tiolowymi cysteiny, nie tylko stabilizują natywną strukturę białka, ale także zapobiegają fałdowaniu się cząsteczki w przypadku nieprawidłowego sparowania reszt cysteinowych [1]. Powszechnie występujące w różnych białkach wiązania disiarczkowe są biosyntetyzowane zarówno w komórkach prokariotycznych, jak i eukariotycznych. Z tego względu trudno przecenić znaczenie wymiany tiol-disiarczek w procesach biochemicznych [2].

Wcześniejsze badania wykazały, że *N*-tlenek 2-merkaptopirydyny po kokrystalizacji z jodem ulega dimeryzacji do obojętnej lub półprotonowanej formy disiarczkowej [3][4]. Także merkaptopirydyny ulegają podobnej spontanicznej kondensacji. Fotoliza może prowadzić do powstawania disiarczków nawet bez dodatku jodu, co potwierdza kokrystalizacja merkaptopirazyny z tiomocznikiem. W wyniku tej reakcji otrzymano tytułowy związek. Poster prezentuje wyniki badań rentgenograficznych oraz analizy konformacyjnej 2,2'-ditiobispirazyny. Celem prowadzonych prac było sprawdzenie czy związek ten może być potencjalnym reagentem dla reakcji wymiany typu tiol-disiarczek zgodnie z mechanizmem S_N2.

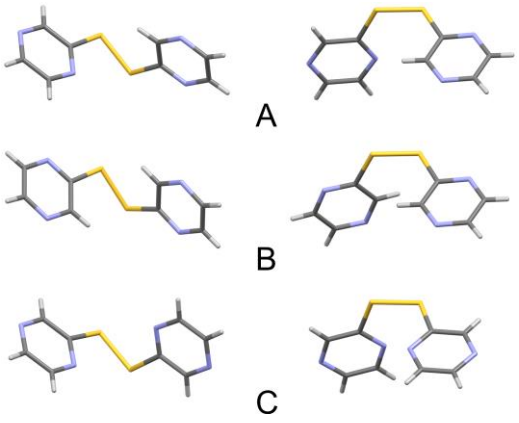

Rys. 1. Struktury przestrzenne trzech różnych konformerów 2,2'-ditiobispirazyny.

Literatura

[1] Sevier, C. S. & Kaiser, C.A., *Nat. Rev. Mol. Cell Biol.*, **3** (2002) 836–847.
[2] Cheng, Z., Zhang, J., Ballou, D. P. & Williams, C. H., *Chem. Rev.*, **111**(9) (2011) 5768–5783.
[3] Witt, D., SYNTHESIS, **16** (2008) 2491–2509.
[4] Wzgarda-Raj, K., Rybarczyk-Pirek**,** A.J., Wojtulewski, S., Pindelska, E. & Palusiak, M., *Structural Chem.*, **30** (2019) 827-833.

A-40

SUPRAMOLECULAR CHEMISTRY OF MAGNESIUM PHTHALOCYANINE WITH ETHYLENEDIAMINE

Jan Janczak

Institute of Low Temperature and Structure Research, Polish Academy of Sciences, Okólna 2, 50-442 Wrocław,

The two axially ligated magnesium phthalocyanine derivatives, MgPc(EDA) and MgPc(H_2O), were obtained directly by thermal reaction of MgPc in ethylenediamine (EDA) solution. Both complexes, MgPc(EDA) and MgPc(H_2O), co-crystallize with the water molecule in the centrosymmetric space group ($P2_1/c$) of the monoclinic system yielding good-quality single crystals **1**. Presence in the crystals **1** the MgPc(H_2O) results from the high affinity of MgPc to trace of water in the solvent as well as due to the high affinity of MgPc to moisture in air. The axially substituted magnesium phthalocyanine derivatives, MgPc(EDA) and MgPc(H_2O), are, as expected, non-planar metallophthalocyanines, and interact with each other through a solvated water molecule to form supramolecular aggregates linked by N–H···O and O–H···N hydrogen bonds (Fig. 1).

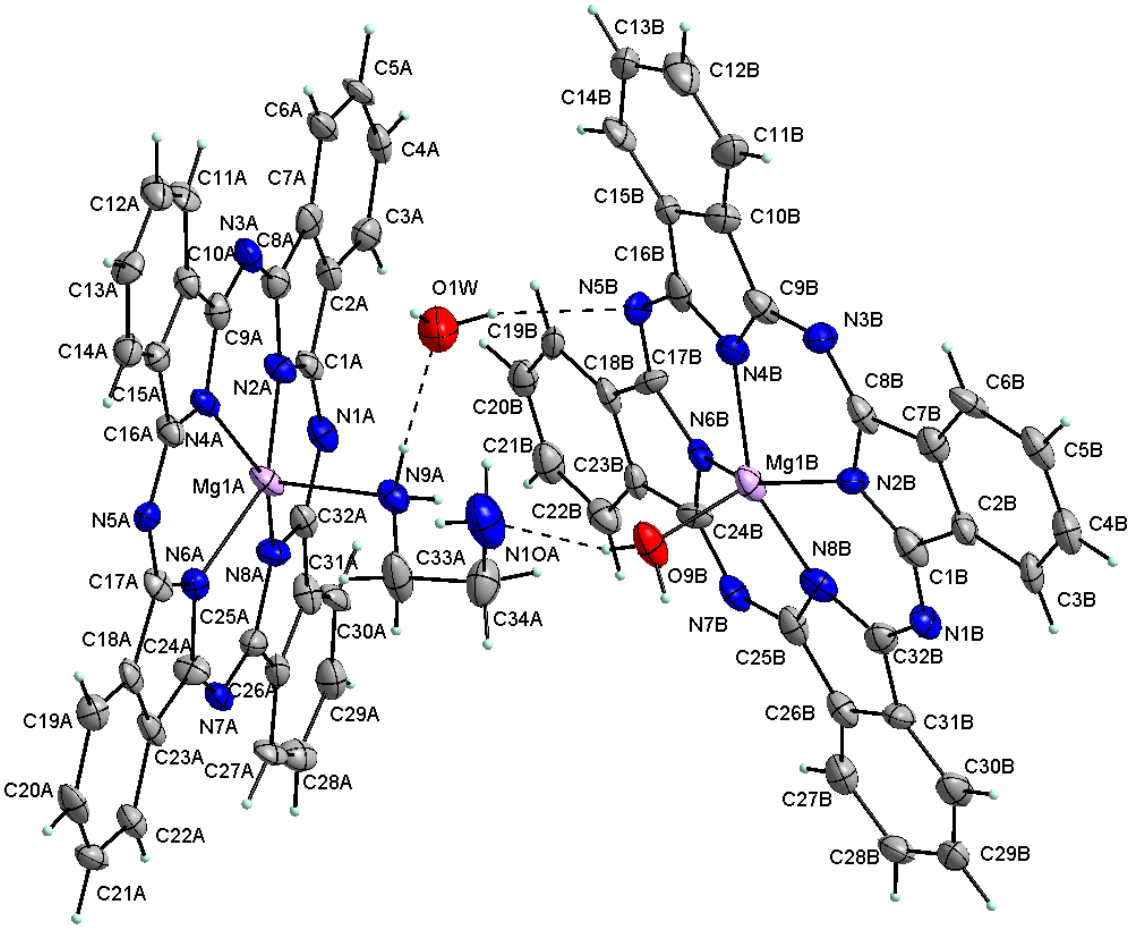

Fig. 1. View of the asymmetric unit of **1** with the labelling scheme. Anisotropic displacement parameters are at the 50% probability level. H atoms represent the circle with arbitrary radii.

The supramolecular arrangement of non-planar MgPc derivatives in the crystal is governed by interactions between the polar ones with the non-zero dipole moment of both molecules, MgPc(EDA) and MgPc(H_2O), and with the lattice water molecules *via* N—H···O and O—H···N hydrogen bonds. Such an arrangement is characterized by the reduction of π···π interactions and the improvement of the inter-system penetration in relation to the parent MgPc, which results in an increase in its solubility and improvement of photophysical and photochemical properties.

The aggregation behavior of the MgPc(EDA) and MgPc(H_2O) complexes building crystals **1** in EDA and ethanol solutions was investigated. The MgPc(EDA) and MgPc(H_2O) complexes building crystals **1** in an ethanol solution are stable, while in the EDA solution, one of them undergoes demetallation with formation of a metal-free phthalocyanine, since the UV-Vis absorption spectrum versus time shown additional electronic absorption band in the region known as the Q-band which is typical for the spectrum of H_2Pc (Fig. 2.).

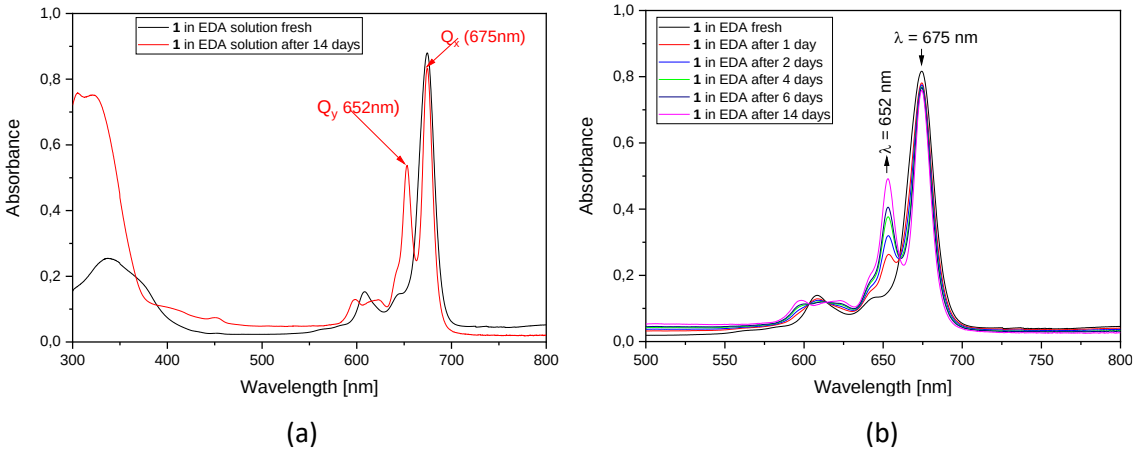

Fig. 2. Optical absorption spectra of **1** in fresh EDA solution and after 14 days (a) and the changes in the Q spectral region after one and after several days (b).

Besides, the UV–Vis spectroscopic characterization of the crystals **1** in solutions, the diffuse reflectance spectroscopic (DSR) characterization on the solid sample of **1** was performed. The DSR spectra of **1** exhibit broad bands with a small blue-shift that might be attributed to a larger exciton coupling resulting from closer contacts between the molecules than in solution. In order to support and verify the experimental results, the DFT and time-dependent (TD) DFT calculations were performed. The results will be discussed and presented.

A-41

INDUKOWANE WROSTEM CIŚNIENIA PRZEJŚCIA FAZOWE TYPU SINGLE-CRYSTAL-TO-SINGLE-CRYSTAL W KOMPLEKSIE ARYLOACETYLENKU ZŁOTA(I) Z TRIETYLOFOSFINĄ

Róża Jastrzębska, Anna Makal

Wydział Chemii Uniwersytetu Warszawskiego, ul. Pasteura 1, 02-093 Warszawa

Jednym z celów pomiarów dyfrakcyjnych pod zwiększonym ciśnieniem jest obserwowanie przejść fazowych typu single-crystal-to-single-crystal (SCSC). Mogą one zajść wtedy, gdy w strukturze związku tworzącego sieć krystaliczną możliwe są zmiany konformacyjne o niskiej energii, wymagające małej zmiany w rozmiarze i kształcie [1]. Skutkuje to powstaniem konformacyjnych polimorfów, których właściwości mogą się między sobą różnić. Istotne więc wydaje się poszukiwanie takich ugrupowań, które umożliwiałyby przejścia SCSC. Przykładowym może być grupa trietylofosfinowa, mogąca przyjąć 7 podstawowych konformacji. W 2009 roku Ellis et al. [2] na podstawie obliczeń zaproponowali niskoenergetyczne ścieżki jej konwersji. W literaturze brakuje jednak potwierdzenia, jak przebiegają zmiany konformacyjne ugrupowania trietylofosfinowego indukowane wzrostem ciśnienia.

W ramach pracy przeprowadzono eksperymenty dyfrakcji rentgenowskiej dla luminescencyjnego kompleksu p-metoksyarylacetylenku złota(I) z trietylofosfiną w zakresie ciśnień 0-3.3 GPa. Zaobserwowano przemiany fazowe typu SCSC przy ok. 0.5 GPa oraz 2.2 GPa. Co ciekawe, druga przemiana fazowa zależy od zastosowanego medium przenoszącego ciśnienie. Podczas sesji plakatowej zostaną przedstawione otrzymane odmiany polimorficzne i różnice między nimi. Analiza obejmie przede wszystkim na zmianach parametrów komórki elementarnej, krystalograficznych elementów symetrii obecnych w strukturze oraz konformacyjnych grupy trietylofosfinowej.

Badania finansowane z grantu OPUS nr DEC-2021/41/B/ST4/02760 Narodowego Centrum Nauki.

Literatura

[1] M. Castro et al., *Acta Cryst. C*, **73** (2017) 731–742.
[2] D. Ellis et al., *Dalton Trans.* (2009) 10436–10445.

A-42

STRUCTURAL STUDIES OF NEW SULFUR DERIVATIVES OF URACIL CONNECTED THROUGH DISULFUR BRIDGE

Michał Dominik Kamiński[1] , Kunal Kumar Jha[1] , Damian Trzybiński[1] , Adam Mieczkowski[1] and Paulina Maria Dominiak[1]

[1] Biological and Chemical Research Centre, Department of Chemistry, University of Warsaw, Żwirki i Wigury 101, 02-089 Warszawa
[2] Institute of biochemistry and biophysics Polish Academy of Sciences, Pawińskiego 5A, 02-106 Warszawa

The pyrimidine bases derivetives are known as medicaments in pharmacological therapies against cancer, insomnia or liver disorders. Howerver, searches for new potential drugs continues. One of new, untypical in their structure derivatives of pyrimidine are oligocyclic uracil sulfur compunds, which pyrimidine rings are bound through disulfur bridges. Thanks to this work we were able to describe three such molecules: F-10, KR2 and KR5 [Fig.1]. The mechanism of their forming is not yet known, however, structural studies of their crystals may play a key role to its understanding.

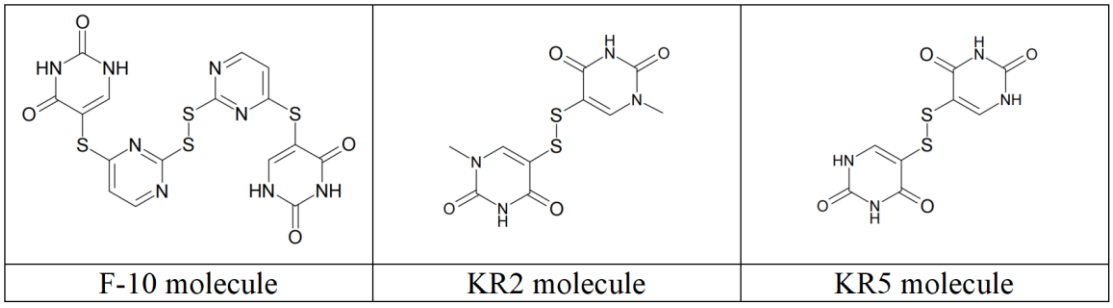

Fig. 1. Atomic structure of F-10, KR2 and KR5 molecules.

In this work, we focused on determining crystal structure of our three uracil sulfur derivatives, including the description of their geometry and non-covalent bonds such as hydrogen, halogen and chalcogen bonds [1]. For this purpose we performed single crystal XRD measurements for crystals of the above molecules. We enriched standard geometry analysis with the Hirshfeld surface analysis [2]. Also, during our study we discovered, that KR2 molecule formed a new polymorph as compared to the structure reported in 1970 [3].

References

[1] Alkorta, I., Elguero, J., Frontera, A., *Crystals*, **10**, 3 (2020) 180.
[2] Tan, S. L., Jotani, M. M., Tiekink, R. T., *Acta Crystallogr. E*, **75**, 3 (2019) 308.
[3] Shefter, E., *J. Chem. Soc. B*, **5** (1970) 903

A-43

CRYSTAL AND MOLECULAR STRUCTURE OF NOVEL PHENOXYACETYLTHIOSEMICARBAZIDES WITH POTENTIAL BIOLOGICAL ACTIVITY

Zbigniew Karczmarzyk[1], Waldemar Wysocki[1], Paweł Kozyra[2] and Monika Pitucha[2]

[1] Faculty of Science, Siedlce University of Natural Sciences and Humanities, 3 Maja 54, 08-110 Siedlce
[2] Independent Radiopharmacy Unit, Medical University of Lublin, Chodzki 4a, PL-20093 Lublin, Poland

Numerous epidemiological studies report an increased risk of developing prostate cancer in patients with melanoma and an increased risk of developing melanoma in patients with prostate cancer [1-3]. Based on our previous studies demonstrating the high anticancer activity of thiosemicarbazides [4,5], we synthesized a series of phenoxyacetylthiosemicarbazide derivatives and some of them acting as potential dual-ligands for both cancer, which was confirmed in vitro tests on four melanoma and prostate cancer cell lines [6].

Here we report the synthesis and crystal and molecular structure of three new phenoxyacetylthiosemicarbazides **1**, **2** and **3** with R = 2-ClC_6H_4, 2-IC_6H_4, 2,4-$Cl_2C_6H_3$, respectively.

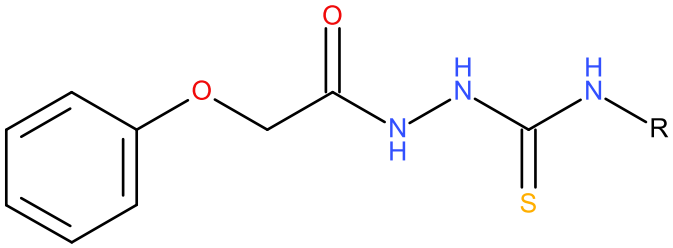

The theoretical calculations using DFT method were undertaken to investigate the energetic, electronic and conformational preferences of searched derivatives.

References

[1] A. Patasius, V. Urbonas, G. Smailyte, *Int J Environ Res Public Health*, **16** (2019) 3915.
[2] S. Caini, M. Boniol, E. Botteri, G. Tosti, B. Bazolli, W. Russell-Edu, F. Giusti, A. Testori, S. Gandini, *Journal of Dermatological Science*, **75** (2014) 3.
[3] P. Acharya, M. Mathur, *Cancer Med*., **9** (2020) 3604.
[4] P. Kozyra, A. Kaczor, Z. Karczmarzyk, W. Wysocki, M. Pitucha, *Struct Chem.* (2023). https://doi.org/10.1007/s11224-023-02152-w.
[5] P. Kozyra, A. Korga-Plewko, Z. Karczmarzyk, A. Hawrył, W. Wysocki, M. Człapski, M. Iwan, M. Ostrowska-Leśko, E. Fornal, M. Pitucha, *Biomolecules* **12** (2022) 151.
[6] P. Kozyra, G. Adamczuk, Z. Karczmarzyk, J. Matysiak, B. Podkościelna, E. Humeniuk, W. Wysocki, A. Korga-Plewko, B. Senczyna, M. Pitucha, *Toxicol. Appl. Pharmacol.* (2023) in press.

A-44

STRUCTURAL DIVERSITY OF HYDRATED TENOFOVIR

Oskar Kaszubowski, Katarzyna Ślepokura

Faculty of Chemistry, University of Wrocław, 14 F. Joliot-Curie, 50-383 Wrocław, Poland

One of the most commonly used groups of antiviral drugs are antimetabolites. These compounds are able to disturb the process of replication or transcription in cells due to their high structural similarity to natural analogues, most often nucleobases, nucleosides or nucleotides [1–3]. One of them is tenofovir (Fig. 1), which has been used to treat HIV infection or hepatitis B for over 20 years [4,5]. Currently, in pharmacy, much attention is paid to the search for new forms of known drugs with improved properties (better solubility or bioavailability). Many of them are solvates, mainly hydrates [6,7].

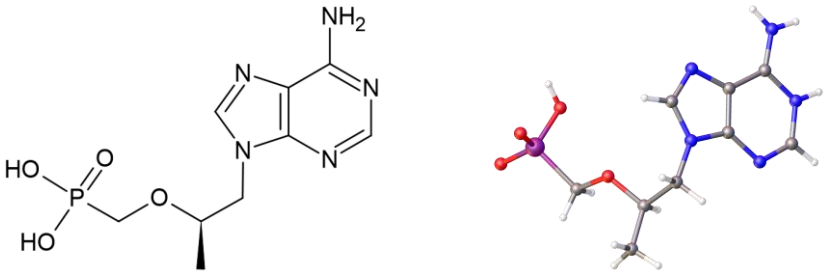

Fig. 1. Chemical (in neutral form; left) and molecular (in zwitterion form; right) structure of tenofovir.

It is worth noting, that the crystal structure of tenofovir has not been reported. Only three crystal structures of its prodrug (disoproxil) are deposited in the Cambridge Structural Database. We obtained several crystalline forms of tenofovir with varying degree of hydration (TEN·xH$_2$O, x: 1–5.5) by crystallization from an aqueous solutions and by thermally induced dehydration. In most of the examined crystals, there was a considerable disorder of water molecules, although in a few of them, including the most hydrated form (TEN·5.5H$_2$O), the disorder of the solvent did not occur. We also observed that solvent disorder seems to affects the crystal architecture, especially within adjacent layers of tenofovir zwitterions and water molecules (Fig. 2).

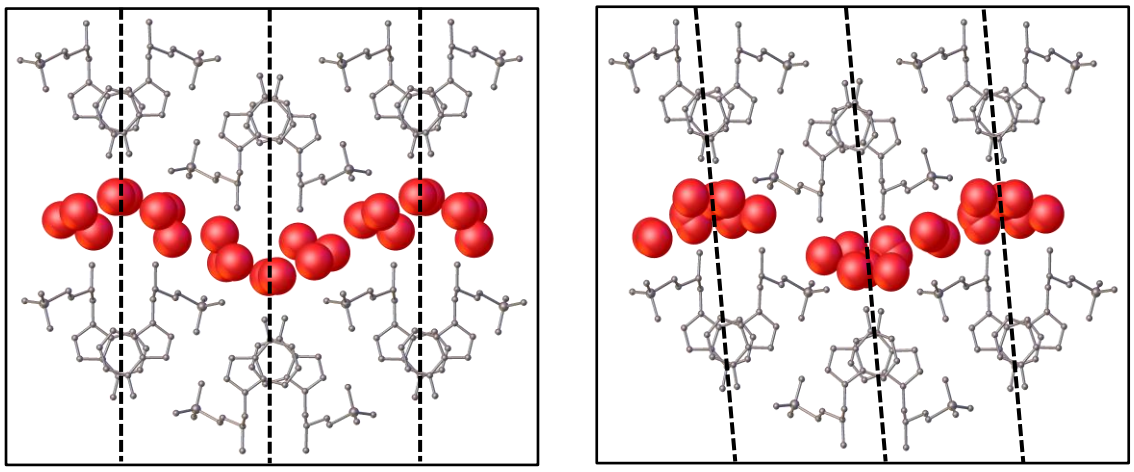

Fig. 2. Relative position of tenofovir zwitterions layers (marked in grey) relative to each other in crystal with ordered (left) and disordered (right) water molecules (marked in red). Both crystals are orthorhombic, $P2_12_12_1$ space group.

References
[1] H. H. Balfour, *NEJM*, **340** (1999) 1255–1268.
[2] E. D. Clercq, *Nat. Rev. Drug Discov*., **1** (2002) 13–25.
[3] D. Warnke, J. Barreto, Z. Temesgen, *J. Clin. Pharmacol*., **47** (2007) 1466–1598.
[4] A. Ustianowski, J. E. Arends, *Infect. Dis. Ther*., **4** (2015) 145–157.
[5] B. P. Kearney, J. F. Flaherty, J. Shah, *Clin. Pharmacokinet*., **43** (2004) 595–612.
[6] A. M. Healy, Z. A. Worku, D. Kumar, A. M. Madi, *Adv. Drug Deliv. Rev*., **17** (2017) 25–46.
[7] E. Jurczak, A. H. Mazurek, Ł. Szeleszczuk, D. M. Pisklak, M. Zielińska-Pisklak, *Pharmaceutics*, **12** (2020) 959.

A-45

CRYSTAL STRUCTURE OF A MONONUCLEAR ZINC(II) COMPLEX WITH SCHIFF BASE

Hubert Kleinschmidt, Anna Dołęga and Magdalena Siedzielnik

Department of Inorganic Chemistry, Faculty of Chemistry, Gdansk University of Technology, G. Narutowicz 11/12, 80-233 Gdańsk

From catalysts to corrosion inhibitors and antiseptics, Schiff bases and their metallic complexes boast a broad range of applications. With each passing year, new synthesis methods with properties of these compounds are discovered by the scientific community. Notably, zinc complexes have demonstrated use in catalyzing polymerization reactions as well as in light-emitting diodes [1-4].

Within this study, new mononuclear complex **C1** with the formula of [Zn(**L1**)$_2$] (**HL1**: 2-(4-methylpyridin-2-ylimino)methyl)-6-methoxyphenol) has been synthesised and characterized by X-ray diffraction analysis.

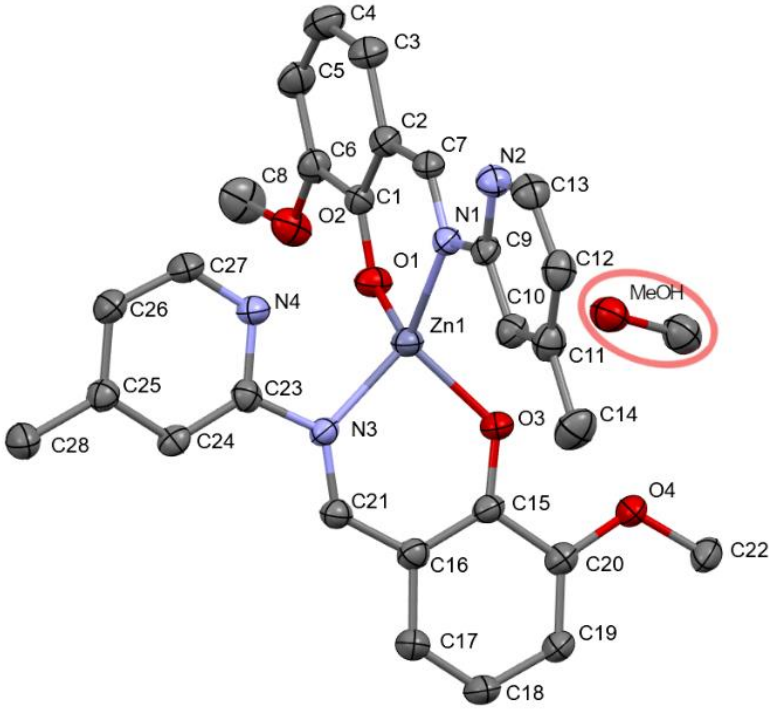

Fig. 1. Molecular structure of **C1**. Thermal ellipsoids at 50%. Hydrogen atoms and have been omitted and a methanol molecule has been highlighted for clarity.

A-45

Table 1. Selected geometric parameters

Bond length [Å]			
N1—Zn1	1.998(3)	O1—Zn1	1.917(3)
N3—Zn1	1.995(3)	O3—Zn1	1.952(3)
Angles [º]			
O1—Zn1—O3	112.72(12)	O1—Zn1—N1	97.55(12)
O1—Zn1—N3	113.15(12)	O3—Zn1—N1	113.80(11)
O3—Zn1—N3	92.55(11)	N3—Zn1—N1	127.81(12)

The compound was obtained by reacting the previously synthesised Schiff base (**L1**) with zinc acetate in methanol followed by the addition of Et_3N. [5] Crystals suitable for X-ray analysis were obtained at +4°C. In the unit cell alongside the complex molecule a methanol molecule is found.

The crystallographic data for the title compound were collected on an STOE IPDS 2T diffractometer at 120.0 K using Mo Kα radiation of a microfocus X-ray source. **C1** crystallizes in a triclinic system in P1 space group. The unit cell parameters are as follows: a = 9.5075(10) Å, b = 11.1738(12) Å, c =14.2108(16)Å, α = 108.585(9), β = 102.931(9)°, γ = 93.804(9), V= 1379.1(3)Å^3 and Z= 2. Quality parameters of the solution are $R_1[I > 2\sigma(I)]$= 0.057, wR_2 = 0.196, R_{int}=0.068, GOOF= 1.13. Asymmetric unit contains complex molecule and one methanol molecule.

Obtained substance is a mononuclear zinc(II) complex, where two imine molecules are coordinated to the zinc as a center atom. Zinc atom forms four bonds to its neighbor atoms in tetrahedral geometry. The lengths of nitrogen-zinc and oxygen-zinc bonds are in accordance with those founded in the literature.

Literature

[1] Prakash, A., & Adhikari, D. (2003). Application of Schiff bases and their metal complexes-A Review.
[2] Afshari, F., Ghomi, E.R., Dinari, M., & Ramakrishna, S. (2023). ChemistrySelect.
[3] Ceramella, J., Iacopetta, D., Catalano, A., Cirillo, F., Lappano, R., & Sinicropi, M.S., *Antibiotics*, **11** (2022) 191.
[4] Gusev, A., Kiskin, M.A., Braga, E.V., Kryukova, M.A., Baryshnikov, G.V., Karaush-Karmazin, N.N., Minaeva, V., Minaev, B.F., Ivaniuk, K., Stakhira, P., Ågren, H., & Linert, W. *ACS Applied Electronic Materials*, **3**(8) (2021) 3436–3444.
[5] Siedzielnik, M., Pawłowska, M., Daśko, M., Kleinschmidt, H., & Dołęga, A. *RSC Advances*, **13** (2023) 8830–8843

A-46

COORDINATION POLYMERS OBTAINED FROM BERGHOF REACTOR

Andrzej Kochel, Kamil Twaróg

Uniwersytet Wrocławski, Wydział Chemii, F. Joliot-Curie 14, Wrocław

Coordination polymers may find application as luminescence materials (sensors, diodes), conductors, magnetic materials (magnets, sensors), as well as ion exchagers or for gas storage and many others. In this study coordination polymers are obtained solvothermally in pressure reactor Berghof BR100. Polydentate ligands are used, mainly aminocarboxylic acids with multiple N/O donor atoms. The starting salts are of d block metals such as Cu or Mn. The synthesis is one-pot and advantegously leads to crystalline products. The sort of obtained products is affected by the sort of reagents, reaction time, reagents" amounts and volumes, pH and temperature values. Thus proper selection of the synthesis parameters allows to predict what type of compound will be obtained and to tune its properties. The figure below shows an example of a luminescent Cu(I,II) coordination polymer.

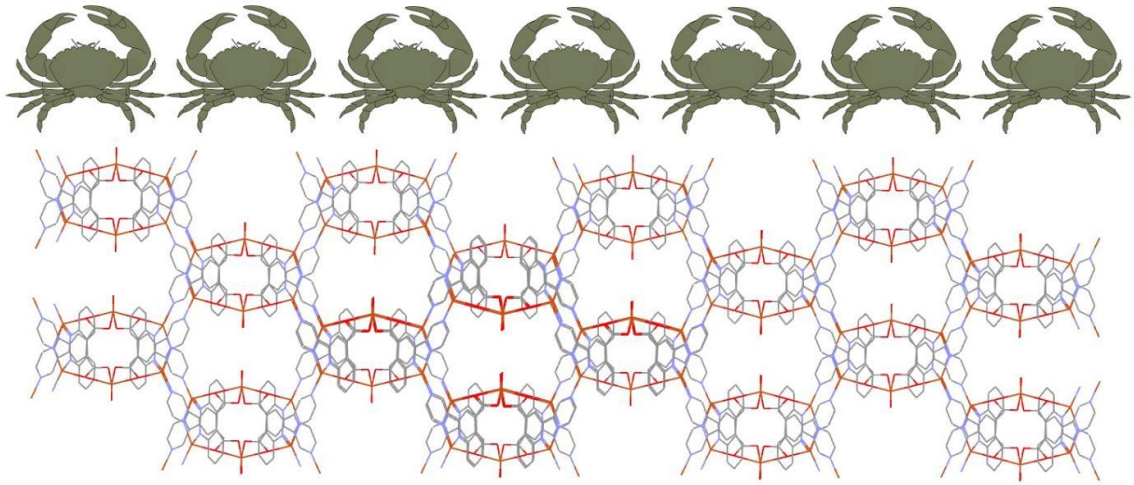

Fig. 1. 3D coordination polymer with aminocarboxylate ligand and Cu(I,II).

A-47

DYNAMICS OF ORGANIC CATIONS IN SWITCHABLE QUINUCLIDINIUM METAL CHLORIDE DIELECTRICS

Dorota A. Kowalska[1], Ewelina Jach[2], Marek A. Gusowski[2], Monika Trzebiatowska[1], Michał Krupinski[3], Wojciech Medycki[4], Jarosław Jędryka[5], Piotr Staniorowski[6], Agnieszka Ciżman[2]

[1] Institute of Low Temperature and Structure Research, Polish Academy of Sciences, Okólna 2, 50-422 Wrocław, Poland
[2] Faculty of Fundamental Problems of Technology, Wrocław University of Science and Technology, Wybrzeże Wyspiańskiego 27, 50-370, Wrocław, Poland
[3] Institute of Nuclear Physics, Polish Academy of Sciences, Walerego Eljasza-Radzikowskiego 152, 31-342 Krakow, Poland
[4] Institute of Molecular Physics, Polish Academy of Science, Smoluchowskiego 17, 60-179 Poznań, Poland
[5] Faculty of Electrical Engineering, Czestochowa University of Technology, Aleja Armii Krajowej 17, 42-218 Czestochowa, Poland
[6] Institute of Experimental Physics, University of Wrocław, plac Maxa Borna 9 50-204 Wrocław, Poland

The series of quinuclidinium-based organic-inorganic hybrids has been synthesised and structurally characterized: Q_2CuCl_4, Q_2CoCl_4, and $Q_4Pb_3Cl_{10}$, where Q = quinuclidinium, $C_7H_{13}NH^+$ [1]. Several methods have been used to investigate the disorder observed in the structure of metal chlorides: single-crystal X-ray diffraction, IR, Raman, NMR, and dielectric spectroscopy. All three compounds undergo phase transitions (PTs) where order-disorder processes take place. The PTs are found at 347/357, 318/329, and 241/246 K on cooling/heating in Q_2CuCl_4, Q_2CoCl_4, and $Q_4Pb_3Cl_{10}$, respectively.

The X-ray single crystal diffraction studies shows that high temperature phase I determined at 365 K and at 340 K for compounds with Cu and Co ions, respectively, is orthorhombic and accommodates *Pnma* space group for both crystals (Fig. 1b,d). Under the temperature lowering the structures undergoes phase transitions to phase II and adapt monoclinic space group $P2_1/c$ and $P2_1/n$ for Q_2CuCl_4 and Q_2CoCl_4, respectively. At 100 K the structures are ordered, whereas Phase I is characterized by disorder of Q cations (Fig. 1a,c).

The crystal of $Q_4Pb_3Cl_{10}$ crystallizes at room temperature (RT) in the disordered orthorhombic *Cmce* structure (phase I), where inorganic part creates 2D network (Fig. 2). After the PT, occurring below RT, the structure adjusts the *Pbcn* space group and the positions of Q ions remain disordered.

The crystals exhibit switchable and tunable properties of the dielectric function between two stable ON/OFF states. The magnetic properties were also investigated over a wide temperature range by measuring the magnetic susceptibility and magnetization as a function of temperature and external magnetic field, which allowed us to demonstrate the competition between the paramagnetic and diamagnetic signals in these compounds. The dynamics probed by NMR has shown a nonequivalence of Q cations in all studied compounds.

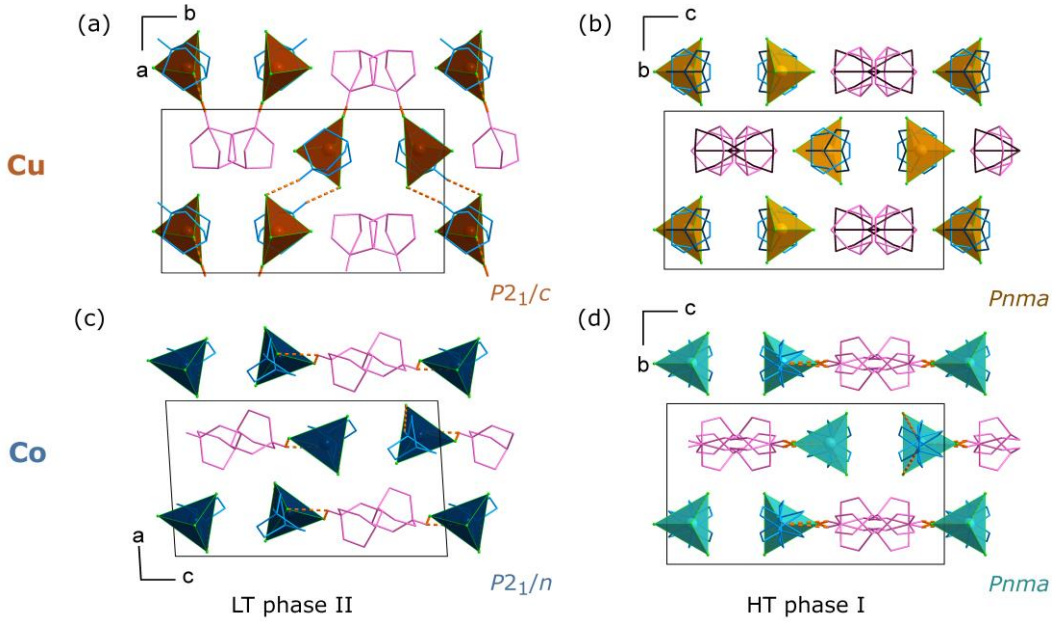

Fig. 1. The comparison of the corresponding crystal views of Q_2CuCl_4 and Q_2CoCl_4 showing the arrangement of ions and N—H···C bonds (orange dashed lines) among them. Two symmetrically different types of Q cations are shown in blue and pink colours. The hydrogen atoms, which do not create N—H···Cl bonds, are removed for the presentation's clarity.

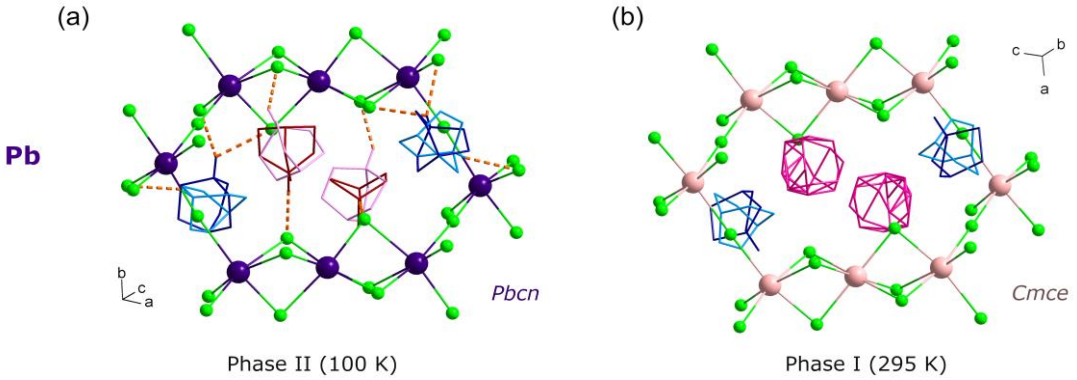

Fig. 2. The comparison of corresponding fragments of $Q_4Pb_3Cl_{10}$ structure in two different phases: (a) phase II, (b) phase I. The Q ions are placed at two positions: one marked in blue colours (light and dark for two disordered positions), the second one marked in dark red and pink colours..

References

[1] E. Jach, D. A. Kowalska, M. A. Gusowski, M. Trzebiatowska, M. Kurpiński, W. Medycki, J. Jędryka, P. Staniorowski, A. Ciżman, *J. Phys. Chem. C*, **127** (2023) 2589–2602.

A-48

SUPRAMOLECULAR HOST-GUEST COMPLEXES OF PENTAMIDINE WITH *P*-SULFONATOCALIX[*N*]ARENES

Kateryna Kravets and Oksana Danylyuk

Institute of Physical Chemistry Polish Academy of Sciences
Kasprzaka 44/52 str., 01-224 Warsaw

Sulfonated calix[*n*]arenes have been widely studied as a class of water-soluble organic macrocycles. These negatively charged calixa[*n*]renes have different cavity sizes. Such cavity's variety allows them to bind to a greater number of cationic and neutral molecules forming host-guest complexes. The host–guest assembly is mainly supported by hydrogen bonds and a set of weak N–H···π, O–H···π, $(C–H)^{+}\cdots O^{-}$ and $(C–H)^{+}\cdots\pi^{-}$, $\pi^{+}–\pi^{-}$ and cation–π interactions, coordination of metals and hydrophobic effect. [1]. The solid-state complexes are interesting from the perspective of formation of supramolecular polymers, cocrystals, vesicles, giant polyhedra, micelles, and supramolecular frameworks.

In this work, we demonstrate the solid-state interactions between biologically active positively charged pentamidine and the negatively charged *p*-sulfonato-calix[*n*]arene. In the host-guest assembles pentamidine appears as a bi-amidine guest. Pentamidine is a water-soluble biologically active drug that is used as an antimicrobial agent and is effective in pneumonia. A more recent analysis shows the antibacterial effect of pentamidine in combination with linezolid, as well as a potential therapeutic effect in vivo on the corresponding CRE infections [2].

p-Sulfonatocalix[4]arene is the smallest representative of the calix[*n*]arene family, which has a rigid cone conformation. The solid-state chemistry of this macrocycle is well-known. The larger *p*-sulfonatocalix[6]arene and *p*-sulfonatocalix[8]arene are more flexible and accept a larg number of conformations in host–guest complexes.

The crystal structures of the *p*-sulfonatocalix[*n*]arene-pentamidine complexes have been determined using the single-crystal X-ray diffraction method. The structural assembly in the solid state is mainly supported by charge-assisted hydrogen bonds between the bi-amidine groups of the pentamidine and the sulfonate groups of the *p*-sulfonatocalix[*n*]arenes. We show the differences between the structures of the host-guest complexes obtained from the water and those obtained from water-cosolvent mixtures.

Literature

[1] O. Danylyuk, K. Suwinska, *Chemical Communication*, **39** (2009) 5799.
[2] M. Tang, C. Quian, X. Zhang et al., *Microbiology Spectrum*, **11** (2023).

A-49

DICYANAMIDE – BRIDGED COBALT(II) COORDINATION POLYMERS WITH PYRAZINE DERIVATIVES AS COLIGANDS

Anna Kryczka, Joanna Palion-Gazda, Barbara Machura, Katarzyna Choroba

University of Silesia in Katowice, Institute of Chemistry, Szkolna 9, 40-006 Katowice

Coordination polymers have been a topic of research since the 18th century. These compounds are of great interest for their potential applications in heterogeneous catalysis, magnetism or luminescence, and even had a direct impact on domestic life and large-scale industrial processes [1-6]. Coordination polymers are made of cations or metal clusters linked by organic or inorganic linkers. Linkers are ligands that allow the polymer network to spread by creating a donor-acceptor bond between the central atoms. Due to the huge choice of coordinating metals, these compounds can have a wide range of structural or magnetic properties.

Compounds, where the central ion was the cobalt(II) cation, ligands were mono- and disubstituted pyrazines and dicyanamide bridges have been synthesized and investigated. New coordination polymers with formulas $[Co_3(dca)_6(2–MeOpyz)_4]_n$ (**1**), $[Co(dca)_2(2–Cl–6–Mepyz)_2]_n$ (**2**), $\{[Co_3(dca)_6(2,3–Me_2pyz)_2(H_2O)_2]\cdot 2(2,3–Me_2pyz)\}_n$ (**3**) were obtained. The crystallographic structures of the polymers were determined by single crystal X-ray diffraction. The main purpose was to study the influence of the type of substituents on the method of pseudohalide ion coordination, dimensionality and topology of the obtained polymer.

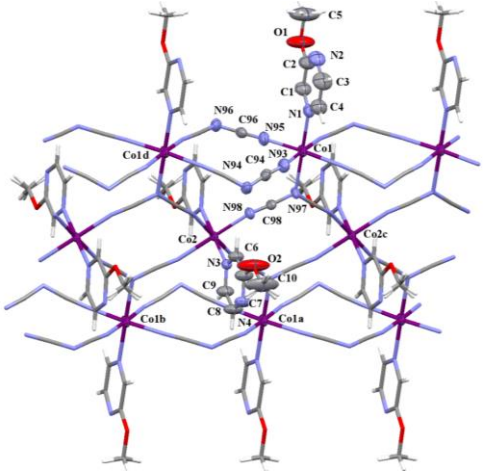

Fig. 1. Two-dimensional coordination network of $[Co_3(dca)_6(2–MeOpyz)_4]_n$ (**1**) – fragment of a triple polymer chain.

Literature

[1] J.Y. Lee, O. K. Farha, J. Roberts, K. A. Scheidt, S.B. T. Nguyen and J. T. Hupp, *Chem. Soc. Rev.*, **38** (2009) 1450–1459.
[2] S. L. James, Metal-organic frameworks, *Chem. Soc. Rev*., **32** (2003) 276–288.
[3] B. Moulton, M.J. Zaworotko, *Chem. Rev*., **101** (2001) 1629–1658.
[4] S. Kitagawa, R. Kitaura, S. Noro, *Angew. Chem. Int. Ed.*, **43** (2004) 2334–2375.
[5] J. L. C. Rowsell, O. M. Yaghi, *Angew. Chem. Int. Ed.*, **44** (2005) 4670–4679.
[6] A. Y. Robin, K. M. Fromm, *Coordination Chemistry Reviews*, **250** (2006) 2127–2157.

A-50

EFFECT OF DIAMINE BRIDGE ON REACTIVITY OF TETRADENTATE ONNO NICKEL(II) COMPLEXES

Kamila Pruszkowska[1,*], Olga A. Stasyuk[1,2], Anna Zep[1], Adam Krówczyński[1], Rafał R. Siciński[1], Miquel Solà[2], Michał K. Cyrański[1]

[1] Faculty of Chemistry, University of Warsaw, Pasteura 1, 02-093 Warsaw
[2] Departament de Química, Universitat de Girona, C/ Maria Aurèlia Capmany 69, 17003 Girona, Catalonia, Spain

**e-mail: kpruszkowska@chem.uw.edu.pl*

Tetradenate ligands such as salens [N,N'-bis(salicylidene)ethylenediamines] and acacens [N,N'-bis(acetylacetone)ethylenediamines] are commonly used in coordination chemistry due to their potential application in memory devices, chemical sensors, and contrast agents for magnetic resonance imaging [1-3]. The presented research concerns four-coordinated ONNO type nickel (II) complexes and the possibility of their reactions with the heterocyclic aromatic amines.

Square planar ONNO type Ni(II) complexes with two and three carbon atoms in the diamine bridge of the ligand (C2_CH_3_Ni and C3_CH_3_Ni, respectively), were characterized by single crystal X-ray diffraction technique. Checking the reactivity of these complexes towards *N*-heterocyclic aromatic amines, it was found that only C3_CH_3_Ni is capable of forming octahedral complexes and changing its spin state upon coordination of axial ligands. In contrast to the previous research, where electronic effect of substituents plays the crucial role in the formation of octahedral Ni(II) complex, in our case it is due to geometric factors [4-7].

References

[1] A. Bousseksou, G. Molnar, L. Salmon, W. Nicolazzi, *Chem. Soc. Rev*., **40** (2011) 3313–3335.
[2] J. Linares, E. Codjovi, Y. Garcia, *Sensors*, **12** (2012) 4479–4492.
[3] M. A. Halcrow, *Spin-Crossover Materials: Properties and Applications*, John Wiley & Sons Ltd, Chichester 2013, p. 564.
[4] H. Kurz, K. Schötz, I. Papadopoulos, F. W. Heinemann, H. Maid, D. M. Guldi, A. Köhler, G. Hörner, B. A. Weber, *J. Am. Chem. Soc*., **143** (2021) 3466–3380.
[5] Q. Meng, J. K. Clegg, K. A. Jolliffe, L. F. Lindoy, M. Lan, G. Wei, *Inorg. Chem. Commun*., **13** (2010) 558–562.
[6] C. Hansch, A. Leo, R. W. Taft, *Chem. Rev*., **91** (1991) 165–195.
[7] K. Pruszkowska, O. A. Stasyuk, A. Zep, A. Krówczyński, R. R. Sicinski, M. Solà, and M. K. Cyrański, *ChemPhysChem*, **23** (2022) e202100741.

A-51

ADVANCING QUANTUM CRYSTALLOGRAPHY REFINEMENT: THE SYNERGY OF HAR AND NOMORE MODELS

Helena Butkiewicz[1], Anders Ø. Madsen[2], Michał Chodkiewicz[1] i Anna A. Hoser[1]

[1] Faculty of Chemistry, University of Warsaw, Pasteura 1, 02-093 Warsaw, Poland
[2] Department of Pharmacy, University of Copenhagen, Universitetsparken 2, Copenhagen, Denmark

X-ray diffraction (XRD) has evolved into a widely utilized and indispensable method for characterizing the structure of materials since the recording of the first diffraction pattern for a single crystal. With advancements in theory, experiments, XRD diffractometers, and detection technology, the collection of highly accurate and precise diffraction patterns has surpassed expectations from just a few years ago. Extracting comprehensive information from experimental results requires sophisticated models due to the dependence of diffracted beam intensity on both electron density and thermal motion. While significant progress has been made in electron density modeling (e.g., Hansen-Coppens multipole model [1], Hirshfeld atom refinement (HAR) [2, 3]), the treatment of thermal motion has remained largely unchanged for a century. In light of this, we have developed a novel method called Normal Mode Refinement (NoMoRe), wherein instead of refining routine atomic displacement parameters (ADPs) against single-crystal X-ray diffraction data, we refine frequencies obtained from periodic *ab-initio* calculations [4]. In this work, we introduce a new model that combines the strengths of the charge density model (HAR) and the thermal motion model (NoMoRe). We will demonstrate the effectiveness of this model by presenting its application to exemplary compounds such as alanine, xylitol, naphthalene, and glycine polymorphs.

Financial support from Polish National Science Centre (SONATA17 grant 2021/43/D/ST4/03136) is kindly acknowledged.

Literature

[1] N. K. Hansen, *Acta Cryst. A.*, **34** (1978) 909.
[2] D. Jayatilaka, B. Dittrich, *Acta Cryst. A.*, **64** (2008) 383.
[3] S. C. Capelli, H. -B. Burgi, B. Dittrich, S. Grabowsky, D. Jayatilaka, *IUCrJ*, **1** (2014) 361.
[4] A. A. Hoser, A. Ø. Madsen, *Acta Cryst. A.*, **72** (2016) 206.

A-52

IMPROVING THERMAL MOTION DESCRIPTION IN HIGH-PRESSURE CRYSTALLOGRAPHY USING QUANTUM CRYSTALLOGRAPHY

Joachim Czapiński, Anna Makal i Anna A. Hoser

Biological and Chemical Research Center, Department of Chemistry, University of Warsaw, ul. Żwirki i Wigury 101, 02-089 Warszawa, Poland.

High-pressure crystallographic experiments conducted using diamond anvil cells (DACs) generally suffer from incomplete data. This limitation introduces errors in the refined crystallographic parameters obtained through conventional models employing anisotropic displacement parameters.

In this study, we aimed to enhance the accuracy of calculated parameters by applying quantum crystallography methods. Our approach involved the utilization of the Normal Mode Refinement (NoMoRe) method [1], which has demonstrated superiority over classical techniques in various crystallographic analyses.

The idea of quantum crystallography is based on the use of quantum mechanics with *ab initio* methods, like density functional theory (DFT) for crystallographic calculations and analysis to provide a more comprehensive understanding of materials' structures. By considering the collective vibrational motions of atoms within a crystal lattice, NoMoRe considers the quantum mechanical behavior of atoms, leading to refined crystallographic models with improved accuracy. It does so by refinement of frequencies of normal modes which are evaluated using *ab-initio* periodic computations against single crystal X-ray data.

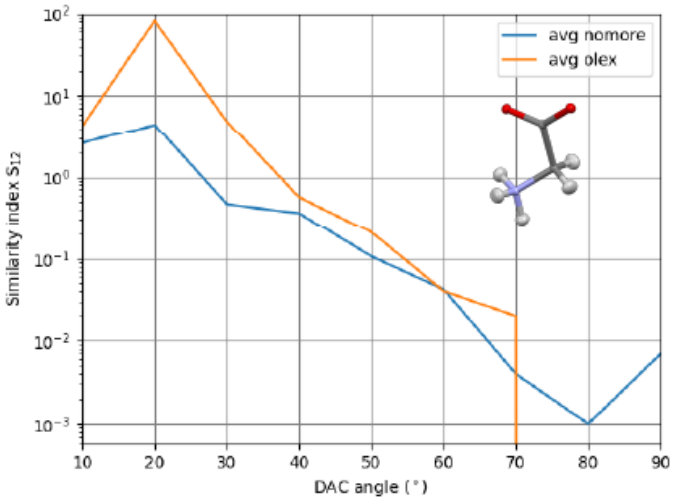

Fig. 1 Comparison of similarity indices for NoMoRe and classical methods for α-glycine.

For two model systems (α-glycine and 4'-hydroksyacetofenon (HAP)) we collected complete single crystal diffraction data. Next, we systematically reduced completeness of dataset to simulate measurements in DAC cells and on each dataset we conducted NoMoRe refinement and routine refinement in OLEX.

Through our implementation of NoMoRe in refining of crystallographic experiments, we successfully reduced the errors associated with calculated parameters (see Fig. 1). The incorporation of this quantum mechanical method offered a more precise description of atomic displacements within the crystal lattice, enhancing the accuracy and precision of our refined crystallographic models. We have observed an increase of accuracy of the anisotropic displacement parameters calculation for the NoMoRe method, compared with commonly used software: OLEX. The similarity index between the obtained parameters for incomplete and complete (no DAC) data for smaller angles was much better when the new approach was utilized.

It should be noted that the effectiveness of NoMoRe may depend on factors such as the crystal system, experimental conditions, and specific research objectives. Further investigations and validations are required to assess the general applicability and limitations of the NoMoRe method in high-pressure crystallography.

Financial support from Polish National Science Centre (SONATA17 grant 2021/43/D/ST4/03136) is kindly acknowledged

Literatura

[1] Hoser A. A., Madsen A. Ø., Acta Cryst A 2016, A72, 206-214

A-53

DIFFERENT MECHANISMS OF PHASE TRANSITIONS IN ANTIFERROELECTRIC SOLID SOLUTIONS BASED ON $PbZrO_3$ AND $PbHfO_3$

Irena Jankowska-Sumara[1], Marek Paściak[2], Jae-Hyeon Ko[3], Andrzej Majchrowski[4]

[1] Institute of Physics, Pedagogical University of Cracow, Kraków, Poland
[2] Institute of Physics of the Czech Academy of Sciences, Prague, Czech Republic
[3] School of Nano Convergence Technology, Hallym University Chuncheon 24252, Korea
[4] Institute of Applied Physics, Military University of Technology, Warsaw, Poland

Antiferroelectric perovskite crystals are technologically important materials with a complex picture of phase transitions. Among the parameters that affect strongly the stability of particular phases are temperature, pressure, and chemical doping. Here are the results of our structural studies to indicate the similarities and differences between the effects of hydrostatic pressure and Sn^{4+} ion doping of lead zirconate and lead hafnate ($PbZrO_3$ and $PbHfO_3$) [1-4].

The latter can be understood as chemical pressure since Sn^{4+} ions have slightly smaller ionic radii than Zr^{4+} as well as Hf^{4+} ions. For this purpose, the solid solutions of $Pb(Zr_{1-x}Sn_x)O_3$ (PZS) and $Pb(Hf_{1-x}Sn_x)O_3$ (PHS) where $0< x<0.3$, were characterized using single-crystal X-ray diffraction, and Raman light scattering in the wide temperature range.

The information on the structure of two intermediate phases (IM and A2), situated between low-temperature antiferroelectric A1 and high-temperature paraelectric (PE) phases has been obtained. The lower-temperature intermediate A2 phase is characterized by incommensurate displacive modulations in the Pb sublattice, while the IM phase is of AFD (antiferrodistorsive) character mainly related to antiphase octahedral tilts. It was found that the resulting IM phase has a long-range order of oxygen octahedral rotations and Pb atomic displacements which are still correlated only on a short range with some signatures of local modulation.

Optical phonons and phase transitions in PZS and PHS single crystals were investigated by temperature-dependent Raman spectra. It was found that several soft modes control the phase transition between two antiferroelectric phases indicating its displacive character, whereas, in the paraelectric phase, soft modes and Rayleigh scattering were observed. Finally, the complete phase diagram of both solid solutions in temperature composition space is presented.

References

[1] I. Jankowska-Sumara, J.-T. Hong, B. W. Lee, J.-H. Ko, M. Podgórna, A. Majchrowski, and A. Piekara, *Journal of Applied Physics*, **125** (2019) 014101.
[2] I. Jankowska-Sumara, M. Paściak, M. Podgórna, A. Majchrowski, M. Kopeckŷ, J. Kub, *APL Mater*., **9** (2021) 021101.
[3] I. Jankowska-Sumara, J-H Ko, A. Majchrowski, *Journal of The American Ceramic Society*, **104** (2021) 5990-6001.
[4] M. A. Kniazeva, A. E. Ganzha, I. Jankowska-Sumara, M. Pasciak, A. Majchrowski, A. V. Filimonov, A. I. Rudskoy, K. Roleder, R. G. Burkovsky, *Phys. Rev. B*, **105** (2022) 014101.

A-54

EXCITED-STATE GEOMETRY OF THE LUMINESCENT [Cu(DMP)(DPPE)]$^+$ COMPLEX IN THE SOLID STATE: THE TIME-RESOLVED LAUE X-RAY DIFFRACTION STUDY

Piotr Łaski[a], Radosław Kamiński[a], Katarzyna N. Jarzembska[a], Michał Hapka[a], Krzysztof Durka[b], Lauren E. Hatcher[c], Robert Henning[d], Wojciech Gadomski[a], Dariusz Szarejko[a], Paul R. Raithby[c]

[a] *Department of Chemistry, University of Warsaw, Żwirki i Wigury 101, Warsaw, PL*
[b] *Department of Chemistry, Warsaw University of Technology, Noakowskiego 3, 00-664, Warsaw, PL*
[c] *Department of Chemistry, University of Bath, Claverton Down, Bath BA2 7AY, UK*
[d] *Consortium for Advanced Radiation Sources, University of Chicago, Chicago, IL 60637, USA*

Application of X-ray diffraction methods to samples excited using some source of UV-Vis light is called most commonly photocrystallography. This way one can track light-induced processes taking place in the solid state via observation of structural changes, as well as very short-lived (lifetimes shorter than microseconds) excited states in crystals. Experiments leading to uncovering structures of the latter species are technically advanced, and the collected data requires novel methods of data handling and analysis. Under such circumstances, studies of short-lived light-induced excited states in crystals of small molecules are currently feasible almost exclusively at high-intensity X-ray sources, such as synchrotrons. The time-resolved (TR) X-ray diffraction Laue method, applied originally for macromolecular samples, constitutes the most efficient approach, as it allows effective single-pulse diffraction experiments thanks to an intense X-ray flux.

In this poster we will present in detail the data collection (BioCARS 14-ID-B APS beamline, Chicago, US), processing and analysis of the TR Laue diffraction performed for the model copper(I) luminescent complex, along with some computational and spectroscopic findings. The choice of the complex was dictated by several factors, such as previous studies using the monochromatic synchrotron technique. Furthermore, copper(I) complexes of this kind constitute a very interesting field of research towards OLEDs or other photo- or electroluminescent devices.

Acknowledgements: P.Ł., R.K. and D.S. acknowledge the SONATA grant (2016/21/D/ST4/03753) of the National Science Centre in Poland for financial support. L.E.H. and P.R.R. are grateful to the Engineering and Physical Sciences Research Council (UK) for funding (grant No. EP/K004956/1). The in-house X-ray diffraction experiments were carried out at the Department of Physics, University of Warsaw, on a Rigaku Oxford Diffraction SuperNova diffractometer, which was cofinanced by the European Union within the European Regional Development Fund (POIG.02.01.00-14-122/09). The authors thank the Wrocław Centre for Networking and Supercomputing (Grant 285) for providing computational facilities. The research also used the resources of the Advanced Photon Source (APS), a U.S. Department of Energy (DOE) Office of Science User Facility operated for the DOE Office of Science by Argonne National Laboratory under contract No. DE-AC02-06CH11357. Use of BioCARS was additionally supported by the National Institute of General Medical Sciences of the National Institutes of Health (NIH) under grant No. R24GM111072 (note: the content is solely the responsibility of the authors and does not necessarily represent the official views of NIH). The time-resolved setup at Sector 14 was funded in part through collaboration with Philip Anfinrud (NIH/NIDDK).

A-55

STRUCTURAL PROPERTIES OF THE HUNTITE TYPE GALLIUM BASED BORATES (REGa$_3$(BO$_3$)$_4$)

Roman Minikayev[1], Andriy A. Prokhorov[2], Leonid F. Chernush[3] and Jan Lančok[2]

[1] Institute of Physics, P.A.S., al. Lotników 32/46, 02-668, Warsaw, Poland
[2] Institute of Physics AS CR, Na Slovance 2, 18221, Prague, Czech Republic
[3] A.A. Galkin Donetsk Institute for Physics and Engineering, R. Luxembourg 72, 83114, Donetsk, Ukraine

Borates which are described by the general formula $REM_3(BO_3)_4$, where *RE* is a rare-earth ion and *M* is Al, Fe, Ga or Cr, crystallize in the huntite type structure o. These materials exhibit good luminescence and nonlinear optical properties and have high thermal, chemical and mechanical stability. Even slight doping of these materials with rare earth ions promotes the suitability of boranes for use in compact lasers. Interest in miniature lasers pumped by light-emitting diodes in the green-blue spectrum is stimulating research into new laser systems based on nonlinear crystals [1-3].

The least studied REGa$_3$(BO$_3$)$_4$ family of boranes (*RE* = Y, Nd, Eu, Gd, Dy, Er) with a huntite structure will be the subject of the presentation. Based on the structure model introduced for the more well-known borates YAl$_3$(BO$_3$)$_4$ [4] and already used for one of the gallium borates (REGa$_3$(BO$_3$)$_4$) [5]. The behavior of cell dimensions, atomic positions and other structural properties will be shown in comparison with the radius of the rare-earth ion introduced into the compound's unit cell.

Literatura

[1] X. Y. Chen, Z. D. Luo, D. Jaque, J. J. Romero, J. G. Sole, Y. D. Huang, A. D. Jiang, and C. Y. Tu, *J Phys-Condens Mat*, **13** (2001) 1171.
[2] D. Jaque, O. Enguita, J. G. Sole, A. D. Jiang, and Z. D. Luo, *Applied Physics Letters*, **76** (2000) 2176.
[3] A. Brenier, C. Y. Tu, Z. J. Zhu, J. F. Li, Y. Wang, Z. Y. You, and B. C. Wu, *Appl Phys Lett*, **84** (2004) 16.
[4] E. L. Belokoneva, L. I. Alshinskaya, M. A. Simonov, N. I. Leonyuk, T. I. Timchenko, and N. V. Belov, *J Struct Chem*, **20** (1979) 461.
[5] E. L. Belokoneva, L. I. Alshinskaya, M. A. Simonov, N. I. Leonyuk, T. I. Timchenko, and N. V. Belov, *J Struct Chem*, **19** (1978) 382.

A-56

HIGH PRESSURE STUDIES OF THE SIMPLEST PRIMARY AMINES

Natalia Sacharczuk[a], Anna Olejniczak[a], Maciej Bujak[b], Marcin Podsiadło[a]

[a] *Faculty of Chemistry, Adam Mickiewicz University, Uniwersytetu Poznańskiego 8, Poznań, 61-614, Poland*
[b] *Faculty of Chemistry, University of Opole, Oleska 48, Opole, 45-052, Poland*

A homologous series of the simplest primary amines: ethylamine (EA), propylamine (PA), butylamine (BA) and pentylamine (PEA) has been studied at high pressure by the single-crystal X-ray diffraction. EA is gaseous, while PA, BA and PEA are liquids at ambient conditions. These primary amines hold significant importance in organic chemistry, and their crystal structures have been previously determined solely at ambient pressure and low temperature.[1] In this studies their structures have been determined, at ambient temperature, from their freezing pressures up to *ca.* 5 GPa. Ethylamine at high pressure crystallizes in the phase II of space group $P2_1/c$, already found at ambient pressure and low-temperature. Interestingly, for the other amines the six new polymorphs have been discovered. At high pressure propylamine exists in two polymorphic phases (II and III), both in space group $P2_1/c$. Butylamine also forms two new polymorphs (phases II and III), both in space group $Pbc2_1$. Similarly, pentylamine shows two new polymorphs (phases II and III), in different space groups, $Pbc2_1$ and $P2_1cn$, respectively. By analysing the intermolecular interactions of NH···N and CH···N, we explained the mechanisms of the structural transformations of primary amines under high pressure.

Acknowledgements: this study was supported by the National Science Centre (grant No. 2020/37/B/ST4/00982).

References

[1] A. G. P. Maloney, P. A. Wood, S. Parsons, *CrystEngComm.*, **16** (2014) 3867−3882.

A-57

FAZY SMEKTYCZNE I KRYSTALICZNE CHIRALNEGO ZWIĄZKU 3F5FPhH6 BADANE Z UŻYCIEM DYFRAKCJI RENTGENOWSKIEJ I METOD KOMPLEMENTARNYCH

Aleksandra Deptuch[1], Małgorzata Jasiurkowska-Delaporte[1], Ewa Juszyńska-Gałązka[1,2], Anna Drzewicz[1], Marcin Piwowarczyk[1], Magdalena Urbańska[3], Stanisław Baran[4]

[1] Instytut Fizyki Jądrowej im. H. Niewodniczańskiego, Polska Akademia Nauk, ul. Radzikowskiego 152, 31-342 Kraków, Polska
[2] Research Center for Thermal and Entropic Science, Graduate School of Science, Osaka University, 560-0043 Osaka, Japan
[3] Instytut Chemii, Wojskowa Akademia Techniczna, ul. Kaliskiego 2, 00-908 Warszawa, Polska
[4] Uniwersytet Jagielloński, Wydział Fizyki, Astronomii i Informatyki Stosowanej, Instytut Fizyki im. M. Smoluchowskiego, ul. Łojasiewicza 11, 30-348 Kraków, Polska

Przemiany fazowe ciekłokrystalicznego związku o akronimie 3F5FPhH6 [1,2] (Rys. 1) są zbadane z użyciem dyfrakcji rentgenowskiej (XRD), różnicowej kalorymetrii skaningowej (DSC), szerokopasmowej spektroskopii dielektrycznej (BDS) i mikroskopii polaryzacyjnej (POM). 3F5FPhH6 wykazuje trzy fazy ciekłokrystaliczne: antyferroelektryczną fazę smektyczną C_A* (SmC_A*) w szerokim zakresie temperatury oraz fazy SmC* i SmA* (odpowiednio ferro- i paraelektryczną) w bardzo wąskim zakresie temperatury. W przeciwieństwie do związków o podobnej strukturze cząsteczkowej [3-5], różniących się jedynie typem fluorowania pierścienia benzenowego, 3F5FPhH6 nie tworzy szkła fazy smektycznej, natomiast łatwo ulega krystalizacji (Rys. 2). Przebieg krystalizacji jest zbadany metodą DSC dla różnych szybkości ochładzania i zanalizowany metodą izokonwersyjną [6] w celu wyznaczenia efektywnej energii aktywacji, co pozwala wyróżnić trzy zakresy temperaturowe, w których kinetyka krystalizacji jest inna. Wyniki DSC i XRD sugerują zachodzenie przejścia szklistego w fazie krystalicznej, która na podstawie widm dielektrycznych i obliczeń DFT w programie Gaussian 16 [7] jest uznana za fazę o nieporządku konformacyjnym (CONDIS), a przypuszczalne przejście szkliste może być związane z zamrożeniem zmian konformacyjnych. Wyniki przedstawione są w publikacji [8].

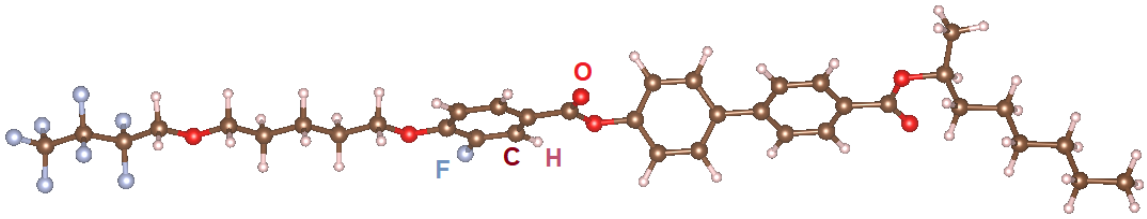

Rys. 1. Molekuła 3F5FPhH6 zoptymalizowana metodą DFT, wizualizacja w programie VESTA [9].

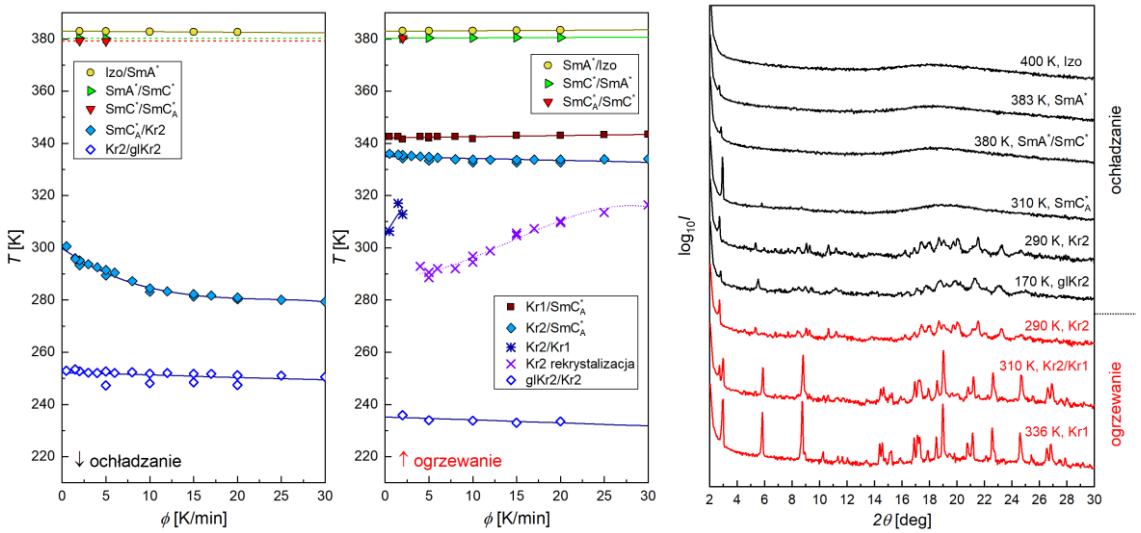

Rys. 2. Przejścia fazowe 3F5FPhH6 dla różnych szybkości ochładzania i ogrzewania, wyznaczone metodą DSC, oraz dyfraktogramy rentgenowskie zebrane podczas ochładzania i ogrzewania.

Podziękowania: Dziękujemy dr hab. Wojciechowi Zającowi (IFJ PAN) za pomoc w obliczeniach DFT, wykonanych na klastrze Prometeusz z Akademickiego Centrum Komputerowego Cyfronet AGH w ramach infrastruktury PL-Grid. Dyfraktometr rentgenowski Empyrean 2 (PANalytical) z przystawką temperaturową Cryostream 700 Plus (Oxford Cryosystems) zostały zakupione ze środków European Regional Development Fund Operational Program Infrastructure and Environment (POIS.13.01.00-00-062/08).

Literatura

[1] M. Żurowska, R. Dąbrowski, J. Dziaduszek, K. Czupryński, K. Skrzypek, M. Filipowicz, *Mol. Cryst. Liq. Cryst.*, **495** (2008) 145/[497].
[2] M. Żurowska, R. Dąbrowski, J. Dziaduszek, K. Garbat, M. Filipowicz, M. Tykarska, W. Rejmer, K. Czupryński, A. Spadło, N. Bennis, J.M. Otón, *J. Mater. Chem.*, **21** (2011) 2144.
[3] A. Deptuch, M. Jasiurkowska-Delaporte, W. Zając, E. Juszyńska-Gałązka, A. Drzewicz, M. Urbańska, *Phys. Chem. Chem. Phys.*, **23** (2021) 19795.
[4] A. Deptuch, M. Jasiurkowska-Delaporte, M. Urbańska, S. Baran, *J. Mol. Liq.*, **368** (2022) 120612.
[5] A. Deptuch, E. Juszyńska-Gałązka, M. Jasiurkowska-Delaporte, A. Drzewicz, M. Piwowarczyk, M. Urbańska, *Phase Trans.*, **96** (2023) 166.
[6] H.L. Friedman, *J. Polym. Sci., Part C: Polym. Symp.*, **6** (2007) 183.
[7] M.J. Frish et al., Gaussian 16, Revision C.01, Gaussian, Inc., Wallingford CT (2019).
[8] A. Deptuch, M. Jasiurkowska-Delaporte, E. Juszyńska-Gałązka, A. Drzewicz, M. Piwowarczyk, M. Urbańska, S. Baran, *J. Phys. Chem. B*, **126** (2022) 6547.
[9] K. Momma, F. Izumi, *J. Appl. Cryst.*, **44** (2011) 1272.

A-58

THIAZOLOTHIAZOLES AS NEW MATERIALS IN OPTOELECTRONICS - STRUCTURAL AND SPECTROSCOPIC CHARACTERIZATION

Karolina Gutmańska[a], Anna Ordyszewska[a], Konrad Szaciłowski[b] and Anna Dołęga[a]*

*[a] Gdańsk University of Technology, Department of Inorganic Chemistry, Narutowicza St. 11/12, 80-233, Gdańsk, Poland, *anna.dolega@pg.edu.pl*
[b] AGH University of Kraków, Academic Centre for Materials and Nanotechnology, A. Mickiewicza Av., 30, 30-059, Kraków, Poland

Thiazolo[5,4-d]thiazoles (TzTz) represent a class of bicyclic compounds based on a thiazole ring. The presence of a flat TzTz system with a high electron affinity renders them highly suitable for electron acceptance. Additionally, their distinctive feature of strong π-π stacking interactions contributes to excellent electron mobility, while their notable oxidative stability holds promise for optoelectronic applications.[1] In addition, the same properties facilitate efficient charge transfer in TzTz, making them particularly appealing in the electronic industry. Given these advantageous characteristics, thiazolothiazoles have found numerous applications in organic electronics, particularly in fields such as photovoltaics (OPV), as organic light-emitting diodes (OLEDs), field-effect transistors (OFETs) or filament memristors.[2] Despite the widespread interest in these compounds, the work carried out to date has resulted in neither a complete structural and spectroscopic knowledge of TzTz nor the optimal methods for their preparation.

In light of this, our current endeavor focuses on refining synthetic approaches to obtain highly pure crystalline products, which should facilitate full structural and spectroscopic (X-ray diffraction, FT-IR, NMR, and UV-Vis) characterization. Based on one of the obtained compounds (Fig. 1), we will discuss salient structural elements, as well as selected spectroscopic properties exhibited by the compound.

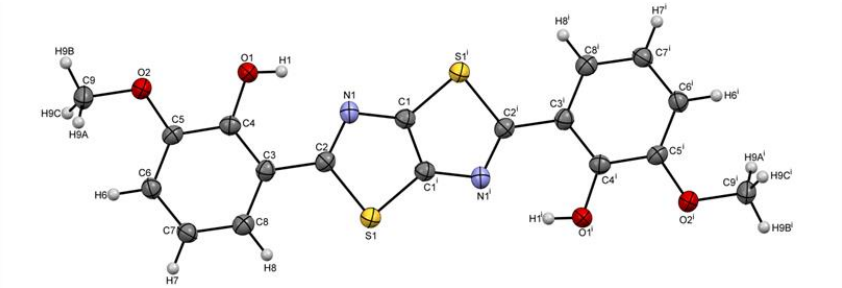

Fig. 1. Molecular structure of 2,5-bis(3-methoxy-2-hydroxyphenyl)[1,3]thiazolo[5,4-d]thiazole.

Studies financed by National Science Centre (Poland, the OPUS project (UMO-2022/47/B/ST4/00728).

References

[1] A.B.S. Santos, A.M. Manfredi, C.A.M. Salla, G. Farias, E. Girotto, J. Eccher, E. Westphal, S.F. Curcio, T. Cazati, I. Malvestiti, E.H.L. Falcão, I.H. Bechtold, H. Gallardo, *J. Mol. Liq.*, **321** (2021) 114887.
[2] D. Bevk, L. Marin, L. Lutsen, D. Vanderzande, W. Maes, *RSC Adv.*, **3** (2013) 11418.

A-59

SYNTHESIS, CRYSTAL STRUCTURE, AND MAGNETIC PROPERTIES OF NEW COORDINATION COMPOUNDS OF COBALT(II) HALIDES WITH 2-METHYLANILINE

Michał Duda[1], Piotr Konieczny[2], Marcin Oszajca[1], Wiesław Łasocha[1]

[1] Faculty of Chemistry, Jagiellonian University, ul. Gronostajowa 2, 30-387 Kraków, Poland

[2] The Henryk Niewodniczański Institute of Nuclear Physics, Polish Academy of Sciences, ul. Radzikowskiego 152, 31-342 Kraków, Poland

In this research, two organic-inorganic coordination compounds of cobalt(II) halides with 2-methylaniline (2-MeA) were synthesized and studied: $CoCl_2(2\text{-MeA})_2$ and $CoBr_2(2\text{-MeA})_2$. The compounds were synthesized using a fast and simple solvo-mechanical method [1], where the corresponding cobalt salt was mixed with an excess of liquid amine in an agate mortar. As a result, intensely blue powders were obtained.

Based on the X-ray powder diffraction patterns (XRPD), crystal structures of the investigated compounds were determined (Table 1). Cell parameters, crystal system, space group, and positions of cobalt and halogen atoms in the unit cell were determined by direct methods using EXPO2014 [2] (indexing was performed using the NTREOR algorithm [3]). The structure model was prepared with the parallel tempering method (a direct space method) using FOX [4]. As building blocks, free-rotating molecules of 2-MeA were used while the positions of cobalt and halogen atoms were fixed. Restrained structure refinement was performed using Jana2006 [5] with the profile method [6-8].

Table 1. Basic crystallographic data for $CoCl_2(2\text{-MeA})_2$ and $CoBr_2(2\text{-MeA})_2$.

chemical formula	$CoCl_2(C_7H_9N)_2$	$CoBr_2(C_7H_9N)_2$
color	dark blue	bright blue
crystal system	orthorhombic	orthorhombic
space group	*Fdd*2	*Fdd*2
a [Å]	24.9270(4)	25.5517(2)
b [Å]	27.1220(4)	26.7524(3)
c [Å]	4.6425(9)	4.76242(5)
V [Å^3]	3138.73(9)	3255.45(6)
Z	8	8
R_p [%]	6.83	4.86
R_{wp} [%]	4.41	4.48
numer of restraints*	17	32

*related to the geometry of the 2-MeA molecules

In both crystal structures, cobalt atoms are surrounded by two halogen cations and two nitrogen atoms from the amine molecules, occupying the corners of the coordination polyhedra (tetrahedra) (Fig. 1). In the structures, there are eight molecules of $CoX_2(2\text{-MeA})_2$ per unit cell (Fig. 2a). The molecules are organized into *pseudo*-ribbons parallel to the [001] crystallographic direction (Fig. 2b) by ionic interactions between Co^{2+} and halogen anions, X^-, and weak N-H···X interactions.

Since cobalt(II) atom has spin S = 3/2, magnetic properties of the compounds were investigated. As the molecules are aligned in *pseudo*-ribbons, it was expected that the compounds could exhibit SCM (Single-Chain Magnet) behavior; however, the

magnetization *vs.* temperature curves dismissed this hypothesis. The ordering temperature calculated for $CoCl_2(2\text{-}MeA)_2$ is ~6.7 K and for $CoBr_2(2\text{-}MeA)_2$: ~6.0 K Difference between ZFC (Zero-Field-Cooled) and FC (Field-Cooled) curves observed in the case of $CoCl_2(2\text{-}MeA)_2$ could indicate that the material underwent an irreversible process (probably degradation) during the measurements. The determined magnetic susceptibility, χT, for the compound with chlorine is ~2,78 $cm^3 \cdot mol^{-1} \cdot K$, and for the compound with bromine: ~2,53 $cm^3 \cdot mol^{-1} \cdot K$. Studies of magnetic properties as a function of pressure are under progress.

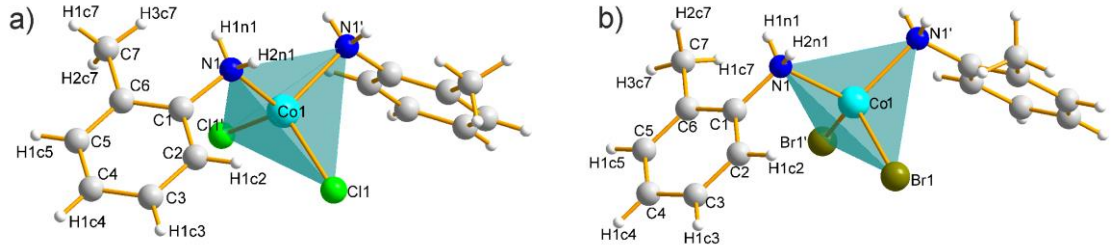

Fig. 1. Single molecule of: a) $CoCl_2(2\text{-}MeA)_2$ and b) $CoBr_2(2\text{-}MeA)_2$ with coordination polyhedra shown.

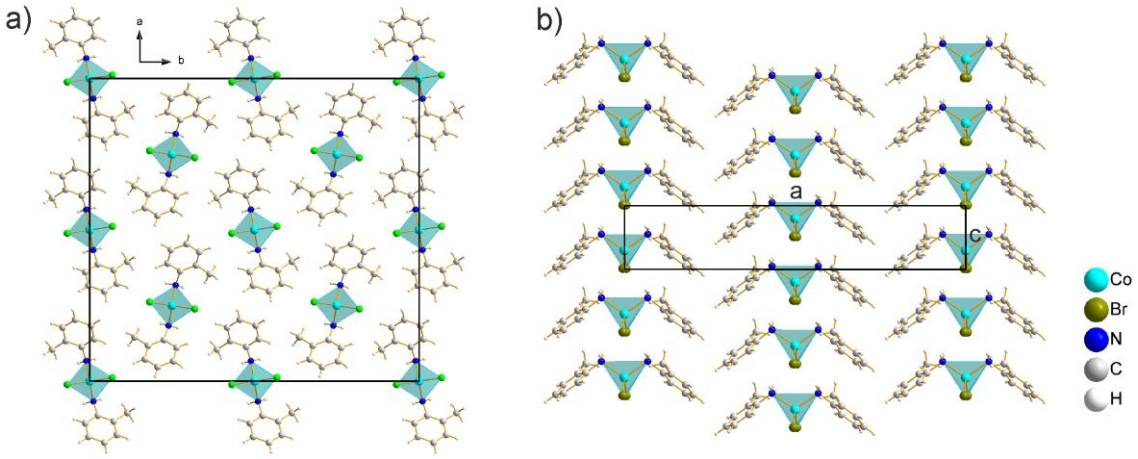

Fig. 2. Structure views of the studied compounds: a) unit cell of $CoCl_2(2\text{-}MeA)_2$ shown along the [001] direction; b) $CoBr_2(2\text{-}MeA)_2$ molecules arranged in *pseudo*-ribbons parallel to the [001] direction (view along the [010] direction).

References

[1] M. Duda, *PhD Thesis*, (2021) 108.
[2] A. Altomare, M. Camalli, C. Cuocci, C. Giacovazzo, A. Moliterni, R. Rizzi, *J. Appl. Cryst.*, **42** (2009) 1197.
[3] A. Altomare, G. Campi, C. Cuocci, L. Eriksson, C. Giacovazzo, A. Moliterni, R. Rizzi, P.-E. Werner, *J. Appl. Cryst.*, **42** (2009) 768.
[4] V. Favre-Nicolin, R. Černý, *J. Appl. Cryst*., **35** (2002) 734.
[5] V. Petříček, M. Dušek, L. Palatinus, *Z. Kristallogr. Cryst. Mater*., **229** (2014) 345.
[6] H.M. Rietveld, *J. Appl. Cryst*., **2** (1969) 65.
[7] B.O. Loopstra, H.M. Rietveld, *Acta Cryst. B*., **25** (1969) 787.
[8] B.O. Loopstra, H.M. Rietveld, *Acta Cryst. B*., **25** (1969) 1420.

A-60

METHANOL AND ETHANOL SOLVATES OF 4-(2,4,6-TRIPHENYL-1-PYRIDINIUM) PHENOLATE

Iga Grześkowiak*, Andrzej Katrusiak, Szymon Sobczak

Department of Materials Chemistry, Faculty of Chemistry, Adam Mickiewicz University, Poznań, Uniwersytetu Poznańskiego 8, 61-614 Poznań

**e-mail: igagrz@st.amu.edu.pl*

The group of N-phenolate pyridinium dyes is well-known of their significant negative solvatochromic effect. Depending on the solvent polarity their absorption maximum shifts towards higher wavelengths. Such intense change in the absorption spectrum is connected to the unique electronic structure of this betaine dyes.[1]

One of the most interesting compound among all group of betaine dyes is 4-(2,4,6-triphenyl-1-pyridinium) phenolate, often abbreviated to as ET(1). Crystallization from metanol:water (1:5vol) mixture allow to obtain a red single crystals of ET(1) water hydrate with 5.78 water molecules per one ET(1). In this hydrated form (space group $C222_1$) the ET(1) molecule is in the zwitterionic form, forming direct H-bonds between phenolate-oxygen atom and two adjacent water molecules.[2]

In order to further investigate the interaction between ET(1) and different solvent molecules, to shed a new light to the solvatochromic mechanism, we implemented a diamond-anvil cell to obtained novel ET(1) solvates. The crystal structures of methanol $C_{29}H_{21}NO{\cdot}4CH_3OH$ (**1**); and ethanol $C_{29}H_{21}NO{\cdot}4C_2H_5OH$ (**2**); solvates were obtained by high-pressure isochoric recrystallization and characterized in-situ by high-pressure X-ray diffraction (XRD).[3] Crystallization from methanol at 0.57GPa and 1.17GPa lead to formation of yellow crystals (space group $P2_1/n$), while form ethanol at 0.24GPa and 0.76GPa lead to red crystals of $R3c$ space group.

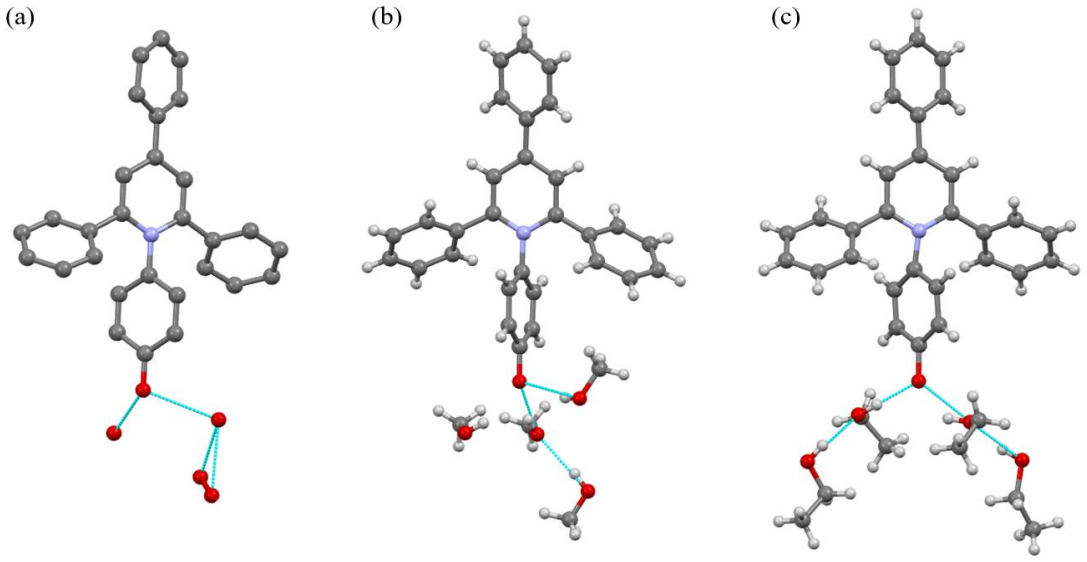

Fig. 1. The asymmetric unit of ET(1) cocrystallized with (a) water ($C_{29}H_{21}NO{\cdot}5.78H_2O$) at ambient conditions[2]; (b) methanol ($C_{29}H_{21}NO{\cdot}4CH_3OH$) at 0.57GPa; and (c) ethanol molecules ($C_{29}H_{21}NO{\cdot}4C_2H_5OH$) at 0.24GPa.

References
[1] Reichardt, C. *Chem. Rev.*, **94** (1994) 2319–2358.
[2] Stadnicka, K., Milart, P., Olech, A., & Olszewski, P. K. *J. Mol. Struct.*, **604** (2002) 9–18.
[3] Katrusiak, A. (2018). *International Tables for Crystallography*, edited by C.J. Gilmore, J.A. Kaduk, H. Schenk, Vol. H, pp. 156–173. New York: John Wiley & Sons.

A-61

HIGH PRESSURE ESTERIFICATION OF BENZOIC ACID AND SIMPLE ALCOHOLS

Paweł Lewkowicz, Andrzej Katrusiak and Szymon Sobczak

Faculty of Chemistry, Adam Mickiewicz University,
Uniwersytetu Poznańskiego 8, 61-614 Poznan, Poland

Due to theirs pleasant smells, esters are one of the most frequently used group of chemical compounds in production of perfumes as well as in food industry. At ambient conditions formation of the ester bond occurs according to the Fisher mechanism, where protonated acid undergoes an electrophilic reaction with alcohol. Usually catalyzed by H_2SO_4 thanks to being strong acid and possessing dehydrating properties.

Recently, some report regarding a direct synthesis of fatty acid esters from alcohols with carboxylic acids at high pressure has been reported.[1] But the mechanism as well as specific conditions required for this reaction are unclear.

In our research we attempt to provide more insights into the process of the high-pressure esterification, in the reaction of the benzoic acid with different alcohols, such as methanol,[2] 1-propanol and 1-butanol in concentration between 30-35% heated between 403-416 K at 0.3-0.35 GPa. High-pressure reactions has been conducted in a diamond-anvil cell,[3] which allowed us for the in-situ investigation of the reaction progress and through the following isochoric recrystallization to obtain a single-crystalline products which were investigated by the X-ray diffraction. As a result of our reaction we provide a novel environmentally-friendly way for obtaining esters without a need of the strong acids acting as a reaction catalyst. Which reduces both reaction time and costs of product purification.

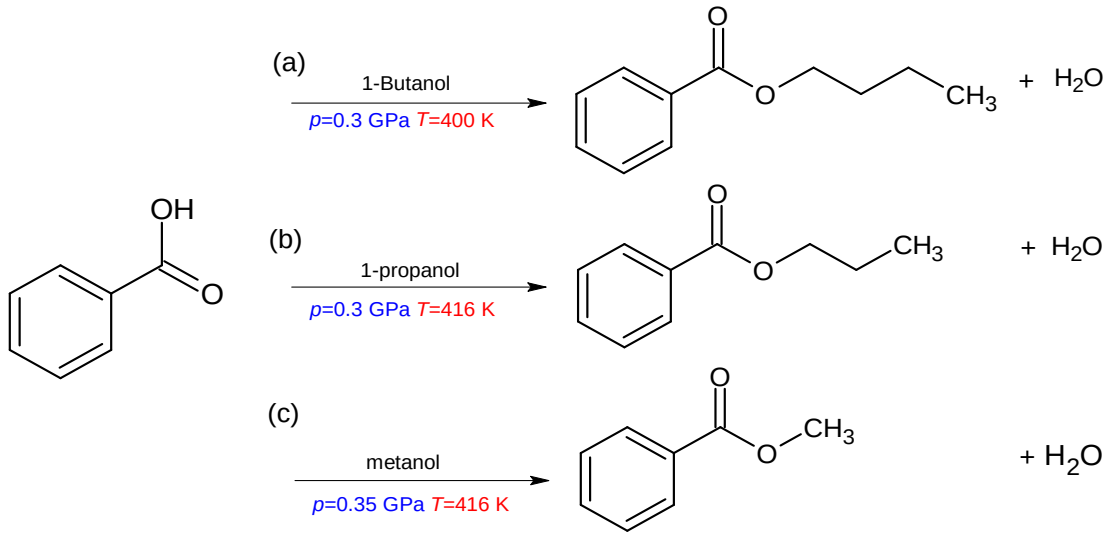

Fig. 1. High-pressure reactions of benzoic acid with (a) 1-butanol, (b) 1-propanol, (c) methanol.

References

[1] Z. Khan, F. Javed, Z. Shamair, A. Hafeez, T. Fazal, A. Aslam, W.B. Zimmerman, F. Rehman, *J. Ind. Eng. Chem.*, **103** (2021) 80–101.
[2] W. Cai, A. Katrusiak *J. Phys. Chem. C*, **117** (2013) 21460–21465.
[3] A. Katrusiak, *Acta Crystallogr. Sect. B*, **75** (2019) 918–926.

A-62

REVEALING THE STRUCTURE-PROPERTY RELATIONSHIP OF PHENYL-SUBSTITUTED PERYLENE DIIMIDE DERIVATIVE (PTCDI-PH) UNDER EXTREME CONDITIONS

Paulina Ratajczyk[1], Szymon Sobczak[1], Przemysław Woźny[1], Angelika Wcisło[1], Tomasz Poręba[2], Andrzej Katrusiak[1]

[1] Faculty of Chemistry, Adam Mickiewicz University, Uniwersytetu Poznańskiego 8, 61-614 Poznań, Poland
[2] European Synchrotron Radiation Facility, 71 Avenue des Martyrs, 38000 Grenoble, France

In recent years, perylene diimide derivatives (PDIs) have emerged as promising organic electronic and optoelectronic materials. They are known for their excellent electron mobility, high absorption coefficients, and exceptional chemical and thermal stability. These characteristics make PDIs ideal electron acceptors for a wide range of organic electronics applications, including organic field-effect transistors (OFETs), organic light-emitting diodes (OLEDs), organic photovoltaics (OPVs), and dye-sensitized solar cells (DSSCs) [1].

Extreme pressure and temperature can be used as effective tools to model structural changes that significantly affect the performance of organic electronics. Even subtle modifications in conformation, bond lengths, angles between atoms and strength of intermolecular interactions induced by extreme conditions can affect the optoelectronic properties of this class of compounds [2]. Therefore, accurate characterization of the effects of structural changes on their properties is of great importance.

To investigate the behavior of this class of materials under extreme conditions, we focused on *N*, *N*'-diphenyl-3,4,9,10-perylenedicarboximide, abbreviated as PTCDI-Ph (Fig. 1). By studying the high-pressure as well as high- and low-temperature effects on the single crystal structure of PTCDI-Ph, we compared the resulting structural changes with the absorption and emission properties of this compound. The investigation employed techniques such as differential scanning calorimetry, X-ray diffraction, UV-Vis absorption, and photoluminescence spectroscopy. Our findings provide valuable insights into the response of PTCDI-Ph to extreme conditions and pave the way for tailoring their optoelectronic properties through controlled structural modifications.

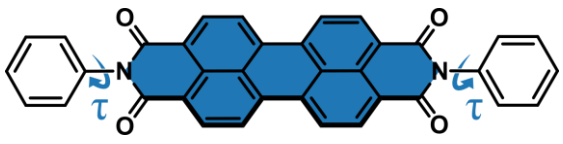

Fig. 1. Molecular structure of PTCDI-Ph.

Acknowledgments
The authors acknowledge the European Synchrotron Radiation Facility (ESRF) for provision of synchrotron radiation facilities. P.R. is a recipient of the Adam Mickiewicz University Foundation scholarship for the 2022/2023 academic year and is grateful to the Polish Ministry of Education and Science (Diamentowy Grant DI2019/0160/49) for their financial support.

A-62

Literature
[1] X. Zhan, A. Facchetti, S. Barlow, T. J. Marks, M. A. Ratner, M. R. Wasielewski, S. R. Marder, *Adv. Mater.*, **23** (2011) 268-284.
[2] M. Szafrański, A. Katrusiak, *J. Phys. Chem. Lett.*, **8** (2017) 2496-2506.

A-63

WPŁYW PODSTAWNIKÓW 2-(4-CHLOROFENYLO)ETYLOWYCH W POZYCJACH IMIDOWYCH NA UPAKOWANIE I WŁAŚCIWOŚCI OPTYCZNE DIIMIDÓW PERYLENOWYCH

Angelika Wcisło, Paulina Ratajczyk, Andrzej Katrusiak, Szymon Sobczak

Zakład Chemii Materiałów, Wydział Chemii, Uniwersytet im. Adama Mickiewicza w Poznaniu, 61-614 Poznań, Polska

Barwniki z grupy diimidów perylenowych (PDI) należą do grupy organicznych materiałów *n*-przewodnikowych. Pochodne tych związków są powszechnie wykorzystywane jako pigmenty do produkcji lakierów samochodowych i farb przemysłowych.[1] Ze względu na unikalne właściwości optoelektroniczne, PDI zaczynają być rozważane jako alternatywa dla tradycyjnych materiałów fotowoltaicznych. Istotne staje się więc zrozumienie zależności między strukturą, a wydajnością i efektywnością tych materiałów. W ostatnich latach, badania prowadzone w warunkach wysokiego ciśnienia i ekstremalnych temperatur, zarówno niskich jak i wysokich, zyskują na znaczeniu, umożliwiając modelowanie deformacji, do których dochodzi w materiałach podczas ich produkcji i eksploatacji.[2]

W celu zbadania związku pomiędzy właściwościami strukturalnymi, a ich wpływem na właściwości optoelektroniczne, przeprowadzono badania nowej pochodnej PDI, zmodyfikowanej przez wprowadzenie grup 2-(4-chlorofenylo)etylowych (Rys. 1) w pozycjach imidowych (4ClPEPTC). Multidyscyplinarne badania łączące metody dyfrakcyjne, spektroskopową analizę UV-Vis oraz skaningową kalorymetrię różnicową, w warunkach ekstremalnego ciśnienia (do 5 GPa) i temperatury (120-400 K), ujawniły wysoką stabilność 4ClPEPTC, krystalizującego w układzie rombowym, o grupie przestrzennej $Pna2_1$. Zmiany strukturalne zostały skorelowane z widmami absorpcji, wykonanymi w zakresie 78-348 K oraz w warunkach wysokiego ciśnienia (0.1 MPa-5.08 GPa), wskazując przesunięcia krawędzi absorpcji wynoszące odpowiednio 4 nm/100 K oraz 22.6 nm/GPa.

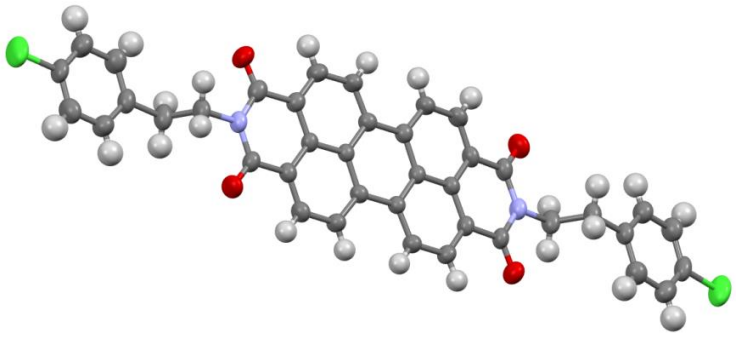

Rys. 1. Cząsteczka pochodnej PDI z podstawnikami 2-(4-chlorofenylo)etylowymi w pozycjach imidowych.

Praca naukowa finansowana ze środków budżetowych na naukę w latach 2020-2024 jako projekt badawczy w ramach programu „Diamentowy Grant” (DI2019/0160/49).

A-63

Literatura
[1] F. Würthner, *Chem. Commun.*, **14** (2004) 1564-1579.
[2] A. Katrusiak, *Acta Crystallogr. Sect. B*, **75** (2019) 918-926.

A-64

BENDING THE BONDS: UNVEILING HALOGEN INTERACTIONS IN ELASTIC POLYMORPH OF 2,5-BIS(3-BROMOPHENYL)FURAN

Konrad Dyk[1,2], Vasyl Kinzhybalo[2], Yuriy Horak[3], Serhii Butenko[3], Miłosz Siczek[4], and Daniel M. Kamiński[1]

[1]Institute of Chemical Sciences, Maria Curie-Sklodowska University, Maria Curie-Sklodowska 3 sqr., 20-031 Lublin, Poland
[2]Institute of Low Temperature and Structure Research, Polish Academy of Sciences, Okolna 2 str., 50-422 Wroclaw, Poland
[3]Ivan Franko National University of Lviv, Kyryla i Mefodiya str. 6, 79005 Lviv, Ukraine
[4]Department of Chemistry, University of Wroclaw, 14 F. Joliot-Curie, 50-383 Wroclaw, Poland

The structural investigation of organic compounds is of paramount importance for understanding their physical and chemical properties. We present a comprehensive analysis of the structural features of 2,5-bis(3-bromophenyl)furan, focusing on the intriguing phenomenon of halogen interactions and their influence on its overall crystal properties.

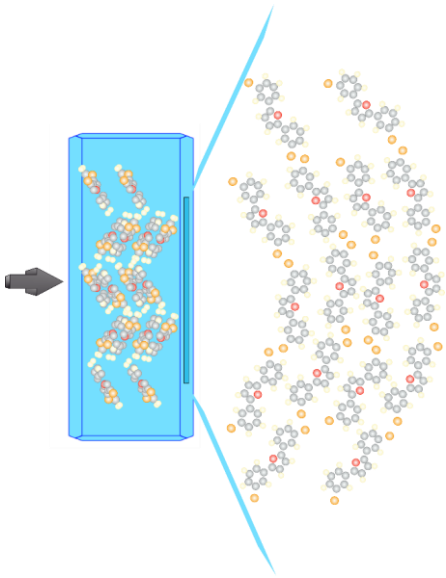

Fig. 1. Unveiling halogen interactions in elastic crystal.

Halogen interactions, particularly those involving bromine atoms, have gained significant attention in recent years due to their unique characteristics and implications in various fields of chemistry. These interactions play a crucial role in the formation of supramolecular assemblies, leading to distinctive crystal packing motifs and influencing the physical properties of the resulting materials. Investigating the influence of halogen interactions on crystal structures is thus essential for understanding and predicting the behavior of organic compounds in a wide range of applications.

A-64

In this study, we employ a combination of X-ray diffraction techniques, crystallographic analysis and computational modeling to elucidate the crystal structures of 2,5-bis(3-bromophenyl)furan polymorphic modifications. Our investigations reveal the presence of intricate halogen interactions between the bromine atoms of neighboring molecules within the crystal lattice. We explore the nature and strength of these interactions, their geometrical preferences, and their impact on the packing arrangement of the molecules.

Furthermore, we delve into the correlation between the observed halogen interactions and the resulting crystal mechanical properties of 2,5-bis(3-bromophenyl)furan. Through a systematic analysis of the crystal packing, we investigate the effects of these interactions on the molecular arrangement, intermolecular forces, and crystallographic parameters such as unit cell dimensions, density and thermal behavior.

Understanding the intricate relationship between halogen interactions and crystal properties in organic compounds has significant implications for materials design, molecular recognition and supramolecular chemistry. The insights gained from this study contribute to the growing body of knowledge on the role of halogen interactions in crystal engineering, providing a foundation for the rational design and synthesis of novel materials with tailored properties.

A-65

INFLUENCE OF Gd ON THE PHASE TRANSFORMATIONS IN IRON OXIDE-BASED NANOPARTICLES OBTAINED BY THE COPRECIPITATION METHOD

Uladzislaw Gumiennik, Janusz Przewoźnik

AGH University of Krakow, Faculty of Physics and Applied Computer Science, Mickiewicza Av. 30, 30-059 Kraków, Poland

Over the past decades, a lot of efforts have been directed to study different iron oxides-based compounds for biomedical applications. In this work, we investigate structure and magnetic properties of intermediate states in the synthesis of nanoparticles (NPs) containing $Gd_xFe_{3-x}O_4$ (x = 0; 0,05; 0,1) core inside mesoporous SiO_2 shell. NPs are sintered by two-stage procedure including coprecipitation method [1], where the molar concentration of ammonia was fixed to 13,3 mol/L, and using $Si(OC_2H_5)_4$ tetraethyl orthosilicate (TEOS) hydrolysis [2].

During coprecipitation, phase transformations occur due to the catalysis process [3]. The sequence of transformations is: Fe^{3+} → β-FeOOH → α-FeOOH → (α/γ-Fe_2O_3) → Fe_3O_4; Fe^{2+} → $Fe(OH)_2$ → [iron valency change from 2+ to 3+] → γ-FeOOH → γ-Fe_2O_3 → Fe_3O_4. Variation of molar concentrations of the reagents makes it possible to suspend the course of the reaction and study of intermediate phase composition.

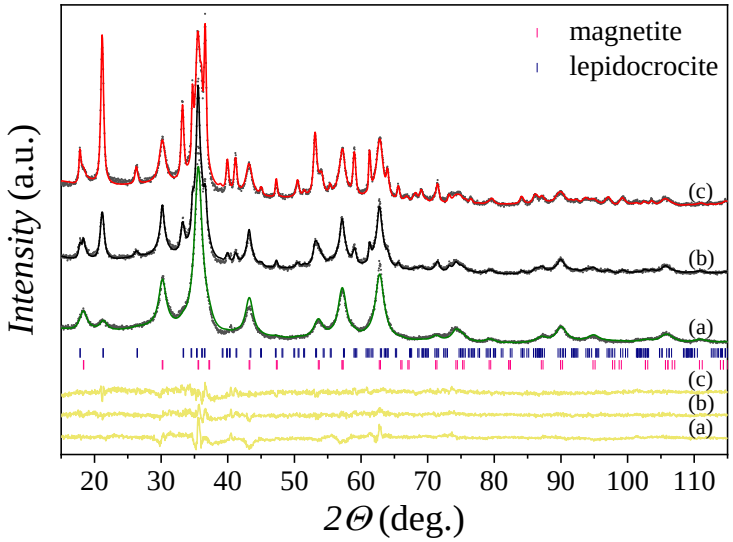

Fig. 1. XRD patterns with Rietveld refinement of $Gd_xFe_{3-x}O_4$ samples with x = 0 (a), 0,05 (b), and 0,1 (c).

The samples are characterized by X-ray diffraction (XRD), scanning electron microscopy, energy-dispersive X-ray spectroscopy, ^{57}Fe Mössbauer spectroscopy (at T = 20 – 300 K), and vibrating sample magnetometry at T = 2 – 300 K and magnetic fields B up to 9 T.

XRD analysis showed that the addition of gadolinium under this synthesis condition leads to increased formation of an additional antiferromagnetic lepidocrocite (γ-FeOOH) phase. However, recalculation of the magnetization at B = 9 T and T = 2 K

only to the mass of the ferrimagnetic $Gd_xFe_{3-x}O_4$ phase shows a clear increase in its saturation with increasing x (1,6 μB/f.u. (x = 0) → 2,0 μB/f.u. (x = 0,05) → 2,3 μB/f.u. (x = 0,1)).

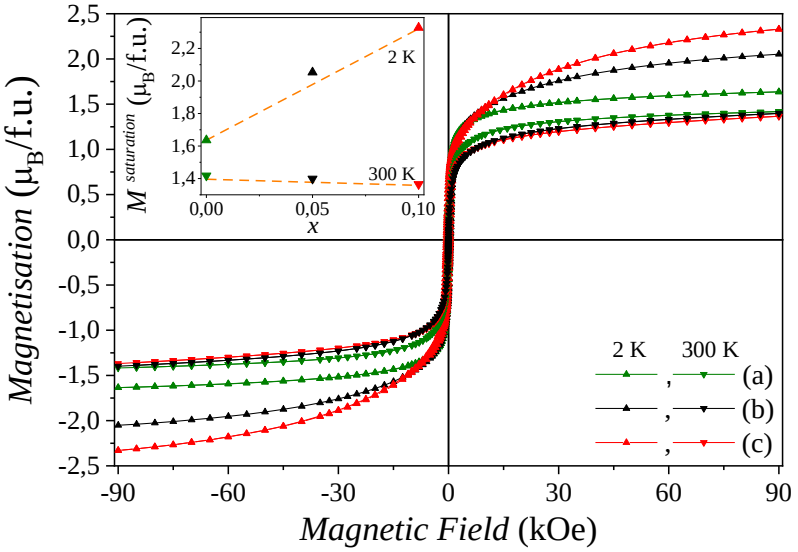

Fig. 2. Magnetisation vs. magnetic field of $Gd_xFe_{3-x}O_4$ samples with x = 0 (a), 0,05 (b), and 0,1 (c).

Literature

[1] R. Massart and V. Cabuil, *J. Chim. Phys.*, **84** (1987) 967.
[2] F. Yang et al., *J. of All. and Comp.*, **728** (2017) 1153–1156.
[3] T. Ahn et al., *J. Phys. Chem. C*, **116** 10 (2012) 6069–6076.

A-66

STRUCTURAL CHARACTERISATION OF Na/Ag ALENDRONATE SOLID SOLUTIONS

Karolina Gutmańska[a], Sebastian Demkowicz[b] and Anna Dołęga[a]

[a] Department of Inorganic Chemistry, Faculty of Chemistry
[b] Department of Organic Chemistry, Faculty of Chemistry
Gdańsk University of Technology, 80-233 Gdansk, Poland

As a result of the series of the reactions of silver precursor with the sodium alendronate we have obtained a number of crystalline products, in which the silver atoms gradually replaced the sodium atoms, while the crystal structure of the sodium alendronate [1] was basically preserved. We were able to find out and conclude that the sodium and silver alendronate are mutually soluble over a complete range of relative concentrations. In the communication we describe the minute changes in the unit cell parameters accompanying the growing concentration of silver in the crystals. We have also observed low R_{int} values for the high Na or Ag content and higher R_{int} for the Na/Ag ratios close to 1:1. However, it must be mentioned that for "the worst" structures the merging error was 3.97% (31.3% of silver atoms and 68.7% of sodium atoms) and 5.09% (60.8% of silver atoms and 39.2% of sodium atoms), which means that the crystals were still of good quality. For the high content of sodium or silver we have obtained and measured crystals with R_{int} values close to or even below 2%.

In Fig. 1 we illustrate the asymmetric unit of sodium/silver alendronate system.

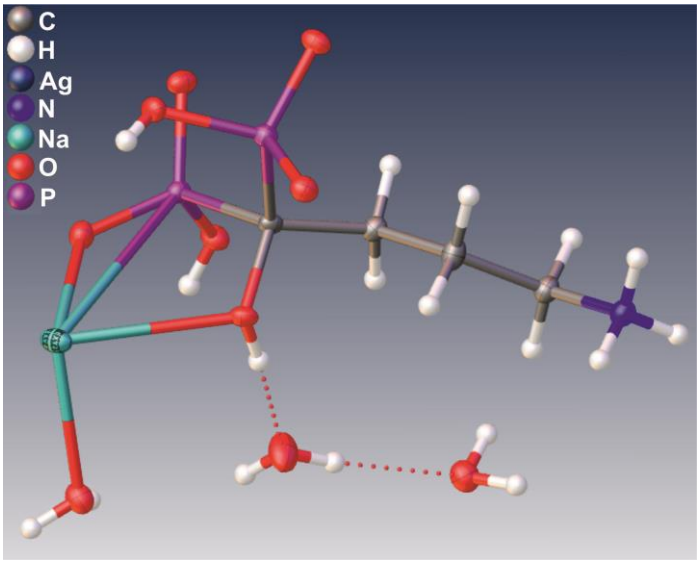

Fig. 1. The asymmetric unit of Na/Ag alendronate crystal structure.

The described feature *i.e.* the ability to form solid solution, provides a way to tailor the properties of the Na/Ag alendronate system for medical applications such as the introduction of antibacterial properties into alendronate/hydroxyapatite composites.

References

[1] D. Vega, R. Baggio, M.T. Garland, *Acta Cryst. C*, **52** (1996) 2198.

A-67

WPŁYW PODSTAWNIKA NA SPOSÓB ASOCJACJI CZĄSTECZEK W SIECIACH KRYSTALICZNYCH POCHODNYCH BENZOFURANU

Ilona Materek[1], Urszula Maciołek[1], Marta Struga[2], Anna E. Kozioł[1]

[1] *Wydział Chemii, Uniwersytet Marii Curie-Skłodowskiej, 20-031 Lublin*
[2] *Katedra Biochemii, Warszawski Uniwersytet Medyczny, 02-097 Warszawa*

Sól to krystaliczna substancja stała zawierająca dwie lub większą liczbę form jonowych. Według innej definicji solami są układy wieloskładnikowe, w których proton zostaje przeniesiony z cząsteczki o charakterze kwasowym na cząsteczkę o charakterze zasadowym, w wyniku czego te substancje występują w postaci jonów [1].

Układ benzofuranu wchodzi w skład budowy wielu związków pochodzenia naturalnego, które charakteryzują się aktywność biologiczną. Wykazują one działanie: przeciwzapalne, przeciwwirusowe, przeciwbakteryjne, przeciwgrzybicze, przeciwgorączkowe, przeciwalergiczne i przeciwcukrzycowe. Ze względu na możliwość modyfikacji struktury, szkielet benzofuranu jest obecnie powszechnie spotykanym fragmentem farmakoforów w cząsteczkach leków [2,3]. Jednocześnie pochodne benzofuranu mogą być użytecznymi koformerami w syntezie kokryształów.

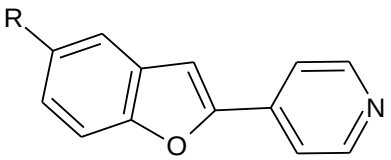

R = H: 4-(1-benzofuran-2-ylo)pirydyna
R = C_2H_5: 4-(5-etylo-1-benzofuran-2-ylo)pirydyna

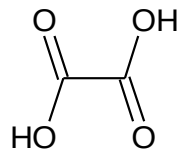

kwas szczawiowy

Rys. 1. Wzory strukturalne ko-formerów.

W prezentowanej pracy określone zostały struktury kryształów: (**a**) pirydylobenzofuranu, (**b**) jego pochodnej etylowej (Rys. 1) oraz szczawianów obu związków.

Badane cząsteczki posiadają w swojej budowie bardzo istotny synton – pierścień pirydyny – wykorzystywany w chemii supramolekularnej do „rozpoznawania" np. grup hydroksylowych czy karboksylowych [4,5].

W sieciach krystalicznych czystych ko-formerów pomiędzy układami pirydyny tworzą się dimery, które są stabilizowane międzycząsteczkowymi wiązaniami wodorowymi C-H…N (Rys. 2). Kryształ **a** zbudowany jest z dwu par cząsteczek, natomiast kryształ **b** jest tworzony przez jedną parę.

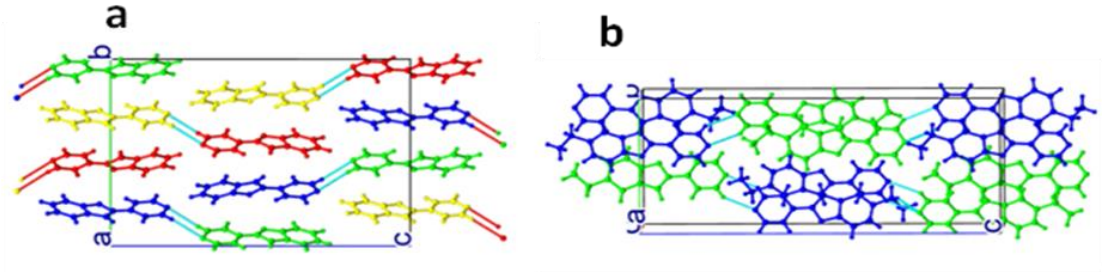

Rys. 2. Upakowanie cząsteczek ko-formerów. Cząsteczki symetrycznie niezależne są ilustrowane różnymi kolorami.

Obie pochodne pirydylobenzofuranu tworzą z kwasem szczawiowym sole o stechiometrii 1:1; proton kwasu jest przyłączany do atomu azotu pirydyny i powstaje układ o bardzo podobnej strukturze − rozpatrywanej na poziomie oddziaływań międzyjonowych (Rys. 3). W obu krystalicznych solach monoaniony szczawianowe tworzą dimery (stabilizowane przez parę wiązań wodorowych O-H…O), natomiast liczne oddziaływania kation…anion to wiązania wodorowe typu C-H…$N_{pirydyl}$ oraz C-H…O.

Taka struktura pirydylobenzofuran–kwas szczawiowy jest dość konserwatywna, o czym świadczy to, że w sieć pochodnej **a** włączona jest cząsteczka rozpuszczalnika (metanolu), która uzupełnia objętość zajmowaną przez podstawnik etylowy w krysztale szczawianu **b**. Jednak w dalszym zasięgu ułożenie asocjatów jest różne (Rys. 4). W sieci szczawianu **a** płaskie asocjaty tworzą warstwy, pomiędzy którymi inkludowane są cząsteczki metanolu; w sieci szczawianu **b** występuje asocjacja w „jodełkę".

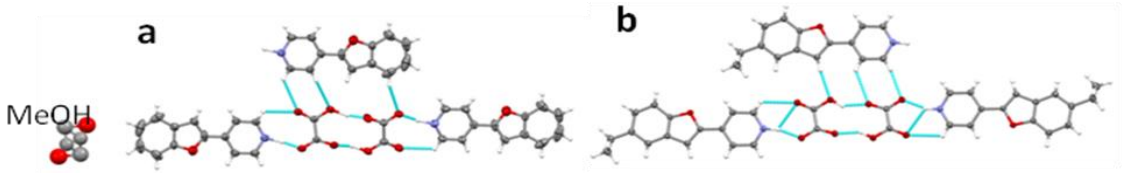

Rys. 3. Oddziaływania anion…anion oraz kation…anion w strukturach szczawianów związków **a** i **b**. W lewym rogu rysunku zaznaczone jest miejsce lokalizacji rozpuszczalnika (nieuporządkowanej cząsteczki metanolu).

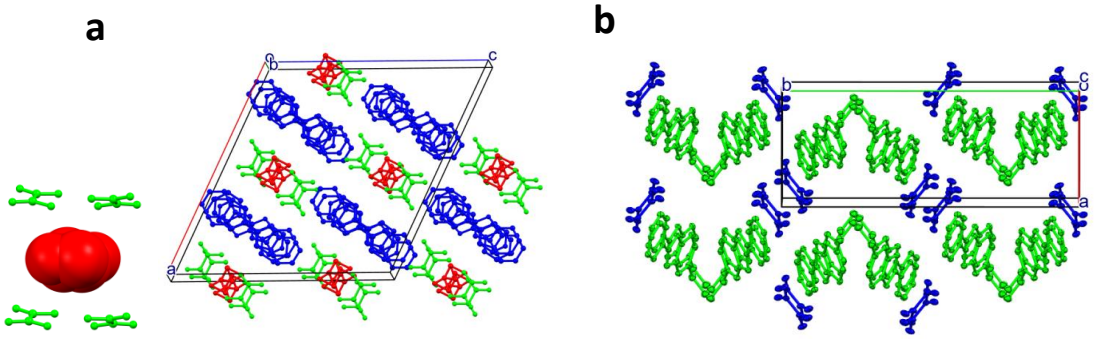

Rys. 4. Upakowanie jonów w sieciach szczawianów.

Literatura

[1] C. B.Aakeröy, M. E. Fasulo, J. Desper, *Mol. Pharmaceutics*, **4** (2007) 317.
[2] S. Nagar, S. Das, M.A. Islam, A. Mukherjee, *Lett. Drug Des. Discov.*, **6** (2009) 38.
[3] E. Hejchman, K. Ostrowska, D. Grzeszczuk, N. Kruk, *Farmacja Współczesna*, **6** (2013) 72.
[4] O. Almarsson, M.J. Zaworotko, *Chem. Commun*., (2004) 1889.
[5] K. Samanta, S. Maji, J. Samanta, R. Natarajan, *Cryst. Growth Des.*, **21** (2021) 6485.

A-68

THE XFEL CENTERS OF EXCELLENCE INITIATIVE

Katarzyna Jarzembska[a], Ryszard Sobierajski[b], Wojciech Gawełda[c,d,e], Radoslaw Kamiński[a], Adam Glinka[c], Jacek Kubicki[c], Maciej Kozak[c], Dagmara Milewska[f]

[a] *Department of Chemistry, University of Warsaw, Żwirki i Wigury 101, Warsaw, PL*
[b] *Institute of Physics, Polish Academy of Sciences, Lotników 32/46, Warsaw, PL*
[c] *Department of Physics, Adam Mickiewicz University, Uniwersytetu Poznańskiego 2, Poznań, PL*
[d] *Autonomous University of Madrid, Campus Universitario Cantoblanco, 28049 Madrid, ES*
[e] *IMDEA Nanoscience Institute, Calle Faraday 9, 28049 Madrid, ES*
[f] *National Centre for Nuclear Research, Andrzeja Sołtana 7, 05-400 Otwock, Świerk, PL*

The network of X-ray Free-Electron Laser Centers of Excellence (XFEL CoE) has been established this year to provide substantive and organizational support to the Polish scientific community in the use of the European X-ray Free-Electron Laser (EuXFEL). There are four XFEL CoE (located in the National Centre for Nuclear Research (NCNR; Świerk/Otwock), Institute of Physics of the Polish Academy of Sciences (IP PAS; Warsaw), Department of Chemistry of the University of Warsaw (UW; Warsaw) and Department of Physics of the Adam Mickiewicz University (AMU; Poznań) that bring together scientists with experience in research using XFELs, whose knowledge and commitment will constitute support for new Polish users of this infrastructure. Ryszard Sobierajski (IP PAS) is the substantive coordinator of the project. The activities planned within the project are aimed at building and development of Polish XFEL users community. They include lectures for postgraduate students, organization of workshops and conferences dedicated to XFEL science, organization and financing of internships at EuXFEL (European XFEL), training in the research techniques related to potential experiments using the EuXFEL source, as well as supporting preliminary research indispensable to prepare high-quality research proposals for measurement time on EuXFEL. The XFEL Centers' leaders will also support researches in preparation of such EuXFEL projects and applications for beamtime.

Hence, the poster will present in detail the above-mentioned initiative, with the introduction of the four Centers of Excellence in Poland, their role and contact people. The exemplary XFEL research perspectives for crystallographers will also be shown.

Acknowledgements: NSC (Poland), Support for Polish EuXFEL Users–Supervision, Part II (2022–26), Ministry of Science and Education (Poland).

A-69

NEW MODULATED PHASE OF FERROCENE DISPLAY MOLECULAR DIPOLE MOMENTS

Andrzej Katrusiak[1], Michalina Rusek[1], Michal Dušek[2], Václav Petříček[2] and Marek Szafrański[3]

[1] Faculty of Chemistry, Adam Mickiewicz University, Uniwersytetu Poznańskiego 8, 61-614 Poznań
[2] Institute of Physics, Czech Academy of Sciences, Na Slovance 2, 182 21 Praha
[3] Faculty of Physics, Adam Mickiewicz University, Uniwersytetu Poznańskiego 2, 61-614 Poznań

The discovery of ferrocene over 70 years ago initiated the rapid development in organometallic chemistry. Today, metalocenes belong to commonly known chemical compounds and precursors, which find multiple applications. While exploring the phase diagram of the prototypic sandwich compound, ferrocene $Fe^{2+}[C_5H_5]^-_2$ ($FeCp_2$), we established that its molecular 5-fold symmetry cannot be reconciled with the dielectric response of this crystal. When cooling the ferrocene crystals below the stability region of phase I, we found its new phase I'', which reveals the relationships between the molecular conformation, intermolecular interactions and electric permittivity of this compound [1]. In room-temperature ferrocene phase I, the cyclopentadienyl rings Cp are orientationally disordered, but the molecule is located on the inversion centre implying its staggered conformation. Between 172.8 and 163.5 K, the conformational disorder of ferrocene molecules is projected onto the incommensurate modulation. The structure of phase I'' is described in the (3+2)-dimensional superspace, where the molecular conformations, rotations and inclinations of the Cp rings, molecular tilts and displacements of the Fe^{2+} cations, the phases between the disordered Cp rings as well as the CH···π bonds in the crystal environment, are modulated. These modulated shifts in atomic positions combine into the geometric distortions of the idealized $FeCp_2$ molecule, for example a significant bending of the line drawn through the centroids of Cp rings and the Fe cation, which breaks the 5-fold symmetry and generates waves of molecular dipole moments with their amplitudes approaching $4 \cdot 10^{-30}$ C·m. The dipole moment of ferrocene molecules is consistent with the dielectric properties of this compound [1].

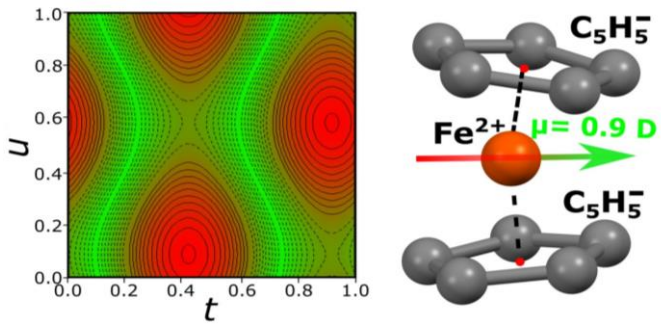

Fig. 1. Modulation map and dipole moment of ferrocene in phase I''.

References

[1] A. Katrusiak, M. Rusek, M. Dušek, V. Petříček, M. Szafrański, *J. Phys. Chem. Lett.*, **14** (2023) 3111–3119.

A-70

DISULFIDE BOND EXCHANGE IN ARYL DISULFIDES AT HIGH-PRESSURE

Szymon Sobczak, Paulina Ratajczyk, Andrzej Katrusiak

Adam Mickiewicz University, Uniwersytetu Poznanskiego 8, 61-614 Poznań, Poland

The aim of 'green' chemistry focuses on improving existing and exploring new techniques leading to the sustainable synthesis of chemical compounds. Traditionally, many materials are manufactured by solvothermal and solution-based methods - both requiring considerable amounts of energy and generating a lot of waste. To overcome these problems inspiration can be taken from nature. Mankind has always been dependent on mineral resources, many of which were formed in the unique high-pressure and high-temperature environment in Earth's crust. What is more, the energy required for compressing a sample to a considerable pressure of about 500 MPa (5 times higher than that at the bottom of the Mariana Trench) is a small fraction, about an order of magnitude less, compared to the energy needed for heating the sample by about 100 K. The highpressure technologies have already paved their way in the food industry, thus it can be expected that mimicking such extreme conditions will soon become more common to synthesize novel materials. too.

The application of pressure in the aryl disulfide exchange reaction allows excluding catalysts or any reducing agents in the process.[1] Owing to the confined reaction space of the high-pressure reactor or diamond anvil-cell, the entropy of the system can be increased in a controlled manner to a stage when the substrates are dissolved and the molecules are excited into high energy conformers, involving rota-vibrational states.[2] The mechanical energy absorbed by homodimeric aryl disulfide molecules allows and facilities the homolytic cleavage of the S-S bonds. Then the unique process of high-entropy nucleation and subsequent kinetic crystallization offsets the thermodynamic equilibrium accelerating the exchange reaction.[3] This combination of effects provides an environmentally responsible method, in which pure heterodimeric disulfides can be attained with high yields, in a form of single crystals, with a smaller number of steps, in shorter times, requiring less energy and producing less or no waste at all.[4]

Literatura

[1] S. Sobczak, W. Drożdż, G. I. Lampronti, A. M. Belenguer, A. Katrusiak, A. R. *Chem. - A Eur. J.*, **24** (2018) 8769–8773.
[2] S. Sobczak, A. Katrusiak, *J. Phys. Chem. C*, **121** (2017) 2539–2545.
[3] S. Sobczak, P. Ratajczyk, A. Katrusiak, *Chem. – A Eur. J.*, **27** (2021) 7069–7073.
[4] S. Sobczak, P. Ratajczyk, A. Katrusiak, *ACS Sustain. Chem. Eng*., **9** (2021) 7171–7178.

PLAKATY – SESJA B
POSTERS – SESSION B

B-1

ANALYSIS OF GLUCOSE/XYLOSE ISOMERASE STRUCTURES OBTAINED UNDER HIGH PRESSURE INDUCED BY DIFFERENT METHODS

Agnieszka Klonecka[1,2,3], Joanna Sławek[1], Katarzyna Kurpiewska[4], Maciej Kozak[1,5]

[1] SOLARIS National Synchrotron Radiation Center, Jagiellonian University, ul. Czerwone Maki 98, 30-392 Kraków
[2] Faculty of Physics, Astronomy and Applied Computer Science, Jagiellonian University, ul. Łojasiewicza 11, 30-348 Kraków
[3] Jagiellonian University, Doctoral School of Exact and Natural Science, Jagiellonian University, Kraków, Poland
[4] Department of Crystal Chemistry and Crystal Physics, Faculty of Chemistry, Jagiellonian University, 30-387 Kraków, Poland
[5] Department of Biomedical Physics, Faculty of Physics, Adam Mickiewicz University in Poznań, ul. Uniwersytetu Poznańskiego 2, 61-614 Poznań.

The findings from the analysis of the crystal packing of glucose/xylose isomerase from *Streptomyces rubiginous* were presented at the 63rd Polish Crystallographic Meeting. Now we are continue this project and results of diffraction experiments under high pressure, which was induced using two different methods will be presented.

The first crystal structure was obtained using a home-source diffractometer (Rigaku XtaLAB Synergy S Dualflex diffractometer) and a diamond anvil cell. The crystal structure of glucose/xylose isomerase in this experiment was successfully determined at the pressure of 288 MPa and the resolution of 2.5 Å.

The second structure was determined on the basis of diffraction data collected at the European Synchrotron Radiation Facility. The protein crystals have been frozen under high pressure (200 MPa) induced by gaseous helium. The resulting structure of glucose/xylose isomerase is characterized by a resolution of 1.33 Å.

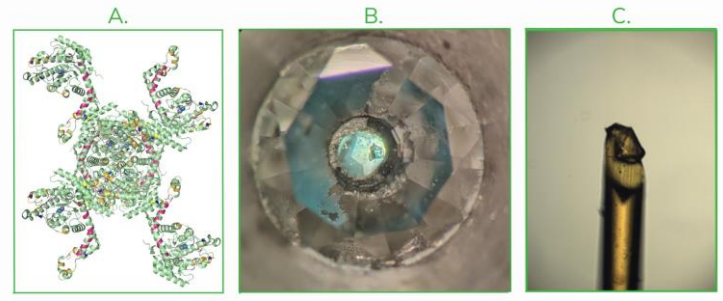

Fig. 1. Crystal packing of glucose/xylose isomerase – the most important contacts (A). Glucose/xylose crystals in the diamond anvil cell (B) and during freezing under high-pressure (C)

In our presentation, we show obtained by us structures of glucose/xylose isomerase and their comparative analysis (2 high pressure structures and 1 reference structure at ambient pressure), focusing on differences in the crystal packing induced by the pressure.

This work was supported by research grant PRELUDIUM BIS (grant ID: 2020/39/O/ST4/03465) from National Science Centre (Poland).

B-2

PURIFICATION AND CRYSTALLIZATION OF THE MURINE TBC1D17

Dominika Krzeszewska, Agnieszka Pietrzyk-Brzezińska, Edyta Gendaszewska-Darmach

Institute of Molecular and Industrial Biotechnology, Lodz University of Technology, ul. Stefanowskiego 2/22, 90-573 Łódź

Rab proteins belong to the superfamily of small GTPases which are responsible for the regulation of the processes related to endocytosis, sorting and transport of cargo across membranes, formation of lysosomes, growth and differentiation, as well as maintaining the homeostasis of the organism by neutralizing pathogens [1]. Their activity is tightly controlled by posttranslational modifications and regulatory proteins, among which the GTP-ase activating proteins (GAPs) can be distinguished. These regulators bind to Rabs in active, GTP-bounded form, and stimulate their intrinsic hydrolytic activity, leading to downregulation of small GTPases [2].

Due to a wide range of the Rab proteins function, their altered activity is often related to occurrence of neurodegenerative, oncologic, immune and metabolic disorders [1]. While type 2 diabetes mellitus, a complex metabolic disorder, affects approximately 463 million adults and cause death of about 1,5 million people per year [2, 3], searching for new methods that could change the activity of key proteins causing disease symptoms is needed. For this purpose, it is necessary to know the spatial structure of the molecular targets such as GAPs.

Literature data indicate that one of the proteins which is crucial for proper glucose metabolism is Rab5 and its level of expression is decreased in physiological conditions conducive to the development of type 2 diabetes [4]. Moreover inhibition of TBC1D17, which is a recently identified GAP for Rab 5, improved glucose uptake by myoblasts [5]. Unfortunately, the structure of TBC1D17 protein is not known so far. Therefore, one of the aims of our project is the determination of the crystal structure of TBC1D17. TBC1D17 was purified using chromatographic techniques and crystallized using vapour diffusion method. However, the obtained crystals require further optimization which is currently underway.

Research is part of the project Preludium Bis-3 (2021/43/O/NZ1/01565) financed by National Science Centre, Poland.

Literature

[1] J. Agola, P. Jim, H. Ward, S. Basuray, A. Wandinger-Ness, *Clin Genet.*, **80**(4) (2011) 305-318.
[2] E. Gendaszewska-Darmach, M. Garstka, K. Błażewska, *J. Med. Chem.*, **64** (2021) 9677-9710.
[3] WHO statistics, 2023.
[4] A. Karvela, E. Kostopoulou, A. Gil, A. Avgeri, A. Papa, V. Barrios, G. Lambrinidis, I. Dimopoulos, G. Georgiou, J. Argente, B. Spiliotis, *Horm. Res. Paediatr.*, **93**(5) (2020) 287-296.
[5] X. Rao, X. Cong, X. Gao, Y. Shi, L. Shi, J. Wang, C-Y. Ni, M. He, Y. Xu, C. Yi, Z-X. M.eng, J. Liu, P. Lin, L. Zheng, Y. Zhou, *Cell Death Differ.*, **28**(12) (2021) 3214-3234.

B-3

FIRST STRUCTURES OF PLANT' ORNITHINE TRANSCARBAMYLASE FROM *ARABIDOPSIS THALIANA* IN THEIR LIGANDED STATE

Maciej Nielipiński, Bartosz Sekuła, Agnieszka Pietrzyk-Brzezińska

Institute of Molecular and Industrial Biotechnology, Lodz University of Technology, ul. Stefanowskiego 2/22, 90-573 Łódź

Function of urea cycle in animals and plants is similar yet different. In both cases it is a central part of nitrogen metabolism, yet the goal for animals is to excrete excess nitrogen by secretion [1], while for pants excess nitrogen is stored – mainly in form of arginine [2]. While plethora of functional studies for plant's urea cycle are present, when it comes to structure only one enzyme out of nine is known. Here we present structures of *Arabidopsis thaliana* ornithine transcarbamylase (OTC) bound to biological ligands.

OTC catalyses reaction of condensation between carbamoyl phosphate' carbamoyl group (CP) and ornithine, yielding citrulline which later can be processed to arginine [2]. Plant's OTC activity is naturally blocked by phaseolotoxin derivative octicidine – produced by *Pseudomonas syringae*, This inhibition lead to disease known as "halo blight" [3].

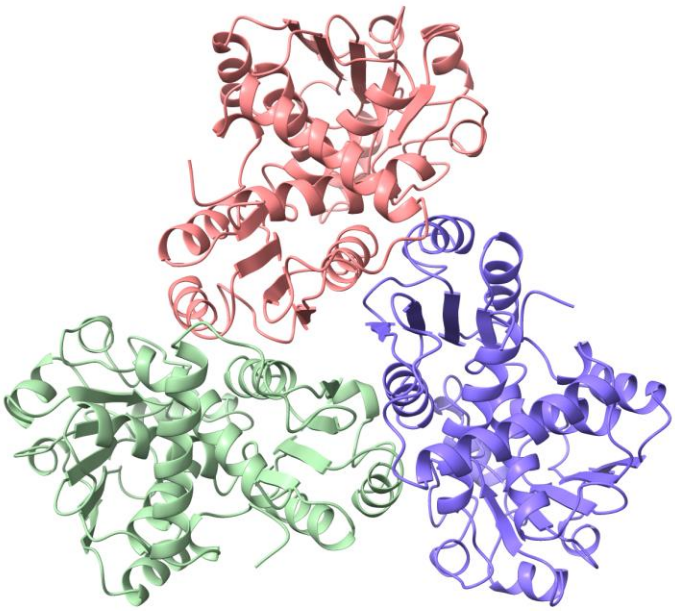

Fig. 1. *Biological assembly of AtOTC.*

*At*OTC shares distinct similarities with OTCs from both eukaryotic and prokaryotic organisms. It is an α/β protein that has 2 distinguishable domains: N-terminal - CP-binding and C-terminal - ornithine binding. Subunits form symetric trimeric assembly (Fig 1.). Both domains share topological similarities, as they are

composed of β-sheet seated between flanking α-helices forming a Rossman-like fold motif. Substrate binding site is located in the cleft between domains. Binding of ornithine causes domain closure by structurization of 300s loop – with both conformations seen in presented structures.

This research was funded by National Science Centre project SONATA17 2021/43/D/NZ1/00486.

Literature

[1] P. A. Wright, *J Exp Biol*, **198 (Pt 2)** (1995) 273–281.
[2] G. Winter, C. D. Todd, M. Trovato, G. Forlani, D. Funck, *Sec. Plant Physiology*, **6** (2015).
[3] C. L. Bender, F. Alarcon-Chaidez, D. C. Gross, *Microbiol Mol Biol Rev*, **63(2)** (1999) 266–292.

B-4

INITIAL CRYSTALLOGRAPHIC STUDIES OF HTRA AND HtrA_ΔPDZ2 PROTEINS FROM *HELICOBACTER PYLORI*

Marta Orlikowska[1], Zofia Kurkiewicz[1], Urszula Zarzecka[2], Joanna Skórko-Glonek[2]

[1] *Wydział Chemii, Uniwersytet Gdański, ul. Wita Stwosza 63, 80-308 Gdańsk*
[2] *Wydział Biologii, Uniwersytet Gdański, ul. Wita Stwosza 59, 80-308 Gdańsk*

Helicobacter pylori infections are widespread worldwide and the infection rates of the human population ranges from approximately 20% to almost 90%. Although these bacteria typically colonies the stomach for many decades without significant consequences, the presence of *H. pylori* is associated with an increased risk for several diseases, including peptic ulcers, non-cardia gastric adenocarcinoma and gastric MALT lymphoma. For these reasons, *H. pylori* is classified as a Group I carcinogen. The virulence determinants of *H. pylori* can be related to the pathogenic processes, including colonization, immune escape and development of disease symptoms. This pathogen requires numerous essential virulence factors to establish infection, including the serine protease HtrA (High Temperature Requirement A).

The *Helicobacter pylori* HtrA protein (HtrAHp) is an important virulence factor involved in the infection process by proteolysis. As a protease and chaperone, HtrAHp is involved in protein quality control, which is particularly important under stress conditions. HtrAHp contains a protease domain and two C-terminal PDZ domains (PDZ1 and PDZ2). In the HtrA protein family, the PDZ domains are proposed to play important roles, including regulation of proteolytic activity.

The aim of our project was to provide details information about the structure of two variants of the HtrA protein from *Helicobacter pylori* (a full-length protein and a protein lacking one PDZ domain – HtrA_ΔPDZ2).

References

[1] Zarzecka *et al*., *Cell Microbiol.* **23** (2021) 13299.
[2] Zarzecka *et al*., *Front Microbiol.*, **10** (2019) 961.

B-5

STRUCTURAL CHARACTERISTICS OF 5-(CHLOROBENZYLIDENE)RHODANINE-3-CARBOXYALKYL DERIVATIVES

Wojciech Nitek[a], Ewa Żesławska[b], Waldemar Tejchman[b]

[a] Faculty of Chemistry, Jagiellonian University, Gronostajowa 2, 30-087 Kraków
[b] Institute of Biology and Earth Sciences, Pedagogical University, Podchorążych 2, 30-084 Kraków

Rhodamine derivatives are known for a wide range of biological activities. They demonstrate antibacterial, antifungal, antiviral, antiparasitic, antidiabetic, antineoplastic and antiinflammatory activity [1].

In our earlier research [2], the antibacterial activity of 5-substituted derivatives of rhodanine-3-carboxyalkyl acids was investigated. At present, our interest is focused on some structural aspects of selected compounds.

The crystal structures of three synthetized compounds were determined: 5-(2'chlorobenzylidene)rhodanine-3-propionic acid (**R1**), 5-(3'chlorobenzylidene)-rhodanine-3-propionic acid (**R2**) and 5-(4'chlorobenzylidene)-rhodanine-3-propionic acid (**R3**). For compound R2 two polymorphs (R2a and R2b) were obtained.

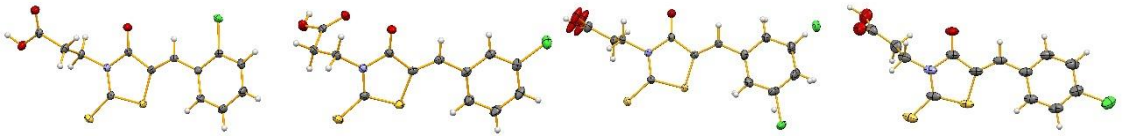

R1 **R2a** **R2b** **R3**

Dominant motif of crystal packing of each studied structure is O-H...O intermolecular H-bonds. It should be noted that presented compounds differ in position of chlorine atom in chlorobenzylidene fragment. Obviously it affects the crystal packing and interactions with the neighbourhood. The comparison of **R2a** and **R2b**, which differ in the orientation of the chlorobenzylidene fragment, shows the involving of chlorine atom in the halogen bond only in **R2b**.

References

[1] D. Kaminskyy, A. Kryshchyshyn, R. Lesyk, *Eur. J. Med. Chem*., **140** (2017) 542.
[2] W. Tejchman, I. Korona-Głowniak, A. Malm, *et al*., *Med. Chem. Res*., **26** (2017) 1316.

B-6

CHARAKTRYSTYKA ODDZIAŁYWAŃ PEPTYDÓW AMYLOIDU BETA Z WYBRANYMI NANOCZĄSTKAMI WĘGLOWYMI

Anna Bisok, Julia Telus, Żaneta Polańska, Maciej Kozak

Zakład Fizyki Biomedycznej, Uniwersytet Adama Mickiewicza,
ul. Uniwersytetu Poznańskiego 2, 61-614 Poznań

Choroba Alzheimera (AD) to nieuleczalne i śmiertelne schorzenie neurodegeneracyjne, które stopniowo degraduje tkankę nerwową mózgu, upośledza pamięć, procesy myślowe, a w końcu nawet zdolność do wykonywania podstawowych czynności. Jego patogeneza nie jest poznana, jednakże postulowana jest hipoteza, nazywana amyloidową, zgodnie z którą, białko prekursorowe amyloidu (APP) jest „cięte" przez enzymy (β- i γ-sekretazy). W efekcie prowadzi to do powstania kilku wariantów oligopeptydów (tzw. peptydów β-amyloidowych), zazwyczaj o długości 40, 42 lub 43 reszt aminokwasowych. Wykazują one tendencję do formowania oligomerów, agregatów i złogów amyloidowych, które deponując się w mózgu prowadzą do stopniowej degradacji neuronów [1].

Dotychczasowe dane wskazują, że różne nanocząstki węglowe mogą modulować procesy agregacji peptydów Aβ [1,2]. Od wielu lat nanocząstki węglowe, takie jak fullereny, są badane w celu określania ich zastosowań w medycynie, technologii i farmacji. Mogą potencjalnie być przydatne w zastosowaniach biomedycznych, co jest związane z ich unikalnymi właściwościami fizykochemicznymi, takim jak dużą powierzchnia czynna przy stosunkowo małym rozmiarze (zwykle poniżej 100 nm) i zdolność do przekraczania bariery krew-mózg [3].

Podejrzewa się, że hydrofobowe powierzchnie nanocząstek węglowych mogą wchodzić w interakcje z amyloidami beta, co jest możliwe do zaobserwowania za pomocą dedykowanych technik spektroskopowych oraz mikroskopii elektronowej i AFM.

Dlatego za cel prezentowanych badań, wybrano zbadanie interakcji między peptydami Aβ a wybranymi nanocząstkami węglowymi. Szczegółowe zrozumienie mechanizmów patologicznej agregacji peptydów Aβ w obecności nanocząstek węglowych powinno pomóc w lepszym zrozumieniu procesów neurodegeneracyjnych.

Badania te zostały częściowo sfinansowane dzięki grantu Study@Research.

Literatura

[1] Ghosh, S., Sachdeva, B., Sachdeva, P. *et al.* Graphene quantum dots as a potential diagnostic and therapeutic tool for the management of Alzheimer's disease. *Carbon Lett.*, **32** (2022) 1381–1394. DOI: 10.1007/s42823-022-00397-9.

[2] Guo F, Li Q, Zhang X, Liu Y, Jiang J, Cheng S, Yu S, Zhang X, Liu F, Li Y, Rose G, Zhang H. Applications of Carbon Dots for the Treatment of Alzheimer's Disease. *Int. J.. Nanomedicine.,* **17** (2022) 6621–6638. DOI: 10.2147/IJN.S388030.

[3] Priyadarsini, S., Mohanty, S., Mukherjee, S. *et al.* Graphene and graphene oxide as nanomaterials for medicine and biology application. *J. Nanostruct. Chem.*, **8** (2018) 123–137. DOI: 10.1007/s40097-018-0265-6.

B-7

THE NATURE-INSPIRED MUTAGENESIS OF THE *E. COLI* L-ASPARAGINASE EcAIII: STRUCTURAL AND BIOINFORMATIC STUDIES

Maciej Janicki[1], Anna Ściuk[2], Andrzej Zielezinski[1], Miłosz Ruszkowski[3], Agnieszka Ludwików[1], Wojciech M. Karłowski[1], Mariusz Jaskolski[3,4], Joanna Loch[2]

[1] *Faculty of Biology, Adam Mickiewicz University, Poznań, Poland*
[2] *Faculty of Chemistry, Jagiellonian University, Krakow, Poland*
[3] *Institute of Bioorganic Chemistry, Polish Academy of Sciences, Poznań, Poland*
[4] *Faculty of Chemistry, Adam Mickiewicz University, Poznań, Poland*

Site-directed mutagenesis is a common approach to elucidate the role of particular residues in protein stability or enzymatic activity. There are many ways to design mutations. We have shown that pangenomic analyses combined with molecular modeling can facilitate the design of new EcAIII variants [1]. We used a recent collection of EcAIII orthologous sequences present in 11,435 bacterial species to generate a position-specific scoring matrix (PSSM). In the close vicinity of the substrate binding site, we observed the highest variability across the orthologs at the position corresponding to Met200 in EcAIII. At this site, in more than half of the orthologs, Met200 was replaced by one of the five residues: W, L, T, K, I (Fig. 1). We produced a series of EcAIII variants and obtained crystals of four mutants: M200I, M200L, M200T, and M200W. Despite many trials, we could not crystallize the M200K mutein, so its structure was predicted with AlphaFold2 [2].

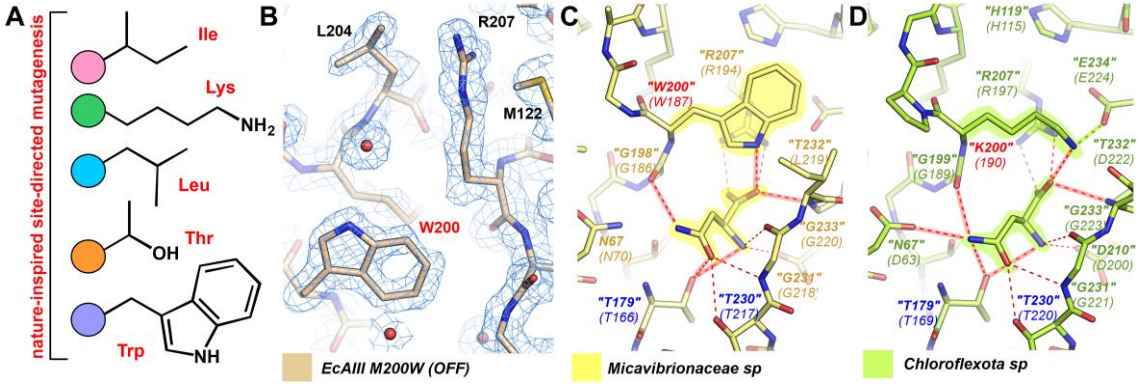

Fig. 1. (A) Site-directed mutagenesis of Met200 in EcAIII protein. (B) Electron density map 2FoFc (1.00σ) around mutation site in M200W mutant in OFF state. Interactions stabilizing substrate in the active site of the predicted structure of EcAIII ortholog from (C) *Micavibrionaceae sp* (sp002789675[1]) and (D) *Chloroflexota sp* (sp011362935[1]). [1]Names from the Genome Taxonomy Database.

We also examined how other natural Ntn-amidohydrolases adapt their active sites to the presence of residues that were selected for EcAIII mutagenesis. We observed that the substitutions "M200W" and "M200K" may be beneficial for substrate stabilization (Fig. 1 C, D), but to achieve such a positive effect, additional mutations should be simultaneously present to prevent large-amplitude fluctuations of "Lys200"

or switching of the enzyme to the OFF-state by “Trp200”. Moreover, we found that in some proteins one of the threonines from the threonine triad was replaced by Ser.

By analyzing sequences and predicted structures of 25 orthologs of EcAIII, originated from different bacterial species, we identified a number of interesting proteins that could be promising targets for future engineering and therapeutic applications. It seems that bacteria living in halophilic and thermophilic environments as well as in the rhizosphere could serve as valuable sources of new L-asparaginases with outstanding properties. As the therapeutic potential of L-asparaginases is not limited to leukemias but can be applied to other types of cancer [3], there is high interest in the design of new therapeutic L-asparaginases.

Work supported by National Science Centre (NCN) grant 2020/38/E/NZ1/00035

References

[1] M. Janicki, A. Ściuk, A. Zielezinski, M. Ruszkowski, A. Ludwików, W. Karlowski, M. Jaskolski, J. Loch, *Protein Sci*., **6** (2023) e4647.
[2] Jumper J, Evans R, Pritzel A, Green T, Figurnov M, Ronneberger et al., *Nature*, **596** (2021) 583-589.
[3] J. Jiang, S. Batra, J. Zhang, *Metabolites*, **11** (2021) 402.

B-8

CUCURBIT[7]URIL-MEDIATED HISTIDINE DIMERIZATION: EXPLORING THE STRUCTURE AND BINDING MECHANISM

Ewelina Zaorska, Maura Malińska

Wydział Chemii, Uniwersytet Warszawski, ul. Pasteura 1, 02-093 Warszawa

Cucurbit[7,8]urils form inclusion complexes with hydrophobic amino acids (Trp, Tyr, Phe, Met) and peptides containing these residues at the N-terminus. However, despite their common use in protein purification, the affinity of histidine (His) residues to cucurbit[7,8]urils have not been extensively studied. X-ray diffraction experiments were performed to explore the binding of histidine residues to the cucurbit[7]uril (CB7) cavity. We obtained crystal structure of CB7 with L-His, D-His and LD-His. Previous computational studies focused on a 1:1 ratio between CB7 and histidine, whereas our results demonstrate that CB7 can simultaneously bind two histidine molecules. The property of binding two guests were previously believed to be preserved in larger cavities. This information expands our understanding of the complexation behavior between CB7 and histidine, emphasizing the importance of considering higher order binding interactions. Histidine dimer is facilitated by the hydrophobic CB7 shell. This close parallel stacking arrangement is unique and not typically observed in crystal structures of small molecules or proteins. Histidine weakly binds to CB7 or CB8; however, isothermal titration calorimetry revealed micromolar equilibrium dissociation constant values for CB7 and CB8 bound to dipeptides containing His at the C-terminus. For those with histidine at the N-terminus, the values were only millimolar. These results show that the receptor CB7 exhibits high selectivity for specific peptide sequences, which may allow its use in biological applications to recognise recombinant proteins containing N-terminal Leu-His affinity tags.

Overall, our study contributes to the comprehensive characterization of histidine's binding properties and provides novel insights into the complexation behavior of histidine with CB7. These findings pave the way for further investigations and potential applications of histidine in molecular recognition and supramolecular chemistry.

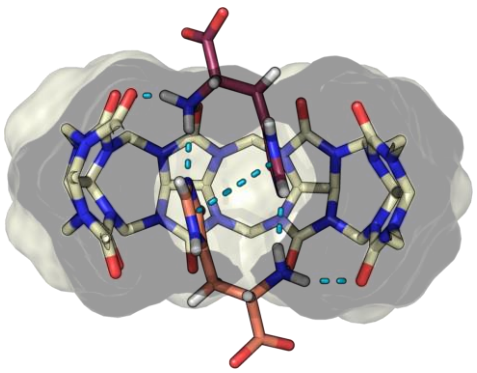

Fig. 1. D-His@CB7 in the asymmetric part of the unit cell of the crystal structure with host-guest ratio 1:2. The CB7 and His molecules were drawn using a stick representation, and the van der Waals surface is shown for CB7. Hydrogen bonds and $\pi...\pi$ stacking interactions are represented as blue dashed lines.

B-9

HOW PRESSURE INFLUENCES THE STRUCTURE OF HIV PROTEASE? – INTRODUCTION TO HIGH-PRESSURE STUDIES

Joanna Sławek, Agnieszka Klonecka, Maciej Kozak

SOLARIS National Synchrotron Radiation Centre, Jagiellonian University, ul. Czerwone Maki 98, 30-392 Kraków, Poland

Research under high pressure is usually associated with the characterization of new materials, minerals as well as geological processes. However, it turns out that this type of research is also very helpful in characterizing biological samples. Depending on the applied pressure, various types of changes in the protein structure can be observed, such as unit cell compression, phase transition, conformational rearrangements, improvement of diffraction quality by reducing disorder, compression of internal pockets and tunnels, changes in the hydration structure or changes in the position and conformation of ligands [1]. The effect of high pressure on the functioning of enzymes remains in the area of basic research (e.g. dynamics of structural elements induced by pressure) and application interest (enzymatic activity in technological processes).

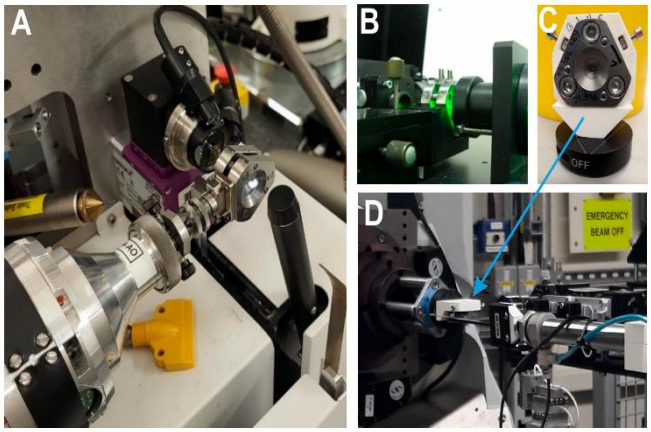

Figure. 1. Diamond anvil cell on the crystallographic beamline ID30B at ESRF (A) and I19 at DIAMOND (B-D). [1]

Proteases are enzymes that play a key role in the viral replication process. They are responsible, among others, for the formation of a mature virion. Due to their function, proteases are often chosen as the target of research into new therapeutic strategies [2-4].

This research focuses on preparing the samples for high-pressure protein crystallography studies of HIV-1 protease, as a part of the MINIATURA 5 project. Literature data suggest that the applied pressure may induce large conformational changes in HIV protease structure, but this has not been confirmed by crystallographic studies so far. [5-6] As an introduction for the high pressure crystallographic studies, this presentation describes the first experimental steps. In particular, this involves protein expression, purification, stability assays and crystallization.

After optimalization of crystallization conditions, the best crystals will be selected for crystallographic studies. Crystals will be pressurized inside of the DAC cell and subjected to the diffraction experiments.

B-9

This work was supported by research grant MINIATURA 5 (grant ID: 2021/05/X/ST5/01496) from National Science Centre (Poland).

Literature

[1] Kurpiewska K et al. (2023) *Crystals* https://doi.org/10.3390/cryst13040560
[2] Silva J.L. et al. (2015) *High Pressure Bioscience*, DOI: 10.1007/978-94-017-9918-8_15
[3] Huang L. et al. (2019) *Sci. Rep*., DOI: 10.1038/s41598-018-36730-4
[4] Włodawer A. et al. (1989) *Science*, DOI:10.1126/science.2548279
[5] Ingr M. et al (2015) *PLOS One*, DOI: 10.1371/journal.pone.0119099
[6] Kutálková E. et al. (2014) *Phys. Chem. Chem. Phys*., DOI:10.1039/C4CP03676J

B-10

CZY KRYSZTAŁY O SŁABYCH ODDZIAŁANIACH MIĘDZYCZĄSTECZKOWYCH MOGĄ MIEĆ WYSOKĄ TEMPERATURĘ TOPNIENIA?

Elżbieta Łastawiecka, Anna E. Kozioł, Marek Stankevič, Daniel M. Kamiński

Katedra Chemii Organicznej i Krystalochemii, Wydział Chemii UMCS, Lublin

Przemiany fazowe, a zwłaszcza temperatury topnienia, są od dawna problemem w nauce i technice, co jest szczególnie istotne w farmacji, naukach o środowisku i inżynierii materiałowej [1-4]. Oprócz bezpośredniego wykorzystania temperatur topnienia do wskazania przejścia fazowego ciało stałe-ciecz, są one również wykorzystywane do oszacowania m.in. rozpuszczalności w wodzie, toksyczności.

Intuicyjnie, wzrost temperatury powoduje wzrost drgań atomów lub cząsteczek, aż pokonają one siły przyciągania scalające kryształ. Termodynamicznie temperatura topnienia to temperatura, w której fazy stała i ciekła czystej substancji współistnieją w równowadze pod ciśnieniem atmosferycznym, przy energii swobodnej przemiany fazowej równej zeru [5].

$$\mathbf{0} = \Delta G = \Delta H_m - T_m \Delta s_m \qquad T_m = \Delta H_m / \Delta s_m$$

Wspomniana zależność wskazuje, że na zachowanie dowolnego kryształu w temperaturze topnienia wpływają zarówno siły oddziaływania związane z entalpią, jak i entropią. Siły entalpii obejmują efekty jonowe, dipolowe, dyspersyjne i wiązania wodorowe, podczas gdy efekty entropowe obejmują wpływ położenia, rotacji, translacji i zmienność konformacyjną (wibracje) cząsteczek.

Zgodnie z teorią topnienia Motta zależność między energią sieci krystalicznej a temperaturą topnienia ($-E_{latt}/T_m$) jest względnie stała, co wykazano doświadczalnie dla metali alkalicznych. Jest to jednak prosty przypadek w porównaniu z cząsteczkami organicznymi (> 10 atomów), w których część entropowa zgodnie z równaniem może mieć znaczący wpływ na destrukcję sieci. Powszechnie wiadomo, że symetria może wpływać na entropię rotacyjną [6], która nie jest uwzględniana w prostych obliczeniach energii spójności kryształu. Cząsteczka, która wykazuje wysoką entropię rotacyjną (niską symetrię) ma niską temperaturę topnienia kryształu.

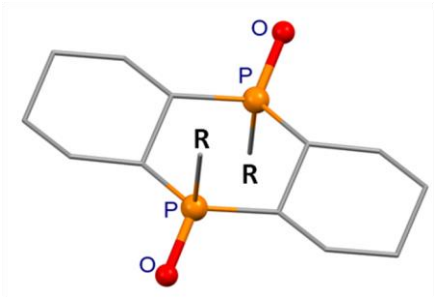

(I) **R** = metyl; tt = 407 °C
(II) **R** = cyklopentyl, tt = 342 °C
(III) **R** = *tert*-butyl, tt = 280 °C

Rys. 1. Temperatury topnienia badanych związków.

W naszym badaniu analizujemy kryształy trzech pochodnych alicyklicznych tlenków fosfin (Rys. 1), w których symetryczne cząsteczki przyciągają się jedynie poprzez oddziaływania dipol-dipol i van der Waalsa. Związki te mają wyjątkowo wysoką temperaturę topnienia jak dla oddziaływań międzycząste-czkowych tego typu (Rys. 2). Taka temperatura topnienia nie może być związana tylko z efektami entalpowymi.

B-10

Sieci kryształów **I** – **III** stabilizowane są głównie przez oddziaływania międzycząsteczkowe H…H i C-H…O (Rys. 3). Na przykład dla związku **I**, o temperaturze topnienia 407 °C, udziały kontaktów wynoszą 81% (H…H) oraz 10 % (C-H…O).

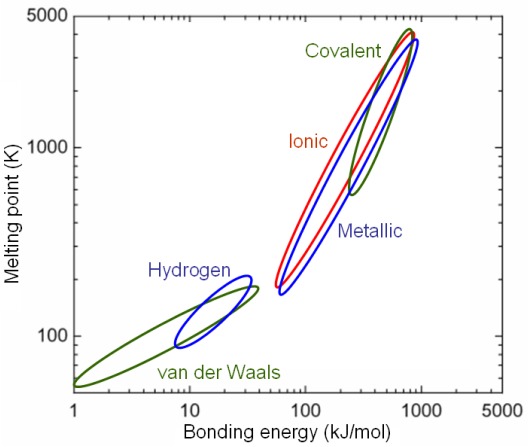

Rys. 2. Zależność temperatury topnienia od rodzaju wiązania [7].

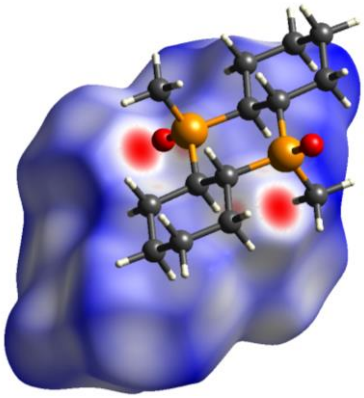

Rys. 3. Powierzchnia Hirshfelda cząsteczki **I**.

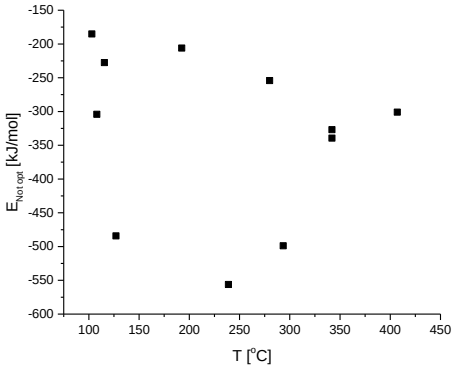

Rys. 4. Zależność temperatur topnienia od energii sieci.

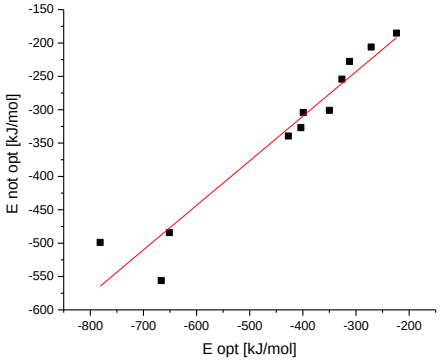

Rys. 5. Zależność pomiędzy energiami sieci zrelaksowanej i niezrelaksowanej.

Pokazujemy, że ignorowanie efektów entropowych prowadzi do niskiej korelacji między temperaturą topnienia a obliczoną energią sieci (Rys. 4). Liniowa zależność E_{opt}-E_{notopt} (Rys. 5) wskazuje, że relaksacja sieci nie ma wpływu na powyższą zależność.

Obliczenia energii sieci zostały wykonane w programie Crystal17 udostępnionego przez Wrocławskie Centrum Obliczeniowe.

Literatura

[1] H.M. Titi, M. Arhangelskis, G.P. Rachiero, T. Friscic, R.D. Rogers. *Angew. Chem. Int. Ed.*, **58** (2019) 18399.
[2] I.V. Tetko, D.M. Lowe, A.J. Williams. *J. Cheminform.*, **8** (2016) 2.
[3] U.P. Preiss, W. Beichel, A.M.T. Erle, Y.U. Paulechka, I. Krossing. *ChemPhysChem*, **12** (2011) 2959.
[4] I.V. Tetko, Y. Sushko, S. Novotarskyi, L. Patiny, I. Kondratov, A.E. Petrenko, L. Charochkina, A.M. Asiri. *J. Chem. Inf. Model.*, **54** (2014) 3320.
[5] S.S. Godavarthy, R.L. Robinson Jr., K.A.M. Gasem. *Ind. Eng. Chem. Res.*, **45** (2006) 5117.
[6] S.H. Yalkowsky. *J. Pharm. Sci.*, **103** (2014) 2629.
[7] *www.globalsino.com/EM/page3239.html*

B-11

ANALIZA STRUKTURALNA NOWYCH FOTOUCZULACZY BODIPY ZAWIERAJĄCYCH UGRUPOWANIE BIS[1]BENZOTIENO[1,4]TIABORINOWE

Paulina H. Marek-Urban[a,b], Karolina Wrochna[a], Karolina Urbanowicz[b], Krzysztof Woźniak[b], Krzysztof Durka[a]

[a]*Wydział Chemiczny, Politechnika Warszawska, ul. Noakowskiego 3, 00-664 Warszawa*
[b]*Wydział Chemii, Uniwersytet Warszawski, ul. Pasteura 1, 02-093 Warszawa*

Reaktywne formy tlenu (ROS, ang. *reactive oxygen species*), z uwagi na swoje silne własności utleniające, znajdują zastosowanie w syntezie organicznej, fotouzdatnianiu wody oraz w medycynie i biologii.[1] Poszukiwanie fotouczulaczy zdolnych do wydajnego generowania ROS jest więc przedmiotem szeroko zakrojonych badań. Na szczególną uwagę zasługują kompleksy BODIPY, które poddane odpowiednim modyfikacjom strukturalnym wykazują zadowalające własności fotouczulające. Jedną ze strategii projektowania efektywnych fotouczulaczy BODIPY, może być przestrzenne rozseparowanie i prostopadłe ułożenie obszaru donora i akceptora w cząsteczce.[2] Dzięki temu, podczas wzbudzenia możliwe jest zachodzenie fotoindukowanego przeniesienia elektronu z fragmentu donora do akceptora (PeT, ang. *photoinduced electron transfer*), co skutkuje tworzeniem się wzbudzonych stanów z przeniesieniem ładunku (CT, ang. *charge transfer*). Singletowe stany CT, podczas wtórnego transferu elektronu mogą tworzyć stany trypletowe, kluczowe do aktywacji cząsteczek tlenu.

Proponowane przez nas podejście zakłada przeniesienie donora na bis[1]benzotieno[1,4]tiaborinowe ugrupowanie boracykliczne (BBTB), podczas gdy akceptor lokalizuje się w obszarze liganda dipirolometanylylidenowego (BDP). Otrzymane dwa izomery boroorganicznych kompleksów BODIPY wykazywały wysokie wydajności generowania ROS (ok. 70 %) oraz cechowały się wysoką fotostabilnością. Wykonana charakterystyka spektroskopowa potwierdziła występowanie emisyjnych stanów CT w roztworach badanych układów. Badania strukturalne potwierdziły wzajemne prostopadłe ułożenie fragmentów donora i akceptora. Co więcej, w strukturach rozpoznano występowanie typowych dla kompleksów BODIPY J-agregatów, które jednak różniły się sposobem ułożenia cząsteczek między izomerami *syn-syn* oraz *anti-anti*. Udało się także otrzymać ko-kryształy solwatów toluenowych dla jednego z izomerów. Geometrie kompleksów uzyskane z badań strukturalnych posłużyły do wykonania obliczeń kwantowo-chemicznych, które pozwoliły zracjonalizować mechanizm generowania ROS przez badane związki. [3]

Finansowanie badań w ramach projektu OPUS 20 (2020/39/B/ST4/02370). Praca zrealizowana w ramach Programu Operacyjnego Wiedza Edukacja Rozwój 2014-2020 współfinansowanego ze środków Europejskiego Funduszu Społecznego.

Literatura

[1] M. C. DeRosa *et. al., Coord. Chem. Rev.*, **233** (2002) 351-371.
[2] Z. Wang, *et al., Chem. Eur., J.* **26** (5) (2020) 1091-1102.
[3] P. H. Marek-Urban, *et al., Chem. Eur. J.*, (2023) e202300680.

B-12

POLYMORPHISM AND CONFORMATIONAL DIVERSITY OF TETRA-*O*-ETHYL-*p*-*tert*-BUTYLCALIX[4]ARENE

Renny Louis Anto Maria Losus, Marek Krzemiński and Liliana Dobrzańska

Nicolaus Copernicus University in Toruń, Faculty of Chemistry, 87-100 Toruń, Poland

Calixarenes have gained significant attention in the field of supramolecular chemistry due to their straightforward synthesis, well-defined and modifiable cavity, selective guest binding capabilities, and structural flexibility. Various derivatives of calixarenes have found applications as hosts, sensors, drug carriers, adsorbents, and more. Extensive research has been conducted to explore their properties in solution and the solid state, including conformational flexibility, packing arrangements, and guest binding properties [1].

In general, calix[4]arenes display four conformations, namely cone, partial cone, 1,2-alternate, and 1,3-alternate. At room temperature, *p-tert*-butylcalix[4]arene (CA4) exhibits the ability to undergo interconversions among its four conformers in solution [2]. The degree of this conformational flexibility depends on the steric hindrance of the substituents, so it can be influenced by structural modifications. For instance, tetra-*O*-*methyl*-*p*-*tert*-butylcalix[4]arene displays a dynamic equilibrium among the four conformers at temperatures already slightly above room temperature, whereas tetra-*O*-*ethyl*-*p*-*tert*-butylcalix[4]arene undergoes the equilibrium process at temperatures exceeding 100°C [3]. In the solid state, CA4 undergoes single-crystal to single-crystal transformations (SCSCs) between the host-guest complex and the apohost phases, resulting in different host-guest complexes and packing arrangements.

This study focuses on the solid-state properties of tetra-*O*-*ethyl*-*p*-*tert*-butylcalix[4]arene (CA4Et). The cone and partial cone conformers of CA4Et were characterized earlier by NMR studies (solution) [4]. We would like to present solid-state characterization results which led to the isolation of two polymorphs of the compound adopting the partial cone conformation (PC1, PC2), and a crystal structure in which the molecules adopt the cone conformation (C1). PC1 and PC2, were obtained from EtOH, whereas crystals of the cone conformer (C1) were obtained from benzene, by slow evaporation. The crystal structures were determined by single-crystal X-ray diffraction (SCXRD).

Both polymorphs (PC1 and PC2) crystallize in the monoclinic $P2_1/c$ space group and display distinct packing arrangements. The presence of these two phases in the initial bulk was confirmed by powder X-ray diffraction (PXRD). Hirshfeld surfaces and fingerprint plots were generated and analyzed for all crystal structures. Furthermore, the crystal lattice energies were calculated using Pixel to elucidate the differences in packing and compare the stability of the obtained phases. In all crystal structures, the stabilization primarily arises from weak CH-π interactions and dispersion forces. Detailed results on the structural characterization of these phases will be presented.

Acknowledgements: RL and LD would like to thank the National Science Centre – Poland for grant no. 2014/14/E/ST5/00611.

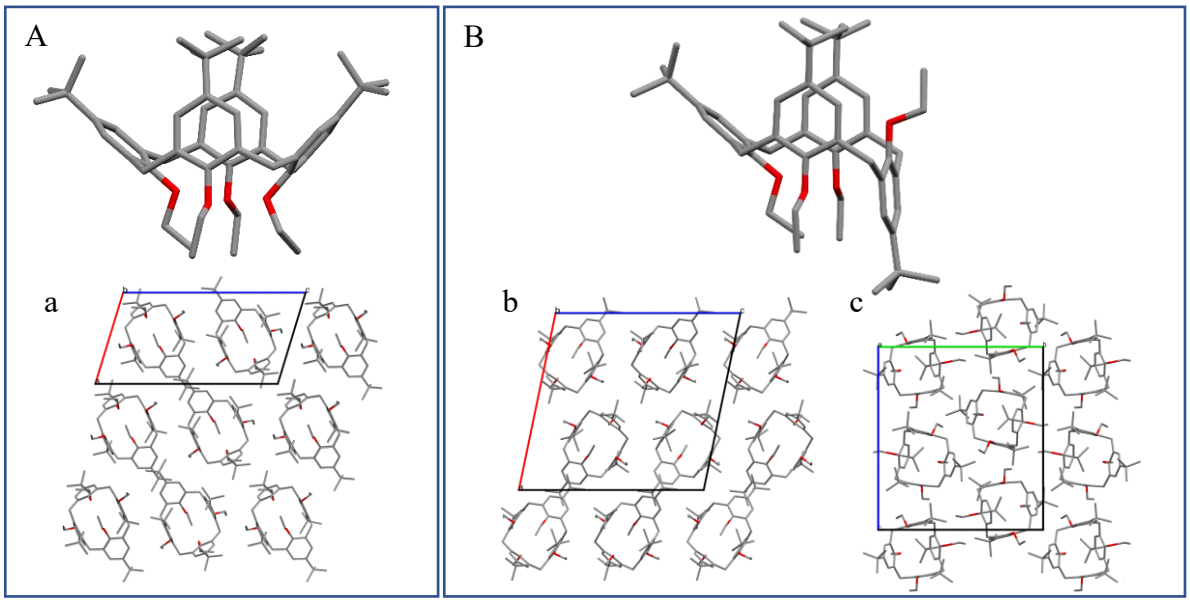

Fig. Crystal structures of tetra-*O*-*ethyl*-*p*-*tert*-butylcalix[4]arene adopting different conformations: cone (A), partial cone (B) and packing diagrams of C1(a), PC1(b) viewed along the *b* axis and PC2(c) viewed along the *a* axis. All hydrogen atoms have been omitted for clarity.

References

[1] P. Neri, J. Sessler, M. X. Wang, Calixarenes and Beyond (2016).
[2] C. D. Gutsche, B. Dhawan, J. A. Levine, K. H. No, L. J. Bauer, Tetrahedron, **39** (1983) 409.
[3] S. E. Matthews, S. Cecioni, J. E. O'Brien, C. J. MacDonald, D. L. Hughes, G. A. Jones, S. H. Ashworth, S. Vidal, Chem. Eur. J., **24** (2018) 4436.
[4] K. Iwamoto, K. Araki, S. Shinkai, J. Org. Chem., **56** (1991) 4955.

B-13

DWA PODEJŚCIA OTRZYMYWANIA FARMACEUTYCZNYCH WIELOSKŁADNIKOWYCH KRYSZTAŁÓW ZAWIERAJĄCYCH NAPROKSEN ORAZ AKRYDYNĘ I JEJ POCHODNE

Artur Mirocki[a,*], Artur Sikorski[a], Mattia Lopresti[b], Luca Palin[b,c], Eleonora Conterosito[b], Marco Milanesio[b]

[a] Uniwersytet Gdański, Wydział Chemii, Katedra Chemii Fizycznej, ul. W. Stwosza 63, 80-308 Gdańsk, Polska
[b] Università del Piemonte Orientale, Dipartimento di Scienze e Innovazione Tecnologica, Viale T. Michel 11, 15121 Alessandria, Italy
[c] Nova Res s.r.l., Via D. Bello 3, 28100 Novara, Italy
**e-mail: artur.mirocki@ug.edu.pl*

Formułowanie aktywnych substancji farmaceutycznych (*z ang. APIs*) jest jednym z kluczowych etapów przekształcania cząsteczki bioaktywnej w lek. Powszechnym sposobem modyfikowania, dostosowywania i kontrolowania właściwości APIs jest wykorzystywanie ich możliwych polimorfów. Bardziej wymagającą, ale intrygującą drogą jest otrzymywanie wieloskładnikowych kryształów (kokryształów, soli, kokryształów soli lub ich solwatów) z udziałem aktywnych substancji farmaceutycznych. W ten sposób można nie tylko modyfikować, ale także uzyskać nowe właściwości substancji, poprzez odpowiedni dobór cząsteczek koformera, a także modyfikację stosunku stechiometrycznego [1-3].

Otrzymywanie i stosowanie wieloskładnikowych kryształów zawierających różne aktywne substancje farmaceutyczne może mieć efekty synergiczne, wykazując lepszą wydajność w odniesieniu do sumy oddzielnych właściwości, na przykład, kokryształ tramadolu-celekoksybu posiada znacznie lepszy profil biofarmakologiczny niż wolna kombinacja dwóch składników lub pojedyncze związki [4].

Na podstawie powyższych przesłanek zbadano właściwości strukturalne kryształów zawierających naproksen i akrydynę oraz 9-aminoakrydynę, aby zrozumieć, jakimi metodami możliwe jest otrzymanie kryształów (dla różnych stosunków stechiometrycznych) i jakie są oddziaływania w upakowaniu sieci krystalicznej.

Podczas gdy krystalizacja kryształów molekularnych na bazie akrydyny była szeroko badana w warunkach roztworu [5-7], potencjał metod bezrozpuszczalnikowych i / lub mechanochemicznych jest nadal nieznany. Aby wypełnić tę lukę, podjęto próbę kokrystalizacji naproksenu z wyżej wymienionymi akrydynami, stosując różne podejścia: obróbkę cieplną suchej mieszaniny mechanicznej oraz mielenie wspomagane cieczą (LAG), jako alternatywę dla tradycyjnego wytrącania. W pierwszym przypadku próba otrzymania kokryształów przebiegała w warunkach suchych pod wpływem temperatury i nie dała rezultatów niezależnie od zastosowanej temperatury, poniżej lub powyżej temperatury topnienia reagentów. W drugim przypadku reakcja była napędzana mechanicznym działaniem mielenia wspomaganym kilkoma kroplami rozpuszczalnika w celu ułatwienia i poprawy reakcji. Próba ta pozwoliła na otrzymanie kryształów molekularnych naproksenu z akrydyną (Rysunek 1). Poprzez krystalizację z roztworu uzyskano dwie struktury – naproksenu z akrydyną oraz naproksenu z 9-aminoakrydyną. Do zbadania stabilności związków zastosowano PXRD, DSC i TGA w zmiennej temperaturze.

B-13

Mając na uwadze przebadane możliwości otrzymywania farmaceutycznych wieloskładnikowych kryształów zawierających naproksen i akrydyny w niniejszej prezentacji przedstawiona zostanie metodyka otrzymywania, charakterystyka strukturalna oraz wyniki analiz termicznych wieloskładnikowych kryształów z udziałem naproksenu, jako niesteroidowego leku przeciwzapalnego oraz akrydyn.

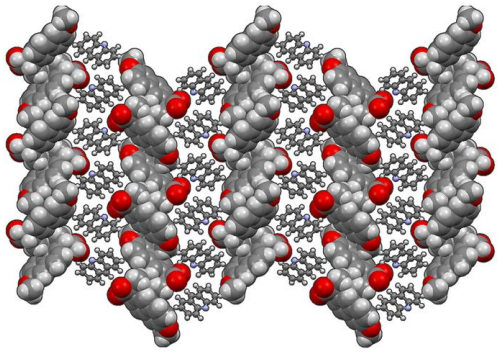

Rys. 1. Upakowanie kokryształu naproksenu z akrydyną (1:1).

Literatura

[1] Mirocki, A.; Lopresti, M.; Palin, L.; Conterosito, E.; Sikorski, A.; Milanesio, M. Exploring the molecular landscape of multicomponent crystals formed by naproxen drug and acridines. *CrystEngComm* **2022**, 24(39), 6839-6853.

[2] Shan, N.; Zaworotko, M. J. The role of cocrystals in pharmaceutical science. *Drug discovery today* **2008**, 13(9-10), 440-446.

[3] Duggirala, N. K.; Perry, M. L.; Almarsson, Ö.; Zaworotko, M. J. Pharmaceutical cocrystals: along the path to improved medicines. *Chemical communications* **2016**, 52(4), 640-655.

[4] Port, A.; Almansa, C.; Enrech, R.; Bordas, M.; Plata-Salamán, C. R. Differential solution behavior of the new API–API co-crystal of tramadol–celecoxib (CTC) versus its constituents and their combination. *Crystal Growth & Design* **2019**, 19(6), 3172-3182.

[5] Mirocki, A.; Sikorski, A. The influence of solvent on the crystal packing of ethacridinium phthalate solvates. *Materials* **2020**, 13(22), 5073.

[6] Mirocki, A.; Sikorski, A. Influence of halogen substituent on the self-assembly and crystal packing of multicomponent crystals formed from ethacridine and meta-halobenzoic acids. *Crystals* **2020**, 10(2), 79.

[7] Sikorski, A.; Trzybiński, D. Networks of intermolecular interactions involving nitro groups in the crystals of three polymorphs of 9-aminoacridinium 2, 4-dinitrobenzoate· 2, 4-dinitrobenzoic acid. *Journal of Molecular Structure* **2013**, 1049, 90-98.

B-14

V-SHAPED DONOR–ACCEPTOR ORGANIC EMITTERS – STRUCTURAL STUDIES

Wojciech Derkowski[1], Dharmandra Kumar[2], Tomasz Gryber[3], Jakub Wagner[1], Maja Morawiak[1], Michał Andrzej Kochman[3], Adam Kubas[3], Przemysław Data[2], Marcin Lindner[1]

[1] *Institute of Organic Chemistry, Polish Academy of Sciences, ul. Kasprzaka 44/52, 01-224 Warsaw, Poland*
[2] *Łódź University of Technology, Department of Chemistry, ul. Żeromskiego 114, 90-543 Łódź, Poland*
[3] *Institute of Physical Chemistry, Polish Academy of Sciences, ul. Kasprzaka 44/52, 01-224 Warsaw, Poland*

Organic molecules demonstrating the thermally activated delayed fluorescence (TADF) [1] phenomenon can theoretically produce 100% internal quantum efficiency (IQE) giving rise to a new class of emitters for OLED applications. These organic emitters are characterized by a new V-shaped [2] steric arrangement, separating the dibezazepine-based acceptor and donor moieties by a phenylene linker. Adopting a new design strategy, we recently demonstrated that a nitrogen-doped polycyclic aromatic hydrocarbon (N-PAH) scaffold incorporating dibenzazepine can provide the basis for efficient TADF emitters [3]. The title compounds 4a–d were assembled within four scalable synthetic steps as depicted in scheme 1 [4,5].

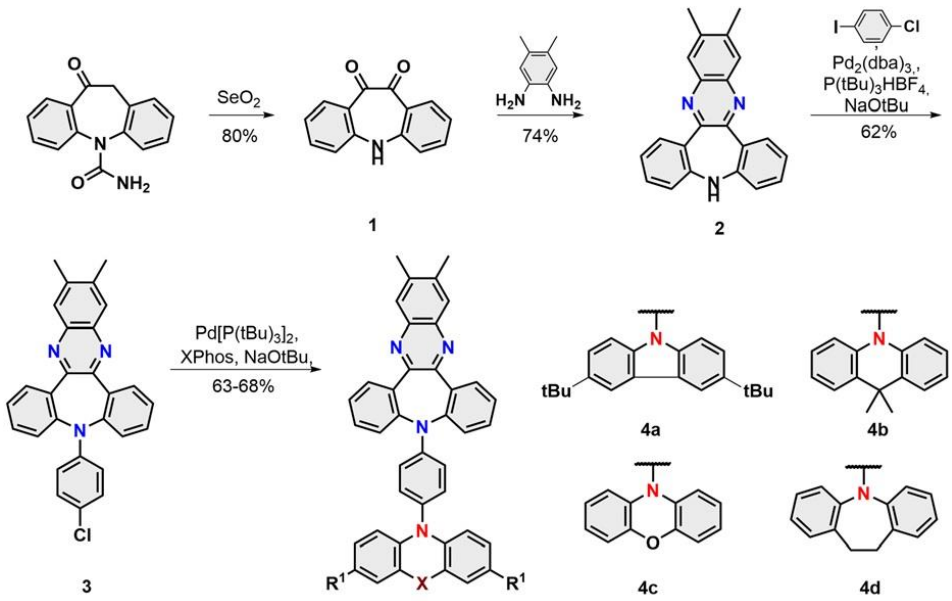

Scheme 1. Synthetic route towards title compounds **4a - d**.

Monocrystalline samples were obtained for three of the four reaction products 4a, 4b and 4d, for which X-ray tests were performed. All obtained products were investigated using techniques such as NMR, absorption, photoluminescence, cyclic voltammetry, and electronic structure calculations were performed.

The non-planar V-shaped conformation within the set of obtained molecules was unambiguously confirmed by X-ray crystallography of 4a,b and 4d (Fig. 1). Analysis of their structures obtained from single crystal diffraction showed that the angle between the planes of segments, namely, dibenzazepine and benzene bridge donors, was found to range from 110.61/110.51 (4a/b) to 112.91 (4d) degrees, consistent with our anticipated topology.

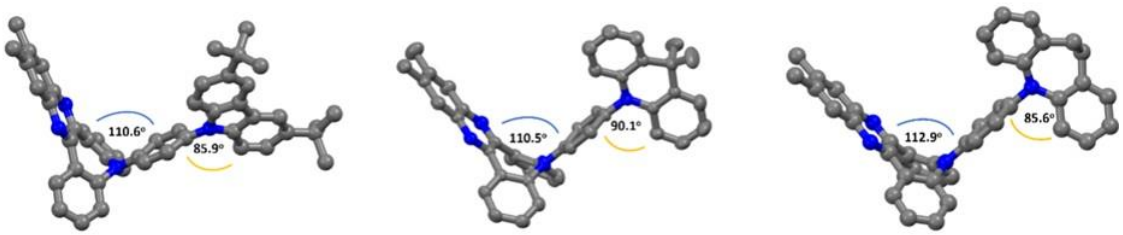

Fig. 1. Single X-ray structure of the dyes **4a**, **b**, and **d**.

As the final stage of the investigation, OLED devices based on 4a–4d were prepared and analysed (Fig. 2).

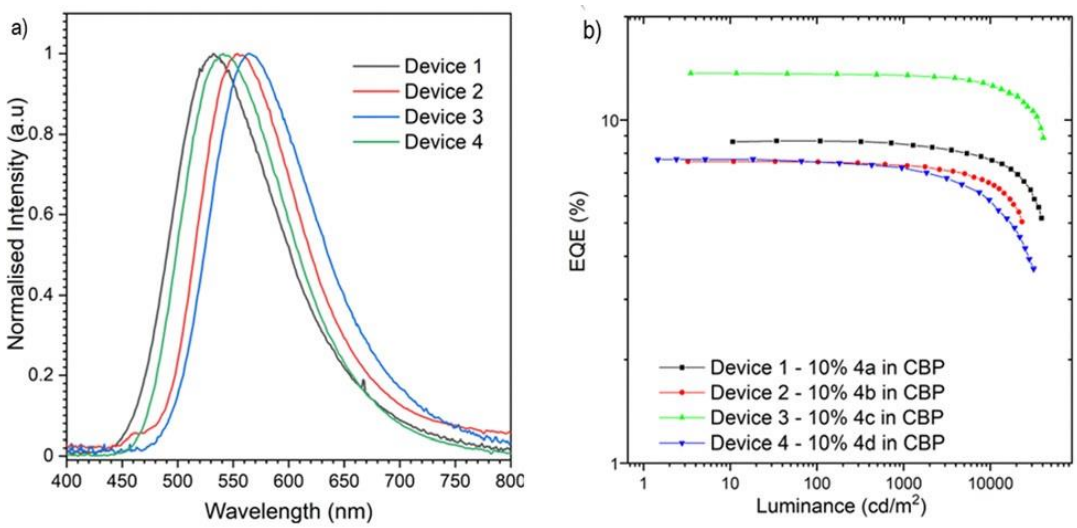

Fig. 2. The characteristics of the OLED devices based on emitters **4a – d**. a) Electroluminescence spectra. b) EQE-luminance characteristics.

References

[1] K. Goushi, K.Yoshida, K.Sato, C. Adachi, *Nat. Photonics*, **6** (2012) 253.
[2] D.W. Lee, J. Hwang, H.J. Kim, H. Lee, J. M. Ha, H. Y. Woo, S. Park, M. J. Cho, D. H. Choi, *ACS Appl. Mater. Inerfaces*, **13** (2021) 49076.
[3] J. Wagner, P. Zimmermann Crocomo, M.A. Kochman, A. Kubas, P. Data, M. Lindner, *Angew. Chem., Int. Ed.*, **61** (2022) e202202232.
[4] C.-T. Chen, J.-S. Lin, M.V.K. Moturu, Y.-W. Lin, W. Yi, Y.-T. Tao, C.-H. Chein, *Chem. Commun.*, (2005) 3980.
[5] P. Ruiz-Castillo, S.L. Buchwald, *Chem. Rev.*, **116** (2016) 12564.

B-15

KONFORMACJA A LUMINESCENCJA – DWA OBLICZA STRUKTUR POLIMORFICZNYCH BOROORGANICZNEGO KOMPLESKU 2-PIRYDYLOFENOLU

Dawid R. Natkowski[a], Paulina H. Marek-Urban[a,b], Karolina Wrochna[a], Krzysztof Woźniak[b], Krzysztof Durka[a]

[a] Wydział Chemiczny, Politechnika Warszawska, ul. Noakowskiego 3, 00-664 Warszawa
[b] Wydział Chemii, Uniwersytet Warszawski, ul. Pasteura 1, 02-093 Warszawa

Zjawisko polimorfizmu może wpływać na szereg właściwości fizykochemicznych danego materiału, takich jak rozpuszczalność, czy temperatura topnienia ale także na własności spektroskopowe. Jednym z kluczowych czynników wpływających na właściwości luminescencyjne ciał stałych jest konformacja molekuł oraz ich otoczenie chemiczne[1]. Warte szczególnej uwagi są układy, które pod wpływem czynników zewnętrznych, np. pod wpływem działania siły mechanicznej, są w stanie zmieniać swoją formę polimorficzną wykazując tym samym mechanochromizm[2].

Niniejsza prezentacja skupia się na opisie dwóch odmian polimorficznych boroorganicznego kompleksu zbudowanego z sulfonowego rdzenia boroorganicznego oraz 2-pirydylofenolu (liganda), dla których zaobserwowano znaczne różnice we właściwościach spektroskopowych. Maksima fluorescencji dla obu form wynoszą odpowiednio 448 nm i 488 nm, a wydajności kwantowe są równe 69 % i 36 %. Co więcej, dla obu odmian polimorficznych zaobserwowano wspomniane zjawisko mechanochromizmu. Materiały w wyniku utarcia wykazują przesunięcie maksimów emisji. Przeprowadzone badania strukturalne posłużyły do scharakteryzowania otrzymanych odmian polimorficznych. Celem zracjonalizowania obserwowanych różnic we właściwościach spektroskopowych oraz stabilności przeprowadzono serię obliczeń teoretycznych DFT, TD-DFT oraz periodycznych obliczeń kwantowochemicznych, a także wykonano badania DFT. Analiza otrzymanych danych doprowadziła do określenia związku pomiędzy konformacją molekuły, jej oddziaływaniami międzycząsteczkowymi, a własnościami luminescencyjnymi.

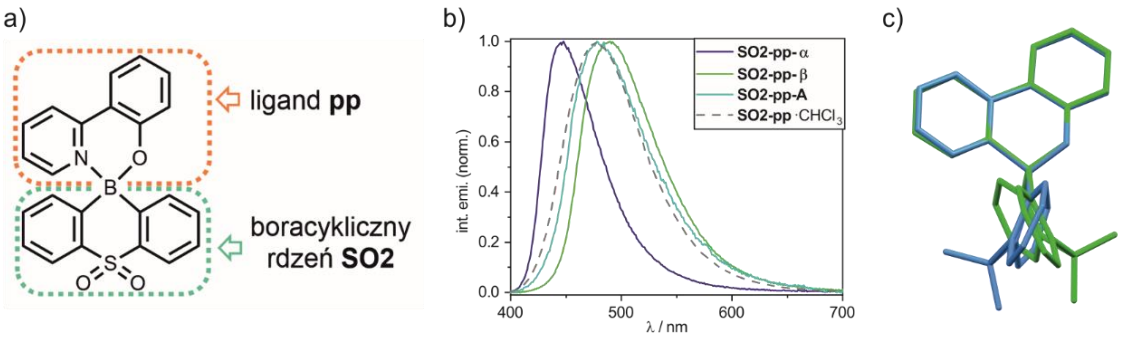

Rys. 1. a) Schemat badanego kompleksu. b) Znormalizowane widma absorbcji, emisji badanych form polimorficznych oraz fazy amorficznej w ciele stałym oraz w roztworze. c) Nałożenie geometrii molekuł dwóch struktur polimorficznych.

B-15

Finansowanie badań w ramach projektu OPUS 20 „Efektywne fotouczulacze oparte na sztywnych układach boroorganicznych jako generatory tlenu singletowego” (2020/39/B/ST4/02370).

Literatura

[1] Z. Zhang, *et al*., *Dyes and Pigments*, **145** (2017) 294-300.
[2] M. Fan, *et al*., *Dyes and Pigments*, **190** (2021) 109311.

B-16

STRUCTURAL CHARACTERISATION OF DARIFENACIN FREE BASE HYDRATE

Przemysław Nowak[1,2], Marta K. Dudek[2], Piotr Paluch[2]

[1] Bio-Med-Chem Doctoral School of University of Lodz and Lodz Institutes of the Polish Academy of Sciences, Matejki 21/23, 90-237 Łódź
[2] Centre of Molecular and Macromolecular Studies, Polish Academy of Sciences, Sienkiewicza 112, 90-363 Łódź

The benzofurane derivatives are important class of compounds with many biological activities. They are used as a antidepressant, anticancer, antiviral, antifungal, antioxidant, anti-psychotic medicines [1]. Darifenacin is one of the benzofurane derivatives used in the treatment of overactive bladder. It is a selective antagonist of the M3 muscarinic receptors that control the contraction of the smooth muscles of the bladder [2].

There are two known crystalline forms of darifenacin free base: a hydrate and a solvate with toluene, characterized only by PXRD, IR spectroscopy and DSC [3]. To date, the only know neat solid form of darifenacin is amorphous [4]. Here we report structural characterisation of darifenacin free base hydrate and a method of its preparation. The hydrate was characterised with the use of IR spectroscopy and solid state NMR spectroscopy. What's more, we have done CSP (Crystal Structure Prediction) calculations to compare possible structures of darifenacin free base and darifenacin free base hydrate. The comparison is used to identify possible supramolecular synthons, as well as to find a justification why darifenacin free base is known only as a amorphous form.

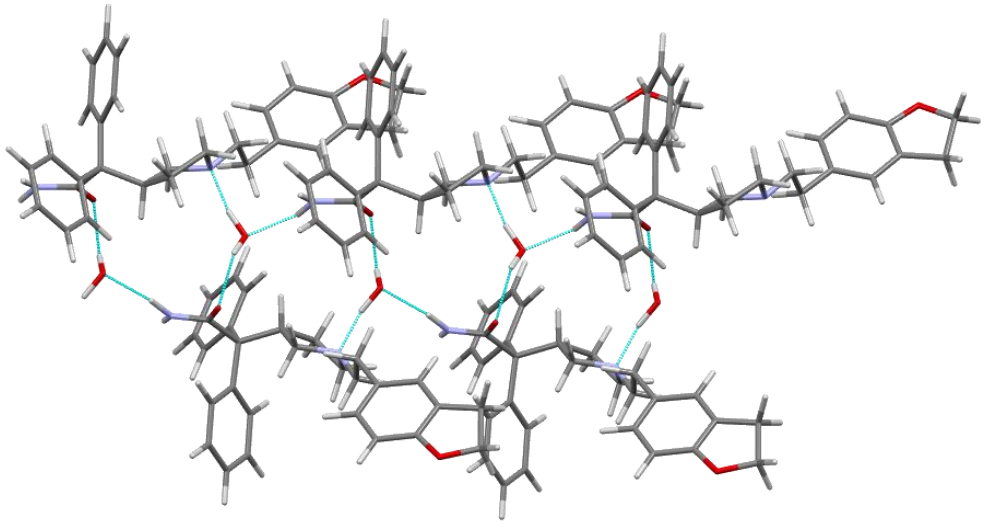

Fig. 1. The structure of darifenacin free base hydrate obtained in CSP calculations. Hydrogen bonds are highlighted in blue. For most structures CSP calculations for darifenacin free base indicate the lack of interactions between molecules in crystal structures.

PLGrid is acknowledged for providing computational resources under the computational grant no. PLG/2022/015813

Literatura

[1] Miao, Y.; Hu, Y.; Yang, J.; Liu, T.; Sun, J.; Wang, X.; Natural source, bioactivity and synthesis of benzofuran derivatives, *RSC Adv.*, **9** (2019) 27510–27540.
[2] Farag, M.M., El-Sebaie, W., Basalious, E.B. *et al*. Darifenacin Self-assembled Liquid Crystal Cubic Nanoparticles: a Sustained Release Approach for an Overnight Control of Overactive Bladder. *AAPS PharmSciTech*, **24**(120) (2023).
[3] Dunn, P. J; Matthews, J. G.; Newbury, T. J.; O'Connor, G.; US 2003/0191176 A1, 2003.
[4] Kodali, E. R.; Medikonduri, S.; Neela, P. K.; Pradhan, N. S.; Valgeirsson, J.; US 2010/0204296 A1, 2010.

B-17

INVESTIGATING THE EFFECT OF DIFFERENT ANIONS OF QUINUCLIDINOLIUM SALTS ON THEIR PLASTIC PHASE TRANSITION BEHAVIORS

Samet Ocak[1,*], Michele R. Chierotti[2], Dario Braga[1], Tommaso Salzillo[3], and Simone d'Agostino[1]

[1] Department of Chemistry "Giacomo Ciamician", The University of Bologna, Via F. Selmi, 2, 40126 Bologna, Italy
[2] Department of Chemistry and NIS Centre, The University of Turin, Via P. Giuria 7, 10125, Torino, Italy
[3] Department of Industrial Chemistry "Toso Montanari", The University of Bologna, Viale del Risorgimento 4, 40124, Bologna, Italy

**e-mail: samet.ocak3@unibo.it*

Plastic crystals are unique substances where the molecules or ions maintain the same center of mass as in a regular crystal lattice but possess the ability to rotate freely. These materials exhibit characteristic transitions between disorder and order, enabling the creation of diverse functional substances. In particular, organic ionic plastic crystals (OIPCs) have attracted considerable interest in recent years due to their potential application as solid-state electrolytes [1-2].

The primary objective of this study encompasses three key aspects. Firstly, our focus is on investigating the influence of counter-anions on the plastic phase transitions within a series of R-(+)-(3)-hydroxyquinuclidinium salts [QH]X. By varying the size, shape, and charge of the anions, we anticipate observing diverse behaviors in terms of plastic phase transition characteristics and types. Secondly, we aim to explore the feasibility of producing crystalline solid solutions, examining how the composition of these resultant materials further impacts the phase transition compared to the pure parent systems. Lastly, we intend to analyze the ionic conductivity behavior of these salts, particularly by comparing their conductivities in both ordered and disordered phases.

In order to achieve this objective, we employ a synthetic approach to create a series of [QH]X salts with diverse counter-anions. These include sulfate (SO_4^{2-}), tetraphenylborate (BPh_4^-), terafluoroborate (BF_4^-), hexafluorophosphate (PF_6^-) in an octahedral arrangement, and methanesulfonate ($SO_3CH_3^-$). The synthesis involves the metathesis reaction between [QH]Cl and metal salts containing the respective counter-anions. A combination of solid-state techniques is employed to investigate the properties of these materials, including variable temperature X-ray diffraction (XRD), thermal analyses, multinuclear solid-state NMR spectroscopy (utilizing nuclei such as ^{11}B, ^{13}C, ^{15}N, ^{19}F, and ^{31}P), variable temperature wideline ^{19}F T_1 relaxation measurements, micro-Raman spectroscopy, and electrochemical impedance spectroscopy (EIS). Through these analyses, we aim to gain insights into the crystal structures, phase transition behavior, and ionic conductivity of the synthesized materials [3].

B-17

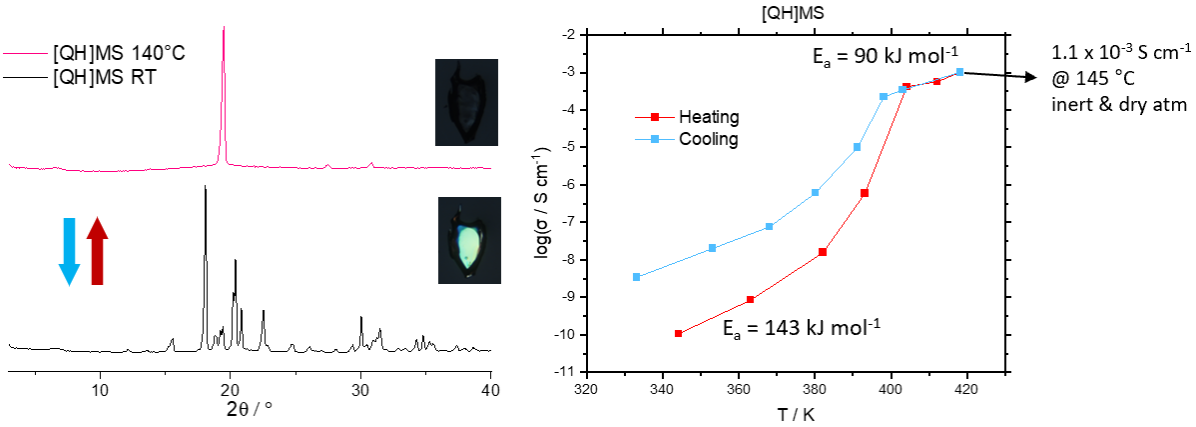

Fig. 1. VT-PXRD and trend of the ionic conductivity of [QH]MS.

Literatura

[1] S. Das et al., Chemical Society Reviews. **2020**, 49(24), 8878-8896.
[2] S. d'Agostino et al., Cryst. Growth & Des. **2019**, 19, 6266-6273.
[3] S. Ocak et al., Mol. Syst. Des. Eng. **2022**, 49(24), 10.1039/d2me0040g.

B-18

ANALIZA WPŁYWU STRUKTURY ORAZ ODDZIAŁYWAŃ MIĘDZYCZĄSTECZKOWYCH NA WŁAŚCIWOŚCI FOTOPRZEŁĄCZALNE KOMPLEKSU PD(II) Z GRUPĄ NITROWĄ

Kacper Paszczyk, Katarzyna N. Jarzembska, Radosław Kamiński, Patryk Borowski, Krystyna A. Deresz, Adam Krówczyński

Wydział Chemii Uniwersytetu Warszawskiego, ul. Żwirki i Wigury 102, 02-089 Warszawa

Foto- i termoprzełączalne związki chemiczne mogą mieć rozmaite zastosowania m.in. w fotowoltaice i fotonice. Głównym celem przeprowadzonych badań oraz analizy było ocena wpływu struktury oraz otoczenia grupy nitrowej na wspomniane właściwości nowego, potencjalnie fotoprzełączalnego kompleksu Pd(II) w formie kryształu (Pd-1a). N,N,O-donorowy kompleks Pd(II) o płasko-kwadratowej geometrii sfery koordynacyjnej centrum metalicznego otrzymano zgodnie z procedurą opisaną w literaturze [1]. Jego strukturę przedstawiono na rysunku 1.

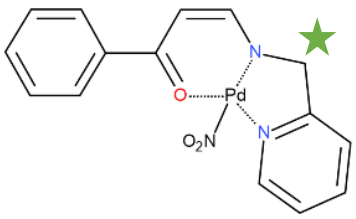

Rys. 1. Struktura badanego kompleksu, Pd-1a.

Dla analizowanego związku przeprowadzono krystalizacje z różnych rozpuszczalników, otrzymując kryształy różnej jakości oraz wielkości. Otrzymano strukturę dominującą, a także pojedyncze kryształy dwóch innych odmian polimorficznych i dwóch solwatomorfów (z DCM oraz CH_3Cl). Ponadto w przypadku krystalizacji z DMF, metanolu i etanolu zaobserwowano kryształy badanego związku z atomem węgla, oznaczonym gwiazdką na rysunku 1, utlenionym do grupy karbonylowej. Wszystkie struktury zbadano metodą monokrystalograficznej dyfrakcji rentgenowskiej, a następnie dla trzech najbardziej obiecujących układów w kontekście właściwości przełączalnych przeprowadzono eksperyment fotokrystalograficzny [2]. Dodatkowo przeprowadzono eksperymenty metodą spektroskopii IR w ciele stałym, w celu określenia stopnia konwersji próbek oraz optymalnych warunków dla reakcji fotoizomeryzacji grupy nitrowej.

Dominujący polimorf związku okazał się najefektywniejszym przełącznikiem molekularnym w ciele stałym z badanej grupy układów Pd-1a. Cząsteczka związku tworzy w tym przypadku strukturę krystaliczną o symetrii $P2_1/n$, w której komórka elementarna zawiera dwie nierównoważne symetrycznie cząsteczki. Naświetlanie światłem LED o długości fali 470 nm okazało się optymalne. W wyniku wzbudzenia tylko jedna cząsteczka w części niezależnej ulega reakcji. Połączenie nitrowe

transformuje się do wiązania typu *endo*-nitrito. Maksymalna uzyskana populacja metastabilnego izomeru wynosi około 85% w100 K i utrzymuje się do temperatury około 180 K.

Podziękowania dla grantu SONATA BIS (2020/38/E/ST4/00400) za wsparcie finansowe.

Literatura

[1] Dabrowski, J.; Krówczyński, A. Ni(II) complexes with bis(β-acylvinyl)amines and (8-quinolyl-β-acylvinyl)amineshome laboratory. *J. Appl. Crystallogr*., **49** (2016) 1383–1387.
[2] Kamiński, R.; Jarzembska, K.N.; Kutyła, S.E.; Kamiński, M.A. portable light-delivery device for in situ photocrystallografic experimets at home laboratory. *J. Appl. Crystallogr*. **49** (2016) 1383–1387.

B-19

RESONANCE-ASSISTED HYDROGEN BOND DEFINED BY P=O···H-O SYNTHON

Anna Pietrzak[a], Przemysław Nowak[b,c], Tomasz Janecki[d] and Wojciech M. Wolf[a]

[a] *Institute of General and Ecological Chemistry, Łódź University of Technology*
[b] *Centre of Molecular and Macromolecular Studies, Polish academy of Sciences, Łódź, Poland*
[c] *Bio-Med-Chem Doctoral School of University of Lodz and Lodz Institutes of the Polish Academy of Sciences, Łódź, Poland*
[d] *Institute of Organic Chemistry, Łódź University of Technology*

Intramolecular interactions are crucial for conformations of molecules. One of such strong intramolecular effects is resonance-assisted hydrogen bond (RAHB) recognized in many chemical compounds. RAHB is applicable as a driving force in the synthesis of different classes of organic compounds and coordination and organometallic complexes. Moreover, RAHB systems may serve as a supporting tool in activating saturated and unsaturated covalent bonds [1]. In most reported systems, donor or/and acceptor is linked to a carbon atom [2-3], while these interactions involving a phosphoryl group as an acceptor are very scarce. Crystallographic structural database (CSD) [4] contains 467 structures stabilized by intramolecular synthon P=O···H-X creating a 6-membered cyclic moiety. This number limits to 92 structures if an alternating single and double bond system characterizes cyclic moiety. Consequently, in CSD there are only 13 structures with a conformation defined by resonance-assisted hydrogen bond defined by P=O···H-O synthon, namely RAHB-P (Fig. 1).

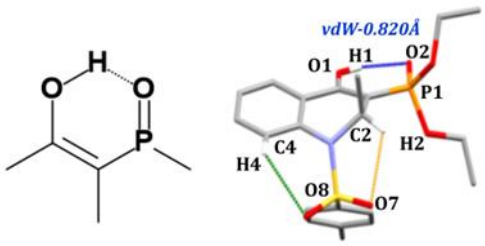

Fig. 1. Structural scheme of RAHB-P (left) and intramolecular interactions stabilizing a conformation of 3-(diethoxyphosphoryl)-1,2-dihydroquinolin-4-ol.

Here we reported RAHB-P stabilizing the conformation of organophosphorus compounds (*i.e.*, derivatives of 3-(diethoxyphosphoryl)-1,2-dihydroquinolin-4-ols). The effect was characterized by SC-XRD analysis supported by ^{1}H NMR studies and NBO calculations.

References

[1] K.T. Muhamudov, B. J. L. Pombeiro, *Chem. Eur. J.*, **22** (2016) 16356.
[2] G. Gilli, F. Bellucci, F. Ferretti, V. Bertolasi, *J. Am. Chem. Soc*., **111** (1989) 1023.
[3] L. Sobczyk, S. J. Grabowski, T. M. Krygowski, *Chem. Rev*., **105** (2005) 3513.
[4] C. R. Groom, I. J. Bruno, M. P. Lightfoot, S. C. Ward, *Acta Cryst. C*, **72** (2016) 171.

B-20

REVERSIBLE LINKAGE ISOMERISM INDUCED UNDER HIGH PRESSURE IN CRYSTALS OF A MODEL NICKEL(II) NITRATE COMPLEX

Kinga Potempa[1], Damian Paliwoda[2], Katarzyna N. Jarzembska[1], Adam Krówczyński[1], Patryk Borowski[1], Radosław Kamiński[1]

[1]University of Warsaw, Department of Chemistry, Żwirki i Wigury 101, 02-089 Warsaw, Poland
[2]European Spallation Source, Partikelgatan 2, 224 84 Lund, Sweden

Linkage isomerism is a phenomenon that occurs for metal complexes with an ambidentate ligand, capable of forming various coordination modes. The isomerisation reaction in the solid state is usually induced by some external factors such as electromagnetic radiation and temperature, which were applied in most of the studies to date [1,2]. The nitrate ligand constitutes a good example of a switchable moiety. In most cases it is found in the nitro form (bound by the nitrogen atom to a metal centre) and after irradiation with light from the UV-Vis range it may undergo the isomerisation process to nitrito form (bound by the oxygen atom). At the moment there are only few reported cases of this photoreaction taking place at room temperature [3] which is crucial for real life applications.

The effect of high pressure on linkage isomerism remains far less investigated. Although some reports on behaviour of metal complexes with nitrate ligand under high pressure were published, [4] none of them presented the isomerisation process of NO_2 under such conditions. Here, we introduce the nickel(II) nitrate complex in which the ambidentate ligands exist in a number of coordination modes depending on the applied pressure. There are two NO_2 groups attached to the metal centre in the molecule which adopt the *exo*-nitrito mode in the ground state. This is very unique as usually it is the least energetically privileged arrangement. Moreover, despite that both moieties differ in a very subtle way, only one of them is able to undergo the isomerisation process.

Crystal packing definitely affects the linkage isomerisation reaction, specifically such factors as intermolecular interactions and steric hindrances. In the presented case linkage isomerism results from the applied mechanical force that leads to structural deformations and/or phase transition. HP crystallographic measurements were conducted in the 0.4-6 GPa pressure range at room temperature. Along with the increased pressure two phase transitions occurred accompanied by the nitrate ligand bonding mode changes. Moreover, the observed process is reversible, which makes it a potential candidate for a pressure sensor.

Acknowledgments
The SONATA BIS(2020/38/E/ST4/00400) of the NCN (Poland) is gratefully acknowledged for financial support. The in-house X-ray diffraction experiments were performed at the Department of Physics,University of Warsaw, on a Rigaku Oxford Diffraction SuperNova diffractometer, which wasco-financed by the European Union within the European Regional Development Fund (POIG.02.01.00-14-122/09). The Wrocław Centre for Networking and Supercomputing (grant No. 285) is gratefully acknowledged for providing computational facilities.

B-20

Literature
[1] Cole, J. M., *Crystallographica Section A Foundations of Crystallography*, **64**(1) (2008) 259–271.
[2] Kutniewska, S. E., Krówczyński, A., Kamiński, R., Jarzembska, K. N., Pillet, S., Wenger, E., Schaniel, D., *IUCrJ*, **7** (2020) 1188-1198.
[3] Deresz, K.A., Kamiński, R., Kutniewska, S. E., Krówczyński, A., Schaniel, D., Jarzembska, K. N. *Chem. Commun.*, **58** (2022) 13439-13442
[4] Zakharov, B. A., Marchuk, A. S., Boldyreva, E. V, *CrystEngComm*, **17** (2015) 8812-8816

B-21

SYNTHESIS AND CRYSTAL STRUCTURE OF $(HGua)_2Na_2(P_2O_6)\cdot 7H_2O$

Paulina Kurowska[1], **Vasyl Kinzhybalo**[2], **Katarzyna Ślepokura**[1]

[1] *University of Wroclaw, Faculty of Chemistry, 14 F. Joliot-Curie, 50-383 Wroclaw*
[2] *Institute of Low Temperature and Structure Research, Polish Academy of Sciences, 2 Okólna, 50-422 Wroclaw*

Guanidine (Gua) is an organic compound that crystallizes as a colourless solid that absorbs water and carbon dioxide from the air. Its salts especially guanidine carbonate and guanidine nitrate crystallize well. X-ray analysis of guanidine crystals has shown that the three nitrogen atoms are not identical, but in compounds where guanidine is protonated the nitrogen atoms due to electron resonance are symmetrically arranged in a plane around the carbon atom [1]. Guanidine shows strong basic properties (pK_b = 0.4). It should be noted that one of the guanidine salts, namely guanidine isocyanate, has been tested against COVID-19 as a lysis buffer [2]. Some of the guanidine derivatives have bactericidal properties. Polyhexamethylene guanidine is well known as a general antiseptic; it is now actively used as a disinfectant, especially against COVID-19.

Inorganic hypodiphosphates are better explored than organic hypodiphosphate salts [3]. In addition, hypodiphosphate salts containing both organic and inorganic cations are virtually unknown. Therefore, we carried out the reaction of $(HGua)_2CO_3$ with $Na_2H_2(P_2O_6)\cdot 6H_2O$ that yielded colourless crystals of double salt $(HGua)_2Na_2(P_2O_6)\cdot 7H_2O$ ($P2/n$, a = 15.419(4), b = 7.048(3), c = 16.449(4) Å, β = 94.36(3)°, V = 1782.4(10) Å^3, T = 100 K).

The asymmetric unit of the $(HGua)_2Na_2(P_2O_6)\cdot 7H_2O$ crystal consists of two guanidinium cations, two sodium cations (one in the general position and two halves on the centres of inversion), two halves of hypodiphosphate tetraanions (on two-fold axes) and seven water molecules (Fig. 1). The Na1 ion coordinates three water molecules and one $P_2O_6^{4-}$ anion (A, bidentately). The Na2 and Na3 ions have an octahedral coordination environment, which consists exclusively of water molecules. The octahedra of Na2 and Na3 are edge-joined by bridging water molecules O4W and O5W into chains running along the *b* axis. Na1 ions are attached to these chains by bridging water molecules O3W. Hypodiphosphate tetraanions A connect the adjacent chains with each other into layers that lie in planes parallel to $(\bar{1}01)$.

Hypodiphosphate anion A coordinates to two sodium ions (Na1) in a chelating manner and is a hydrogen bond acceptor from four guanidine cations and ten water molecules. In contrast, anion B is not involved in coordination to sodium ions. Instead, it is the hydrogen bond acceptor from as many as six guanidinium cations and ten water molecules.

Guanidinium cation A is a hydrogen bond donor to two anions and two water molecules. In contrast, guanidinium cation B is a hydrogen bond donor to three anions and one water molecule.

B-21

Most intriguing feature of the reported structure is concerned with Na1 coordination environment (Fig. 1, inset). Contrary to Na2 and Na3 coordination environments which are octahedral, Na1 is pentacoordinated with tetragonal pyramidal polyhedron. The sixth coordination site is occupied by guanidinium (A) nitrogen atom (N1) at the quite short distance of 3.034(1) Å. The survey of CSD didn't reveal such close contacts between sodium and guanidinium cations.

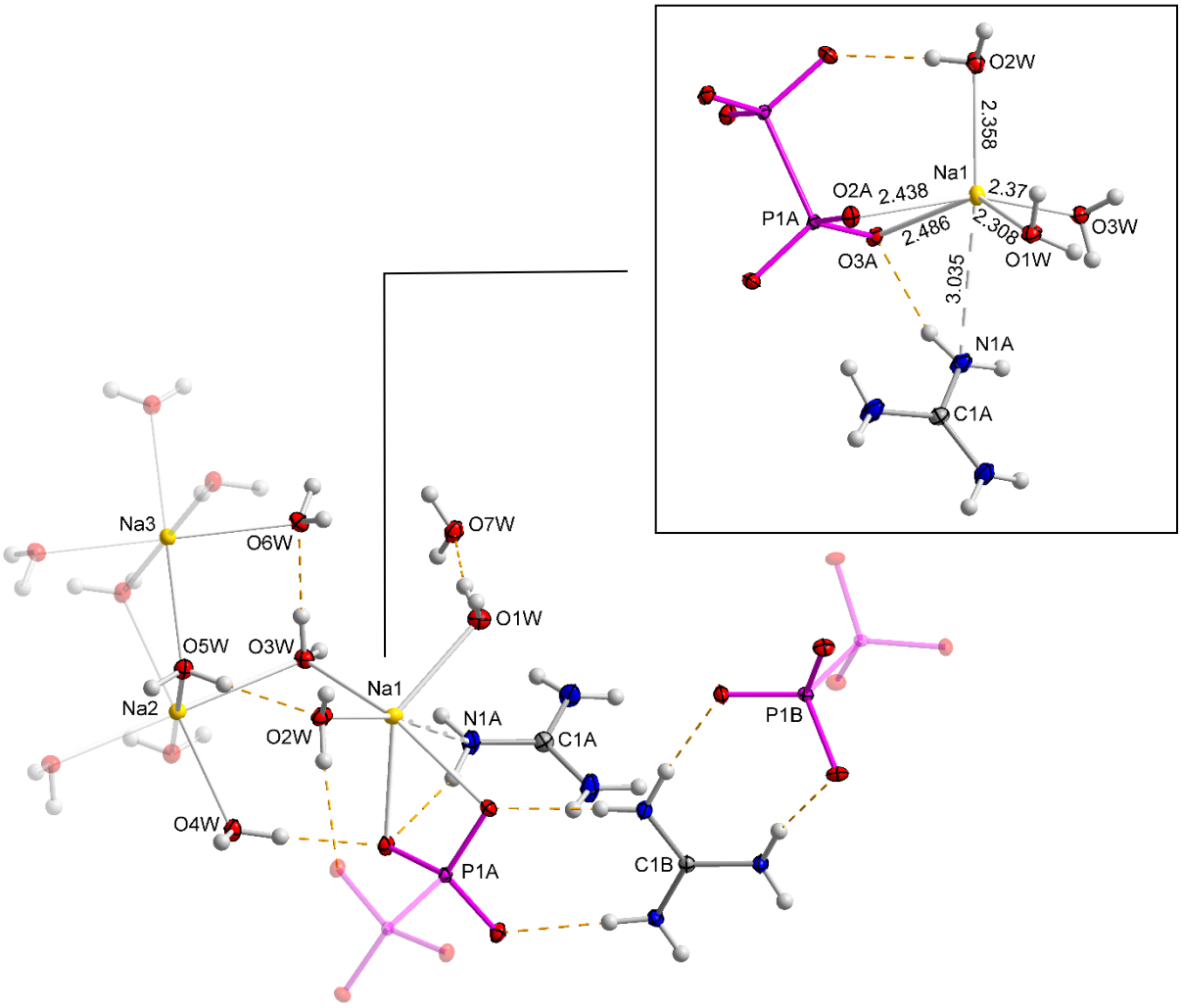

Fig. 1. Fragment of the crystal structure along with the selected atom labels; ellipsoids are shown at 50% probability level. Symmetry-dependent moieties are shown as transparent. Inset: Coordination environment of Na1 ion along with sodium–ligand distances (Å).

Literature

[1] T. Yamada, X. Liu, U. Englert, H. Yamane, R. Dronskowski, *Eur. J. Chem.*, **15** (2009) 5651–5655.
[2] E. Z. Ong, Y. F. Z. Chan, W. Y. Leong, N. M.Y. Lee, S. Kalimuddin, S. M. H. Mohideen, K. S. Chan, A. T. Tan, A. Bertoletti, E. E. Ooi, J. G. H. Low, *Cell Host Microbe*, **27** (2020) 879–882.
[3] V. Kinzhybalo, M. Otręba, K. Ślepokura, T. Lis, *Wiad. Chem*., **75** (2021) 423–466.

B-22

ISOMORPHOUS CRYSTALS OF AMINALS, 2-AMINOPYRIDINE DERIVATIVES

Anna Kwiecień[1], Anna Pyra[2] and Zbigniew Ciunik[2]

[1] Department of Basic Chemical Sciences, Faculty of Pharmacy, Wroclaw Medical University, Borowska 211a, 50-556 Wroclaw, Poland
[2] Faculty of Chemistry, University of Wrocław, 14 Joliot-Curie, 50-383 Wrocław, Poland

Nucleophilic addition reactions are one of the most important reaction of the carbonyl group of aldehydes or ketones. In these reactions a negatively polarised atom or group of atoms (e.g. water, hydrogen cyanide, alcohols, primary amines, secondary amines) attacks the positively charged carbon atom of the carbonyl group (leading to germinal diols, cyanohydrins, acetals, imines, enamines, respectively) [1].

Nucleophilic addition of primary amines to carbonyl group is a two-step process (Fig.1.). In the first step a hemiaminal, tetrahedral addict is formed. This intermediate is usually unstable and undergo further dehydration reaction [1]. In some special conditions the hemiaminal product is stable enough to be isolated [2-4]. Occasionally a reaction analogue to the acetal formation can occur, and one mole of carbonyl compound react with two moles of amine to give germinal diamines known as aminals [5].

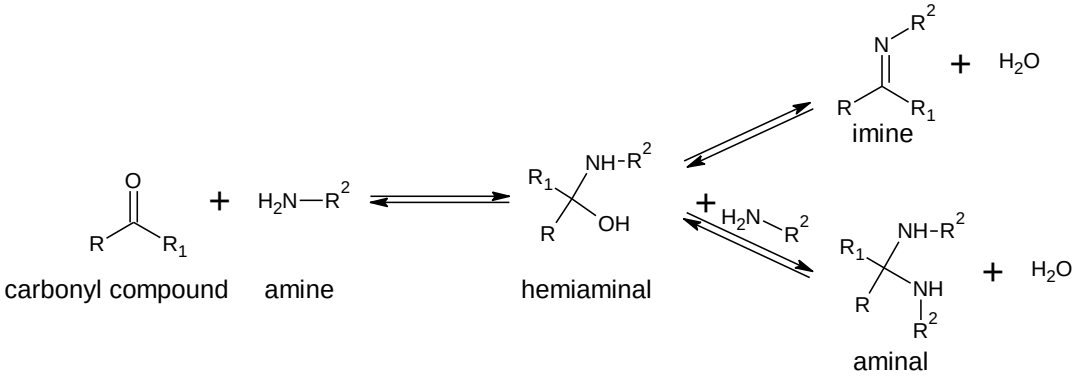

Fig. 1. Nucleophilic addition of primary amines to carbonyl group.

In current work two isomorphous crystals of aminals obtained in the nucleophilic addition of 2-amine-4-methylpyridin to carbonyl group of benzaldehydes substituted with strongly deactivating nitro- or cyano- group in *meta*- position are presented (Fig.2.).

Crystal data of *N*,*N*'-bis(4-methylpyridin-2-yl)-1-(3-nitrophenyl)methanediamine (**Compound I**): $C_{19}H_{19}N_5O_2$, M = 349.39, crystal system: orthorhombic, space group: *Pbca*, a = 21.0958(5)Å, b = 15.8859(4)Å, c = 21.1225(5)Å, V = 7078.7(3)Å^3, Z = 16, R_{int} = 0.0428, R_1 = 0.0475, wR_2 = 0.1300, GoF = 1.021.

Crystal data of 3-{bis[(4-methylpyridin-2-yl)amino]methyl}benzonitrile (**Compound II**): $C_{20}H_{19}N_5$, M = 329.40, crystal system: orthorhombic, space group:

Pbca, a = 21.0468(5)Å, b = 15.8915(4)Å, c = 21.3503(5)Å, V = 7140.9(3)Å^3, Z = 16, R_{int} = 0.0251, R_1 = 0.0377, wR_2 = 0.0974, GoF = 1.026.

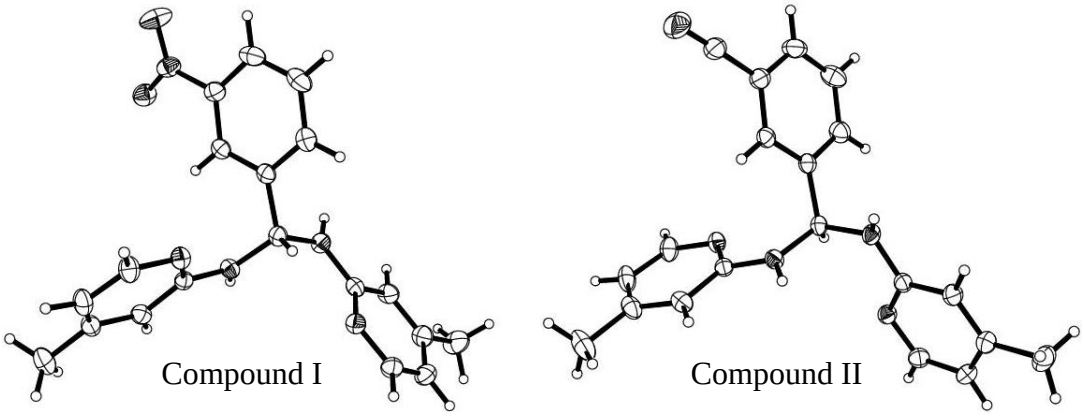

Fig. 2. Molecular structures of obtained compounds.

In the crystal structures of both compounds the N-H$\cdots$N$_{pyrudune}$ type hydrogen bonds links molecules into infinite chains. Furthermore, these chains are parallel to the shortest lattice vector.

References

[1] F.A. Carey, *Organic Chemistry*, 4th edition, The McGraw-Hill Companies, (2000) 661–677.
[2] M. Barys, Z. Ciunik, K. Drabent, A. Kwiecień, *New J. Chem.*, **34** (20100 2605–2611.
[3] A. Kwiecień, M. Barys, Z. Ciunik, *Molecules*, **19** (2014) 11160–11177.
[4] A. Kwiecień, Z. Ciunik, *Molecules*, **20** (2015) 14365–14376.
[5] F. H. Allen, *Acta Cryst.*, **B58** (2002) 380–388.

B-23

A STRUCTURAL STUDY OF THE ISOMERS OF AMINOPYRIDINE USING NON-SPHERICAL ATOMIC FORM FACTORS

Irina S. Konovalova[1,2] and Guido J. Reiss[1]

[1] Bioinorganic Chemistry, Heinrich-Heine-Universität Düsseldorf, Germany
[2] SSI "Institute for Single Crystals", National Academy of Science of Ukraine, 60 Nauky ave., Kharkiv, 61001, Ukraine

Aminopyridines possessing biological activities are of general interest. For example, the 4-aminopyridine is used in MS therapy. The structures of the three isomers of amino-pyridine are known since the 70th of the last century [1-3]. Re-determinations with quality data are limited to two cases [4, 5]. New crystallographic methods like the usage of non-spherical atom form factors [6] for quality standard datasets opens the possibility to do redeterminations on a higher level. Thus we have collected new diffraction data for the three isomers of aminopyridine (*ap*) and re-refined the structures using the NoSpherA2 option of the OLEX2 program system (see Figure 1).

Our previous crystal structure organization analysis for the isomers of mono-aminopyridines (2-*ap*, 3-*ap*, 4-*ap*) were studied using an approach based on comparison of interaction energies between molecules calculated by *ab initio* quantum chemical methods [7]. The presence of the pyridine nitrogen atom causes the formation of N–H···N$_{pyr}$ hydrogen bond which is the strongest in all the studied structures. The donor acceptor distances for the N–H···N hydrogen bonds are 2.9773(8) Å for 4-*ap*, 3.0699(8) Å for 2-*ap and* 3.09773(8) Å for 3-*ap*. Being amphiphilic in hydrogen bond formation, the amino group possesses acceptor properties only in the *meta*-position in mono-aminopyridines. Additionally, C/N–H···π hydrogen bonds were observed in all isomers of aminopyridines. It should be noted that stacking interactions are absent in mono-aminopyridines despite the presence of the aromatic π-system.

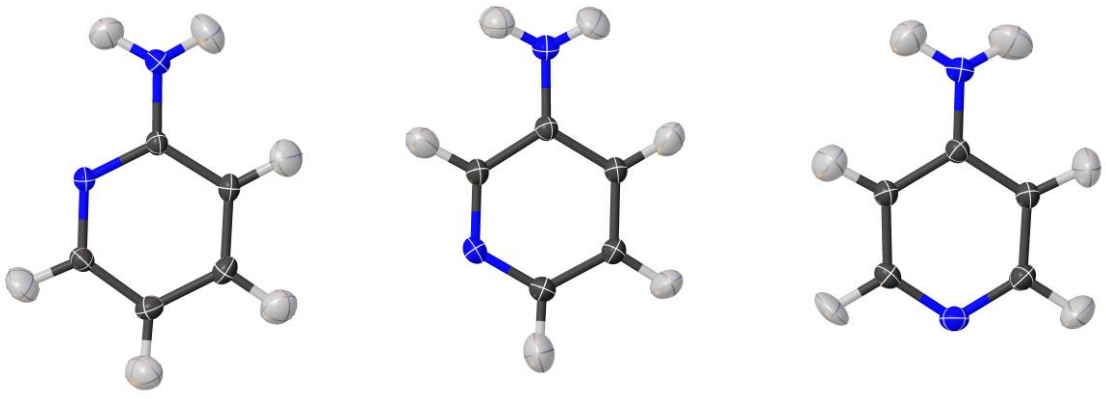

Fig. 1. The aminopyridine isomers (2-*ap*, 3-*ap*, 4-*ap*) redetermined from standard diffraction datasets using non-spherical atom form factors.

Literature

[1] M. Chao, E. Schempp, R. D. Rosenstein, *Acta Crystallogr. B*, **31** (1975) 2922.
[2] M. Chao, E. Schempp, R. D. Rosenstein, *Acta Crystallogr. B*, **31** (1975) 2924.

[3] M. Chao, E. Schempp, *Acta Crystallogr. B*, **33** (1977) 1557.
[4] A. Ilyukhin, P. Koroteev, CCDC 2170593: *Experimental Crystal Structure Determination*, 2022.
[5] F .P. Anderson, J. F. Gallagher, P. T. M.Kenny, A .J. Lough, *Acta Crystallogr. E*, **61** (2005) o1350.
[6] L. Midgley, L. J. Bourhis, O. V. Dolomanov, S. Grabowsky, F. Kleemiss, H. Puschmann and N. Peyerimhoff, *Acta Crystallogr. A*, **77** (2021) 519.
[7] I. S. Konovalova, E. N. Muzyka, V. V. Urzhuntseva, S.V. Shishkina, *Struct. Chem*., **32** (2021) 235.

B-24

APPLICATION OF HIERARCHICAL CLUSTERING OF ATOMIC ELECTRON DENSITY PARAMETERS FOR CONSTRUCTION OF THE MATTS DATA BANK

Paulina Maria Rybicka[a], Marta Kulik[a], Michał Leszek Chodkiewicz[a] i Paulina Maria Dominiak[a]

Biological and Chemical Research Centre, University of Warsaw
ul. Żwirki i Wigury 101, 02-089 Warsaw

Interpretation of experimental data from X-ray diffraction requires the use of a valid electron density model. The Multipole Model (MM) assumes the asphericity of the electron density of atoms, including deformations resulting from the presence of lone electron pairs and covalent bonds.[1] Atoms of the same element, located in a similar chemical environment, have almost identical electron density parameters, which makes it possible to transfer multipole parameters between chemically equivalent atoms. With this concept, banks of aspheric atom types defined by averaging over chemically equivalent atoms are constructed.[2] The MATTS (Multipolar Atom Types from Theory and Statistical Clustering) data bank collects multipole parameters specific to different atom types in proteins, nucleic acids and molecules based on experimental geometries from the Cambridge Structural Database (CSD).[3]

Using data analysis methods such as clustering, we captured similarities in electron density distributions for atom types from the MATTS data bank (651 types) and determined which factors most influenced the multipole parameters of their electron density.[4] The observed similarities and differences between atom types created a the potential to improve the quality of the MATTS bank by modifying the parameterization, definitions and local coordinate systems. The current analysis covers a wider range of data and is conducted on the atoms present in the CSD-derived molecules (about 90000 atoms). In addition, the improved clustering method gives more accurate results by implementing a hierarchical clustering algorithm. By using a greatly expanded dataset, as well as considering different probable orientations of the local coordinate system and chirality, we can improve the quality of the MATTS databank. The introduction of atom types at different levels of generality and specificity will allow the extension of the MATTS databank so that it is possible to reconstruct the electron density of any molecule.

We acknowledge the support from the National Centre of Science (Poland) through grant OPUS No. NCN UMO-2020/39/I/ST4/02904.

Literatura

[1] N. K. Hansen, P. Coppens, *Acta Cryst. A*, **34** (1978) 909–921.
[2] C. P. Brock, J. D. Dunitz, F. L. Hirshfeld, *Acta Crystallogr. Sect. B.*, **47**(5) (1991) 789–797.
[3] K. K. Jha, B. Gruza, P. Kumar, M. L. Chodkiewicz, P. M. Dominiak, *J. Chem. Inf. Model.*, **62**(16) (2022) 3752–3765.
[4] P. M. Rybicka, M. Kulik, M. L. Chodkiewicz, P. M. Dominiak, *J. Chem. Inf. Model.*, **62**(16) (2022) 3766–3783.

B-25

STRUCTURAL STUDIES OF UREA CLATHRATES WITH ALIPHATIC MONOAMINES

Anna Sadocha, Kamila Urbaniak, Michał K. Cyrański and Arkadiusz Ciesielski

University of Warsaw, Faculty of Chemistry, Pasteura 1 02-093 Warsaw

Urea, the first naturally occurring compound synthesized by F. Wöhler nearly 200 years ago, continues to attract considerable interest[1]. Its derivatives find applications in various fields, ranging from cosmetology[2] to the production of explosives[3]. Due to its low toxicity and wide availability, urea is widely utilized in organic synthesis. The ability of urea molecules to form hydrogen bonds enables the creation of intricate three-dimensional supramolecular structures. These structures include both macrocyclic molecules and clathrates, which are crystal systems with channel-like structures that encapsulate guest molecules within urea frameworks.

Urea clathrates, initially discovered in the 1940s, have received relatively limited attention in research[4]. Among the most prevalent clathrate arrangements are those forming infinite channels resembling honeycombs, capable to accommodate linear-shaped guest molecules that typically remain in a disordered state. Importantly, urea can also form clathrates with channels of varying lengths, depending on the guest molecule. Such systems are often sealed by a small molecule, and the guest molecule itself exhibits high order within the channel structure.

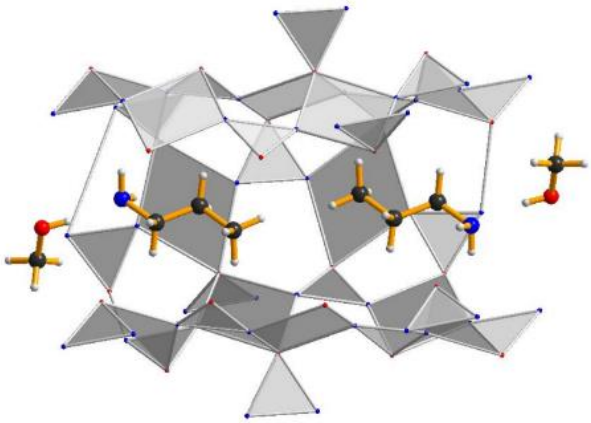

Fig. 1. Urea clathrate with 1-aminopropane.

The current study focuses on the structural analysis of finite urea clathrates formed with aliphatic monoamines. A total of eight structures were obtained using a series of successive amines from 1-aminopropane to 1-aminodecane. Given the high volatility of low molecular weight amines, these compounds exhibit relatively low stability, therefore research need to be conducted at low temperatures. In all obtained systems, two amine molecules are present within the urea channel, with their hydrophobic tails oriented towards the interior. A hydrophilic amino group extends from the channel and forms a hydrogen bond with the closing molecule, methanol. Notably, a significant correlation between the length of the amine chain, represented by the number of carbon atoms, and the lattice constant ***c*** is observed. Most of the studied

B-25

STRUCTURAL STUDIES OF UREA CLATHRATES WITH ALIPHATIC MONOAMINES

Anna Sadocha, Kamila Urbaniak, Michał K. Cyrański and Arkadiusz Ciesielski

University of Warsaw, Faculty of Chemistry, Pasteura 1 02-093 Warsaw

Urea, the first naturally occurring compound synthesized by F. Wöhler nearly 200 years ago, continues to attract considerable interest[1]. Its derivatives find applications in various fields, ranging from cosmetology[2] to the production of explosives[3]. Due to its low toxicity and wide availability, urea is widely utilized in organic synthesis. The ability of urea molecules to form hydrogen bonds enables the creation of intricate three-dimensional supramolecular structures. These structures include both macrocyclic molecules and clathrates, which are crystal systems with channel-like structures that encapsulate guest molecules within urea frameworks.

Urea clathrates, initially discovered in the 1940s, have received relatively limited attention in research[4]. Among the most prevalent clathrate arrangements are those forming infinite channels resembling honeycombs, capable to accommodate linear-shaped guest molecules that typically remain in a disordered state. Importantly, urea can also form clathrates with channels of varying lengths, depending on the guest molecule. Such systems are often sealed by a small molecule, and the guest molecule itself exhibits high order within the channel structure.

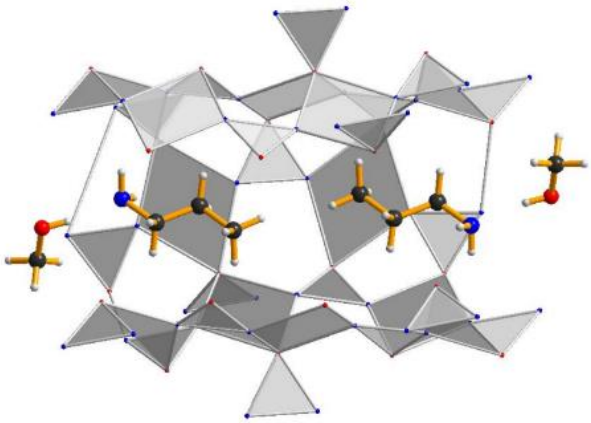

Fig. 1. Urea clathrate with 1-aminopropane.

The current study focuses on the structural analysis of finite urea clathrates formed with aliphatic monoamines. A total of eight structures were obtained using a series of successive amines from 1-aminopropane to 1-aminodecane. Given the high volatility of low molecular weight amines, these compounds exhibit relatively low stability, therefore research need to be conducted at low temperatures. In all obtained systems, two amine molecules are present within the urea channel, with their hydrophobic tails oriented towards the interior. A hydrophilic amino group extends from the channel and forms a hydrogen bond with the closing molecule, methanol. Notably, a significant correlation between the length of the amine chain, represented by the number of carbon atoms, and the lattice constant ***c*** is observed. Most of the studied

systems crystallize in the *C2/c* space group, except for the clathrates with 1-aminopropane and 1-aminoheptane, which belong to the $P2_1/c$ group. This distinction is most likely due to the adjustment of the clathrate tube length to the size of the guest molecule. The binding energy of the urea molecule within the channel was found to be approximately at the level of -30 kcal/mol.

References

[1] J. Meessen, *Chemie Ingenieur Technik*, **86** 12 (2014) 2180.
[2] D. Voegeli, *Derm. in Practice*, **18** (2012) 13.
[3] R. Matyas , J. Selesovsky, V. Pelikan, et. al., Explosive Properties and Thermal Stability of Urea Hydrogen Peroxide Adduct, Propellants, Explosives, Pyrotechnics, Wiley-VCH Verlag GmbH & Co. KGaA, Weinheim, (2016).
[4] M. F. Bengen, *Angew. Chem*., **6** (1951) 207.

B-26

COMBINATION OF QUANTUM-CHEMICAL CALCULATIONS AND X-RAY DIFFRACTION STUDY FOR INVESTIGATION OF TAUTOMERISM

Mariia Shyshkina[a], Dmitry Lega[b], Liudmyla Shemchuk[b], Irina Starchikova[b] and Leonid Shemchuk[b]

[a] State Scientific Institution, "Institute for Single Crystals" of the National Academy of Sciences of Ukraine, 60 Nauky Ave., Kharkiv 61072, Ukraine
[b] National University of Pharmacy, 4 Valentynivska St., Kharkov 61168, Ukraine

The title compound, $C_{27}H_{26}N_2O_6S_2$ (Fig. 1), possesses potential antimicrobial, analgesic, and anti-inflammatory activity.

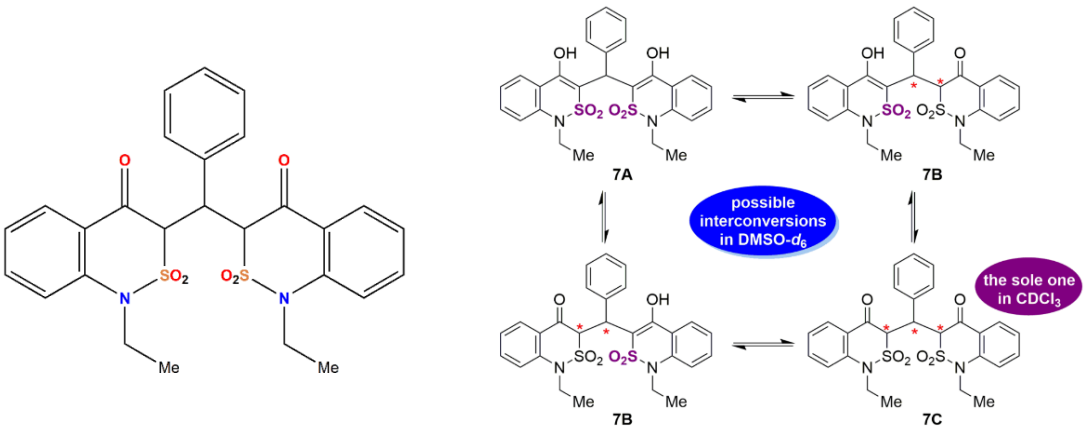

Fig. 1. The scheme of the title compound (on the left). Possible tautomeric forms of the title compound (on the right).

This compound has three tautomeric forms: dienol form **7A**, keto–enol form **7B**, and diketo form **7C** (Fig. 1). We recorded an unexpected ^{1}H NMR spectrum (DMSO-d6, 200 MHz) with a complicated set of numerous signals [1]. Such a spectroscopic picture could be the result of a tautomeric conversion cycle of the title compound initiated by proton movement in the dihydroxy tautomer **7A** (Fig. 1). The prototropic transformations are apparently facilitated by the slight basic properties of the solvent [2]. From the proton spectrum, one can conclude that the mixture contains the monohydroxy tautomer **7B** (a singlet at 11.13 ppm) and diketo form **7C**. We would like to emphasize that tautomers **7B** and **7C** contain several asymmetric carbon atoms and can exist as various optical isomers.

All these tautomers and stereoisomers were optimized by the M06–2X/cc-pVTZ method in a vacuum, using the PCM model with chloroform and DMSO as solvent (Table 1).

Table 1. Relative energies (kcal mol^{-1}) of tautomeric and stereoisomeric forms, calculated by the M06–2X/cc-pVTZ method.

Tautomer/ stereoisomer	Vacuum	PCM model (DMSO)	PCM model (chlorophorm)
	ΔE (kcal mol^{-1})	ΔE (kcal mol^{-1})	ΔE (kcal mol^{-1})
7A	5.66	14.67	16.82
7B	8.58	6.52	7.23
7C (*R, R, R*)	3.21	0	0
7C (*S, R, S*)	0	0	0
7C (*R, R, S*)	0	0	0

The diketo form of the title compound proved to be the most energetically favourable as compared to the keto–enol or dienol forms. The diketo form can exist as three possible stereoisomers with the same configuration of one stereogenic center at the C11 atom and different configurations of the stereogenic centers at two other atoms: (***R, R, R***), (***S, R, S***) and (***R, R, S***). The (***R, R, S***) stereoisomer was found in the crystal phase (Fig. 2).

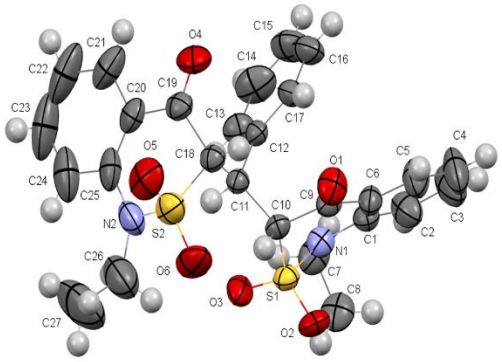

Fig. 2. Molecular structure of the title compound according to X-ray diffraction data. Thermal ellipsoids are shown at the 50% probability level.

It was revealed that the thiazine rings of equivalent benzothiazine fragments have different conformations, (a sofa or a half-chair). The two bicyclic fragments connected through the phenylmethylene group are oriented almost orthogonal to each other, subtending a dihedral angle of 82.16(7).

Literature

[1] M. O. Shyshkina, D. A. Lega, L. M. Shemchuk, I. L. Starchikova, L. A. Shemchuk, *Acta Cryst. E.*, **79** (2023) 349.
[2] W. S. MacGregor, *Ann. NY Acad. Sci.*, **141** (1967) 3.

B-27

CRYSTAL STRUCTURE OF THE TRINUCLEAR COBALT(II) COMPLEX WITH 3-AMINOPYRIDINE AND CHLORIDE LIGANDS

Magdalena Siedzielnik, **Anna Dołęga**

Department of Inorganic Chemistry, Faculty of Chemistry, Gdansk University of Technology, G. Narutowicz 11/12, 80-233 Gdańsk

Aminopyridines are an important class of compounds used as a research tool for characterizing subtypes of the potassium channels.[1] These compounds are widely used in the pharmaceutical industry, *e.g.* as a drug for symptomatic treatment of multiple sclerosis (4-aminopyridine), as a non-steroidal drug to relieve the symptoms of painful, inflammatory conditions like arthritis (2-aminopyridine).[1] Used as ligands, they readily react with transition metal salts to form colourful complexes.[2, 3]

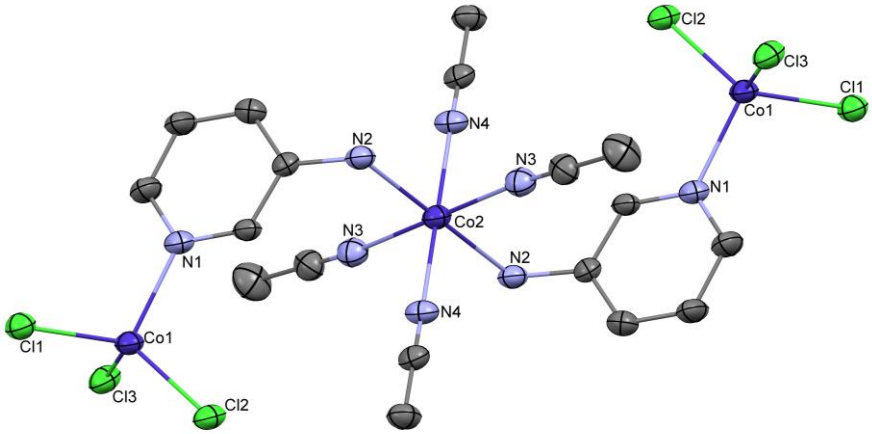

Fig. 1. Molecular structure of **C1**. Thermal ellipsoids at 30%. Numbering given for the cobalt and heteroatoms. Hydrogen atoms were omitted for clarity. Important bond lengths/distances [Å]: Co1—N1 2.038(6); Co1—Cl3 2.251(2); Co1—Cl2 2.255(2); Co1—Cl1 2.260(2); Co2—N4^{i} 2.095(6); Co2—N4 2.095(6); Co2—N3^{i} 2.132(7); Co2—N3 2.132(7); Co2—N2^{i} 2.178(6); Co2—N2 2.178(6); Important angles [^{o}]: N1—Co1—Cl3 106.3(2); N1—Co1—Cl2 106.45(19); Cl3—Co1—Cl2 113.91(8); N1—Co1—Cl1 107.40(18); Cl3—Co1—Cl1 108.10(9); Cl2—Co1—Cl1 114.15(8); N4^{i}—Co2—N4 180.0(3); N4^{i}—Co2—N3 91.0(3) N4—Co2—N3 89.0(3); N4^{i}—Co2—N3^{i} 89.0(3); N4—Co2—N3^{i} 91.0(3); N3—Co2—N3^{i} 180; N4^{i}—Co2—N2^{i} 90.2(2); N4—Co2—N2^{i} 89.8(2); N3—Co2—N2^{i} 85.6(2); N3^{i}—Co2—N2^{i} 94.4(2); N4^{i}—Co2—N2 89.8(2); N4—Co2—N2 90.2(2); N3—Co2—N2 94.4(2); N3^{i}—Co2—N2 85.6(2); N2^{i}—Co2—N2 180; i= -x+1, -y+1. -z+1.

We have isolated several new Co(II) complexes as side products during the synthesis of imine complexes with Co(II). Later, to fully characterize the complexation reaction we stared the purposeful synthesis of the species. Our studies confirmed that the molar ratio of the reactants as well as the temperature of crystallization significantly influences the stoichiometry of the complexes, their molecular geometry as well as their nuclearity. The reaction of $CoCl_2$ with 3-aminopyridine at the ratio 1:2, proceeded with the formation of mononuclear, tetrahedral cobalt(II) complex. The ratio of $CoCl_2$ to 3-aminopyridine 2:1 allowed the isolation of a trinuclear compound (**C1**, Fig.1). Crystals

suitable for X-ray analysis were obtained at room temperature by slow evaporation of the solvent. The crystallographic data for the title compound were collected on an STOE IPDS II diffractometer. at 120 K using Mo K_α radiation of a microfocus X-ray source.

C1 crystallizes in a monoclinic system in $P2_1/c$ space group. The unit cell parameters are as follows: a= 10.026(4) Å; b= 10.283(2) Å, c= 14.737(5) Å; α= 90.0°; β= 91.48(3)°; γ= 90.0°; V= 1521.0 Å^3 and Z= 2. Quality parameters of the solution are $R_1[I>2\sigma(I)]$= 0.080; wR_2 (all data)= 0.284; R_{int}= 0.091, GOOF= 0.968. Asymmetric unit contains half of the molecule. Each of the terminal cobalt atoms is coordinated by three chloride atoms and pyridyl nitrogen atom derived from 3-aminopyridine. The central cobalt atom is coordinated by four molecules of solvent (acetonitrile) and two molecules of 3-aminopyridine. This central Co(II) assumes octahedral coordination.

Literature

[1] M. Kumar Trivedi, A. Branton, D. Travedi, G. Nayak, R. Mishra, S. Jana, Sci. J. Anal. Chem., **3** (2015) 127.
[2] J.R. Allan, G.M. Baillie, H.J. Bowley, D.L. Gerrard, *Eur. Polym. J.*, **24** (1988) 1149.
[3] D.H. Brown, K.P. Forrest, R.H. Nuttall, D.W.A. Sharp, *J. Chem. Soc. A,* (1968) 2146.

B-28

UNRAVELING THE COMPLEX NATURE OF INTERMOLECULAR INTERACTIONS IN QUINOLINE AND ISOQUINOLINE SYSTEMS

Tomasz Sierański

Institute of General and Ecological Chemistry, Lodz University of Technology, Żeromski 116, 90-924 Łódź

Stacking interactions involving N-heterocyclic aromatic rings have recently emerged as a crucial area of study. These systems exhibit a variety of interaction patterns such as π-stacking and hydrogen bonds, contributing significantly to structures of biomolecules, molecular recognition, crystal engineering, and nanoengineering. Given their biological importance and application in designing supramolecular structures, a comprehensive understanding of these interactions is indispensable. While previous research has provided some insight, comprehensive understanding of these interactions, crucial for their biological relevance and application, remains unachieved due to limited exploration of non-stationary configurations[1-4].

This work fills this knowledge gap by examining the potential energy surfaces of model quinoline and isoquinoline dimers[5,6], using dispersion-corrected density functional to calculate interaction energies across numerous systems. Findings were cross-verified with the Cambridge Structural Database[7], and advanced techniques, including natural bond orbital and energy decomposition analyses, were employed.

This multidmensional analysis provides profound insights into the interaction energy landscape of quinoline and isoquinoline systems. The comprehensive approach reveals the complex nature of the intermolecular interactions, offering a novel view of present interaction patterns. The results indicate that intermolecular interactions, particularly stacking, are a combination of multiple sources of interaction energy. This information could play a vital role in predicting crystal structures and modeling crystals with desired properties.

Literatura

[1] T. Sierański, *J Mol Model*, **23** (2017) 338.
[2] T. Sierański, Theor Chem Acc, 139 (2020) 153.
[3] M. Jacobs, L. Greff Da Silveira, G. Prampolini, P.R. Livotto, I. Cacelli, *J. Chem. Theory Comput*., **14** (2018) 543–556.
[4] R.G. Huber, M.A. Margreiter, J.E. Fuchs, S. von Grafenstein, C.S. Tautermann, K.R. Liedl, T. Fox, *J. Chem. Inf. Model*., **54** (2014) 1371–1379.
[5] X.-F. Shang, S.L. Morris-Natschke, Y.-Q. Liu, X. Guo, X.-S. Xu, M. Goto, J.-C. Li, G.-Z. Yang, K.-H. Lee, *Med Res Rev*, **38** (2018) 775–828.
[6] M. Iranshahy, R.J. Quinn, M. Iranshahi, *RSC Adv*., **4** (2014) 15900–15913.
[7] C. R. Groom, I. J. Bruno, M. P. Lightfoot, S. C. Ward, *Acta Cryst*., (2016).

B-29

SYNTHON TRANSFERABILITY IN CRYSTAL STRUCTURES CONTAINING QUINOLINE ANTIMALARIALS

Agnieszka Skórska-Stania, Weronika Sarnowska, Wojciech Nitek and Marlena Gryl

Jagiellonian University, Faculty of Chemistry, Gronostajowa 2, 30-387 Kraków

For many years, quinoline drugs like *Cinchona* alkaloids and then mefloquine (Scheme 1) used to be first line medicines used in the treatment of malaria. Unfortunately, they are no longer recommended by the World Health Organization (WHO) because there are other substances that are equally effective with fewer side effects [1].

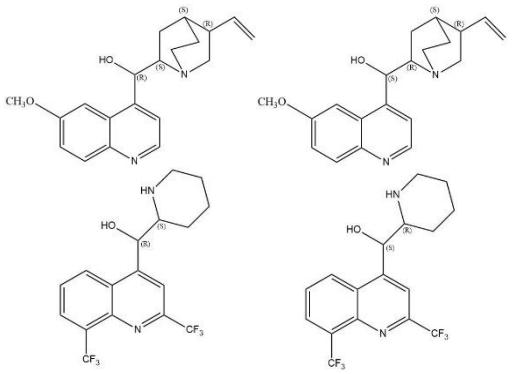

Scheme 1. Chemical diagrams of quinine, quinidine and racemic mixture of mefloquine.

Quinoline drugs are basic amines and are usually provided as salts, *e.g.* sulfates or hydrochlorides. So, the question remains whether it's worth giving up well-established old drugs especially after the global pandemic experience. Maybe it is more prudent to change the formulation of drugs to limit side effect. In the last few years, the remedy for these global problems was found in modified properties of the active pharmaceutical ingredients (API's) through cocrystallization. Combining one or more API's with coformer in the crystal structure can influence the properties of parent drug such as: solubility, polarity, tabletability, melting point and through those the overall bioaviability.

In our research, we have selected API's like quinine, quinidine and mefloquine with coformer- (E)-cyanoxime (CyOx). As weak bases, *Cinchona* alkaloids and mefloquine, have two nitrogen atoms – quinuclidine/pyridine N1 and quinoline N13 and a hydroxyl oxygen atom O12, which can be involved in the formation of hydrogen bonds. The goal of our research was to examine hydrogen bond systems and other weak interactions in the multicomponent crystals containing these API's. For this purpose, we have utilized *in sillico* crystal design methods (CSDMaterials) Hirshfeld surface analysis with QTAIM calculations [2-4]. Employing a wide scope of statistical and quantum chemical methods allowed us to discover and analyze of repeatable synthon formation. Percentage of contributions of interactions as well as their energies were compared for all structures. Based on those results we were able to propose a mechanism allowing to modify the analyzed crystal structures.

References

[1] A. Dondorp, F. Nosten, K. Stepniewska, N. Day, N. White (2005). Artesunate versus quinine for treatment of severe falciparum malaria: a randomised trial. *Lancet*, **366** (9487).
[2] P. R. Spackman, M. J. Turner, J. J. McKinnon, S. K. Wolff, D. J. Grimwood, D. Jayatilaka, & M. A. Spackman, *J. Appl. Cryst.*, **54**(3) (2021) 1006–1011.
[3] R. F. W Bader Atoms in molecules, A Quantum Theory. NewYork: Oxford University Press, (2003).
[4] C. R. Groom, I. J. Bruno, M. P. Lightfoot and S. C. Ward, *Acta Cryst*. *B*, **72** (2016) 171–179.

B-30

SOLID-STATE FLUORESCENCE STUDY OF NEW ORGANIC FLUOROPHORES BASED ON PHENYLHYDRAZONES

Paulina Sobczak, Agata Trzęsowska-Kruszyńska

Institute of General and Ecological Chemistry, Faculty of Chemistry, Lodz University of Technology, Żeromskiego 116, 90-924 Łódź

Solid-state fluorescence is a collective phenomenon of molecules that can be modulated through controlling molecular packing and the electronic conjugation of fluorophores [1]. Organic compounds exhibiting fluorescent properties in the solid-state are of significant importance because their structure can be modified, resulting in the production of switchable and tunable fluorescent materials. Such compounds are considered as potential candidates for optoelectronic [2], forensic [3], and biomedical [4] applications. One of the solid-state emissive organic chromophores design strategies is the minimalization of π···π stacking interactions consisting in the chemical modification of compounds by introducing additional functional groups into their structure, which may significantly increase their usefulness. The factors by which the substituents exert such a great influence on the intensity of the fluorescent properties are the dipole moment of the molecule, the position of the functional group substitution, and the presence of electron withdrawing substituents (EWS) or electron donating substituents (EDS). It was found that the nature of observed absorption and emission can be changed by adjusting the electron withdrawing and electron donating groups by altering the electron density distribution or extending the coupling in the aromatic system [5].

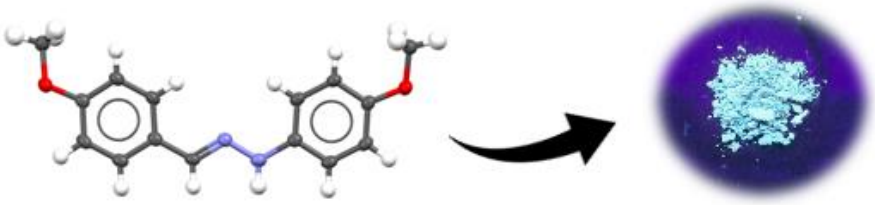

Rys. 1. Molecular structures of phenylhydrazone exhibiting fluorescence.

The main aim of the research was to design and synthesize new effective fluorophores that emit light in the solid-state and to investigate the influence of introducing different substituents into the molecular structure on the fluorescence properties.

The study includes the syntheses of phenylhydrazones and their structural, and spectroscopic characterization using X-ray diffraction, infrared (IR), and fluorescence spectroscopy methods (including excitation—emission matrix—EEM).

References

[1] C. Wang, Z. Li, *Materials Chemistry Frontiers*, **1** (2017) 2174–2194.
[2] A. Uslu, S.O. Tumay, S. Yesilot, *Journal of Photochemistry and Photobiology C: Photochemistry Reviews*, **53** (2022) 100553.
[3] A. A. Ansari, K. M. Aldajani, A.N. AlHazaa, H. A. Albrithen, *Coordination Chemistry Reviews*, **462** (2022) 214523.
[4] J.V. Jun, D.M. Chenoweth, E.J. Petersson, *Organic & Biomolecular Chemistry*, **18** (2020) 5747–5763.
[5] S.P. Anthony, *ChemPlusChem*, **77** (2012) 518–531.

B-31

STRUCTURES OF NEW THIOSEMICARBASIDE DERIVATIVES

Jaroslaw Sukiennik[a], Katarzyna Gobis[b], Izabela Korona-Glowniak[c], Andrzej Fruzinski[a], Andrzej Olczak[a], Malgorzata Szczesio[a]

[a] Institute of General and Ecological Chemistry, Faculty of Chemistry, Lodz University of Technology, Zeromskiego 116, 90-924 Lodz, Poland
[b] Department of Organic Chemistry, Medical University of Gdansk, M. Sklodowskiej-Curie 3a, 80-210 Gdansk, Poland
[c] Department of Pharmaceutical Microbiology, Medical University of Lublin Chodzki 1, 20-093 Lublin, Poland

Thiosemicarbaside derivatives are useful building block. Connected with picoline compounds can create tuberculostatic agents [1]. Additionally, that group of compound show antibacterial [2] and anticancer [3] properties. Presented compound (Table, Scheme) have promising activity against gram-positive bacteria and yeasts. Similarity of compounds provide a small study of comparison between structure and activity.

No	a, b, c [Å]	α, β, γ [°]	Space group	R [%]
1	16.4576 (1) 11.9645 (1) 23.8781 (2)		$Pca2_1$	6.2
2	10.6953 (2) 12.8703 (3) 15.4917 (3)	95.1570 (17) 107.466 (2) 97.8737 (18)	$P\bar{1}$	3.1
3	13.1063 (3) 12.8414 (2) 15.6327 (3)	98.255(2)	$P2_1/c$	3.9

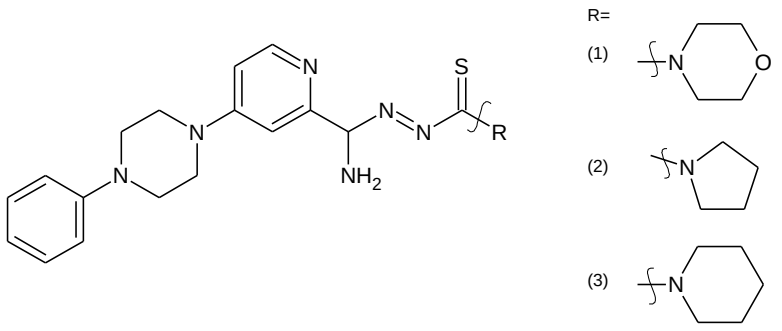

Literature

[1] M. Krause, H. Foks, D. Ziembicka, E. Augustynowicz-Kopeć, A. I. Głogowska, I. Korona-Głowniak, K. Bojanowski, D. Siluk, K. Gobis, *Eur J Med Chem*, **190** (2020) 112106.
[2] A. Kowalczyk, A. Paneth, D. Trojanowski, P. Paneth, J. Zakrzewska-Czerwińska, P. Stączek,, *Int J Mol Sci*, **22** (2021) 8.
[3] R. Chen, L. Huo, Y. Jaiswal, J. Huang, Z. Zhong, J. Zhong, L. Williams, X. Xia, Y. Liang, Z. Yan, *Molecules*, **20** (2019) 11.

B-32

AMIDRAZONE DERIVATIVES - STRUCTURE AND ACTIVITY

Mateusz Romański[a], Katarzyna Gobis[b], Izabela Korona Głowniak[c], Malwina Krause[b], Katarzyna Suśniak[c], Andrzej Olczak[a], Małgorzata Szczesio[a]

[a] *Institute of General and Ecological Chemistry, Faculty of Chemistry, Lodz University of Technology, 116 Żeromskiego Street, 90-924 Lodz, Poland*
[b] *Department of Organic Chemistry, Medical University of Gdansk, M. Skłodowskiej-Curie 3a Street, 80-210 Gdansk, Poland*
[c] *Department of Pharmaceutical Microbiology, Medical University of Lublin, Chodźki 1, 20-093 Lublin, Poland*

Amidrazones and their derivatives exhibit a broad spectrum of biological activity, e.g., antibacterial, antifungal, antimalarial, antiviral, anti-inflammatory, analgesic, anticonvulsant. They also have established antitubercular activity [1]. To determine the relationship between structure and activity of the compounds studied, a series of tests and measurements were performed. Structure was determined for three compounds using diffraction studies, liquid and solid NMR and ab-initio calculations (Fig.1). Activity predictions showed antibacterial and antitumour activity.

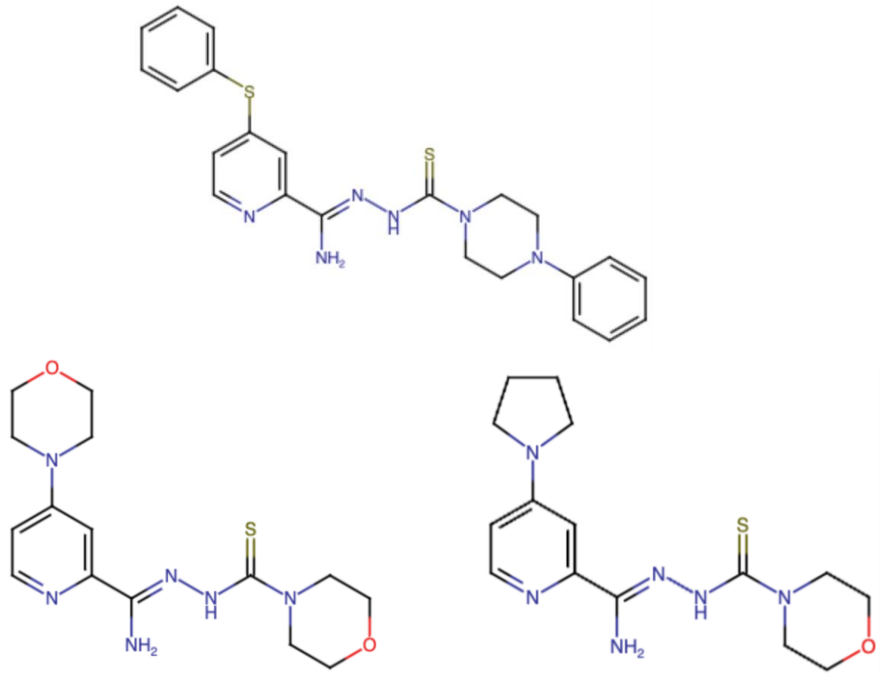

Fig.. 1. Formulas of the compounds.

Literature

[1] R. Paprocka, M. Wiese-Szadkowska, A. Helmin-Basa, L. Mazur, J. Kutkowska, J. Michałkiewicz, J Modzelewska-Banachiewicz, L. Pazderski Monatsh Chem., Vo. 149, 2018, s. 1493-1500.

B-33

SYNTHESIS AND STRUCTURAL ELUCIDATION OF SUBSTITUTED 4-(DIARYLPHOSPHORYL)CHROMAN-2-ONES

Katarzyna Szwaczko, Daniel Kamiński

Department of Organic Chemistry and Crystallochemistry, Institute of Chemical Sciences, Faculty of Chemistry, Maria Curie-Sklodowska University in Lublin

Dihydrocoumarin scaffold is an important structural unit present in a wide range of naturally occurring and synthetic molecules. 3,4-Dihydrocoumarin, i.e. chroman-2-one, is a subclass of this group exhibiting a wide range of biological profiles, including antioxidant, cytotoxic, anticancer, immunomodulatory, anticoagulant, and antimicrobial activities [1-3]. In addition, it is also a useful building block in the synthesis of some other important compounds [4].

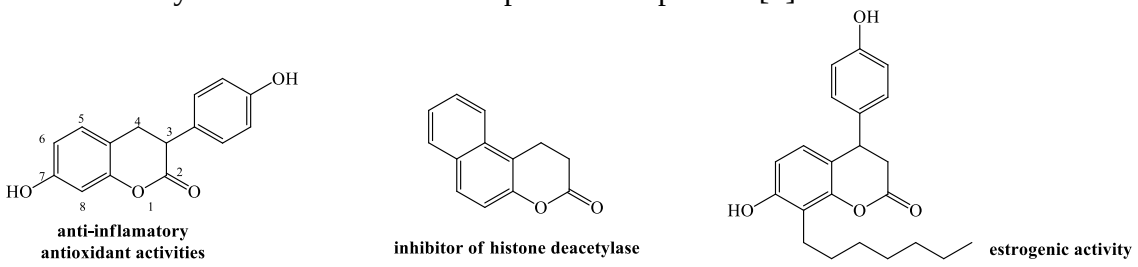

Fig. 1. 3,4-Dihydrocoumarin-based pharmaceuticals.

Phosphorus functionalized organic molecules, in turn, have also found useful applications in the areas of industrial, agricultural, materials and medicinal chemistry [5]. The synthesis of hydrib compounds that are a combination of 3,4-dihydrocoumarin backbone and a phosphoryl moiety could be an interesting solution that opens a route to a new class of organophosphorus compounds.

In this post, we will present a new route for the synthesis of 4-(diarylphosphoryl)chroman-2-ones and their crystallographic analyses.

References

[1] J. Modranka, A. Albrecht, R. Jakubowski, H. Krawczyk, M. Różalski, U. Krajewska, A. Janecka, A. Wyrębska, B. Różalska, T. Janecki, *Bioorg. Med. Chem.*, **20** (2012) 5017.
[2] F. Roelens, K. Huvaere, W. Dhooge, M. Van Cleemput, F. Comhaire, D. De Keukeleire, *Eur. J. Med. Chem.*, **40** (2005) 1042.
[3] J. Posakony, M. Hirao, S. Stevens, J. A. Simon, A. Bedalov, *J. Med. Chem*., **47** (2004) 2635.
[4] E. Ballerini, L. Minuti, O. Piermatti, F. Pizzo, *J. Org. Chem*., **47** (2009) 4311.
[5] S. Demkowicz, J. Rachon, M. Daśkoa, W. Kozak, *RSC Adv*., **6** (2016) 7101.

B-34

DEHYDRATION OF cAMP CALCIUM SALTS FORCES MOVEMENTS IN A CRYSTAL

Aleksandra R. Sokołowska, Katarzyna Ślepokura

University of Wroclaw, Faculty of Chemistry, F. Joliot-Curie 14, 50-383 Wroclaw

Adenosine 3′:5′-cyclic monophosphate (cAMP, Fig. 1) is a vital molecule in every organism, as it plays a role of second messenger in signal transduction pathways[1]. Despite almost 80 years since its discovery, only 7 crystal structures can be found in *Cambridge Structural Database* (CSD). These are cAMP hydrates and sodium salts. Most cAMP zwitterions/anions are *anti* conformers. The base orientation is tuned by ribose pucker (either *envelope* or *twist*) and phosphate moiety, which in most cases adopts *chair* conformation[2].

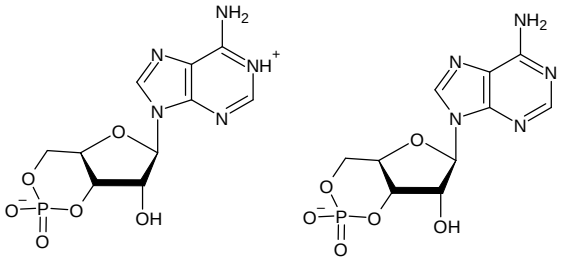

Fig. 1. Scheme of cAMP structure; (on the left) zwitterionic form, (on the right) anionic one.

Here we present a number of different hydrates of cAMP calcium salts: isomorphic series of $[Ca(cAMP)_2(H_2O)_2]\cdot xH_2O$, x = 0, 0.8, 1.5, 2 composition (orthorhombic, $P2_12_12_1$) and $[Ca_2(cAMP)_4(H_2O)_3]\cdot 5H_2O$ (triclinic, $P1$) along with the anhydrous form obtained by dehydration of $[Ca(cAMP)_2(H_2O)_2]\cdot 2H_2O$, i.e. $Ca(cAMP)_2$). All of the currently presented crystalline forms reveal a rare O/P/O/C/C/C *skew* conformation. Calcium cation coordination environment undergoes tremendous changes on water removal to produce very uncommon and rarely-occurring penta-coordinated calcium ion *via* dehydration of orthorhombic modification (Fig. 2). The full story of the crystal: from hydrated *via* dehydrated to rehydrated forms will be presented.

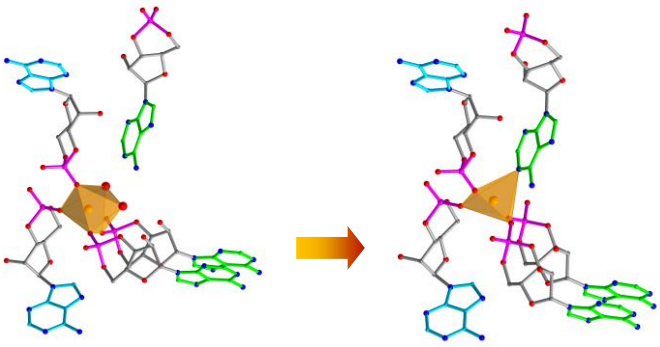

Fig. 2. Structural units of (on the left) $Ca(cAMP)_2\cdot 4H_2O$ and (on the right) $Ca(cAMP)_2$.

References

[1] H. Rehmann, A. Wittinghofer, J. L. Bos, *Mol. Cell Biol.*, **8** (2008) 63-73.

[2] R. P. Newton, C. J. Smith, *Phytochemistry*, **65** (2004) 2423-2437.

B-35

STRUCTURAL ISOMERISM IN ZINC FORMATE AND 1,10-PHENANTHROLINE SYSTEM: STRUCTURE-PROPERTY INTRICACIES

Marcin Świątkowski

Institute of General and Ecological Chemistry, Lodz University of Technology, Zeromskiego 116, 90-924 Lodz

Structural isomerism of coordination compounds is a type of isomerism where two or more compounds have the same molecular formula but different arrangements of atoms or bonds. Structural isomers can be divided into three categories: ionization, coordination, and linkage isomers. Ionization isomers occur when a ligand bound to the metal center exchanges places with an anion or neutral molecule that was initially outside the coordination entity [1]. In practical applications, understanding this form of isomerism has notable implications. For instance, a study on coordination compounds of cobalt butyrate and isobutyrate demonstrated that subtle changes in molecular structure can considerably affect the properties of the compounds, such as the size of formed particles and their spectroscopic and thermal properties [2]. The special type of ionization isomerism is solvate or hydrate isomerism, which arises from the replacement of a coordinated group by a solvent molecule. For example, chromium chloride may contain 4, 5, or 6 coordinated water molecules, resulting in different compounds with distinct colors [1]. These examples highlight how isomerism can notably affect the physical properties of coordination compounds.

The current work presents two new zinc formate coordination compounds with 1,10-phenanthroline, which exhibit structural isomerism (Fig. 1). The isomerism arises from the competition between formate anions and water molecules for the place in the inner coordination sphere. These isomers were investigated for their fluorescent and thermal properties, and the differences observed in these properties were correlated with structural variances.

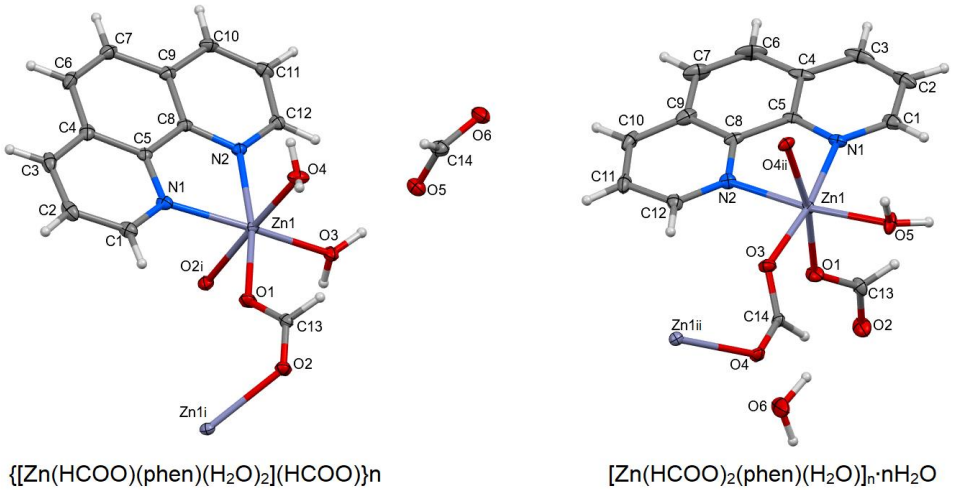

{[Zn(HCOO)(phen)(H_2O)$_2$](HCOO)}n [Zn(HCOO)$_2$(phen)(H_2O)]$_n$·nH_2O

Fig. 1. Molecular structures of zinc structural isomers. The equivalent atoms were generated according to symmetry transformations: (i) -x+0.5, y+0.5, -z+1.5; (ii) -x+1, -y+1, z+0.5.

References

[1] R.H. Petrucci, W.S. Harwood, G.F. Herring, J.D. Madura. *General Chemistry: Principles and Modern Applications: 9th Ed.*, New Jersey: Pearson (2007).
[2] M. Swiatkowski, T. Sieranski, M. Bogdan, R. Kruszynski, *Molecules*, **24** (2019) 3357.

B-36

WYSOKOCIŚNIENIOWA ANALIZA KOMPLEKSU FERROCENYLOACETYLENKU ZŁOTA (I) Z TRIETYLOFOSFINĄ

Bartłomiej Trojanowski, Anna Makal

Uniwersytet Warszawski, Wydział Chemii Uniwersytetu Warszawskiego, 02-089 Warszawa, ul. Żwirki i Wigury 101

Wykonywanie pomiarów pod zwiększonym ciśnieniem pozwala na obserwację przejść fazowych *single-crystal-to-single-crystal* (SCSC) oraz poszukania materiałów o anomalnej ściśliwości (NLC - *negative linear compressibility*). Przykładowymi zastosowaniami materiałów NLC jest zastosowanie ich jako elementów sensorów ciśnieniowych [1] lub materiałów półprzewodnikowych i nadprzewodnikowych zależnych od zwiększającego się ciśnienia [2]. SCSC wykazują związki posiadające w swojej budowie między innymi pochodne fosfiny [3] . Efekt NLC jest dość często spotykany w cząsteczkach posiadających fragment ferrocenowy [4]. Badany kompleks posiada oba powyższe fragmenty w swojej budowie a dodatkowo w jego centrum znajduje się atom złota, który dodatkowo zwiększa szansę na występowanie anomalnej ściśliwości [5]. W sferze badań wysokociśnieniowych nie figuruje jednak wiele pozycji w których występują związki mające w swojej budowie wszystkie takie fragmenty. Nie jest dostępne również wiele pozycji literaturowych omawiających zmiany w ugrupowaniach trietylofosfinowych indukowanych podwyższeniem ciśnienia.

Prezentowane badania są kontynuacją eksperymentów z 2018 roku [6] w których badany związek był analizowany pod względem przejść fazowych w zmiennej temperaturze (110 K – 200 K). W tej prezentacji będą zmiany strukturalne indukowane zwiększonym ciśnieniem. Eksperymenty dyfrakcji rentgenowskiej dla monokryształu ferrocenyloacetylenku złota (I) z trietylofosfiną zostały przeprowadzone zakresie ciśnień 0.3 GPa - 7.3 GPa (pomiary wykonane w Europejskim Ośrodku Promieniowania Synchrotronowego w Grenoble na stacji ID 15b). Powyżej 2.0 GPa zaobserwowano anomalną ściśliwość komórki elementarnej w kierunku **a**. Przedstawione zostaną wyniki badań strukturalnych z wyszczególnieniem zmian konformacyjnych trietylofosfiny oraz przesunięć na pierścieniu ferrocenowym.

Badania finansowane z grantu OPUS nr DEC-2021/41/B/ST4/02760 Narodowego Centrum Nauki.

Literatura

[1] Joseph N Grima, Daphne Attard, Roberto Caruana-Gauci, and Ruben Gatt. *Scripta Materialia*, **65**(7), (2011).
[2] Yuzhu Song, Naike Shi, Shiqing Deng, Xianran Xing, and Jun Chen. *Progress in Materials Science*, **121**:100835 (2021).
[3] Castro, Miguel, et al. *Acta Cryst Chemistry*, **73**(9) (2017).
[4] Paliwoda, Damian, Michael Hanfland, and Andrzej Katrusiak. *TJoPC*, **123**(42) (2019).
[5] Woodall, Christopher H., et al. *Angewandte Chemie*, **125**(37) (2013).
[6] Makal, Anna. *Acta Cryst*, **74**(5) (2018).

B-37

POLYMORPHISM AND STABILITY OF BROMOACETOPHENONE HYDRAZONE: A CASE STUDY

Agata Trzęsowska-Kruszyńska, Marcin Świątkowski, Tomasz Sierański, Marta Bogdan i Paulina Sobczak

Department of X-Ray Crystallography and Crystal Chemistry, Institute of General and Ecological Chemistry, Lodz University of Technology, Żeromskiego 116, 90-924 Lodz, Poland

Polymorphism is a phenomenon in which the same compound can exist in different crystal structures, called polymorphs. Polymorphism is important for pharmaceutical and other applications because different polymorphs can have different physical and chemical properties, such as solubility, dissolution rate, bioavailability, stability, hardness, color, etc. For example, rifaximin and mefenamic acid are two examples of drugs that show different bioavailability in humans depending on their polymorphic forms [1, 2]. Therefore, it is essential to understand the factors that affect the formation and stability of polymorphs, and to develop reliable techniques to identify and characterize them.

The stability of polymorphs is determined by the balance between thermodynamics and kinetics. Thermodynamics dictates that the most stable polymorph is the one with the lowest free energy at a given temperature and pressure. Kinetics dictates that the formation and transformation of polymorphs depend on the rate of nucleation and growth, which can be influenced by various factors. Therefore, the polymorph that crystallizes first may not be the most stable one, and may undergo a polymorphic transition to a more stable form over time. Besides thermodynamics and kinetics, there are other factors that can affect the formation and stability of polymorphs, such as solvent, temperature, pressure, impurities and pressure.

In this poster presentation, we will report the findings of study on the stability of polymorphic forms of bromoacetophenone hydrazone. The results on the correlation between the crystal structure and stability of individual polymorphs will be presented. Stability was determined by differential scanning calorimetry and hot stage microscopy. To gain more insight into the stability of crystal structures, energy calculations of conformers and crystal lattice were performed.

Literature

[1] G.C. Viscomi, M. Campana, M. Barbanti, F. Grepioni, M. Polito, D. Confortini, G. Rosini, P. Righi, V.Cannata, D. Braga, *Cryst. Eng. Commun.*, **10** (2008) 1074.
[2] S. SeethaLekshmi, T.N. Guru Row, *Cryst. Growth Des.*, **12** (2012) 4283.

B-38

SYNTEZA, WŁAŚCIWOŚCI STRUKTURALNE I SPEKTROSKOPOWE KRYSZTAŁU ZAWIERAJĄCEGO KATION KOORDYNACYJNY $[Cu(L\text{-}ARG)(BPY)]^{2+}$

Zuzanna Walkowiak[a], Anna Gągor[b], Maria Jerzykiewicz[c], Magdalena Fitta[d], Agnieszka Wojciechowska[a]

[a] Wydział Chemiczny, Politechnika Wrocławska, Wydział Chemiczny, ul. C. K. Norwida 4/6, 50-373 Wrocław
[b] Instytut Niskich Temperatur i Badań Strukturalnych PAN, ul. Okólna 2, 50-422 Wrocław
[c] Wydział Chemii, Uniwersytet Wrocławski, ul. F. Joliot-Curie 14, 50-383 Wrocław
[d] Instytut Fizyki Jądrowej PAN, ul. W. Eljasza-Radzikowskiego 152, 31-342 Kraków

Kwas 2-amino-5-guanidynopentanowy, zwyczajowo nazywany L-argininą, tworzy połączenia z jonami miedzi(II) typu $[Cu(L\text{-}Arg)^2]^{2+}$ lub $[Cu(L\text{-}Arg)(A)]^{2+}$ (A = 2,2'–bipirydyl (bpy); 1,10–fenantrolina (phen)), które są szeroko badane pod kątem właściwości strukturalnych, magnetycznych oraz biologicznych [1]. Budowa strukturalna utworzonych związków w dużym stopniu zależy od rodzaju wprowadzonego anionu (organicznego jak i nieorganicznego) równoważącego ładunek kationów koordynacyjnych. Dla związków zawierających kationy koordynacyjne typu $[Cu(L\text{-}Arg)(bpy)]^{2+}$ dostępne są jedynie dane dla struktury z jonami chlorkowymi [2].

W trakcie przeprowadzonych przeze mnie badań nad wpływem anionów o różnej symetrii na krystalizację, właściwości strukturalne oraz spektroskopowe związków koordynacyjnych typu [Cu(L-Arg)(bpy)]X (X= Br^-, Cl^-, NO_3^-, SO_4^{2-}, SeO_4^{2-}, $HCOO^-$, CH_3COO^-) otrzymałam dobrej jakości kryształy związku o wzorze $[CuBr(L\text{-}Arg)(bpy)]Br\cdot 2H_2O$.

Jego budowa oraz właściwości nie zostały wcześniej opisane w literaturze. Związek krystalizuje w centrosymetrycznej grupie przestrzennej P-1 o parametrach komórki a = 7.033(1) Å, b = 10.069(1) Å, c = 15.780 (2) Å, α = 99.28(1)°, β = 100.26 (1)°, and γ = 90.51(1)° i Z = 2. Jon miedzi(II) jest chelatowany aminowym atomem azotu i karboksylowym atomem tlenu pochodzącymi od L-Argininy oraz dwoma atomami azotu od cząsteczki bpy. Pięcio-koordynacyjną sferę centrum metalicznego uzupełnia skoordynowany anion bromkowy, a drugi jon bromkowy równoważy ładunek kationu koordynacyjnego $[CuBr(L\text{-}Arg)(bpy)]^+$. Właściwości spektroskopem związku zbadano przy użyciu metod: FT-IR, FIR, Raman oraz EPR (X- and Q-bands). Podatność magnetyczna (2-300 K, 1kOe) wykazuje zachowanie typowe dla paramagnetyka, a niezerowa ujemna wartość θ_{CW} wskazuje na słabe antyferromagnetyczne sprzężenie momentów magnetycznych kompleksu.

B-38

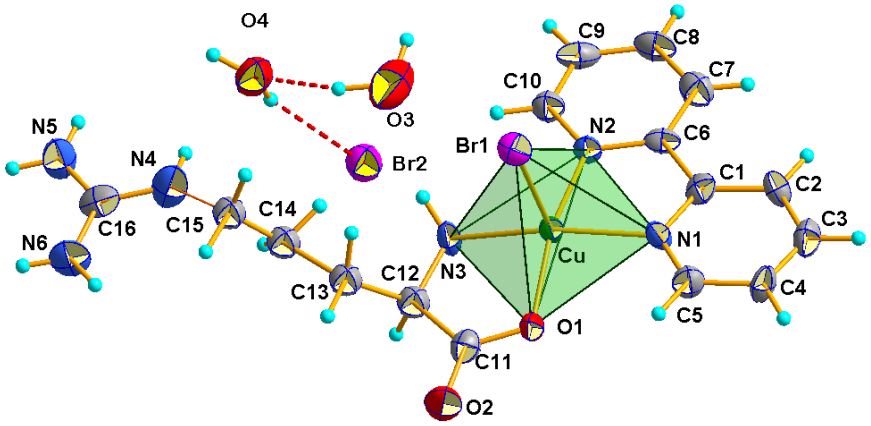

Rys. 1. Budowa kationu koordynacyjnego $[CuBr(L–Arg)(bpy)]^{+}$.

Literatura

[1] N. Ohata, H. Masuda, O. Yamauchi, *Inorg. Chimica Acta*, **300-302** (2000) 749-761.
[2] N. Ohata, H. Masuda, O. Yamauchi, *Inorg. Chimica Acta*, **286** (1999) 37-45.

B-39

SYNTEZA I ROZDZIAŁ ENANCJOMERYCZNIE CZYSTYCH OKTAHYDROPIRYDO[1,2-C][1,3,2]OKSAZAFOSFONINÓW Z RACEMICZNYCH SUBSTRATÓW

Adam Włodarczyk*, Marek Stankevič i Daniel Kamiński

Katedra Chemii Organicznej i Krystalochemii, Instytut Nauk Chemicznych, Wydział Chemii Uniwersytetu Marii Curie-Skłodowskiej w Lublinie ul. Gliniana 33, 20-614 Lublin

**e-mail: adam.wlodarczyk@mail.umcs.pl*

Synteza chiralnych molekuł stanowi ciągle wyzwanie preparatywne. Dlatego każda metoda pozwalająca osiągnąć postęp na tym obszarze jest istotna i wyczekiwana. Znane ścieżki dostępu do optycznie czynnych związków zakładają wykorzystanie chiralnych cząsteczek – nosicieli informacji stereochemicznej, które mogą być włączone w strukturę produktu jako bloki budulcowe lub wymuszają powstawanie molekuł o określonej konfiguracji np. w reakcjach katalizy asymetrycznej. Możliwe jest także wykorzystanie racemicznych mieszanin substratów aby otrzymać diasteromerycznie-wzbogacone lub czyste produkty. Warunkiem jest tworzenie związków, które mają możliwość epimeryzacji centrów stereogenicznych i równowagowanie energetycznie uprzywilejowanych molekuł. (*mached-mismached pair*).

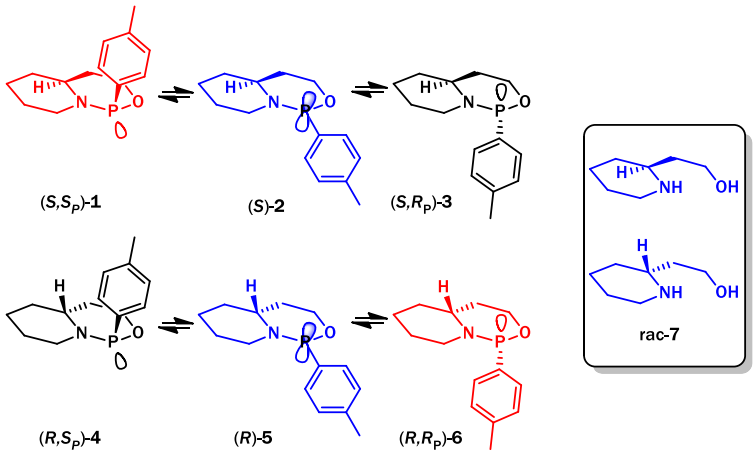

Rys. 1. Epimeryzacja centrum stereogenicznego na atomie fosforu.

Powstające produkty są stosunkowo proste i możliwe do analizy przy pomocy np. NMR o ile wykorzystujemy substraty o znanej konfiguracji. W omawianej syntezie wykorzystywaliśmy racemiczny aminoalkohol **7** a konfigurację powstających produktów można było ustalić jedynie dzięki analizie rengenostrukturalnej.

Literatura

[1] Juge S., Genet J.P. *Tetrahedron Letters*, **30**(21) (1989) 2783–2786.
[2] Jugé S., Stephan M., Merdès R., Genet J. P., Halut-Desportes S *Journal of the Chemical Society, Chemical Communications*, **6** (1993) 531–533.

B-40

KORELACJA STRUKTURA REAKTYWNOŚĆ: KOMPLEKSY AZA-BODIPY OPARTE NA RDZENIACH BORACYKLICZNYCH JAKO FOTOUCZULACZE TLENU SINGLETOWEGO

Karolina Wrochna[a,*], Paulina H. Marek-Urban[a,b], Krzysztof Woźniak[b], Krzysztof Durka[a]

[a] *Wydział Chemiczny, Politechnika Warszawska, ul. Noakowskiego 3, 00-664 Warszawa*
[b] *Wydział Chemii, Uniwersytet Warszawski, ul. Pasteura 1, 02-093 Warszawa*

**e-mail: wrochna.karolina@o2.pl*

Tlen singletowy ($^1O_2$) to wysoce reaktywne indywiduum chemiczne, które znajduje zastosowanie jako silny utleniacz np. w procesach oczyszczania wody, fotoinaktywacji mikroorganizmów oraz terapii fotodynamicznej. Jedną z metod generowania tlenu singletowego jest zastosowanie związków o właściwościach fotouczulających.[1] Badania wykonane w zespole wskazują na skuteczność metody zakładającej projektowanie kompleksów boroorganicznych o budowie *spiro* zbudowanych z odseparowanych przestrzennie części liganda (akceptora) oraz fragmentu boracyklicznego (donora).[2]

Niniejsze badania skupiają się na analizie wpływu budowy kompleksów aza-BODIPY na ich właściwości fotokatalityczne, by umożliwić bardziej świadome projektowanie efektywnych fotouczulaczy. Układy zostały otrzymane z bloków budulcowych: (i) liganda aza-BODIPY podstawionego czterema pierścieniami fenylowymi w pozycji 1, 3, 5 i 7 oraz (ii) różnych układów boracyklicznych takich jak borafluoren czy 6-członowe układy dibenzoheterobirinowe. Do wyjaśnienia właściwości fotokatalitycznych otrzymanych kompleksów wykorzystano dane strukturalne oraz obliczenia kwantowo-chemiczne (DFT oraz TD-DFT). Dodatkowo, przeprowadzona analiza porównawcza struktur krystalicznych pozwoliła określić zakres labilności strukturalnej kompleksów aza-BODIPY oraz typowe oddziaływania międzycząsteczkowe w jakie mogą być one angażowane w sieci krystalicznej.

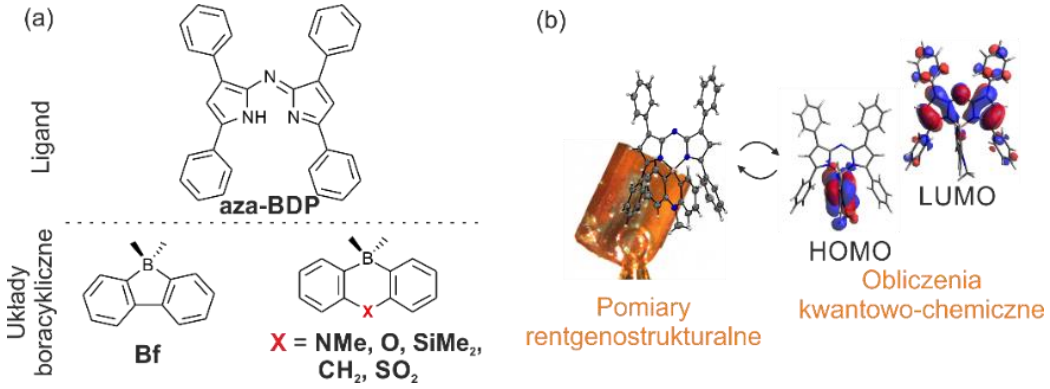

Rys. 1. (a) Schemat analizowanych kompleksów, (b) badania rentgenostrukturalne oraz obliczenia kwantowo-chemiczne.

Finansowanie badań w ramach projektu OPUS 20 „Efektywne fotouczulacze oparte na sztywnych układach boroogranicznych jako generatory tlenu singletowego” (2020/39/B/ST4/02370).

B-40

Literatura
[1] S. Qi, *et al.*, *Chem. Sci.*, **11** (2020) 6479–6484.
[2] P. H. Marek-Urban, *et. al*, *J. Org. Chem.*, **86** (2021) 12714–12722.

B-41

MONONUCLEAR DYSPROSIUM(III) COORDINATION SPECIES OF HOMOCHIRAL 3+3 HEXAAZA MACROCYCLE

Karol Wydra, Tadeusz Lis, Jerzy Lisowski

University of Wrocław, Department of Chemistry, 14. F. Joliot-Curie, 50-383 Wrocław

Single-ion magnets (SIMs) represent a fascinating family of molecular materials that may retain magnetization in the absence of a magnetic field. Without a doubt, the search of SMMs that would exhibit their unique properties above the boiling temperature of liquid nitrogen appears to be one of the most challenging goals of the scientific community [1]. In this regard, the mononuclear Dy(III) coordination compounds play a key role in the development of high-performance SIMs owing to their significant magnetic anisotropy arising from the unquenched orbital angular momentum, strong spin-orbital coupling and ligand-field perturbation [2]. However, the rational synthesis of these compounds constitutes a difficult task due to poor complexing ability and lack of coordination preferences of the Dy(III) ions. Thus, a number of the Dy(III) SIMs have been obtained by incorporation of the dysprosium(III) ions into the core of suitable macrocyclic ligands [3].

Here we present the synthesis, characterization and preliminary magnetic results of mononuclear Dy(III) coordination species of homochiral 3+3 hexaaza macrocycle $H_3\mathbf{L}^{\boldsymbol{R}}$ composed of three phenolic and three diamine units. The single crystal X-ray diffraction measurements revealed the co-crystallization of three coordination forms $[Dy(H_2\mathbf{L}^{\boldsymbol{R}})(NO_3)_2]$, $[Dy(H_2\mathbf{L}^{\boldsymbol{R}})(NO_3)(CH_3OH)](NO_3)$ and $[Dy(H_2\mathbf{L}^{\boldsymbol{R}})(NO_3)(H_2O)](NO_3)$ in a 1:0.5:0.5 molar ratio.

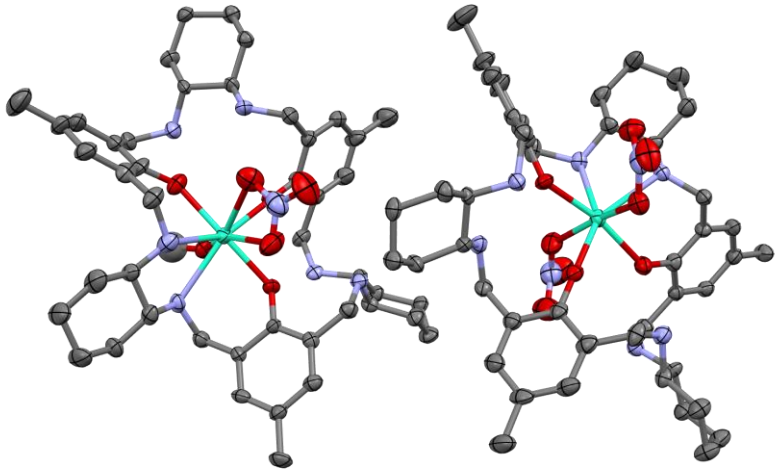

Fig. 1. The X-ray crystal structure of $[Dy(H_2\mathbf{L}^{\boldsymbol{R}})(NO_3)_2][Dy(H_2\mathbf{L}^{\boldsymbol{R}})(NO_3)(CH_3OH)_{0.5}(H_2O)_{0.5}]$. The hydrogen atoms, counterion and solvent molecules were removed for clarity.

Literature

[1] C. A. Gould *et al.*, *Science*, **375** (2022) 198–202.
[2] C. A. P. Goodwin, F. Ortu, D. Reta, N. F. Chilton, D. P. Mills, *Nature*, **548** (2017) 439–442.
[3] S.-Y. Lin, C. Wang, L. Zhao, J. Wu, J. Tang, *Dlaton Trans.*, **44** (2015) 223–229.

B-42

SYNTEZA I STRUKTURA KRYSTALICZNA 1-(4-CHLOROFENYLO)-5-(4-METYLOFENYLO)-SULFONYLOIMINO-1*H*,6*H*-2,3-DIHYDROIMIDAZO[2,1-C][1,2,4]TRIAZOLU

Waldemar Wysocki[1], Zbigniew Karczmarzyk[1], Dariusz Matosiuk[2]

[1] Instytut Nauk Chemicznych,Uniwersytet Przyrodniczo-Humanistyczny w Siedlcach, ul. 3 Maja 54, 08-110 Siedlce
[2] Katedra i Zakład Syntezy i Technologii Chemicznej Środków Leczniczych, Uniwersytet Medyczny w Lublinie, ul. Chodźki 4a, 20-09 Lublin

Pochodne imidazotriazolu stanowią interesującą grupę związków chemicznych o dużym znaczeniu farmakologicznym wykazujących m.in. aktywność przeciwdrobno–ustrojową, przeciwgrzybiczną czy przeciwwirusową [1].

W prezentowanym komunikacie przedstawiamy syntezę i strukturę krystaliczną 1-(4-chlorofenylo)-5-(4-metylofenylo)-sulfonyloimino-1*H*,6*H*-2,3-dihydroimidazo[2,1–c][1,2,4]triazolu. Związek ten otrzymuje się w wyniku termicznej cyklizacji odpowiedniego 1-arylo-2-imidazolinylometylotiosemikarbazydu w temperaturze powyżej 200 °C z wydzieleniem cząsteczki metylotiolu (Rys. 1), przy czym cyklizacja ta zachodzi także spontanicznie w czasie procesu krystalizacji.

We wstępnych badaniach farmakologicznych związek ten wykazuje aktywność hipoglikemiczną.

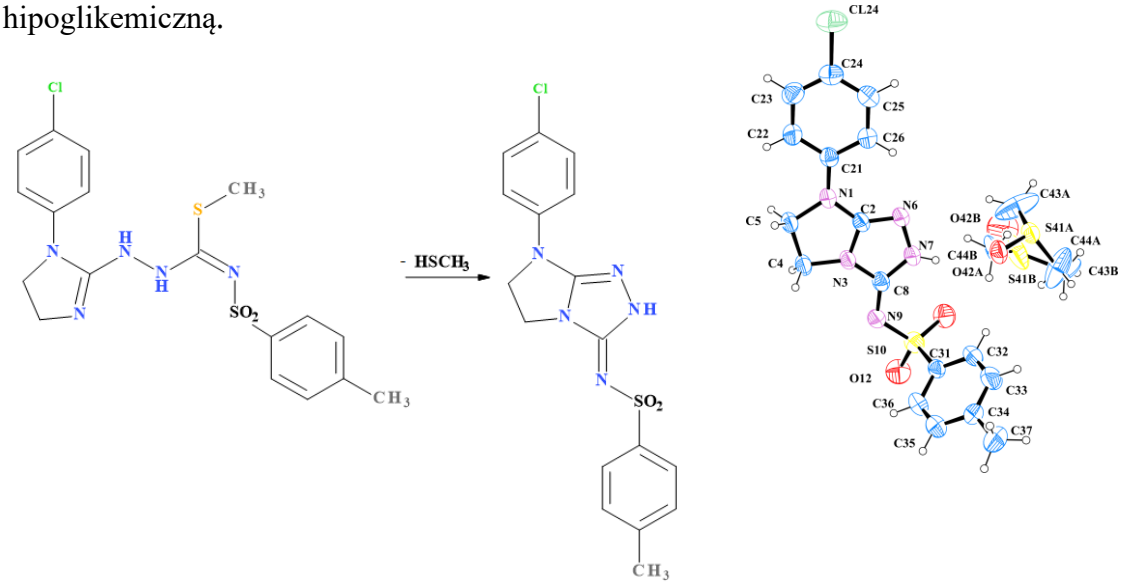

Rys. 1. Schemat reakcji cyklizacji tytułowego związku chemicznego.

Dane krystalograficzne: $C_{17}H_{16}ClN_5O_2S*C_2H_6OS$, M_r = 467.99, układ trójskośny, $P\bar{1}$, a = 8.5048(8), b = 9.0674(8), c = 14.8766(11) Å, α = 74.276(7), β = 86.226(7), γ = 82.337(7)°, V = 1093.91(17) Å^3, Z = 2, D_x = 1.421 gcm^{-3}, μ = 0.397 mm^{-1}, *MoKα*, λ = 0.71073 Å, T = 296(2) K, R = 0.0570 dla 2871 refleksów.

Literatura

[1] Ł. Balewski, F. Sączewski, P. J. Bednarski, L. Wolff, A. Nadworska, M. Gdaniec, A. Kornicka, *Molecules*., **25** (2020) 5924.

B-43

OPEN CAGE-LIKE LITHIUM SILSESQUIOXANE

Patrycja Wytrych, Józef Utko, Tadeusz Lis, Łukasz John

Wydział Chemii Uniwersytetu Wrocławskiego, ul. F. Joliot-Curie 14, 50-383 Wrocław

Polyhedral oligomeric silsesquioxanes (POSS) are organosilicon compounds with the general classification $[RSiO_{1.5}]_n$, where **n** is the number of silicon atoms, and **R** is a substituent on a silicon atom [1,2]. POSS compounds are built of a silicon-oxygen core with dimensions of 1-3 nm, which may consist of 6, 8, 10, and even 12 silicon atoms connected by oxygen bridges [3]. The substituents in the corners of the cage can be reactive or non-reactive functional groups. Their amount and type affect the solubility of cage silsesquioxane and its catalytic activity, thermal stability, and mechanical strength [4].

Both functionalized polyhedral oligomeric silsesquioxanes and incompletely condensed POSS cages are an exciting group of ligands in coordination chemistry, often showing unexpected reactivity in the complexation reaction [5]. Open cages are usually used to obtain metalasilsesquioxanes POMS (Polyhedral Oligomeric MetalloSilsesquioxane) [6], in which a metal atom has replaced one silicon atom in the corner of the cage. On the other hand, functionalized arms of caged silsesquioxanes may have donor atoms coordinating metal ions [7,8].

So far, only two crystal structures composed of open cages, POSS and lithium cations, have been described. The compounds were obtained in reactions with an incompletely condensed POSS cage and lithium amide [9] or *n*-butyllithium [10]. Whereas the present compound (fig. 1) of the formula **[$Li_6(POSS)_2(THF)_3$]** was an unexpected result of the reaction of a functionalized mono-POSS with lithium metal.

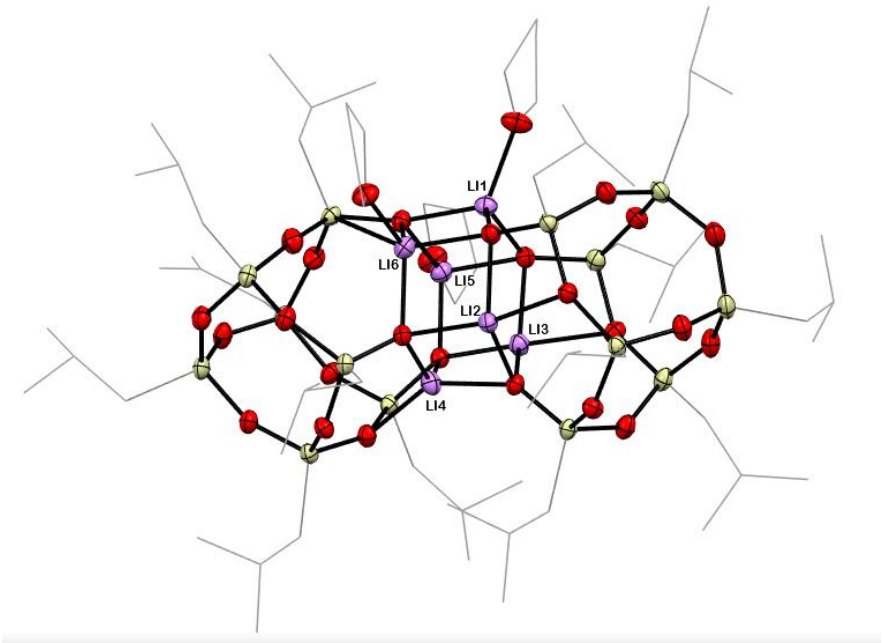

Fig. 1. Molecular structures of $[Li_6(POSS)_2(THF)_3]$. Hydrogen atoms are omitted for clarity

B-43

Literature
[1] Walczak M,; Januszewski R.; Franczyk A.;, Marciniec B., *J. Organomet. Chem.*, **872** (2018) 73.
[2] Chan K. L.; Sonar P.;Sellinger A., *J. Mater. Chem.*, **19** (2009) 9103.
[3] Janowski B.; Pielichowski K., **53** (2008), 87.
[4] Lee H.; Hong S. H., *Applied Catalysis A, General*, **560** (2018) 21.
[5] Piec K.; Kostera S.; Jędrzkiewicz D.; Ejfler J.; John Ł., *New J. Chem*., **44** (2020) 10786.
[6] Guillo P.; Lipschutz M. I.; Fasulo M. E.; Don Tilley T., *ACS Catal*., **7** (2017) 2303.
[7] Di Iulio C.; Jones M. D.; Mahon M.F.; Apperley. D. C., *Inorg. Chem*., **49** (2010) 10232.
[8] Wytrych P.; Utko J.; Stefanski M.; Kłak J.; Lis T.; John Ł., *Inorg. Chem*., **62** (2023) 2913.
[9] Lorenz V., Gießmann S., Gun'ko Y. K., Fischer A. K., Gilje J. W., Edelmann F. T., *Angew. Chem. Int. Ed*., **43** (2004) 4603.
[10] García C., Gómez M., Gómez-Sal P., Hernández J. M., *Eur. J. Inorg. Chem*., (2009) 4401.

B-44

CO-CRYSTALS OF GENISTEIN WITH COFORMERS CONTAINING *N*-HETEROCYCLIC AROMATIC UNIT

Anna Zep[1,*], Arkadiusz Ciesielski[2], Anna Sadocha[2], Anna Rosa[1], Katarzyna Gibuła[1], Michał K. Cyrański[2], Marta Zezula[1]

[1]Łukasiewicz – Industrial Chemistry Institute, Rydygiera 8, 01-793 Warsaw
[2]Faculty of Chemistry, University of Warsaw, Pasteura 1, 02-093 Warsaw

**e-mail: anna.zep@ichp.lukasiewicz.gov.pl*

Investigation on the bioavailability of drugs and active pharmaceutical ingredients (API) along with research on improving their physicochemical properties became the subject of interest in pharmaceutical industry. Low water solubility and low bioavailability decreased potential of possible application in pharmaceutical formulations. Poorly bioavailable drugs after oral administration often do not reach the minimum effective concentration required to achieve the intended pharmacological effect. One of the method of increasing the solubility and bioavailability, which are key factors determining drug effectiveness, is synthesis of co-crystals consisting of an active substance and a suitable coformer [1, 2].

Herein, we present structural analysis and solubility studies of newly obtained co-crystals of genistein with coformers containing *N*-heterocyclic aromatic unit. Co-crystal with 4-dimethylaminopyridine (DMAP) exhibit higher solubility than the pure genistein. An increasing of the rate of permeability of genistein in co-crystal form compared to pure genistein have been observed on the basis of biological permeability studies. The stability of solid drug substance in conditions of elevated temperature and humidity is important in the production process, packaging and storage. Accelerated stability and forced degradation studies confirmed the stability of the drug molecule for the obtained cocrystal of genistein with DMAP.

The improved permeation rate and solubility of co-crystal of genistein, allows us to preliminarily assume that the bioavailability of the substance present in co-crystal will be improved over its uncomplexed form.

References

[1] G. R. Desiraju, J. J. Vittal, A. Ramanan, *Crystal Engineering - a Textbook*, World Scientific Publishing Co. Pte. Ltd. 2011.
[2] M. Guo, X. Sun, J. Chen, T. Cai, *Acta Pharm Sin B.*, **11(8)** (2021) 2537.

B-45

ANALIZA STRUKTURALNA W PROJEKTOWANIU I CHARAKTERYZACJI NOWYCH EMITERÓW TADF

Adam Zuba, Krzysztof Durka i Sergiusz Luliński

Wydział Chemiczny Politechniki Warszawskiej, ul. Noakowskiego 3, 00-664 Warszawa

Emitery termicznie aktywowanej fluorescencji (ang. *thermally activated delayed fluorescence*, TADF) są wykorzystywane do konstrukcji diod typu OLED III generacji. Zjawisko TADF umożliwia promienisty odzysk energii cząsteczek znajdujących się we wzbudzonym stanie trypletowym na drodze odwrotnego przejścia interkombinacjnego (ang. *reverse intersysytem crossing*, rISC), czyli przejścia ze stanu T1 do S1, a następnie fluorescencji. Aby proces ten był możliwy, cząsteczka powinna posiadać orbitale graniczne rozseparowane przestrzennie w dużym, ale niezerowym stopniu. Sprzyja temu architektura molekuł typu donor-akceptor oraz ortogonalne położenie jednostek: donorowej i akceptorowej względem siebie, a także wprowadzenie grupy pośredniczącej ze sprzężonym układem wiązań typu π.

W ramach prowadzonych badań poszukiwane są donory do emiterów światła niebieskiego, opartych na jednostce **SO2B** o bardzo silnych właściwościach akceptorowych i jednostce pośredniczącej **Dipp**. Przeprowadzono syntezę emitera posiadającego donor pochodzący od 2-metylotiofenu – **MeThi-Dipp-SO2B**. Scharakteryzowano również jego strukturę poprzez pomiar dyfrakcji promieniowania rentgenowskiego na monokrysztale (rys. 1).

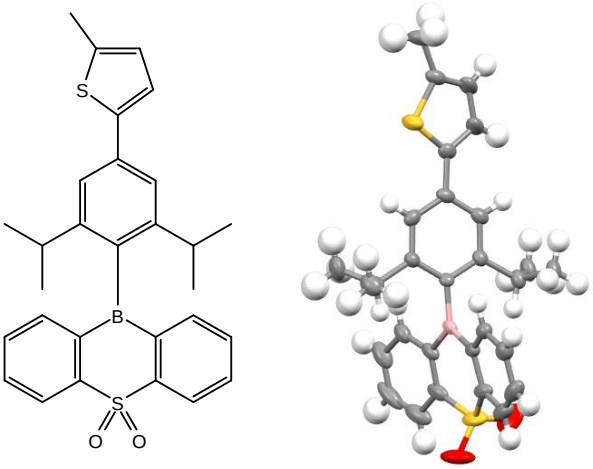

Rys. 1. **MeThi-Dipp-SO2B** – wzór strukturalny oraz struktura cząsteczki w sieci krystalicznej

Badania luminescencji związku potwierdziły, że wykazuje on opóźnioną fluorescencję. Analiza geometrii molekuły oraz wyników obliczeń kwantowych dla cząsteczek z kilkoma potencjalnymi donorami pozwoliła jednak także wskazać czynniki strukturalne, których uwzględnienie przy projektowaniu kolejnych emiterów może pozwolić na zwiększenie wydajności zjawiska TADF.

Badania zostały sfinansowane z projektu Technologie Materiałowe 3 ID-UB pt. "Wydajne emitery TADF oparte na nowych elektronoakceptorowych rdzeniach boracyklicznych i ich zastosowanie w diodach OLED".

B-46

ANALIZA ODDZIAŁYWAŃ MIĘDZYCZĄSTECZKOWYCH W STRUKTURZE 1,3-DIACETYLOPIRENU NA PODSTAWIE DYFRAKCJI W ZMIENNYCH WARUNKACH TEMPERATURY ORAZ CIŚNIENIA

Aleksandra Zwolenik, Anna Makal

Uniwersytet Warszawski, Wydział Chemii, Ludwika Pasteura 1, 02-093 Warszawa

Pochodne pirenu wykazują ciekawe właściwości elektroniczne i fotofizyczne, dlatego są intensywnie badane pod kątem szerokiego zakresu zastosowań. Dzięki obecności oddziaływań typu π-stacking są dobrym przykładem półprzewodników organicznych, a ich właściwości fluorescencyjne sprawiają, że są powszechnie stosowane jako barwniki, m.in. do badań strukturalnych białek, DNA lub błon lipidowych. Diacetylopochodne pirenu wykazują wiele odmian polimorficznych, co dodatkowo zwiększa możliwość ich zastosowań. Są to dobre układy modelowe co sprawia, że ich analiza może pomóc w zrozumieniu jak działają podobne, ale większe i bardziej skomplikowane układy.

Pierwotnie w literaturze znana była tylko jedna odmiana polimorficzna 1,3-diacetylopirenu [1]. Udało się otrzymać nową odmianę tego związku, wykonać eksperyment dyfrakcyjny oraz stworzyć model jego struktury krystalicznej z wykorzystaniem udokładnienia z użyciem asferycznych atomowych czynników rozpraszania. W tej pracy skupiono się na przeanalizowaniu oddziaływań międzycząsteczkowych występujących w strukturze 1,3-diacetylopirenu oraz sprawdzenie, jak ich zmiany wpływają na zmiany właściwości fizykochemicznych. W tym celu, wykonano serię eksperymentów dyfrakcyjnych w szerokim zakresie temperatur (od 90 do 390 K), a także umieszczono badany związek w kowadełku diamentowym typu Merilla-Basseta i wykonano eksperymenty pod zwiększonym ciśnieniem (od 0 do 1.7 GPa przyłożonego ciśnienia). Struktury eksperymentalne uzyskane pod zwiększonym ciśnieniem porównano z teoretycznymi strukturami (z zakresu od 0 do 4.08 GPa przyłożonego ciśnienia), które uzyskano z obliczeń periodycznych wykonanych w programie crystal17. Policzono również wartości energii oddziaływań za pomocą metod przybliżonych w programie CrystalExplorer. Wyniki kluczowych punktów pomiarowych zostały zwizualizowane m.in. za pomocą tzw. „Energy frameworks” [2], co pozwoliło na powiązanie najważniejszych oddziaływań z kierunkami maksymalnej I minimalnej ściśliwości. Na podstawie zebranych danych stwierdzono, które oddziaływania najbardziej stabilizują strukturę 1,3-diacetylopirenu oraz jak zmiany tych oddziaływań pod wpływem działania siły zewnętrznej wpływają na właściwości fizykochemiczne badanego związku, np. jego barwy czy widma luminescencji.

Literatura

[1] S. K. Rajagopal, A. M. Philip, K. Nagarajan, M. Hariharan, *Chem. Commun.*, **50**(63) (2014) 8644–8647.

[2] C. F. Mackenzie, P.R. Spackman, D. Jayatilaka, M. A. Spackman, *IUCrJ*, **4**(5) (2017) 575–587.

Finansowanie projektu: dotacja wewnętrzna nr PSP 501-D112-01-1120000 zlecenie 5011000317

B-47

INFLUENCE OF FLUORINE SUBSTITUENT POSITION ON THE CRYSTAL AND MOLECULAR STRUCTURES OF 5-(FLUOROBENZYLIDENE)IMIDAZOL-4-ONE DERIVATIVES

Ewa Żesławska[1], Wojciech Nitek[2], Jadwiga Handzlik[3]

[1] Institute of Biology and Earth Sciences, Pedagogical University, Podchorążych 2, 30-084 Kraków
[2] Faculty of Chemistry, Jagiellonian University, Gronostajowa 2, 30-387 Kraków
[3] Jagiellonian University Medical College, Department of Technology and Biotechnology of Drugs, Medyczna 9, 30-688 Kraków

Multidrug resistance (MDR) is a global problem in the treatment of various diseases such as cancer, bacterial, fungal and parasitic infections. An interesting approach in the search for the ways to overcome MDR are so called adjuvants, i.e. the compounds able to block at least one mechanism of resistance. Some previously studied the 2-amine derivatives of 5-arylideneimidazol-4-one showed a potency of adjuvants for antibiotic and chemotherapeutic agents [1,2]. In the search for new adjuvants able to block bacterial and/or cancer multidrug resistance, new derivatives of 2-amineimidazol-4-one were synthesized.

We have performed new crystal structure analysis for three derivatives containing fluorine substituent in 5-benzylidene moiety at position *ortho* (**1**), *meta* (**2**) and *para* (**3**).

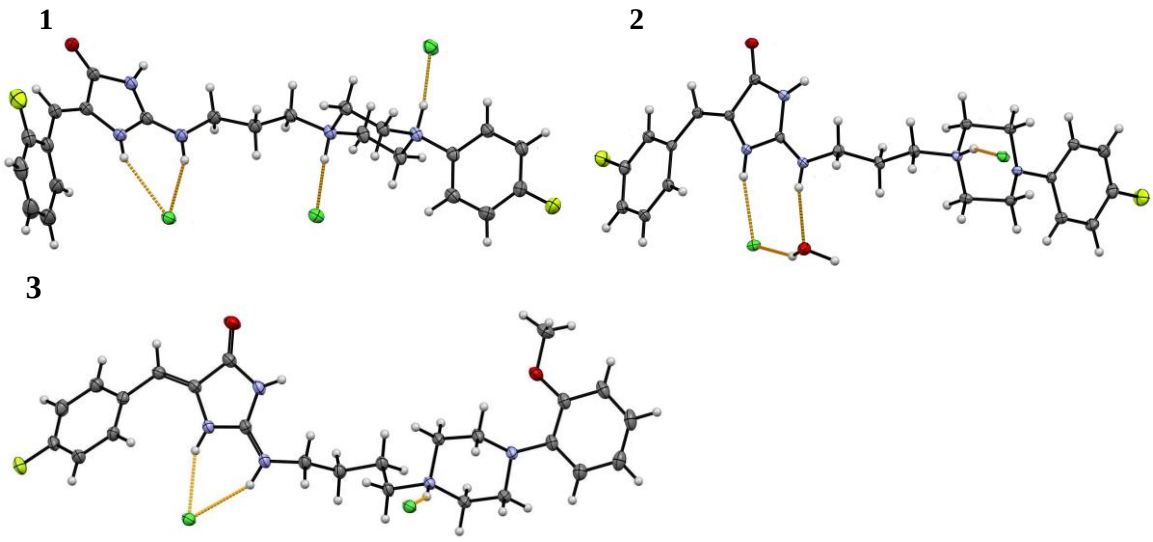

Compound **1** is three times protonated, while **2** and **3** two times. Additionally, **2** crystallizes with water molecule. In the presented crystal structures, we have analyzed the influence of the location of fluorine substituent on the geometry of molecules and intermolecular interactions.

References

[1] A. Kaczor, K. Witek *et al*. *Molecules*., **24** (2019) 438.
[2] A. Kaczor, K. Witek *et al*. *Int. J. Mol. Sci.*, **22** (2021) 2062.

B-48

NEW COPPER(II) COMPLEXES WITH THE 5-FLUOROOROTATE LIGAND: X-RAY STRUCTURES, INFRARED AND RAMAN SPECTRA

Tamara J. Bednarchuk[a], Katarzyna Helios[b,*]

[a] *Institute of Low Temperature and Structure Research, Polish Academy of Sciences, Okólna 2, 50-422 Wrocław, Poland*
[b] *Faculty of Chemistry, Wrocław University of Science and Technology, Smoluchowskiego 23, 50-370 Wrocław, Poland*

**e-mail: katarzyna.helios@pwr.edu.pl*

5-Fluoroorotic acid (5-FH_3Or) is a synthetic derivative of naturally occurring orotic acid (6-carboxyuracil, vitamin B_{13}). In coordination chemistry, orotic acid is an interesting multidentate ligand, since coordination to metal ions can occur via two deprotonated pyrimidine nitrogen atoms, two carbonyl oxygen atoms, and also two carboxylate oxygen atoms. As an extension of our earlier studies on metal complexes with orotic acid we have focused our attention on the coordination properties of the 5-nitroorotate [1,2] and 5-fluoroorotate [3] ligands. "Comprehensive studies on new isomorphous Co(II) and Zn(II) complexes with 5-nitroorotate ligand" (published in Ref. [1], O-4, 2022) was presented at the 63rd Polish Crystallographic Meeting.

Here, we present the results from our work on two novel Cu(II) complexes with 5-fluoroorotate ligand:

- tetraaqua(5-fluoroorotato)copper(II) monohydrate, $[Cu(5\text{-}FHOr)(H_2O)_4]\cdot H_2O$ (**1**), Fig. 1a,
- diammineaqua(5-fluoroorotato)copper(II), $[Cu(5\text{-}FHOr)(H_2O)(NH_3)_2]$ (**2**), Fig. 1b.

Additionally, we have obtained the ammineaqua(5-fluoroorotato)copper(II) complex, $[Cu(5\text{-}FHOr)(H_2O)(NH_3)]_n$ (**3**), structurally characterized by Schneider *et al.* [4].

All three complexes have been thoroughly characterized by FT-IR and Raman spectroscopy. The obtained detailed band assignment will be very helpful for the interpretation of the vibrational spectra of other metal complexes with the 5-fluoroorotate ligand.

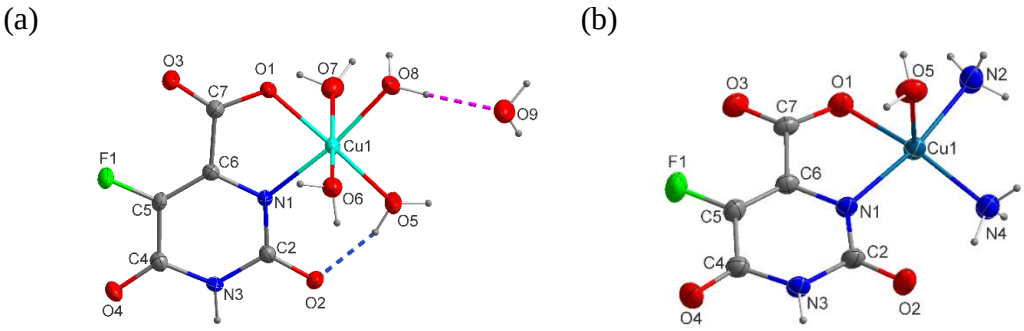

Fig. 1. The molecular structures of (a) compound (**1**) and (b) compound (**2**), showing the atom-numbering schemes.

Single crystal X-ray diffraction analysis has revealed that crystals (**1**) and (**2**) crystallize in the triclinic space group *P-1*. Each metal ion is chelated by the carboxylate oxygen (O1) and the deprotonated nitrogen (N1) atoms of the 5-fluoroorotate ligand. Moreover, in:

(1) four water molecules complete the distorted octahedral coordination sphere around the metal center with elongated axial M–O bonds. The solvent water molecule (O9) is involved in an intermolecular hydrogen bonding with the oxygen atom (O8) of the coordinated water molecule.

(2) two nitrogen atoms (N2 and N4) of two ammonia groups complete a slightly distorted square-planar environment of the copper atom. The coordination sphere of copper is extended to five by the water molecule.

In both complexes (**1**) and (**2**), intermolecular O–H···O and N–H···O hydrogen bonds link two Cu^{II} cations into centrosymmetric dimers.

Complex (**3**), Fig. 2, crystallizes in the monoclinic space group $P2_1/n$. One carboxylate oxygen (O61) atom and the deprotonated nitrogen (N1) atom of the 5-fluoroorotate ligand, one aqua molecule and one ammonia group forms the slightly distorted square pyramidal coordination sphere. The fifth position of the pyramid apex is occupied by the other carboxyl oxygen atom (O62)' of a neighbouring 5-fluoroorotate unit [4].

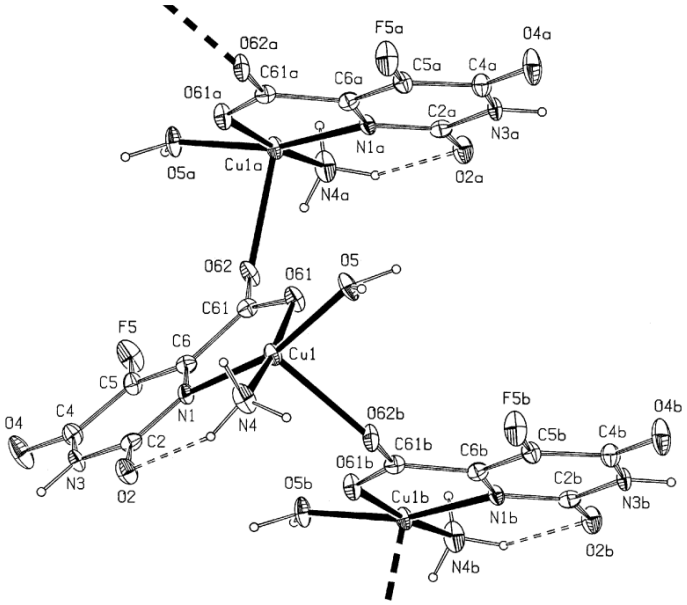

Fig. 2. The molecular structure of (**3**) with the atom-numbering scheme [4].

Literature

[1] K. Helios, T. J. Bednarchuk, R. Wysokiński, M. Duczmal, A. Wojciechowska, A. Łukowiak, A. Kędziora, M. Małaszczuk, D. Michalska, *Polyhedron* (2022) 115830.
[2] K. Helios, M. Duczmal, A. Pietraszko, D. Michalska, *Polyhedron*, **49** (2013) 259.
[3] M. Malik-Gajewska, J. Trynda, W. Zierkiewicz, K. Helios, R. Latajka, J. Wietrzyk, D. Michalska, *J. Mol. Struct.*, **1171** (2018) 155.
[4] A. G. Schneider, H. W. Schmalle, F. Arod, E. Dubler, *J. Inorg. Biochem.*, **89** (2002) 227.

B-49

SHAPE-MEMORY EFFECT TRIGGERED BY π-π INTERACTIONS IN A FLEXIBLE TERPYRIDINE METAL-ORGANIC FRAMEWORK

Wiktoria Gromelska[a], Filip Formalik[b], Alessia Giordana[c], Luca Andreo[c], Ghodrat Mahmoudi[d], Volodymyr Bon[e], Stefan Kaskel[e], Leonard J. Barbour[f], Agnieszka Janiak[a], Emanuele Priola[c], Kornel Roztocki[a]

[a]*Faculty of Chemistry, Adam Mickiewicz University, 61-614 Poznan, Poland*
[b]*Department of Chemical and Biological Engineering, Northwestern University, Evanston, Illinois, 60208, United States*
[c]*Dipartimento di Chimica, Università degli Studi di Torino, Via Pietro Giuria 7, 10125, Torino, Italy*
[d]*Department of Chemistry, Faculty of Science, University of Maragheh, P.O. Box 55136-83111, Maragheh, Iran*
[e]*Chair of Inorganic Chemistry, Technische Universität Dresden, Bergstrasse 66, 01062 Dresden, Germany*
[f]*Department of Chemistry and Polymer Science, University of Stellenbosch, Private Bag X1, Matirland 7602, South Africa*

Shape-memory polymers and alloys can change from a distorted, metastable phase to their original, energetically favorable phase in response to external stimuli. In the context of metal-organic frameworks, the ability of a switchable framework to stabilize the reopened pore phase following the first switching transition is referred to as shape memory.[1,2]

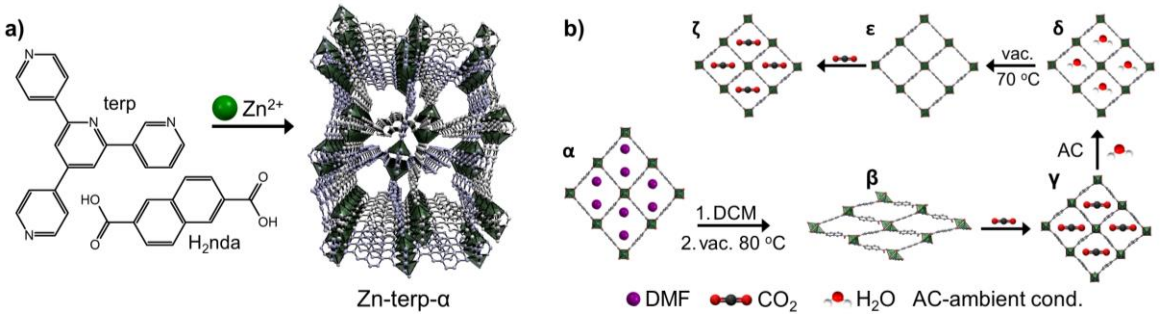

Fig. 1. a) Synthetic route and structural features of as-synthesized Zn-terp-α. b) Schematic illustration of the phase transformation triggered by several subsequent stimuli; for clarity, one subframework representing the doubly interpenetrated Zn-terp-x: x = α − $[Zn_2(nda)_2(terp)]\cdot 2DMF$, β − $[Zn_2(nda)_2(terp)]$, γ − $[Zn_2(nda)_2(terp)]\cdot 3CO_2$, δ − $[Zn_2(nda)_2(terp)]\cdot 2H_2O$ and ε − $[Zn_2(nda)_2(terp)]$; ζ − $[Zn_2(nda)_2(terp)]\cdot CO_2$. nda^{2-} − 2,6-naphthalenedicarboxylate, terp − 6′-(pyridin-4-yl)-3,2′:4′,4″-terpyridine, DCM – dichloromethane.

Herein, we present a novel flexible terpyridine MOF that undergoes a transformation from a porous structure to a nonporous one upon desolvation. When exposed to CO_2 at 195 K, it reopens into a shape-memory phase.[3] Based on extensive in situ experimental studies (SC-XRD and PXRD) and DFT energetic considerations combined with literature reports, we propose classifying shape-memory MOFs into two

groups: responsive and nonresponsive, depending on the transformability of the gas-free reopened pore phase into the collapsed phase.

References

[1] Y. Sakata, S. Furukawa, *et al*. *Science*, **339** (2013) 193−196.
[2] H. Yang, T. X. Trieu, *et al*. *Angew. Chem., Int. Ed.*, **58** (2019) 11757−11762.
[3] K. Roztocki, W. Gromelska, *et al*. *ACS Materials Lett.*, **5**(4) (2023) 1256–1260.

Acknowledgment: National Science Centre (NCN, Poland; Grants no. 2020/36/C/ST4/00534).

B-50

TUNING THE GUEST-INDUCED SPATIO-TEMOPORAL RESPONSE OF ISOSTRUCTURAL DYNAMIC FRAMEWORKS TOWARDS EFFICIENT GAS SEPARATION AND STORAGE

Szymon Sobczak[a,*], Arkadiusz Smaruj[a], Anna Walczak[a], Mateusz Gołdyn[a], Volodymyr Bon[b], Stefan Kaskel[b], Artur Stefankiewicz[a], Kornel Roztocki[a]

[a] *Faculty of Chemistry, Adam Mickiewicz University, Uniwersytetu Poznańskiego 8, 61-614 Poznań, Poland*

[b] *Chair of Inorganic Chemistry, Technische Universität Dresden, Bergstrasse 66, 01062 Dresden, Germany*

**e-mail: szysob@amu.edu.pl*

Understanding and control of the spatiotemporal stimuli-responsiveness of the flexible metal-organic frameworks are crucial for the development of novel adsorbents for gas storage and separation technologies. Herein, we report two isostructural pillared-layer dynamic frameworks that differing only in one atom that bridges benzeno-dicarboxylate linker. Through a synthetic approach, we transform stepwise CO_2-induced transformation into a continuous one (**Fig 1**). Our findings are proved by equilibrium and time-resolved *in situ* powder X-ray diffraction collected during CO_2 adsorption at 195 K. Finally, we use high-pressure single and multi-gas adsorption experiments to show superiority of continuous breathing in CH_4 storage and CH_4/CO_2 separation at 298 K. This report demonstrates that the desirable mechanism of flexible frameworks can be readily achieved through single-atom exchange enabling efficient gas separation and storage.

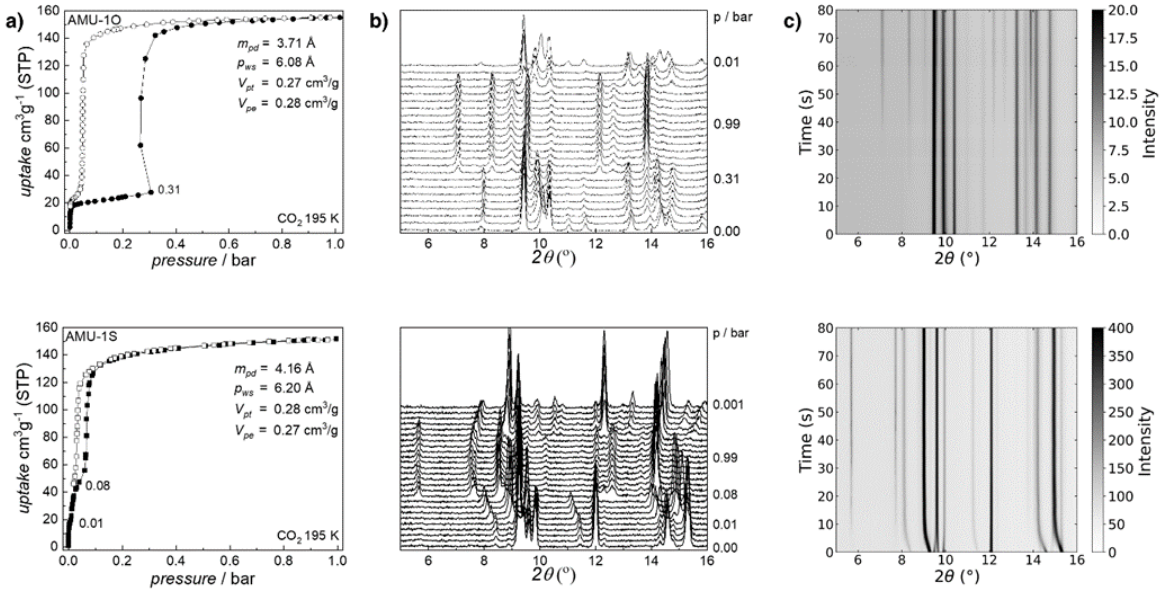

Fig. 1. Mechanistic understanding of CO_2-driven structural transformation in AMU-1X (O – top row; S – bottom row): **a**) CO_2 adsorption (full symbols) and desorption (open symbols) at 195 K juxtaposed with **b**) corresponding in situ PXRD patterns collected at selected pressure (λ = 1.540599 Å);. **c**) in situ time-resolved PXRD during the CO_2 adsorption at 195K (λ = 0.6199 Å, for consistency data were converted to λ = 1.540599 Å).

B-50

References
[1] Roztocki, K; Sobczak, S; Smaruj, A; Walczak, A; Bon, V; Kaskel, S; Stefankiewicz, R (submitted).

Acknowledgment: National Science Centre (NCN, Poland; Grants no. 2020/36/C/ST4/00534).

B-51

WPŁYW WYSOKIEGO CIŚNIENIA NA KOKRYSZTAŁY OPARTE NA 1,2-BIS(4-PIRYDYLO)ETANIE I KWASIE BURSZTYNOWYM

Kornelia Szymańska, Ewa Patyk-Kaźmierczak

Zakład Chemii Materiałów, Wydział Chemii, Uniwersytet im. Adama Mickiewicza w Poznaniu, ul. Uniwersytetu Poznańskiego 8, 61-614 Poznań

W ostatnich latach coraz więcej uwagi poświęca się kokryształom, ponieważ mogą one wykazywać korzystniejsze właściwości fizykochemiczne w porównaniu do kryształów jednoskładnikowych. Są one szczególnie ciekawe w kontekście przemysłu farmaceutycznego, gdzie poprzez odpowiedni dobór koformerów otrzymuje się formy krystaliczne substancji aktywnych leków wykazujące polepszoną rozpuszczalność czy wchłanianie.[1] Dzięki temu możliwe jest opracowanie leków alternatywnych do obecnie stosowanych. Należy jednak pamiętać, że kluczowe jest dokładne poznanie stabilności i możliwych przemian fazowych danej formy krystalicznej zanim zostanie ona wprowadzona na rynek.

Jednym z czynników mogących wpływać na strukturę krystaliczną jest ciśnienie. W warunkach wysokiego ciśnienia (powyżej 0,1 GPa) zachodzić mogą przejścia fazowe, reakcje chemiczne (np. polimeryzacja), przemiany konformacyjne i strukturalne cząsteczek, czy też możliwe jest otrzymywanie nowych form krystalicznych (np. odmian polimorficznych czy solwatów).[2] Pomimo znaczącego rozpowszechnienia w ostatnich dekadach technik wysokociśnieniowych, oraz zwiększonego zainteresowania kokryształami, istnieje znacznie mniej danych na temat wpływu wysokiego ciśnienia na ich strukturę w porównaniu do kryształów jednoskładnikowych. Dlatego, celem niniejszej pracy było zbadanie wpływu wysokiego ciśnienia na kokryształy oparte na 1,2-bis(4-pirydylo)etanie i kwasie bursztynowym.

W pracy eksperymentalnej zastosowano komorę wysokociśnieniową z kowadełkami diamentowymi Merrilla-Bassetta.[3] Badany kokryształ umieszczono w komorze z rubinem służącym do pomiaru ciśnienia oraz z olejem Daphne 7575 pełniącym rolę medium hydrostatycznego. Pomiary dyfrakcji rentgenowskiej przeprowadzono w ciśnieniu do 3,80 GPa (co około 0,50 GPa) przy użyciu dyfraktometru 4-kołowego wyposażonego w lampę molibdenową i detektor CCD EOS.

W wyniku badań wykazano istnienie wysokociśnieniowej odmiany polimorficznej kokryształu 1,2-bis(4-pirydylo)etanu i kwasu bursztynowego w ciśnieniu powyżej 2,92 GPa. Przemiana fazowa zachodzi bez zmiany symetrii kryształu, jednak w jej wyniku odwrócony zostaje trend ściśliwości w kierunku [100], co sprawia, że w fazie wysokociśnienowej występuje rzadkie zjawisko negatywnej liniowej ściśliwości.[4]

Badania zostały sfinansowane przez Narodowe Centrum Nauki w ramach grantu SONATA nr 2020/39/D/ST4/00260.

Literatura

[1] N. K. Duggirala, M. J. Perry, O. Almarsson, M. J. Zaworotko, *Chem. Commun.*, **52** (2016) 640–655.
[2] A. Katrusiak, *Acta. Cryst. B.*, **76** (2019) 918–926.
[3] L. Merrill, W. A. Bassett, *Rev. Sci. Instrum.*, **45** (1974) 290–294.
[4] A. B. Cairns, A. L. Goodwin, *Phys. Chem. Chem. Phys.*, **17** (2015) 20449–20465.

B-52

DETECTION OF PHOTOINDUCED SHORT-LIVED EXCIMER IN FLUORESCENT RHODIUM COMPLEX MONOCRYSTAL VIA TIME-RESOLVED LAUE PHOTOCRYSTALLOGRAPHY AND LUMINESCENCE SPECTROSCOPY

P. Łaski[1], L. Bosman[2], J. Drapała[1,3], R. Kamiński[1], A. Brink[2], D. Szarejko[1], P. Borowski[1], A. Roodt[2], K. N. Jarzembska[1]

[1] Department of Chemistry, University of Warsaw, Żwirki i Wigury 101, Warsaw, Poland
[2] Chemistry Department, University of the Free State, Nelson Mandela Drive, Bloemfontein, South Africa
[3] Department of Chemistry, Warsaw University of Technology, Noakowskiego 3, 00-664 Warsaw, Poland

The development of new photoactive materials with specific properties is an important and pressing concern in modern chemical research. These materials have various scientific and commercial applications, such as photocatalysts, light emitters, biological markers, and optoelectronic devices. Coordination compounds containing transition metal centers with d8−d10 electronic configurations are particularly interesting in this regard. These metal centers have a tendency to form short metal-metal contacts within and/or between molecules, which play a crucial role in determining the properties of the lowest energy emissive states.

In this study, a novel rhodium coordination compound was synthesized and its structure was confirmed using single-crystal X-ray diffraction. The compound exhibited a tendency to form dimeric structures, with the rhodium atoms of two molecules in close proximity (Fig. 1). The spectroscopic properties of the compound in both solid-state and solution samples were analyzed using UV-Vis absorption spectroscopy and time-resolved solid-state emission spectroscopy. The compound was found to be fluorescent upon excitation with near-UV light. The emission maximum occurred at around 570 nm at room temperature and 100 K, with an emission lifetime in the nanosecond range within this temperature range.

Subsequently, time-resolved Laue diffraction photocrystallographic experiments were performed at the 14-ID-B BioCARS synchrotron beamline at the APS. The resulting data was processed using the recently developed LaueProc software, which was specifically designed for analyzing time-resolved Laue data of small molecules. The photodifference maps (Fig. 1) and the refined excited-state structure were compared to the ground-state structure. Furthermore, extensive quantum-mechanical computations and modeling were conducted, including TDDFT and QM/MM calculations for the ground-state (S0), first excited-state (S1), and triplet excited-state (T1). These calculations evaluated theoretical energies, electronic transitions, charge-transfer dynamics, and geometries for both the ground-state and excited-states, providing a comprehensive interpretation of the experimentally observed structural changes and spectroscopic behaviour.

SONATA BIS grant (No. 2020/38/E/ST4/00400) from the National Science Centre in Poland, the funding support from the South African National Research Foundation (SA-NRF) (Grant No.: 137759) and the Wrocław Centre for Networking and Supercomputing, Wrocław, Poland (Grant No. 285) for providing computational facilities are acknowledged. The research used resources of the Advanced Photon Source, a US Department of Energy (DOE) Office of Science User Facility, Argonne National Laboratory. Use of BioCARS was also supported by the National Institute of General Medical Sciences of the National Institutes of Health (NIH) (grant No. R24GM111072). Time-resolved setup at Sector 14 was funded in part through collaboration with Philip Anfinrud (NIH/NIDDK).

B-53

REAL SPACE STRUCTURE SOLUTION OF QUASICRYSTALS

Ireneusz Bugański, Radosław Strzałka, Janusz Wolny

AGH University of Krakow, Faculty of Physics and Applied Computer Science, Kraków Poland

The atomic structure of quasicrystals is predominantly solved with mathematical tools requiring embedding the structure in the higher-dimensional direct space where atoms are represented by closed domains. The real space atomic structure is retrieved when the higher-dimensional domain, called the occupation domain, intersects the real space, incommensurately oriented with respect to the higher-dimensional periodic lattice. The distribution of atomic elements within the domain, as well as the specific shape of the domain is the subject of the structural solution.

In the group of prof. Janusz Wolny, the structure solution of quasicrystals and further refinement is done by finding the initial atomic model in the real space directly [1]. The model is based on the atomic decoration of the aperiodic tiling chosen specifically for the type of quasicrystal. Particularly, the decagonal quasicrystal is solved using the Penrose tiling and the icosahedral quasicrystal is very well described with the Ammann-Kramer-Neri tiling.

The achievements of the real-space approach will be discussed in details. The emphasis will be put on two most recent structural models of quasicrystals, i.e. the structure of the icosahedral Tsai-type $Cd_{5.7}Yb$ [2] that is very similar to the atomic structure of the Bergman-type $Zn_{69.5}Mg_{20.9}Tm_{9.6}$ (Fig. 1.) [3] and the mineral with the decagonal symmetry $Al_{71}Ni_{24}Fe_5$ called decagonite [4]. Steps taken toward achieving the final solution of each structure will be presented comparatively by putting an accent on methodological differences. Icosahedral quasicrystals are truly 3D quasicrystals whereas decagonal phases are periodic in one dimension collinear with the 10-fold axis, therefore the approach to both structures differs.

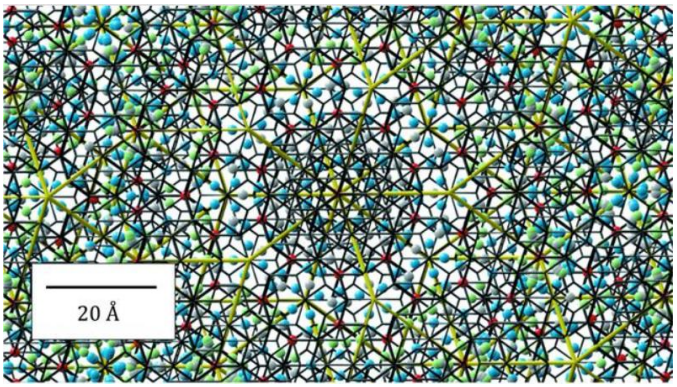

Fig. 1. The structure of i-ZnMgTm seen along 5-fold axis with the Ammann-Kramer-Neri tiling (yellow) and the rhombic triacontahedral Tsai cluster (black) being plotted.

References

[1] J. Wolny, I. Buganski, R. Strzalka, *Cryst. Rev.*, **24** (2018) 22-64.
[2] To be published.
[3] I. Buganski, J. Wolny, H. Takakura, *Acta Cryst.*, *A***76** (2020) 180-196.
[4] I. Buganski, L. Bindi, *IUCrJ*, **8** (2021) 87-101.

B-54

BAZY PRZEMIAN FAZOWYCH W NANOKRYSZTAŁACH

Paweł E. Tomaszewski

Instytut Niskich Temperatur i Badań Strukturalnych, Polska Akademia Nauk,
ul. Okólna 2, 50-422 Wrocław

Coraz popularniejsze badania nanokryształów i obserwowanych przemian fazowych skłoniły do prób systemowego spojrzenia na poprzez podjęcie próby klasyfikacji strukturalnych przemian fazowych wywołanych zmianą wielkości krystalitów.

Schemat diagramu fazowego pokazany jest na Rys. 1.

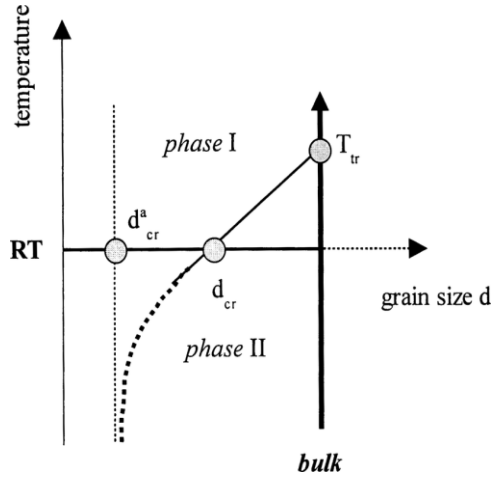

Rys. 1.

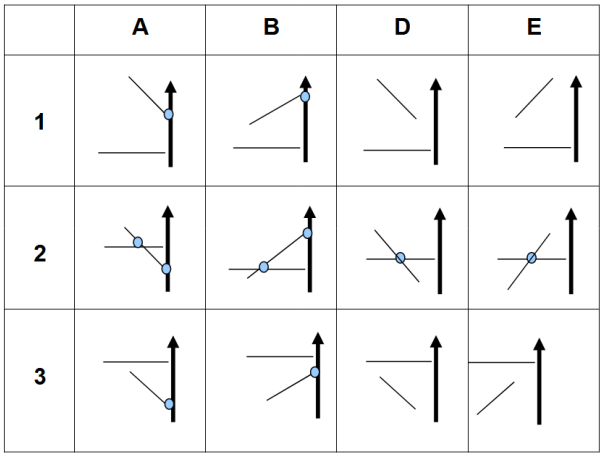

Rys. 2.

Systematyka przemian rozmiarowych wymagała zebrania dotychczasowych wyników w postaci bazy danych. Podstawowe typy przemian schematycznie pokazane zostały na Rys. 2. Z kolei poniższa tabela przedstawia częstość występowania określonego typu (w nawiasach podany został procentowy udział danego typu).

	A	**B**	**D**	**E**	**suma**	**X**
1	23 (3.8)	59 (9.8)	8 (1.3)	8 (1.3)	**98 (16.3)**	---
2	11 (1.8)	109 (19.0)	100 (16.6)	0	**220 (36.5)**	84 (13.9)
3	46 (7.6)	115 (19.1)	24 (4.0)	16 (2.7)	**198 (32.8)**	---
Σ	**80 (13.3)**	**283 (46.9)**	**129 (21.4)**	**24 (4.0)**	**519**	**84**

Szczególnym rodzajem przemian są te zakwalifikowane to typu X, który opisywany jest tzw. diagramem wyspowym (Rys. 3). Tutaj istotne jest rozróżnienie między „temperaturą" a „temperaturą wygrzewania, T_{calc}". Podana liczba 84 takich przemian rozmiarowych jest tylko wartością szacunkową. należy bowiem przebadać literaturę pod kątem sposobu otrzymania badanej próbki. Wydaje się, że wiele

przemian, zwłaszcza tych z „odwrotną” kolejnością faz (wyższa symetria dla niższych temperatur) powinno być rozpatrywaniach w modelu wyspowym. Niestety, nikt dawniej nie badał wielkości krystalitów dla takich faz co uniemożliwia poprawny opis przemiany.

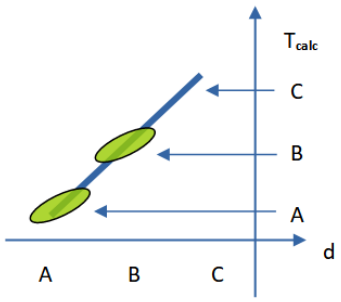

Rys. 3.

Osobną bazę danych opracowano dla przemian występujących pod ciśnieniem. Tu możliwe są trzy warianty diagramu fazowego *ciśnienie-rozmiar* oznaczone literami A, B i C (Rys. 4).

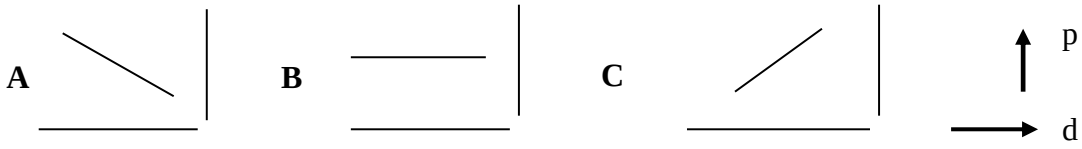

Rys. 4.

Statystyka występowania typów przemian ujęta została w poniższej tabelce.

A	**B**	**C**	**---**
83	4	42	55

Ze względu na jakość pomiarów aż w 55 przypadkach nie udało się jednoznacznie przypisać typu obserwowanej przemianie rozmiarowej.

B-55

STRUCTURAL PARAMETERS AND BULK MODULUS OF ALUMINATE SPINELS AS A FUNCTION OF THE INVERSION PARAMETER

Jan Jakub Leon Stasiczak and Paweł Piszora

Department of Materials Chemistry, Faculty of Chemistry, Adam Mickiewicz University, Uniwersytetu Poznańskiego 8, 61-614 Poznań, Poland

Lattice parameter, *a*, and oxygen parameter, *u*, define crystal structure of spinels. Meanwhile, bulk modulus is one of the most fundamental parameters defining their elastic properties. The oxygen parameter, *u*, was modeled separately for the shell as well as the core for each model, since all of the applied potential libraries assume a core-shell model for oxygen atoms [1]. The value of the *u* parameter decreases with the increasing inversion parameter. This does not happen, however, at the same rate for core and shell, so that the functions for both intersect at inversion parameter of about 0.9. Bulk modulus, which for the spinel lattice takes the same values calculated according to Reuss and Voigt, for each of the modeled spinels increases with the inversion parameter.

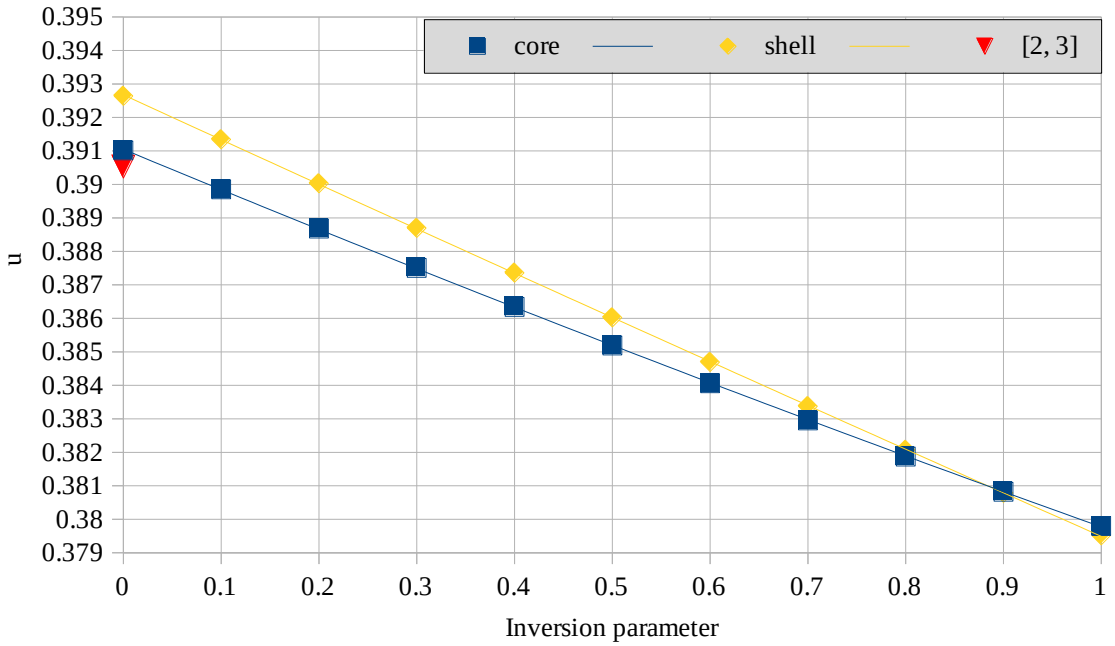

Fig. 1. Oxygen parameter, *u*, calculated for $ZnAlCrO_4$ spinel. The triangle represents average value of *u* for $ZnAl_2O_4$ [2] and $ZnCr_2O_4$ [3].

References

[1] J. D. Gale, A. L. Rohl, *Mol. Simul.*, **29** (2003) 291.
[2] M. Ardit, G. Cruciani, M. Dondi, *Am. Mineral.*, **97** (2012) 1394.
[3] D. Levy, V. Diella, A. Pavese, M. Dapiaggi, A. Sani, *Am. Mineral.*, **90** (2005) 1157.

B-56

EXPLORING THE CRYSTAL STRUCTURE OF $CeSi_{1.2}Ga_{0.8}$ ALLOY: INSIGHTS FROM EXPERIMENTAL AND COMPUTATIONAL ANALYSIS

Karol Synoradzki[1], Przemysław Skokowski[1], Łukasz Frąckowiak[1], Mykhaylo Koterlyn[2], Jakub Sebesta[3], Dominik Legut[3], Tomasz Toliński[1]

[1] *Institute of Molecular Physics, Polish Academy of Sciences, Poznań, Poland*
[2] *Institute of Physics, K. Wielkiego University, Bydgoszcz, Poland*
[3] *IT4Innovations, VSB - Technical University of Ostrava, Ostrava, Czech Republic*

Ce-based compounds display numerous intriguing physical properties stemming from the unique electron structure of cerium. Unlike other elements, cerium's *f* electrons are not strongly localized, nor are they effectively shielded from external influences by the conduction electrons. As a result, there is a significant degree of hybridization between the *f* electrons and the conduction electrons, leading to the partial or complete delocalization of the 4*f* shell electrons. This phenomenon gives rise to various remarkable phenomena such as magnetic ordering, spin fluctuations, the heavy-fermion state, the Kondo effect, and mixed valence. In addition to their significance in fundamental studies, Ce-based compounds are currently under investigation for various applications. Particularly, they are being explored in the context of hydrogen storage, magnetocaloric effects, and thermoelectric effects.

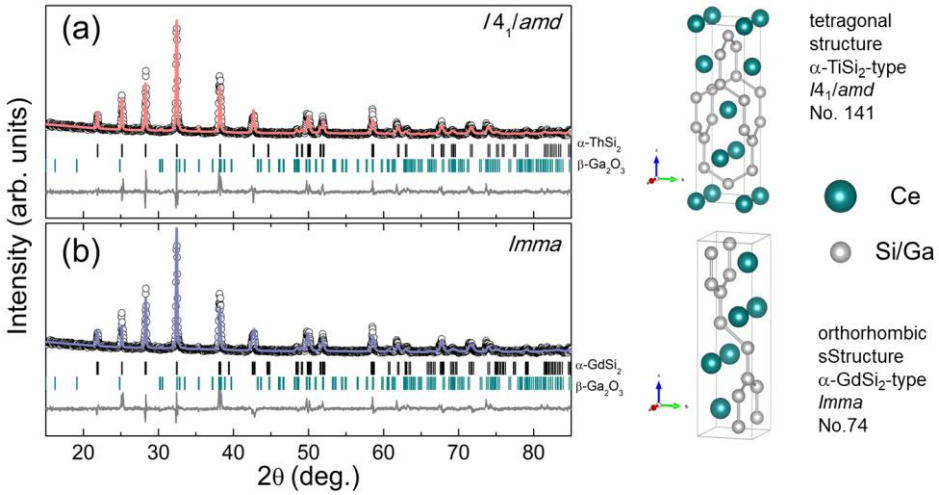

Fig. 1. X-ray diffraction pattern of $CeSi_{1.2}Ga_{0.8}$ alloy obtained at room temperature. Open circles represents experimental points and solid line represents the Rietveld refined patterns (a) for tetragonal α-$ThSi_2$-type ($I4_1/amd$, No. 141) and (b) for orthorhombic α-$GdSi_2$-type structure (*Imma*, No.74). The gray lines at the bottom represent the difference between the fit and the experimental results. The Bragg peaks for α-$ThSi_2$-type, α-$GdSi_2$-type structure, and β-Ga_2O_3 impurity phase are marked by short vertical lines. The right side of the figure shows the unit cells for α-$ThSi_2$-type (top) and α-$GdSi_2$-type (bottom) structures. Dark cyan spheres represent Ce atoms and gray spheres represent Si and Ga atoms.

In this work, we study the crystallographic structure of the $CeSi_{1.2}Ga_{0.8}$ alloy belonging to the $CeSi_{2-x}Ga_x$ series. Depending on the chemical composition, two different structures are observed in these compounds. The starting compound $CeSi_2$ crystallizes in a tetragonal α-$TiSi_2$-type structure (space group $I4_1/amd$, No. 141), while

$CeGa_2$ crystallizes in a hexagonal AlB_2-type structure (space group *P*6/*mmm*, No. 191) [2]. As the concentration changes in the $CeSi_{2-x}Ga_x$ series, the structure of the alloys will change. It has been shown in the literature that for $0 < x < 1.3$ the alloys crystallize in an α-$TiSi_2$-type structure [3].

The obtained results for our polycrystalline $CeSi_{1.2}Ga_{0.8}$ sample from powder X-ray diffraction can be fitted with very good agreement assuming that this alloy crystallizes in the α-$TiSi_2$-type structure, see Fig. 1(a). Apart from the peaks attributed to the main phase, we have detected additional peaks stemming from a minor presence of gallium oxide β-Ga_2O_3, which is considered an impurity phase. Interestingly, we found that an equally good fit could be obtained assuming that this alloy crystallizes in orthorhombic α-$GdSi_2$-type structure (space group *Imma*, No. 74), see Fig. 1(b). The two structures are quite similar, the α-$GdSi_2$-type structure can be considered as a slightly deformed α-$TiSi_2$-type structure, therefore fitting results for both structures are very similar. The parameters determining the quality of the fit (R_B - Bragg factor and R_F - structure factor) are close for each structure, with those for the α-$TiSi_2$-type structure being slightly lower (R_B = 12.8, R_F = 11.0) than those for α-$GdSi_2$-type (R_B = 19.2, R_F = 12.4). On the other hand, the *ab inito* SPR-KKR calculations revealed that the α-$GdSi_2$-type structure possesses the formation energy lower by about 81.6 meV/atom than the α-$ThSi_2$-type one [4]. The densities of states for the two structures are very similar as can be seen in Fig.2. In both cases, Ce 4*f* states dominate, forming an intense peak near the Fermi level.

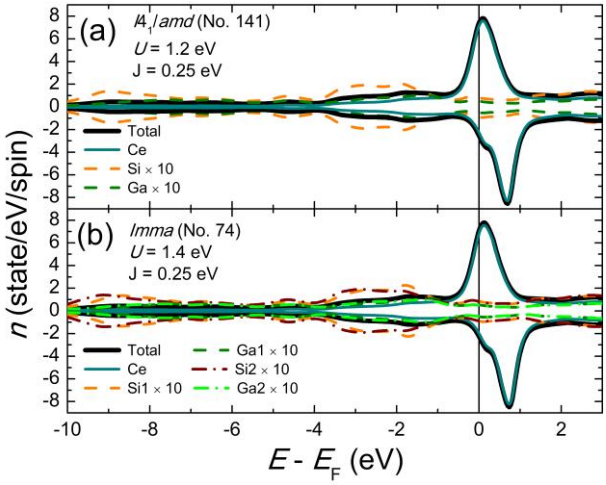

Fig. 2. The densities of states (DOS) of $CeSi_{1.2}Ga_{0.8}$ for (a) $I4_1/amd$ (No.141) and (b) *Imma* (No. 74) crystal structure.

Based on our findings, it is not possible to definitively determine the exact crystal structure of $CeSi_{1.2}Ga_{0.8}$. As a result, further measurements utilizing high-quality single crystals and a suitable equipment, such as a synchrotron, would be required to resolve this issue conclusively.

Literature

[1] S.F. Matar, Progress in *Solid State Chemistry*, **41** (2013) 55–85.
[2] R. Pottgen, B. Chevalier, *Zeitschrift Für Naturforschung B*, **70** (2015) 695–704.
[3] H. Mori, N. Sato, T. Sato, *Solid State Commun*., **49** (1984) 955–958.
[4] K. Synoradzki, P. Skokowski, Ł. Frąckowiak, M. Koterlyn, J. Sebesta, D. Legut, T. Toliński, *J. Magn. Magn. Mater.*, **547** (2022) 168833.

B-57

UNVEILING THE STRUCTURAL ADAPTABILITY OF CALF-20 METAL-ORGANIC FRAMEWORK

Joanna Drwęska, Filip Formalik, Kornel Roztocki, Randall Q. Snur, Leonard J. Barbour, Agnieszka Janiak

Faculty of Chemistry, Adam Mickiewicz University, Uniwersytetu Poznańskiego 8, 61-614 Poznań, Poland

Calgary Framework 20 (CALF-20) is a readily obtained and reproducible zinc-based metal-organic framework that exhibits excellent durability in the CO_2 sorption process [1]. Previous reports indicate that the stability of materials may be attributed to their potential flexibility [1,2]. To verify this, we found the proper conditions for single-crystal-to-single-crystal phase transition of CALF-20, hereafter referred to as CALF-20α_s (s – solvent molecule). A new phase dubbed CALF-20β_s is formed after heating CALF-20α_s at 80°C for seven days, during which a water molecule is statistically ligated to half of the zinc cations in the MOF. This phenomenon causes changes in the 3-D framework, resulting in a decrease in porosity.

To better understand the nature of the CO_2 sorption process at the atomic level, we carried out *in situ* single-crystal X-ray diffraction experiment under controlled CO_2 gas pressure using an environmental gas cell, thus obtaining CALF-20α_{CO2}. The experiment revealed that no structural changes occur upon the gas sorption and allowed us to identify real carbon dioxide positions in the framework. We also determined that CO_2 interacts with CALF-20 through electrostatic interactions.

Theoretical analysis of CALF-20 flexibility proved that the water molecule is a key factor in stabilizing the structure, resulting in exceptional stability of the framework in the presence of bases, acids, and steam. Nevertheless, under anhydrous conditions, the energetically favourable phase is CALF-20α, which is also reflected in the experimental results. Furthermore, we predict the presence of an additional CALF-20β contracted phase, which can only exist at very low temperatures.

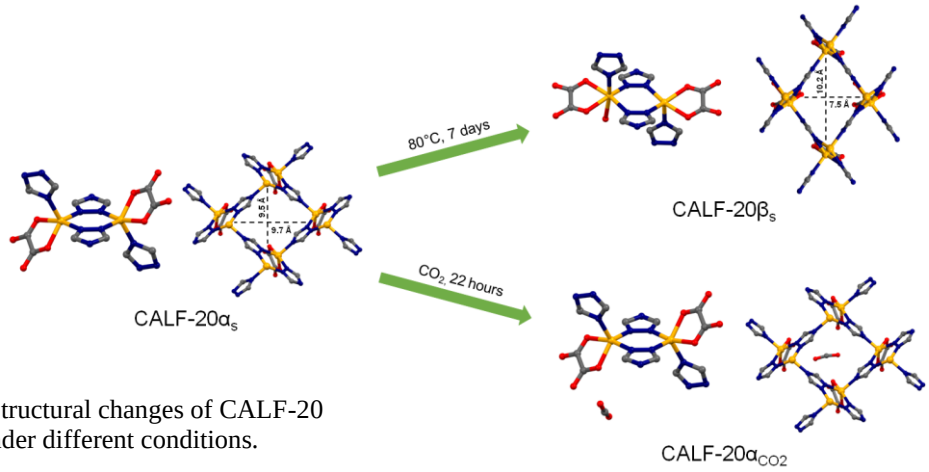

Fig. 1. Structural changes of CALF-20 under different conditions.

References

[1] J.-B. Lin et al., *Science*, **374** (2021) 1464.

[2] Y. Wei et al., *RSC Adv.*, **12** (2022) 18224.

B-58

EFFECT OF BLADE GEOMETRY ON γ′ LATTICE PARAMETER AND PRIMARY ORIENTATION OF SINGLE-CRYSTALLINE CORED TURBINE BLADES

Jacek Krawczyk* and Włodzimierz Bogdanowicz

Institute of Materials Engineering, Faculty of Science and Technology, University of Silesia in Katowice, 75 Pułku Piechoty 1a St., 41-500 Chorzów, Poland

**e-mail: jacek.krawczyk@us.edu.pl*

Gas turbine engines used in aerospace are among the most complex mechanical systems. The engines operate at increasingly high turbine temperatures to satisfy ever-increasing working demands. Turbine blades work in temperatures close to the melting point of the material they are made of. They are internally cooled by the air passing through intricate passages within the blade geometry to decrease the blade temperature during operation. The complex geometry of the blades may contribute to the formation of different types of crystal defects related, e.g., to the material thickness.

Currently, commonly used materials for blade production are superalloys characterized by an imposing combination of high-temperature strength, phase stability, and resistance to high-temperature oxidation. The complex loads during the service of the blades mean that they must be resistant to high-temperature tensile strain and creep; these requirements are met by CMSX-4 superalloy. The single-crystalline casts of CMSX-4 superalloy have high phase stability, homogeneity of the dendritic microstructure, and resistance to high-temperature corrosion.

The single-crystalline cored turbine blades made of CMSX-4 superalloy were obtained by directional crystallization using the Bridgman technique. The withdrawal rate was 3 mm/min. The groups of dendrites formed during crystallization typically create an array with a preferred crystal orientation of [001]-type, which should be parallel to the withdrawal direction and the vertical axis Z of the blade.

The lattice parameter $a_{\gamma'}$ of the γ′-phase creating the single-crystalline alloy, and the α angle - defining the primary crystal orientation were measured in the areas located near the selector situated asymmetrically, considering the top view of the blade. The distributions of the $a_{\gamma'}$ and the α angle were determined along the lines parallel to the vertical blade axis Z using X-ray diffraction methods. The relations between changes in the $a_{\gamma'}(Z)$ and $\alpha(Z)$ were analyzed on the Z levels where the shape of the blade's cross-section changes. The local increase in $a_{\gamma'}(Z)$ was found near the root-airfoil connection level and certain other root levels, which is related to the change in blade section shapes on such levels. The local extremes in $\alpha(Z)$, representing the dendrite bends, were observed at these levels. The increase in the $a_{\gamma'}(Z)$ with the local bending of dendrites was discussed concerning the local redistribution of alloying elements and local residual stresses of the γ-dendrites. For the first time, a method of analyzing the local bending of the dendrites was proposed by studying the behavior of the $\alpha(Z)$.

References

[1] J. Krawczyk,, W. Bogdanowicz, J. Sieniawski, *Materials*, **16** (1) (2023) 112.

B-59

HETEROMETALLIC ZIF MATERIALS

Łukasz Kurowski[1], Szymon Piekarski[1], Martina Basilicata[2], Mattia Lopresti[2], Marco Milanesio[2], Magdalena Siedzielnik[1], Anna Dołęga[1]

[1] Gdańsk University of Technology, Chemical Faculty, Department of Inorganic Chemistry, Narutowicza St. 11/12, 80-233 Gdańsk, Poland
[2] Università del Piemonte Orientale "A Avogadro", Dipartimento di Scienze e Innovazione Tecnologica, Via Michel 11, 15100 Alessandria - Italy

ZIFs or Zeolitic Imidazolate Frameworks are a type of 3D coordination polymers that are composed of imidazolate anions and metal ions. Over 100 ZIF topologies were reported in the literature. Their interesting feature is relatively easy transformation into the glassy state. ZIFs are investigated as catalysts [1], CO2 capturing materials [2], or in medical applications. [3] The example of the cobalt ZIF material is shown in Fig. 1 [4]

Whereas homometallic ZIFs are well-recognized and their properties widely described in the literature, there are relatively few known heterometallic ZIFs. Here we describe a simple method of synthesis and properties of several heterometallic systems.

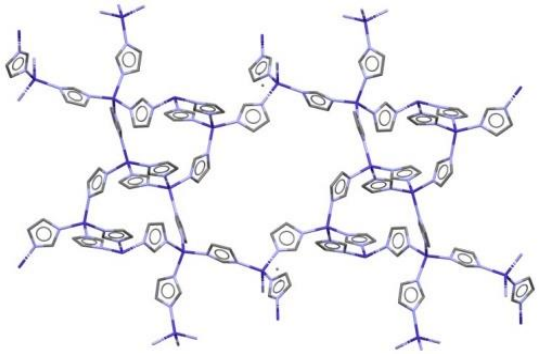

Fig. 1. Molecular structure of Co ZIF [4].

In the poster we present the results obtained for the synthesis of Zn-Co, Zn-Ag and Co-Ag ZIF materials. We described very simple method of ZIFs synthesis. In the case of zinc and cobalt each ratio of metal ions in the reaction mixture returns a stable phase in which the metal ions may replace one another. In the case of zinc/cobalt and silver only one stable material with a defined stoichiometry of metal ions is formed. The crystal structure of Co-Zn ZIF was derived from powder diffraction data.

Literatura

[1] W. Xue, Q. Zhou, F. Li, B. S. Ondon (2019) Zeolitic imidazolate framework-8 (ZIF-8) as robust catalyst for oxygen reduction reaction in microbial fuel cells, *J. Power Sources*, **423** (2019) 9–17.
[2] A. Phan, C. J. Doonan, Uribe- F. J. Romo, C. B. Knobler, M. O'Keeffe, O. M. Yaghi. Synthesis, Structure, and Carbon Dioxide Capture Properties of Zeolitic Imidazolate Frameworks. *Acc. Chem. Res*., **43** (2010) 58–67.
[3] R. Ettlinger, N. Moreno, D. Volkmer, K. Kerl, H. Bunzen, Zeolitic Imidazolate Framework-8 as pH-Sensitive Nanocarrier for "Arsenic Trioxide" Drug Delivery. *Chem. Eur. J*., **25** (2019) 13189–13196.
[4] Y.-Qi Tian, C.-X. Cai, Y. Ji, X.-Z. You, S.-M. Peng, G.-H. Lee [Co5(im)10·2 MB]∞: A Metal-Organic Open-Framework with Zeolite-Like Topology. *Angew. Chem.*, **114** (2002) 1442–1444.

B-60

THE MULTI-SCALE ANALYSIS OF STRUCTURAL DEFECTS IN SINGLE-CRYSTALLINE TURBINE BLADES

Robert Paszkowski, Włodzimierz Bogdanowicz

University of Silesia in Katowice, Faculty of Science and Technology, Institute of Materials Engineering, 1a 75 Pułku Piechoty St., 41-500 Chorzów, Poland

**e-mail: robert.paszkowski@us.edu.pl*

The nickel-based superalloys are the most widely used materials for producing single-crystalline (SX) turbine components, commonly used in the aerospace and energy industry sectors. Because of complex loading conditions, these materials must meet many requirements concerning their quality, for example, heat and corrosion resistance and high mechanical strength on complex loads [1]. These high requirements are met by the second generation of single crystalline CMSX-4.

Due to the specific dendrite structure of superalloys and the complex shape of the blades, various growth defects, such as low-angle boundaries [2], dislocations [1], vacancies [3], and inhomogeneity of alloying elements, which cause the formation of residual stresses [4], may be formed during the crystallization process. The turbine blades casts are divided into two main parts — bulk root and fine airfoil. These root defects are inherited by the airfoil during crystallisation of the blade and often do not disappear even after heat treatment is applied on production lines [4]. For this reason, it is important to analyse the as-cast structural heterogeneity of the blades.

The as-cast single-crystalline blades made of industrial nickel-based superalloy of CMSX-4 were studied. Single-crystalline turbine blades were produced by directional solidification using the Bridgman technique with a 3 mm/min withdrawal rate. The ALD Vacuum Technologies furnace in Research and Development Laboratory for Aerospace Materials, Rzeszów University of Technology, was used. A coupling of scanning electron microscopy and X-ray diffraction topography allowed the visualization of dendritic arrays and surface defects in the root part of the blades. The characterization of defects on a microscopic scale was performed using Positron Annihilation Lifetime Spectroscopy.

Based on the results, character of inhomogeneity was described. There are differences in the size of dendrite arms, most frequently depending on the location relative to the selector. X-ray topography studies on thin samples allowed the observation of contrast inversions and areas where internal stresses occur. The registered positron lifetimes ascribed to defects are outstandingly higher than typical defects found in metals and their alloys reported in the literature. These long lifetimes were ascribed to micro-voids that probably occur at the dendrite-matrix connection, originating from the shrinking of liquid metal enclosed in inter-dendritic regions during solidification.

References

[1] R.C. Reed, The Superalloys, Fundamentals and Applications, Cambridge University Press, 2006.
[2] W. Bogdanowicz, J. Krawczyk, R. Paszkowski, J. Sieniawski, *Materials*, **12** (2019) 4126.
[3] J. Krawczyk, R. Paszkowski, W. Bogdanowicz, A. Hanc-Kuczkowska, J. Sieniawski, B. Terlecki, *Materials*, **12** (2019) 870.
[4] J. Krawczyk, W. Bogdanowicz, A. Hanc-Kuczkowska, A. Tondos, J. Sieniawski, *Met. Mater. Trans.A*, **49** (2018) 4353.

B-61

CRYSTALLITE SIZE AND SINTERING TEMPERATURE AS POTENTIAL CAUSES OF DISCREPANCIES IN THE VALUES OF LATTICE PARAMETERS OF COPPER-ZINC FERRITES

Jolanta Darul and Paweł Piszora

Department of Materials Chemistry, Faculty of Chemistry, Adam Mickiewicz University, Uniwersytetu Poznańskiego 8, 61-614 Poznań, Poland

Following the dependences of the lattice parameter on the zinc content available in the literature, it is difficult to clearly determine the monotonicity of such changes. The function describing such a relationship can be increasing, non-decreasing or non-monotonic. It is difficult to indicate literature data that would confirm the validity of Vegard's law in the entire range of concentrations for this series of solid solutions.

Zinc ferrite is normal while copper ferrite is inversed spinel. As a result, although the ionic radius of zinc is larger than the ionic radius of copper, the distribution of cations between the tetrahedral and octahedral positions has a large influence on the lattice parameter change in this series of solid solutions. The distribution of cations depends on the parameters of the synthesis reaction, such as temperature, oxygen partial pressure, and sample cooling rate.

Here we report a problem with finding a linear function describing the dependence of the lattice parameter on the zinc content in zinc-copper ferrite. In particular, we are looking for the relationship between the size of crystallites and changes in the lattice parameter as a function of x in $Cu_{1-x}Zn_xFe_2O_4$.

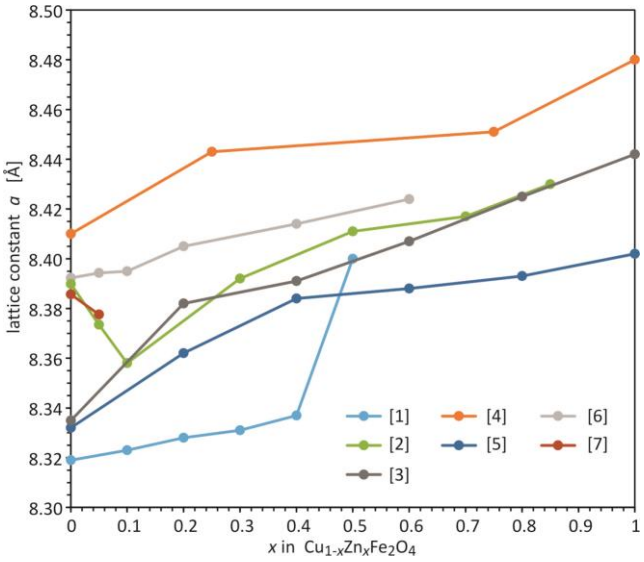

Fig. 1. Lattice constant verses Zn concentration for $Cu_{1-x}Zn_xFe_2O_4$.

References

[1] A. T. Dhiwahar, M. Sundararajan, P. Sakthivel et al., *J. Phys. Chem. Solids*, **138** (2020) 109257.
[2] A. Subha, M. G. Shalini, S. Rout, S. C. Sahoo, *J. Supercond. Nov. Magn.*, **33** (2020) 3577.
[3] S. Güner, S. Esir, A. Baykal, A. Demir, Y. Bakis, *Superlattice Microst.*, **74** (2014) 184.
[4] M. U. Rana, M. U. Islam, T. Abbas, *Mater. Chem. Phys.*, **65** (2000) 345.

[5] T. M. Hammad, J. K. Salem, A. A. Amsha, N. K. Hejazy, *J. Alloy Compd.*, **741** (2018) 123.
[6] S. K. Jena, D. C. Joshi, Z. Yan, Y. Qi, S. Ghosh, S. Thota, *J. Appl. Phys.*, **128** (2020) 073908.
[7] J. Darul, W. Nowicki, *Radiat. Phys. Chem.*, **78** (2009) S109.

B-62

STRUCTURAL PROPERTIES OF ANTIMONY(III) IODIDES CRYSTALLIZING WITH METHYLHYDRAZINIUM

Magdalena Rowińska[a,*], Tamara J. Bednarchuk[a], Anna Piecha-Bisiorek[b], Ryszard Jakubas[b], Anna Gągor[a]

[a] *W. Trzebiatowski Institute of Low Temperature and Structure Research Polish Academy of Sciences, Okólna 2, 50-950 Wrocław, Poland*
[b] *Faculty of Chemistry, University of Wrocław, F. Joliot-Curie 14, 50-383, Wrocław, Poland*

**e-mail: m.rowinska@intibs.pl*

Halometallates constitute an important class in the field of hybrid, organic-inorganic materials. Many crystallize in polar space groups exhibiting non-linear optical, piezo- and ferroelectric properties. The narrow energy bandgaps and broadband absorption make them suitable for applications in solar cells. Lead-iodide compounds incorporating methylamine [1] are well-known examples, featuring a perovskite crystal structure and superior energy absorption. Despite evident advantages, these materials are chemically unstable when exposed to average humidity and light.

As a result, ongoing research is actively exploring organic-inorganic hybrids with alternative amines and metal centres [2,3]. Here we focus on hybrid compounds comprising methylhydrazine and antimony iodide with a stoichiometry of $(MHy)_2[SbI_5]$, synthesized using a direct method. It has been confirmed that this specific stoichiometry has the potential to yield a ferroelectric behaviour [4].

The single-crystal x-ray diffraction measurements revealed that the studied compounds exhibit two room-temperature polymorphs. In both compounds, the crystal structure consists of one-dimensional (1D) polymeric anionic $[SbI_5]_\infty^{2-}$ cis-chains built of SbI_6 corner-sharing octahedra. The cations, which are dynamically disordered and located within the crystal voids, interact with the chains through weak hydrogen bonds.

Polymorph **1** crystallizes in the monoclinic $P2_1/n$ space group, possesses a large unit cell with a = 8.641(3), b = 37.238(9), c = 10.663(4) Å, β = 91.29(3)°, V = 3430.2(19) Å^3. In turn, compound **2** crystallizes in the orthorhombic symmetry with a chiral $P2_12_12_1$ space group and smaller unit cell with a = 8.835(3), b = 10.550(4), c = 18.395(5) Å, V = 1714.6(10) Å^3.

In the following poster the detailed structural peculiarities of both polymorphs as well as their physicochemical properties will be discussed.

The research was funded by the National Science Centre as part of the OPUS 22 project (grant number: 2021/43/B/ST5/01172).

Literature

[1] A. K. Jena, M. Ikegami, T. Miyasaka *ACS Energy Lett*., **2**(8) (2017) 1760–1761.
[2] D. Drozdowski, A. Gągor, D. Stefańska, J. K. Zaręba, K. Fedoruk, M. Mączka, A. Sieradzki *J. Phys. Chem. C*, **126**(3) (2022) 1600–1610.
[3] P. Szklarz, A. Gągor, R. Jakubas, P. Zieliński, A. Piecha-Bisiorek, J. Cichos, M. Karbowiak, G. Bator, A. Ciżman. *J. Mater. Chem. C*, **7** (2019) 3003–3014.
[4] R. Jakubas, M. Rok, K. Mencel, G. Bator, A. Piecha-Bisiorek *Inorg. Chem. Front.*, **7** (2020) 2107–2128.

B-63

THE $CsPbBr_3$ PEROVSKITE CORE – GLASS CLADDING OPTICAL FIBER - FABRICATION AND PROPERTIES

Paweł Socha[1], Dariusz Pysz[1], Karol Bartosiewicz[2], Andrzej Lechna[1], Robert Tomala[3], Maksym Buryi[4], Robert Kral[4], Alicja Anuszkiewicz[1], Michał K. Cyrański[5], Ryszard Buczyński [1,6]

[1] Łukasiewicz Research Network - Institute of Microelectronics and Photonics, ul. Wólczyńska 133, 01-919 Warsaw
[2] Department of Physics, Kazimierz Wielki University, ul. Powstańców Wielkopolskich 2, 85-090 Bydgoszcz
[3] Institute of Low Temperature and Structure Research, ul. Okólna 2, 50-422 Wrocław
[4] Institute of Physics of Czech Academy of Sciences, Cukrovarnická 10/112 162 00 Prague 6
[5] Department of Chemistry, University of Warsaw, Pasteura 1, 02-093 Warsaw
[6] Department of Physics, University of Warsaw, Pasteura 5, 02-093 Warsaw

Optical fibers are very desirable in a wide range of applications like telecommunication, lasers, sensors, photovoltaics, medicine, etc. due to their small size and various properties. One example of functional optical fibers is crystalline core – glass cladding fibers, which take benefits from both crystalline and glass materials. The promising candidates for the crystalline core are halide perovskites (HPs) (ABX_3; e.g. A = Cs^+, CH_3NH^{3+}; B = Pb^{2+}, Sn^{2+}; X= Cl^-, Br^-, I^-) with their various properties [1]. HPs exhibit e.g. luminescence, tunable bandgaps, large absorption coefficient, high carrier mobility, and production costs of these materials are relatively low. Therefore, they are used in many optoelectronic devices like solar cells, light-emitting diodes, lasers, photodetectors, etc. However, several challenges still have to be faced. HPs are very sensitive to humidity, and their composition is not environmentally friendly. Using glass cladding can solve both problems by isolation the crystalline core from external conditions.

Perovskite core fibers (PCF) were obtained before by perovskite crystallization directly inside the hollow core fiber [2]. Crystals growth rates in this research were about mm/day and resulted in good quality crystalline cores. However, fibers with an internal diameter below 300 um have growth limitations due to limited ion diffusion.

In this report, we present the fabrication and properties of $CsPbBr_3$ perovskite core - glass cladding fibers (Fig.1) obtained with the Molten-Core Method (MCM). MCM is commonly used to obtain crystal core – glass cladding fibers [3], nonetheless this method was not previously used to obtain PCF. For this technique is crucial to fit the thermal parameters of crystals and glass - crystalline material must be completely melted while the glass is soft enough for fiber drawing at the same temperature. When the fiber leaves the furnace the molten core crystallizes again. The advantage of this method is the possibility to produce very long fibers (up to hundreds of meters) in a relatively short time. Furthermore, the synthesis of HPs can be performed during the drawing process. The crystallization process is spontaneous, thus the fiber core quality was carefully investigated with single-crystal X-ray diffraction, scanning electron microscope imaging, and energy-dispersive X-ray analysis. Obtained fibers were also characterized with transmission measurements, and photoluminescence excitation and

emission spectroscopy. Experiments confirmed, that the crystalline core is $CsPbBr_3$ perovskite cubic phase exhibiting green photoluminescence at UV excitation.

Fig. 1. $CsPbBr_3$ perovskite core optical fibers.

References

[1] J. S. Manser, J. A. Christians, P. V. Kamat, *Chem. Rev.*, **116** (2016), 12956–13008.
[2] Y. Zhou, M. A. Parkes, J. Zhang, Y. Wang, M. Ruddlesden, H. H. Fielding, L. Su, *Sci. Adv*. **8**, eabq8629 (2022).
[3] J. Ballato, A. C. Peacock, *APL Photonics* **3** 120903 (2018)

B-64

CRYSTALLOGRAPHIC PROPERTIES OF $Pb_{1-x}Sn_xTe$ AND SnTe LAYERS GROWN ON CdTe/GaAs(001) SUBSTRATES

Adrian Sulich[1], Krzysztof Dybko[1,2], Wojciech Wołkanowicz[1], Elżbieta Łusakowska[1], Piotr Dziawa[1], Janusz Sadowski[1], Badri Taliashvili[1], Tomasz Wojtowicz[2], Tomasz Story[1,2], and Jaroslaw Z. Domagala[1]

[1] Institute of Physics, Polish Academy of Sciences, Aleja Lotnikow 32/46, PL 02 668 Warsaw, Poland
[2] International Research Centre MagTop, Institute of Physics, Polish Academy of Sciences, Aleja Lotnikow 32/46, PL 02 668 Warsaw, Poland

$Pb_{1-x}Sn_xTe$ and SnTe are intensively studied narrow-gap semiconductors, potentially useful, among others, as topological, photosensitive, thermoelectric or superconducting materials [1-6]. For our research we selected heterostructures composed of $Pb_{1-x}Sn_xTe$ or SnTe rock-salt layers and CdTe(001) buffer grown on commercially available substrate, 2° off-cut GaAs(001). Extended-defect structure of these heterostructures, the unit cell parameters and crystal lattice strain in each layer were investigated. As the experimental technique laboratory high-resolution X-ray diffraction based on $CuK_{\alpha 1}$ irradiation ($\lambda = 1.5404$Å) was applied.

The results show that CdTe buffer is relaxed in all of the samples but $Pb_{1-x}Sn_xTe$ and SnTe layers are partially strained (the percentage relaxation is at the range of 86-98%). We assessed the general crystallographic quality of the studied materials as good (comparable with the results published in literature); however, some misorientation between the substrate, the buffer and the main layer, as well as unit cell distortion and anisotropy of the azimuthal defects distribution in CdTe, $Pb_{1-x}Sn_xTe$ and SnTe have been detected. In the most cases the distortion is tetragonal but in some samples alternative, monoclinic distortion of the SnTe layer occurs which may affect its topological properties, secured by crystal symmetry.

This research was partially supported by the Foundation for Polish Science through the IRA Programme co financed by EU within SG OP and by the NCN Grants: UMO 2017 /27/B/ST3/02470 and UMO 2019/35/B/ ST3/03381.

Literature

[1] P. Dziawa, B. J. Kowalski, K. Dybko, R. Buczko, A. Szczerbakow, M. Szot, E. Łusakowska, T. Balasubramanian, B. M. Wojek, M. H. Berntsen, O. Tjernberg, T. Story, *Nat. Mater.*, **11** (2012) 1023.
[2] G. Tan, F. Shi, S. Hao, H. Chi, T. P. Bailey, L. D. Zhao, C. Uher, Ch Wolverton, V. P. Dravid, M. G. Kanatzidis, *J. Am. Chem. Soc.*, **137** (2015) 11507.
[3] A.S. Tarasov, D.V. Ishchenko, I.O. Akhundov, V.A. Golyashov, A.E. Klimov, S. P. Suprun, E. V. Fedosenko, V.N. Sherstyakova, A.G. Rybkin, O.Yu. Vilkov, O. E. Tereshchenko, *Applied Surface Science*, **569** (2021) 150930.
[4] Y. Tanaka, Z. Ren, T. Sato, K. Nakayama, S. Souma, T. Takahashi, K. Segawa, Y. Ando, *Nat. Phys.*, **8** (2012) 800.
[5] R. D. Zhong, J. A. Schneeloch, T. S. Liu, F. E. Camino, J. M. Tranquada, G. D. Gu, *Physical Review B*, **90** (2014) 020505.
[6] A. Sulich, E. Łusakowska, W. Wołkanowicz, P. Dziawa, J. Sadowski, B. Taliashvili, T. Wojtowicz, T. Story, J. Z. Domagala, *Journal of Materials Chemistry C*, **10** (2022) 3139.

B-65

WPŁYW DOKŁADNOŚCI FUNKCJI FALOWEJ NA JAKOŚĆ MULTIPOLOWEJ REPREZENTACJI CZĄSTECZKI

Vladislav Ignatev, Paulina M. Dominiak

Biological and Chemical Research Centre, Wydział Chemii, Uniwersytet Warszawski, ul. Żwirki i Wigury 101, 02-089, Warszawa, Polska

Najprostszym oraz najczęściej używanym modelem w udokładnianiu danych dyfrakcji rengenowskiej jest model niezależnych atomów (independent atom model, IAM), w którym atomy są traktowane jako sferyczne centra rozpraszania. Bardziej zaawansowane modele przedstawiają rozpraszające atomy jako asferyczne obiekty, i jednym z najlepszych przykładów takiego modelu jest Model Multipolowy (MM) [**1**], który używa sumę harmonik sferycznych (t.z. ekspansja multipolowa) do przedstawienia gęstości elektronowej atomu. Model multipolowy jest podstawą banku MATTS (Multipolar Atom Types from Theory and Statistical clustering) [**2**], banku danych asferycznych typów atomów, którę reprezentują uśrednione parametry atomów w pewnym otoczeniu chemicznym i mogą być użyte do szybkiej i dokładnej rekonstrukcji gęstości elektronowej cząsteczki.

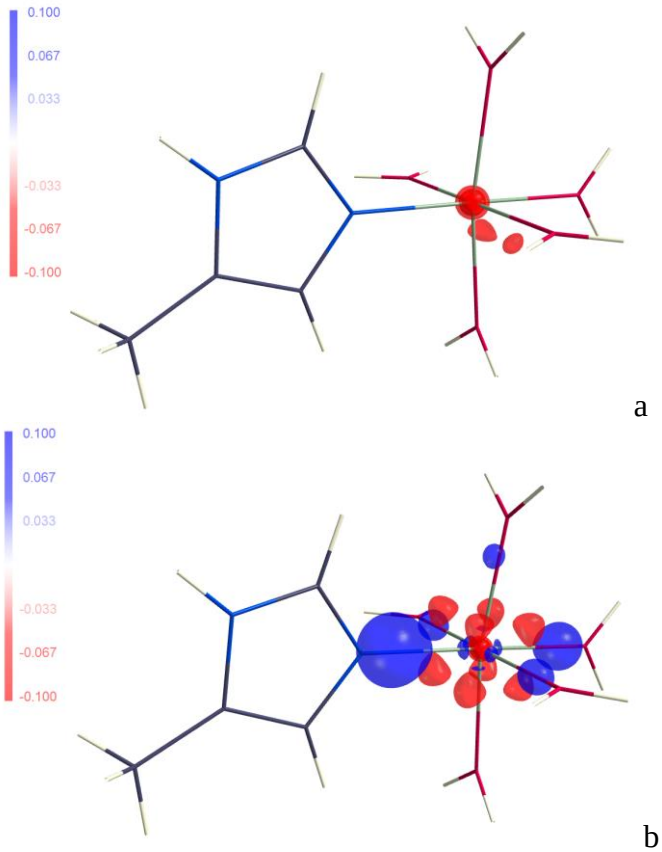

Rys. 1. Gęstość deformacyjna (MM minus IAM, odcięcie 0.1 e/Å^3) atomu Mg w kompleksie $[Mg(H_2O)_5His]^{2+}$; **a** – na podstawie obliczeń w bazie 6-31G**, **b** - na podstawie obliczeń w bazie UGBS1P.

B-65

Jednym z kroków dodawania danych do banku MATTS jest wyznaczenie gęstości elektronowej cząsteczek modelowych przy użyciu obliczeń kwantowo-chemicznych. Okazuję się, że poziom teorii używanej do obliczenia funkcji falowej znacznie wpływa na uzyskiwane parametry multipolowe.

W tym badaniu sprawdzaliśmy wpływ bazy (zestaw funkcji reprezentujący elektronową funkcje falową) w ramach metody DFT z funkcjonałem B3LYP i różnych strategii udokładniania na jakość multipolowej reprezentacji cząsteczki. Obiektem badań były oktaedryczne międzycząsteczkowe kompleksy Mg^{2+}. Jednym z najważniejszych wyników pracy jest wniosek, że w ramach metod używanych przez nas najbardziej odpowiednimi bazami są bazy typu split-valence triple-zeta [**3**].

Literatura

[1] Hansen, N. K., Coppens, P. *Acta Cryst. Section A,* **34** (6) (1978) 909–921, https://doi.org/10.1107/S0567739478001886

[2] Paulina M. Rybicka, *et. al*., *J. Chem. Inf. Model*., **62** (16) (2022) 3766–3783, https://doi.org/10.1021/acs.jcim.2c00145

[3] Jensen, F., *WIREs Comput. Mol. Sci*., **3**(3) (2012) 273–295. doi:10.1002/wcms.1123.

Podziękowania

This research was funded by National Science Centre, Poland 2020/39/I/ST4/02904.

B-66

CIF PROSTY PROGRAM DO WIZUALIZACJI PLIKÓW CIF NA URZĄDZENIA Z SYSTEMEM ANDROID

Daniel M. Kamiński

Katedra Chemii Organicznej i Krystalochemii, Wydział Chemii UMCS Lublin

CIF to prosty program do wizualizacji struktur kryształów zapisanych w formacie *.cif na urządzenia z systemem Android. Program może pokazywać część asymetryczną komórki elementarnej, powielać ją przez elementy symetrii oraz rozbudowywać ją translacyjnie w kierunkach x, y, z. Dodatkowo w programie można dokonywać prostych pomiarów odległości (długości wiązań), kątów oraz wyszukiwać wiązania wodorowe. Program pozwala prezentować dane w postaci sfer, kulek, prętów oraz elipsoid (Rys. 1). Otrzymane obrazy można zapisać bezpośredni do pamięci urządzenia.

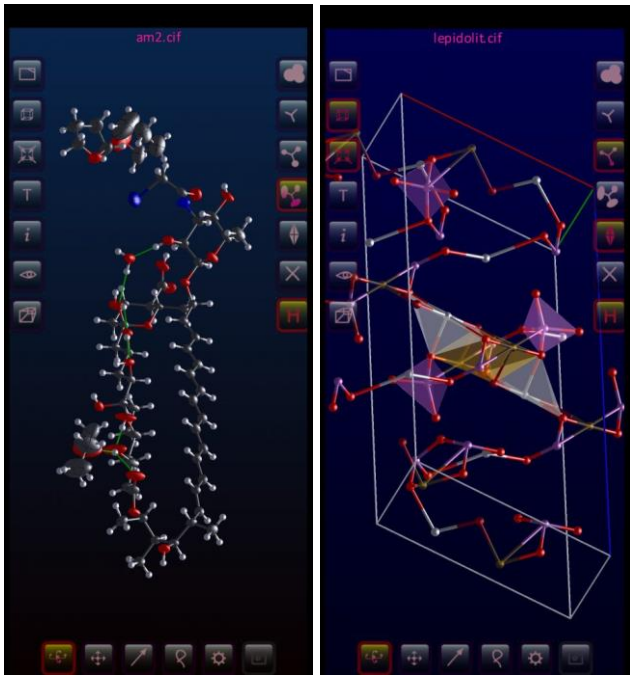

Rys. 1. Przykładowe zrzuty z ekranu programu CIF.

Głównym zadaniem projektu jest udostępnienie kodu umożliwiającego tworzenie własnych aplikacji związanych z krystalografią (np. odczyt plików CIF, wprowadzenie operacji na grupach przestrzennych oraz prawidłową prezentację obliczeń 3D). Licencja GNU projektu umożliwia wykorzystanie jego bibliotek we własnych programach [1]. Więcej informacji o projekcie można znaleźć na stronie programu [2].

Literatura

[1] www.github.com/DanielKami/cf
[2] www.dkami.umcs.pl/programs/cif/

B-67

CRYOMICROSCOPY AND ELECTRON DIFFRACTION CORE FACILITY – HIGH QUALITY DATA WITH GLACIOS MICROSCOPE

Szymon Sutuła,[1,2,3] Tomasz Góral,[1] Barbara Olech,[1,2,3] Krzysztof Woźniak[1,2,3]

[1] Cryomicroscopy and Electron Diffraction Core Facility, Centre of New Technologies, University of Warsaw, Banacha 2C, 02-097 Warsaw, Poland
[2] Biological and Chemical Sciences Research Centre, University of Warsaw, Żwirki i Wigury 101, 02-089 Warsaw, Poland
[3] Department of Chemistry, University of Warsaw, Pasteura 1, 02-093 Warsaw, Poland

In 2019 University of Warsaw installed one of the first cryo-EM microscopes in the country – the 200kV Glacios equipped with a Falcon3EC camera and a phase plate solution. In the next few years the Cryomicroscopy and Electron Diffraction Core Facility has been established and started providing many local structural biologists and chemists with a direct access to this ground-breaking and Noble-winning cryo-EM technology. To date, there have been only two cryo-EM Core Facilities operating in Poland which provide services in all cryo-EM modalities.

We show the current possibilities of our Core Facility and a range of services which are offered to our users. We follow the open-access policy and welcome users from both national and international academic institutions as well as industry. Our recent developments include benchmarking the Single Particle Analysis reconstruction of apoferritin at the 1.92Å level with local resolution reaching 1.65Å (Fig. 1) and 2.27Å reconstruction of the AbiK bacterial polymerase. The results are further enhanced with the upgrade of the microscope to the micro-ED functionality allowing for a structure determination of small molecules based on electron diffraction data. Even with a kinematic approach it is possible to successfully refine crystal structures with no needed restraints with only microcrystals available (Fig. 2). On top of that, we have recently started a process of building €0.5M-worth IT infrastructure support for the cryo-EM data storage (up to 1.6 PB) and expanding on the data processing capabilities which will be a unique set-up of its kind not only in Poland but also in Central Europe. We also show that being able to offer all cryo-EM modalities in one instrument significantly boosts a research potential and opens up new application possibilities.

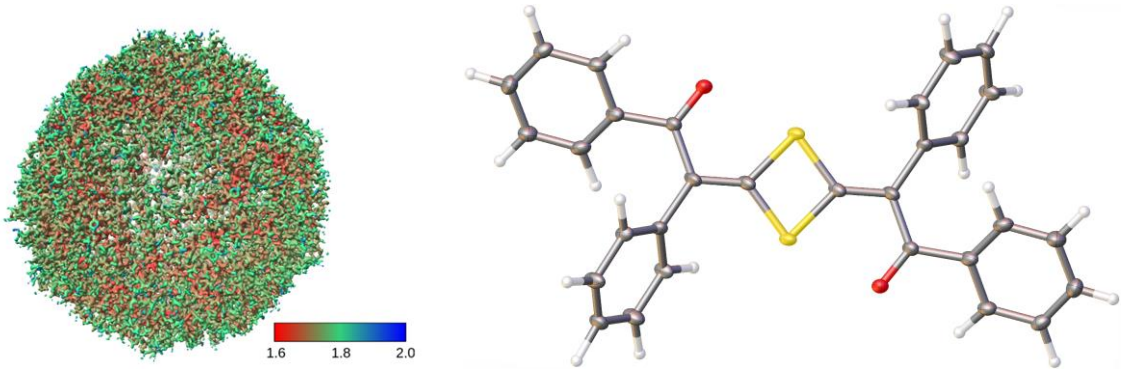

Fig. 1. Reconstruction of apoferritin at 1.92Å resolution reaching locally 1.65Å (left) and refined structure based on micro-ED microcrystal experiment (right).

B-68

CRYSTAL STRUCTURE OF $Ni_{2.894}Te_2$

Lubomir Gulay[1], Marek Daszkiewicz[2], Adam Pietraszko[2]

[1] Department of Chemistry and Technology, Lesya Ukrainka Volyn National University, Lutsk 43009, Ukraine
[2] Institute of Low Temperature and Structure Research, Polish Academy of Sciences, Okólna 2, 50-950 Wrocław, Poland

The existence of several phases at ~Ni_3Te_2 composition has been reported in Refs. [1, 2]. A metal deficient Cu_2Sb structure type (space group *P4/nmm*) for $Ni_{3\pm q}Te_2$ exists above 573 K. The orthorhombic phase related to tetragonal one (Cu_2Sb structure type) has been observed between 423 and 573 K. Below 423 K the monoclinic and orthorhombic $2a\times b\times c$ or tetragonal $2a\times c$ superstructures were observed. Crystal structure of monoclinic and orthorhombic $2a\times b\times c$ superstructures has been determined in Ref. [3]. Tetragonal $2a\times c$ superstructure was observed for slowly cooled sample with composition $NiTe_{0.69}$ (~$Ni_{59}Te_{41}$).

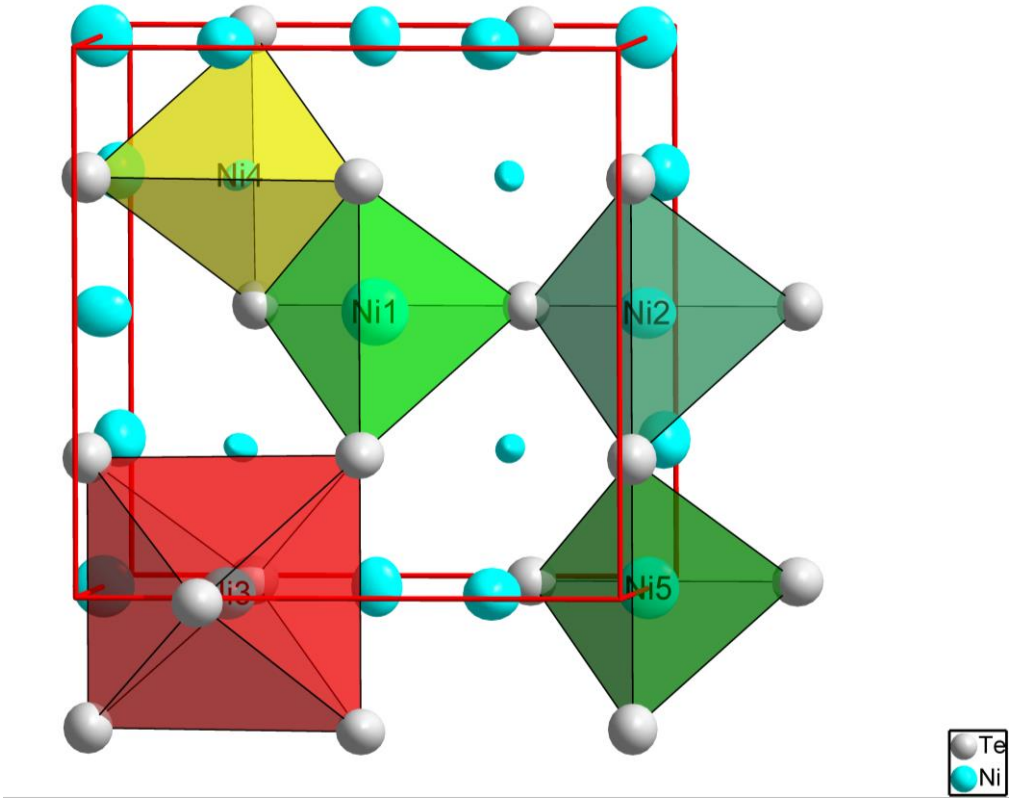

The alloy with the $Ni_{59}Te_{41}$ composition was prepared by fusion of the high purity elements (Ni - 99.92 wt. %, Te - 99.99 wt. %) in evacuated quartz ampoule. The synthesis was realized in a shaft furnace with the heating rate of 30 K/h. The maximal temperature of the synthesis was about 1370 K. The sample was kept at maximal temperature during 4 hours and cooled slowly (10 K/h) to room temperature.

B-68

Small single crystal suitable for crystal structure investigation was selected. The composition of single crystal was confirmed by EDX analysis (EDAX PV9800 microanalyzer). The X-ray intensities data were collected on a KUMA Diffraction KM-4 four-circle diffractometer equipped with a CCD camera (graphite-monochromatized MoK_α radiation, λ = 0.71073 Å). The raw data were treated with the CrysAlis Data Reduction program taking into account an absorption correction. The intensities of the reflections were corrected for Lorentz and polarization factors. The crystal structure determination was performed using JANA2006 program [4].

The $Ni_{2.894}Te_2$ compound crystallizes in tetragonal unit cell (space group *P*-4*m*2, *a* = 7.4937(6), *c* = 6.0275(5) Å, *R*1 = 0.0326, *wR*2 = 0.0755). $Ni_{2.894}Te_2$ represents a 2*a* × *c* superstructure of a metal deficient Cu_2Sb-related structures. The ordering of the Ni atoms and vacancies take place in the structure of $Ni_{2.894}Te_2$. The Te atoms in $Ni_{2.894}Te_2$ are stacked in a close-packed arrangement with layers in the sequence *ABC* (distorted cubic close packing). The Ni atoms (Ni3) occupy half of octahedral interstices formed by Te atoms. Remaining Ni atoms (Ni1, Ni2, Ni4 and Ni5) are located in half of tetrahedral interstices formed by Te atoms and occupy ~47 % of them.

Literature

[1] J. Barstad, F. Grønvold, E. Røst, E. Vestersjø, *Acta Chem. Scand*., **20** (1966) 2865.
[2] A.L.N. Stevels, *Philips Res. Rep. Suppl.*, **9** (1969) 1–128.
[3] L. D. Gulay, I. D. Olekseyuk, *J. Alloys Compd.*, **376** (2004) 131.
[4] V. Petricek, M. Dusek, L. Palatinus, *Z. Kristallogr*., **229**(5) (2014) 345.

B-69

PHASE TRANSITIONS IN MIXED-CATION $MA_{1-x}EA_xPbI_3$ PEROVSKITES

Anna Gągor*[a], Dawid Drozdowski[a], Mirosław Mączka[a], Mantas Simenas[b]

[a] W. Trzebiatowski Institute of Low Temperature and Structure Research Polish Academy of Sciences, Okólna 2, 50-950 Wrocław, Poland
[b] Faculty of Physics, Vilnius University, Sauletekio 3, LT-10257Vilnius, Lithuania

**e-mail: a.gagor@intibs.pl*

Hybrid methylammonium (MA) lead halide perovskites have gained significant attention as efficient photovoltaic materials. They exhibit remarkable power conversion efficiency and possess key physical properties that contribute to their high performance [1]. However, the dynamics of molecular cations and structural phase transitions can influence their properties and device operation. Mixing different A-site cations in perovskite compositions enhances both performance and stability [2]. Despite numerous studies on mixed lead halide perovskites, the effects of cation mixing on structural phases, phase transitions, and cation dynamics remain less understood.

This study investigates the mixed-cation $MA_{1-x}EA_xPbI_3$ perovskite system. The inclusion of ethylammonium (EA) cations in the hybrid compounds offers improved stability and photovoltaic performance. Pure EA-based perovskite crystallizes in orthorhombic symmetry, but its structural phase transitions are not well-documented. In contrast, the phase transitions of pure MA-based perovskite are well-known. The research reveals that mixing $MA_{1-x}EA_xPbI_3$ stabilizes the cubic phase and significantly reduces the temperatures of structural phase transitions. At higher EA concentrations ($x \gtrsim 0.3$) , the low-temperature phase transition is completely suppressed, resulting in the formation of a new tetragonal phase with a different symmetry. Upon further increase of x, the phase separation is observed, indicating that the EA solubility limit in $MAPbI_3$ is about 40% [3]. The investigation of crystal structure and phase transitions in hybrid perovskites, similar to conventional oxide perovskites, poses challenges due to intricate twinning caused by symmetry breaking, and additionally, the intricate amine ordering process with temperature lowering. Here we use the combined powder and single crystal x-ray diffraction to solve the (x,T) phase diagram for $MA_{1-X}EA_XPbI_3$.

The presence of EA in the structure increases the rotation barrier of the MA cations and tunes the dielectric permittivity values. However, the permittivity value at low temperatures remained relatively high ($\varepsilon' \sim 50$), indicating the lattice's polarizability by the lone-pair electrons of the lead cations. This behaviour appears to be universal among lead-based hybrid perovskites. For the highest EA levels, the signatures of the dipolar glass phases are observed.

Literature

[1] Snaith, H. J. Perovskites: The Emergence of a New Era for Low-Cost, High-Efficiency Solar Cells. *J. Phys. Chem. Lett.*, **4** (2013) 3623–3630, DOI: 10.1021/jz4020162.
[2] Wu, C.; Chen, K.; Guo, D. Y.; Wang, S. L.; Li, P. G. Cations Substitution Tuning Phase Stability in Hybrid Perovskite Single Crystals by Strain Relaxation. *RSC Adv*., **8** (2018) 2900– 2905, DOI: 10.1039/c7ra12521f.
[3] Simenas, M., Balciunas, S., Gągor, A., (..) Mączka, M., and Banys, J., *Chem. Mater*., **34**(22) (2022) 10104–10112; https://doi.org/10.1021/acs.chemmater.2c02807.

B-70

FROM STRUCTURE TO EMISSION: A DEEP DIVE INTO THE FLUORESCENCE PROPERTIES OF 8-HYDROXYQUINOLINE AND 5,7-DICHLORO-8-HYDROXYQUINOLINE OIHMS

Marta Bogdan, Tomasz Sierański, Marcin Świątkowski i Agata Trzęsowska-Kruszyńska

Instytut Chemii Ogólnej i Ekologicznej, Politechnika Łódzka, ul. Żeromskiego 116, 90-924 Łódź

The study of organic-inorganic hybrid materials (OIHMs) based on 8-hydroxyquinoline (8-hq) and 5,7-dichloro-8-hydroxyquinoline (8-hqCl_2) offers a promising avenue for advancing our understanding of luminescent materials and their potential applications. Our studies have provided valuable insights into the luminescent properties of these compounds. By focusing on non-covalent interactions, the supramolecular approach has emerged as an effective way to design structures with variable luminescent properties. The fluorescence properties of these materials can be fine-tuned by controlling non-covalent interactions, such as hydrogen bonding, π-π interactions, and ion-π interactions. These OIHMs present a fascinating study in structural and electronic diversity, with their fluorescence characteristics varying to reflect their properties[1].

8-hq, a small and planar molecule, is an example of a structure with a broad spectrum of applications in medicine[2], analytical chemistry[3], and optoelectronic materials[4]. However, its fluorescence properties can be significantly altered by factors such as the presence of water molecules in the crystal lattice, which can quench fluorescence[5,6]. The use of inorganic species significantly changes the spectroscopic and luminescent properties of 8hq-based systems. Similarly, 8hqCl_2 demonstrates fluorescence properties[7,8], making it an interesting candidate for diverse applications, including utilization in light-emitting diodes (LEDs) and sensors. The intricate relationships between different types of interactions, such as hydrogen bonding, π-π stacking, ion-π and solvent interactions, can dramatically influence the photophysical properties of a system.

For 8-hq compounds, fluorescence is observed in most cases, with two fluorescence maxima characterized by different excitation wavelengths and the same emission wavelength. The unprotonated 8-hq, however, does not exhibit fluorescence in the solid state due to the ESIPT process resulting from intramolecular O-H•••N hydrogen bonding[9]. On the other hand, 8-hqCl_2 compounds show varying fluorescence characteristics, with some demonstrating two emission maxima and others only one. The fluorescence process is associated with the π-π* excitations involving the electron density of the entire 8-hqCl_2 ligand. A notable difference is observed in the fluorescence intensity of its salts: 8-hqCl_2HBr and 8-hqCl_2HCl, with the latter exhibiting complete fluorescence quenching due to the presence of water molecules in the solid-state structure. Interestingly, in zinc, mercury, and cadmium 8-hqCl_2 compounds, the fluorescence intensity of bromides exceeds that of chlorides, attributed to pronounced anion-π interactions and subtly distinct interactions with water molecules.

Our research underscores the importance of understanding the complex interplay between various factors that can influence fluorescence. The findings hold potential

implications for the design and optimization of systems for specific optical applications, providing a basis for the development of new materials with tailored properties and the manipulation of existing systems to achieve improved or novel functionality.

Literatura

[1] M. Bogdan, T. Sierański, M. Świątkowski, A. Trzęsowska-Kruszyńska, *CrystEngComm*, **20** (2023) 1993.
[2] V. Prachayasittikul, S. Prachayasittikul, S. Ruchirawat, V. Prachayasittikul, *Drug Des. Devel. Ther*., **7** (2013) 1157.
[3] T. Moeller, A. Cohen, *Anal. Chem*., **22** (1950) 686.
[4] M. Albrecht, M. Fiege, O. Osetska, *Coord. Chem. Rev*., **8-9** (2008) 812.
[5] J. Maillard, K. Klehs, C. Rumble, E. Vauthey, M. Heilemann, A. Fürstenberg, *Chem. Sci*., **12** (2021) 1352.
[6] R. Ayscue, V. Vallet, J. Bertke, F. Réal, K. Knope, *Inorg. Chem*., **60** (2021) 9727.
[7] Y. Fazaeli, M. Amini, E. Najafi, E. Mohajerani, M. Janghouri, A. Jalilian, S. Ng, *J. Fluoresc*., **22** (2012) 1263.
[8] Z. Yang, D. Shao, G. Zhou, *J. Chem. Eng. Data*, **64** (2019) 5057.
[9] Y. Liu, S. Wang, C. Zhu, S. Lin, *New J. Chem*., **41** (2017) 8437.

SESJA NAUKOWA
SEKCJI MŁODYCH KRYSTALOGRAFÓW PTKryst
SCIENTIFIC SESSION OF THE PCA
YOUNG CRYSTALLOGRAPHERS SECTION

CRYSTAL STRUCTURE OF A MONONUCLEAR ZINC(II) COMPLEX WITH SCHIFF BASE

Hubert Kleinschmidt, Anna Dołęga and Magdalena Siedzielnik

Department of Inorganic Chemistry, Faculty of Chemistry, Gdansk University of Technology, G. Narutowicz 11/12, 80-233 Gdańsk

From catalysts to corrosion inhibitors and antiseptics, Schiff bases and their metallic complexes boast a broad range of applications. With each passing year, new synthesis methods with properties of these compounds are discovered by the scientific community. Notably, zinc complexes have demonstrated use in catalyzing polymerization reactions as well as in light-emitting diodes [1-4].

Within this study, new mononuclear complex **C1** with the formula of [Zn(**L1**)$_2$] (**HL1**: 2-(4-methylpyridin-2-ylimino)methyl)-6-methoxyphenol) has been synthesised and characterized by X-ray diffraction analysis.

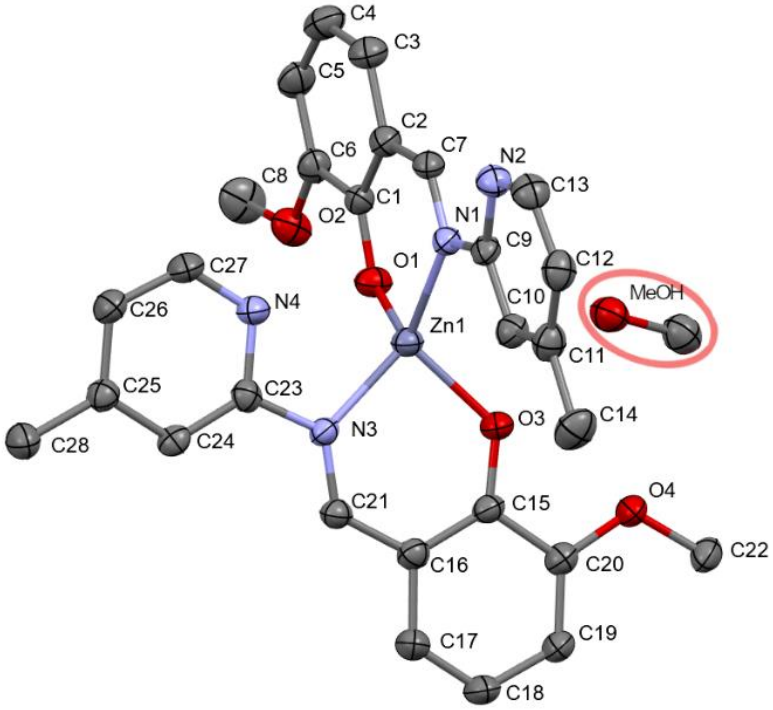

Fig. 1. Molecular structure of **C1**. Thermal ellipsoids at 50%. Hydrogen atoms and have been omitted and a methanol molecule has been highlighted for clarity.

Table 1. Selected geometric parameters

Bond length [Å]			
N1—Zn1	1.998(3)	O1—Zn1	1.917(3)
N3—Zn1	1.995(3)	O3—Zn1	1.952(3)
Angles [º]			
O1—Zn1—O3	112.72(12)	O1—Zn1—N1	97.55(12)
O1—Zn1—N3	113.15(12)	O3—Zn1—N1	113.80(11)
O3—Zn1—N3	92.55(11)	N3—Zn1—N1	127.81(12)

The compound was obtained by reacting the previously synthesised Schiff base (**L1**) with zinc acetate in methanol followed by the addition of Et_3N. [5] Crystals suitable for X-ray analysis were obtained at +4°C. In the unit cell alongside the complex molecule a methanol molecule is found.

The crystallographic data for the title compound were collected on an STOE IPDS 2T diffractometer at 120.0 K using Mo Kα radiation of a microfocus X-ray source. **C1** crystallizes in a triclinic system in P1 space group. The unit cell parameters are as follows: a = 9.5075(10) Å, b = 11.1738(12) Å, c =14.2108(16)Å, α = 108.585(9), β = 102.931(9)°, γ = 93.804(9), V= 1379.1(3)Å^3 and Z= 2. Quality parameters of the solution are $R_1[I > 2\sigma(I)]$= 0.057, wR_2 = 0.196, R_{int}=0.068, GOOF= 1.13. Asymmetric unit contains complex molecule and one methanol molecule.

Obtained substance is a mononuclear zinc(II) complex, where two imine molecules are coordinated to the zinc as a center atom. Zinc atom forms four bonds to its neighbor atoms in tetrahedral geometry. The lengths of nitrogen-zinc and oxygen-zinc bonds are in accordance with those founded in the literature.

Literature

[1] Prakash, A., & Adhikari, D. (2003). Application of Schiff bases and their metal complexes-A Review.
[2] Afshari, F., Ghomi, E.R., Dinari, M., & Ramakrishna, S. (2023). ChemistrySelect.
[3] Ceramella, J., Iacopetta, D., Catalano, A., Cirillo, F., Lappano, R., & Sinicropi, M.S., *Antibiotics*, **11** (2022) 191.
[4] Gusev, A., Kiskin, M.A., Braga, E.V., Kryukova, M.A., Baryshnikov, G.V., Karaush-Karmazin, N.N., Minaeva, V., Minaev, B.F., Ivaniuk, K., Stakhira, P., Ågren, H., & Linert, W. *ACS Applied Electronic Materials*, **3**(8) (2021) 3436–3444.
[5] Siedzielnik, M., Pawłowska, M., Daśko, M., Kleinschmidt, H., & Dołęga, A. *RSC Advances*, **13** (2023) 8830–8843

S-2

ANALIZA WŁAŚCIWOŚCI FOTOPRZEŁĄCZALNYCH NOWO OTRZYMANYCH KOMPLEKSÓW Ni(II) I Pd (II) ZAWIERAJĄCYCH GRUPĘ NITROWĄ ORAZ N,N,O-DONOROWY LIGAND POMOCNICZY

Kacper Paszczyk, Katarzyna N. Jarzembska, Adam Krówczyński

Wydział Chemii Uniwersytetu Warszawskiego, ul. Żwirki i Wigury 102, 02-089 Warszawa

Foto- i termoprzełączalne związki chemiczne mogą mieć rozmaite zastosowania m.in. w fotowoltaice i fotonice. Głównym celem przeprowadzonych badań oraz analizy było zbadanie wspomnianych właściwości w przypadku dwóch nowych, potencjalnie fotoprzełączalnych kompleksów w formie kryształów. N,N,O-donorowe kompleksy Ni(II) oraz Pd(II) o płasko-kwadratowej geometrii sfery koordynacyjnej centrum metalicznego otrzymano zgodnie z procedurą opisaną w literaturze [1]. Ich struktury przedstawiono na rysunku 1.

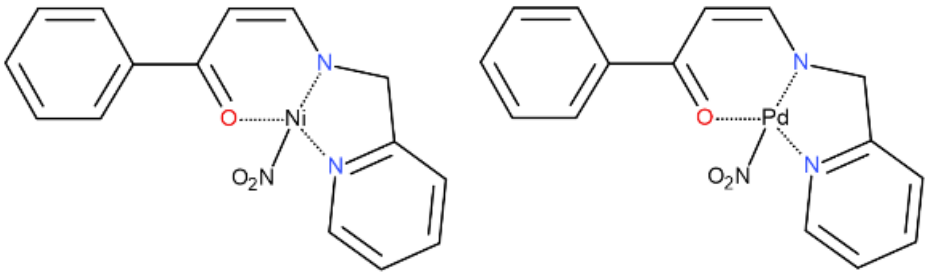

Rys. 1. Struktury badanych kompleksów, Ni-1a oraz Pd-1a.

Dla obu analogów przeprowadzono krystalizacje z kilku rozpuszczalników otrzymując kryształy różnej jakości oraz wielkości. W przypadku obu kompleksów jedna forma krystaliczna okazała się dominująca. Warto zaznaczyć, że dla Pd-1a otrzymano również pojedyncze kryształy dwóch innych odmian polimorficznych i dwóch solwatomorfów (z DCM oraz CH_3Cl).

Podstawowe formy krystaliczne zbadano przy pomocy spektroskopii IR w ciele stałym pod kątem właściwości fotoprzełączalnych. Bazując na tych wynikach zaplanowano i przeprowadzono serie eksperymentów fotokrystalograficznych [2]. Kryształy związków niklowego (Ni-1a) i palladowego (Pd-1a) naświetlano światłem o długości fali odpowiednio w 530 nm i 470 nm w różnych temperaturach, aby oszacować maksymalną konwersję oraz zbadać relaksację czasową i temperaturową. W przypadku Ni-1a potwierdzono bliską całkowitej fototizomeryzację w przypadku obu metod, natomiast dla Pd-1a potwierdzono całkowitą fotoizomeryzację w cienkim filmie za pomocą spektroskopii w podczerwieni i uzyskano ponad 85%-ową konwersję w przypadku próbki monokrystalicznej. W kryształach obu związków obserwuje się transformację grupy nitrowej do połączenia *endo*-nitrito. Dla podstawowej struktury Pd-1a w komórce elementarnej o symetrii $P2_1/n$ znajdują się dwie cząsteczki nierównoważne symetrycznie, z których tylko jedna ulega fotoizomeryzacji.

S-2

Podziękowania dla grantu SONATA BIS (2020/38/E/ST4/00400) za wsparcie finansowe.

Literatura

[1] Dabrowski, J.; Krówczyński, A. Ni(II) complexes with bis(β-acylvinyl)amines and (8-quinolyl-β-acylvinyl)amineshome laboratory. *J. Appl. Crystallogr.*, **49** (2016) 1383–1387.
[2] Kamiński, R.; Jarzembska, K.N.; Kutyła, S.E.; Kamiński, M.A. portable light-delivery device for in situ photocrystallografic experimets at home laboratory. *J. Appl. Crystallogr*., **49** (2016) 1383-1387.

S-3

POLIMORFIZM I MECHANOCHROMIZM – RÓŻNORODNOŚĆ LUMINESCENCJI BOROORGANICZNEGO KOMPLESKU 2-PIRYDYLOFENOLU

Dawid R. Natkowski[a], Paulina H. Marek-Urban[a,b], Karolina Wrochna[a], Krzysztof Woźniak[b], Krzysztof Durka[a]

[a] *Wydział Chemiczny, Politechnika Warszawska, ul. Noakowskiego 3, 00-664 Warszawa*
[b] *Wydział Chemii, Uniwersytet Warszawski, ul. Pasteura 1, 02-093 Warszawa*

Badania nad czterokoordynacyjnymi kompleksami boroorganicznymi opartymi na rdzeniu sulfonowym (**SO2**) i 2-pirydylofenolu (**pp**) uwidoczniły tworzenie się dwóch form polimorficznych tego kompleksu. Wyznaczone przy użyciu obliczeń periodycznych energie kohezji oraz przeprowadzone badania DSC pozwoliły określić formę alfa jako kinetyczną oraz beta jako termodynamicznie trwalszą. Wyodrębnione formy krystaliczne wykazywały istotne różnice we właściwościach luminescencyjnych takich jak maksima emisji fluorescencji, wynoszące odpowiednio 448 nm (niebieska emisja) i 488 nm (zielona emisja), oraz wydajności kwantowe na poziomie 69 % i 36 %. Kluczowym czynnikiem wpływającym na właściwości luminescencyjne opisywanych form jest odmienna, znacząco się różniąca konformacja molekuł, co potwierdzono na drodze obliczeń DFT i TD-DFT. Obie z form polimorficznych wykazują niezależnie zjawisko mechanochromizmu. Co ciekawe, maksimum pasma emisji formy alfa ulega hipsochromowemu, podczas gdy formy beta batochromowemu przesunięciu podczas ucierania, w obu przypadkach prowadząc do otrzymania materiału o turkusowej barwie emisji. Powrót do czystych form alfa i beta jest możliwy po ogrzaniu próbek. Obserwacje udało się zracjonalizować częściową amorfizacją materiału proszkowego zachodzącą podczas ucierania. Forma amorficzna kompleksu **SO2-pp** charakteryzuje się bowiem odmiennymi własnościami luminescencyjnymi od obu form krystalicznych (478 nm, emisja turkusowa).

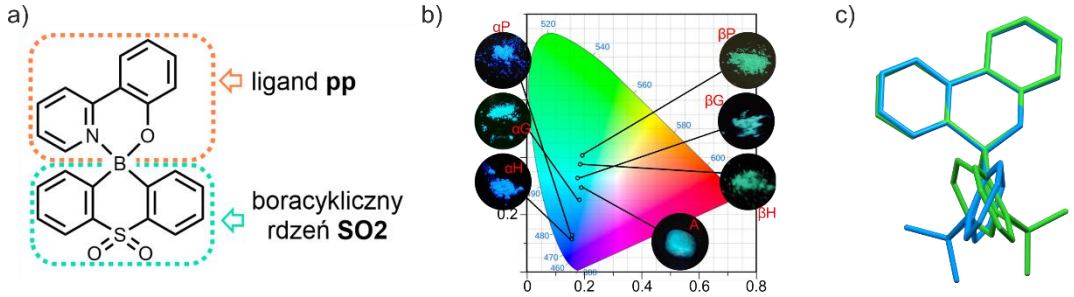

Rys. 1. a) Schemat badanego kompleksu. b) Diagram CIE 1931 ze zdjęciami badanych odmian kompleksu w świetle UV (360 nm). c) Nałożenie geometrii molekuł dwóch struktur polimorficznych.

Finansowanie badań w ramach projektu OPUS 20 „Efektywne fotouczulacze oparte na sztywnych układach boroorganicznych jako generatory tlenu singletowego” (2020/39/B/ST4/02370).

S-4

ANALIZA ODDZIAŁYWAŃ MIĘDZYCZĄSTECZKOWYCH W STRUKTURZE 1,3-DIACETYLOPIRENU NA PODSTAWIE DYFRAKCJI W ZMIENNYCH WARUNKACH TEMPERATURY ORAZ CIŚNIENIA.

Aleksandra Zwolenik, Anna Makal

Uniwersytet Warszawski, Wydział Chemii, Ludwika Pasteura 1, 02-093 Warszawa

Pochodne pirenu wykazują ciekawe właściwości elektroniczne i fotofizyczne, dlatego są intensywnie badane pod kątem szerokiego zakresu zastosowań. Dzięki obecności oddziaływań typu π-stacking są dobrym przykładem półprzewodników organicznych, a ich właściwości fluorescencyjne sprawiają, że są powszechnie stosowane jako barwniki, m.in. do badań strukturalnych białek, DNA lub błon lipidowych. Diacetylopochodne pirenu wykazują wiele odmian polimorficznych, co dodatkowo zwiększa możliwość ich zastosowań. Są to dobre układy modelowe co sprawia, że ich analiza może pomóc w zrozumieniu jak działają podobne, ale większe i bardziej skomplikowane układy.

Pierwotnie w literaturze znana była tylko jedna odmiana polimorficzna 1,3-diacetylopirenu [1]. Udało się otrzymać nową odmianę tego związku, wykonać eksperyment dyfrakcyjny oraz stworzyć model jego struktury krystalicznej z wykorzystaniem udokładnienia z użyciem asferycznych atomowych czynników rozpraszania. W tej pracy skupiono się na przeanalizowaniu oddziaływań międzycząsteczkowych występujących w strukturze 1,3-diacetylopirenu oraz sprawdzenie, jak ich zmiany wpływają na zmiany właściwości fizykochemicznych. W tym celu, wykonano serię eksperymentów dyfrakcyjnych w szerokim zakresie temperatur (od 90 do 390 K), a także umieszczono badany związek w kowadełku diamentowym typu Merilla-Basseta i wykonano eksperymenty pod zwiększonym ciśnieniem (od 0 do 1.7 GPa przyłożonego ciśnienia). Struktury eksperymentalne uzyskane pod zwiększonym ciśnieniem porównano z teoretycznymi strukturami (z zakresu od 0 do 4.08 GPa przyłożonego ciśnienia), które uzyskano z obliczeń periodycznych wykonanych w programie crystal17. Policzono również wartości energii oddziaływań za pomocą metod przybliżonych w programie CrystalExplorer. Wyniki kluczowych punktów pomiarowych zostały zwizualizowane m.in. za pomocą tzw. „Energy frameworks” [2], co pozwoliło na powiązanie najważniejszych oddziaływań z kierunkami maksymalnej I minimalnej ściśliwości. Na podstawie zebranych danych stwierdzono, które oddziaływania najbardziej stabilizują strukturę 1,3-diacetylopirenu oraz jak zmiany tych oddziaływań pod wpływem działania siły zewnętrznej wpływają na właściwości fizykochemiczne badanego związku, np. jego barwy czy widma luminescencji.

Literatura

[1] S. K. Rajagopal, A. M. Philip, K. Nagarajan, M. Hariharan, *Chem. Commun.*, **50**(63) (2014) 8644–8647.

[2] C. F. Mackenzie, P.R. Spackman, D. Jayatilaka, M. A. Spackman, *IUCrJ*, **4**(5) (2017) 575–587.

Finansowanie projektu: dotacja wewnętrzna nr PSP 501-D112-01-1120000 zlecenie 5011000317

S-5

KOMPLEKSY BODIPY O BUDOWIE *SPIRO* Z ROZBUDOWANYM UKŁADEM WIĄZAŃ SPRZĘŻONYCH – DROGA DO SKUTECZNEJ TERAPII FOTODYNAMICZNEJ

Karolina Wrochna[a,*], Paulina H. Marek-Urban[a,b], Karolina Urbanowicz[a], Krzysztof Woźniak[b], Krzysztof Durka[a]

[a] *Wydział Chemiczny, Politechnika Warszawska, ul. Noakowskiego 3, 00-664 Warszawa*
[b] *Wydział Chemii, Uniwersytet Warszawski, ul. Pasteura 1, 02-093 Warszawa*

**e-mail: wrochna.karolina@o2.pl*

Terapia fotodynamiczna (PDT) to innowacyjna metoda leczenia zmian nowotworowych,[1] która wykorzystuje trzy czynniki: światło, tlen oraz fotouczulacz.[2] Wzbudzone cząsteczki fotouczulaczy przechodzą do stanów trypletowych, dzięki czemu mogą oddziaływać z cząsteczkami tlenu generując jego reaktywne formy (ROS). Kluczowym jest odpowiednie zaprojektowanie fotouczulacza, by zwiększyć efektywność przejścia międzysystemowego (ISC), zapewnić odpowiednią rozpuszczalność w środowisku biologicznym i możliwość wzbudzania światłem czerwonym („optyczne okno tkanki").[3] Badania prowadzone w zespole dowodzą o wysokich wydajnościach generowania $^1O_2$ kompleksów BODIPY o budowie *spiro* zawierających rdzeń 9-borafluorenu.[4]

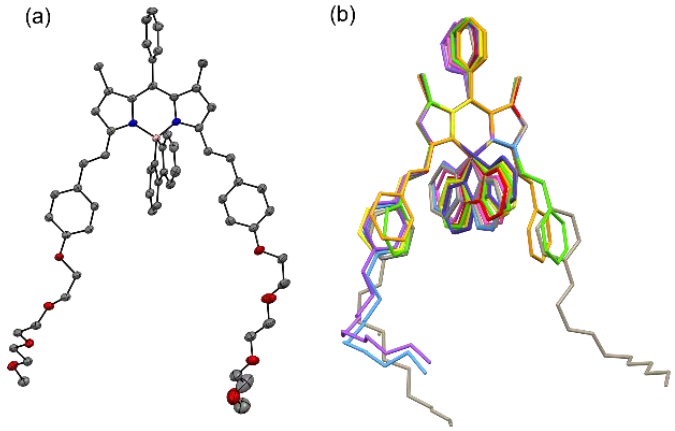

Rys. 1. (a) Rysunek ORTEP jednej z analizowanych struktur oraz (b) nałożenia struktur analizowanych kompleksów.

W odpowiedzi na wyzwania stawiane przez PDT zaprojektowaliśmy oraz otrzymaliśmy nowe kompleksy BODIPY o budowie *spiro*, cechujące się rozszerzonym układem wiązań π-sprzężonych oraz zwiększoną wodorozpuszczalnością. Przeprowadzone przez nas badania fotokatalityczne i fotostabilności, pozwoliły na ocenę potencjału fotouczulaczy. Istotnym elementem charakterystyki było określenie struktur krystalicznych otrzymanych związków. Zaobserwowano, że badane układy wykazują tendencję do tworzenia form polimorficznych. Podjęto próbę celowej hodowli różnych form krystalicznych kompleksów, w wyniku czego udało się scharakteryzować 9 struktur, w tym 3 pary form polimorficznych oraz pierwszy ko-kryształ molekularny dwóch

różnych kompleksów BODIPY. Analiza porównawcza pozwoliła uwidocznić istotność tworzenia się J-agregatów w strukturach, których kąt poślizgu udało się skorelować z obecnością słabych oddziaływań C–H…C(π). Charakterystykę strukturalną uzupełniono o obliczenia DFT.

Finansowanie badań w ramach projektu OPUS 20 „Efektywne fotouczulacze oparte na sztywnych układach boroogranicznych jako generatory tlenu singletowego” (2020/39/B/ST4/02370).

Literatura

[1] C. A. Robertson, *et.al*, *J. Photochem. Photobiol. B*, **96 (**2009) 1–8.
[2] P. Agostinis, *et.al*, *CA. Cancer J. Clin.*, **61** (2011) 250–281.
[3] A. Kamkaew, *et.al*, *Chem Soc Rev*, **42** (2013) 77–88.
[4] P. H. Marek-Urban, *et.al*,, *J. Org. Chem.*, **86** (2021) 12714–12722.

S-6

TYRAMINE AS A PROLIFIC COFORMER IN CRYSTAL ENGINEERING

Szymon Grabowski[a,b] and Marlena Gryl[a]

[a]Faculty of Chemistry, Jagiellonian University, Gronostajowa 2, Kraków, 30-387 Poland
[b]Doctoral School of Exact and Natural Sciences, Jagiellonian University, Prof. Łojasiewicza 11, Kraków, 30-348 Poland

Prolific cofomers in crystal engineering can be defined as building blocks showing a remarkable ability to create multicomponent solids (co-crystals/salts) with various components. Such molecules are extremely interesting from the crystal engineering perspective as they enable the design of materials containing molecules unwilling to cocrystallize. It is vital to understand the nature of prolific coformers, particularly the interactions formed in their structures. This analysis might lead to a better understanding and controlling the crystallization process.[1,2,3]

Tyramine is a molecule that crystallizes with many components[4], creating a variety of salts and co-crystals reported in the Cambridge Structural Database. Here we present crystal structures of two new organic salts containing tyramine: I – with L-pyroglutamic acid; III – with aminohippuric acid. Results were compared with the known crystal phase of tyraminium (R)-mandelate. Asymmetric units are shown in Fig. 1. In each case, proton transfer occurred between carboxylic and amino groups.

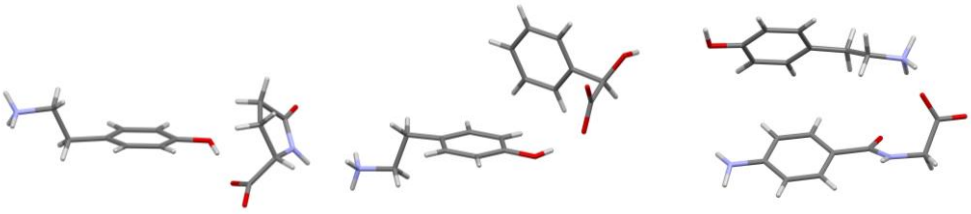

Figure 1. Asymmetric units of (I) – left, (II) – middle and (III) – right.

Structure analysis results showed that the tyramine alkyl chain's conformational flexibility contributes to its prolific performance. In (I), (II) and (III), the torsion angle between atoms in tyramine alkyl chain is different, which indicates the capability of tyraminium cation to fit to another component during molecular self-organization. For each structure also Hirshfeld surface analysis was performed and results were compared to examine possible interaction schemes created by tyramine. Fingerprint plots are shown in Fig. 2.

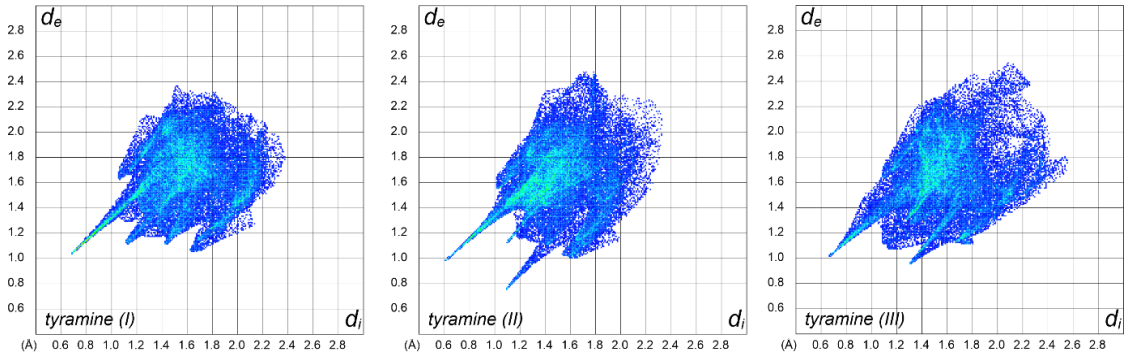

Figure 2. Fingerprint plots for tyramine cation in (I), (II) and (III).

Some differences are visible in the low d_i and d_e values region, where the characteristic spikes should occur. $O_i \cdots H_e$ interactions nature varies in each case: for (I) they are hydrogen bonds, for (II) – weak C—H···O interactions and for (III) – both of them.

For (I) and (II), experimental and theoretical electron density analysis was performed to quantify intermolecular interactions. For (III), only topological analysis based on theoretical data was conducted because the obtained crystals were unsuitable for high-resolution X-ray diffraction measurements. Estimated interaction energies and values of electron density at critical points differed for tyramine cation in each structure. Especially for (II), tyramine···acid interactions are of less importance for crystal packing than for (I) and (III), where these interactions are crucial. It shows that tyramine demonstrates not only conformational but also synthon formation flexibility which is another vital factor causing its prolific abilities.[5]

Literature

[1] Zhang, S.-W. & Yu, L. (2015). Vol. *Advances in Organic Crystal Chemistry: Comprehensive Reviews 2015*, edited by R. Tamura & M. Miyata. pp. 337–353. Springer.
[2] Zhang, S. W., Harasimowicz, M. T., De Villiers, M. M. & Yu, L. (2013). *J. Am. Chem. Soc.* **135**, 18981–18989.
[3] Zhang, S. W., Kendrick, J., Leusen, F. J. J. & Yu, L. (2014). *J. Pharm. Sci.* **103**, 2896–2903.
[4] Briggs, N. E. B., Kennedy, A. R. & Morrison, C. A. (2012). *Acta Crystallogr. Sect. B Struct. Sci.* **68**, 453–464.
[5] Grabowski, S. & Gryl, M., in preparation for publication

S-7

ANALYSIS OF GLUCOSE/XYLOSE ISOMERASE STRUCTURES OBTAINED UNDER HIGH PRESSURE INDUCED BY DIFFERENT METHODS

Agnieszka Klonecka[1,2,3], Joanna Sławek[1], Katarzyna Kurpiewska[4], Maciej Kozak[1,5]

[1] SOLARIS National Synchrotron Radiation Center, Jagiellonian University, ul. Czerwone Maki 98, 30-392 Kraków
[2] Faculty of Physics, Astronomy and Applied Computer Science, Jagiellonian University, ul. Łojasiewicza 11, 30-348 Kraków
[3] Jagiellonian University, Doctoral School of Exact and Natural Science, Jagiellonian University, Kraków, Poland
[4] Department of Crystal Chemistry and Crystal Physics, Faculty of Chemistry, Jagiellonian University, 30-387 Kraków, Poland
[5] Department of Biomedical Physics, Faculty of Physics, Adam Mickiewicz University in Poznań, ul. Uniwersytetu Poznańskiego 2, 61-614 Poznań.

The findings from the analysis of the crystal packing of glucose/xylose isomerase from *Streptomyces rubiginous* were presented at the 63rd Polish Crystallographic Meeting. Now we are continue this project and results of diffraction experiments under high pressure, which was induced using two different methods will be presented.

The first crystal structure was obtained using a home-source diffractometer (Rigaku XtaLAB Synergy S Dualflex diffractometer) and a diamond anvil cell. The crystal structure of glucose/xylose isomerase in this experiment was successfully determined at the pressure of 288 MPa and the resolution of 2.5 Å.

The second structure was determined on the basis of diffraction data collected at the European Synchrotron Radiation Facility. The protein crystals have been frozen under high pressure (200 MPa) induced by gaseous helium. The resulting structure of glucose/xylose isomerase is characterized by a resolution of 1.33 Å.

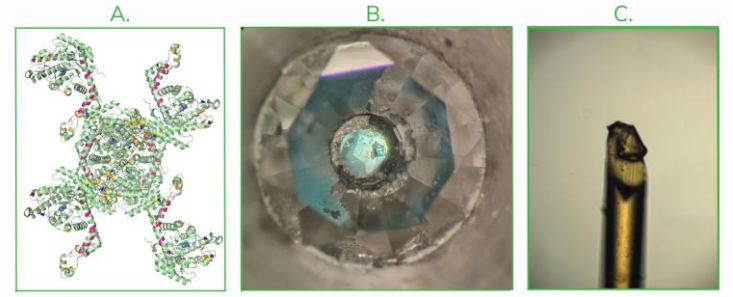

Fig. 1. Crystal packing of glucose/xylose isomerase – the most important contacts (A). Glucose/xylose crystals in the diamond anvil cell (B) and during freezing under high-pressure (C)

In our presentation, we show obtained by us structures of glucose/xylose isomerase and their comparative analysis (2 high pressure structures and 1 reference structure at ambient pressure), focusing on differences in the crystal packing induced by the pressure.

This work was supported by research grant PRELUDIUM BIS (grant ID: 2020/39/O/ST4/03465) from National Science Centre (Poland).

S-8

STRUCTURAL AND FUNCTIONAL STUDIES OF EcAIII MUTANTS POSSESSING DIFFERENT SUBSTITUTIONS AT THE ENTRANCE TO THE ACTIVE SITE

Anna Ściuk[1,2], Krzysztof Lewiński[1], Mariusz Jaskolski[3,4], Joanna Loch[1]

[1] Faculty of Chemistry, Jagiellonian University, Krakow, Poland
[2] Jagiellonian University, Doctoral School of Exact and Natural Sciences, Krakow, Poland
[3] Institute of Bioorganic Chemistry, Polish Academy of Sciences, Poznan, Poland
[4] Faculty of Chemistry, A. Mickiewicz University, Poznan, Poland

L-asparaginases are enzymes that catalyze the decomposition of L-Asn into L-Asp and ammonia. L-asparaginases are used in the treatment of acute lymphoblastic leukemia. However, due to their severe side effects, new therapeutic L-asparaginases are highly needed. Class 2 L-asparaginases belong to the Ntn-hydrolase family and develop enzymatic activity in the autoproteolytic maturation process. Although their affinity for the substrate is relatively low, genetic engineering, in particular site-directed mutagenesis, could potentially improve it. Some studies of structure-function relationships in Class 2 L-asparaginases are available; however, many aspects of the maturation process or catalytic mechanism remain unresolved. Therefore, the main objective of our project was to explore the role of selected residues in the activity of Class 2 L-asparaginases.

To design new variants, sequence conservation near the catalytic threonine triad was analyzed using pangenomic analysis and methodology described previously [1]. Five of the most preferred substitutions at position 200 in the EcAIII sequence were identified. Next, a series of EcAIII new variants, i.e., M200I, M200L, M200K, M200T, and M200W were produced. For purified proteins, biochemical, biophysical, and structural studies were performed. The nanoDSF experiment showed reduced T_m for variants M200K and M200L. It was possible to crystallize most of the new variants, and the determined crystal structures revealed interesting rearrangements of the active site, especially in variant M200W. Crystallographic studies were supported by extensive bioinformatic analysis to discover the origins of structural changes and substrate affinity observed in EcAIII mutants.

Work supported by National Science Centre (NCN) grant 2020/38/E/NZ1/00035

References

[1] A. Zielezinski, J.I. Loch, W.M. Karlowski, M. Jaskolski, *Sci Rep* **12**, (2022) 15797.

S-9

STRUCTURAL STUDIES OF HOST-GUEST COMPLEXES OF SULFONATED CALIXARENES

Kateryna Kravets and Oksana Danylyuk

Institute of Physical Chemistry Polish Academy of Sciences
Kasprzaka 44/52 str., 01-224 Warsaw

Sulfonated calix[*n*]arenes have been widely studied as a class of water-soluble organic macrocycles. These negatively charged calixa[*n*]renes have different cavity sizes. Such cavity's variety allows them to bind to a greater number of cationic and neutral molecules forming host-guest complexes. The host–guest assembly is mainly supported by hydrogen bonds and a set of weak N–H···π, O–H···π, $(C–H)^{+}\cdots O^{-}$ and $(C–H)^{+}\cdots\pi^{-}$, $\pi^{+}–\pi^{-}$ and cation–π interactions, coordination of metals and hydrophobic effect. [1]. The solid-state complexes are interesting from the perspective of formation of supramolecular polymers, cocrystals, vesicles, giant polyhedra, micelles, and supramolecular frameworks.

In this work, we demonstrate the solid-state interactions between biologically active positively charged pentamidine and the negatively charged *p*-sulfonatocalix[*n*]arene. In the host-guest assembles pentamidine appears as a bi-amidine guest. Pentamidine is a water-soluble biologically active drug that is used as an antimicrobial agent and is effective in pneumonia. A more recent analysis shows the antibacterial effect of pentamidine in combination with linezolid, as well as a potential therapeutic effect in vivo on the corresponding CRE infections [2].

p-Sulfonatocalix[4]arene is the smallest representative of the calix[*n*]arene family, which has a rigid cone conformation. The solid-state chemistry of this macrocycle is well-known. The larger *p*-sulfonatocalix[6]arene and *p*-sulfonatocalix[8]arene are more flexible and accept a larg number of conformations in host–guest complexes.

The crystal structures of the *p*-sulfonatocalix[*n*]arene-pentamidine complexes have been determined using the single-crystal X-ray diffraction method. The structural assembly in the solid state is mainly supported by charge-assisted hydrogen bonds between the bi-amidine groups of the pentamidine and the sulfonate groups of the *p*-sulfonatocalix[*n*]arenes. We show the differences between the structures of the host-guest complexes obtained from the water and those obtained from water-cosolvent mixtures.

Literature

[1] O. Danylyuk, K. Suwinska, *Chemical Communication*, **39** (2009) 5799.
[2] M. Tang, C. Quian, X. Zhang et al., *Microbiology Spectrum*, **11** (2023).

S-10

HYDRATED TENOFOVIR – HOW A SLIGHT CHANGE IN WATER CONTENT CAN AFFECT THE CRYSTAL STRUCTURE

Oskar Kaszubowski, Katarzyna Ślepokura

Faculty of Chemistry, University of Wrocław, 14 F. Joliot-Curie, 50-383 Wrocław, Poland

One of the most commonly used groups of antiviral drugs are antimetabolites. These compounds are able to disturb the process of replication or transcription in cells due to their high structural similarity to natural analogues, most often nucleobases, nucleosides or nucleotides [1–3]. One of them is tenofovir (TEN, Fig. 1), which has been used to treat HIV infection or hepatitis B for over 20 years [4,5]. Currently, in pharmacy, much attention is paid to the search for new forms of known drugs with improved properties (better solubility or bioavailability). Many of them are solvates, mainly hydrates [6,7].

It is worth noting, that the crystal structure of tenofovir has not been reported. Only three crystal structures of its prodrug (disoproxil) are deposited in the Cambridge Structural Database. We obtained several crystalline forms of tenofovir with varying degree of hydration (TEN·xH$_2$O, x = 1–5.5) by crystallization from an aqueous solutions. In most of the examined crystals, there was a considerable disorder of water molecules, although in a few of them, including the most hydrated form (TEN·5.5H$_2$O), the disorder of the solvent did not occur.

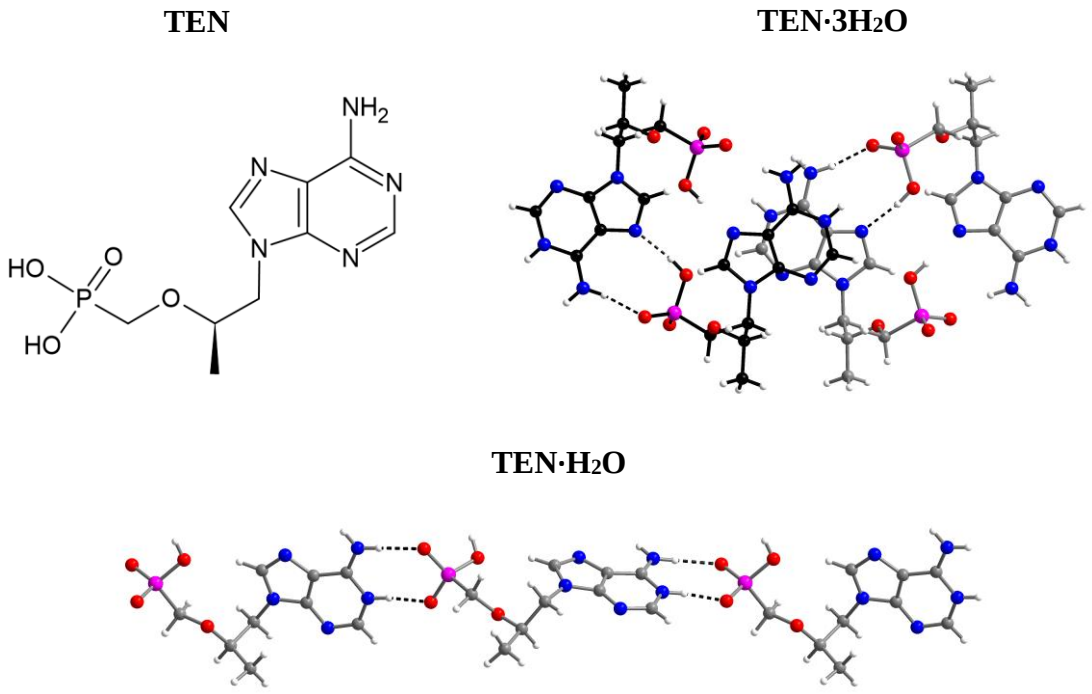

Fig. 1. Structural formula of tenofovir (TEN; neutral form) and the main TEN···TEN interactions in the crystals of TEN·3H$_2$O and TEN·H$_2$O with different architecture (both from the TEN·xH$_2$O, x = 1–5.5 series).

We have found that exposure most of them to elevated temperature leads to the formation of another monohydrate form (which was never obtained by crystallization from solution). Importantly, the process is running without destroying the crystals, through the *single crystal*-to-*single crystal* (*SC*-to-*SC*) transformation. We also observed that partial dehydration of crystals characterized by high disordered water molecules can lead to monohydrate form with better diffraction quality (and free of disorder), which potentially could be one of the solutions to the difficulties in interpreting structural data of crystals with high solvent disorder.

References

[1] H. H. Balfour, *NEJM*, **340** (1999) 1255–1268.
[2] E. D. Clercq, *Nat. Rev. Drug Discov*., **1** (2002) 13–25.
[3] D. Warnke, J. Barreto, Z. Temesgen, *J. Clin. Pharmacol*., **47** (2007) 1466–1598.
[4] A. Ustianowski, J. E. Arends, *Infect. Dis. Ther*., **4** (2015) 145–157.
[5] B. P. Kearney, J. F. Flaherty, J. Shah, *Clin. Pharmacokinet*., **43** (2004) 595–612.
[6] A. M. Healy, Z. A. Worku, D. Kumar, A. M. Madi, *Adv. Drug Deliv. Rev*., **17** (2017) 25–46.
[7] E. Jurczak, A. H. Mazurek, Ł. Szeleszczuk, D. M. Pisklak, M. Zielińska-Pisklak, *Pharmaceutics*, **12** (2020) 959.

S-11

WPŁYW DOKŁADNOŚCI FUNKCJI FALOWEJ NA JAKOŚĆ MULTIPOLOWEJ REPREZENTACJI CZĄSTECZKI

Vladislav Ignatev, Paulina M. Dominiak

Biological and Chemical Research Centre, Wydział Chemii, Uniwersytet Warszawski, ul. Żwirki i Wigury 101, 02-089, Warszawa, Polska

Najprostszym oraz najczęściej używanym modelem w udokładnianiu danych dyfrakcji rengenowskiej jest model niezależnych atomów (independent atom model, IAM), w którym atomy są traktowane jako sferyczne centra rozpraszania. Bardziej zaawansowane modele przedstawiają rozpraszające atomy jako asferyczne obiekty, i jednym z najlepszych przykładów takiego modelu jest Model Multipolowy (MM) [**1**], który używa sumę harmonik sferycznych (t.z. ekspansja multipolowa) do przedstawienia gęstości elektronowej atomu. Model multipolowy jest podstawą banku MATTS (Multipolar Atom Types from Theory and Statistical clustering) [**2**], banku danych asferycznych typów atomów, którę reprezentują uśrednione parametry atomów w pewnym otoczeniu chemicznym i mogą być użyte do szybkiej i dokładnej rekonstrukcji gęstości elektronowej cząsteczki.

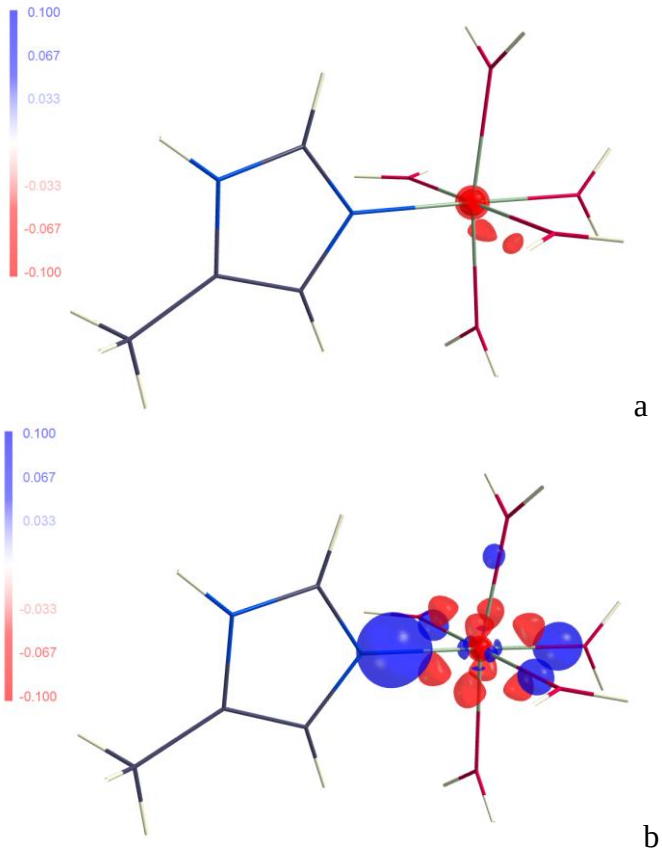

Rys. 1. Gęstość deformacyjna (MM minus IAM, odcięcie 0.1 e/Å^3) atomu Mg w kompleksie $[Mg(H_2O)_5His]^{2+}$; **a** – na podstawie obliczeń w bazie 6-31G**, **b** - na podstawie obliczeń w bazie UGBS1P.

S-11

Jednym z kroków dodawania danych do banku MATTS jest wyznaczenie gęstości elektronowej cząsteczek modelowych przy użyciu obliczeń kwantowo-chemicznych. Okazuję się, że poziom teorii używanej do obliczenia funkcji falowej znacznie wpływa na uzyskiwane parametry multipolowe.

W tym badaniu sprawdzaliśmy wpływ bazy (zestaw funkcji reprezentujący elektronową funkcje falową) w ramach metody DFT z funkcjonałem B3LYP i różnych strategii udokładniania na jakość multipolowej reprezentacji cząsteczki. Obiektem badań były oktaedryczne międzycząsteczkowe kompleksy Mg^{2+}. Jednym z najważniejszych wyników pracy jest wniosek, że w ramach metod używanych przez nas najbardziej odpowiednimi bazami są bazy typu split-valence triple-zeta [**3**].

Literatura

[1] Hansen, N. K., Coppens, P. *Acta Cryst. Section A,* **34** (6) (1978) 909–921, https://doi.org/10.1107/S0567739478001886

[2] Paulina M. Rybicka, *et. al*., *J. Chem. Inf. Model*., **62** (16) (2022) 3766–3783, https://doi.org/10.1021/acs.jcim.2c00145

[3] Jensen, F., *WIREs Comput. Mol. Sci*., **3**(3) (2012) 273–295. doi:10.1002/wcms.1123

Podziękowania

This research was funded by National Science Centre, Poland 2020/39/I/ST4/02904.

S-12

THE LOCAL STRUCTURE OF AMMONIA BORANE DESCRIBED BY PAIR DISTRIBUTION FUNCTION METHOD

Anna Piekara, Wojciech Sławiński

Faculty of Chemistry, University of Warsaw, Pasteura 1, 02-093 Warsaw

Ammonia Borane is material of great interest due to its potential use as a hydrogen storage material realized by high gravimetric and volumetric hydrogen contents - 19.6 wt% and 0.145 kg L^{-1}.[1] The low temperature phase of BH_3NH_3 is describe by orthorhombic structure with the space group $Pmn2_1$ (Z = 2, a = 5.541 Å, b = 4.705 Å, and c = 5.020 Å). The phase transition occurred at 225 K[1,2]. At room temperature ammonia borane characterize by a tetragonal structure with the space group $I4mm$ (Z = 2, a = b = 5.263 Å, c = 5.050 Å)[1,2]. The high-temperature phase is more disordered what causes plasticity of the crystals, piezoelectric and pyroelectric properties[2]. The B–N bond lies along a 4-fold rotational axis what is conflicting with the 3-fold symmetry expected from the tetrahedral $–BH_3$ and $–NH_3$ groups. For this reason it is difficult to describe the local structure by using standard diffraction methods.

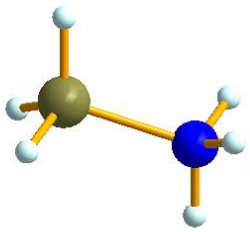

Fig. 1. Molecule of Ammonia Borane.

Pair Distribution Function analysis is a powerful technique employed to study the atomic structure of materials. This method proves particularly valuable when traditional crystallographic approaches face limitations. While Bragg diffraction provides an accurate description of the average structure, it fails to reveal the specific local atomic arrangements contributing to this average. The atomic Pair Distribution Function, known as PDF or G(r), offers a simple one-dimensional function that contains vital information about structural correlations within a material[3].

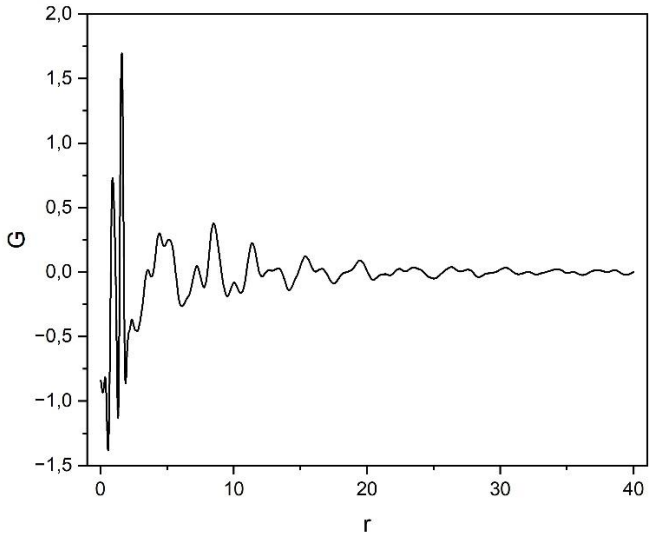

Fig. 2. PDF diagram for Ammonia Borane at room temperature.

The X-ray measurements performed using specifically designed for the Pair Distribution Function (PDF) beamlines gave data which was analysed using specialized software. The next step was to use Reverse Monte Carlo (RMC) modelling which is a general method of structural modelling based on experimental data. The objective is to construct a structural model, typically referred to as a configuration, that aligns with one or multiple sets of experimental data, considering the associated errors and adhering to a set of constraints. These errors are considered to be purely statistical and follow a normal distribution. The aim is to develop a model that best captures the experimental observations while accounting for the uncertainties inherent in the data[4].

Literature

[1] Demirci, U. B. Ammonia borane, a material with exceptional properties for chemical hydrogen storage. *International Journal of Hydrogen Energy* vol. 42 9978–10013 Preprint at https://doi.org/10.1016/j.ijhydene.2017.01.154 (2017).
[2] Bowden, M. E., Gainsford, G. J. & Robinson, W. T. Room-temperature structure of ammonia borane. *Aust J Chem*, **60** (2007) 149–153.
[3] Terban, M. W. & Billinge, S. J. L. Structural Analysis of Molecular Materials Using the Pair Distribution Function. *Chem Rev*, **122** (2022)1208–1272.
[4] Tucker, M. G., Keen, D. A., Dove, M. T., Goodwin, A. L. & Hui, Q. RMCProfile: Reverse Monte Carlo for polycrystalline materials. *Journal of Physics Condensed Matter* **19**, (2007).

S-13

INFLUENCE OF Gd ON THE PHASE TRANSFORMATIONS IN IRON OXIDE-BASED NANOPARTICLES OBTAINED BY THE COPRECIPITATION METHOD

Uladzislaw Gumiennik, Janusz Przewoźnik

AGH University of Krakow, Faculty of Physics and Applied Computer Science, Mickiewicza Av. 30, 30-059 Kraków, Poland

Over the past decades, a lot of efforts have been directed to study different iron oxides-based compounds for biomedical applications. In this work, we investigate structure and magnetic properties of intermediate states in the synthesis of nanoparticles (NPs) containing $Gd_xFe_{3-x}O_4$ (x = 0; 0,05; 0,1) core inside mesoporous SiO_2 shell. NPs are sintered by two-stage procedure including coprecipitation method [1], where the molar concentration of ammonia was fixed to 13,3 mol/L, and using $Si(OC_2H_5)_4$ tetraethyl orthosilicate (TEOS) hydrolysis [2].

During coprecipitation, phase transformations occur due to the catalysis process [3]. The sequence of transformations is: Fe^{3+} → β-FeOOH → α-FeOOH → (α/γ-Fe_2O_3) → Fe_3O_4; Fe^{2+} → $Fe(OH)_2$ → [iron valency change from 2+ to 3+] → γ-FeOOH → γ-Fe_2O_3 → Fe_3O_4. Variation of molar concentrations of the reagents makes it possible to suspend the course of the reaction and study of intermediate phase composition.

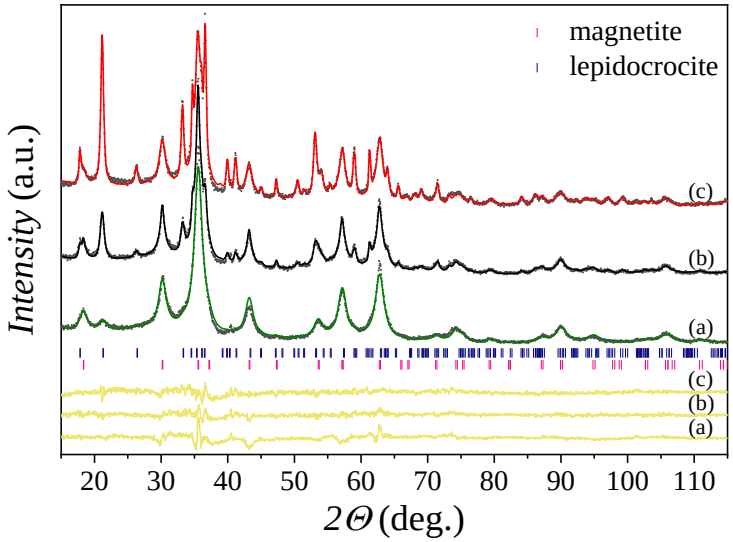

Fig. 1. XRD patterns with Rietveld refinement of $Gd_xFe_{3-x}O_4$ samples with x = 0 (a), 0,05 (b), and 0,1 (c).

The samples are characterized by X-ray diffraction (XRD), scanning electron microscopy, energy-dispersive X-ray spectroscopy, ^{57}Fe Mössbauer spectroscopy (at T = 20 – 300 K), and vibrating sample magnetometry at T = 2 – 300 K and magnetic fields B up to 9 T.

XRD analysis showed that the addition of gadolinium under this synthesis condition leads to increased formation of an additional antiferromagnetic lepidocrocite (γ-FeOOH) phase. However, recalculation of the magnetization at B = 9 T and T = 2 K

only to the mass of the ferrimagnetic $Gd_xFe_{3-x}O_4$ phase shows a clear increase in its saturation with increasing x (1,6 μB/f.u. (x = 0) → 2,0 μB/f.u. (x = 0,05) → 2,3 μB/f.u. (x = 0,1)).

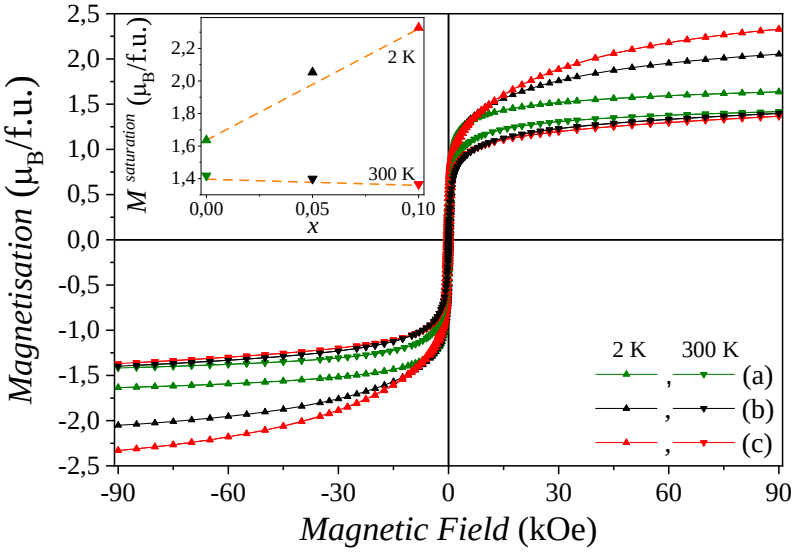

Fig. 2. Magnetisation vs. magnetic field of $Gd_xFe_{3-x}O_4$ samples with x = 0 (a), 0,05 (b), and 0,1 (c).

Literature

[1] R. Massart and V. Cabuil, *J. Chim. Phys.*, **84** (1987) 967.
[2] F. Yang et al., *J. of All. and Comp.*, **728** (2017) 1153–1156.
[3] T. Ahn et al., *J. Phys. Chem. C*, **116** 10 (2012) 6069–6076.

S-14

EFFECT OF HIGH CONCENTRATION OF VACANCIES ON TWINNING IN FCC NANOPARTICLES

Ilia Smirnov[a], Zbigniew Kaszkur[a], Armin Hoell[b]

[a] *Institute of Physical Chemistry, ul. Kasprzaka 44/52, 01-224 Warsaw, Poland*
[b] *Helmholtz-Zentrum Berlin für Materialien und Energie, Hahn-Meitner-Platz 1, 14109 Berlin, Germany*

TEM observations shows that FCC nanoparticles (NPs) possess a variety different morphologies: cuboctahedron (CUB), decahedral (DEC), or icosahedral (ICO). The two latter perfect morphologies are special cases of multitwinned structures. It is thought that the appearance of one or another morphology is depended on the minimum free energy per atom. Meanwhile, the exact mechanism that triggers the twinning is unknown.

We developed a computational simulation approach allowing to simulate the twinning: a regular CUB model is saturated with a large number of vacancies undergoes the relaxation. This leads to the transformation of normal CUB into multitwinned one (with a XRD pattern similar to DEC).

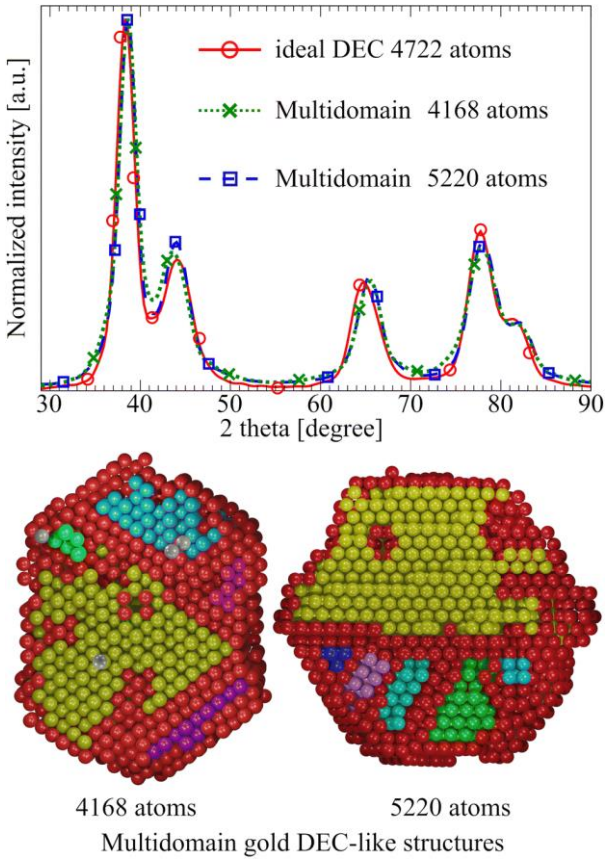

Fig. 1. Comparison of XRD diffraction patterns of an ideal relaxed DEC and relaxed irregular Au multidomain structures consisting of approximately 5 domains (cross sections are shown). Red atoms correspond to the surface/twin plane and neighbouring defect atoms; all other colours represent ideal fcc domains.

S-14

Synchrotron in-situ SAXS and WAXS techniques were applied to verify this concept. Gold NPs (average size ~2.3 nm) were irradiated with X-ray beams. Depending on the X-ray flux intensities, two types of nanoparticle growth were found:

- ***for low-flux***: WAXS & SAXS analysis shows an increase in mean particle size and decrease of NPs density. These observation can be interpreted as an **accumulation of vacancies** inside NPs.

- ***for high-flux:*** WAXS & SAXS analysis shows a decrease in mean particle size and growth of NPs density. These observation can be interpreted as an quick **accumulation** followed by **release** of vacancies under intense X-ray beam.

These indirect observations of vacancies is an important step to understand the development and evolution of NPs morphology.

S-15

SYNTHESIS, CRYSTAL STRUCTURE, AND MAGNETIC PROPERTIES OF NEW COORDINATION COMPOUNDS OF COBALT(II) HALIDES WITH 2-METHYLANILINE

Michał Duda[1], Piotr Konieczny[2], Marcin Oszajca[1], Wiesław Łasocha[1]

[1] Faculty of Chemistry, Jagiellonian University, ul. Gronostajowa 2, 30-387 Kraków, Poland
[2] The Henryk Niewodniczański Institute of Nuclear Physics, Polish Academy of Sciences, ul. Radzikowskiego 152, 31-342 Kraków, Poland

In this research, two organic-inorganic coordination compounds of cobalt(II) halides with 2-methylaniline (2-MeA) were synthesized and studied: $CoCl_2(2\text{-MeA})_2$ and $CoBr_2(2\text{-MeA})_2$. The compounds were synthesized using a fast and simple solvo-mechanical method [1], where the corresponding cobalt salt was mixed with an excess of liquid amine in an agate mortar. As a result, intensely blue powders were obtained.

Based on the X-ray powder diffraction patterns (XRPD), crystal structures of the investigated compounds were determined (Table 1). Cell parameters, crystal system, space group, and positions of cobalt and halogen atoms in the unit cell were determined by direct methods using EXPO2014 [2] (indexing was performed using the NTREOR algorithm [3]). The structure model was prepared with the parallel tempering method (a direct space method) using FOX [4]. As building blocks, free-rotating molecules of 2-MeA were used while the positions of cobalt and halogen atoms were fixed. Restrained structure refinement was performed using Jana2006 [5] with the profile method [6-8].

Table 1. Basic crystallographic data for $CoCl_2(2\text{-MeA})_2$ and $CoBr_2(2\text{-MeA})_2$.

chemical formula	$CoCl_2(C_7H_9N)_2$	$CoBr_2(C_7H_9N)_2$
color	dark blue	bright blue
crystal system	orthorhombic	orthorhombic
space group	*Fdd*2	*Fdd*2
a [Å]	24.9270(4)	25.5517(2)
b [Å]	27.1220(4)	26.7524(3)
c [Å]	4.6425(9)	4.76242(5)
V [Å^3]	3138.73(9)	3255.45(6)
Z	8	8
R_p [%]	6.83	4.86
R_{wp} [%]	4.41	4.48
numer of restraints*	17	32

*related to the geometry of the 2-MeA molecules

In both crystal structures, cobalt atoms are surrounded by two halogen cations and two nitrogen atoms from the amine molecules, occupying the corners of the coordination polyhedra (tetrahedra) (Fig. 1). In the structures, there are eight molecules of $CoX_2(2\text{-MeA})_2$ per unit cell (Fig. 2a). The molecules are organized into *pseudo*-ribbons parallel to the [001] crystallographic direction (Fig. 2b) by ionic interactions between Co^{2+} and halogen anions, X^-, and weak N-H···X interactions.

Since cobalt(II) atom has spin S = 3/2, magnetic properties of the compounds were investigated. As the molecules are aligned in *pseudo*-ribbons, it was expected that the compounds could exhibit SCM (Single-Chain Magnet) behavior; however, the

magnetization *vs.* temperature curves dismissed this hypothesis. The ordering temperature calculated for $CoCl_2(2\text{-}MeA)_2$ is ~6.7 K and for $CoBr_2(2\text{-}MeA)_2$: ~6.0 K Difference between ZFC (Zero-Field-Cooled) and FC (Field-Cooled) curves observed in the case of $CoCl_2(2\text{-}MeA)_2$ could indicate that the material underwent an irreversible process (probably degradation) during the measurements. The determined magnetic susceptibility, χT, for the compound with chlorine is ~2,78 $cm^3 \cdot mol^{-1} \cdot K$, and for the compound with bromine: ~2,53 $cm^3 \cdot mol^{-1} \cdot K$. Studies of magnetic properties as a function of pressure are under progress.

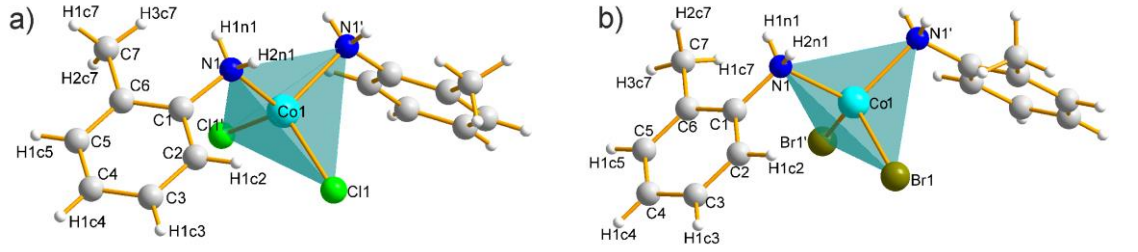

Fig. 1. Single molecule of: a) $CoCl_2(2\text{-}MeA)_2$ and b) $CoBr_2(2\text{-}MeA)_2$ with coordination polyhedra shown.

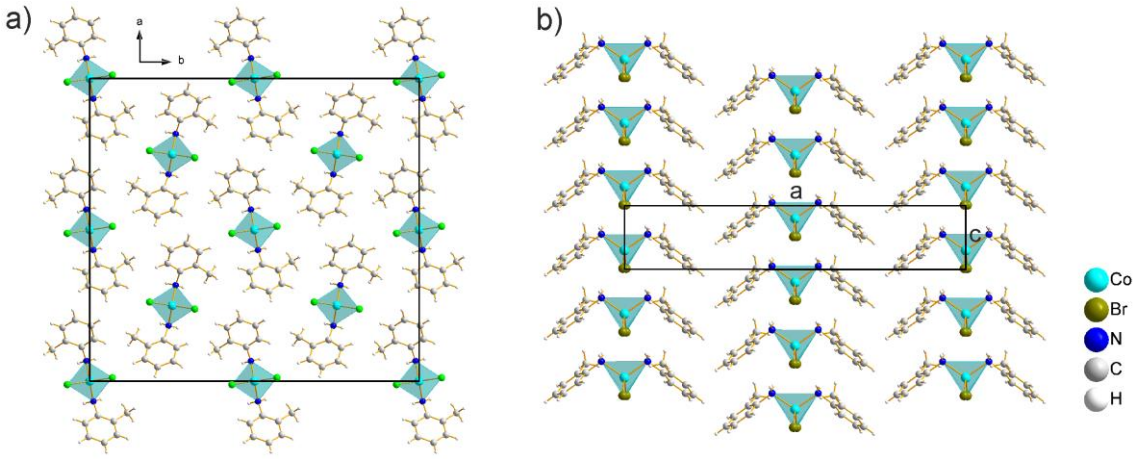

Fig. 2. Structure views of the studied compounds: a) unit cell of $CoCl_2(2\text{-}MeA)_2$ shown along the [001] direction; b) $CoBr_2(2\text{-}MeA)_2$ molecules arranged in *pseudo*-ribbons parallel to the [001] direction (view along the [010] direction).

References

[1] M. Duda, *PhD Thesis*, (2021) 108.
[2] A. Altomare, M. Camalli, C. Cuocci, C. Giacovazzo, A. Moliterni, R. Rizzi, *J. Appl. Cryst.*, **42** (2009) 1197.
[3] A. Altomare, G. Campi, C. Cuocci, L. Eriksson, C. Giacovazzo, A. Moliterni, R. Rizzi, P.-E. Werner, *J. Appl. Cryst.*, **42** (2009) 768.
[4] V. Favre-Nicolin, R. Černý, *J. Appl. Cryst*., **35** (2002) 734.
[5] V. Petříček, M. Dušek, L. Palatinus, *Z. Kristallogr. Cryst. Mater*., **229** (2014) 345.
[6] H.M. Rietveld, *J. Appl. Cryst*., **2** (1969) 65.
[7] B.O. Loopstra, H.M. Rietveld, *Acta Cryst. B*., **25** (1969) 787.
[8] B.O. Loopstra, H.M. Rietveld, *Acta Cryst. B*., **25** (1969) 1420.

S-16

THE $CsPbBr_3$ PEROVSKITE CORE – GLASS CLADDING OPTICAL FIBER - FABRICATION AND PROPERTIES

Paweł Socha[1], Dariusz Pysz[1], Karol Bartosiewicz[2], Andrzej Lechna[1], Robert Tomala[3], Maksym Buryi[4], Robert Kral[4], Alicja Anuszkiewicz[1], Michał K. Cyrański[5], Ryszard Buczyński [1,6]

[1] Łukasiewicz Research Network - Institute of Microelectronics and Photonics, ul. Wólczyńska 133, 01-919 Warsaw
[2] Department of Physics, Kazimierz Wielki University, ul. Powstańców Wielkopolskich 2, 85-090 Bydgoszcz
[3] Institute of Low Temperature and Structure Research, ul. Okólna 2, 50-422 Wrocław
[4] Institute of Physics of Czech Academy of Sciences, Cukrovarnická 10/112 162 00 Prague 6
[5] Department of Chemistry, University of Warsaw, Pasteura 1, 02-093 Warsaw
[6] Department of Physics, University of Warsaw, Pasteura 5, 02-093 Warsaw

Optical fibers are very desirable in a wide range of applications like telecommunication, lasers, sensors, photovoltaics, medicine, etc. due to their small size and various properties. One example of functional optical fibers is crystalline core – glass cladding fibers, which take benefits from both crystalline and glass materials. The promising candidates for the crystalline core are halide perovskites (HPs) (ABX_3; e.g. A = Cs^+, CH_3NH^{3+}; B = Pb^{2+}, Sn^{2+}; X= Cl^-, Br^-, I^-) with their various properties [1]. HPs exhibit e.g. luminescence, tunable bandgaps, large absorption coefficient, high carrier mobility, and production costs of these materials are relatively low. Therefore, they are used in many optoelectronic devices like solar cells, light-emitting diodes, lasers, photodetectors, etc. However, several challenges still have to be faced. HPs are very sensitive to humidity, and their composition is not environmentally friendly. Using glass cladding can solve both problems by isolation the crystalline core from external conditions.

Perovskite core fibers (PCF) were obtained before by perovskite crystallization directly inside the hollow core fiber [2]. Crystals growth rates in this research were about mm/day and resulted in good quality crystalline cores. However, fibers with an internal diameter below 300 um have growth limitations due to limited ion diffusion.

In this report, we present the fabrication and properties of $CsPbBr_3$ perovskite core - glass cladding fibers (Fig.1) obtained with the Molten-Core Method (MCM). MCM is commonly used to obtain crystal core – glass cladding fibers [3], nonetheless this method was not previously used to obtain PCF. For this technique is crucial to fit the thermal parameters of crystals and glass - crystalline material must be completely melted while the glass is soft enough for fiber drawing at the same temperature. When the fiber leaves the furnace the molten core crystallizes again. The advantage of this method is the possibility to produce very long fibers (up to hundreds of meters) in a relatively short time. Furthermore, the synthesis of HPs can be performed during the drawing process. The crystallization process is spontaneous, thus the fiber core quality was carefully investigated with single-crystal X-ray diffraction, scanning electron microscope imaging, and energy-dispersive X-ray analysis. Obtained fibers were also characterized with transmission measurements, and photoluminescence excitation and

emission spectroscopy. Experiments confirmed, that the crystalline core is $CsPbBr_3$ perovskite cubic phase exhibiting green photoluminescence at UV excitation.

Fig. 1. $CsPbBr_3$ perovskite core optical fibers.

References

[1] J. S. Manser, J. A. Christians, P. V. Kamat, *Chem. Rev.*, **116** (2016), 12956–13008.
[2] Y. Zhou, M. A. Parkes, J. Zhang, Y. Wang, M. Ruddlesden, H. H. Fielding, L. Su, *Sci. Adv*. **8**, eabq8629 (2022).
[3] J. Ballato, A. C. Peacock, *APL Photonics* **3** 120903 (2018)

LISTA ZAREJESTROWANYCH UCZESTNIKÓW KONWERSATORIUM
LIST OF THE REGISTERED PARTICIPANTS

Jan	**Adamek**		Warszawa	Wydział Chemiczny, Politechnika Warszawska
Julia	**Alberska**		Warszawa	Wydział Chemii, Uniwersytet Warszawski
Piotr Józef	**Bardziński**	dr inż.	Wrocław	Uniwersytet Wrocławski, Wydział Chemii
Elżbieta	**Bartoszak-Adamska**	dr hab.	Poznań	Department of Crystallography, Faculty of Chemistry, Adam Mickiewicz University, Poznań
Tamara	**Bednarchuk**	dr	Wrocław	Instytut Niskich Temperatur i Badań Strukturalnych PAN
Anna	**Bisok**		Poznań	Uniwersytet Adama Mickiewicza
Teresa	**Bizoń**	inżynier	Warszawa	Uniwersytet Warszawski, Wydział Chemii
Marta	**Bogdan**	magister	Łódź	Politechnika Łódzka, Wydział Chemiczny
Patryk	**Borowski**	Doktorant	Warszawa	Uniwersytet Warszawski, Wydzial Chemii
Iwona	**Bryndal**	Dr	Wrocław	Uniwersytet Medyczny we Wrocławiu
Krzysztof	**Brzeziński**	dr hab.	Poznań	Instytut Chemii Bioorganicznej PAN
Armand	**Budzianowski**	doktor	Otwock	Narodowe Centrum Badań Jądrowych
Ireneusz	**Bugański**	Dr inż.	Kraków	AGH University of Krakow
Anna	**Bujacz**	Dr hab. inż.	Łódź	Institute of Molecular and Industrial Biotechnology, Faculty of Biotechnology and Food Sciences, Lodz University of Technology
Grzegorz	**Bujacz**	Prof. dr hab. inż.	Łódź	Institute of Molecular and Industrial Biotechnology, Faculty of Biotechnology and Food Sciences, Lodz University of Technology
Helena	**Butkiewicz**	doktor	Warszawa	Wydział Chemii, Uniwersytet Warszawski
Magdalena	**Ceborska**	dr hab.	Warszawa	Wydział Matematyczno-Przyrodniczy, Uniwersytet Kardynała Stefana Wyszyńskiego w Warszawie
Lilianna	**Chęcińska**	dr hab.	Łódź	Uniwersytet Łódzki
Jarosław	**Chojnacki**	Profesor	Gdańsk	Politechnika Gdańska
Anna	**Ciborska**	Dr inż.	Gdańsk	Katedra Chemii Nieorganicznej, Wydział Chemiczny, Politechnika Gdańska
Arkadiusz	**Ciesielski**	doktor	Warszawa	Uniwersytet Warszawski, Wydział Chemii
Bartosz	**Cieśla**	Inżynier	Gdańsk	Politechnika Gdańska, Wydział Chemiczny, Katedra Chemii Nieorganicznej
Jerzy	**Czachórski**		Warszawa	Malvern Panalytical B.V. Sp. z o.o. Oddział w Polsce
Joachim	**Czapiński**	Inżynier	Warszawa	University of Warsaw
Patryk	**Czapnik**	magister	Łódź	Uniwersytet Łódzki, Wydział Chemii, Katedra Chemii Fizycznej, Zakład Chemii Biofizycznej

Oksana	**Danylyuk**	dr hab.	Warszawa	Instytut Chemii Fizycznej Polskiej Akademii Nauk
Marek	**Daszkiewicz**	dr hab.	Wrocław	Instytut Niskich Temperatur i Badań Strukturalnych PAN we Wrocławiu
Aleksandra	**Deptuch**	dr.	Kraków	Instytut Fizyki Jądrowej PAN
Lei	**Ding**	PhD	Holandia (Almelo)	Malvern Panalytical
Grygoriy	**Dmytriv**	Dr.	Ukraina (Lwów)	Ivan Franko National University of Lviv
Anna	**Dołęga**	Dr hab.	Gdańsk	Politechnika Gdańska, Wydział Chemiczny, Katedra Chemii Nieorganicznej
Dawid	**Drozdowski**	Mgr inż.	Wrocław	Instytut Niskich Temperatur i Badań Strukturalnych Polskiej Akademii Nauk
Joanna	**Drwęska**	mgr	Poznań	Faculty of Chemistry, Adam Mickiewicz University
Michał	**Duda**	Dr	Kraków	Uniwersytet Jagielloński w Krakowie
Marta	**Dudek**	dr hab.	Łódź	Center of Molecular and Macromolecular Studies, Polish Academy of Sciences
Wojciech	**Dudziak**	Inżynier	Wrocław	Uniwersytet Wrocławski, Wydział Chemii
Konrad	**Dyk**	Mgr	Lublin	University of Maria Curie-Sklodowska in Lublin
Mariya	**Dzevenko**	PhD	Ukraina (Lwów)	Kruty Heroes Lviv Lyceum with Intensive Military and Physical Training
Maciej	**Ejnik**	Student	Gdańsk	Politechnika Gdańska
Julia	**Fiszer**	licencjat	Wrocław	Wydział Chemii, Uniwersytet Wrocławski
Sławomir	**Frynas**	dr	Lublin	Zakład Chemii Organicznej i Krystalochemii UMCS
Michał	**Gacki**	dr inż	Łódź	Politechnika Łódzka
Emilia	**Ganczar**	dr	Wrocław	Wydział Chemii Uniwersytet Wrocławski
Anna	**Gągor**	dr hab.	Wrocław	Instytut Niskich Temperatur i Badań Strukturalnych im. Włodzimierza Trzebiatowskiego Polskiej Akademii Nauk
Maria	**Gdaniec**	Prof. dr hab.	Poznań	Wydział Chemii UAM, Poznań
Mirosław	**Gilski**	dr hab.	Poznań	Zakład Krystalografii, Wydział Chemii, Uniwersytet im. A. Mickiewicza w Poznaniu
Marek	**Gnypek**		Warszawa	LABSOFT Sp. z o.o. / Bruker AXS GmbH
Antonina	**Gonet**	licencjusz (magistrantka)	Poznań	Uniwersytet A.Mickiewicza w Poznaniu Instytut Chemii Bioorganicznej PAN, Poznań
Szymon	**Grabowski**	Magister	Kraków	Wydział Chemii, Uniwersytet Jagielloński
Wiktoria	**Gromelska**	Mgr	Poznań	Uniwersytet im. Adama Mickiewicza w Poznaniu, Wydział Chemii, Zakład Krystalografii
Marlena	**Gryl**	dr hab.	Kraków	Uniwersytet Jagielloński w Krakowie, Wydział Chemii, Zakład Krystalochemii i Krystalofizyki
Magdalena	**Grzegórska**	Magister	Toruń	Uniwersytet Mikołaja Kopernika w Toruniu
Iga	**Grześkowiak**	Student	Poznań	Uniwersytet im. Adama Mickiewicza w Poznaniu
Uladzislaw	**Gumiennik**	M.Sc.	Kraków	AGH University of Krakow

Karolina	**Gutmańska**	Mgr inż.	Gdańsk	Katedra Chemii Nieorganicznej, Wydział Chemiczny, Politechnika Gdańska
Natalia	**Halaba**	licencjat	Łódź	Wydział Chemii Uniwersytetu Łódzkiego
Katarzyna	**Helios**	dr inż.	Wrocław	Politechnika Wrocławska / Wrocław University of Science and Technology
Neda	**Heydari**	PhD student	Iran (Zandżan)	University of Zanjan
Andrzej	**Hilczer**	Dr	Poznań	Instytut Fizyki Molekularnej Polskiej Akademii Nauk
Anna	**Hoser**	dr	Warszawa	Uniwersytet Warszawski, Wydział Chemii
Valeryia	**Hushcha**	Licencjat	Łódź	Katedra Chemii Fizycznej, Wydział Chemii, Uniwersytet Łódzki
Natallia	**Husik**	Magister - studentka	Łódź	Uniwersytet Łódzki
Vladislav	**Ignatev**	Magister	Warszawa	Uniwersytet Warszawski
Piotr	**Jakieła**	mgr	Warszawa	Malvern Panalytical B.V. Sp. z o.o. Oddział w Polsce
Natasza	**Jakubik**	Student	Warszawa	Wydział Chemii Uniwersytetu Warszawskiego
Jan	**Janczak**	prof. dr hab.	Wrocław	Instytut Niskich Temperatur i Badań Strukturalnych, PAN
Agnieszka	**Janiak**	dr hab.	Poznań	Wydział Chemii, Uniwersytet im. Adama Mickiewicza
Irena	**Jankowska-Sumara**	profesor	Kraków	Uniwersytet Pedagogiczny w Krakowie
Katarzyna	**Jarzembska**	dr hab.	Warszawa	Uniwersytet Warszawski
Róża	**Jastrzębska**	Inżynier	Warszawa	Wydział Chemii Uniwersytetu Warszawskiego
Izabela	**Jendrzejewska**	dr hab.	Katowice	Uniwersytet Śląski w Katowicach, Instytut Chemii
Justyna	**Kalinowska-Tłuścik**	dr hab.	Kraków	Wydział Chemii Uniwersytet Jagielloński w Krakowie
Karolina	**Kałduńska**	magister	Toruń	Wydział Chemii, Uniwersytet Mikołaja Kopernika w Toruniu
Daniel	**Kamiński**	dr hab.	Lublin	UMCS
Radosław	**Kamiński**	dr	Warszawa	University of Warsaw
Michał	**Kamiński**	student	Warszawa	Uniwersytet Warszawski
Zbigniew	**Karczmarzyk**	dr hab. inż.	Siedlce	Uniwersytet Przyrodniczo-Humanistyczny w Siedlcach
Marta	**Karpiel**	mgr	Kraków	Uniwersytet Jagielloński
Zbigniew	**Kaszkur**	prof. dr hab.	Warszawa	Instytut Chemii Fizycznej PAN
Oskar	**Kaszubowski**	Magister	Wrocław	Uniwersytet Wrocławski, Wydział Chemii
Andrzej	**Katrusiak**	Prof.	Poznań	Adam Mickiewicz University
Marta	**Kilichowska**	mgr	Kraków	Wydział Chemii Uniwersytetu Jagiellońskiego w Krakowie
Agnieszka	**Kiliszek**	dr hab.	Poznań	Instytut Chemii Bioorganicznej Polska Akademia Nauk
Vasyl	**Kinzhybalo**	dr	Wrocław	Instytut Niskich Temperatur i Badań Strukturalnych PAN

Hubert	**Kleinschmidt**	Student 1 stopnia	Gdańsk	Politechnika Gdańska
Agnieszka	**Klonecka**	Magister	Kraków	Narodowe Centrum Promieniowania Synchrotronowego SOLARIS
Andrzej	**Kochel**	dr hab.	Wrocław	Uniwersytet Wrocławski, Wydział Chemii
Irina	**Konovalova**	Dr.	Ukraina (Charków)/ Niemcy (Düsseldorf)	SSI "Institute for Single Crystals", National Academy of Science of Ukraine, Kharkiv Bioinorganic Chemistry, Heinrich-Heine-University Dusseldorf
Dorota	**Kowalska**	dr inż.	Wrocław	Instytut Niskich Temperatur i Badań Strukturalnych im. Włodzimierza Trzebiatowskiego Polskiej Akademii Nauk
Andrzej	**Kowalski**	Dr	Wrocław	Rigaku Polska, sp. z o.o.
Maciej	**Kozak**	prof. dr hab.	Kraków	SOLARIS, National Synchrotron Radiation Centre, Jagiellonian University
Anna	**Kozakiewicz-Piekarz**	doktor	Toruń	Wydział Chemii, Uniwersytet Mikołaja Kopernika w Toruniu
Marcin	**Kozieł**	doktor	Kraków	Uniwersytet Jagielloński
Anna	**Kozioł**	prof.	Lublin	Wydział Chemii Uniwersytet Marii Curie-Skłodowskiej, Lublin
Kateryna	**Kravets**	Magister	Warszawa	Instytut Chemii Fizycznej Polskiej Akademii Nauk
Jacek	**Krawczyk**	dr	Katowice	Institute of Materials Engineering, Faculty of Science and Technology, University of Silesia in Katowice
Monika	**Krawczyk**	doktor	Wrocław	Instytut Fizyki Doświadczalnej Uniwersytet Wrocławski
Marta	**Krawczyk**	doktor	Wrocław	Wydział Farmaceutyczny, Uniwersytet Medyczny im. Piastów Śląskich we Wrocławiu
Agnieszka	**Krawiec**	lic	Katowice	Uniwersytet Śląski w Katowicach
Katarzyna M.	**Krupka**	Licencjat	Wrocław	Uniwersytet Wrocławski
Anna	**Kryczka**	lic	Katowice	Uniwersytet Śląski w Katowicach
Dominika	**Krzeszewska**	mgr inż.	Łódź	Politechnika Łódzka, Instytut Biotechnologii Molekularnej i Przemysłowej
Szymon	**Krzywda**	dr hab.	Poznań	UAM
Maria	**Książek**	doktor	Katowice	Instytut Fizyki, Uniwersytet Śląski
Maciej	**Kubicki**	Prof	Poznań	Uniwersytet im. Adama Mickiewicza w Poznaniu
Paulina	**Kurowska**	licencjat	Wrocław	Uniwersytet Wrocławski
Łukasz	**Kurowski**		Gdańsk	Politechnika Gdańska
Joachim	**Kusz**	profesor	Katowice	Instytut Fizyki, Uniwersytet Śląski
Anna	**Kwiecień**	dr	Wrocław	Uniwersytet Medyczny we Wrocławiu, Wydział Farmaceutyczny, Katedra i Zakład Podstaw Nauk Chemicznych
Paweł	**Lewkowicz**	Student I stopnia	Poznań	Zakład chemii materiałów, UAM, Poznań
Janusz	**Lipkowski**	Profesor	Warszawa	Emeryt
Tadeusz	**Lis**	Profesor	Wrocław	Wydział Chemii, Uniwersytet Wrocławski

Joanna	**Loch**	dr	Kraków	Uniwersytet Jagielloński, Wydział Chemii
Piotr	**Łaski**	MSc	Warszawa	Uniwersytet Warszawski
Elżbieta	**Łastawiecka**	dr	Lublin	UMCS
Sebastian	**Machowski**	mgr	Radlin	Testchem sp. z o.o.
Urszula	**Maciołek**	dr inż.	Lublin	Uniwersytet Marii Curie-Skłodowskiej
Anna	**Makal**	dr hab.	Warszawa	Wydział Chemii Uniwersytetu Warszawskiego
Maura	**Malińska**	dr	Warszawa	Wydział Chemii, Uniwersytet Warszawski
Magdalena	**Małecka**	dr hab.	Łódź	Katedra Chemii Fizycznej Uniwersytet Łódzki
Paulina	**Marek-Urban**	mgr inż.	Warszawa	Wydział Chemiczny, Politechnika Warszawska
Renny Louis Anto	**Maria Losus**	M.Sc	Toruń	Nicolaus Copernicus University in Torun
Eddy	**Martin**	PhD	Warszawa	LABSOFT Sp. z o.o. / Bruker AXS GmbH
Volodymyr	**Medviediev**	PhD	Ukraina (Charków)	SSI "Institute for Single Crystals" of the National Academy of Sciences of Ukraine
Roman	**Minikayev**	Dr.	Warszawa	Instytut Fizyki PAN
Natalia	**Miodowska**	Mgr inż.	Wrocław	Politechnika Wrocławska
Artur	**Mirocki**	Doktor	Gdańsk	Wydział Chemii, Uniwersytet Gdański
Maja	**Morawiak**	dr inż.	Warszawa	Instytut Chemii Organicznej PAN
Tadeusz	**Muzioł**	dr	Toruń	Faculty of Chemistry Nicolaus Copernicus University in Toruń
Dawid	**Natkowski**	Student	Warszawa	Politechnika Warszawska
Maciej	**Nielipiński**	mgr inż.	Łódź	Politechnika Łódzka, Instytut Biotechnologii Molekularnej i Przemysłowej
Wojciech	**Nitek**	doktor	Kraków	Uniwersytet Jagielloński, Wydział Chemii
Przemysław	**Nowak**	Magister inżynier	Łódź	Centrum Badań Molekularnych i Makromolekularnych PAN
Maurycy	**Nowak**	Student Chemii Medycznej	Warszawa	Wydział Chemii Uniwersytetu Warszawskiego
Samet	**Ocak**	PhD student	Włochy (Bolonia)	University of Bologna
Andrzej	**Olczak**	dr hab.	Łódź	Politechnika Łódzka
Paweł	**Ołówek**	Magister	Niemcy (Neu-Insenburg)	Rigaku Europe SE
Marta	**Orlikowska**	dr	Gdańsk	Wydział Chemii Uniwersytetu Gdańskiego
Marcin	**Oszajca**	dr	Kraków	Wydział Chemii Uniwersytetu Jagiellońskiego
Kacper	**Paszczyk**	student, II rok stud. lic.	Warszawa	Kolegium MISMaP, Uniwersytet Warszawski
Wojciech	**Paszkowicz**	Profesor	Warszawa	Institute of Physics, Polish Academy of Sciences
Robert	**Paszkowski**	PhD Eng.	Katowice	University of Silesia in Katowice Faculty of Science and Technology Institute of Materials Engineering
Natalia	**Pawłowska**	lic	Łódź	Wydział Chemii Uniwersytetu Łódzkiego

Anna	**Pietrzak**	dr	Łódź	Instytut Chemii Ogólnej i Ekologicznej, Politechnika Łódzka
Agnieszka	**Pietrzyk-Brzezińska**	Dr inż.	Łódź	Politechnika Łódzka, Instytut Biotechnologii Molekularnej i Przemysłowej
Paweł	**Piszora**	dr hab.	Poznań	Department of Materials Chemistry, Faculty of Chemistry, Adam Mickiewicz University
Kinga	**Potempa**	MSc	Warszawa	University of Warsaw
Aleksandra	**Półrolniczak**	Magister	Poznań	Adam Mickiewicz University
Kamila	**Pruszkowska**	mgr	Warszawa	Wydział Chemii, Uniwersytet Warszawski
Anna	**Pyra**	Dr	Wrocław	Uniwersytet Wrocławski
Paulina	**Ratajczyk**	mgr/doktorant	Poznań	Uniwersytet im. Adama Mickiewicza w Poznaniu
Guido	**Reiss**	Dr.	Niemcy (Düsseldorf)	Bioinorganic Chemistry, Heinrich-Heine-University Düsseldorf, Germany
Piotr	**Rejnhardt**	Doktor	Warszawa	Uniwersytet Warszawski Wydział Chemii
Kinga	**Roszak**	dr	Poznań	Faculty of Chemistry, Adam Mickiewicz University, Poznań, Poland
Magdalena	**Rowińska**	magister	Wrocław	Instytut Niskich Temperatur i Badań Strukturalnych Polskiej Akademii Nauk
Kornel	**Roztocki**	dr	Poznań	Uniwersytet Adama Mickiewicza w Poznaniu
Michalina	**Rusek**	Dr	Poznań	Adam Mickiewicz University
Paulina	**Rybicka**	mgr	Warszawa	Uniwersytet Warszawski
Urszula	**Rychlewska**	profesor senior	Poznań	Uniwersytet im. Adama Mickiewicza w Poznaniu
Natalia	**Sacharczuk**	magister chemii/doktorant	Poznań	Wydział Chemii, Uniwersytet im. Adama Mickiewicza w Poznaniu
Anna	**Sadocha**	magister	Warszawa	Uniwersytet Warszawski, Wydział chemii
Bartosz	**Sekuła**	dr inż.	Łódź	Politechnika Łódzka, Instytut Biotechnologii Molekularnej i Przemysłowej
Jarosław	**Serafińczuk**	dr hab. inż.	Wrocław	Katedra Nanometrologii, Politechnika Wrocławska, Sieć Badawcza Łukasiewicz - PORT Polskie Centrum Rozwoju Technologii, Wrocław, Polska
Svitlana	**Shishkina**	PhD	Ukraina (Charków)	SSI "Institute for Single Crystals" of the National Academy of Sciences of Ukraine
Mariia	**Shyshkina**	PhD student	Ukraina (Charków)	SSI "Institute for Single Crystals" of the National Academy of Sciences of Ukraine
Magdalena	**Siedzielnik**	mgr inż.	Gdańsk	Politechnika Gdańska, Wydział Chemiczny, Katedra Chemii Nieorganicznej
Tomasz	**Sierański**	Doktor inżynier	Łódź	Instytut Chemii Ogólnej i Ekologicznej, Politechnika Łódzka
Tymoteusz	**Skadorwa**	student	Wrocław	Uniwersytet Wrocławski
Agnieszka	**Skórska-Stania**	dr	Kraków	Uniwerystet Jagielloński, Wydział Chemii, Zakład Krystalochemii i Krystalofizyki
Joanna	**Sławek**	dr inż.	Kraków	Narodowe Centrum Promieniowania Synchrotronowego SOLARIS
Ilia	**Smirnov**	MSc	Warszawa	Institute of Physical Chemistry, PAS, Warsaw
Vernon	**Smith**	Dr	Warszawa	LABSOFT Sp. z o.o. / Bruker AXS GmbH
Paulina	**Sobczak**	mgr inż.	Łódź	Politechnika Łódzka

Szymon	**Sobczak**	Doktor	Poznań	Uniwersytet im. Adama Mickiewicza w Poznaniu
Szymon	**Sobczak**	Magister	Poznań	Uniwersytet im. Adama Mickiewicza w Poznaniu, Wydział Chemii, Zakład Krystalografii
Paweł	**Socha**	PhD	Wrocław	Łukasiewicz Research Network - Institute of Microelectronics and Photonics
Jan Jakub Leon	**Stasiczak**	MSc	Poznań	Adam Mickiewicz University in Poznań
Szymon	**Stolarek**	MSc eng.	Francja (Grenoble)	Xenocs SAS
Jarosław	**Sukiennik**	magister, inżynier	Łódź	Instytut Chemii Ogólnej i Ekologicznej Wydział Chemiczny Politechniki Łódzkiej
Adrian	**Sulich**	Dr	Warszawa	Institute of Physics PAS
Szymon	**Sutuła**	doktor	Warszawa	Uniwersytet Warszawski
Kinga	**Suwińska**	profesor	Warszawa	Uniwersytet Kardynała Stefana Wyszyńskiego w Warszawie
Karol	**Synoradzki**	PhD	Poznań	Institute of Molecular Physics of the Polish Academy of Sciences
Małgorzata	**Szczesio**	dr hab. inż.	Łódź	Instytut Chemii Ogólnej i Ekologicznej Wydział Chemiczny Politechnika Łódzka
Katarzyna	**Szwaczko**	dr	Lublin	Uniwersytet Marii Curie-Skłodowskiej
Kornelia	**Szymańska**	Student	Poznań	Wydział Chemii Uniwersytet Adama Mickiewicza w Poznaniu
Anna	**Ściuk**	magister	Kraków	Uniwersytet Jagielloński
Katarzyna	**Ślepokura**	dr hab.	Wrocław	Faculty of Chemistry, University of Wrocław
Joanna	**Śmietańska**	mgr	Kraków	Akademia Górniczo-Hutnicza im. Stanisława Staszica w Krakowie, Wydział Fizyki i Informatyki Stosowanej
Marcin	**Świątkowski**	doktor inżynier	Łódź	Instytut Chemii Ogólnej i Ekologicznej, Politechnika Łódzka
Julia	**Telus**		Poznań	Uniwersytet im. Adama Mickiewicza w Poznaniu
Paweł	**Tomaszewski**	dr	Wrocław	INTiBS PAN
Bartłomiej	**Trojanowski**	Inżynier	Warszawa	Uniwersytet Warszawski
Agata	**Trzęsowska-Kruszyńska**	dr hab. inż.	Łódź	Politechnika Łódzka, Wydział Chemiczny
Jakub	**Tyborowski**	Student	Warszawa	Politechnika Warszawska
Kamil	**Urbański**	Mgr Inż	Warszawa	Anton Paar Poland
Zuzanna	**Walkowiak**	Inżynier	Wrocław	Politechnika Wrocławska
Angelika	**Wcisło**		Poznań	Uniwersytet im. Adama Mickiewicza w Poznaniu
Adam	**Włodarczyk**	mgr	Lublin	UMCS
Paulina	**Wojciechowska**	Student I-go stopnia	Wrocław	Politechnika Wrocławska
Jakub	**Wojciechowski**	Dr	Niemcy (Neu-Insenburg)	Rigaku Europe SE
Andrzej	**Wojtas**	Dr	Wrocław	PROTO Manufacturing Europe

Wojciech	**Wolf**	prof. dr hab. inż.	Łódź	Instytut Chemii Ogólnej i Ekologicznej, Politechnika Łódzka
Marek	**Wołcyrz**	Prof.	Wrocław	Instytut Niskich Temperatur i Badań Strukturalnych PAN
Karolina	**Wrochna**	Student	Warszawa	Politechnika Warszawska, Wydział Chemiczny
Patryk	**Wróbel**	mgr	Warszawa	LABSOFT Sp. z o.o. / Bruker AXS GmbH
Karol	**Wydra**	magister	Wrocław	Wydział Chemii Uniwersytetu Wrocławskiego
Waldemar	**Wysocki**	dr	Siedlce	Uniwersytet Przyrodniczo-Humanistyczny w Siedlcach
Patrycja	**Wytrych**	magister	Wrocław	Wydział Chemii Uniwersytetu Wrocławskiego
Anna	**Zep**	Dr	Warszawa	Sieć Badawcza Łukasiewicz – Instytut Chemii Przemysłowej imienia Profesora Ignacego Mościckiego w Warszawie
Adam	**Zuba**	inżynier	Warszawa	Wydział Chemiczny Politechniki Warszawskiej
Maja	**Zupancic**	Dr	Holandia (Alkmaar)	Technobis Crystallization Systems
Aleksandra	**Zwolenik**	lic.	Warszawa	Uniwersytet Warszawski, Wydział Chemii
Ewa	**Żesławska**	dr hab.	Kraków	Uniwersytet Pedagogiczny

INDEKS AUTORÓW PRAC / INDEX OF AUTHORS

Czcionką pogrubioną zaznaczono autorów prezentujących, *czcionką pochyłą* współautorów.
Presenting authors are shown in **bold font**, co-authors *in italics*.

Katarzyna	*Gibuła*	*B-44*
Mirosław	**Gilski**	*A-03*, *O-20*, O-21
Alessia	*Giordana*	*B-49*
Roman	*Gladyshevskii*	*A-30*
Adam	*Glinka*	*A-68*
Christian	*Göb*	*O-13*
Katarzyna	*Gobis*	*B-31*, *B-32*
Mateusz	*Gołdyn*	*A-09*, *B-50*
Antonina	**Gonet**	A-04
Tomasz	*Góral*	*B-67*
Szymon	**Grabowski**	A-35, S-6
Wiktoria	**Gromelska**	B-49
Tomasz	*Gryber*	*B-14*
Marlena	*Gryl*	*A-35*, *B-29*, *O-31*, *S-6*
Marta	*Grzechowiak*	*O-20*
Magdalena	**Grzegórska**	A-15
Iga	**Grześkowiak**	A-60
Maciej	*Grzywa*	*O-14*
Gonzalez	*Guillen*	*O-31*
Lubomir	Gulay	B-68
Uladzislaw	**Gumiennik**	A-65, S-13
Marek	*Gusowski*	*A-47*
Karolina	**Gutmańska**	*A-31*, *A-58*, A-66
Natalia	**Halaba**	A-36
Jadwiga	*Handzlik*	*B-47*
Michał	*Hapka*	*A-54*
Lauren E.	*Hatcher*	*A-54*
Katarzyna	Helios	B-48
Felix	*Hennersdorf*	*O-13*
Robert	*Henning*	*A-54*
Neda	**Heydari**	*A-15*, *A-17*, A-37
Andrzej	**Hilczer**	A-11
Armin	*Hoell*	*O-33* *S-14*
Anna A.	**Hoser**	*A-10* *A-51* *A-52* O-28
Valeryia	**Hushcha**	A-38
Natallia	**Husik**	A-39
Vladislav	**Ignatev**	B-65, S-11
Barbara	*Imiołczyk*	*O-20*
Ewelina	*Jach*	*A-47*
Ryszard	*Jakubas*	*B-62*

Tomasz	*Kołodziej*	*O-27*
Anna	*Komasa*	*A-09*
Piotr	*Konieczny*	*A-59*, *S-15*
Irina S.	**Konovalova**	*B-23*, O-11
Izabela	*Korona-Głowniak*	*A-34*, *B-31*, *B-32*
Mykhaylo	*Koterlyn*	*B-56*
Dorota	**Kowalska**	A-47
Maciej	**Kozak**	*A-68*, *B-01*, *B-06*, *B-09*, O-27, *S-7*
Anna	**Kozakiewicz-Piekarz**	*A-15*, A-17
Anna E.	**Kozioł**	A-67, *B-10*, *O-10*
Paweł	*Kozyra*	*A-43*
Robert	*Kral*	*B-63*, *S-16*
Malwina	*Krause*	*B-32*
Kateryna	**Kravets**	*A-28*, A-48, S-9
Marta	**Krawczyk**	A-18
Jacek	**Krawczyk**	B-58
Monika	**Krawczyk**	O-30
Adam	*Krówczyński*	*A-50*, *B-18*, *B-20*, *S-2*
Michał	*Krupinski*	*A-47*
Anna	**Kryczka**	A-49
Marek	*Krzemiński*	*B-12*
Dominika	**Krzeszewska**	B-02
Maria	**Książek**	O-25
Adam	*Kubas*	*B-14*
Jacek	*Kubicki*	*A-68*
Maciej	*Kubicki*	*O-21*
Marta	*Kulik*	*B-24*
Dharmandra	*Kumar*	*B-14*
Zofia	*Kurkiewicz*	*B-04*
Paulina	**Kurowska**	B-21
Łukasz	**Kurowski**	B-59
Katarzyna	*Kurpiewska*	*B-01*, *S-7*
Joachim	*Kusz*	*O-25*
Marcin	*Kuśmierz*	*O-10*
Anna	**Kwiecień**	B-22
Jan	*Lančok*	*A-55*
Daria	*Larowska-Zarych*	*A-09*
Hien Quy	*Le*	*A-22*
Andrzej	*Lechna*	*B-63*, *S-16*
Dmitry	*Lega*	*B-26*

Firmy uczestniczące w konferencji

Rigaku Europe SE

nanotechnology experts

ISBN 978-83-966642-1-1